Stereoselective Palladium-Catalysed C(sp^3)–H Functionalisation of Saturated Heterocycles at Unactivated C3 Positions

A Thesis Submitted by

Amalia-Sofia Piticari

In partial fulfilment of the requirements for the degree of

Doctor of Philosophy

Department of Chemistry

Imperial College London

Molecular Sciences Research Hub

White City Campus

London W12 0BZ

United Kingdom

2022

Declarations

Declaration of Originality

I, Amalia-Sofia Piticari declare that this thesis and the work presented herein has been generated by me as a result of my own original research. Where I have consulted the published work of others this is clearly attributed. Where the thesis is based on work done by myself jointly with others, I have made clear exactly what was done by others and what I have contributed myself.

Copyright Declaration

The copyright of this thesis rests with the author. Unless otherwise indicated, its contents are licensed under a Creative Commons Attribution-NonCommercial 4.0 International Licence (CC BY-NC).

Under this licence, you may copy and redistribute the material in any medium or format. You may also create and distribute modified versions of the work. This is on the condition that: you credit the author and do not use it, or any derivative works, for a commercial purpose.

When reusing or sharing this work, ensure you make the licence terms clear to others by naming the licence and linking to the licence text. Where a work has been adapted, you should indicate that the work has been changed and describe those changes.

Please seek permission from the copyright holder for uses of this work that are not included in this licence or permitted under UK Copyright Law.

Acknowledgements

May 2018 is when I received the news that my last PhD application had been rejected. With pursuing a PhD in Organic Synthesis being my biggest dream at the time, this sent me in a downwards spiral at quite a high speed. With rock bottom in sight, I approached James, though I was quite skeptical about my chances of securing a PhD position in his group. Not only did he say yes to me at that time, thinking I was a suitable candidate, but he continued to believe in my abilities with the same enthusiasm throughout my whole degree – even at times when I doubted myself. Thank you, James, for taking a chance on me and for your continuous advice, optimism and fantastic support throughout the years. I will be forever grateful for having received this opportunity and I wouldn't have bounced back if it weren't for your help.

I would also like to thank the members of the Bull group – past and present, for being the best company I could have asked for. Despite lab days sometimes being long, you have made the years seem so short. Thank you for your kindness, great humour, pub trips and, of course, for coping with the Piticari tantrums throughout the years. Thank you to Daniele Antermite for passing on his C–H functionalisation knowledge to me and helping with the mammoth job of assembling the fragment library, as well as to Sahra, Joe, Natalia and Harry with whom I've been collaborating. Many thanks to AbbVie for providing funding for this project and to Matt Webster for insightful discussions.

I am very grateful to Pete Haycock for running a considerable number of NMR samples at high temperatures, as well as to Corey Fulop for teaching me the intricacies of manually operating an NMR machine. I also thank Lisa Haigh for running all the mass spec analysis.

Big thank you to the wardening team that I was part of during my time in Woodward Halls. I will always remember with great fondness both our fun and challenging moments and I would do it all over again if I could.

For her incredible kindness and support and having gone the extra mile to help me pursue this PhD position – special thanks to my best friend Andreea.

A big thank you to Phil Hathaway for showing me the way "home" when I was lost.

Last but not least, I would like to thank my parents for always encouraging me to keep my chin up and my eyes pointed to the sky. There are no words to express my gratitude for the love and care you have for me and for sticking with me through thick and thin. This thesis is dedicated to you.

Abstract

Saturated heterocycles are widespread pharmacophores in marketed therapeutics and are advantageous scaffolds for the elaboration of new drugs. Their attractive properties include a low molecular weight and a high sp^3 character, which result in improved physicochemical profiles. However, there are limited tools to enable elaboration of building blocks from common feedstock such as intact heterocyclic rings. The ability to selectively probe any of the potential 3D exit vectors running along the C(sp^3)–H bonds would be extremely valuable in terms of modulating ligand-target complementarity, as well as generating molecules with new topologies in uncharted chemical space. Catalytic C–H functionalisation offers the potential to aid expansion along C(sp^3)–H bonds of choice. However, with C–H bonds remote from the heteroatom being less acidic and less distinguishable, achieving regio- and stereoselectivity is a challenge. This thesis presents a strategy for accessing a novel stereodefined 3,4-disubstitution pattern on 6-membered heterocycles by Pd-catalysed directed functionalisation.

Section 2.1 describes the mono-arylation at the C(3) position on unbiased saturated 6-membered heterocycles with a C(4) aminoquinoline amide directing group. Excellent conversions and selectivities for the *cis* diastereomer were achieved at unprecedently mild temperatures for this type of transformation (<50 °C), with access to single *trans* diastereomers enabled by a facile one-pot arylation-epimerisation.

Section 2.2 describes the removal of the aminoquinoline directing group in a divergent fashion to unveil polar functionalities such as nitriles, amides, carboxylic acids and alcohols. This allowed the assembly of a fragment library with a range of substitution patterns and a diversity of binding elements.

Section 2.3 illustrates the generation of building blocks for DNA-encoded libraries. Tri- and even tetrafunctional scaffolds with novel designs could be accessed using the functionalisation protocol.

Finally, section 2.4 presents the development of the first enantioselective C(sp^3)–H functionalisation at an unactivated position in saturated heterocycles.

Table of Contents

i. Glossary of Acronyms and Abbreviations 8
ii. Stereochemical Notation 11
1 Introduction **12**
1.1 An Overview of the Drug Development Process **12**
1.1.1 The Typical Drug Discovery Stages 12
1.1.2 Screening Methods in Drug Discovery 13
1.1.3 Desirable Properties of Drug Candidates 16
1.1.3.1 General Physicochemical Guidelines 16
1.1.3.2 Lipophilicity and Molecular Weight 17
1.1.3.3 Shape and Complexity 18
1.1.4 The Importance of Synthesis in Drug Discovery 19
1.2 6-Membered Saturated Heterocycles in Medicinal Chemistry **19**
1.3 Accessing Saturated Heterocycles with Defined Substitution Patterns **20**
1.3.1 Derivatisation of Pre-Functionalised Intact Rings 21
1.3.2 C(sp^3)–H Functionalisation at Activated Positions 23
1.3.3 Transition Metal Catalysed C(sp^3)–H Functionalisation at Unactivated Positions 25
1.3.3.1 General Considerations 25
1.3.3.2 Heterocycle Functionalisation with a C(2) Directing Group 29
1.3.3.3 Heterocycle Functionalisation with a C(3) Directing Group 35
1.3.3.4 Transannular Heterocycle Functionalisation Examples 38
1.3.3.5 Heterocycle Functionalisation with a C(4) Directing Group 39
1.4 Project Aims **41**
2 Results and Discussion **43**
2.1 Highly Regio- and *cis* Stereoselective C3 Functionalisation of Unbiased 6-Membered Heterocycles Using a C4 Directing Group **43**
2.1.1 Methodology Development 43
2.1.1.1 Directing Group Screen 43
2.1.1.2 Stereochemical Assignment of Reaction Products 45
2.1.1.3 Implementation of Mild Temperature Conditions 50
2.1.1.4 A Design of Experiment Driven Optimisation 57
2.1.2 Reaction Scope 64
2.1.2.1 *N*-Protecting Group and Aryl Iodide Scope 64
2.1.2.2 Hetero- and Carbocycle Reaction Scope 67
2.1.3 Studies on the Origin of Side-Product Formation 68
2.1.3.1 Diarylation Studies 68
2.1.3.2 Deuteration Studies 70
2.1.4 A One-Pot Arylation-Epimerisation 70
2.1.5 Conclusion 71

2.2 Directing Group Deprotection and Fragment Library Synthesis 73
2.2.1 Desirable Fragment Properties 73
2.2.2 Reported Syntheses of Shape Diverse Fragment Libraries 74
2.2.3 Project Aims 76
2.2.4 Aminoquinoline Deprotection on the 2,3-Disubstitution Pattern 77
2.2.4.1 Large Scale Arylation of Pyrrolidines and Piperidines 77
2.2.4.2 Synthesis of Primary Amide Derivatives 79
2.2.4.3 Synthesis of Carboxylic Acid Derivatives 81
2.2.4.4 Synthesis of Alcohol Derivatives 85
2.2.5 Aminoquinoline Deprotection on the 4,3-Disubstitution Pattern 86
2.2.5.1 Large Scale Arylation of 6-Membered Hetero- and Carbocycles 86
2.2.5.2 Accessing *trans* Diastereomers 87
2.2.5.3 Synthesis of Carboxylic Acid Derivatives 88
2.2.5.4 Synthesis of Amide and Nitrile Derivatives 89
2.2.5.5 Synthesis of Alcohol Derivatives 91
2.2.5.6 Boc Deprotection of Piperidine Derivatives 93
2.2.6 Fragment Library Overview and Property Analysis 94
2.2.6.1 General Overview and Physicochemical Property Analysis 94
2.2.6.2 Shape Analysis 98
2.2.7 Conclusions 104
2.3 Synthesis of Building Blocks for DNA-Encoded Libraries (DEL) 105
2.3.1 Strategies for Construction of DEL Building Blocks 105
2.3.2 Project Aims 107
2.3.3 Synthesis of Arylated Precursors 109
2.3.3.1 Large Scale Synthesis of a Bespoke Trifunctional Aryl Iodide 109
2.3.3.2 Large Scale C(3) Arylation of 6-Membered Heterocycles 110
2.3.3.3 Accessing *trans* Diastereomers 114
2.3.4 Synthesis of Trifunctional DEL Building Blocks 117
2.3.4.1 *N*-Boc Piperidine Building Blocks 117
2.3.4.2 Tetrahydropyran and Cyclic Sulfone Building Blocks 119
2.3.5 Synthesis of Tetrafunctional DEL Building Blocks 122
2.3.6 DEL Building Block Library Overview and Conclusions 124
2.4 Enantioselective C(sp^3)–H Functionalisation of Piperidines Bearing a C4 Directing Group 126
2.4.1 A Chiral Ligand Strategy 126
2.4.1.1 Reported Use of Monodentate Directing Groups and Chiral Ligands 127
2.4.1.2 Reported Use of Bidentate Directing Groups and Chiral Ligands 129
2.4.2 Project Aims 132
2.4.3 Methodology Development 133
2.4.3.1 Exploring Chiral Phosphoric Acid (CPA) Ligands 133
2.4.3.2 A 2-(Pyridin-2-yl)isopropyl Amine (PIP) Directing Group 136

2.4.3.3 Exploring Bidentate BINOL Ligands 138
2.4.3.4 Reaction Optimisation 142
2.4.4 Reaction Scope 147
2.4.5 Mechanistic Considerations 148
2.4.6 Conclusion 153
3 Conclusions and Future Work 155
4 Experimental Details and Characterisation Data 158
4.1 General Experimental Considerations 158
4.2 Compounds for Chapter 2.1 160
4.2.1 Directing Group Screen 160
4.2.2 Scope of *N*-Protecting Group and Aryl Iodide 167
4.2.3 Heterocycle Scope 184
4.2.4 Gram-Scale Arylation of Piperidine Amide 29a 187
4.2.5 Tetrahydropyran Arylation 189
4.2.6 Diarylation Studies 193
4.2.7 Deuteration Studies 196
4.2.8 One-Pot Arylation Epimerisation 197
4.3 Compounds for Chapter 2.2 199
4.3.1 Aminoquinoline Deprotection on the 2,3-Disubstitution Pattern 199
4.3.2 Aminoquinoline Deprotection on the 4,3-Disubstitution Pattern 210
4.3.3 Synthesis of Building Blocks for DNA Encoded Libraries (DEL) 227
4.4 Compounds for Chapter 2.3 242
4.4.1 Synthesis of Amides 242
4.4.2 Representative Procedures for the Synthesis of Racemic Compounds 244
4.4.3 General Procedure for the Synthesis of Enantioenriched Compounds 247
4.4.4 Palladacycle Formation 250
4.4.5 HPLC Traces for Enantioenriched 3,4-Disubstituted Piperidines 252
References 258
Appendix 1 - Optimisation Screen in the Presence of 2-(Methylthio)aniline Directing Group 270
Appendix 2 – List of Default Reagents Used in LLAMA Scaffold Decoration 271

i. Glossary of Acronyms and Abbreviations

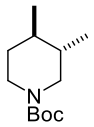
Ac	Acetyl
ADMET	Absorption, Distribution, Metabolism, Excretion, Toxicity
APAQ	Acetyl-protected aminoethyl quinoline
aq.	Aqueous
AQ	Aminoquinoline
APCI	Atmospheric pressure chemical ionisation
Ar	Aryl
BBB	Blood brain barrier
BINOL	1,1'-Bi-2-naphthol
BNPPA	1,1'-Binaphthalene-2,2'-diyl hydrogen phosphate
Boc	*tert*-Butoxycarbonyl
Bu	Butyl
Cbz	Benzyloxycarbonyl
CNS	Central nervous system
CMD	Concerted metalation deprotonation
COPD	Chronic obstructive pulmonary disease
CPA	Chiral phosphoric acid
***m*CPBA**	*m*-Chloroperbenzoic acid
dba	Dibenzylideneacetone
DBU	1,8-Diazabicyclo[5.4.0]undec-7-ene
DCE	Dichloroethane
DFT	Density-functional theory
DG	Directing group
DIPEA	*N*,*N*-Diisopropylethylamine
DMAP	4-(Dimethylamino)pyridine
DMF	*N*,*N*-Dimethylformamide
DMS	Dimethyl sulfide
DMSO	Dimethyl sulfoxide
DNA	Deoxyribonucleic acid
DoE	Design of experiment
DPPA	Diphenylphosphoryl azide
d.r.	Diastereomeric ratio
EDC	1-Ethyl-3-(3-dimethylaminopropyl)carbodiimide
ee	Enantiomeric excess
e.r.	Enantiomeric ratio
ESI	Electrospray ionisation
FDA	Food and Drug Administration

Fsp^3	Fraction of sp^3 carbons
FBDD	Fragment-based drug discovery
GSK	GlaxoSmithKline
HATU	Hexafluorophosphate azabenzotriazole tetramethyl uranium
HBA	Hydrogen Bond Acceptor
HBD	Hydrogen Bond Donor
HFIP	Hexafluoroisopropanol
HMDS	Hexamethyldisilazane
HOBt	1-Hydroxybenzotriazole
HPLC	High performance liquid chromatography
HRMS	High resolution mass spectroscopy
HTS	High throughput screening
IBX	2-Iodoxybenzoic acid
KIE	Kinetic isotope effect
clogP	Calculated partition coefficient
LLAMA	Lead-Likeness and Molecular Analysis
Me	Methyl
MesCOOH	2,4,6-Trimethylbenzoic acid (mesityl carboxylic acid)
mp	Melting point
MW	Molecular weight
NHC	*N*-Heterocyclic carbene
NMP	*N*-Methyl-pyrrolidone
NMR	Nuclear magnetic resonance spectroscopy
NPR	Normalised principal moment of inertia
NROT	Number of rotatable bonds
OA	Oxidative addition
PBF	Plane of best fit
PCR	Polymerase chain reaction
PG	Protecting group
Ph	Phenyl
PIDA	Phenyliodine(III) diacetate ((diacetoxyiodo)benzene)
PIP	2-Pyridinylisopropyl
Piv	Pivaloyl
pK_a	Negative logarithm of the acid dissociation constant K_a
PMI	Principal moment of inertia
ppm	Parts per million
Pr	Propyl
PROTAC	Proteolysis-targeting chimera
PSA	Polar surface area
Q	Quinolin-8-yl

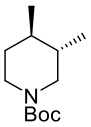
quat	Quaternary carbon
Ro5	Rule of 5
rpm	Revolutions per minute
RSM	Recovered starting material
rt	Room temperature
sat.	Saturated (referring to solutions)
SPINOL	Spirobiindan-7,7'-diol
***t*-amylOH**	2-methylbutan-2-ol (*tert*-amyl alcohol)
THF	Tetrahydrofuran
TIPSY	3,3'-Bis(triphenylsilyl)-1,1'-binaphthyl-2,2'diyl hydrogenphosphate
TMB	1,3,5-Trimethoxybenzene
TRIP	3,3'-Bis(2,4,6-triisopropylphenyl)-1,1'-binaphthyl-2,2'-diyl hydrogenphosphate
VANOL	3,3'-Diphenyl-2,2'-bi-1-naphthalol
VAPOL	2,2'-Diphenyl-(4-biphenanthrol)
X, Y	Generic atom or substituent

ii. Stereochemical Notation

Stereochemistry will be represented in this thesis according to Maehr notation.[1] Solid and broken bold lines will be used to denote relative configuration, whereas solid and broken wedges will denote absolute configuration. Where relative configuration is illustrated, the corresponding compound has been prepared as a racemate. Conversely, where absolute configuration is shown, the corresponding compound has been prepared in the enantioenriched form or as a single enantiomer.



relative configuration



absolute configuration

1 Introduction

1.1 An Overview of the Drug Development Process

1.1.1 The Typical Drug Discovery Stages

The development of new drugs has undoubtedly improved global health and wellbeing over the past decades, being a major contributor to increasing the life expectancy at birth from 66.8 years in 2000 to 73.3 years in 2019.[2] Scientific and technological advances, such as the sequencing of the human genome,[3] functional genomics,[4] as well as the emergence of machine learning and artificial intelligence have led to a more in-depth understanding of disease mechanisms.[5] This has in turn enabled a more informed selection of targets for the development of new therapeutics, nurturing hope that a number of currently untreatable diseases would be cured within our lifetime, with recent notable milestones reached for instance in the treatment of HIV.[6] On the other hand, phenotypic and pathway profiling platforms have also allowed the discovery of efficient drugs in the absence of a fully known disease mechanism.[7] In front of challenges posed by emergent diseases and drug resistance[8,9] these innovations are fuelling the pursuit of excellence in developing new therapeutics faster, cheaper and better tailored to patient needs.

However, drug discovery is far from being a streamlined process, requiring numerous stages, as well as significant time and resources. Being based on a "lock-and-key" analogy, large libraries of compounds are generally screened against a validated biological target, which is often a protein, in order to identify hits (Figure 1.1).[10] Further assays would then assess and rank the hits in terms of selectivity and efficacy, with one or multiple leads selected as a result.[11] To improve their potency, leads would undergo structural optimisation by derivatisation or synthesis of related analogues, aiming to also achieve a balanced profile in terms of potency and physicochemical properties. Depending on available synthetic tools, lead optimisation cycles can be lengthy, often creating a bottleneck in the progression to clinic.[12] The resulting drug candidate(s) may then enter clinical trials, with additional challenges present at each of the three phases in terms of proving a desirable safety and efficacy profile in humans.



Figure 1.1 Schematic representation of the drug discovery stages.

With obstacles to be overcome, launching a single therapeutic on the market may require up to 20 years and cost on average $2.8 bn from target identification to drug approval.[13] Despite the significant resource investment, as well as the increase in the number of approved drugs in recent years,[14] high attrition rates in late stages of drug discovery are still common issues in the pharmaceutical industry.[15,16]Although selection of a single candidate requires screening of thousands of other compounds, this currently has on average a less than 10% chance of entering Phase I clinical trials.[15] Between 2000-2010, 40% of the drug candidates from four top pharmaceutical companies were terminated before reaching clinical trials due to non-clinical toxicity, with a further 25% showing

unfavourable clinical safety, pharmacokinetics and/or bioavailability in subsequent studies.[17] Similar trends were observed by Kola and Landis for a series of candidates from 1991–2000.[18] Overall, the major reasons halting progression through clinical stages in 2016-2018 remained the lack of efficacy and/or safety in 79% of the cases.[15,19] Understanding the causes of the high failure rate is crucial, with suggestions including the unsuitable selection of biological targets, the lack of robust and diverse lead optimisation tools, as well as the low coverage of chemical and physicochemical property space in screening libraries to start with.[20,21,18] There is therefore high potential to tackle some of these issues through the development of novel and tailored synthetic tools for drug discovery.[22]

1.1.2 Screening Methods in Drug Discovery

A variety of screening strategies have been developed to suit a wide range of biological targets. The type of method used dictates the selection of libraries based on molecular weight and other specific properties, as well as influencing the swiftness of finding hits and the quality of the ligand-target interaction observed.

High Throughput Screening (HTS) has been the most employed strategy by pharmaceutical companies since 1980 and consists of testing very large collections, comprising of hundreds of thousands to millions of molecules against a target of interest.[23] This requires significant effort in acquiring and maintaining high quality physical collections of compounds, which would then be tested in automated assays, using plates of 384 wells and above.[24] Due to the relatively high molecular weight of the components, on average between 400 and 650 Da, hits at the limit of the Lipinski rules are often found,[25] limiting subsequent optimisation stages (Figure 1.2). Moreover, hits with only low to medium complementarity to the target are most common, since coverage of the chemical space is restricted by the huge number, in the range of billions, of possible molecules of the molecular weight considered. With criticism towards the 'numbers game' implied by HTS,[26] a shift is seen nowadays towards conducting smaller and more focused screens based on computer-assisted designs and prior understanding of pharmacophores suited for certain targets.[27]

Conversely, with the availability of X-ray crystallography and NMR, as well as the emergence of new sensitive biophysical methods for detecting low affinity hits, the screening of smaller molecules known as **fragments** has been possible. [28,29,30] By contrast to HTS, compounds of a maximum MW of 300 Da are screened, defining a chemical space of a more manageable size. Since the number of possible molecules of MW 300 is at least 10^7 smaller than those of MW 400,[30] unexplored areas of chemical space could be more efficiently sampled through judicious fragment design. Moreover, expanding fragment hits by linking or growth would further enhance the structural diversity achievable, leading to molecules more tailored to the geometrical particularities of the target that would exhibit higher complementarity and affinity compared to HTS-derived leads. (Figure 1.2).[31] However, challenges are associated with the correct identification of fragment hits, as well as with the availability of synthetic tools for enabling flexible expansion of hits along desired vectors and efficient further chemical space exploration.[30] A more detailed discussion of FBDD will be provided in Section 2.2.1.

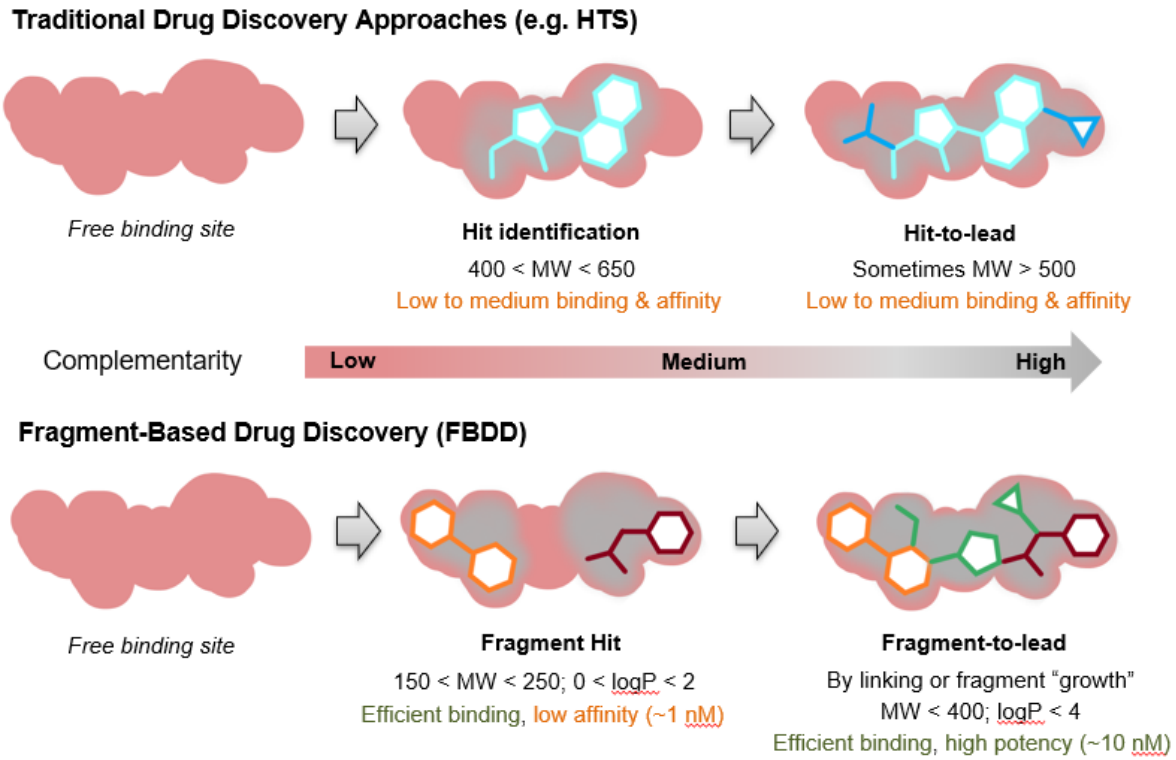


Figure 1.2 Schematic representation of the identification and optimisation of hits arising from traditional drug discovery approached such as HTS, compared to the FBDD strategy.

Phenotypic screening is another drug discovery strategy that can be conducted in the absence of a known target, having been widely employed before the development of HTS, but also recently, especially in the development of antiobiotics.[32,33] In this case, compounds are screened, most often in cell-based assays, for their ability to induce a change in the phenotype of the diseased cell. Having identified successful classes of compounds, the mechanism of action can then be elucidated to allow more informed future screens to be performed.[34]

DNA-encoded libraries (DEL) have also emerged with the potential to revolutionise drug discovery, by enabling the assembly of collections of compounds larger than ever before in a single test tube and obviating the need for large physical storage locations.[35] The concept of DEL was introduced by Brenner and Lerner in 1992 and takes advantage of innovations in DNA sequence amplification.[36,37] An illustrative example of DEL synthesis is shown in Figure 1.3 and involves initial tagging of parent molecules with unique identifying DNA headpieces. The resulting molecules would then be split into wells and further functionalised by addition of building blocks, provided suitable synthetic handles are present. For instance, BB_1 can be attached in well A to all parent compounds, and BB_2 in well B to the same entities, overall achieving all possible combinations between starting materials and reagents. Crucially, another DNA tag identifying the second building block would be appended to existent strands.

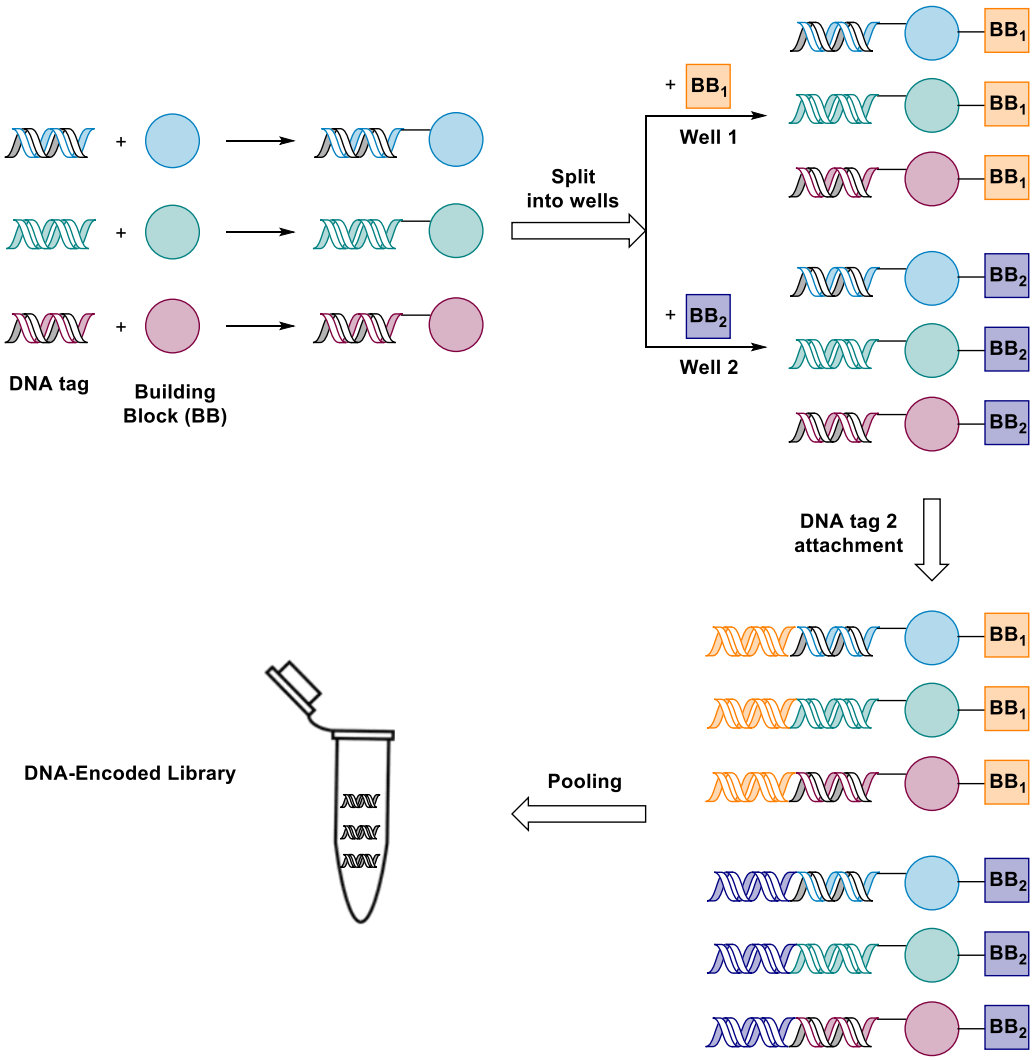


Figure 1.3 Schematic representation of the construction of a DEL library.

Combining the products, termed pooling, and repeating the process could generate considerably sized libraries, each compound bearing a unique DNA strand that 'encodes' its structural particularities. Mixing the library with the target of interest, followed by washing would reveal the binding entities, with amplification of the corresponding DNA barcodes through PCR enabling structural elucidation of the tagged compounds. Despite the operational ease, challenges are present with regard to the availability of DNA-compatible synthetic tools for attachment of various building blocks.[38] Moreover, binding affinity values can only be calculated upon hit validation, with false positives being common. Nevertheless, this method is significantly more time efficient than HTS, with the whole library being screened at once instead of requiring one individual step per compound.

On the other hand, ***in silico* screening methods** have been estimated to allow development of a drug 0.8 years faster and saving approximately $130 million throughout the discovery process.[39] Virtual libraries of compounds can be computationally docked and/or aligned with known protein structures to test the molecular recognition of specific compound classes.[40] The information can then be used to generate more focused HTS libraries for screening in physical assays, helping to concentrate efforts and resources on compounds more likely to result in hits. Alternatively, hit-to-leads may be

computationally designed and tested, enabling prediction of key characteristics prior to their physical synthesis.

1.1.3 Desirable Properties of Drug Candidates

Potency alone is not sufficient to determine the success of a drug candidate, with the interplay of a combination of factors crucial in ensuring progression through the later discovery stages. To achieve the desired therapeutic effect in the human body, a drug needs to be present in the bloodstream at a specific concentration, for a given amount of time. This concept, defined as bioavailability, depends on the aqueous solubility of the drug, with orally administered therapeutics additionally requiring a suitable lipophilicity in order to be absorbed from the gastrointestinal tract. Moreover, distribution to the target must be selective and accompanied by an appropriate clearance rate in order to avoid side-effects and toxicity. Conversely, care must be taken with regard to metabolism, with some drugs being rapidly converted to metabolites that are either toxic or too rapidly excreted. All of these desired behaviours are strongly related to the chemical nature of the molecule, and more intimately to its physicochemical properties. The ability to understand how these measurable and/or predictable physicochemical properties influence ADMET (Absoprtion, Distribution, Metabolism, Excretion and Toxicity) and pharmacokinetics is key to enabling the design of drugs with higher chances of clinical success.

1.1.3.1 General Physicochemical Guidelines

The most widely employed set of guidelines for the assessment of drug-likeness is the Lipinski's Rule of 5 (Ro5), developed in 1997 based on the analysis of the physicochemical properties of approved oral drugs at the time.[41] This stipulates that molecules with MW < 500 Da, clogP <5, less than 5 hydrogen bond donors (HBD) and less than 10 hydrogen bond acceptors (HBA) present solubility and permeability profiles that increase their chances of becoming orally bioavailable drugs. Nevertheless, deviations from these guidelines are increasingly common nowadays, with PROTAC degraders successfully formulated as orally bioavailable drugs despite numerous Lipinski rule violations.[42] Whereas other restricting guidelines have been described such as the GSK "4/400" (clogP/MW)[43] and Pfizer "3/75" (clogP/PSA),[44] the latter also accounting for molecular rigidity as a descriptor, limits on MW and clogP remain of utmost importance in most cases.

As analysed by Churcher, lead optimisation is often accompanied by an increase in MW and lipophilicity, and an initial hit follows the typical progression through Lipinski space depicted in Figure 1.4.[45] Starting with smaller and less lipophilic molecules is therefore essential in anticipation of the physicochemical property inflation. Hence, Churcher defines a "lead-like" space of defined MW and clogP limits (MW = 200–350 and clogP = 0–3), suggesting that compounds in this area have a higher chance of fitting within the optimum drug-like space after elaboration. Additionally, a trend towards the introduction of flat aromatics is common during lead optimisation, given the abundance of sp^2-sp^2 cross-coupling methods. Starting from more 3-dimensional compounds that bear less than 3 aromatic rings is expected to offer better chances for developing successful drugs in novel chemical space. Similar concepts can be translated to FBDD, which requires even smaller molecules for development of a lead (see Section 2.2 for desirable fragment properties).

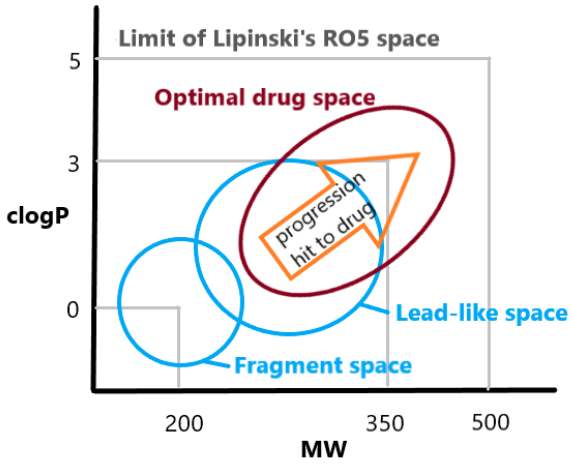


Figure 1.4 Typical hit-to-drug progression within the RO5 space, as identified by Churcher's analysis. Figure adapted from ref. 45.

1.1.3.2 Lipophilicity and Molecular Weight

As illustrated in the previous section, high importance is attached to the physicochemical properties of a drug, since these could influence the efficacy and ADMET (Absorptions, Distribution, Metabolism, Excretion and Toxicity) profile, and consequently also the attrition rate.[46] Unsurprisingly, lipophilicity and molecular weight have the most pronounced effect on ADMET parameters, since these determine the permeability, distribution and solubility behaviours, as well as the routes of drug clearance.[47,48]

Firstly, **lipophilicity** is defined as the affinity of a drug for a non-polar environment such as lipids, being most often quantified by the logarithm of the octanol/water partition coefficient (logP). LogP is therefore a representation of the ratio between the concentration of the drug between the two phases (octanol and water) at equilibrium, with its computational prediction also possible through a variety of descriptors (such as clogP).[49] Lipophilic compounds tend to permeate more easily through cell membranes, enhancing drug absorption. However, a high lipophilicity would correlate with a low aqueous solubility, decreasing the concentration of drug available in the systemic circulation that is able to induce a pharmacological response.[50] Although solubility is also influenced by ionisability at physiological pH, an analysis of 44,584 GSK compounds by Gleeson suggests that candidates with clogP < 4 are most likely to exhibit a good balance between permeability and solubility.[43]

The pursuit towards enhanced potency has been unavoidably associated with increased lipophilicity, since new hydrophobic interactions between the ligand and the target are often generated.[51] This can pose significant toxicity risks, with clearance of the drug becoming more challenging and accumulation in adipose tissues more likely. Moreover, other lipophilic targets can be engaged in a non-specific fashion, leading to undesired side-effects. Interestingly, a study by Leeson and Springthorpe found a link between compounds with clogP > 3 and increased chances of off-target promiscuity.[46] On the other hand, highly lipophilic drugs may be easily metabolised, since interactions with enzymes are facilitated. However, these might be fragmented into smaller polar compounds that are readily eliminated, negatively impacting bioavailability.[52,53] **Molecular weight** plays an important role, either individually or in combination with lipophilicity. Larger molecules tend to have lower permeability due to the presence of multiple heavy atoms, rotatable bonds and higher polar surface area (PSA).[54] It has been suggested

that candidates with MW = 350 – 400 generally show optimum permeability,[48] whilst the same study by Gleeson argued that MW values below 400 are best for tuning the aqueous solubility.[43]

1.1.3.3 Shape and Complexity

Success rates in drug discovery have also been influenced by the molecular shape and complexity of candidates, which impact the target-ligand complementarity, in addition to some ADMET aspects.

Firstly, the presence of hydrogen bond donors and acceptors (**HBD and HBA**, respectively) enables a good communication with the target *via* H-bond interactions. However, excessive hydrogen bonding may reduce the ability of the molecule to cross the cell membrane, affecting bioavailability.[41]

Moreover, the presence of electronegative heteroatoms as HBA would increase the **polar surface area** of a molecule (PSA), impacting once again permeability.[54] PSA is of particular importance in developing CNS drugs, since molecules with low polar surfaces (60-70 $Å^2$) are able to cross the blood-brain barrier (BBB).[55] In this regard, intuitive models (such as BOILED-egg) have recently been designed to estimate drug absorption and brain penetration as a function of PSA and clogP.[56,57] Apart from CNS drugs, the Pfizer "3/75" rule accounts for PSA as a factor influencing later stage toxicity. According to the study by Hughes, candidates with clogP < 3 and PSA > 75 $Å^2$ exhibited lower toxicities in pre-clinical trials.[44]

The overall flexibility of the molecule can also influence permeability. This is quantified by the **number of rotatable bonds**, NROT, which includes any single, non-cyclic and non-amide bonds attached to a non-terminal heavy atom. With more degrees of rotational freedom, a larger number of conformations are energetically accessible. Consequently, restricting the molecule to a conformation that allows transfer across the membrane would result in a high entropic penalty. More rigid compounds are therefore favoured, with NROT ≤ 10 and PSA ≤ 140 Å being associated with good permeability and oral bioavailability.[54]

In addition to the parameters above, there is a recent drive to increase **saturation** and architectural complexity in screening libraries.[58] Arguably, saturation increases **3-dimensionality** at a small MW expense, in turn allowing for a better fit between the ligand and the 3D biological target. As an implication, specificity for the desired target may also be increased.[59] In support of this, empirical observations by Lovering showed a positive correlation between the fraction of sp^3 hybridised carbons (Fsp^3 = number of sp^3 carbons / total carbon count) and the rate of success in later stages of drug discovery.[58] Moreover, saturated compounds with chiral centres may resemble the complexity of natural products and enable a more even exploration of chemical space, and discovery of hits with improved selectivity, activity and pharmacological profiles.

On the other hand, a high **aromatic ring count** (> 3) leads to an increase in lipophilicity and a decrease in solubility, being correlated with drug attrition.[60] Increasing saturation on the other hand has been commonly accompanied by an increase in aqueous solubility.[61] Ritchie and MacDonald argued in favour of increased saturation – however at the same time suggesting that heteroaromatic rings have only a limited negative impact compared to their carbocycle counterparts.[62] In their analysis, replacement of aromatics with saturated heterocycles improved aspects of the ADMET profile, while maintaining at least a similar "developability" compared with the parent molecule. Interestingly, a later matched molecular

pair analysis at Merck showed that saturated benzene analogues can promote interactions with the target that are similar in magnitude to π-π stacking.[63]

1.1.4 The Importance of Synthesis in Drug Discovery

Given the improved understanding of the properties that make better drugs, a good command of synthetic tools becomes crucial in accessing and/or tailoring molecules to exhibit desired characteristics.[64,65]

Over-reliance on the same set of well-established medicinal chemistry tools, such as amide couplings, nucleophilic aromatic substitution and cross-couplings involving sp^2 centres has unintentionally limited the structural diversity explored in screening libraries..[66,67] These procedures, despite being easily amenable to process scale-up, have led to the predominant exploration of aryl-rich compounds.[58] To tackle newer or less 'druggable' targets, for instance protein-protein interactions, solutions may be sought in the heavily uncharted areas of chemical space, comprising of more saturated molecules that present additional opportunities for 3-dimensional elaboration.[68,45] Development of new and robust synthetic protocols is crucial in steering the focus towards these novel screening motifs with improved properties. For instance, despite arguments in the favour of saturated heterocycles, their exploration is limited by the scarcity of methods for accessing defined ring substitutions (see Section 1.3 for a more detailed analysis).

Furthermore, lead optimisation is also limited by the breadth of synthetic methodologies available. The absence of suitable elaboration handles could halt progression of candidates, whereas time-consuming routes towards analogues may result in significant stagnation at this stage. Synthetic methodology development has the potential to overcome these challenges and transform drug discovery, with ongoing efforts in this respect.[22] We are closer than ever to the idea of functionalising any organic molecule along any C–H bond of choice in a selective manner, eliminating the limitation to traditional exit vectors.[69] It is envisioned that further developments in metal-catalysed cross-couplings and C–H activation would help push the current boundaries in terms of accessing saturated compounds with defined substitution patterns, generating large libraries of highly diverse compounds, as well as late-stage functionalisation.[22] Moreover, with modern drug discovery approaches focusing on the screening of smaller molecules, the development of highly stereoselective C(sp^3)–H activation synthetic tools and their application in generating these types of fragments and building blocks will be of high value to medicinal chemistry.

1.2 6-Membered Saturated Heterocycles in Medicinal Chemistry

A significant number of marketed drugs are centred on heterocyclic motifs, with an analysis by Ndjarson showing that more than 50% of the approved small-molecules therapeutics up to 2014 contained an *N*-heterocycle.[70] Moreover, out of the top 5 most commonly used rings, three were saturated heterocycles, with a continuous drive nowadays to increase saturation in screening libraries.[58,62] Out of these, piperidine was found to be most prevalent, with a range of well-known marketed drugs containing this as a central scaffold (Figure 1.5). Other 6-membered heterocycles are also represented, with blockbuster Simvastatin containing a tetrahydropyran motif, as does one of the most recently approved

pain treatment agents Oliceridine.[71] However, the diversity of saturated heterocycles is conditioned by the availability of synthetic tools for their construction. Increasing the diversity of saturated heterocycles employed may be extremely important in probing new binding modes and achieving a variety of desirable physicochemical profiles.

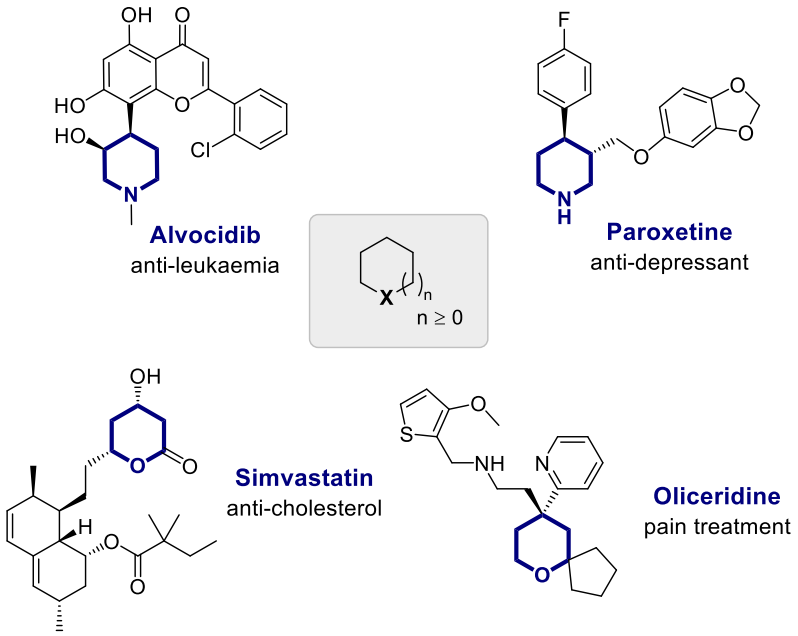


Figure 1.5 Overview of well-known drugs containing 6-membered *N*- and *O*-heterocycles.

Notably, all the drugs in Figure 1.5 bear a stereodefined substitution pattern, being marketed as single enantiomers. Since unsubstituted rings have a high number of energetically accessible conformations, the substitution pattern plays an important role in restricting the inherent flexibility of these rings, counteracting the entropic penalty upon binding.[72] Additionally, substituents could favourably contribute towards the enthalpy of binding. Synthetic methods to allow custom substituted heterocycles to be generated in single diastereomeric and/or enantiomeric forms from common feedstocks would therefore be of significant value for drug discovery.

1.3 Accessing Saturated Heterocycles with Defined Substitution Patterns

One of the most developed methodologies for accessing 6-membered substituted heterocycles relies on the cyclisation of suitably functionalised precursors, *via* either C–C or C–heteroatom bond formation,[73,74] with asymmetric variants also reported.[75] Whereas this has been a broad field of investigation with a multitude of strategies developed, it relies on the presence of pre-existent functionalities such as halides, alkenes and carbonyls, limiting the structural diversity that can be achieved using readily available reagents. More recently, direct amination of C–H bonds has been disclosed as a powerful alternative.[76] However, a more detailed discussion of ring-closure strategies is outside the scope of this thesis and will not be provided here.

Other traditional methods include hydrogenation of unsaturated heterocycles or cycloadditions.[77,78] However, achieving high regio- and stereocontrol in these cases is particularly challenging and relies on existent steric or electronic biases on the substrates.

Since intact rings are very often readily available feedstocks, there is a recent drive to develop selective methods for their functionalisation in desired fashions.[79] This section will present strategies for achieving defined substitution patterns on intact saturated heterocycles, with a focus on arylations, which are relevant to this thesis.

1.3.1 Derivatisation of Pre-Functionalised Intact Rings

Taking advantage of pre-existent diversification handles on the ring such as halides, carbonyl groups or alcohols, substituents can be installed in a modular fashion, leading to a diversity of substituted analogues.

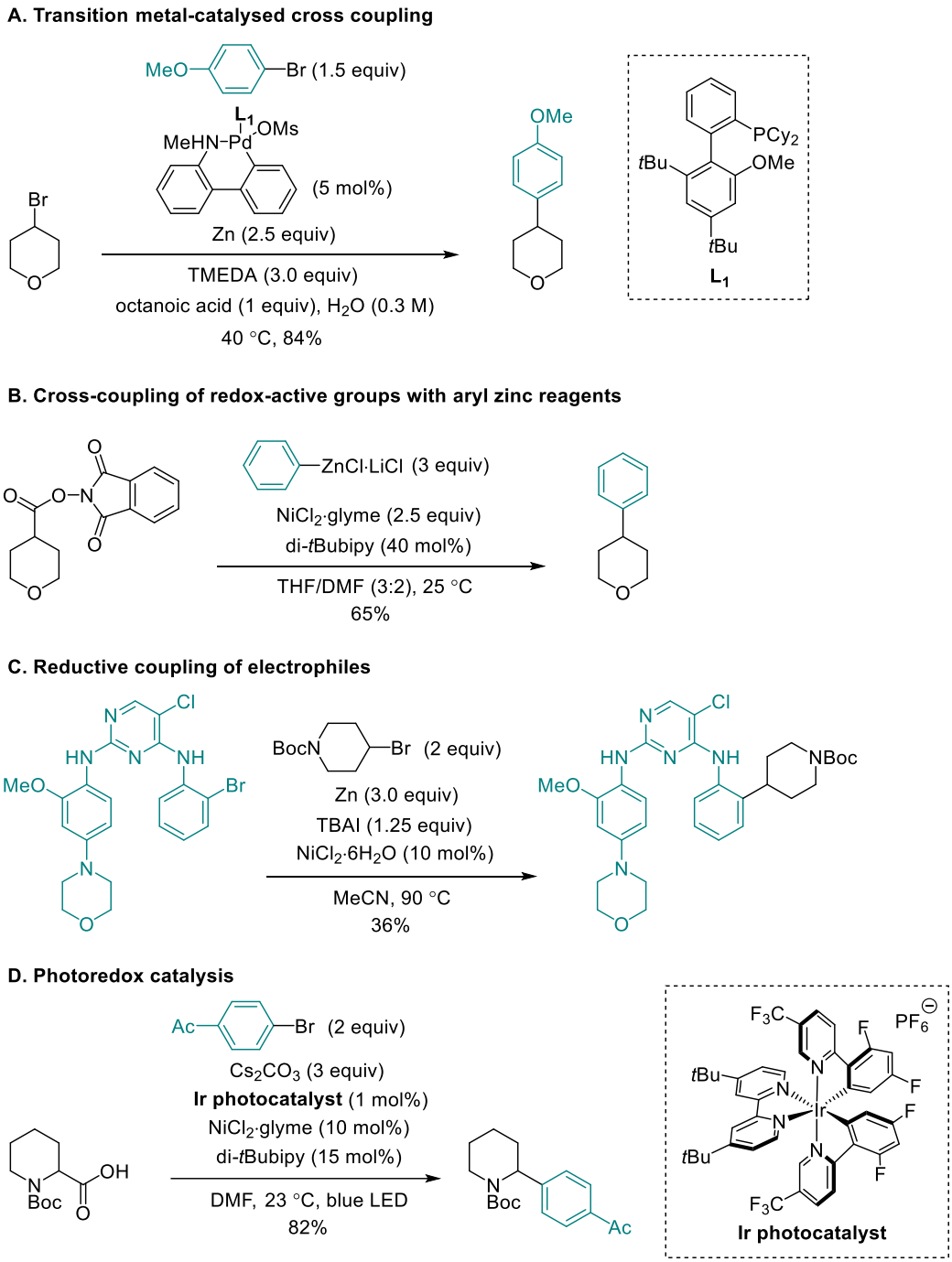
A variety of strategies have been reported for the direct installation of arenes in this fashion, one of the most employed being the transition metal catalysed cross-coupling between halogenated rings and an organometallic. Reactions such as Suzuki and Hiyama couplings were successfully employed in seminal works by Fu,[80,81] with further developments in ligand design preventing competing β-hydride elimination and allowing Pd-catalysed Negishi couplings on piperidines.[82] Additionally, Kumada couplings have also been enabled between halide-substituted heterocycles and Grignard reagents, using either Ni, Co or Fe catalysts.[83] Buchwald showcased a Pd-catalysed Lipshutz-Negishi cross-coupling that could be conducted under aqueous conditions,[84] whereby 4- to 6-membered alkylzinc-substituted heterocycles, generated from the corresponding bromides were successfully coupled to aryl halides or triflates (Scheme 1.1A).

On the other hand, Baran has more recently exploited carboxylic acid functionalities to form redox active groups, such as NHPI (*N*-hydroxyphthalimide) esters.[85] These could undergo fragmentation by a single-electron-transfer (SET) mechanism to forge sp^3-sp^2 bonds under various transition metal catalysed cross-coupling conditions with electrophiles such as aryl zinc reagents, Grignard reagents or boronic acids.[86] For instance, the NHPI ester derived from tetrahydropyran-4-carboxylic acid underwent decarboxylative cross-coupling in the presence of an aryl zinc reagent and a Ni catalyst to provide the corresponding C(4) arylated analogue in 65% yield (Scheme 1.1B).[85] Later studies identified alternative redox active groups based on nitrogen or sulfur, as well as methods to achieve this transformation with high stereoselectivity at tertiary centres.[87]

The reductive coupling of electrophiles has also emerged as a useful strategy for the functionalisation of saturated heterocycles, eliminating the need for organometallic reagents.[88,89,90] Electrophiles such as bromides, tosylates or sulfones could be coupled in the presence of a Ni(II) catalyst – however, excess loadings of reductants such as Zn or Mn are required. An example enabling the late-stage attachment of a piperidine ring to a drug molecule has been recently achieved by Merck and consisted of a reductive coupling between the corresponding bromides (Scheme 1.1C).[91]

Last, but not least, advances in photoredox catalysis have enabled sp^3-sp^2 couplings between saturated heterocycles bearing substituents which are radical precursors and aromatics with orthogonal functional handles.[92] Typically, these transformations are mediated by visible light and employ an Ir catalyst to

promote formation of a reactive radical, with radical precursors often including commonly available carboxylic acids.



Scheme 1.1 Strategies for the direct arylation of prefunctionalised intact rings.

MacMillan reported an example of a dual Ir/Ni catalytic system for the decarboxylative coupling of acids with aryl bromides.[93] In this case, the radical formed from the carboxylic acid under visible light irradiation in the presence of an Ir complex is intercepted by the Ni(II) aryl complex to give a Ni(III) aryl alkyl species, which would then deliver a new C–C bond upon reductive elimination. Compared to previous cross-couplings, this avoids the challenging transmetallation process, as well as the possibility for competing β-hydride elimination. Conducting this transformation on piperidine C(2) carboxylic acid in

the presence of 1-acetyl-4-bromobenzene afforded the corresponding C(2) arylated product in an excellent 82% yield (Scheme 1.1D).

On the other hand, the ability to selectively use any of the ubiquitous C–H bonds in these compounds as handles for further elaboration would be extremely powerful in terms of constructing even more diverse heterocycle libraries without being restricted by the availability of certain substituted precursors. Efforts are being made in this regard, with an overview of current methods illustrated in the next sections.

1.3.2 C(sp^3)–H Functionalisation at Activated Positions

The selective direct functionalisation of C(sp^3)–H bonds in saturated heterocycles has attracted increased attention. A plethora of methodologies have demonstratedfunctionalisation at the α position with respect to the heteroatom, since the corresponding C–H bonds display a higher reactivity compared to those remote from the heteroatom towards either homolytic or heterolytic cleavage, being termed "activated".[94] This is due to both a lower bond dissociation energy of these C–H bonds adjacent to the heteroatom,[95] as well as a higher acidity, reflected by the significantly reduced pKa value (Figure 1.6).[96] These distinct properties have allowed functionalisation *via* either α-carbanion, α-carbocation or α-radical intermediates, as well as by transition metal catalysed C–H activation.

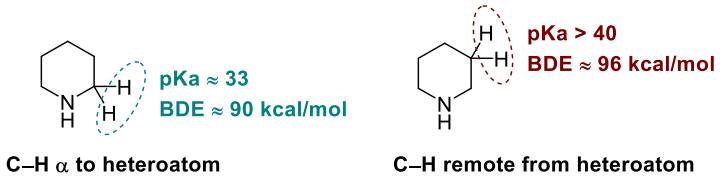
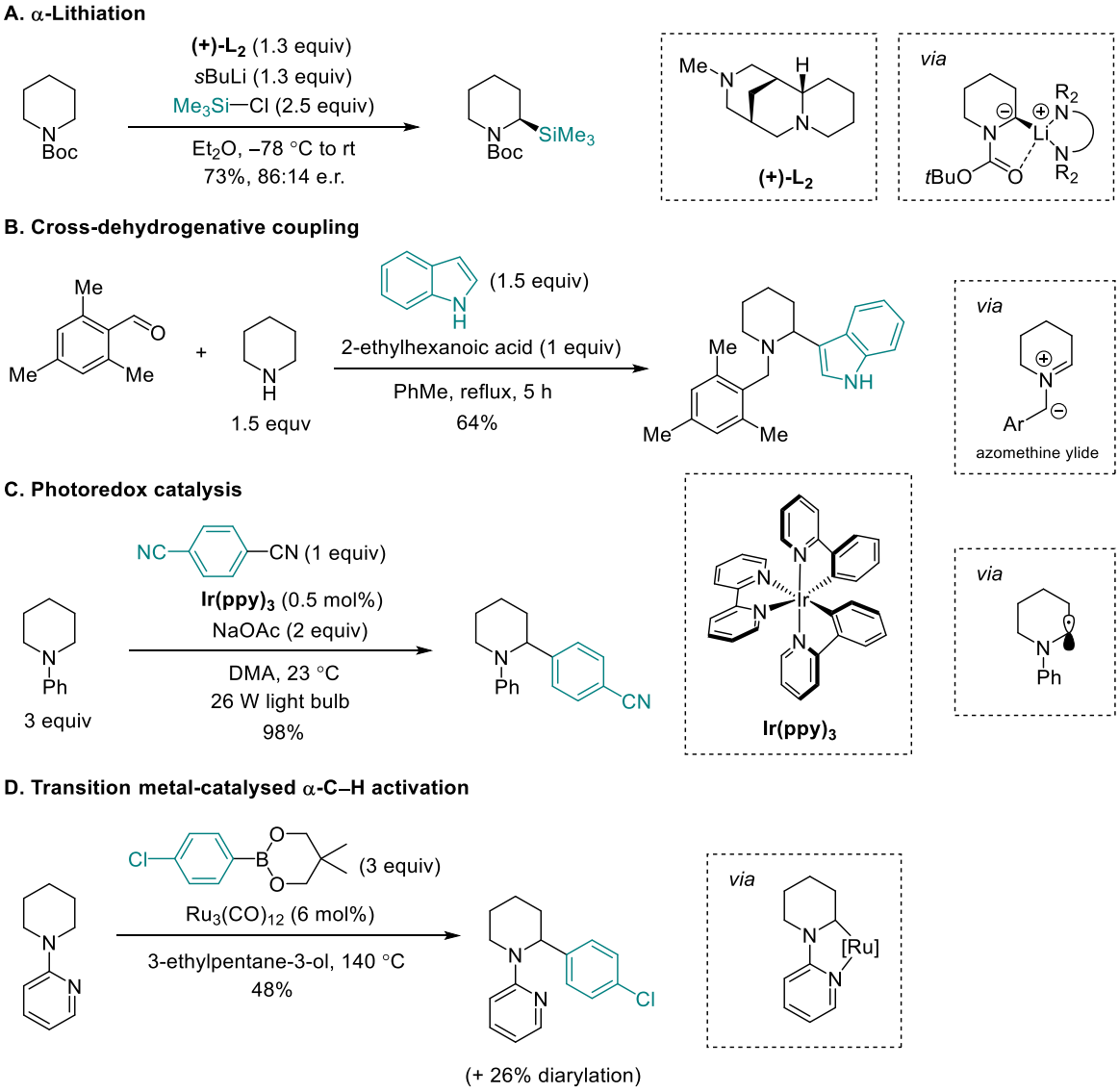


Figure 1.6 pKa and BDE difference between activated C(2)–H bonds and C–H bonds remote from the heteroatom.

The formation of an α-carbanion has usually been achieved by deprotonation with an organolithium base, followed by trapping with an electrophile. A variety of methods have been reported, with asymmetric deprotonation also made possible by employing a chiral diamine such as sparteine to coordinate to the lithium cation.[97] Recent work by O'Brien, Campos and collaborators employed react IR monitoring and mechanistic investigations to drive the development of a high yielding lithiation-trapping of piperidines.[98] Resorting to the use of *s*-BuLi in conjunction with (+)-sparteine surrogate **(+)-L_2**, C(2)-substituted piperidines could be synthesised in high enantioselectivities by reaction with electrophiles such as Me_3SiCl, Bu_3SnCl or various acyl chlorides, with an example of silylation illustrated in Scheme 1.2A.

Cross-dehydrogenative coupling has emerged as an alternative route for functionalising the C(2) position through an α-carbocation intermediate (e.g. iminium or oxonium), followed by reaction with a nucleophile. Metal catalysts such as Fe, Cu, and V species have been employed to generate the carbocation in conjunction with an oxidant, enabling Friedel-Crafts reactions with a variety of aromatics.[99] Nevertheless, metal-free conditions enabled by catalytic amounts of Lewis or Brønsted acids have also been demonstrated, involving hydride transfers to a pre-existing electrophilic moiety, such as an internal carbonyl.[100] Most often, the resulting carbocation is reacted with an organometallic to furnish the corresponding C(2)-substituted rings, though reactions with other nucleophiles are known.

As an interesting example, Seidel achieved C–C bond formation between the C(2) position on an intact piperidine ring and the C(3) on indole (Scheme 1.2B).[101] In this case, an imine is initially formed by piperidine condensation with sterically demanding mesitylaldehyde. This enables intramolecular hydride transfer to form an azomethine ylide which gets captured by the nucleophile.



Scheme 1.2 Overview of different strategies towards functionalisation of the intact ring at activated C(2) positions.

Homolytic cleavage of C–H bonds has also been employed to generate α-radical intermediates, one of the most notable strategies involving photoredox-mediated reactions. MacMillan first reported the photoredox catalysed arylation of saturated unsubstituted *N*-heterocycles at the activated C(2) position, with an example on a piperidine substrate illustrated in Scheme 1.2C.[102] In the above transformation, a single-electron transfer (SET) takes place from the activated Ir(III) catalyst species formed in the presence of visible light to the electron poor aryl coupling partner, resulting in formation of radical anion. Ir(IV) can then be reduced to Ir(III) by undergoing SET with the amine, generating the corresponding α-amino radical in the presence of a base. Finally, radical-radical coupling affords the corresponding C(2)-substituted piperidine. Notably, using a terephthalonitrile-derived radical anion led in this case to almost

quantitative yield of C(2) substituted piperidine. Dual Ir/Ni catalytic systems were also later developed by Doyle and MacMillan to allow the coupling of *N*-heterocyclic α-amino radical species with various aryl halides.[103] On the other hand, various photoredox protocols have been found to enable Minisci-type reactions between the same α-heteroatom radicals and more electron-poor heteroaromatics.[104]

Last, but not least, a significant number of studies have been dedicated to the transition metal catalysed C–H functionalisation at these more activated positions, due to the greater ease of metal insertion into these C(sp^3)–H bonds. Following pioneering work by Sames on pyrrolidine rings,[105] Maes reported the first C(2) functionalisation of piperidines, achieved in the presence of a Ru catalyst and using a pyridyl N(1) substituent (Scheme 1.2D).[106] It was suggested that the N(1) group dictated oxidative addition of Ru(0) into the C(2)–H bond, forming a thermodynamically favourable 5-membered metallacycle, which then underwent transmetallation with the boronate coupling partner. After reductive elimination, C(2) mono-substituted piperidines were isolated in up to 48% yields, though issues of mono- *vs* di-arylation were observed.

1.3.3 Transition Metal Catalysed C(sp^3)–H Functionalisation at Unactivated Positions

1.3.3.1 General Considerations

Given the previously discussed activated nature of the C–H bonds adjacent to the heteroatom, selective functionalisation at other positions on saturated heterocycles represents a significant challenge. Gratifyingly, advances in transition metal catalysis are paving the way towards activating these more inert bonds and envisaging new disconnections that would have otherwise not been viable.[107]

Mechanistically, transition metal catalysed C–H functionalisation involves an initial activation step, in which the metal inserts into a C–H bond, leading to formation of an organometallic species. From here, functionalisation with a coupling partner is possible to form new bonds between either carbon centres or a carbon and a heteroatom. The nature of the catalyst employed dictates the type of C–H bond cleavage taking place during the activation (Figure 1.7).[108] For instance, early transition metals in their highest oxidation state would promote σ-bond metathesis, since they lack additional coordination sites. On the other hand, electron-rich low-valent metals would promote oxidative addition, increasing their oxidation state and coordination number. Electron deficient late transition metals favour electrophilic substitution, whereas group 8-10 metals have been proposed to promote a concerted metalation-deprotonation (CMD) without formal change in the oxidation or coordination number.

With previous and current development of Pd catalysed C–H functionalisation methodologies on sp^2 and sp^3 systems, the mechanism of Pd insertion into the C–H bond (also termed C–H activation or metalation) was proposed to occur *via* several pathways.[109] Early studies supported an electrophilic activation mechanism in which Pd activates aromatic substrates to form Wheland-type intermediates from which proton abstraction occurs.[110,111] However, later Hammet parameter analysis by Davies and MacGregor did not support electrophilic activation of the aromatic ring by Pd in some cases, particularly when employing a dimethylaniline substrate and instead suggested an oxidative addition process, in which an initial agostic interaction takes place between the metal centre and the C–H bond.[112] This was

further argued to increase the acidity of the C–H bond to be activated, facilitating its abstraction by a base *via* a thermodynamically and kinetically favourable 6-membered intermediate.

However, a CMD mechanism was overall found to explain the C–H cleavage process over the widest range of systems.[113,114] This implies a transition state in which proton abstraction mediated by a base occurs concomitantly with formation of a new carbon–metal bond. Early studies by Fagnou on the Pd-catalysed benzene arylation demonstrated the direct involvement and importance of anionic ligands or bases in the C–H abstraction process, as well as the occurrence of a proton transfer pathway instead of S_EAr or radical processes.[115] Fagnou also showed that the CMD process correctly predicted the functionalisation reactivity and regioselectivity of entire spectra of electronically-diverse arenes, including some of the electron-rich examples for which S_EAr had previously been proposed.[116] Moreover, little or no deviation from the concerted nature of the C–H activation event was seen when changing the electronic nature of the aromatic substrate, especially in the case of Pd^{II}-carboxylate assisted transformations.[117] Mechanistic investigations by the same author further revealed a favourable CMD pathway also for the case of Pd-catalysed C(sp^3)–H bond cleavage, which explained general regioselectivity trends seen in the activation of aliphatic substrates.[118]

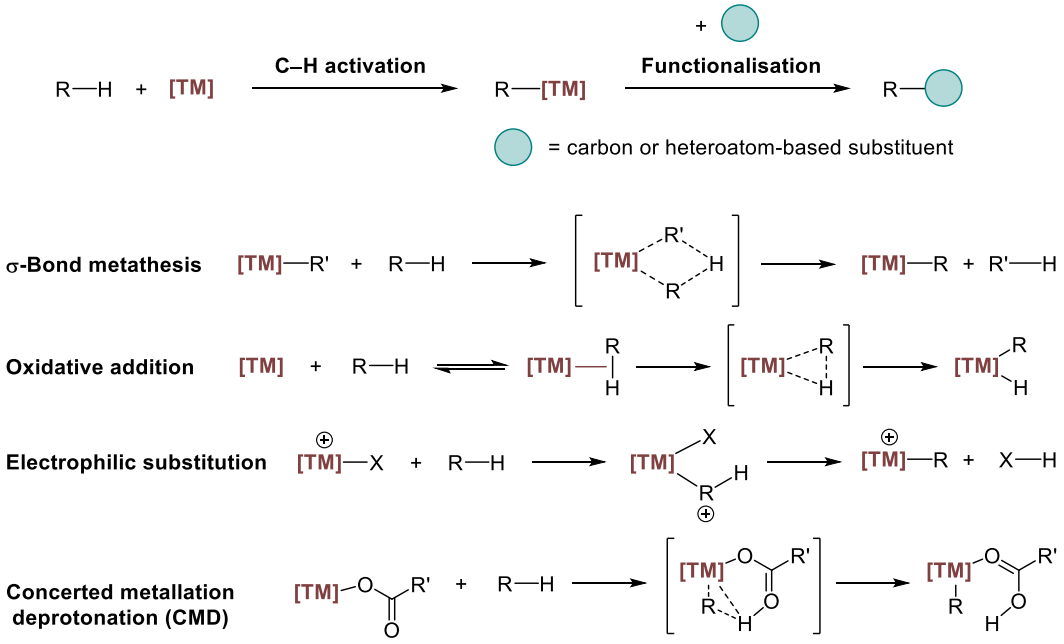
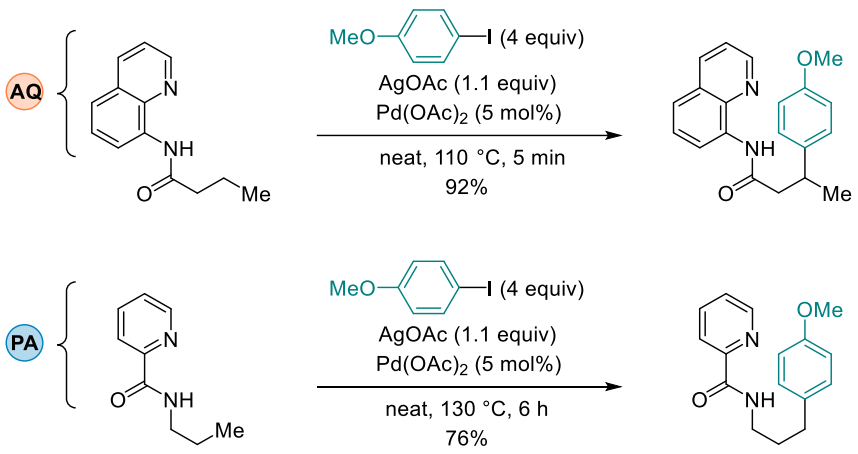


Figure 1.7 Overview of the type of mechanisms encountered in transition metal catalysed activation of C–H bonds.

Carboxylates and carbonates are commonly employed bases for facilitating proton abstraction, being introduced in the reaction as either anionic ligands of the metal source itself or through external reagents. Of the latter, silver bases are often preferred due to the additional roles of Ag in increasing turnover such as acting as halide scavenger (see below), and/or oxidant,[119,120] but also even as a partner in formation of heterobimetallic complexes with the catalyst which promote alternative and more energetically favourable C(sp^3)–H activations pathways.[121] Whereas the base is usually coordinated to the metal centre during the CMD, resulting in an inner-sphere deprotonation, examples are known in which outer-sphere anions promote proton abstraction.[122] On the other hand, certain bases or ligands

can be introduced in the reaction as additives, since they may decrease the activation energy barrier towards C–H abstraction and even promote an almost barrier-less C–H activation on certain substrates.[115,117] Interestingly, soluble organic additives have been used as co-catalysts to shuttle the protons to a stoichiometric insoluble base and prevent reversing the C–H deprotonation.[115]

Nevertheless, difficulties are met when trying to activate chemically similar C–H bonds, especially in the absence of biases inherent to the substrate, such as the presence of markedly more acidic sites and/or steric hindrance. To address this, the concept of directed C–H functionalisation has been developed, consisting of the use of auxiliaries which coordinate to the catalyst and position it in proximity of specific sites on the molecule, guiding activation at these position(s).[123] Significant strides have been made in the C(sp^2)–H functionalisation of aromatics, enabling regioselective functionalisations at various positions with respect to the directing group.[124] However, the activation of C(sp^3)–H bonds has been more challenging, due to questions of both regio- and stereocontrol, as well as the lower acidity of these bonds and absence of orbitals of suitable energies to easily interact with the metal. In 2005 Daugulis reported a notable achievement in the regioselective functionalisation of methylene groups on linear aliphatic substrates, by use of a removable bidentate directing group.[125] In this work, an 8-aminoquinoline (AQ) group was installed on aliphatic carboxylic acids *via* amide coupling, acting as an *N*,*N*-ligand for the Pd catalyst and dictating activation of the β-C(sp^3)–H with respect to the carbonyl *via* a thermodynamically favoured 5-membered Pd-cycle. In the presence of aryl iodide coupling partners, arylation at the β methylene was therefore selectively achieved in high yields (Scheme 1.3). Crucially, the mode of binding and the electronic properties of the aminoquinoline auxiliary were essential to stabilising the metal centre at high valences in order to effect the C–H insertion and subsequent catalytic steps (see below). Alternatively, using picolinamide as an "inverted" directing group binding to the aliphatic chain *via* an amine resulted in selective γ-C(sp^3)–H arylation.



Scheme 1.3 Daugulis' C(sp^3)–H functionalisation directed by removable bidentate auxiliaries (8-aminoquinoline and picolinamide).

The functionalisation mechanism was agreed to involve a Pd(II)/Pd(IV) manifold, with subsequent mechanistic investigations supporting this hypothesis (Figure 1.8).[126,127] Upon Pd coordination to the directing group, cyclopalladation was proposed to occur by concerted metalation-deprotonation (CMD) assisted by acetate, with both the catalyst and the silver base being sources of acetate. A 5,5-bicyclic palladacycle was the thermodynamically favourable intermediate, being generated by insertion of Pd

into the β-C(sp^3)–H bond. This intermediate was suggested to undergo oxidative addition with the aryl iodide coupling partner to form a Pd(IV) species. The possibility of forming this high valent species was later confirmed by the isolation and characterisation of a Pd(IV) complex from treatment of a related AQ-coordinated Pd(II) metallacycle with Br_2 at low temperatures (–78 °C).[128] Subsequent reductive elimination and halide abstraction aided by silver, followed by Pd decomplexation would then regenerate the active Pd(II) species and afford the β–arylated product.

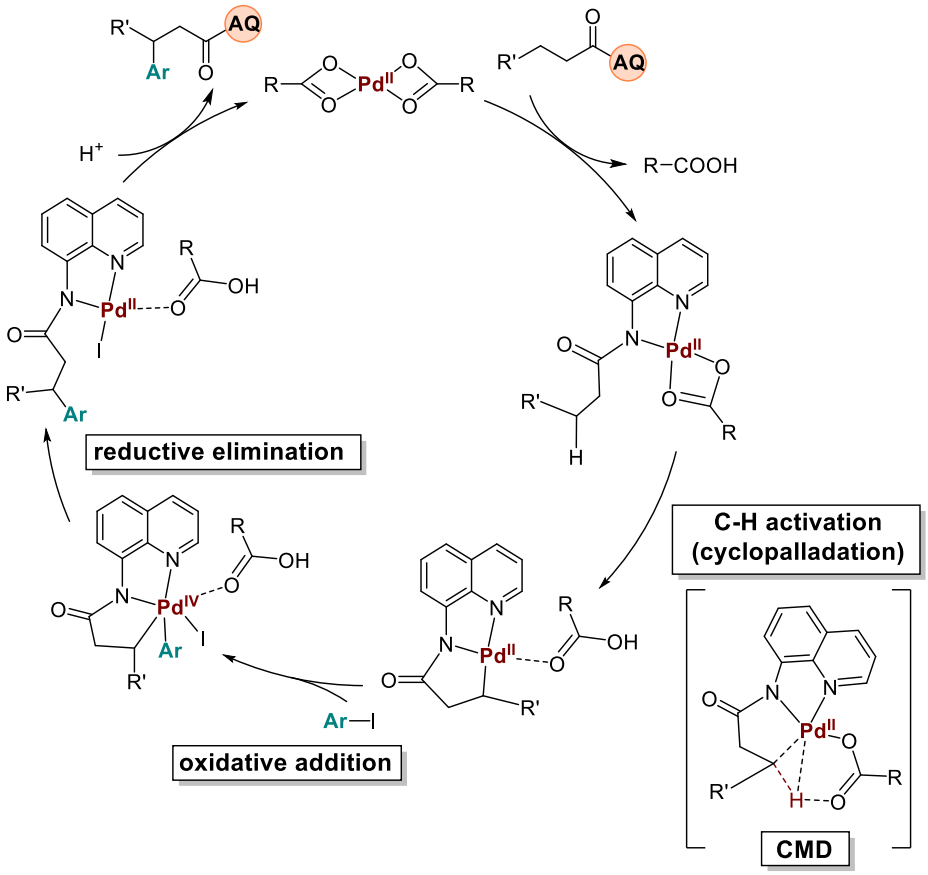


Figure 1.8 Pd^{II}/Pd^{IV} catalytic cycle proposed for the arylation of C(sp^3)–H bonds in the presence of an 8-AQ directing group.

Since this pioneering work, significant developments have been made in guiding selective C(sp^3)–H functionalisation on a variety of substrates with the aid of directing groups, notable examples including the arylation of aminoacids,[129] peptide macrocycles,[130] as well as facilitating total syntheses of natural products.[131] Interestingly, functionalisations occurring by alternative catalytic pathways are known, such as Pd^0/Pd^{II} manifolds (see Section 2.4.1.2 for an example),[269] as well as some mediated by binuclear Pd^{III} species.[132] Moreover, a variety of directing groups with different coordination abilities have been developed to cater for the electronic requirements of certain transformations and open opportunities for functionalisation at a variety of sites.[133] Weakly coordinating monodentate directing groups have also been successfully employed in conjunction with bespoke ligands to stabilise the metal centre and fine-tune aspects related to reactivity and selectivity, including enantioselectivity.[151,263]

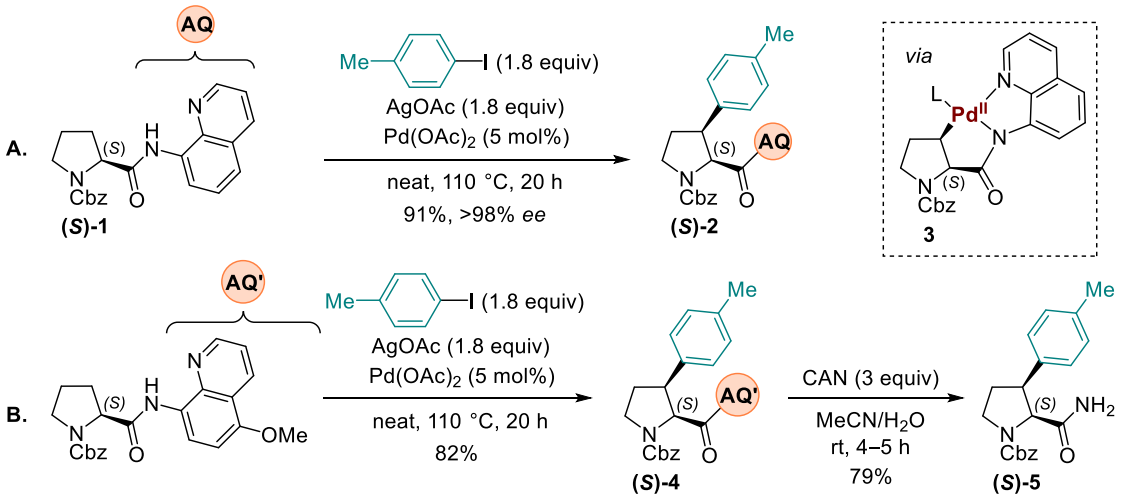
Nevertheless, the use of bidentate directing groups remains the most widely employed strategy, holding promise for addressing the challenges in the functionalisation of intact saturated heterocycles at

unactivated positions. An overview of the current directed methodologies for activation at positions remote from the heteroatom will be presented in the next sections, focusing on 5- and 6-membered *N*-heterocycles for which significantly more developments exist. Additionally, approaches for directing group deprotection will also be discussed in cases where this is achieved.

1.3.3.2 Heterocycle Functionalisation with a C(2) Directing Group

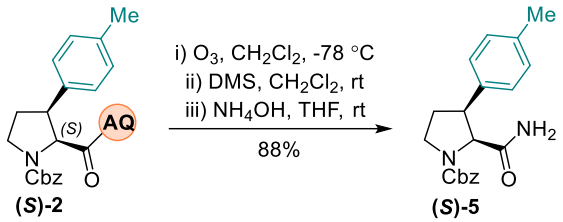
Following examples of alkynylation and arylation at remote positions on THP substrates by Yu,[163,164] the Bull group reported in 2014 the first directed arylation of unactivated C(sp^3)–H bonds in saturated *N*-heterocycles (Scheme 1.4A).[134] Using the carboxylic acid handle on the readily available *N*-Cbz (*S*)-proline aminoacid, the 8-aminoquinoline auxiliary was installed at C(2) by amide coupling to form **(*S*)-1**. In the presence of Pd catalysis, a highly regio- and stereoselective C(3) arylation was achieved with a range of aryl iodide coupling partners, affording access to *cis*-2,3-disubstituted pyrrolidines such as **(*S*)-2** in up to 91% yield under solvent-free conditions. The fused 5,5,5-tricyclic palladacycle intermediate **3** was thought to be responsible for both the observed diastereoselectivity, as well as the observed retention of (*S*)–proline enantiomeric excess. Interestingly, the *N*-protecting group used to prevent unwanted substrate-catalyst coordination was found to significantly impact conversion, with lower reactivity observed for the *N*-Boc pyrrolidine compared to the *N*-Cbz analogue.

Given the hindered nature of the strong amide bond, removal of the aminoquinoline auxiliary proved challenging. Employing 5-OMe-AQ instead as a higher electron density directing group was the only successful strategy to unveil the corresponding C(2) free amide **(*S*)-5**, by enabling CAN-mediated cleavage of the quinolyl motif from **(*S*)-4** (Scheme 1.4B). Moreover, this directing group, firstly employed by Chen,[135] promoted moderate to good yields in the C(3) arylation step.



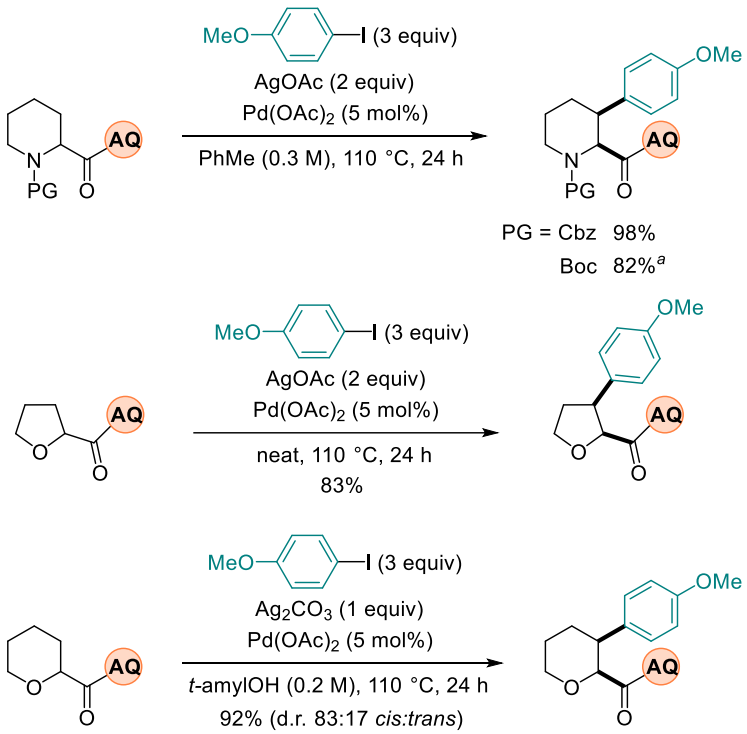
Scheme 1.4 A. C(sp^3)–H functionalisation of *N*-Cbz proline with a C(2) aminoquinoline amide (AQ) or 5-OMe-AQ (AQ') directing group. B. Removal of AQ' in the presence of CAN to unveil a free amide.

In a subsequent publication by Maulide, removal of AQ from **(*S*)-1** was demonstrated by ozonolytic cleavage, followed by treatment with aqueous ammonia to generate **(*S*)-5** in 88% yield (Scheme 1.5).[225]



Scheme 1.5 Ozonolysis protocol reported by Maulide for the removal of AQ to the corresponding free amide.

The Bull group also demonstrated the compatibility of a range of 5- and 6-membered *N*- and *O*-heterocycles with the previous C(3) functionalisation strategy, with a concise optimisation of the reaction conditions conducted for each substrate (Scheme 1.6).[169] Compared to pyrrolidines, piperidines exhibited a higher reactivity, with yields up to 98% obtained for the arylated product, though a decreased reactivity was seen again when using an *N*-Boc protecting group. Tetrahydrofurans and tetrahydropyrans were also arylated in excellent yields, however, formation of the *trans* diastereomer could be observed in the latter case, with the desired *cis* products isolated in up to 83:17 d.r. For the C(3) functionalisation of tetrahydrofurans, a similar aminoquinoline-directed strategy has also been reported by Babu, with excellent tolerance demonstrated for a range of heteroaryl iodide coupling partners.[136]

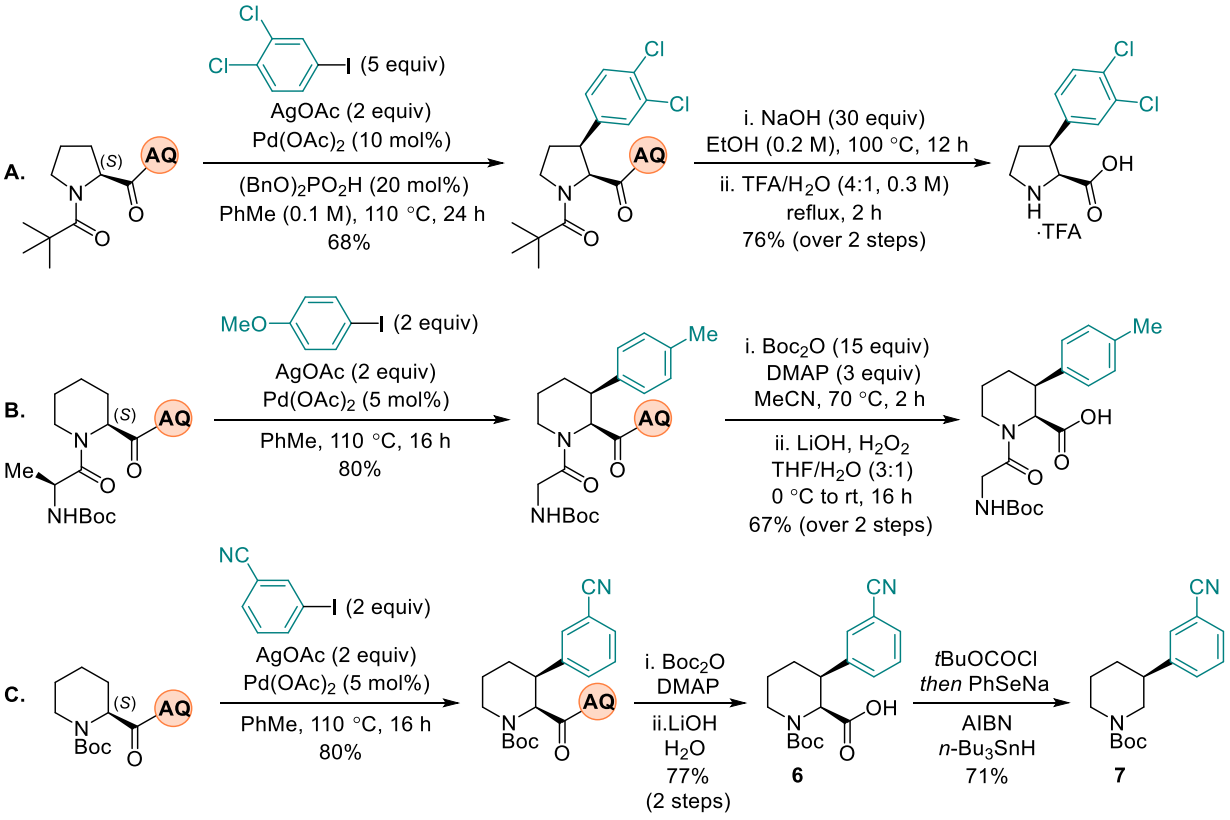


Scheme 1.6 Optimised conditions for C(3) functionalisation of piperidines, tetrahydrofurans and tetrahydropyrans bearing a C(2) AQ directing group.[a] Using Ag_2CO_3 (1 equiv) instead of AgOAc, as well as PivOH (30 mol%) and no solvent.

Numerous AQ-directed C(3) functionalisation protocols have been developed since on saturated 5- and 6-membered substrates, allowing the preparation of compounds with medicinal chemistry applications.

To enable AQ removal under strong basic conditions, Liu optimised the C(3) functionalisation of pyrrolidines in the presence of an *N*-pivaloyl protecting group (Scheme 1.7A).[137] To overcome the lower reactivity of this system, up to 5 equivalents of aryl iodide were used, in conjunction with a phosphate additive. Interestingly, the subsequent AQ removal step occurred without epimerisation at C(2) despite a large excess of NaOH being used.

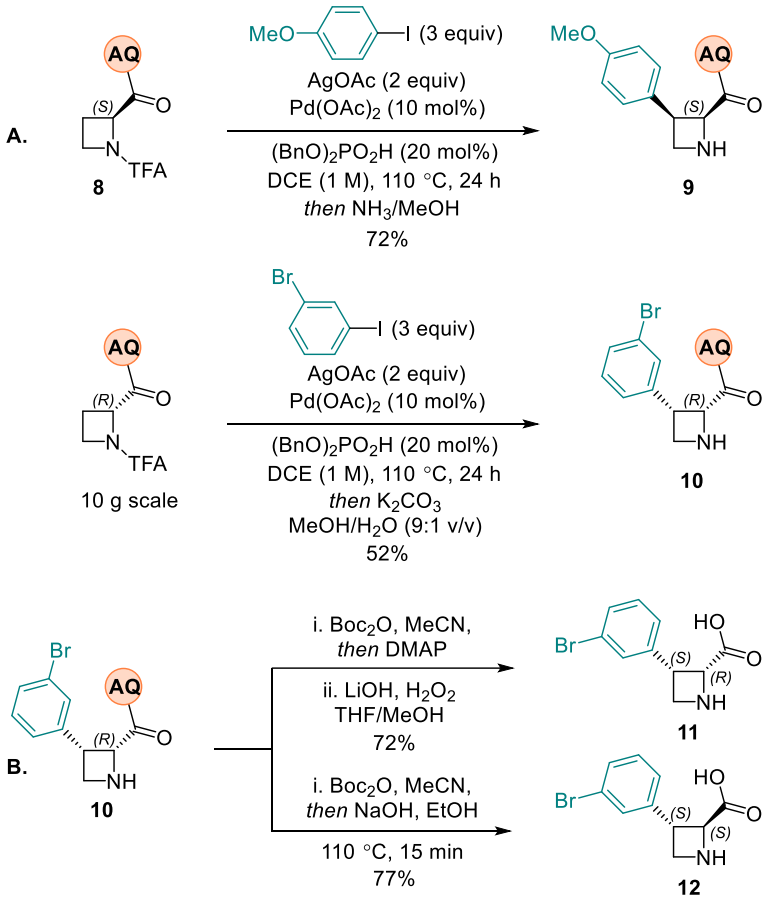
To open the opportunity for late-stage modification of peptides, the C(3) arylation of proline and pipecolinic acid moieties contained in di- and tripeptides has also been demonstrated by Kazmaier (Scheme 1.7B).[138] An aminoquinoline auxiliary installed at C(2) afforded high yields and retention of configuration at all stereogenic centres. The directing group was removed by amide activation with Boc_2O, followed by LiOOH hydrolysis to unveil the parent carboxylic acids and enable further diversification from *C*-terminus. A similar AQ removal strategy was employed by Wu after optimising a protocol for the C(3) arylation of *N*-Boc protected (*S*)-pipecolinic acid (Scheme 1.7C).[139] In this case, complete removal of the C(2) substituent was achieved by radical decarboxylation of **6** to generate neuroleptic drug analogue **7**. Later on, Wu also expanded the scope of the C(3) functionalisation to include alkoxylation and acyloxylation, with the nature of solvent and/or oxidant used determining the outcome.[140] Other AQ directed C(3) functionalisations involving coupling partners different from aryl iodides are known on 5- and 6-membered *N*-heterocycles, such as alkylations (using bromoacetates or phosphonated alkyl iodides),[141,142] fluorinations (using NFSI or Selectfluor in conjunction with the less coordinating PIP DG),[143,144] as well as alkynylations (using 1-bromo-2-triisopropylsilylacetylene).[145]



Scheme 1.7 Directed C(3) arylation of 5- and 6-membered *N*-heterocycles, followed by AQ removal to synthesise biologically relevant compounds.

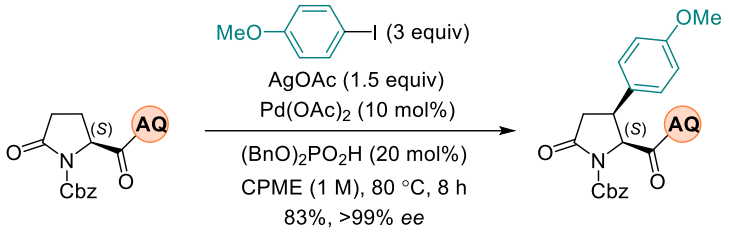
On the other hand, with tools available for reverting back to the carboxylic acid functionality after conducting an AQ-directed arylation, Baran, Yu, Schreiber and coworkers reported a formal C_β–H/C_α-C activation of 4-, 5- and 6-membered enantiopure aminoacids.[146] In this approach, a stereocontrolled *cis*-C(3) activation was followed by AQ removal and a highly *trans*-selective decarboxylative cross-coupling (dCC) to generate *trans*-2,3-difunctionalised carbon frameworks with high enantiopurities (>96% *ee*).

Moving to smaller ring sizes, Schreiber reported the C(3) arylation of commercially available enantiopure *S*-azetidine-2-carboxylic acid **8** (Scheme 1.8).[248] Using an AQ amide installed at C(2), an *N*-TFA protecting group was deemed best for encouraging high reactivity and affording *cis*-C(3) arylated azetidines in up to 72% yields and with high stereoselectivities. Notably, the TFA group could be hydrolysed in the same pot as the functionalisation, demonstrating an elegant and direct entry to free azetidine products (**9**, **10**). With a wide substrate scope, arylation in the presence of 3-bromoiodobenzene could be demonstrated on even a 10 g scale. This generated useful quantities of the 2,3-disubstituted azetidine intermediate **10** which could be converted to carboxylic acid building blocks **11** and **12** by AQ removal *via* Boc_2O activation, followed by basic hydrolysis (Scheme 1.8B). These carboxylic acids had various applications in the construction of a DEL library (see Section 2.3.1),[247] as well as in streamlining the synthesis of previously identified antimalarials.[147]



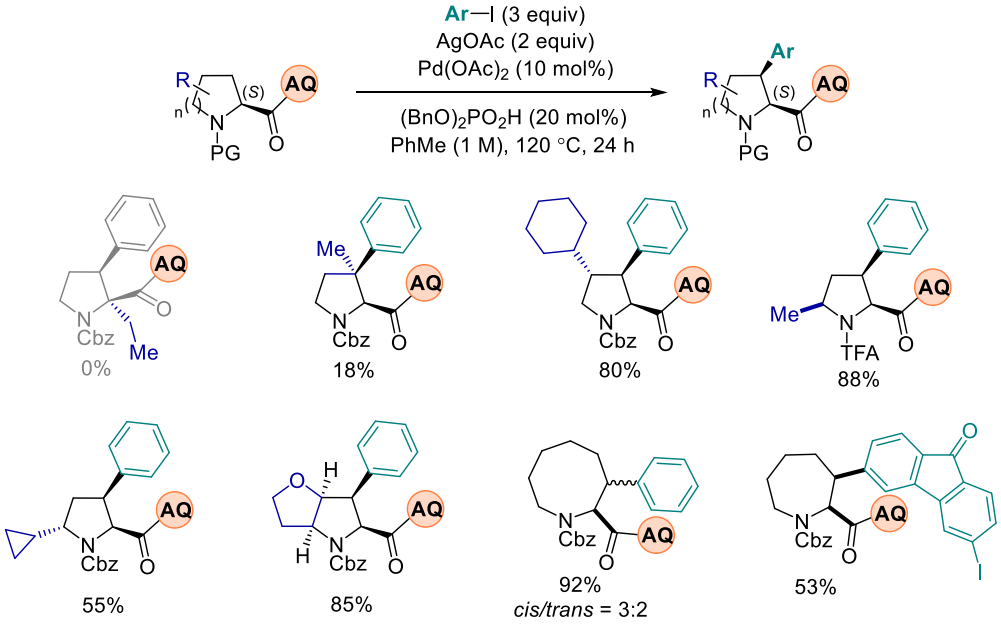
Scheme 1.8 A. AQ directed C(3) arylation of *S*-azetidine-2-carboxylic acid derivatives, with same-pot heteroatom deprotection. B. Example AQ deprotection by amide activation, followed by basic hydrolysis.

The aminoquinoline auxiliary could also be used to direct C–H functionalisation at traditionally unreactive sites on electronically and sterically biased substrates, such as pyroglutamic acids. With C(2) and C(4) positions being most accessible, Schreiber and coworkers managed to direct the arylation at C(3) through a similar strategy to the one used before on azetidines, but opting for the use of CPME as a solvent with improved safety profile (Scheme 1.9).[148] Besides Cbz, the reaction was tolerant of a range of electron-deficient *N*-protecting groups without a significant decrease in yield.



Scheme 1.9 C(3) functionalisation of pyroglutamic acids using a C(2) AQ directing group.

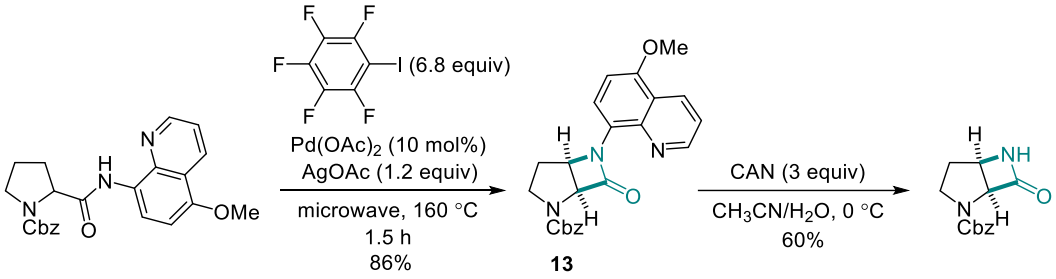
Similar to this, the directed C(3) functionalisation of pyrrolidines bearing a variety of pre-existent linked or fused alkyl or cycloalkyl substituents was studied more extensively by Mykhailiuk (Scheme 1.10).[149] To start with, an ethyl group geminal to the C(2) aminoquinoline amide auxiliary led to no transformation, presumably due to hindering the substrate from adopting a conformation conducive to C–H abstraction. On the other hand, a methyl group present at this position was found to be susceptible to functionalisation alongside the C(3) methylene. A pre-existent C(3) methyl allowed arylation at the same position to occur, albeit in low yield (18%). C(4) substituents *trans* with respect to the directing group were well tolerated, leading to up to 80% isolated yield of 2,3,4-trisubstituted pyrrolidines.



Scheme 1.10 Study of the influence of pre-existent ring substituents upon the yield of AQ directed C(3) arylation of proline. Directed arylation proven on variously sized saturated *N*-heterocycles.

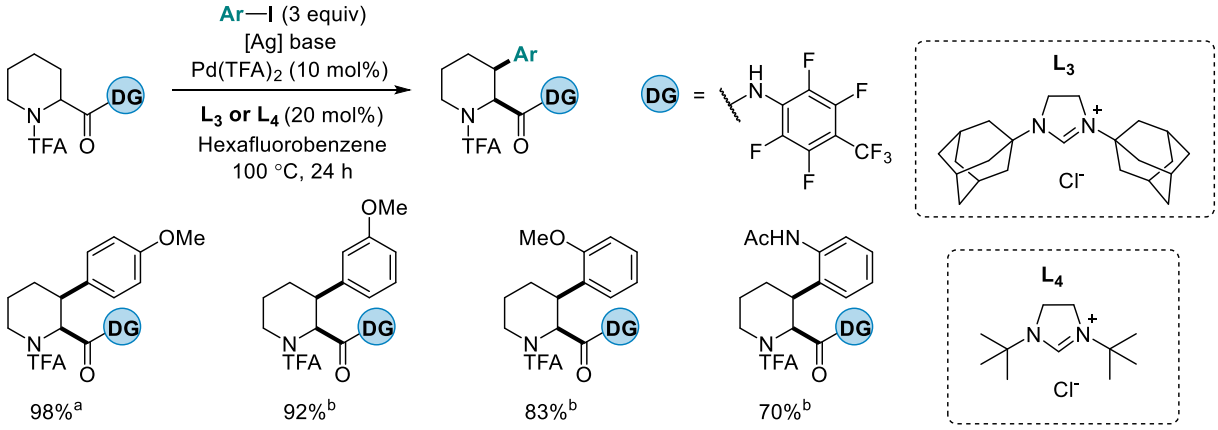
A similar behaviour was seen with distal C(5) groups, either *cis* or *trans* with respect to AQ, as well as with the presence of 4,5-fused rings. Finally, C(3) arylation of larger rings, such as 7- and 8-membered *N*-Cbz saturated heterocycles could be demonstrated with a range of aryl iodides, including a diiodinated fluoren-9-one, for which reactivity at only one iodine site was seen. However, formation of *trans*-arylated products was generally more prevalent with increasing ring size, lowering the *cis*-diastereoselectivity

The directed C(3) functionalisation of pyrrolidines and piperidines could also be promoted in an intramolecular fashion by Wu to generate valuable natural product-like lactams (Scheme 1.11).[150] To achieve this, the electronic properties of the aryl iodide coupling partner were modified to favour formation of a C–N bond with the amide nitrogen in the reductive elimination step instead of a C–C bond. Employing the electron-withdrawing pentafluoroiodobenzene, as well as microwave irradiation, *cis* fused β-lactam derivatives such as **13** could be obtained with high regio- and stereoselectivity, with removal of the pendant quinoline moiety possible in the presence of ceric ammonium nitrate (CAN) (Scheme 1.11).



Scheme 1.11 Stereoselective C(3) intramolecular amination using 5-methoxy-quinoline as both directing group and coupling partner, followed by quinoline removal by CAN oxidation for the generation of *cis*-fused β-lactams.

Monodentate directing groups have also been reported to direct functionalisation on saturated heterocycles. Using a C(2) perfluorinated aryl amide and an *N*-heterocyclic carbene (NHC) ligand to enhance σ-donation to the metal centre, C(3) arylation could be effected in excellent yields on *N*-TFA piperidines in the presence of a wide range of aryl iodides (Scheme 1.12).[151]



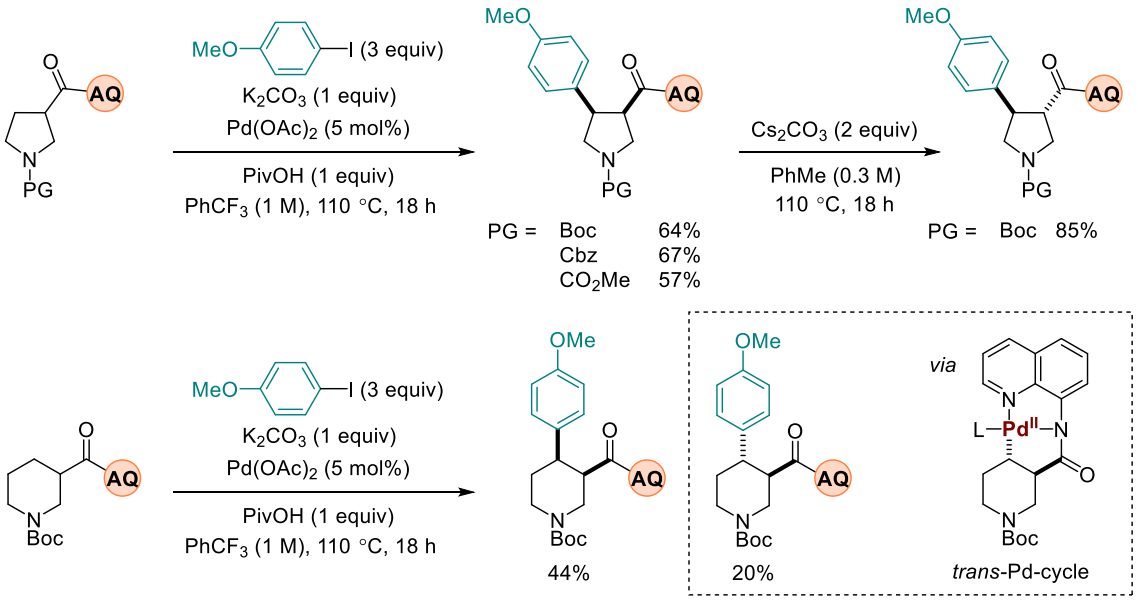
Scheme 1.12 NHC-mediated C(3) functionalization of *N*-TFA protected piperidines with a C(2) monodentate directing group. [a]Using **L$_3$**, Ar-I (2 equiv) and AgOAc (3.0 equiv). [b]Using **L$_4$**, Ar-I (3 equiv) and Ag_2CO_3 (2.0 equiv).

Moreover, the products were formed with high *cis* stereoselectivity, whereas fine-tuning the steric and electronic features of the NHC ligand enabled installation of previously challenging substituents, such as *meta*- and *ortho*-substituted arenes in high yields (>70%). Mechanistic investigations revealed this to be the first example of C(sp^3)–H activation promoted by a Pd^{II}/NHC complex, with an overall Pd^{II}/Pd^{IV} manifold in operation.

1.3.3.3 Heterocycle Functionalisation with a C(3) Directing Group

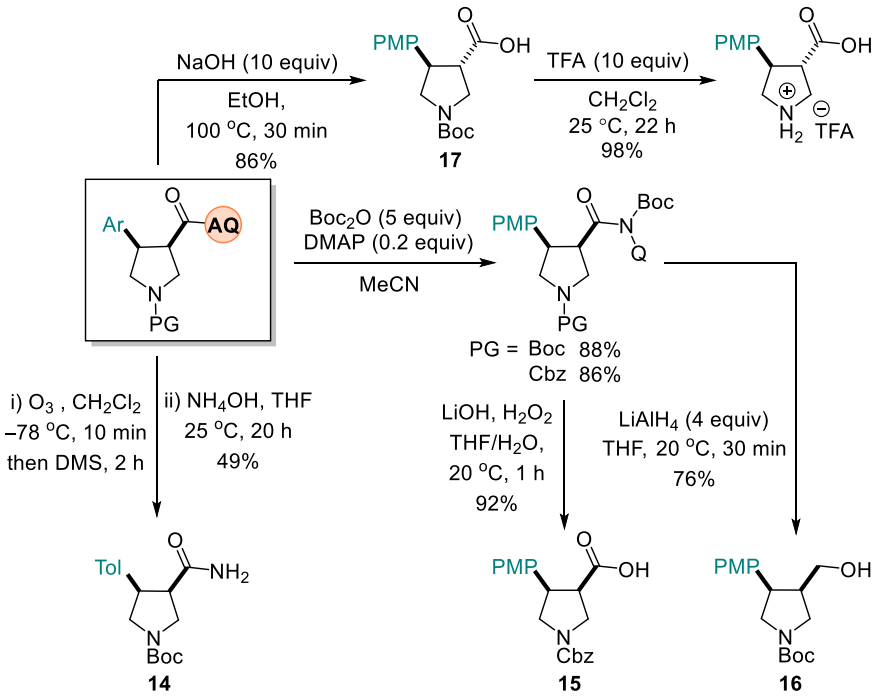
5- and 6-Membered heterocycles with directing groups installed at C(3) pose selectivity questions in their functionalisation, since two different β-methylene environments are available.

In work conducted by the Bull group, *N*-Boc pyrrolidines and piperidines bearing a C(3) aminoquinoline amide were subjected to Pd-catalysed arylation in the presence of various aryl iodides.[168] Surprisingly, despite the more acidic C(2) position, arylation at C(4) was selectively observed in both cases, most likely due to the steric hindrance imposed by the carbamate protecting group (Scheme 1.13). Further reaction optimisation resulted in the used of silver-free conditions, by employing K_2CO_3 as base in conjunction with PivOH additive, with these conditions completely inhibiting formation of the minor C(2) arylated side product. Yield of up to 67% were achieved with a diversity of aromatics bearing medicinally relevant functionalities and/or diversification handles such as NHBoc, CF_3 or SMe, as well as with various *N*-protecting groups. Moreover, high *cis* stereoselectivity was seen in the arylation of pyrrolidines, although the products could be converted to the corresponding *trans* diastereomers by a facile Cs_2CO_3 epimerisation. Alternatively, starting from the enantiopure substrate resulted in retention of *ee* and isolation of single *cis* enantiomers, which could be further epimerised to enantioenriched *trans*-3,4-disubstituted products. Under adapted conditions, piperidines led also to *cis* stereoselective C(4) arylation, although formation of *trans*-configured side-products was observed in varying amounts with *para*- and *meta*-substituted aryls. Interestingly, mechanistic investigations revealed the origin of a side-product from competing *trans*-palladacycle formation rather than epimerisation.



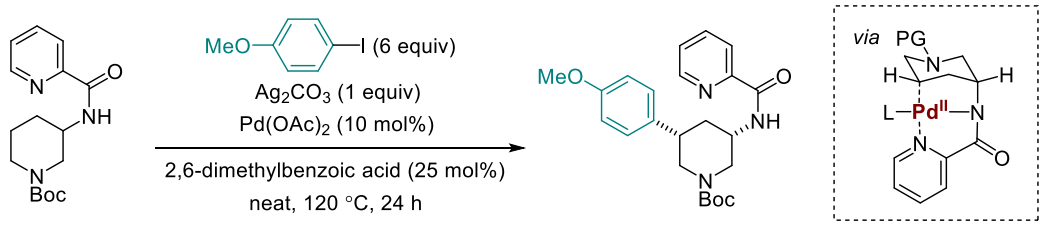
Scheme 1.13 C(4) selective arylation of pyrrolidines and piperidines using a C(3) AQ directing group. Piperidine *trans*-arylated side-product arising from a *trans*-palladacycle.

Divergent aminoquinoline removal was also demonstrated to unveil free polar functionalities (Scheme 1.14). Amide **14** could be unveiled by adapting Maulide's ozonolysis protocol,[225] whereas Boc-activation of the directing group allowed entry to *cis* carboxylic acid **15** upon treatment with LiOOH and *cis* alcohol **16** after reduction with $LiAlH_4$. By contrast to the 2,3-disubstituted heterocycles, AQ hydrolysis with excess NaOH promoted concomitant epimerisation, affording *trans*-acid **17** directly in an excellent 86% yield.



Scheme 1.14 Divergent AQ removal to unveil free polar functionalities.

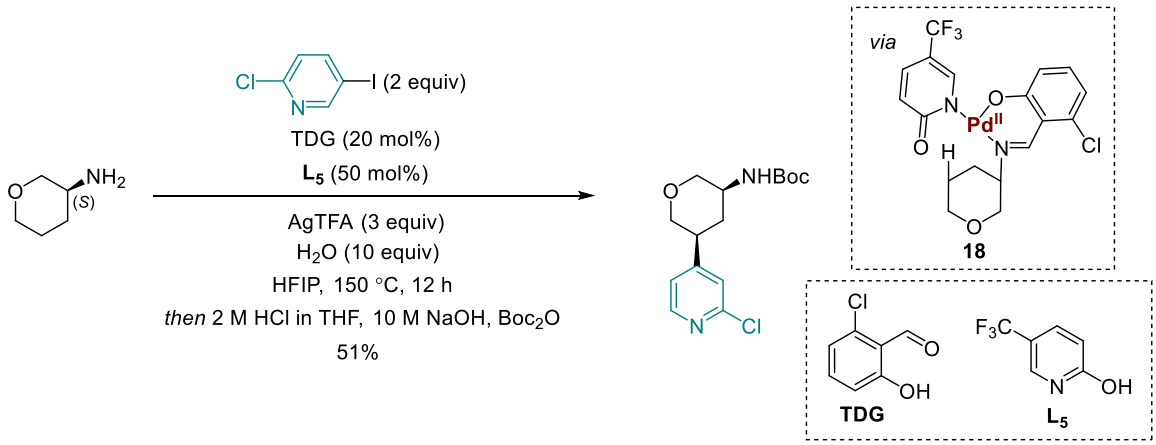
Auxiliaries attached through amine functionalities have also been used to direct ring functionalisation. Maes reported the use of a C(3) picolinamide directing group on piperidine substrates.[152] In this case, a 5-membered bridged palladacycle is thermodynamically favourable, engaging the C(5) position and resulting in stereospecific γ-*cis*-arylation with respect to the amine (Scheme 1.15). As in previous examples, an *N*-Boc protecting group was opted for, since it was best in preventing intramolecular coordination of the ring nitrogen to Pd and allowing the productive C(5)–H insertion instead. The picolinoyl auxiliary could be removed by basic hydrolysis with retention of dr to revert to the parent C(3) amine for further derivatisation. Later on, Maes reported the C(5) olefination of piperidines and tetrahydropyrans using the same directing group, as well as olefination coupled with intramolecular amidation with the picolinoyl auxiliary to generate bridged bicyclic scaffolds.[153]



Scheme 1.15 Regio- and stereoselective C(5) arylation using a C(3) amine-linked picolinamide auxiliary.

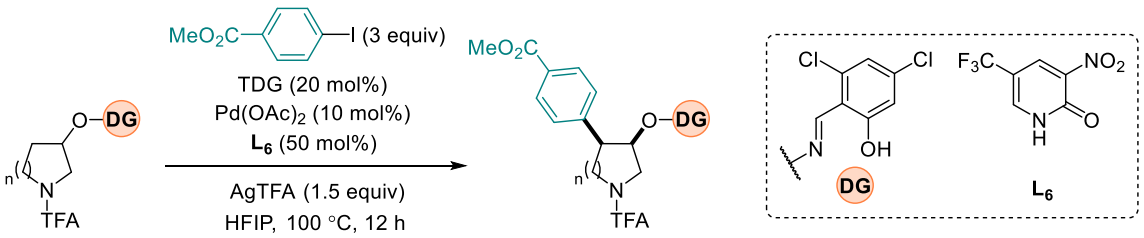
Examples of γ-alkynylation directed by the picolinamide group have been reported on *N*-Boc piperidines by Balaraman.[154]

Using pre-existent amine handles, the formation of transient imine directing groups has also been reported. Transient directing groups (TDGs) represent advantageous strategies in C–H functionalisation, by obviating the extra steps needed for installation and cleavage of the metal-coordinating auxiliary.[155] Yu reported the assembly of imines from free amines and hydroxybenzaldehydes, resulting in transient bidentate coordinating groups that would form 6-membered Pd(II) chelates.[156] One of these TDGs formed with a C(3) free amine group on tetrahydropyran was successfully employed in promoting functionalisation at C(5) with 2-chloro-pyridine in 51% yield and with high *cis* stereoselectivity (Scheme 1.16). A 2-pyridone ligand (**L$_5$**) acted as an acetate surrogate to accelerate the C–H cleavage step, whereas regioselectivity arose from formation of a fused 6,5-bicyclic palladacycle intermediate (**18**). The corresponding 3,5-*cis*-disubstituted product could be isolated as the *N*-Boc protected amine after acidic work-up to cleave the imine, followed by basic extraction and Boc protection.



Scheme 1.16 Heteroarylation of tetrahydropyran at C(5) using a C(3) transient imine directing group.

Yu has also demonstrated the use of alcohol-linked directing groups for the functionalisation of 4-, 5- and 6-membered saturated *N*-heterocycles.[157] The directing group was installed by reacting oxaziridine or dichlorosalicylaldehyde derivatives with the corresponding C(3) alcohol and afforded *cis* stereoselective β-arylation at C(4) under Pd-catalysed conditions (Scheme 1.17).



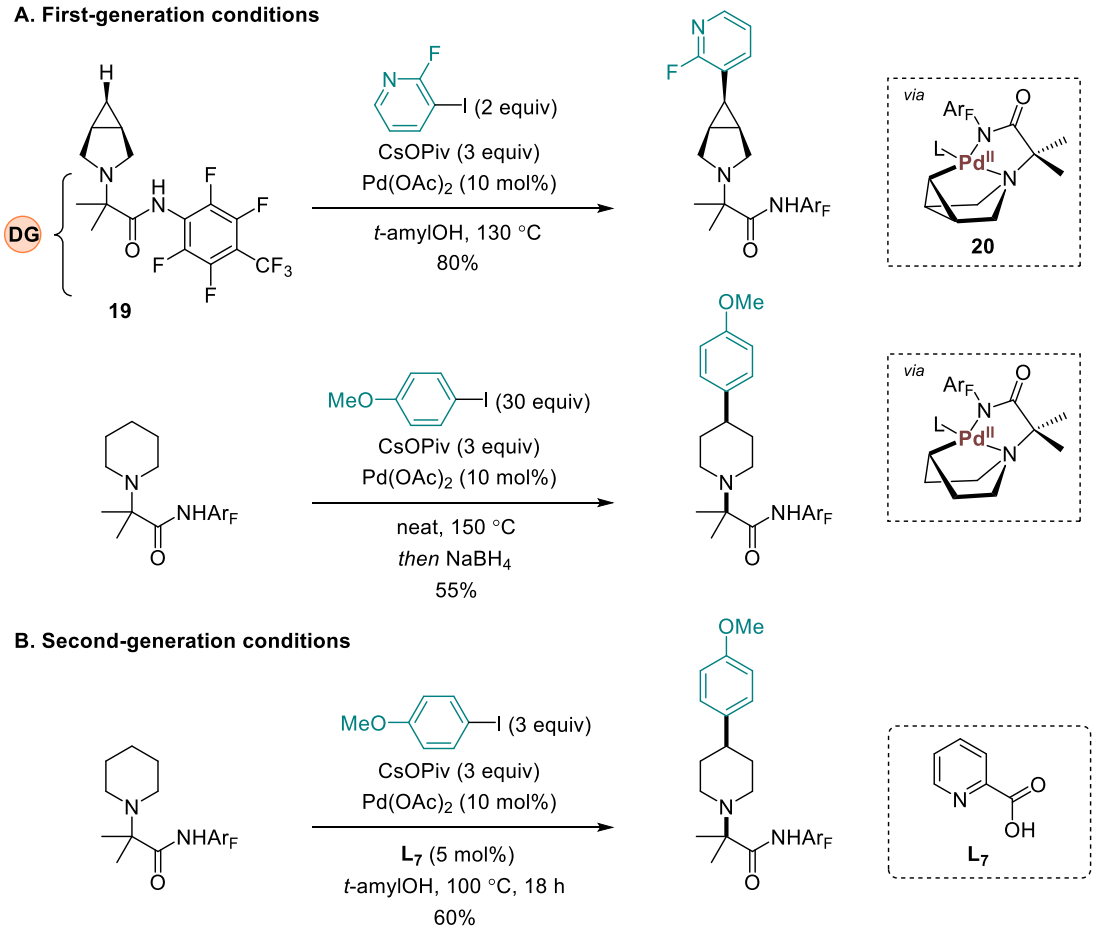
n = 0 45% (mono:di = 6.5:1), >20:1 d.r
1 42%, >20:1 d.r.
2 61%, 2:1 d.r.

Scheme 1.17 C(4) functionalisation with a C(3) alcohol-linked directing group.

Similar to the transient directed activation, regioselectivity was given by the formation of a fused 6,5-bicyclic palladacycle, with the directing group coordinating to the metal centre in a 6-membered chelate fashion. Compared to carboxylic acid-linked directing groups, lower selectivity for mono-arylation was seen for azetidines, whereas a significant drop in diastereoselectivity was seen for piperidines.

1.3.3.4 Transannular Heterocycle Functionalisation Examples

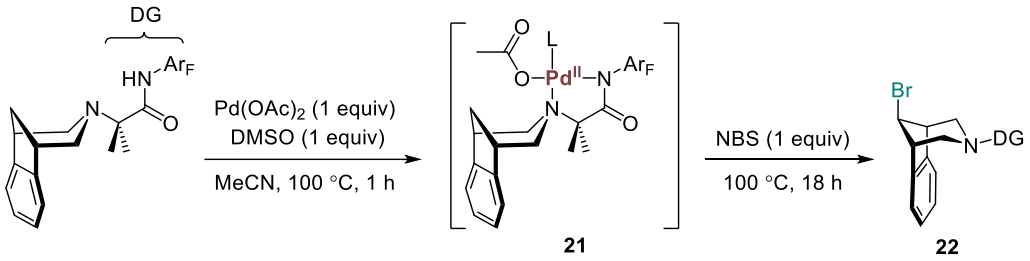
Using an N(1)-linked directing group, Sanford achieved the arylation of alicyclic amine cores in a transannular fashion.[158] Bidentate coordination to the metal centre was proposed *via* the endocyclic *N* atom and the perfluorinated tolylamide motif attached (Scheme 1.18A). This allowed formation of a 5-membered palladacycle with the distal C(4) position *via* a boat-like intermediate (**20**), with mechanistic studies confirming this proposal.[159] The transannular arylation occurred in excellent yields on model substrate **19**, which was judiciously chosen for the availability of cyclopropyl C(4)–H bonds, as well as for the increased tendency to adopt a boat conformation. The methodology could remarkably be applied to simple piperidine substrates to achieve C(4) arylation, however, significantly higher aryl iodide loadings and temperatures were required.



Scheme 1.18 Transannular arylation at the distal C(4) position with respect to the N(1) directing group, using first- or second-generation catalyst systems.

To enhance functionalisation of challenging substrates such as piperidine, Sanford developed a second-generation catalyst system, consisting of the addition of pyridine and quinoline carboxylate ligands to prevent the early deactivation of catalyst.[160] Notable improvements were seen in terms of substrate and aryl iodide tolerance, and the functionalisation of piperidine occurred in 60% yield in the presence of only 3 equivalents aryl iodide compared to 30 equivalents under the first-generation conditions (Scheme 1.18B). Later on, Dandapani expanded the scope of heteroaryl coupling partner even further for the transannular strategy.[161]

Recently, Sanford demonstrated a transanular methodology for the formation of bonds other than C–C, to either halogens, nitrogen, oxygen, sulfur or boron, requiring stoichiometric Pd.[162] To overcome the preference for the more activated C(2) position of the highly reactive oxidants, substrate-Pd(II) complex **21** was preassembled and then reacted with the electrophile of choice. For example, treatment of **21** with NBS afforded γ-brominated **22** as the single regioisomer, with high *cis* stereoselectivity (Scheme 1.19). A wide electrophile scope was tolerated, opening possibilities for flexible late-stage functionalisation of some of these underexplored motifs.



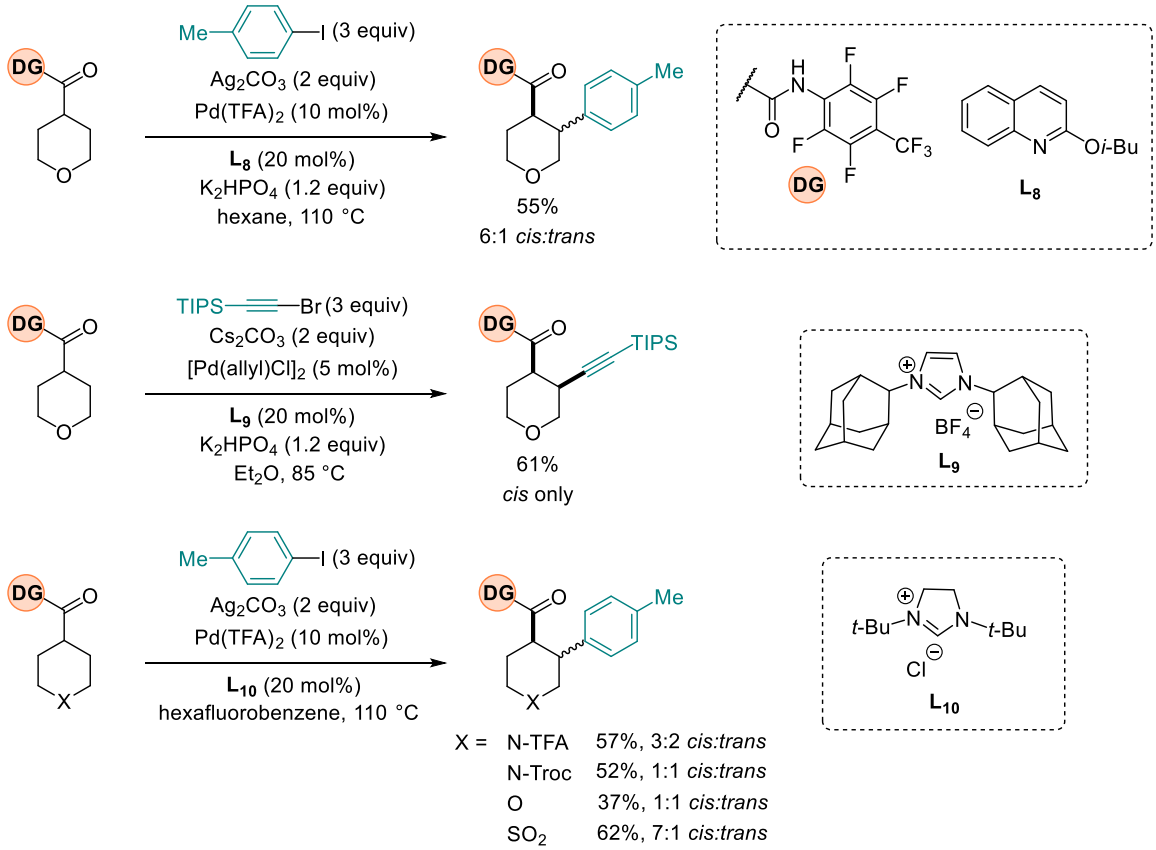
Scheme 1.19 2-Step one-pot procedure for transannular γ-bromination *via* substrate pre-complexation to Pd.

1.3.3.5 Heterocycle Functionalisation with a C(4) Directing Group

In all the C(sp^3)–H functionalisation examples discussed so far, regio- and diastereoselectivity were enhanced by electronic and steric biases on the substrate. Fewer methodologies are currently known to achieve stereoselective monofunctionalisation when a set of equivalent methylene groups are present. For instance, the functionalisation of 6-membered rings bearing a C(4) directing group poses significant challenges due to the presence of 4 equivalent β-C(3)–H bonds prone to C–H activation in an indiscriminate fashion.

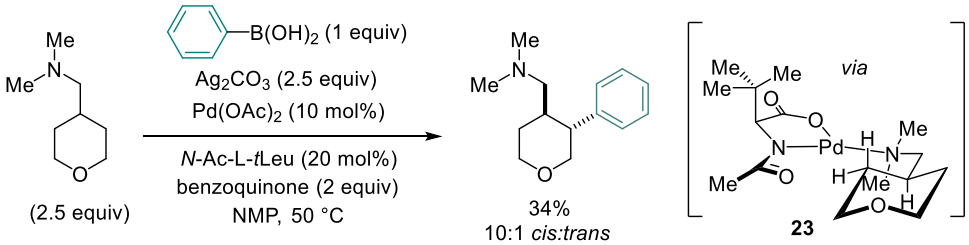
A few isolated attempts at this more challenging functionalisation have been reported by Yu, however, low diastereoselectivity was observed in all cases (Scheme 1.20). Using the Yu-Wasa auxiliary at C(4) and a 2,6-dialkoxypyridine ligand, tetrahydropyran was reacted with *p*-tolyl iodide to provide the C(3) mono-arylated product as a 6:1 *cis*:*trans* diastereomeric mixture.[163] Later, alkynylation of the same substrate with TIPS-alkynyl bromide was trialled. An NHC stabling ligand and a Pd^0/Pd^{II} strategy were employed, this time leading to isolation of the single *cis* diastereomer in 61% yield.[164] Arylation was reattempted by Yu in 2016 using an NHC ligand and Pd^{II}/Pd^{IV} catalysis and, despite high monofunctionalisation yields (52-57%) seen with *N*-TFA and *N*-Troc piperidine substrates, low or no diastereocontrol was achieved on either *N*- or *O*-heterocycles.[151] Only the 6-membered cyclic sulfone showed an improved *cis*-selectivity profile, due to *trans*-C–H functionalisation being hindered by the

bulky sulfonyl group. Recently, Yu also reported the use of an *O*-linked directing group, with an example of employing it at C(4) to effect C(3) functionalisation of *N*-TFA piperidine, albeit in a low 2:1 *cis*:*trans* d.r. (Scheme 1.17).[157]



Scheme 1.20 C(3) arylation trials by Yu on unbiased 6-membered heterocycles using a C(4) directing group.

Interestingly, Gaunt reported a C(3) mono-arylation example of tetrahydropyran in the presence of a dimethyl amine functionality. This was found to proceed *via* a favoured Pd insertion into the *trans*-C–H bond with respect to the alkyl amine in intermediate **23** (Scheme 1.21).[165] Despite an increased diastereoselectivity, in this case in favour of the *trans* isomer, a modest 34% yield was observed.



Scheme 1.21 Stereoselective *trans* C(3)-arylation of tetrahydropyran using a pendant tertiary alkylamine group.

On the other hand, using C(4) amine-linked directing groups has raised selectivity questions in the arylation of the activated C(2) position(s). Using a picolinamide directing group on a glycoside ring, Messaoudi addressed the challenge of achieving highly regio- and *cis* stereoselective C(sp^3)–H mono-functionalisation at the anomeric position.[166] Using a modified picolinamide auxiliary, Sheppard also reported an example of *cis* stereoselective C(2) arylation on tetrahydropyran.[167]

1.4 Project Aims

The work described in this thesis was aimed at developing highly stereoselective Pd-catalysed methodologies for the functionalisation of unbiased 6-membered heterocycles at unactivated C(3) positions. Aiming also to demonstrate the applicability of these tools to drug discovery, the synthesis of novel fragments and building blocks with attractive properties for medicinal chemistry were targeted.

A bidentate acid-linked directing group would be installed on readily available C(4) carboxylic acids (Figure 1.9A). These would then be employed to direct β-C–H arylation *via* a 5-membered palladacycle in the presence of an aryl iodide and generate a novel 3,4-disubstitution pattern with defined stereochemistry. With the question of selectivity arising from the presence of equivalent methylene groups adjacent to the auxiliary, a mono-*cis* configured product would be aimed for, since this would possess valuable fragment-like properties and might enable facile access to corresponding *trans* diastereomers by epimerisation. Optimisation would first be conducted on piperidine, the most widespread saturated heterocyclic scaffold in marketed drugs, and a removable *N*-Boc protecting group would be used to prevent undesired Pd coordination to the ring heteroatom. Compatibility with a range of 6-membered heterocycles would be targeted, as it would not only afford a wide diversity of currently underexplored medicinal chemistry motifs, but would also expand the ability to elaborate common pharmacophores along less explored vectors.

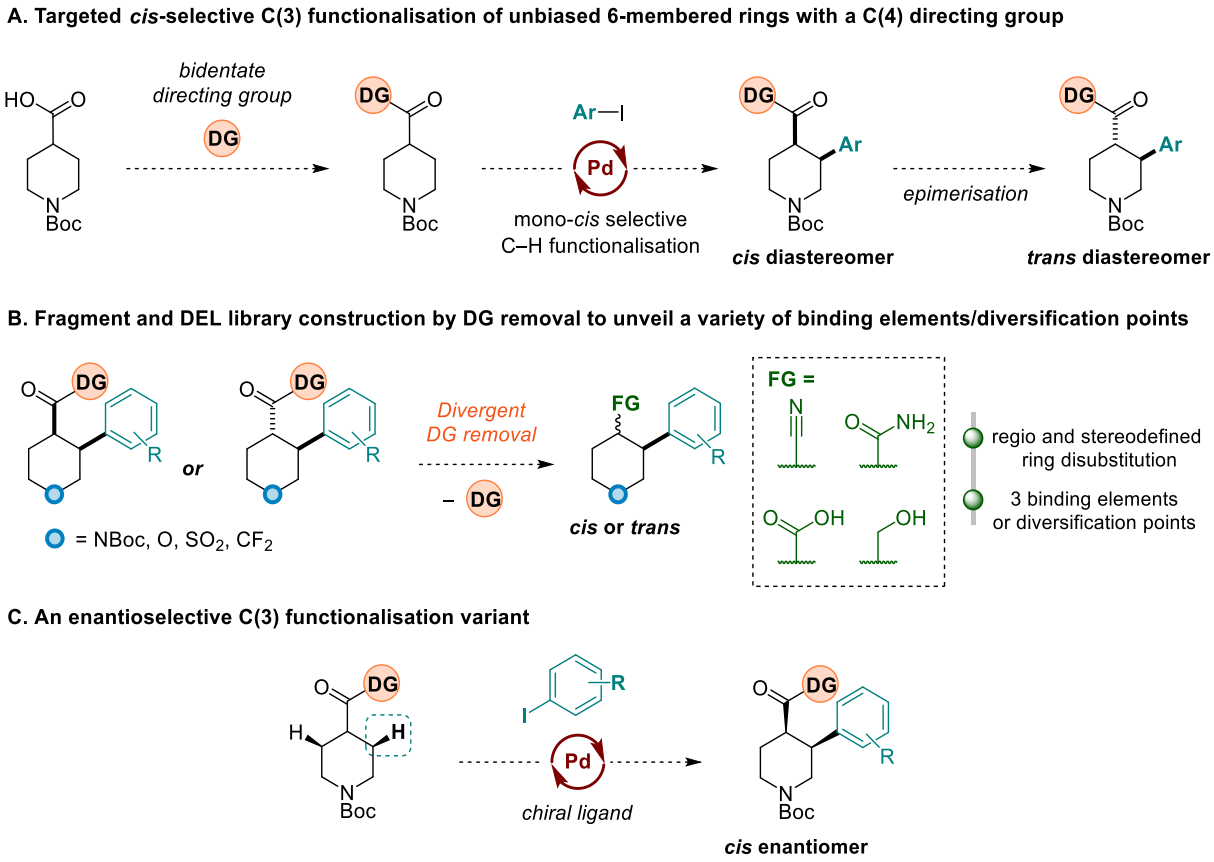


Figure 1.9 Summary of project aims.

The next goal was the facile and divergent removal of the strongly coordinating directing group to unmask a range of polar functionalities that would act as either binding elements or handles for downstream elaboration (Figure 1.9B). The targeted compounds would be highly shape-diverse fragments with attractive physicochemical properties for FBDD screening, as well as with a design that features the presence of at least 3 different binding elements: an aryl group, a C(4) free polar group and an endocyclic heteroatom. Moreover, a similar design, but with allowing a diversity of elaboration handles on the aryl group would be envisaged to allow the generation of DEL building blocks with up to 3 diversification points.

Finally, desymmetrisation of the four equivalent C(3)–H bonds in the presence of a suitable chiral ligand was envisaged to achieve the first enantioselective functionalisation at an unactivated position on a saturated heterocycle (Figure1.9C). High diastereo- and enantiomeric ratios were targeted on the challenging unbiased piperidine substrate, intending to maintain the use of the same bidentate directing group for which removal strategies would have already been established.

To summarise, the following 3 objectives would be followed:

1. The *cis* stereoselective C(3) mono-functionalisation of unbiased 6-membered heterocycles using a C(4) bidentate directing group (Section 2.1)
2. The use of the methodology from 1. to assemble fragment and DEL libraries in underrepresented chemical space, characterised by 3-dimensionality and diversity of binding elements/diversification points and their spatial distribution (Sections 2.2 and 2.3)
3. The development of a highly enantioselective variant of the methodology from 1. using a chiral ligand (Section 2.4)

2 Results and Discussion

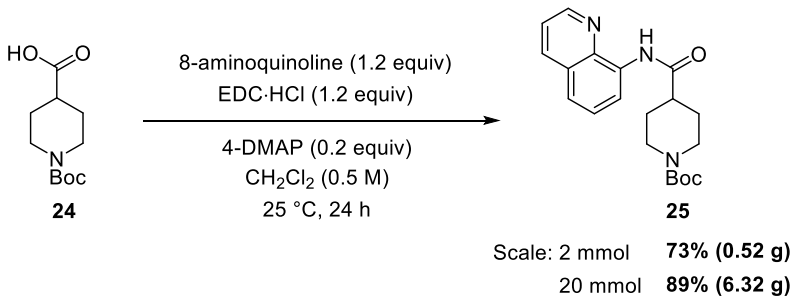
2.1 Highly Regio- and *cis* Stereoselective C3 Functionalisation of Unbiased 6-Membered Heterocycles Using a C4 Directing Group

A concise account of this work can be found in *Advanced Synthesis & Catalysis*.[168]

2.1.1 Methodology Development

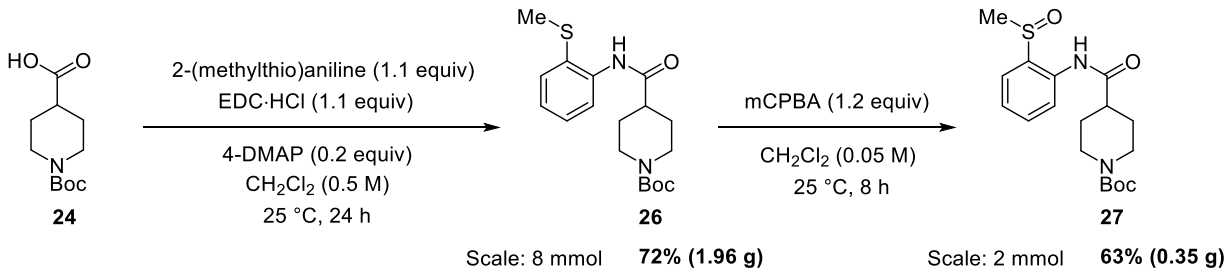
2.1.1.1 Directing Group Screen

Based on the high reactivity of *N*-Boc piperidines in previous directed functionalisations,[169,170] readily available *N*-Boc piperidine-4-carboxylic acid **24** was chosen for investigation as a model substrate. A series of bidentate directing groups were selected based on their precedented success in promoting β-C–H functionalisation when installed as amides using a pre-existent carboxylic acid handle.[126,171] Using EDC·HCl and DMAP, the 8-aminoquinoline auxiliary could be installed in >70% yield by amide coupling with **24** under ambient conditions, with the preparation of multigram quantities of product **25** possible (Scheme 2.1).



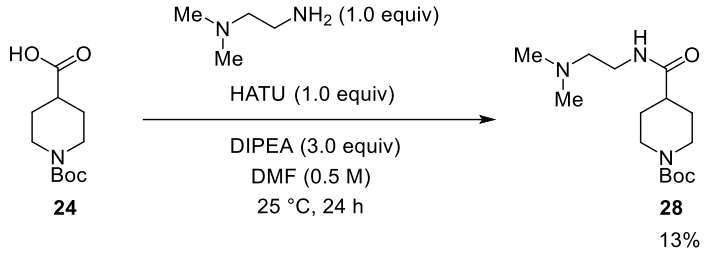
Scheme 2.1 Aminoquinoline installation at piperidine C4.

Under similar conditions, 2-(methylthio)aniline could also be installed in 72% yield to give **26**, whereas subsequent *m*CPBA oxidation also allowed access to **27** bearing the 2-(methylsulfinyl)aniline auxiliary (Scheme 2.2).



Scheme 2.2 2-(methylthio)aniline installation at piperidine C4, followed by conversion to sulfoxide.

Finally, *N*,*N*-dimethylenediamine was installed using HATU as coupling reagent, however, a challenging purification due to the increased polarity of this substrate resulted in a modest yield of **28** (Scheme 2.3).

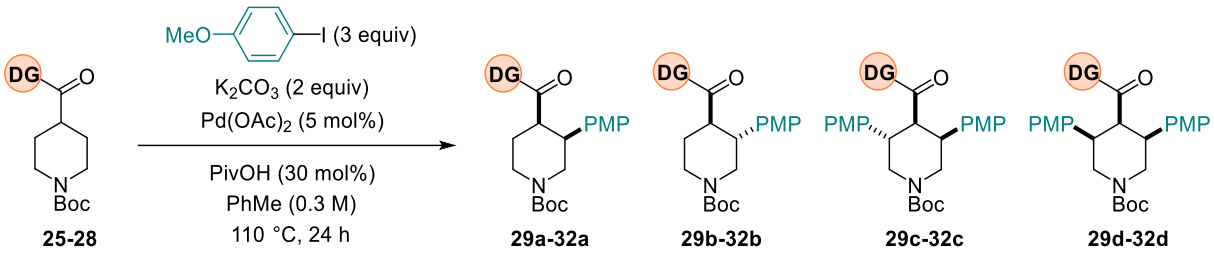


Scheme 2.3 Installation of dimethylethylenediamine directing group at piperidine C(4).

With useful quantities of each substrate available, their individual reactivities in the directed arylation were assessed. Initial conditions were based on the literature precedent of C(4) functionalisation of *N*-heterocycles in the presence of a C(3) directing group.[170] At 110 °C in toluene, arylation in the presence of 4-iodoanisole and $Pd(OAc)_2$ catalyst afforded a high >80% conversion of aminoquinoline amide **25** (Table 2.1, entry 1). Four different functionalisation products were identified after purification (see Section 2.1.2.2): the mono-arylated *cis* and *trans* isomers **29a** and **29b**, as well as the diarylated *cis*-*trans* **29c** and *cis*-*cis* **29d**. Mono-*trans* and di-*cis*-*cis* isomers were observed in similarly high yields, with no apparent preference for either *cis* or *trans* arylation. 2-(Methylthio)aniline displayed lower reactivity, affording only mono-*trans* arylated **30b** in 25% yield (entry 2). Interestingly, the sulfoxide-based directing group led to no observable conversion to arylated products, with starting **27** almost quantitively recovered (entry 3). Presumably, increasing the oxidation level at sulfur weakens its coordination to palladium, or forces a different coordination mode (i.e. through oxygen) that prevents formation of the thermodynamically favourable 5-membered palladacycle in the C-H activation stage. As a non-aromatic auxiliary, ethylenediamine led to only trace amounts of products (<10% combined yield), posing purification challenges (entry 4).

Given the high stereoselectivity achieved with 2-(methylthio)aniline, the use of this auxiliary was initially investigated. Despite affording exclusively the opposite diastereomer to the one desired, *trans* **30b** could be arising from *cis*-arylation to **30a** followed by a rapid complete epimerisation. To probe this, a range of bases were trialled, none of which led to any observable *cis* arylated product (See *Appendix 1*). Alternatively, increasing the amount of PivOH additive to up to 2 equivalents did not offset the exclusive formation of **30b** (for the full range of conditions trialled see *Appendix 1*). Most likely, lower energy barriers are associated in this case with transition state(s) leading to *trans* arylation, although the stereodetermining step is unknown. Interestingly, the yield of *trans* arylation still could not be increased beyond 25%, even at temperatures exceeding 130 °C.

Based on these results, it was decided to instead focus on the more reactive aminoquinoline auxiliary, aiming to steer the reactivity towards formation of mono-*cis* **29a**.



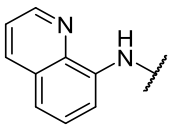
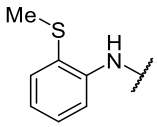
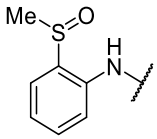
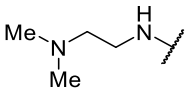
Entry	Directing Group	RSM (%)[a]	Observations[b]
1		**25** (18)	**29a** (18%) **29b** (26%) **29c** (10%) **29d** (24%)
2		**26** (67)	**30b** (25%)
3		**27** (92)	**27** (92%)
4		**28** (88)	<10% inseparable arylation products

Table 2.1 Reactivity outcomes in the presence of various bidentate directing groups. Reaction scale: 0.5 mmol. [a]Calculated by ^{1}H NMR using 1,3,5-trimethoxybenzene as internal standard.[b]Isolated yields.

2.1.1.2 Stereochemical Assignment of Reaction Products

The relative configurations of the 3,4-disubstituted piperidine products from the previous section were determined based on key coupling constants (*J* values) in ^{1}H NMR. With a partially restricted rotation around the carbamate C–N bond in the *N*-Boc protecting group, rotamers are present in solution at room temperature, complicating NMR analysis. To promote free bond rotation and coalescence of rotameric signals, NMR experiments were conducted at 100 °C (373 K) in DMSO-d_6. This allowed visualisation of products as single entities, with well-resolved splitting patterns for each multiplet signal.

In all cases, the coupling constants (*J* values) between vicinal protons followed the general trend given by the Karplus equation in relationship with their dihedral angle (θ), validating a piperidine chair conformation.[172,173,174,175] Preferred substituent orientations (axial or equatorial) and consequently

product configurations could be deduced from couplings of protons at the C(3) and C(4) positions, with other *J* values on the ring calculated to support the findings.

The workflow for the stereochemical assignment of **29a** is illustrated in full below, with all other products following this example. Firstly, HSQC enabled identifying the signals corresponding to aliphatic protons at tertiary carbon centres (H_a and H_b, Figure 2.1). The most deshielded signal of the two (δ 3.30 ppm) was assigned to the α-carbonyl proton (H_a), since it also showed COSY correlations to the least deshielded methylene protons in the ^{1}H NMR, corresponding to H_g and H_h (2.04 ppm and 1.90 ppm, respectively, Figure 2.2).

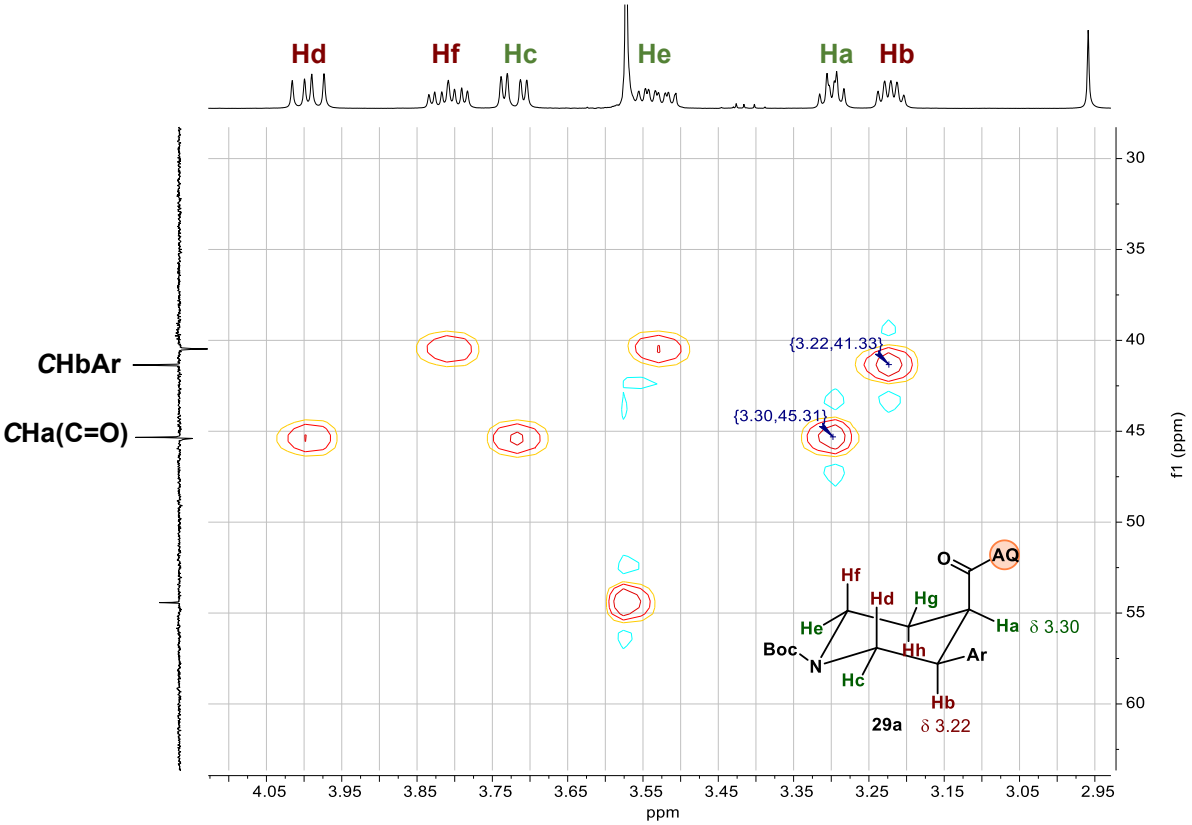


Figure 2.1 HSQC spectrum in DMSO-d_6 at 373 K, showing carbon-proton correlations for tertiary centres. DEPT-135 on vertical axis.

Multiplet analysis revealed a mutual *J* = 6.7 Hz between H_a and H_b (Figure 2.2). This was slightly larger than expected compared to a typical axial-equatorial coupling in piperidines (2–6 Hz), but well below values reported for axial-axial couplings (8-13 Hz).[175,176] An axial-equatorial coupling was therefore assumed between the two, especially given that deviations from the original Karplus equation are common with varying the electronic properties of the substituents.[173] To validate this, couplings to neighbouring protons were analysed. From the outset, proton H_b clearly adopted an axial orientation, with a large *J* = 8.7 Hz with respect to H_d. In turn, H_d appeared as a doublet of doublets with 2 large couplings, one to geminal H_c and one to vicinal H_b. Axial H_d also resonated at higher frequency compared to equatorial H_c, consistent with behaviours observed for geminal protons in 6-membered saturated chair structures.[177] The chemical shift difference δ_{ae} = 0.45 ppm is within the reported range for cyclohexane methylene protons (δ_{ae} = 0.4 – 0.5 ppm, where $\delta_{ae} = \delta_{axial} - \delta_{equatorial}$). Moreover, ring heteroatoms such as nitrogen have been shown to enhance this difference, by exhibiting an axial lone

pair of electrons that has a deshielding effect on neighbouring axial protons.[178,179] In this case, H_d is also the most deshielded aliphatic proton, supporting an additional anisotropic effect introduced by the axial carbonyl group of the aminoquinoline auxiliary.[180] Furthermore, proton H_a displayed only couplings smaller than 6.7 Hz with H_b, H_g and H_h, validating its equatorial position, whereas the chemical shifts and splitting patterns of remaining H_e and H_f were consistent with all the previous assignments. Overall, a *cis* configuration was demonstrated for **29a** with an axial directing group and an equatorial aryl (Figure 2.3), in agreement with the higher reported A-values for phenyl groups (>3.0 kcal/mol) compared to carboxylate substituents on cyclohexane (approx. 1.3 kcal/mol for CO_2Me).[181]

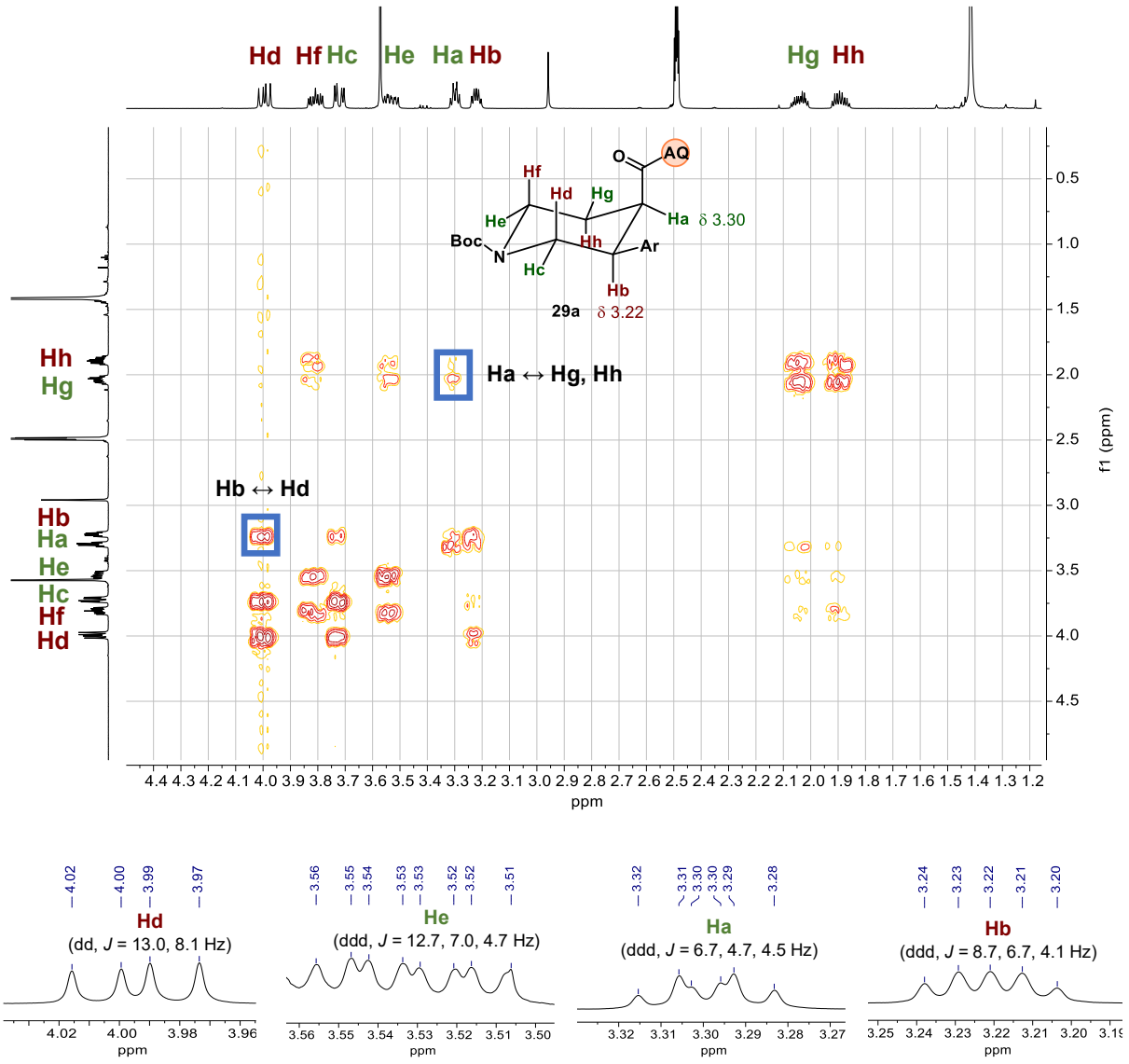


Figure 2.2 COSY in DMSO-d_6 at 373 K, highlighting relevant proton-proton correlations. Expanded ^{1}H NMR multiplets for calculation of relevant *J* values.

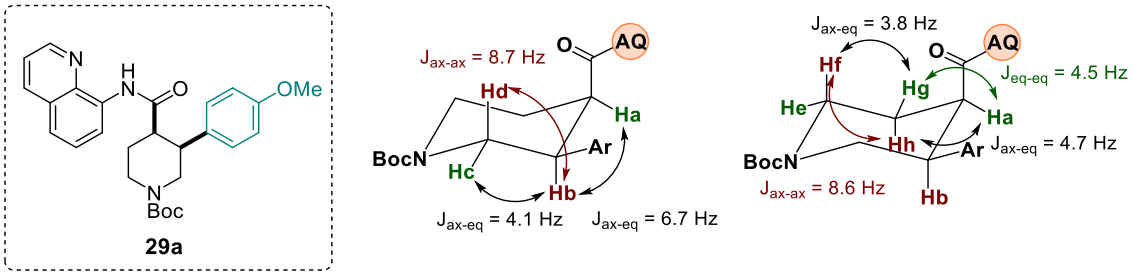
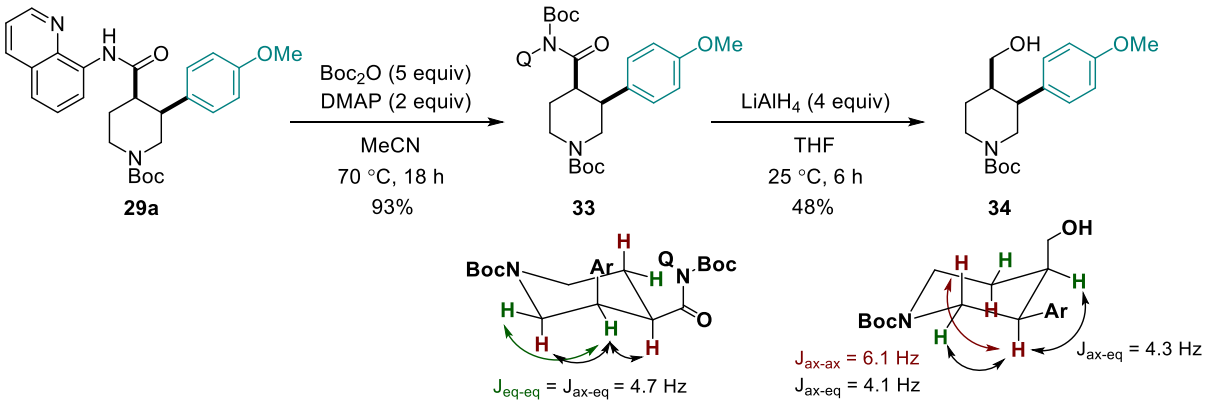


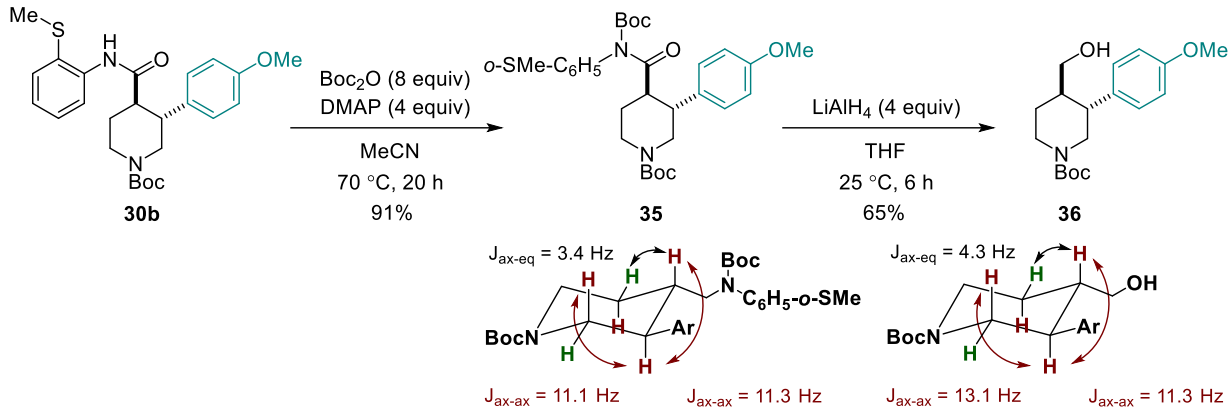
Figure 2.3 Final stereochemical assignment of **29a**, with selected *J* values shown.

This stereochemical assignment was further probed against the *trans* configured piperidine **30b** obtained with the 2-(methylthio)aniline directing group. The two directing groups were removed under reductive conditions to unveil the corresponding primary alcohols **34** and **36** (Schemes 2.4 and 2.5). Providing our assumptions regarding starting materials **29a** and **30b** were correct, **34** and **36** should be diastereomers. First, to enhance the electrophilicity of the carbonyl group, withdrawing electron-density from the amide C–N bond was necessary. This was achieved by Boc protection of the amide group using excess Boc_2O and DMAP, which proceeded in high yields (>90%). Interestingly, the larger amide now occupies the equatorial position in **33**, forcing the aryl group to adopt an axial orientation, as illustrated by the *J* values in Scheme 2.4. Conversely, **35** adopts the thermodynamically favourable diequatorial conformation. Upon $LiAlH_4$ treatment, Boc-protected intermediates **33** and **35** each afforded a distinct alcohol product.



Scheme 2.4 Removal of the aminoquinoline directing groups under reductive conditions. Selected *J* values shown.

A higher yield was observed in the latter case for the formation of **36**, presumably due to the higher accessibility of the carbonyl group when situated next to a *trans* substituent. As expected, comparison of the high-temperature ^{1}H-NMR spectra of alcohol products **34** and **36** demonstrated a diastereomeric relationship, with similar proton environments resonating at different chemical shifts across the two species. The most pronounced differences of up to 0.8 ppm were seen for the C(2) methylene peaks adjacent to CHAr, as well as for the CH_2OH and C*H*CH_2OH signals (Figure 2.4).



Scheme 2.5 Removal of the 2-(methylthio)aniline directing groups under reductive conditions. Selected *J* values shown.

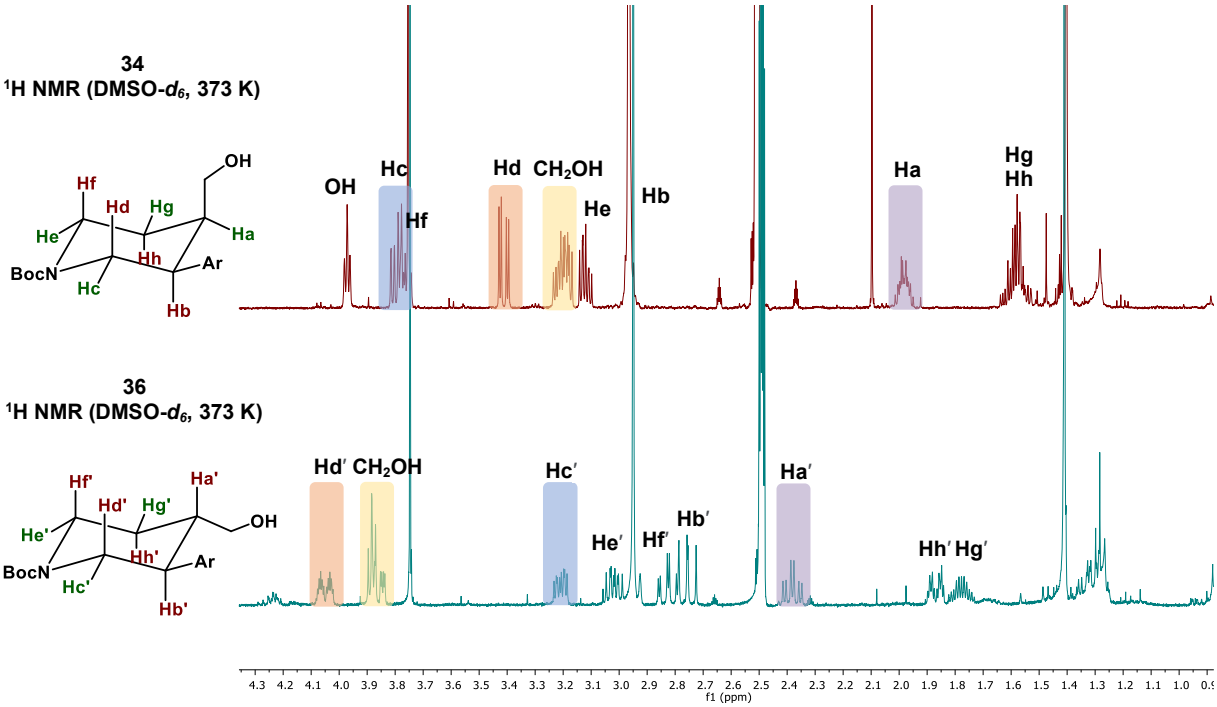


Figure 2.4 High temperature ^{1}H NMR comparison of **34** and **36** (expanded aliphatic region shown). The protons in the highlighted pairs exhibit significantly different chemical shifts, indicative of a diastereotopic relationship between the two corresponding compounds.

The *trans* side-product **29b** of the aminoquinoline amide directed reaction also adopted the most favourable diequatorial conformation, as indicated by analysis of *J* values (Figure 2.5). Diarylated **29c** exhibited an equatorial aminoquinoline amide, with one axial and one equatorial aryl substituent. In *cis-cis* **29d** both aryls favour equatorial positions, given their higher predicted A value compared to the amide (see above),[181] placing the directing group in an axial position.

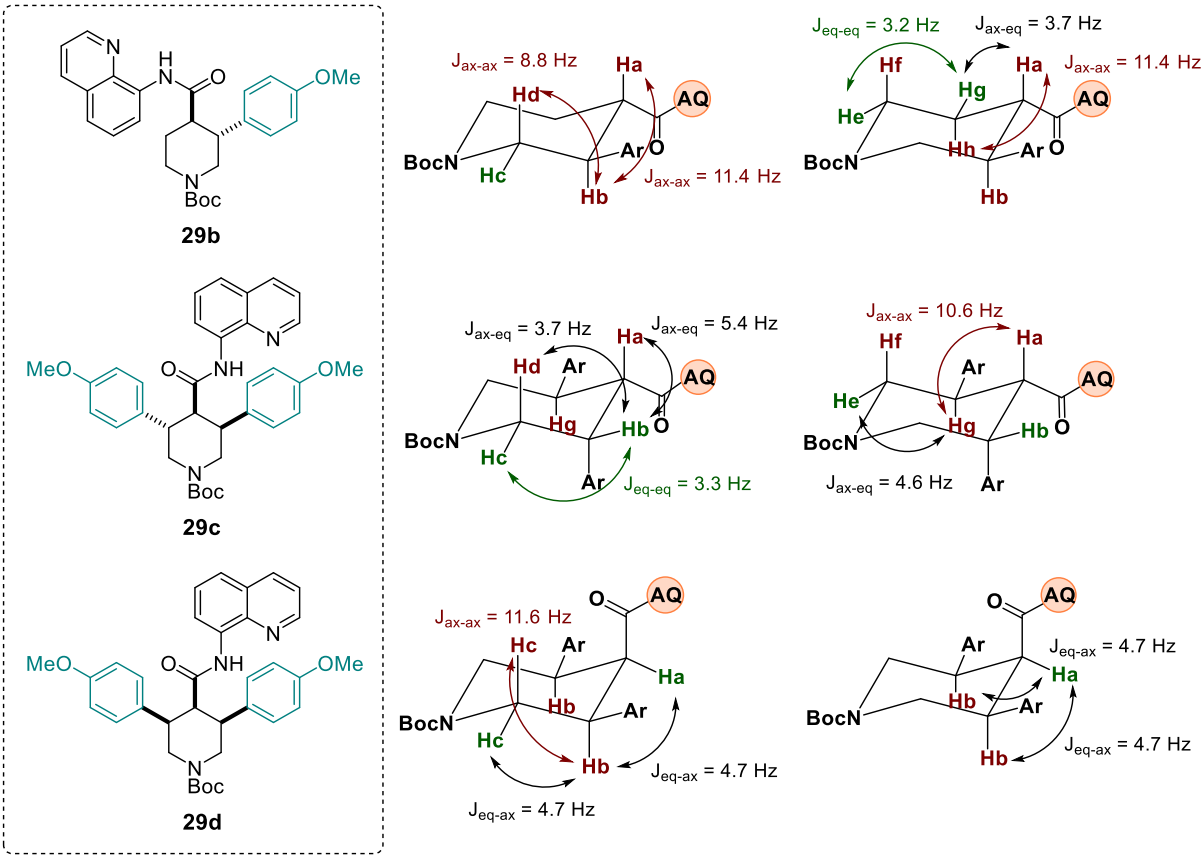
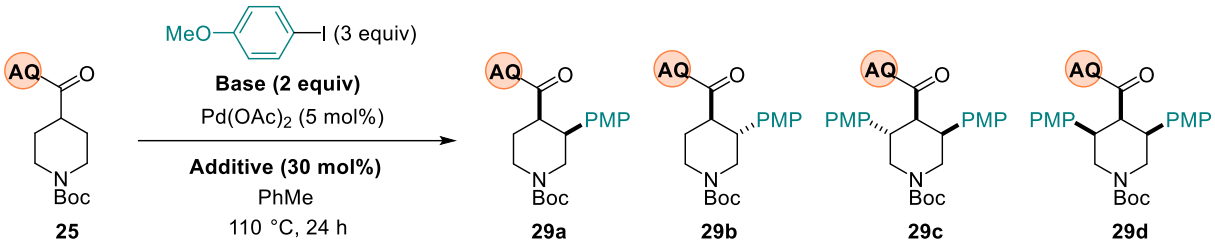


Figure 2.5 Stereochemical assignment of side products **29b-d**, with representative *J* values shown.

2.1.1.3 Implementation of Mild Temperature Conditions

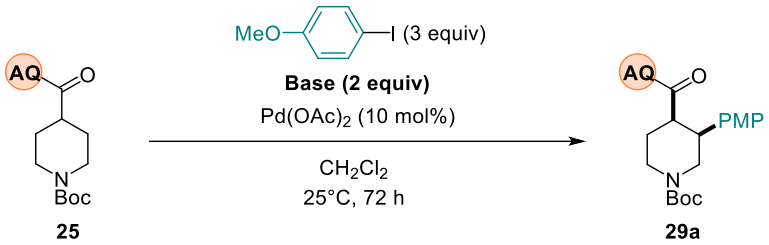
Using the aminoquinoline-amide substrate **25**, reaction optimisation was carried out in order to maximise the yield of mono-*cis* functionalised **29a** whilst minimising the competing side-arylation processes. Starting from the previous reaction at 110 °C (Section 2.1.1.2), a range of acetate and carbonate bases were trialled, in an effort to identify conditions that might promote a selective *cis* or *trans* functionalisation. K_2CO_3 was still found to promote the highest reactivity, with near-complete consumption of starting material when increasing the concentration from 0.3 M to 3 M – however, selectivity still remained an issue. Silver carbonate was unable to promote arylation despite addition of PivOH additive. On the other hand, acetates (AgOAc, CsOAc) gave selective *cis* arylation in up to 36% yield and <9% yield of each of the other three side-products **29a-d**. Unfortunately, attempts to further increase the mono-*cis* yield by employing an additive or increasing the substrate concentration were unsuccessful, with significant diarylation observed instead (Table 2.2, entries 1-3). Alternatively, since K_2CO_3 led to considerable side reactivity, a drop in temperature was hoped to increase selectivity for either of the mono-arylated products. However, opting for a temperature of 80 °C still afforded products **29a-d** in an indiscriminate fashion, but in lower individual yields (<10%, entry 4).



Entry	Concentration (M)	Base	Additive	yield (%)[a]					
				29a	29b	29c	29d	RSM	Total
1	1	AgOAc	None	21	10	12	17	34	94
2	1	CsOAc	None	25	13	11	20	27	96
3	0.3	AgOAc	PivOH	33	5	6	6	41	91
4[b]	0.3	K_2CO_3	PivOH	5	3	6	9	68	90

Table 2.2 Trials to modulate functionalisation selectivity (changes in concentration, additives, temperature). Reaction scale: 0.2 mmol. [a]Calculated by ^{1}H NMR using 1,3,5-trimethoxybenzene as internal standard. [b]Conducted at 80 °C.

For the directed mono-functionalisation of unbiased cyclopentane substrates, Chen had previously reported the use of ambient temperature conditions and chlorinated solvents.[182] Repeating the K_2CO_3 mediated reaction in CH_2Cl_2 at only 25 °C led in this case to the formation of desired **29a** exclusively, albeit in <5% yield (Table 2.3). A screen of carbonate and acetate bases was carried out under these new conditions, increasing the reaction time to 72 h and the catalyst loading to 10 mol% to match Chen's optimised protocol. Gratifyingly, Ag_2CO_3 led to **29a** in 33% yield without formation of any other arylation side-products (entry 2), whereas other bases did not promote any reactivity (entries 3-5). Finally, increasing substrate concentration in increments in the presence of Ag_2CO_3 was found to enhance neither the yield of **29a** or the overall conversion (entries 6-9).

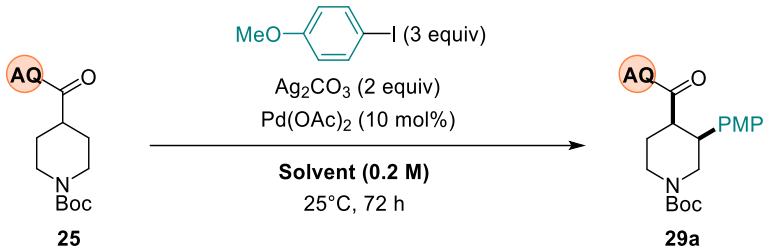


25 **29a**

Entry	Concentration (M)	Base	yield (%)[a]		
			29a	RSM	Total
1	0.2	K_2CO_3	3	88	92
2	0.2	Ag_2CO_3	33	55	88
3	0.2	Cs_2CO_3	0	78	78
4	0.2	AgOAc	0	80	80
5	0.2	CsOAc	0	91	91
6	0.8	Ag_2CO_3	33	57	90
7	1	Ag_2CO_3	35	56	89
8	2	Ag_2CO_3	35	55	90
9	3	Ag_2CO_3	37	57	94

Table 2.3 Base screen for the functionalisation of **25** under ambient temperature conditions in CH_2Cl_2. Reaction scale: 0.2 mmol. [a]Calculated by ^1H NMR using 1,3,5-trimethoxybenzene as internal standard. Only **29a** observed as product.

With Ag_2CO_3 as base, a series of solvents were screened, aiming to trial examples of aromatic, polar protic and polar aprotic environments (Table 2.4). Besides previously used dichloromethane, further halogenated solvents were tested (entries 1-8). Trifluorotoluene ($PhCF_3$), chosen due to the close resemblance to CH_2Cl_2 in terms of dielectric constants (ε_{PhCF_3} = 9.18 vs $\varepsilon_{CH_2Cl_2}$ = 9.04),[183] performed best in terms of both yield and selectivity for *cis* arylation (40% **29a**, Entry 5). This solvent also displays a higher boiling point compared to CH_2Cl_2, motivating its choice in later temperature studies (see Table 2.5). HFIP, a solvent commonly used in C–H functionalisations led to no arylation,[184] and combining it with $PhCF_3$ in a 3:1 ratio led to no improvement compared to the use of $PhCF_3$ alone (entry 7). Trifluoroethanol provided a low yield of **29a** (entry 8), whereas opting for a non-halogenated aromatic solvent such as toluene failed to promote any reactivity at room temperature (entry 9). *t*-AmylOH exhibited a similar behaviour as the polar protic trifluoroethanol, as did the polar aprotic 2-MeTHF (entries 10 and 12, respectively). No reaction occurred in dioxane, whereas other polar aprotic solvents (MeCN, DMF, NMP) led to modest or no functionalisation yields, likely due to competition for coordination at Pd with the carbonate and acetate ligands involved in CMD (entries 13-15).

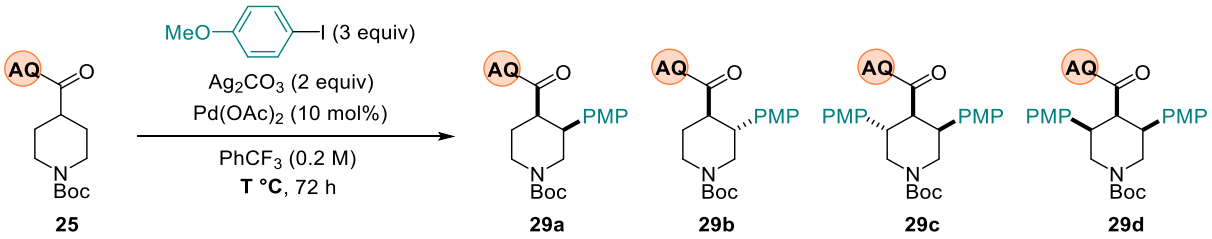


25 **29a**

Entry	Solvent	yield (%)[a]		
		29a	**RSM**	**Total**
1	CH_2Cl_2	33	55	88
2	DCE	34	48	82
3	PhCl	31	57	88
4	*o*-DCB	27	62	89
5	$PhCF_3$	40	52	92
6	HFIP	0	88	88
7	$PhCF_3$/HFIP (3:1)	38	50	88
8	Trifluoroethanol[b]	12	69	83
9	PhMe	0	89	89
10	*t*-amylOH	16	79	85
11	Dioxane	0	82	82
12	2-MeTHF	11	73	84
13	MeCN	0	78	78
14	DMF	5	79	84
15	NMP[b]	22	45	71

Table 2.4 Solvent screen for the functionalisation of **25** under ambient temperature conditions. Reaction scale: 0.2 mmol. [a]Calculated by ^{1}H NMR using 1,3,5-trimethoxybenzene as internal standard. Only **29a** observed as product. [b]Trace amounts (<5%) **29b** observed.

$PhCF_3$ was chosen as solvent, especially due to its higher boiling point which allowed carrying out the next temperature studies. The temperature was increased in increments of 10 °C, observing changes in the overall conversion and product distribution (Table 2.5). A steady increase in the yield of **29a** was initially observed, with a peak of 46% achieved at 45 °C (entries 1-3). Further increasing the temperature above 45 °C was unsuccessful in encouraging higher levels of starting material conversion, and instead enhanced formation of other side-products at the expense of **29a** (entries 4-7).

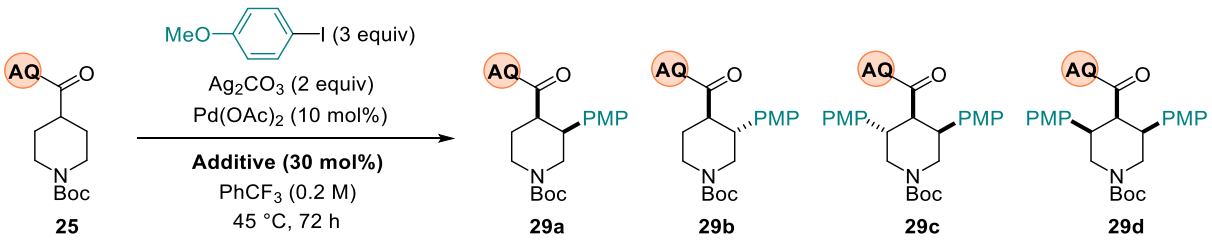


25 29a 29b 29c 29d

Entry	Temperature (°C)	yield (%)[a]					
		29a	29b	29c	29d[b]	RSM	Total
1	25	36	0	0	<5	48	84
2	35	41	6	7	<5	35	89
3	45	46	5	4	<5	37	92
4	55	36	5	6	<5	32	79
5	65	42	7	8	<5	38	95
6	75	37	6	8	<5	37	89
7	85	31	8	13	<5	40	92

Table 2.5 Temperature screen for the functionalisation of **25**. Reaction scale: 0.2 mmol. [a]Calculated by ^{1}H NMR using 1,3,5-trimethoxybenzene as internal standard. [b]Trace amounts (<5%) **29d** observed, difficult to quantify due to peak overlap with starting material in ^{1}H NMR.

Having identified the impact of temperature upon selectivity, a series of additives were tested to further enhance consumption of **25** (Table 2.6). Good yields and selectivities were seen with aliphatic and aromatic acids bearing sterically bulky backbones, suggesting that the stereodetermining step benefits from a degree of steric hindrance imposed by the additive (entries 2-5). Outstandingly, mesityl carboxylic acid (MesCOOH) promoted full consumption of starting **25** (entry 5). This is in marked contrast with the reaction conducted in the absence of additives, which led to 37% unreacted starting material (entry 1). Phosphoric acids also promoted excellent reactivities, with diphenylphosphoric acid ($(PhO)_2PO_2H$) promoting again full starting material consumption, albeit with modest selectivity for desired **29a** (entries 6,7). Coordinating ligands such as pyridines and pyridones were also studied, since these could stabilise high-valent Pd(IV) species, in addition to assisting with Pd decomplexation at the end of the catalytic cycle and preventing catalyst deactivation (entries 8-10).[163,185]



25 29a 29b 29c 29d

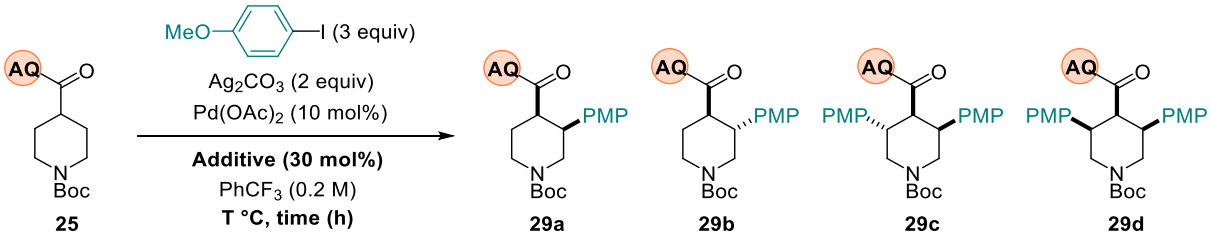
Entry	Additive	yield (%)[a]					
		29a	29b	29c	29d[b]	RSM	Total
1	None	48	6	3	<5	37	94
2	PivOH	44	5	4	<5	38	91
3	*i*PrCOOH	39	6	8	<5	19	74
4	AdCOOH	46	3	10	<5	41	99
5	MesCOOH	45	6	11	20	0	82
6	$(BnO)_2PO_2H$	55	12	15	<5	14	96
7	$(PhO)_2PO_2H$	31	11	36	21	0	99
8	Pyridine	0	0	0	0	98	98
9	5-CF_3-2-pyridone	13	7	4	<5	45	69
10	5-Me-2-pyridone	13	6	3	<5	63	84
11	$Cu(OAc)_2$	32	4	0	<5	42	78
12	KF	27	10	7	<5	26	70

Table 2.6 Additive screen for the functionalisation of **25**. Reaction scale: 0.2 mmol. [a]Calculated using 1,3,5-trimethoxybenzene as internal standard. [b]The trace amounts (<5%) observed were difficult to quantify due to peak overlap with starting material in ^{1}H NMR.

Unfortunately, pyridine completely inhibited the reaction, whereas neither electron-rich nor electron-poor pyridones led to significant extents of *cis* arylation (entries 8-19). $Cu(OAc)_2$ was employed to re-oxidise any quantities of Pd black arising from catalyst poisoning,[160,186] however, no improvement in reactivity was seen (entry 11). Finally, KF was trialled for the ability of fluoride salts to promote initial amide N–H activation during Pd coordination to the directing group, as well as lead to formation of catalytically active Pd-Ag heterobimetallic complexes.[187] Nevertheless, modest yields and *cis* selectivity were observed (entry 12).

Having identified MesCOOH and $(PhO)_2PO_2H$ as promoting increased starting material consumption, experiments were aimed at improving the selectivity for **29a** in these reactions. The currently long reaction time (72 h) was seen as a major hindrance to achieving stereocontrol, since prolonged exposure to base and excess aryl iodide would promote the likelihood of epimerisation or overreaction. Indeed, reducing the reaction time to only 24 h in the presence of MesCOOH led to 57% NMR yield of **29a** and small percentages of **29b-29d** and **25** (Table 2.7, entry 1). Again, this seems to indicate **29a** as

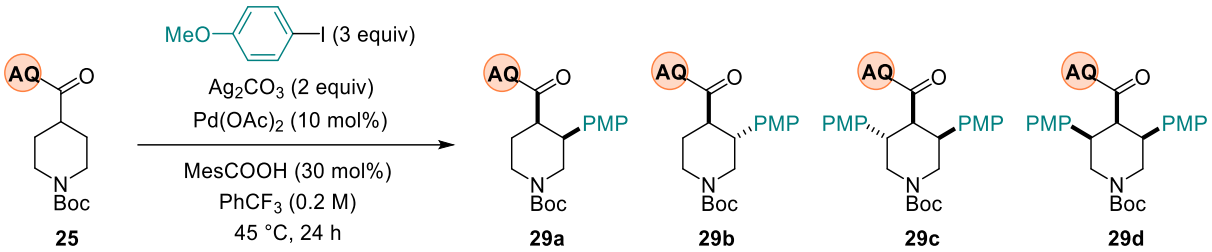
common precursor for the formation of other arylated piperidines, with a full explanation provided in Section 2.1.3. Diphenyl phosphate gave **29a** in comparable yield after 24 h, albeit significant diarylation still occurred in this case (entry 2). Conversely, opting for a 72 h reaction time, but instead reducing the temperature to 25 °C resulted in only moderate *cis* arylation yields (<43%) with the two additives (entries 3,4).



Entry	Additive	Time (h)	Temperature (°C)	yield (%)[a]					
				29a	29b	29c	29d[b]	RSM	Total
1	MesCOOH	24	45	57	10	11	9	9	96
2	$(PhO)_2PO_2H$	24	45	58	11	18	12	0	99
3	MesCOOH	72	25	34	3	0	0	55	92
4	$(PhO)_2PO_2H$	72	25	43	10	2	<5	35	93

Table 2.7 Time and temperature adjustments using either MesCOOH or $(PhO)_2PO_2H$ as additives. Reaction scale: 0.2 mmol. [a]Calculated by ^1H NMR using 1,3,5-trimethoxybenzene as internal standard.

Opting for the use of MesCOOH at 45 °C under the 24 h conditions, next changes were aimed at reducing reagent loadings (aryl iodide, base catalyst) (Table 2.8). Halving the silver base loading led to formation of **29a** in over 60% yield with improved selectivity (entry 2). However, substoichiometric amounts of base led to a marked drop in reactivity (entry 3). Pleasingly, decreasing the aryl iodide loading from 3 to 2 equivalents also improved the selectivity profile, with yield of **29a** maintained above 50%. Using 1 equivalent of coupling partner induced excellent *cis* selectivity at 45 °C, however, modest conversion was seen after 24 h (entry 5). A similar effect is seen when halving the Pd loading to 5 mol% (entry 6). Finally, by combining the positive effects of reducing both the base loading to 1 equivalent and the aryl iodide loading to 2 equivalents, desired **29a** could be obtained in 68% isolated yield and good selectivity (entry 7). This suggested that a broader understanding of the factor interactions rather than individual changes in a single variable at a time may be key to unlocking the maximum achievable yield and selectivity in this reaction.



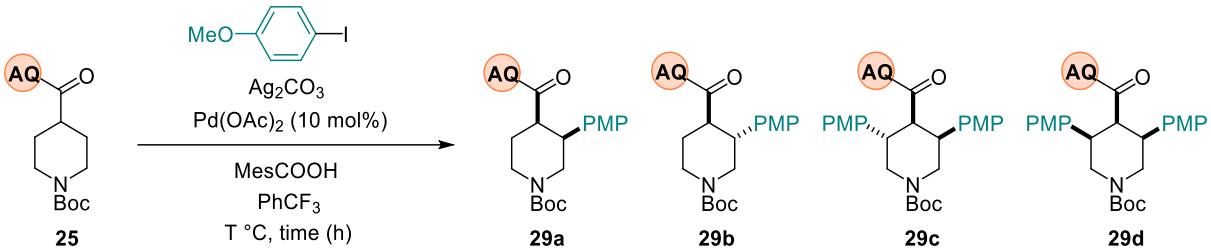
25 29a 29b 29c 29d

Entry	Changes to conditions	yield (%)[a]					
		29a	29b	29c	29d	RSM	Total
1	None	57	10	11	9	9	96
2	Ag_2CO_3 (1 equiv)	64	7	8	8	7	94
3	Ag_2CO_3 (0.5 equiv)	58	4	2	0	21	85
4	ArI (2 equiv)	54	8	9	7	16	94
5	ArI (1 equiv)	46	3	0	0	45	94
6	$Pd(OAc)_2$ (5 mol%)	47	3	2	0	38	91
7	Ag_2CO_3 (1 equiv) **and** ArI (2 equiv)	68 (64)	8	7	0	11	94

Table 2.8 Studying the effects of reducing reagent loadings. Reaction scale: 0.2 mmol. [a] Calculated by ^{1}H NMR using 1,3,5-trimethoxybenzene as internal standard. Isolated yield in parenthesis.

2.1.1.4 A Design of Experiment Driven Optimisation

To study the effects of factor interactions upon the maximum achievable yield of **29a**, a Design of Experiment (DoE) study was conducted. The JMP Pro 14 software was used to create experimental designs and perform statistical analysis.[188] By contrast to the OFAT (one factor at a time) method, a fraction of all possible experiments were now judiciously sampled, with the outcomes used to statistically predict reaction behaviour over entire defined areas of experimental space. Based on the number of factors considered (n), surface plots of desired responses (e.g yield) could be modelled in n dimensions, allowing identification of local/absolute maxima and the conditions under which these can be achieved. The DoE study was aimed at maximising the yield of **29a** and was carried out in two stages, comprising of a definitive screening and a custom design. Firstly, a definitive screening design allowed scanning the continuous factors in the reaction for their ability to impact the desired response. Besides individual effects, changes in desired response as result of factor interactions would also be identified using this design, up to second order effects. As illustrated in Table 2.9, factor limits were chosen to allow exploration of the wider experimental space surrounding the local maximum previously inferred by OFAT, which afforded 68% **29a**. However, upper limits were also selected to maintain reagent loadings and temperature within desirable values that would ensure resource economy and a cost-effective process.



Factor	Lower Limit	Upper Limit	Presumed Optimum Based on OFAT
Ag_2CO_3 equiv (Base)	0.5	2	1
PMP–I equiv (Ar-I)	1	3	2
Temperature (°C)	35	55	45
Time (h)	15	45	24
Concentration (M)	0.1	1.1	0.2
MesCOOH Loading (mol%) (additive)	20	60	30

Table 2.9 Overview of definitive screening design settings.

Out of 2^6 (=64) possible runs in a full factorial design, a set of 16 experiments was opted for (quarter fraction). Compared to a half fraction design, this model poses a higher risk of incorrectly distinguishing two-factor interactions. However, sparsity and heredity principles would aid identifying discrepancies, since significant interactions would contain factors that are themselves individually significant.[189] Therefore, this constituted a highly time-efficient manner for screening out least impactful factors before a more in-depth optimisation round. Based on the experimental findings for the 16 runs, the variation in mono-*cis* **29a** yield was fitted to the statistical model used for prediction. An excellent fit between experimental and expected yield was observed for runs at temperatures below 55 °C (R^2 = 0.99) (Figure 2.5). However, at and above 55 °C, a clear lack of fit was observed, presumably due to other reactivity pathways that override previous factor effects.

Considering runs at below 55 °C, the most impactful factors could be depicted from the Main Effects Residual Plot, by analysis of their corresponding gradient (Figure 2.6). With the steepest positive gradients, the base and aryl iodide loadings were predicted to impact the yield in a directly proportional fashion. Conversely, the steep negative slope for time suggested a significant and inversely proportional effect of this parameter on yield. Most importantly, additive loading was found to bear the least influence on reaction response, motivating a fixed value of this parameter to be employed in further studies (*vide infra*), whilst no significant second order interactions were observed.

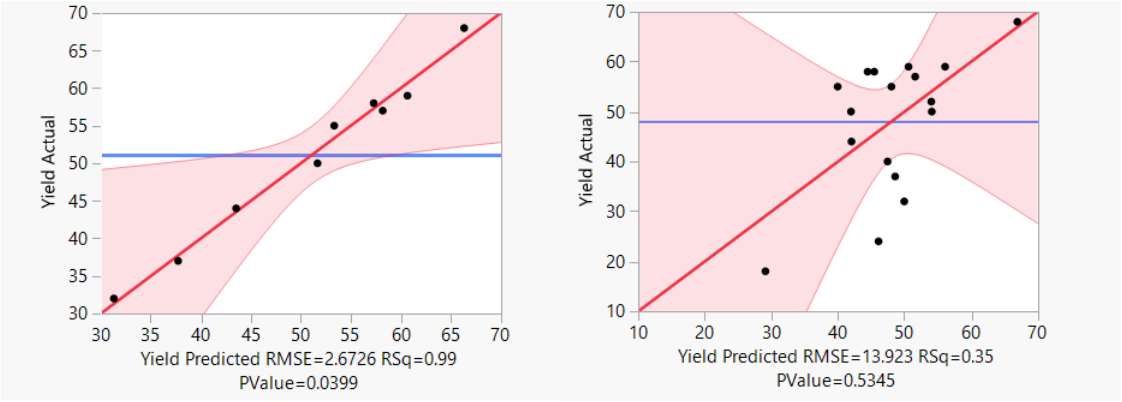


Figure 2.5 Fitting experimental data (black data points) to the statistical model predicted yield (red line) in a Definitive Screening Design. Left: runs at T < 55 °C considered. Right: Runs with T = 55 °C included.

A peak in yield at 60% was predicted after a 15 h reaction time when using 2 equivalents Ag_2CO_3 and 3 equivalents of aryl iodide. Although this is matched by the experimental value (62% determined by NMR), the design failed to account for known maxima towards the centre of the chosen experimental space, such as the outcome of the OFAT-derived settings.

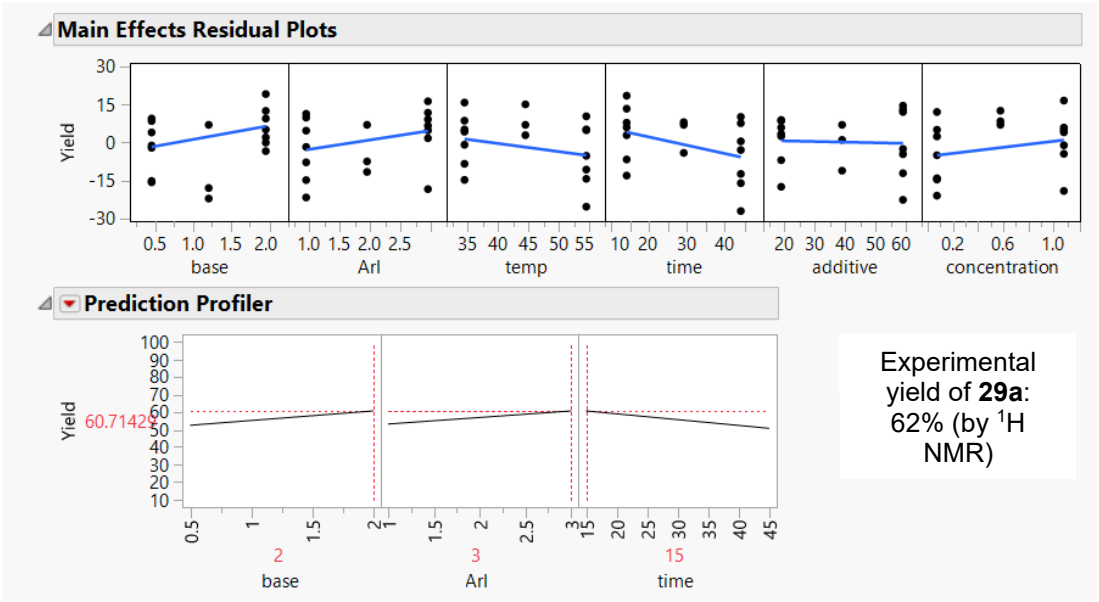
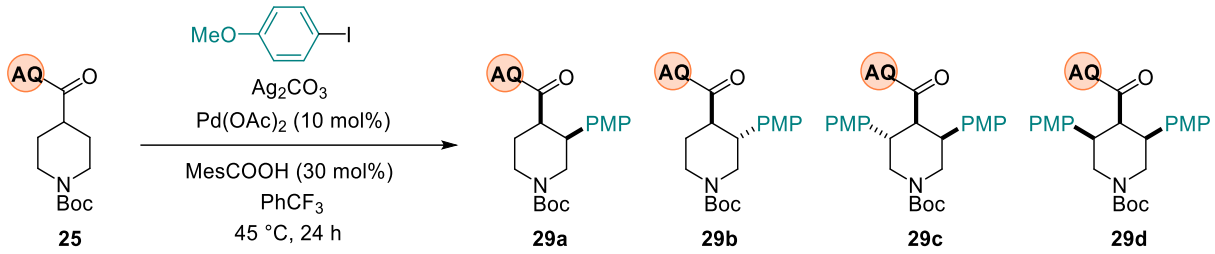


Figure 2.6 Variation in yield across the factor ranges chosen and prediction profiler showing most impactful factors and predicted optimum settings.

Expanding further along the suggested directions (higher base and aryl iodide loading, lower time) was found to reduce the yield by as much as 20% by facilitating diarylation. Since an increase in reagent loading would nevertheless be undesirable from an economical point of view, efforts continued with a second stage of DoE investigation aimed at yield optimsation.

Opting for a custom design, the maximum yield of **29a** was sought, this time with temperature, time and additive loading fixed at the most desirable values. A temperature of 45 °C was chosen in order to minimise extensive side-reactivity that impacts model fitting, and a 24 h time and a 30 mol% additive loading were considered operationally convenient. Smaller ranges for the remaining 3 factors (aryl iodide

and base loadings, and concentration) were considered, in order to gain a higher resolution of the experimental area surrounding the previously inferred maximum (Table 2.8, entry 7 and Table 2.10).



Factor	Lower Limit	Upper Limit	Presumed Optimum Based on OFAT
Ag_2CO_3 equiv (Base)	1	1.5	1
PMP–I equiv (Ar-I)	1.5	2.5	2
Concentration (M)	0.1	0.3	0.2

Table 2.10 Overview of definitive screening design settings.

Given the reduced number of factors, it became viable to study all possible interactions (individual factors, 2nd order and 3rd order interactions), with a half fraction design including relevant repeats and 3 centre points now requiring only 17 runs. With a custom design chosen for this purpose, an excellent fit between experimental data and the statistical model was now observed (Figure 2.7, $R^2 = 0.99$), providing confidence in the prediction accuracy.

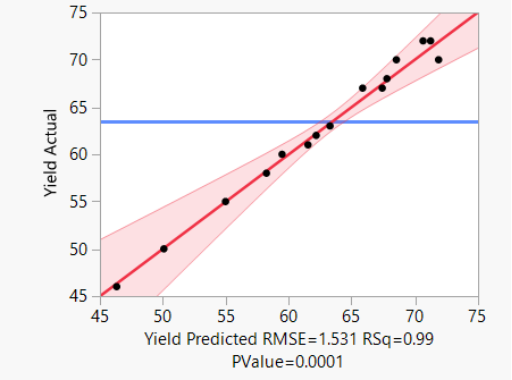


Figure 2.7 Left: Fitting experimental data (black data points) to the statistical model predicted yield (red line) in a Custom Design. Right: Main factors/interactions.

The prediction profiler illustrated the extent to which statistically relevant factors impact the desired response. Judging by the shape of the individual plots, concentration was found to have the most significant effect, with small variations in solvent volume dramatically affecting the desired yield. Again, no second or higher order interactions between distinct factors could be identified. By maximising desirability, the highest achievable yield of **29a** was predicted as 73% under the conditions shown in red in Figure 2.8. Crucially, at least a local maximum within the desirable reagent loadings was successfully

captured, as proven by the dome-shaped graphs of each variable. Interestingly, concentrations lower than 0.2 M result in the steepest decrease in yield, whereas other changes in parameters, including increasing the concentration to 0.3 M does not appear as detrimental.

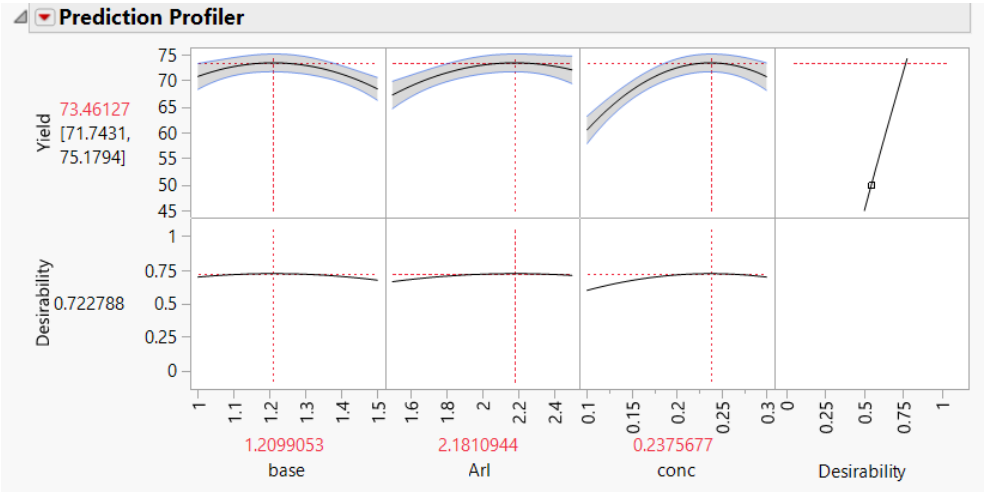


Figure 2.8 Prediction Profiler showing variation in predicted yield with changes in chosen factors. Plot showing the maximized desirability (yield) scenario, with grey areas representative of prediction error.

Additionally, other desired responses could be added to the model, such as the levels of diarylation. For instance, the yield of di-*cis-trans* arylation, which usually tends to be more significant than di-*cis-cis* arylation for any of the trialed conditions, can be decreased to only 2% by reducing base loading and concentration (Figure 2.9). However, the best possible compromise between reducing diarylation and increasing mono-*cis* functionalisation would result in a 10% predicted drop in desired **29a** yield.

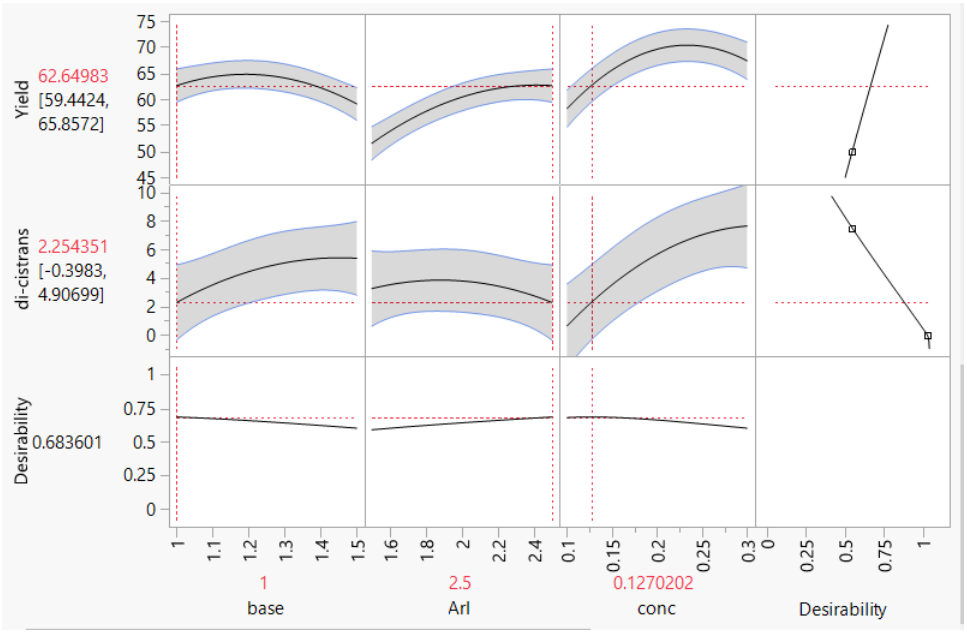


Figure 2.9 Prediction Profiler modelling concomitant optimisation of two desired responses: increasing yield of mono-*cis* **29a** (top) and decreasing yield of di-*cis-trans* **29c** (bottom).

Reactions were run to confirm the above DoE findings, employing conditions corresponding to plateau values of 70-74% in predicted yield (Table 2.11). Excellent agreement was found between experimental and predicted results, with up to 72% *in-situ* yields observed. Settings minimising the reagent loadings could be found, which led to a 68% isolated yield and the highest overall conversion (entry 3). These were selected as the final optimised conditions, subsequently employed in reaction scope studies (see Section 2.1.2)

Entry	Base equiv	ArI equiv	Conc (M)	Yield (%)[a]					
				29a	29b	29c	29d	RSM	Total
1	1	2	0.2	69(64)	6	7	2	14	97
2	1.2	2.2	0.24	72(67)	7	9	2	9	99
3	1.25	2	0.3	72(68)	8	9	2	7	98
4	1.25	2.5	0.2	72(66)	6	8	5	7	98

Table 2.11 Sampling design space points corresponding to the plateau in maximum yield (70-74%). Reaction scale: 0.2 mmol. [a]Calculated by ^{1}H NMR using 1,3,5-trimethoxybenzene as internal standard. Isolated yields shown in parenthesis.

The DoE study findings could be translated to a 3D plot of predicted yield vs. any chosen 2 factors. Fixing the concentration at the optimum 0.3 M, the reaction response surface could be visualised against aryl iodide and Ag_2CO_3 loadings (Figure 2.10) revealing a defined dome-shaped figure, with a plateau at 73% yield.

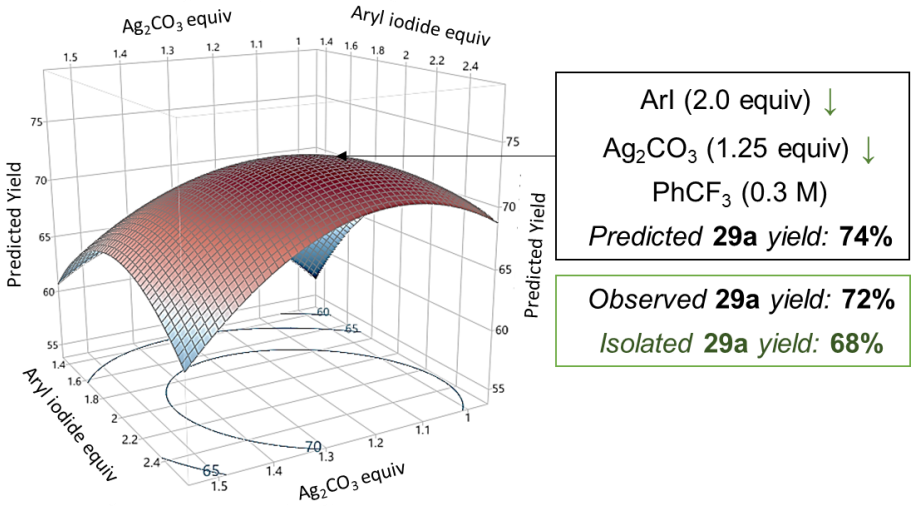
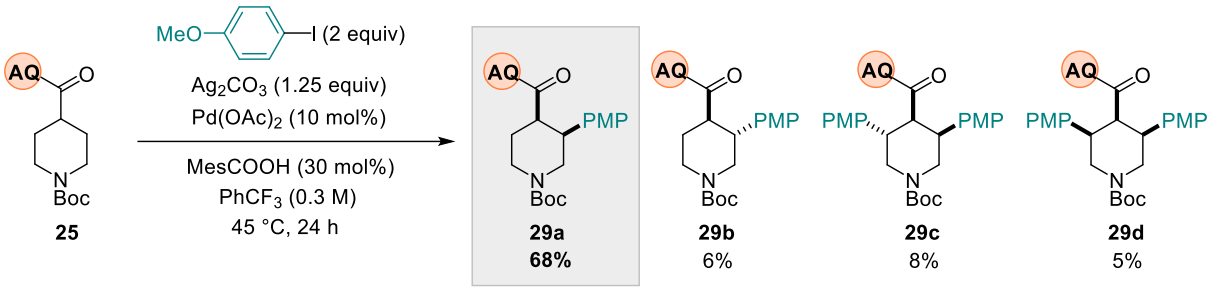


Figure 2.10 Reaction response surface with respect to aryl iodide and Ag_2CO_3 loadings, visualised at a fixed 0.3 M concentration. DoE reaction optimisation using a Definitive Screening and refined by a Custom Design.

Overall, the maximum achievable yield of **29a** could be correctly predicted under the most desirable temperature and time settings (45 °C and 24 h, respectively) using a DoE approach. Crucially, the optimum outcome could now be achieved by lowering the amounts of coupling partner and silver carbonate compared to the previous OFAT-derived conditions (Table 2.7, entry 1). The changes in

reagent loadings led also to an improved selectivity profile, with only 5-8% yields of each of the possible side-arylation products **29b-d** (Scheme 2.6).

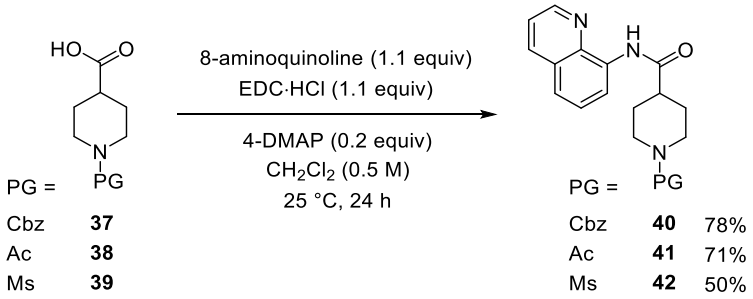


Scheme 2.6 Final optimised reaction conditions. Isolated yield shown for **29a**. Yields for **29b-29d** calculated by ^{1}H NMR using 1,3,5-trimethoxybenzene as internal standard.

2.1.2 Reaction Scope

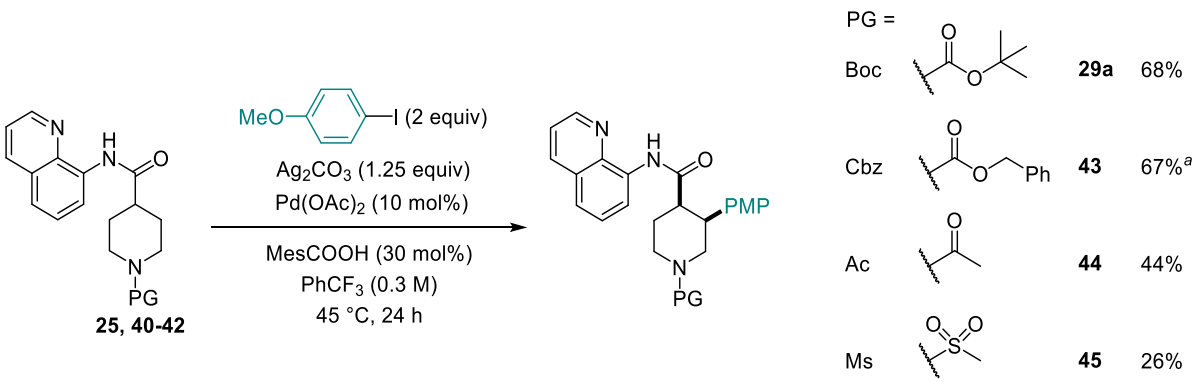
2.1.2.1 *N*-Protecting Group and Aryl Iodide Scope

With the optimised conditions, the reaction scope was evaluated. First, a series of commercially available piperidine 4-carboxylic acids bearing different *N*-protecting groups were sourced. The aminoquinoline directing group was then installed by EDC coupling, the amide formation proceeding in good yields to furnish **40-42** (Scheme 2.7).



Scheme 2.7 Aminoquinoline installation on a range of *N*-protected piperidines.

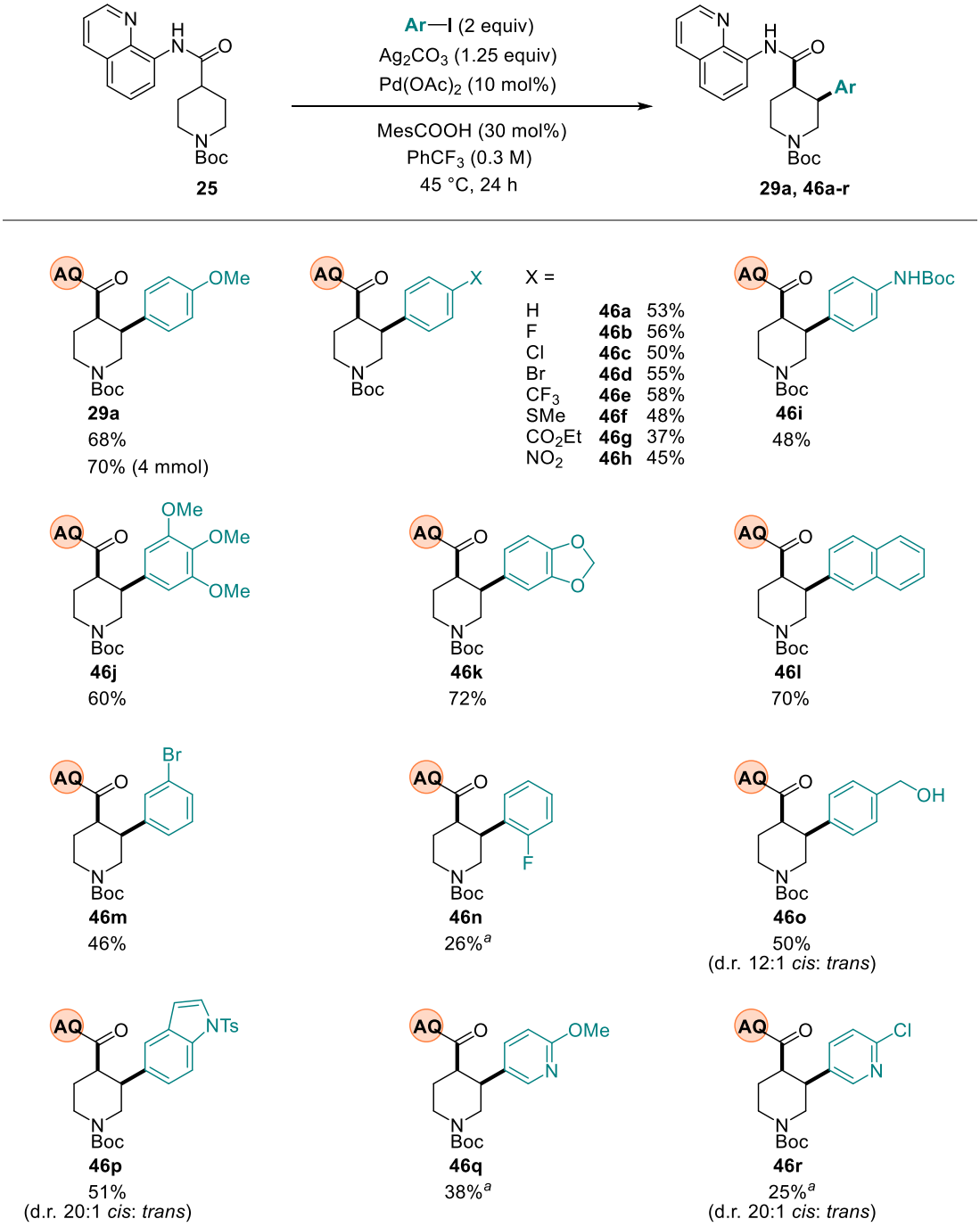
With amides **40**-**42** in hand, the arylation conditions were applied using 4-iodoanisole as coupling partner (Scheme 2.8). Both *N*-Boc and *N*-Cbz substrates **25** and **40** gave comparably high yields of *cis*-arylated product, however, significant purification difficulties were experienced in the presence of the Cbz group (**43**). Acetate (**41**) and mesyl (**42**) groups were tolerated and afforded exclusive *cis* arylation, albeit in lower yields (**44**, **45**).



Scheme 2.8 Aminoquinoline installation on a range of *N*-protected piperidines. Reaction scale: 0.4 mmol. [a]Product inseparable from starting amide by standard chromatographic methods, yield calculated by ^{1}H NMR using 1,3,5-trimethoxybenzene as internal standard

With *N*-Boc as the protecting group of choice, aryl iodides with a range of electronic and steric properties could be successfully employed (Scheme 2.9). In most cases, single *cis* diastereomers were isolated unless the d.r. is specified. Using 4-iodoanisole, the reaction could be run on 4 mmol scale, affording an excellent 70% yield and enabling preparation of gram-quantities of **29a**. Various *p*-aryl substituents were well tolerated, including halogens (**46b**-**e**) and the more electron-withdrawing ester and nitro functionalities (**46g-h**), affording yields between 37-58%. An *N*-Boc protected aniline was successfully installed in 48% yield, introducing an additional handle for further elaboration (**46i**). The highest yields,

up to 72%, were generally observed with electron-rich aryls such as trimethoxybenzene and benzodioxole derivatives (**46j-k**). Naphthalene could also be installed in 70% yield (**46l**).

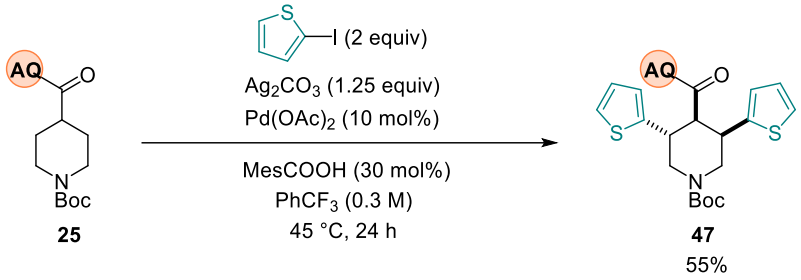


Scheme 2.9 Aryl iodide scope in the directed C3 arylation of piperidines Reaction scale: 0.4 mmol. d.r. shown for inseparable *cis*:*trans* mixtures, with single *cis* diastereomers isolated in all other cases. [a]3.0 equiv ArI and $PhCF_3$ (0.2 M).

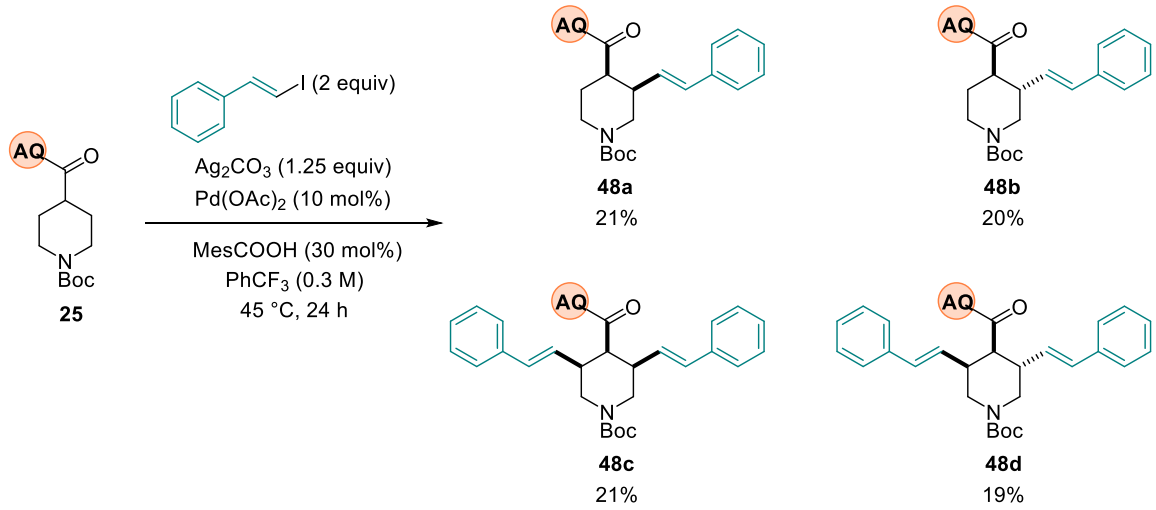
These observations, together with the moderate yields seen with electron deficient substrates may support reductive elimination as a rate-determining step, since electron-donating substituents better facilitate this step.

Meta- and even *ortho*- substituted aromatics were tolerated, with up to 46% yield obtained with 3-bromoiodobenzene (**46m**). However, the steric demands of 2-fluoroiodobenzene required the use of excess aryl iodide and determined a drop in yield to slightly below 30% (**46n**). The reaction was tolerant of functional groups susceptible to oxidation in the presence of silver, and pleasingly even an unprotected benzyl alcohol could be installed in 50% yield (**46o**), besides the previous examples of methyl sulfide and benzodioxole. Moreover, heteroarenes were compatible with the reaction conditions, with *N*-Ts protected indole affording 51% yield (**46p**). Pyridines with either electron-donating or withdrawing substituents could be employed, leading to reduced, but synthetically useful yields of at least 25% (**46q-r**).

2-Iodothiophene and styryl iodide were found to give unusually high reactivity (Scheme 2.10). In the former case, *cis-trans* arylated **47** formed as major product in 55% yield, with only trace amounts of mono-arylation observed. Conversely, (*E*)-β-styryl iodide led to full starting material consumption but led to loss of selectivity with the four mono- and dialkenylated piperidines **48a-d** each formed in approximately equal yields (Scheme 2.11). Notably, the (*E*) alkene geometry was preserved in all products. Both the smaller thiophene ring and the alkene would release steric hindrance when coordinated at a Pd(IV) centre compared to the other aryl iodides trialled, motivating their higher reactivity. It could be therefore argued that either oxidative addition or reductive elimination are stereodetermining, since these are both catalytic steps sensitive to the steric demands of the coupling partner.



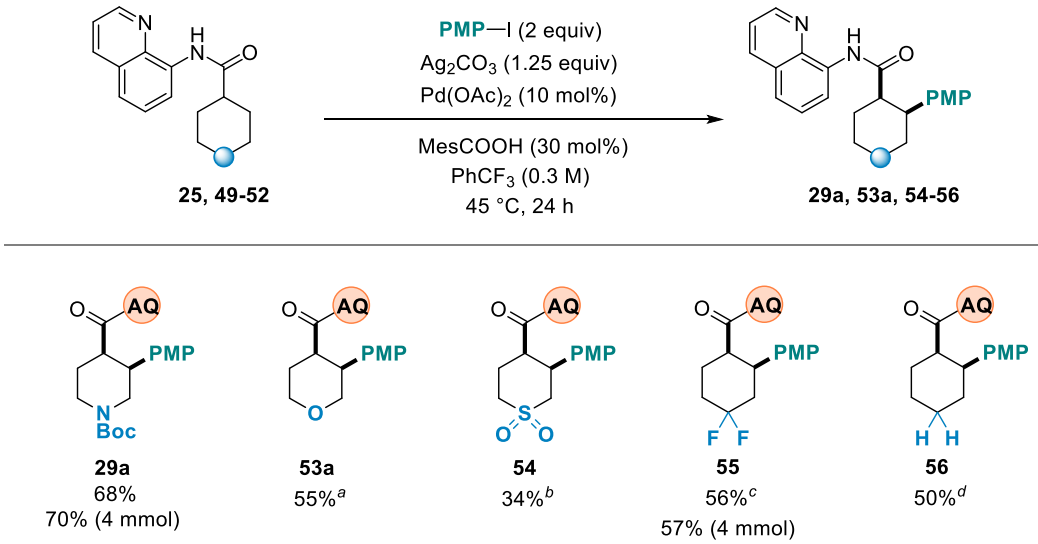
Scheme 2.10 Diarylation outcome in the presence of 2-iodothiophenol.



Scheme 2.11 Loss of selectivity when using styryl iodide as coupling partner.

2.1.2.2 Hetero- and Carbocycle Reaction Scope

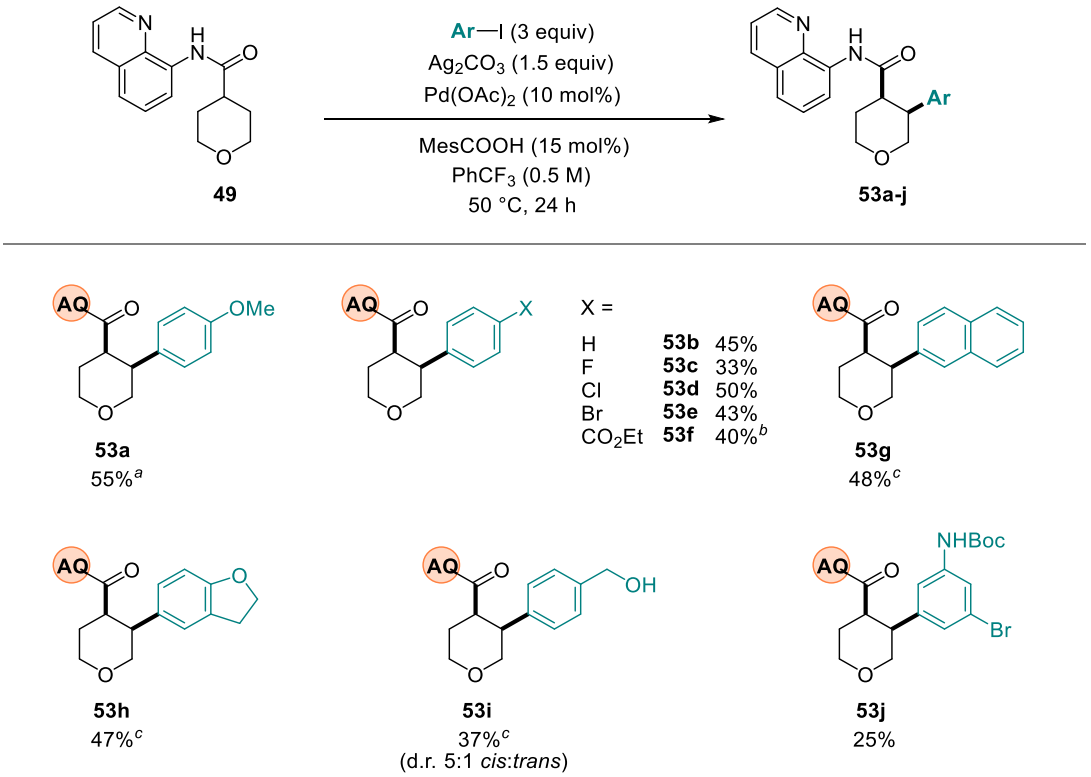
The optimised protocol could be applied with only few modifications to the selective C(3) *cis*-arylation of a range of 6-membered saturated hetero- and carbocycles bearing a C(4) aminoquinoline amide directing group (Scheme 2.12). Using 4-iodoanisole, tetrahydropyran could be functionalised in up to 55% yield, with a brief DoE study conducted by MSci student Harry Moore to fine-tune the reaction parameters.[190] A decreased general reactivity was observed in this case. With diarylation occurring to smaller extents, increases in concentration (0.5 M), aryl iodide loading (3 equiv) and temperature (50 °C) were employed to enhance *cis* product **53a** formation. The 6-membered cyclic sulfone could be arylated in 34% yield to give **54**, but requiring 3 equivalents or aryl iodide and a temperature of 75 °C. The lower reactivity could be due to 1,3-repulsion between the pseudo-axial S=O and an incoming C(3) substitutent.[151] Without deviations from the original conditions, 1,1-difluorocyclohexane afforded consistent 56-57% yields on small and large scale, with 0.96 g of **55** produced from 4 mmol of corresponding **51**. Finally, mono-*cis* arylation of cyclohexane could be promoted in similar yield. In this case, no *trans* configured products were observed, but desired **56** underwent a facile second *cis* arylation. To offset this, only 1 equivalent of aryl iodide was used, whereas the reaction time was increased to 48 h to provide **56** in 50% yield alongside 25% yield of *cis*-*cis* analogue.



Scheme 2.12 Hetero- and carbocycle C3 *cis* functionalisation scope. Reaction scale: 0.4 mmol unless otherwise stated. [a]DoE optimisation and reaction conducted by Harry Moore (MSci). Using PMP–I (3 equiv), Ag_2CO_3 (1.5 equiv), MesCOOH (15 mol%), $PhCF_3$ (0.5 M), 50 °C. [b]PMP–I (3 equiv), 75 °C. [c]Reaction conducted by Natalia Larionova (PDRA). [d]Using PMP–I (1 equiv), 48 h.

For tetrahydropyran, the coupling partner scope was expanded (Scheme 2.13). Aryl iodides previously used with *N*-Boc piperidine (see Section 2.1.3.1) were similarly tolerated, with *p*-substituted phenyl groups installed in 33-55% yields. Halogens and electron-withdrawing substituents were tolerated (**53c-f**), whereas naphthalene and benzofuran afforded some of the highest yields (**53g-h**). The unprotected benzyl alcohol was compatible again with the conditions, though led to increased *trans* arylation and an inseparable mixture of *cis* and *trans* diastereomers in 5:1 d.r. (**53i**). Notably, a *meta* disubstituted aryl iodide could be successfully employed to provide **53j** in 25% yield. Compared to

previous examples, the lower observed yield might arise from aniline coordination to Pd. Interestingly, products arising from an oxidative addition into the C–Br bond were not observed, neither in this case, nor for other brominated aryls used. With an *N*-Boc protected amine and a bromide as further functionalisation handles, the applications of this product and similar products will be discussed in Section 2.3.4.

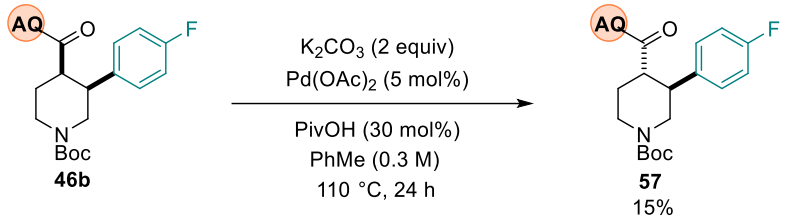


Scheme 2.13 Expanding the aryl iodide scope for tetrahydropyran functionalisation. Reactions on 0.4 mmol scale. [a]Reaction run by Harry Moore (MSci student). [b]Inseparable mixture of *cis* and *cis-cis* isomers (8:1 molar ratio, respectively) [c]Reactions run by Joe Higham (PhD steudent).

2.1.3 Studies on the Origin of Side-Product Formation

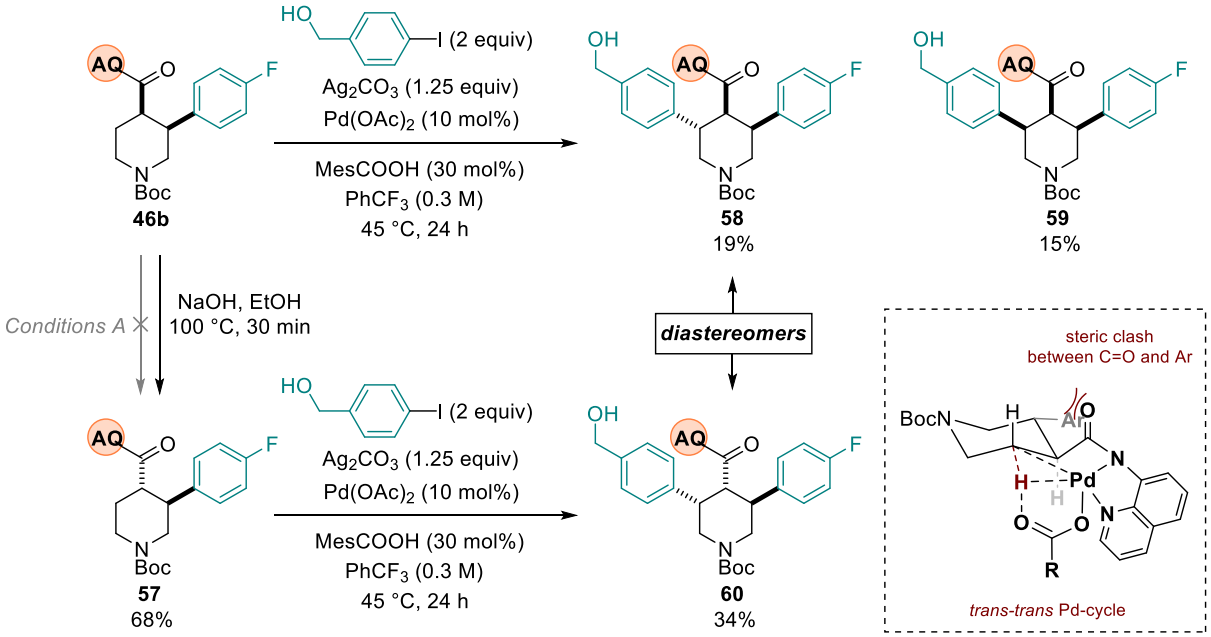
2.1.3.1 Diarylation Studies

Investigations were next conducted into the pathways leading to the minor arylation products. Considering the apparent consumption of the *cis* arylated product at elevated temperatures in favour of forming *trans* and diarylated piperidines, an epimerisation process was suspected to take place. To probe this, the *cis*-configured product **46b** was resubjected to the reaction conditions in the absence of aryl iodide. Under the initial conditions at 110 °C using K_2CO_3 as base, 15% of the starting material epimerised, this process being potentially enhanced if *trans* **57** was immediately consumed in a subsequent second arylation (Scheme 2.14).



Scheme 2.14 *Cis* to *trans* epimerisation under the high temperature reaction conditions. An estimated 80% unreacted **46b** accounted for the mass balance.

However, under the optimised conditions in the absence of coupling partner, **46b** does not undergo any transformation, being quantitatively recovered (Conditions A, Scheme 2.15). This suggests that besides the lower temperature of 45 °C, the acid additive (MesCOOH) could also play a role in reducing the basicity of the reaction environment. To also test epimerisation in the presence of a coupling partner, a second arylation on **46b** was performed, this time using a different aryl iodide to provide a stereochemical marker. In the presence of 4-iodobenzyl alcohol, di-*cis*-*trans* **58** and di-*cis*-*cis* **59** formed in 19% and 15% yields, respectively. Crucially, the existing relative stereochemistry on the ring was unaffected, with the second aryl group installed in either a *cis* or a *trans* fashion with respect to the directing group. Therefore, arylation in a *trans* fashion to form either the mono- or diarylated side-products must be the result of *trans* palladacycle formation.[169,191,192]



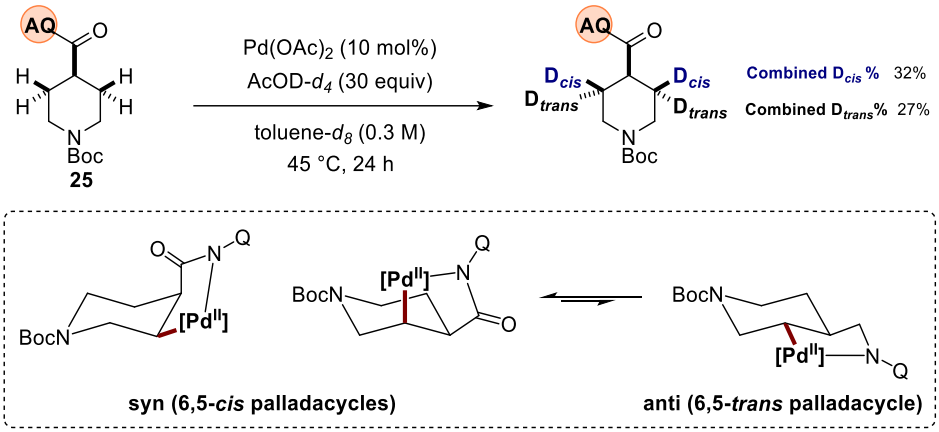
Scheme 2.15 Studies elucidating the origin of minor arylation products under optimised conditions and hypothetical palladacycle precursor to *trans-trans* arylation. Conditions A: **46b** (1 equiv), Ag_2CO_3 (1.25 equiv), $Pd(OAc)_2$ (10 mol%), MesCOOH (30 mol%), $PhCF_3$ (0.3 M), 45 °C, 24 h.

To further probe the previous stereochemical assignments, **46b** was deliberately epimerised to **57** by treatment with NaOH. Subjecting **57** to arylation with 4-iodobenzyl alcohol now led to *cis*-*trans*-arylated **60**, which was found by NMR analysis to be a diastereomer of **58**, confirming previous deductions on the stereochemistry of the first *cis*-*trans* isomer. Interestingly, formation of a *trans*-*trans*-arylated piperidine was not observed under any conditions, as the palladacycle precursor to this transformation

would present significant strain in its all-equatorial conformation and possible steric clash between the directing group and the pre-existing aryl group, being energetically unfavourable.

2.1.3.2 Deuteration Studies

To prove activation of both *cis* and *trans* C(3)–H bonds with respect to the directing group, deuteration studies were performed. This involved mixing aminoquinoline amide **25** with the catalyst of choice ($Pd(OAc)_2$) to promote formation of a palladacycle, whilst excess AcOD-d_4 was used to promote displacement of Pd by deuterium at the activated positions (Scheme 2.16). After evaporation of the organics, the crude product was analysed by ^1H NMR in $CDCl_3$ and contrasted to the starting material. Deuteration occurred exclusively at C(3), in similar percentages at both the *cis* and *trans* diastereotopic positions (32% D_{cis} and 27% D_{trans}, respectively). Moreover, no deuterium incorporation was observed α to the amide carbonyl, indicating no epimerisation *via* enolate formation. These results suggest formation of both *cis* and *trans* palladacycle species in equilibrium, implying that the stereodetermining step is downstream of C–H activation. Presumably, the *cis* palladacycle most easily overcomes subsequent activation energy barrier(s) in the catalytic cycle at 45 °C to lead to the major product, pushing the equilibrium in favour of its formation.



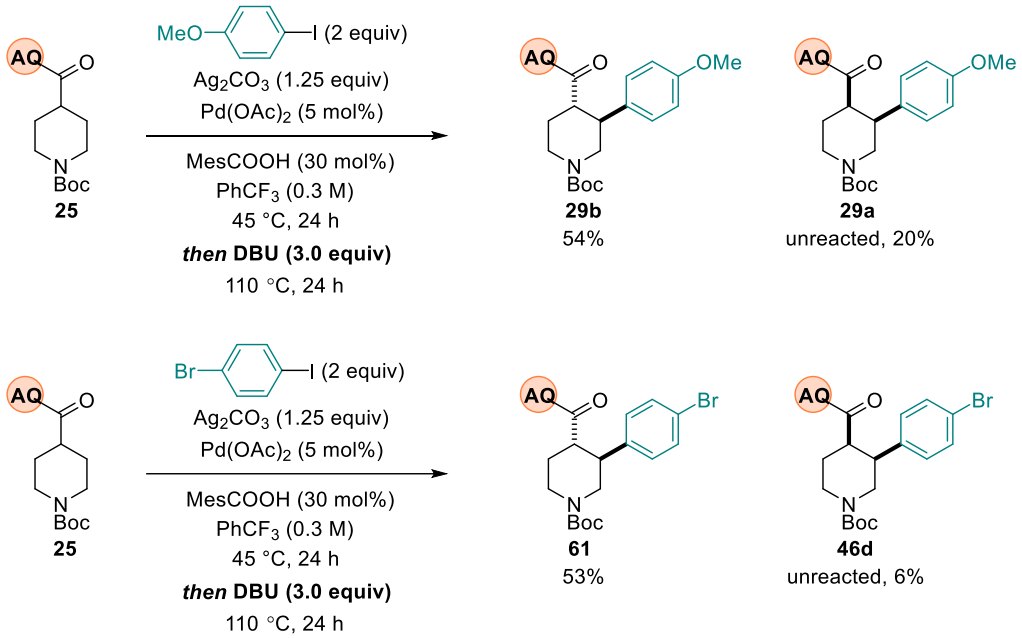
Scheme 2.16 Deuteration studies on aminoquinoline amide **25**, supporting formation of both *cis* and *trans* palladacycles in the C–H activation step.

Based on studies described in this section it follows that the minor *trans* diastereomer forms as result of *trans*-C(3)–H activation, while the major *cis* isomer undergoes a second arylation to furnish the *cis*-*cis* diarylated side-product. Finally, the *cis*-*trans* product can arise from a second arylation of either monoarylated isomers *via* either a *cis* or a *trans* palladacycle.

2.1.4 A One-Pot Arylation-Epimerisation

Epimerisation of the *cis* product was previously achieved in a discrete step using NaOH (see Section 2.1.4.1). However, developing an *in-situ* epimerisation was deemed extremely valuable, offering the opportunity of selecting the stereochemical outcome of the reaction at will. Addition of a soluble base to the crude reaction mixture post arylation was envisaged to effect *cis* to *trans* conversion, in addition to shutting down potential diarylation pathways by coordinating to and inactivating the metal catalyst.

Pleasingly, employing DBU at 100 °C led to high levels of epimerisation, with *trans* diastereomers isolated in only one step from amide **25** (Scheme 2.17). Similar to the original procedure, the one-pot arylation-epimerisation was easily scalable. On 2 mmol scale, **29b** is formed in 54% yield after 24 h after epimerisation of 70% of the amount of *cis* isomer formed *in situ* . With the *p*-bromophenyl substituent on the ring, epimerisation occurred more readily, and with 90% conversion, to provide **61** in 53% yield.



Scheme 2.17 A DBU-mediated one-pot arylation-epimerisation protocol. Reaction scale: 2 mmol. Products isolated as single *trans* diastereomers in the yields shown, with yields of non-epimerised *cis* products calculated by ^{1}H NMR using 1,3,5-trimethoxybenzene as internal standard.

2.1.5 Conclusion

A Pd-catalysed methodology has been developed for the mono-functionalisation of 6-membered saturated heterocycles in a highly regio- and diastereoselective fashion.

Using a C(4) aminoquinoline amide directing group, high stereocontrol was achieved for the *cis* C(3) position despite the presence of 4 equivalent C(3)–H sites. Mild temperatures (45–50 °C) were key to the observed selectivity, this being the first example of saturated heterocycle functionalisation at an unactivated position to not require temperatures above 100 °C (Figure 2.11). A DoE study was conducted to gain an advanced understanding of the reaction behaviour with changes in continuous parameters and allowed selection of conditions that maximised the *cis* arylation yield. Mono-*cis* arylated piperidines were isolated as single diastereomers in up to 72% yields, with only small percentages (<10%) of *trans*- and diarylated side-products. The reaction was scalable to 4 mmol, affording >1 g of *cis*-functionalised product. A wide coupling partner scope was demonstrated, with over 20 different electron-rich and electron-poor substrates tolerated, including heteroaryl iodides. The methodology was applicable to *N*, *O* and *S*-heterocycles, as well as to carbocycles, affording synthetically useful yields of *cis*-arylated building blocks of relevance to medicinal chemistry (see Sections 2.2 and 2.3 for applications).

No *cis* to *trans* epimerisation was found to take place under the reaction conditions, with the *trans* side-product proposed to arise from the corresponding *trans*-palladacycle intermediate. Deuteration studies confirmed activation of both *cis* and *trans* C(3)–H positions to similar extents, suggesting C–H abstraction is not stereodetermining. Base epimerisation of the *cis* product could be promoted in the same pot as the arylation by subsequent addition of DBU, affording direct and facile entry to *trans* diastereomers at will.

Strategies for the divergent removal of the aminoquinoline directing group will be discussed in the next chapter, together with applications of the resulting products in medicinal chemistry, for generation of fragment libraries and DNA-encoded library (DEL) building blocks with attractive properties.

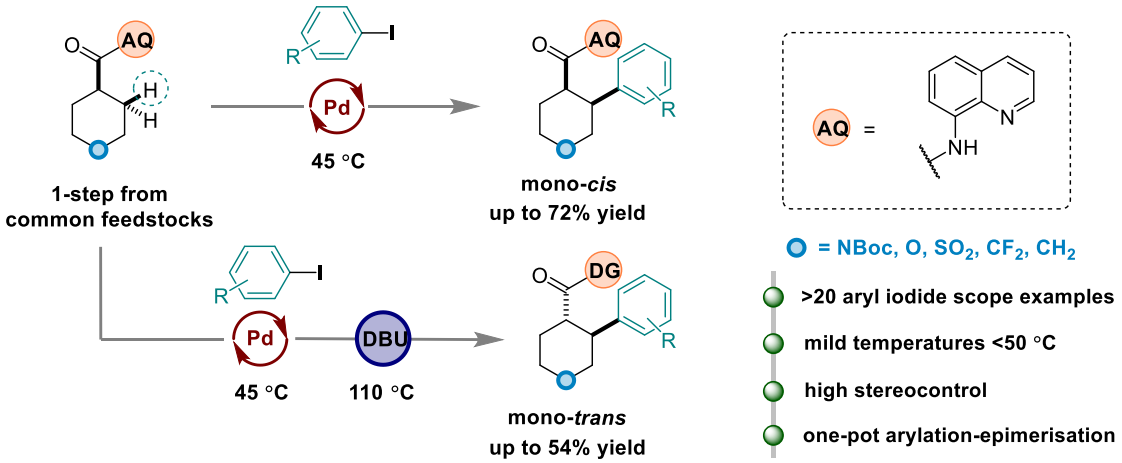


Figure 2.11 A directed methodology for highly stereoselective *cis*-C(3) functionalisation of saturated unbiased heterocycles, with direct access to *trans* diastereomers by one-pot arylation-epimerisation.

2.2 Directing Group Deprotection and Fragment Library Synthesis

2.2.1 Desirable Fragment Properties

Focused on screening molecules of relatively low MW (<300 Da), fragment-based drug discovery has enabled the generation of drugs more suited to highly 3-dimensional biological targets and has played an increasing role in producing clinical candidates over the past 20 years.[30,193] Besides the practicalities of screening smaller libraries, this has also allowed the identification of new binding modalities with challenging targets that could not be unveiled by traditional high-throughput approaches.[194,195] Notably, Vemurafenib is the first approved drug originating from FBDD, as well as the first selective inhibitor of the oncogenic BRAF kinase, showing a considerably improved efficacy compared to active compound classes previously derived from extensive HTS.[196] The development of Vemurafenib was based upon the identification of a relatively simple 3-substituted aza-indole fragment hit, followed by SAR exploration and elaboration from the C(3) aryl substituent (Figure 2.12).[197]

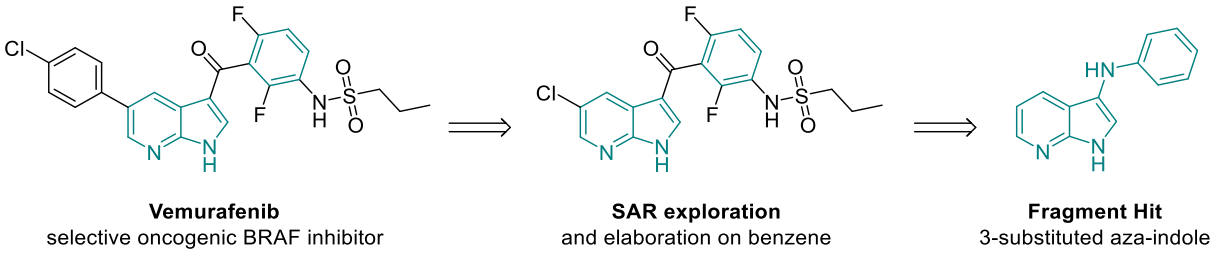


Figure 2.12 Development of Vemurafenib from an aza-indole fragment hit.

However, fragments pose challenges in screening due to their small size, exhibiting only low affinities (K_d > 0.1 mM) and requiring specialised biophysical techniques to identify their binding, such as surface plasmon resonance, thermal shift assay, microscale thermophoresis and isothermal titration calorimetry.[195,198,209] Moreover, these experiments often require high costs, high concentrations and implicitly amounts of pure protein and result in a low throughput. Whereas NMR can also be employed for rapidly identifying binding fragments from a cocktail, X-ray analysis of ligand-target co-crystal structures is needed for identification and validation, especially forvery low molecular weight hits.[199] For the latter case, numerous repeat experiments might be needed to deconvolute ligand-to-target binding, especially when a fragment cocktail yields multiple hits. Moreover, high quality crystallised proteins are needed, in addition to the requirement for these to be robust enough (i.e. not undergo major conformational changes) during fragment soaking experiments. On the other hand, false positives are a common occurrence, given that small molecules need to be screened at high concentrations in DMSO/water – this implies ensuring a good fragment solubility, although at the same time it increases the chances of aggregation and non-specific effects during screening..[194,200] Additionally, some false positives termed pan-assay interference compounds (PAINS) can arise due to the presence of functionalities that react with the protein target itself, hence careful selection of fragments must consider any potential reactivity.[198]

Beyond the requirement to ensure a good solubility for screening, the physicochemical properties of fragments influence the 'lead-likeness' of compounds generated by growth/linking or elaboration during

hit optimisation (see Introduction Section 1.1.3.1 for a schematic representation of lead-like space). Astex defined a 'Rule of 3', proposing fragment selection criteria that allow for efficient lead discovery. According to this, molecules with clogP < 3, MW < 300, HBA ≤ 3, HBD ≤ 3, NROT ≤ 3 and PSA ≤ 60 Å have most chances of being successful hits, as well as being developed into leads with desirable profiles.[201] The 'rule' was later revised within Astex, stipulating that a reduction in size (to MW < 200) and lipophilicity (to clog P < 2), together with an increase in 3-dimensionality would be most beneficial in the design of fragment libraries, although interactions may only be identifiable by X-ray crystallography.[202,203]

The ability to attach substituents at specific positions on the fragment, known as development along growth vectors has been highlighted as an important factor in determining progression of a fragment hit throughout drug discovery stages.[202] The lack of synthetic tractability along certain growth vectors can significantly decelerate optimisation to lead or even halt further progression. Moreover, elaboration alongside traditional vectors such as polar functionalities, for which a multitude of synthetic tools exist, would result in preventing the binding interactions of these groups with the target. While synthetic strides are made to respond to the increasing demands of medicinal chemistry programs, with developments in transition metal catalysed couplings,[204] photocatalysis,[205] C–H activation[206] and high throughput experimentation,[207] attention has been paid to the design of the fragment compounds themselves.[208,209] For instance, Brennan introduced the concept of 'poised fragments', defining small molecules that can be deconstructed into synthons and reacted with commercially available building blocks in a parallel fashion to generate analogue libraries.[210] Recently, Astex and collaborators proposed the idea of selecting fragments based on their "sociability", invoking the use of graph data structures similar to the ones employed by social media applications.[211,212] According to their classification, "sociable" fragments would have synthetic tractability alongside each growth vector, as well as commercially available close analogues, prompting their inclusion in screening libraries. On the other hand, a recent trend has been towards maximising the spatial distribution of functionalisation handles and creating new means to exploit them in order to expediently generate stereodefined structures with custom geometries.[68]

The recognised benefits of increasing the level of saturation in screening libraries is also guiding fragment design (see Introduction Section 1.1.3).[213,214] In this respect, sp^3 centres can act as vectors for elaboration in an out-of-plane fashion from the parent fragment, with growth in 3-dimensions associated with increased chances of producing a successful lead.[215]

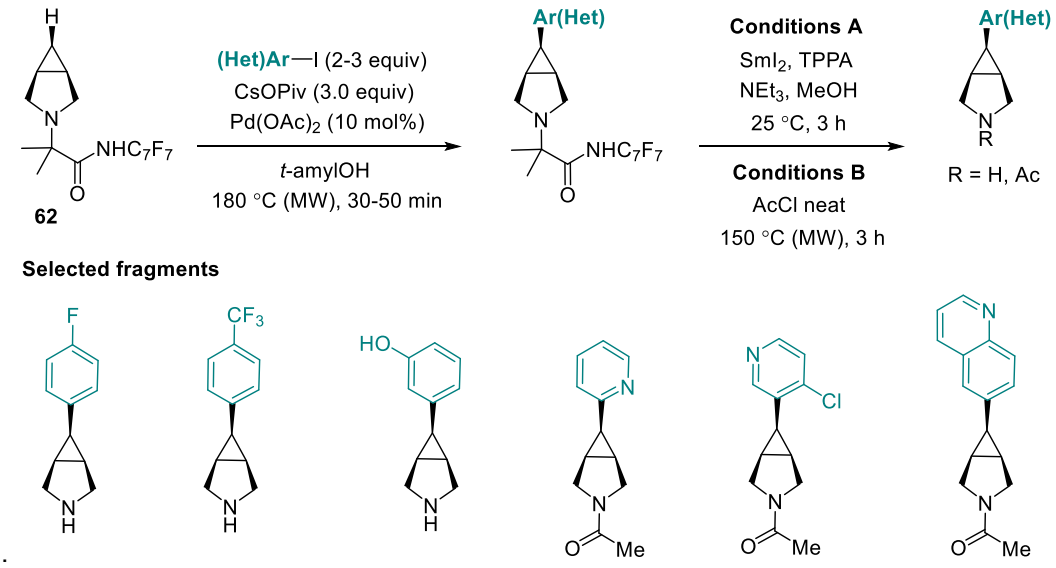
Besides these characteristics, the accessibility of starting materials for fragment generation should be considered, as well as the tractability of the synthetic route, given that access to a diversity of analogues might be required. Finally, the structural novelty of fragments has been recognised as desirable from at least the context of IP protection. This is due to observations that significantly different targets can sometimes be bound by the same or by closely related small molecules.[216,217]

2.2.2 Reported Syntheses of Shape Diverse Fragment Libraries

Based on all the above considerations, there is a strong focus to include underrepresented and more 3-dimensional compounds in fragment libraries, but also a drive to balance complexity with potency and developability, while maintaining desirable physicochemical properties. A series of strategies have been

employed for generating fragment libraries with these desired characteristics, [215] based on diversity-oriented synthesis,[218,219,220] diversification of readily available/synthesised scaffolds[221] or computationally driven design.[223] Interestingly, some of the methodologies used to construct and diversify fragment libraries have started to be recognised for their suitability to also enable fragment-to-lead optimisation.

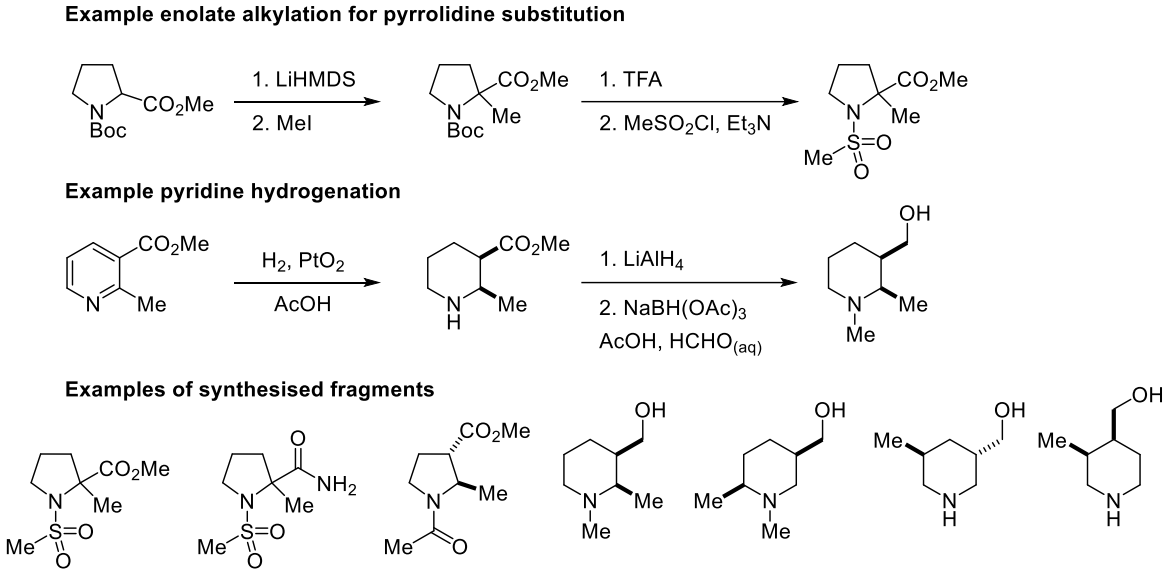
C–H functionalisation could enable expedient and divergent decoration of readily available scaffolds to generate attractive fragment-like compounds focused on design simplicity. Moreover, high scaffold and stereochemical diversity could potentially be achieved by methodologies that are highly stereoselective and compatible with a wide range of substrates. In collaboration with AbbVie, Sanford illustrated the synthesis of 3D fragments by the directed transannular arylation of 3-azabicyclo[3.1.0] hexane (Scheme 2.18).[222] Besides the choice of a relatively low MW substrate, the original conditions were adapted to enhance throughput and suitability for medicinal chemistry use. 14 fragments were assembled from commercially available bicyclic scaffold **62** in a divergent fashion. These showed optimal physicochemical properties within the Rule of 3 space, as well as a degree of 3-dimensionality higher than 90% of the AbbVie fragments, as assessed through consideration of both the average principal moment of inertia (PMI) and plane of best fit (PBF).



Scheme 2.18 Transannular C–H arylation of 3-azabicyclo[3.1.0]hexane core and adapted directing group removal for the synthesis of a fragment collection.

A recent computationally driven approach reported by O'Brien further supported the advantages of simple scaffold designs in generating shape-diverse libraries.[223] Aiming to include common pharmacophores with desirable physicochemical properties, a virtual enumeration of simple yet underrepresented disubstituted pyrrolidines and piperidines (including regio- and stereoisomers) was performed, with a focus on accessible functionalisation handles. Shape analysis was conducted on both the virtual fragments, as well as on their computationally calculated conformations up to 1.5 kcal/mol higher in energy, motivated by the probability of accessing these conformations *in vivo*. Synthetic targets were then chosen based on structures and/or conformers judged to be most 3-dimensional by analysis of the corresponding principal moments of inertia. By further fine-tuning the selection based on synthetic

accessibility, a set of 56 fragments were targeted by methodologies such as enolate alkylation and pyridine hydrogenation (Scheme 2.19). The final synthesised library was found to have increased shape-diversity compared to 6 commercial libraries.



Scheme 2.19 Illustrative synthesis of computationally designed pyrrolidine and piperidine fragments with a high degree of 3-dimensionality.

Overall, there are still clear difficulties in accessing any substitution pattern of choice on sp^3 systems,[224] which promise to enhance desirable properties in screening libraries. There is an increasing demand for robust and expedient synthetic tools to both assemble these small molecules, as well as further elaborate them along any growth vectors of choice.

2.2.3 Project Aims

Common pharmacophores such as 5- to 6-membered saturated heterocycles present valuable opportunities for the assembly of fragments, such as a low molecular weight, presence of sp^3 centres and availability of growth vectors in 3 dimensions.

This work aimed to demonstrate the assembly of a diverse library of heterocyclic fragments in underexplored chemical space using a directed C(sp^3)–H functionalisation strategy. As key features, inexpensive feedstocks such as intact saturated heterocycles would be used as starting materials, whereas fragments would be designed to possess three different binding elements in order to enhance binding enthalpy with the target and increase the rate of genuine hits. As illustrated in Figure 2.13, the design would feature: (i) an endocyclic heteroatom part of the ring, capable of promoting H-bonding interactions, (ii) an aryl group with a small and polar substituent such as -OMe or -F, capable of promoting π-π stacking interactions and (iii) a polar functionality for inducing either H-bonding or ionic interactions. Moreover, a stereodefined substitution pattern would be targeted to reduce the conformational freedom of the ring and minimise the entropic penalty upon binding, all whilst maintaining structural simplicity.

Starting from commercially available carboxylic acids of general structure **63**, aminoquinoline would be installed as directing group. Corroborating all previous group protocols, as well as the methodology

described in Section 2.1, C(sp^3)-H arylation would then be performed to target the synthesis of 5- and 6-membered saturated heterocycles bearing any possible vicinal disubstitution pattern (**64-66**). Notably, given these are *cis* stereoselective methodologies, expanding the stereochemical diversity of the library by base-mediated epimerisation would provide the corresponding *trans* diastereomers. Finally, with the aryl substituent installed, the other two binding elements would be unveiled by: (i) divergent directing group removal to generate a range of polar coordinating functionalities that would include alcohols, carboxylic acids, amides and/or nitriles (ii) deprotection of the endocyclic heteroatom where necessary. Overall, the fragment library was designed to feature structural novelty and simplicity, diversity of binding elements and their spatial distribution, as well as representation of underexplored pharmacophores. Most importantly, the C(sp^3)–H functionalisation strategy used for its construction would demonstrate how growth vectors of choice can be selectively probed, allowing for further applicability in fragment elaboration. Last, but not least, the unique profiles and suitability for FBDD of the synthesised compounds would be demonstrated by shape and physicochemical property analysis.

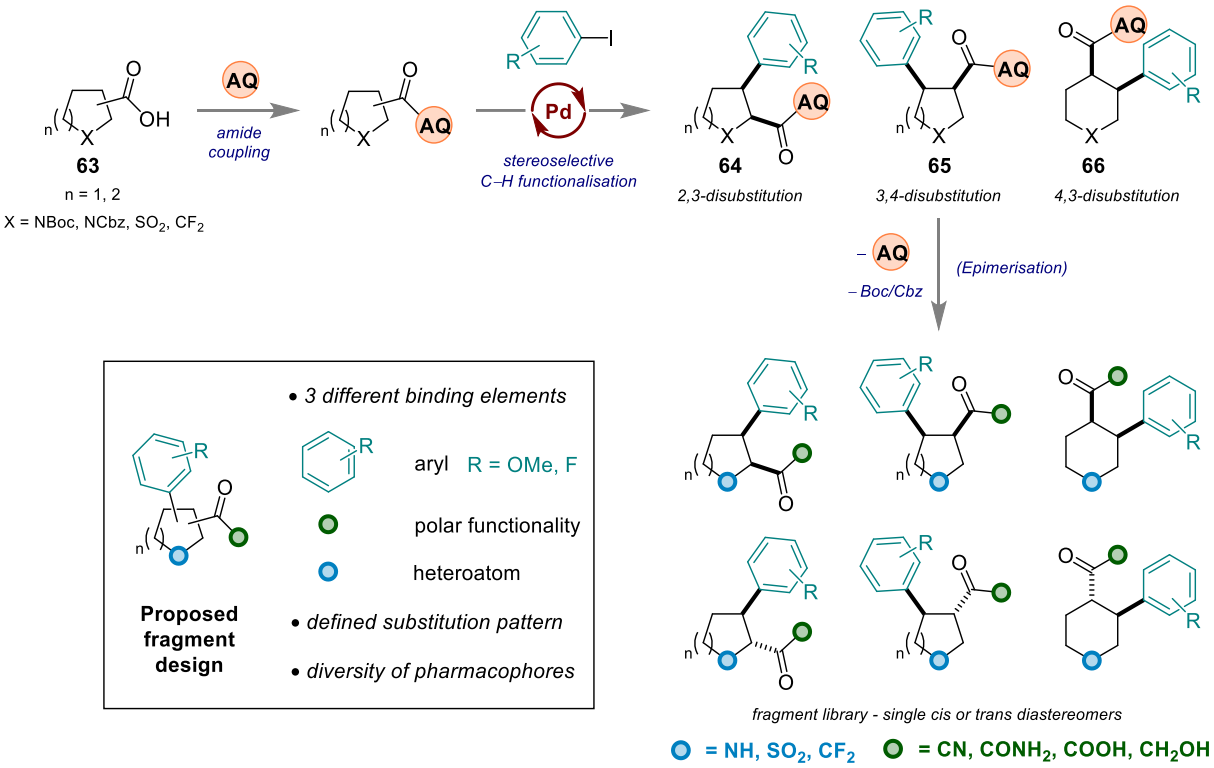


Figure 2.13 Proposed fragment design and desired synthetic route involving regio- and stereoselective C(sp^3)-H functionalisation, followed by divergent removal of directing group to unveil polar binding elements.

2.2.4 Aminoquinoline Deprotection on the 2,3-Disubstitution Pattern

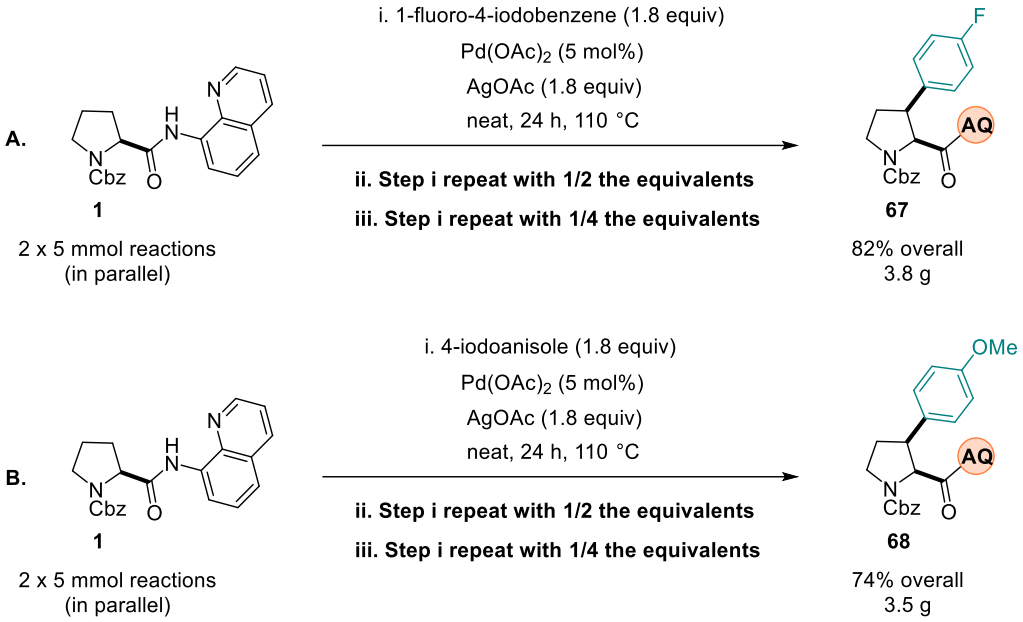
2.2.4.1 Large Scale Arylation of Pyrrolidines and Piperidines

The previously developed protocol for the C(3) arylation of pyrrolidines and piperidines in the presence of a C(2) aminoquinoline amide directing group were successful on reaction scales up to 0.5 mmol.[169,134] With no reported scale-up procedure to date, the challenge of synthesising gram-quantities of C(3) functionalised heterocycles was addressed.

Firstly, 5 mmol of *N*-Cbz DL-proline **1** was subjected to the original arylation conditions in the presence of 1-fluoro-4-iodobenzene (Scheme 2.20A). Unfortunately, only 50% conversion was observed and standard chromatographic procedures failed to separate the desired product cleanly from the resulting equimolar mixture of **67** and unreacted **1**. Since C(3) is the only reactive site and no side-products were formed, resubjecting the crude mixture to the reaction conditions was employed as a solution to achieve full consumption of the starting material. Notably, residual metals were removed beforehand by filtration of crude mixtures through a Celite plug. Half of the previous equivalents in each reagent were used, to match remaining **1** observed by ^{1}H NMR, leading to a further 25% consumption in **1**. Finally, another resubjection, this time using quarter of the initial reagent equivalents promoted conversion of any remaining **1**, leading to isolation of **67** in 83% yield (1.26 g). The 5 mmol functionalisation could be performed multiple times in parallel, in separate vials, with the final crude mixtures combined before conducting a single purification. Running these processes two times in parallel led to 3.8 g **67** in 82% overall yield.

Following a similar workflow, *N*-Cbz DL-proline was also functionalised in the presence of 4-iodoanisole to afford 3.5 g of the *p*-methoxyphenyl analogue **68** in 74% yield (Scheme 2.20B).

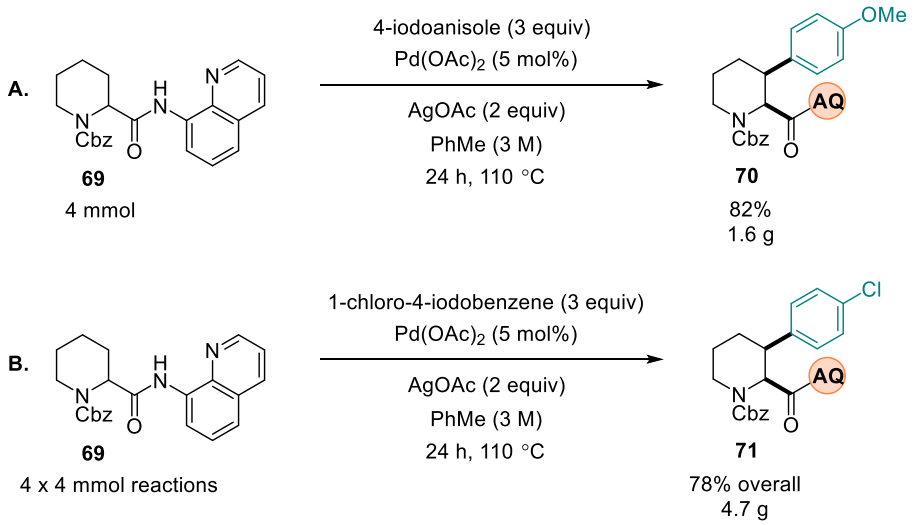
Interestingly, later investigations revealed the importance of reagent addition order, with up to 75% conversion seen after a single run when charging the reaction tube in the following sequence: aryl iodide, AgOAc, $Pd(OAc)_2$ and amide **1**. In particular, addition of **1** as the last reagent was crucial for the observed outcome. This is presumably due to the viscosity of this reagent, which prevents efficient mixing and stirring under the neat reaction conditions once it is deposited on the interior walls of the reaction vial.



Scheme 2.20 Large scale C(3) arylation of pyrrolidine with A. 1-fluoro-4-iodobenzene and B. 4-iodoanisole. 5 mmol reaction conducted 3 times in parallel, with crude mixtures combined and purified once.

N-Cbz piperidine **69** exhibited higher reactivity for C(3) functionalisation, with the original protocol having enabled the use of toluene as solvent without impacting the yield.[169] Scaling up the reaction to 4 mmol, the concentration in toluene was increased from 0.3 M to 3 M to allow containing the reaction volume in

the maximum sized sealed vial available (25 mL). In the presence of 4-iodoanisole, 1.6 g arylated **70** was isolated (82% yield) without any resubjection to reaction conditions (Scheme 2.21A). Using 1-chloro-4-iodobenzene and conducting 4 x 4 mmol single runs in parallel led to a total of 4.7 g of **71** after purification of the combined crude reaction mixtures (78% overall yield, Scheme 2.21B).

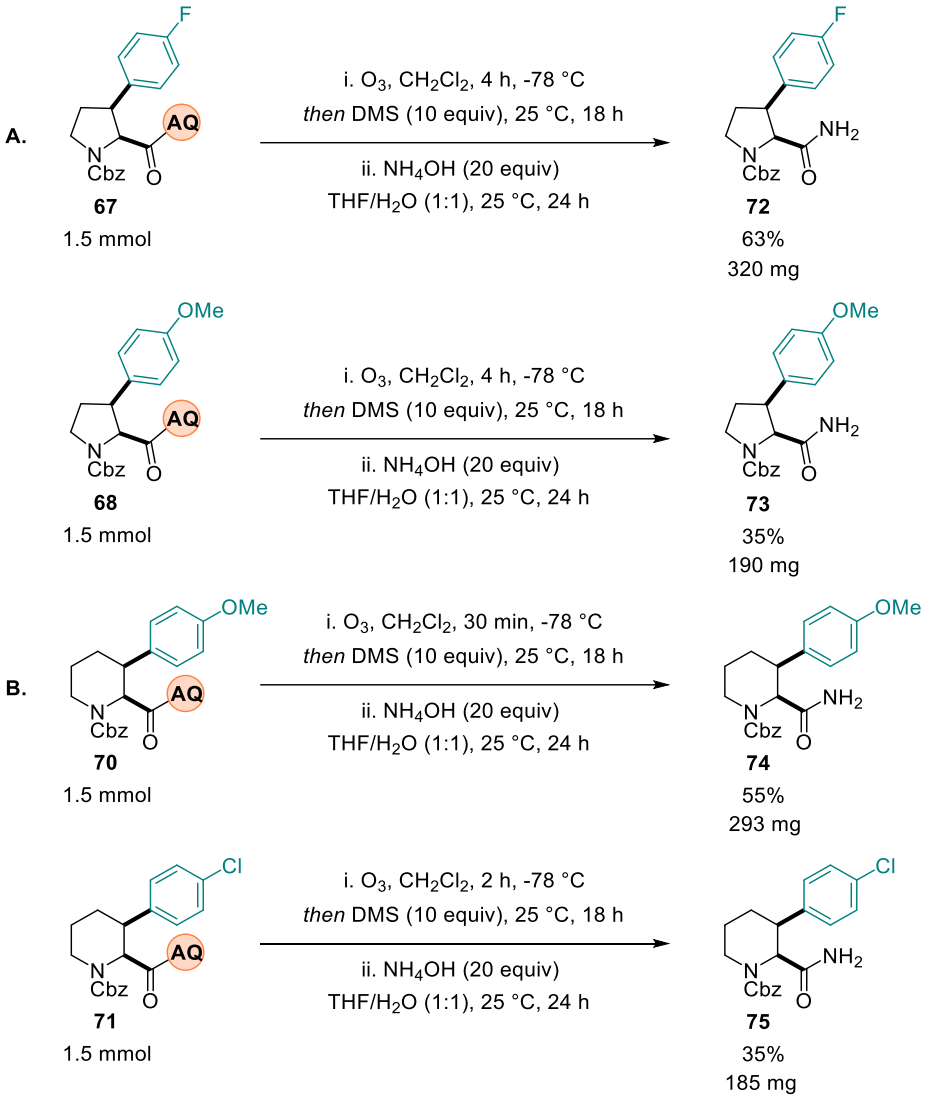


Scheme 2.21 Large scale C(3) arylation of piperidine with A. 4-iodoanisole and B. 1-chloro-4-iodobenzene. For B, 4 mmol scale reactions conducted 4 times in parallel, with crude mixtures combined and purified once.

2.2.4.2 Synthesis of Primary Amide Derivatives

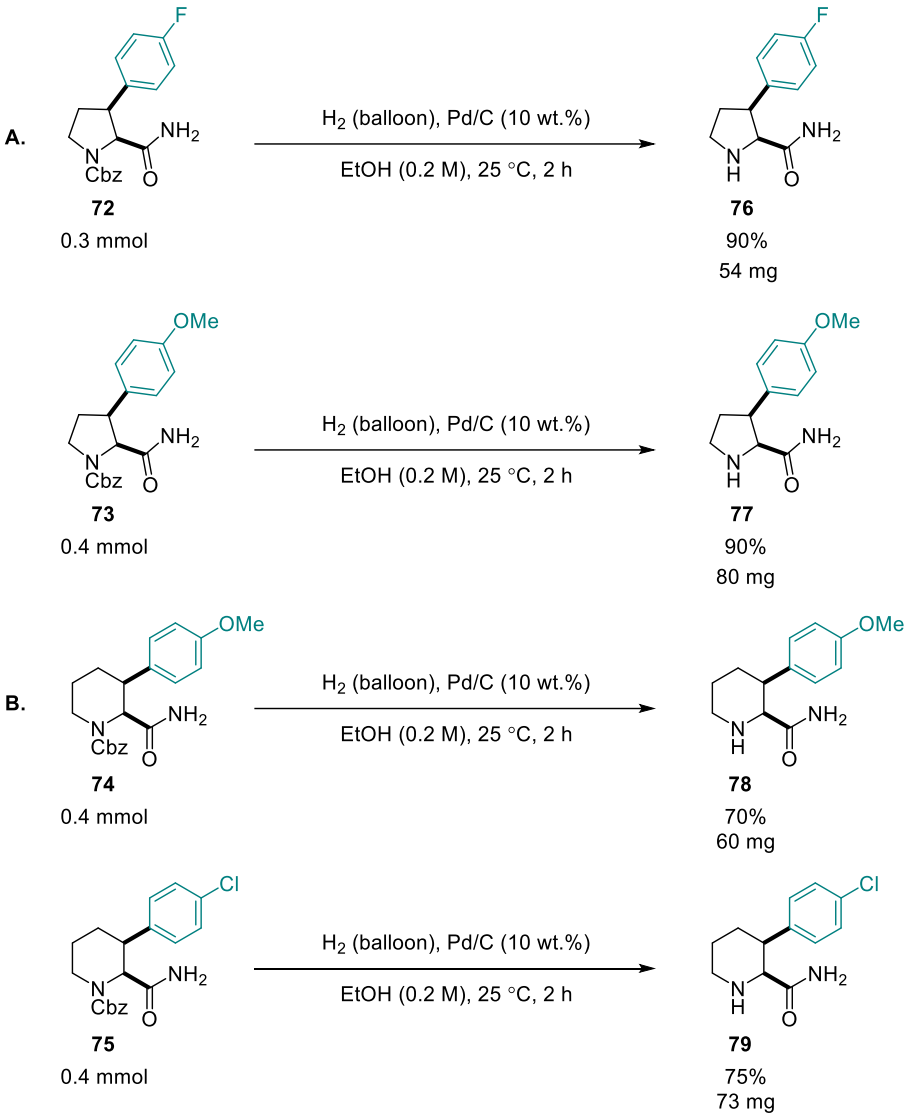
Adapting a procedure reported by Maulide,[225] ozonolytic cleavage of the directing auxiliary was performed on the arylated pyrrolidine substrates, followed by treatment with 28% aq. NH_4OH to unveil corresponding C(2) amides. By contrast to previous unsuccessful attempts which resulted in the electronic modulation of the directing group itself to enable its removal,[134,,226] 8-aminoquinoline could now be derivatised into a free amide in moderate to high yields (Scheme 2.22A). However, the desired products were UV inactive, with ninhydrin staining serving best for identification and purification purposes. *p*-Fluoroarylated **72** was obtained in an excellent 63% yield from **67**, whereas the *p*-methoxyarylated substrate **68** gave a lower 35% yield of corresponding amide **73**, as expected due to the potential for off-site oxidation of the electron-rich aryl substituent.

Similarly, the ozonolysis procedure was applied to previously synthesised piperidines to afford the corresponding C(2) amides (Scheme 2.22B). Faster oxidation was observed, with shorter reaction times needed to observe the colour change specific to the presence of excess ozone in solution. *p*-Chloroarylated **75** was obtained in 35% yield after a 2 h ozone treatment and subsequent work-up, whereas **70** underwent directing group oxidation in only 30 min, with subsequent procedures affording **74** in 55% yield. The faster rate of aminoquinoline oxidation in the latter case contributed to minimising associated degradation of the *p*-methoxyphenyl moiety, enabling a higher amide yield compared to the 5-membered analogue.



Scheme 2.22 Ozonolytic cleavage of aminoquinoline, followed by NH_4OH work-up to unveil free amides on C(3) functionalised pyrrolidines and piperidines.

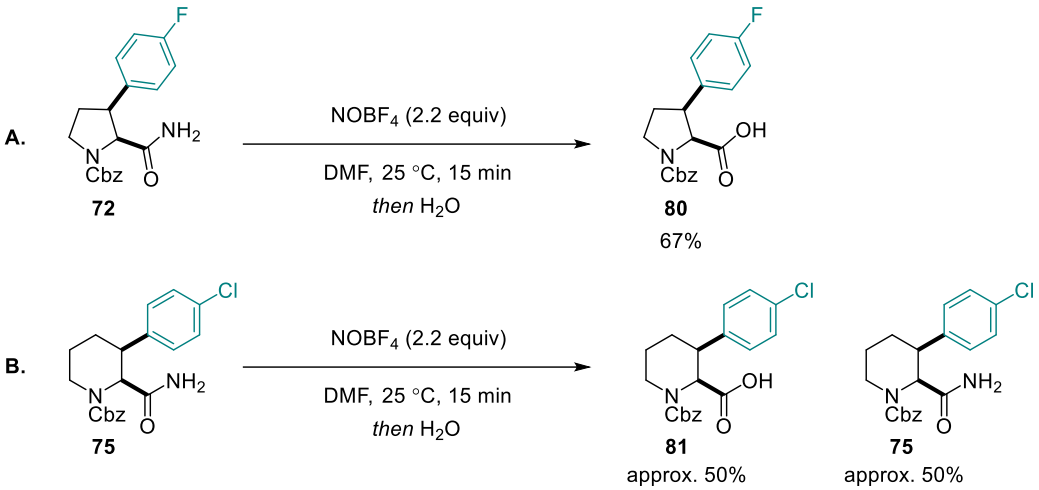
Subsequent Cbz deprotection was achieved by hydrogenation in excellent yields (>70%) to afford the desired pyrrolidine and piperidine amide fragments (**76-79**, Scheme 2.23).



Scheme 2.23 Cbz deprotection by hydrogenation to synthesise pyrrolidine amide fragments.

2.2.4.3 Synthesis of Carboxylic Acid Derivatives

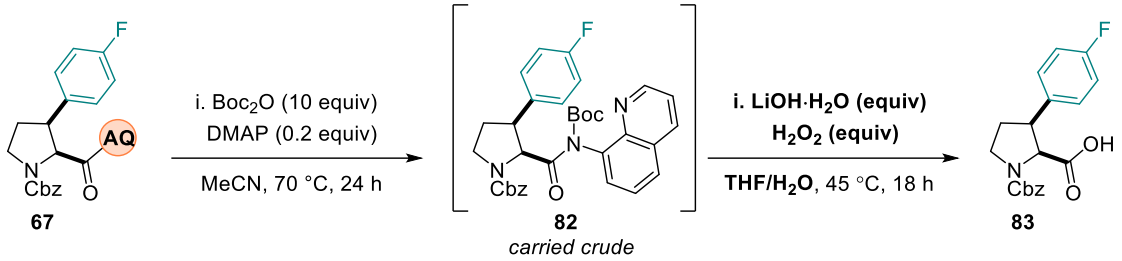
Two viable routes were identified for derivatisation of functionalised pyrrolidines to C(2) carboxylic acids. Firstly, amide **72** previously prepared could be subjected to $NOBF_4$ treatment, followed by hydrolysis of the resulting nitrosylated intermediate to generate corresponding acid **80** in 67% yield (34% from **72** over 3 steps, Scheme 2.24A). Unfortunately, applying the strategy to piperidine **75** resulted in an 1:1 molar mixture of carboxylic acid **81** and unreacted amide (Scheme 2.24B). Furthermore, desired **81** could not be separated by standard chromatographic techniques due to the similarity in polarity with the amide, as well as the lack of UV activity of both compounds. Resubjection to reaction conditions, even at 45 °C did not further increase the conversion. Presumably, the C(3) aryl exhibits increased steric hindrance upon the free amide in the 6-membered ring, preventing approach by the nitrosonium ion.



Scheme 2.24 Nitrosylation of amides, followed by hydrolysis to generate corresponding carboxylic acids.

Alternatively, activation of the aminoquinoline amide towards hydrolysis was attempted, as inspired by earlier group work on the 3,4-disubstitution pattern.[170] Despite this strategy proving unsuccessful in the past on the 2,3-disubstitution pattern,[226] recent reports have highlighted the need for large excesses of reagents for the activation of more sterically hindered amides.[146] Boc protection in the presence of excess Boc_2O was envisaged to generate a labile imide, which would undergo LiOOH-mediated hydrolysis in a similar manner to Evans auxiliary removal. [227,228] However, careful modulation of the reagent equivalents would in this case be required to achieve good conversion over the two steps.

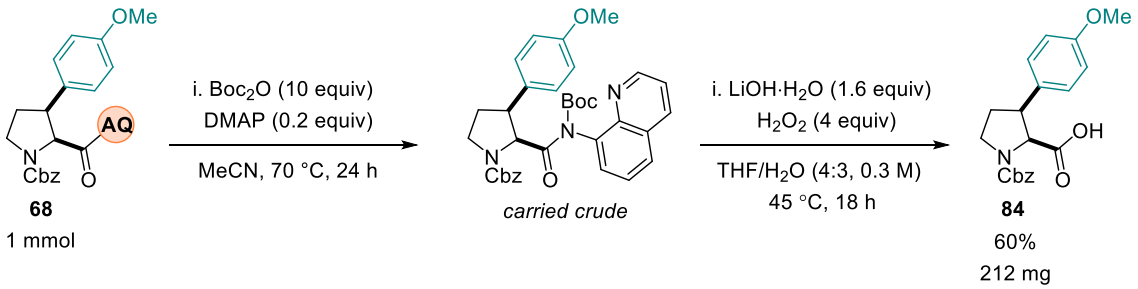
In the presence of 5 equivalents of Boc_2O, 5-membered **67** underwent amide Boc protection in less than 30%, as calculated by the decrease in the amide peak intensity in ^1H NMR. Conversely, treating **67** with 10 equivalents of Boc_2O and catalytic amounts of DMAP resulted in a satisfactory 75% conversion to **82** by NMR after 24 h at 70 °C. Special precautions were taken to avoid rapid generation of CO_2 in the sealed vial, such as allowing sufficient headspace and gentle heating to the target temperature on an oil bath. The Boc-protected intermediate was carried as crude to the next step, in which LiOOH was generated *in-situ* from LiOH and H_2O_2. Unfortunately, previously reported conditions on the pyrrolidine 3,4-disubstitution pattern were not compatible with this substrate,[170] leading to no detectable formation of acid **83** (Table 2.12, entry 1). Increasing the percentage of water in the solvent mixture promoted hydrolysis in 15% yield, most likely by enhancing LiOH solubility (entry 2). Opting for almost equal volumes of THF and water (4:3 ratio THF:H_2O) led to a marked increase in the yield of **83** to 40%. Whilst increasing the equivalents of LiOH was undesirable due to the potential for C(2) epimerisation, employing additional equivalents of H_2O_2 with respect to LiOH (in a 2.5:1 ratio, respectively) afforded **83** in 52% yield (entry 4). Maintaining the 2.5:1 H_2O_2:LiOH ratio, but decreasing the individual loadings in these reagents further improved the yield (entry 5). From here, changes in substrate concentration were detrimental to the yield, hence 0.3 M was judged as being most suitable.



Entry	$LiOH·H_2O$ equiv	H_2O_2 equiv	THF/H_2O (v/v, conc)	83 yield %
1	2	3	6:1, 0.3 M	0
2	2	3	7:3, 0.3 M	15
3	2	3	4:3, 0.3 M	40
4	2.4	6	4:3, 0.3 M	52
5	1.6	4	4:3, 0.3 M	60
6	1.6	4	4:3, 0.2 M	55
7	1.6	4	4:3, 0.4 M	50

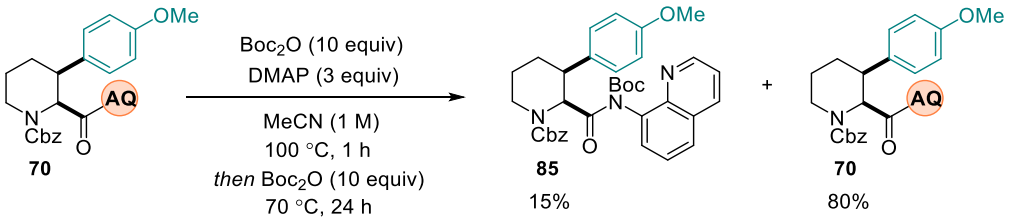
Table 2.12 Optimisation of the LiOOH mediated hydrolysis on the pyrrolidine substrate bearing a Boc-activated C(2) aminoquinoline amide. Reactions on 0.4 mmol. **83** isolated by acid-base workup involving $NaHCO_3$ and HCl.

The optimised procedure also afforded 60% yield of carboxylic acid **84** starting from *p*-methoxyphenyl substituted pyrrolidine **68**, this product being easily isolated by acid-base work-up (Scheme 2.25).



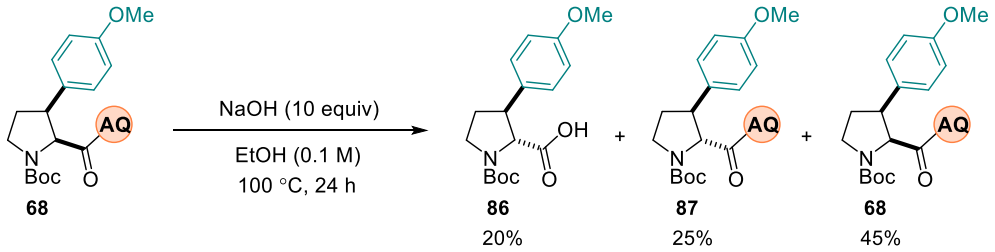
Scheme 2.25 Aminoquinoline deprotection on *p*-methoxyphenyl substituted pyrrolidine by an optimised amide activation/basic hydrolysis sequence.

Unfortunately, amide Boc protection on the 6-membered ring proved elusive, with only 15% conversion to **85** despite sequential addition of up to 20 equivalents of Boc_2O and implementation of harsher reaction conditions (Scheme 2.26).

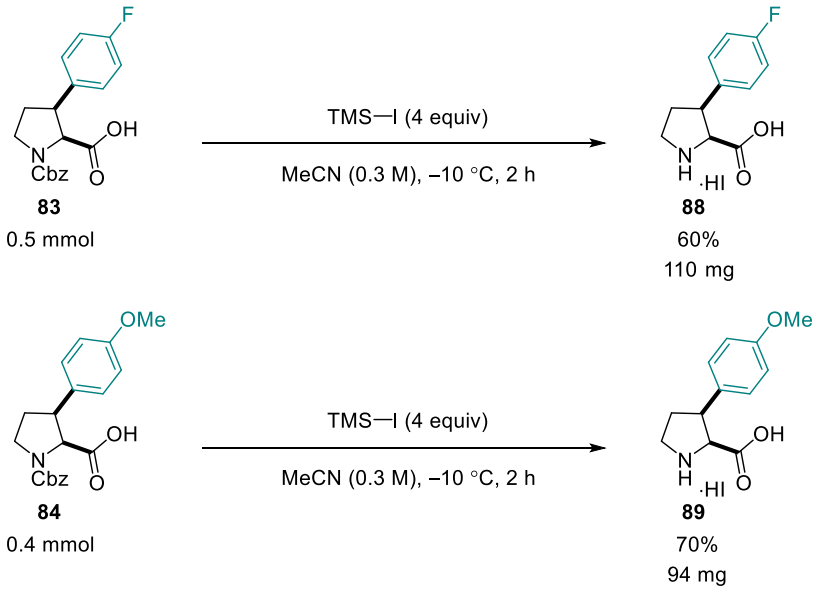


Scheme 2.26 Attempted aminoquinoline amide Boc protection on piperidine **70**. Yields determined by ^{1}H NMR using 1,3,5-trimethoxybenzene as internal standard.

Finally, hydrolysis in the presence of excess NaOH was attempted, to promote both C(2) epimerisation and amide hydrolysis for direct entry to *trans* carboxylic acids.[170] Whereas no reaction was observed on the 6-membered ring, with starting material quantitatively recovered, 5-membered **68** underwent partial epimerisation to **87** at 100 °C, with aminoquinoline amide hydrolysis to **86** occurring only to a small extent (20%, Scheme 2.27). Increasing the reaction time and/or NaOH loading was not found to improve this outcome, with the steric demands of the 2,3-disubtituted pyrrolidines and piperidines clearly impacting the ease of AQ auxiliary removal and the ability to synthesise useful quantities of **86**.



Scheme 2.27 Attempted NaOH mediated epimerisation-hydrolysis on pyrrolidine **68**. Isolated yield for **86**, after acid-base work-up. **87** and **68** yields determined by ^{1}H NMR using 1,3,5-trimethoxybenzene as internal standard.



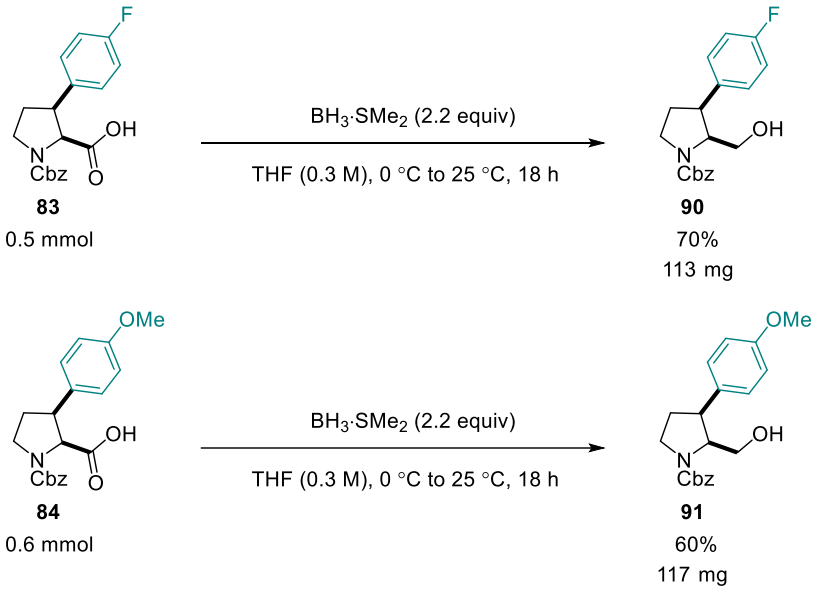
Scheme 2.28 Cbz deprotection in the presence of TMS iodide to synthesise 5-membered amino acid fragments.

Interestingly, the standard hydrogenation procedure for Cbz deprotection was completely inhibited in the presence of a carboxylic acid, presumably due to the coordinating and/or poisoning effect of this

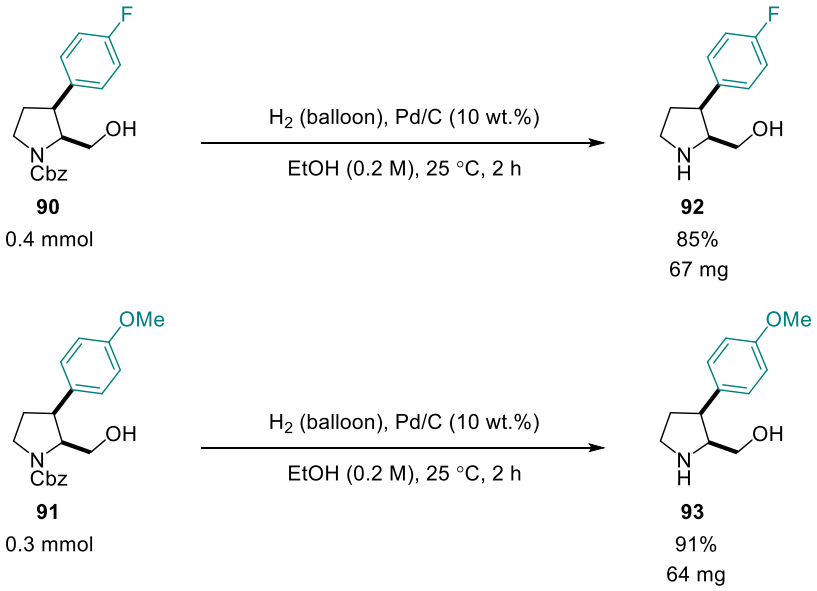
functionality on the Pd catalyst. Gratifyingly, an alternative procedure involving TMS iodide [229] afforded the desired aminoacids **88** and **89** as the hydroiodide salts from the corresponding pyrrolidines **83** and **84**, respectively (Scheme 2.28). Notably, exclusive selectivity for Cbz removal over demethylation was observed in the case of **84** under the selected temperature conditions (– 10 °C).

2.2.4.4 Synthesis of Alcohol Derivatives

To expand the diversity of polar binding groups in the fragment collection, carboxylic acids **83** and **84** were reduced to the corresponding alcohols **90** and **91**, repsectively using $BH_3 \cdot SMe_2$. Excellent yields >60% were observed, with no C(2) epimerisation under these mild conditions (Scheme 2.29). Hydrogenolysis of the Cbz group in the presence of Pd/C proceeded smoothly to afford the pyrrolidine amino alcohol fragments **92** and **93** in >60 mg quantities each (Scheme 2.30).



Scheme 2.29 $BH_3 \cdot SMe_2$ mediated reduction of carboxylic acids to corresponding alcohols.



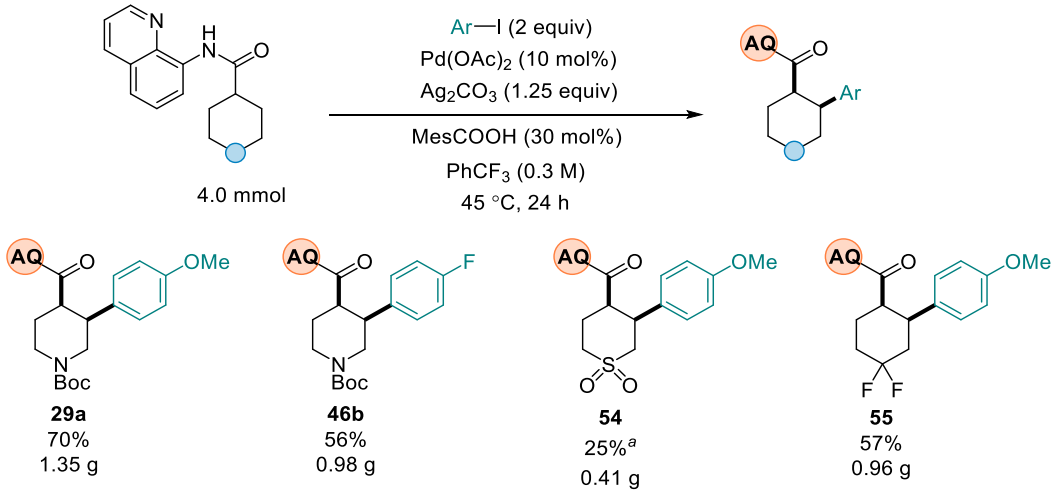
Scheme 2.30 Cbz removal to afford 5-membered amino alcohol fragments.

2.2.5 Aminoquinoline Deprotection on the 4,3-Disubstitution Pattern

2.2.5.1 Large Scale Arylation of 6-Membered Hetero- and Carbocycles

As previously demonstrated, the highly selective *cis* C(3) mono-functionalisation could be applied to a range of 6-membered saturated heterocycles bearing the C(4) aminoquinoline amide directing group. Aiming to generate larger quantities of arylated products for derivatisation into fragments with a range of polar functionalities, 4 mmol scale functionalisations were conducted on the *N*-Boc, SO_2 and CF_2 substrates in the presence of either 4-iodoanisole or 4-fluoroiodobenzene (Scheme 2.31). Good to excellent yields (25-70%) were observed, with gram-scale preparations of desired products **29a**, **46b**, **54** and **55** possible. Notably, reactions could now be transitioned to round bottom flasks of various sizes whilst maintaining reproducibility, as opposed to being limited by the sealed vial size in the case of high temperature reactions.

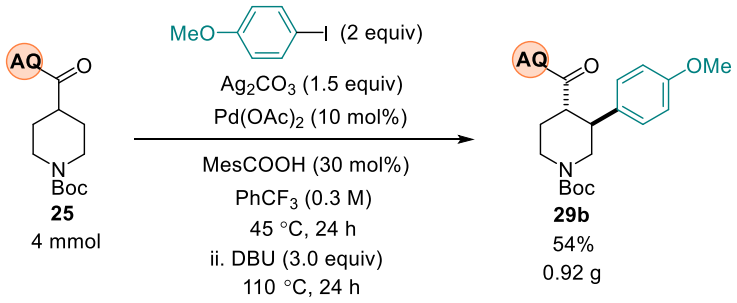
Challenges were observed in the separation between the *cis* **46b** and its corresponding *trans* diastereomer, with small percentages of the latter (5-7%) coeluting after a 5-10% Et_2O/CH_2Cl_2 gradient. A second purification using a gradient of 2-20% acetone in pentane resolved the issue – however, the initial Et_2O/CH_2Cl_2 gradient was still crucial for separating the mono-arylated products from small amounts (8-10%) of diarylated analogues. As reported in the heterocycle reaction scope, the cyclic sulfone exhibited a lower reactivity, prompting a raise in temperature from 45 °C to 75 °C, as well as in the equivalents of Ag_2CO_3 and coupling partner.



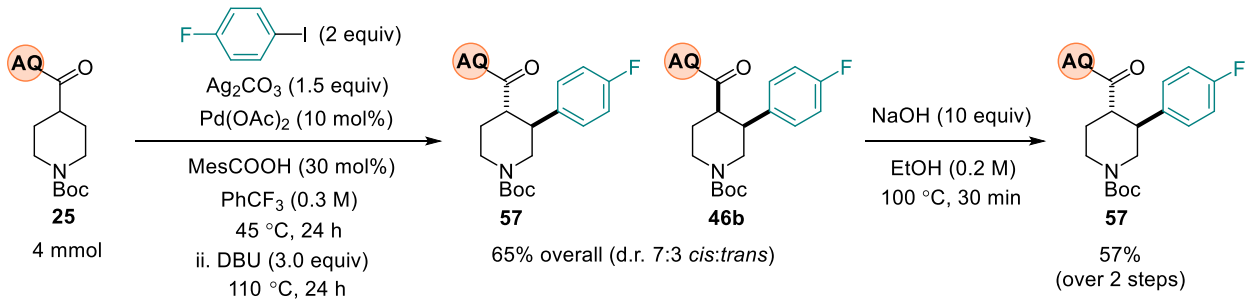
Scheme 2.31 Arylation of 6-membered saturated heterocycles on 4 mmol scale. Reactions conducted in a round bottom flask fitted with suba seal, under Ar atmosphere (balloon). [a] ArI (3.0 equiv), Ag_2CO_3 (2.0 equiv), 75 °C.

2.2.5.2 Accessing *trans* Diastereomers

With the recently developed one-pot arylation epimerisation, *trans* **29b** bearing a *p*-methoxyphenyl group at C(3) could be generated directly from amide **25** (Scheme 2.32). A 24 h reaction time at 110 °C after DBU addition was sufficient to promote ≥90% of the formed *cis* isomer to epimerise, affording **29b** in 54% yield on 4 mmol scale. Achieving a similarly high extent of epimerisation proved more challenging for the *p*-fluorophenyl substituted piperidine, with only 35% yield of *trans* **57** observed under the same one-pot conditions as before (Scheme 2.33). Increasing the epimerisation time to 48 h or 72 h did not further improve the outcome, hence the mixture of *trans* **57** and *cis* **46b** isomers, isolated in 65% combined yield, was further subjected to NaOH treatment at 100 °C. Any remaining *cis* isomer was converted to **57**, which was obtained in 57% yield over the two steps.

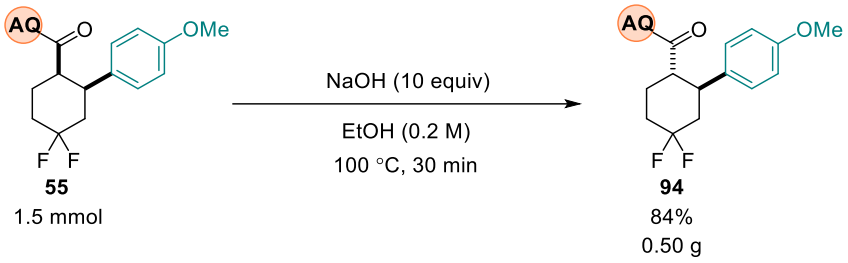


Scheme 2.32 Epimerisation of *p*-methoxyphenyl substituted piperidine.



Scheme 2.33 Epimerisation of *p*-fluorophenyl substituted piperidine.

Excess NaOH could also be employed to promote rapid epimerisation of any leftover mono-*cis* arylated product. Using 10 equivalents of NaOH, difluorocyclohexane **55** was epimerised in 84% yield after only 30 minutes, affording **94** in >95% purity without chromatographic purification (Scheme 2.34).

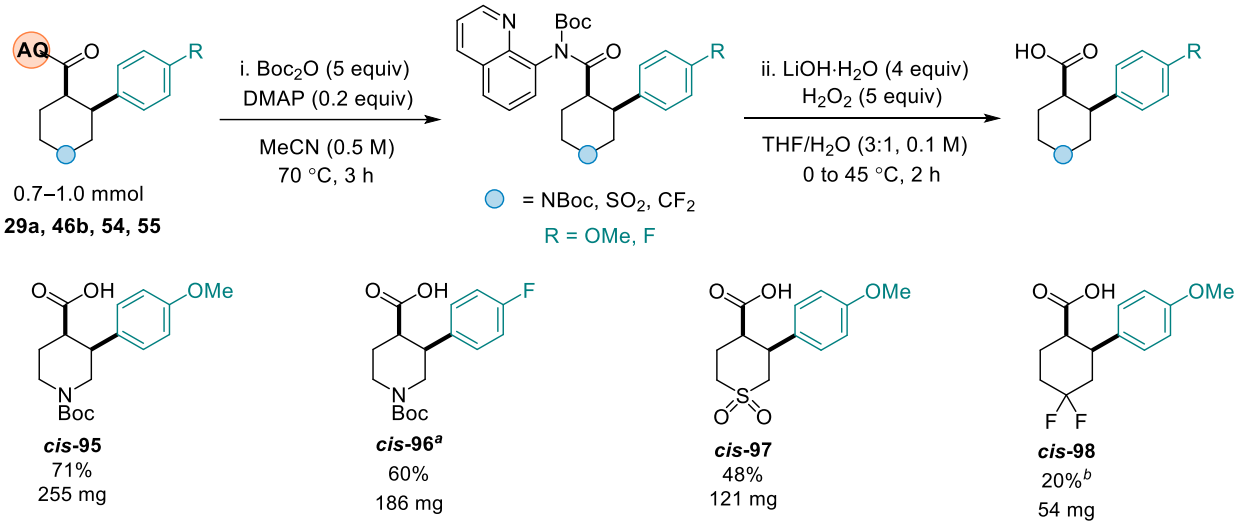


Scheme 2.34 NaOH mediated epimerisation of C(3) *p*-methoxyphenyl substituted difluorocyclohexane.

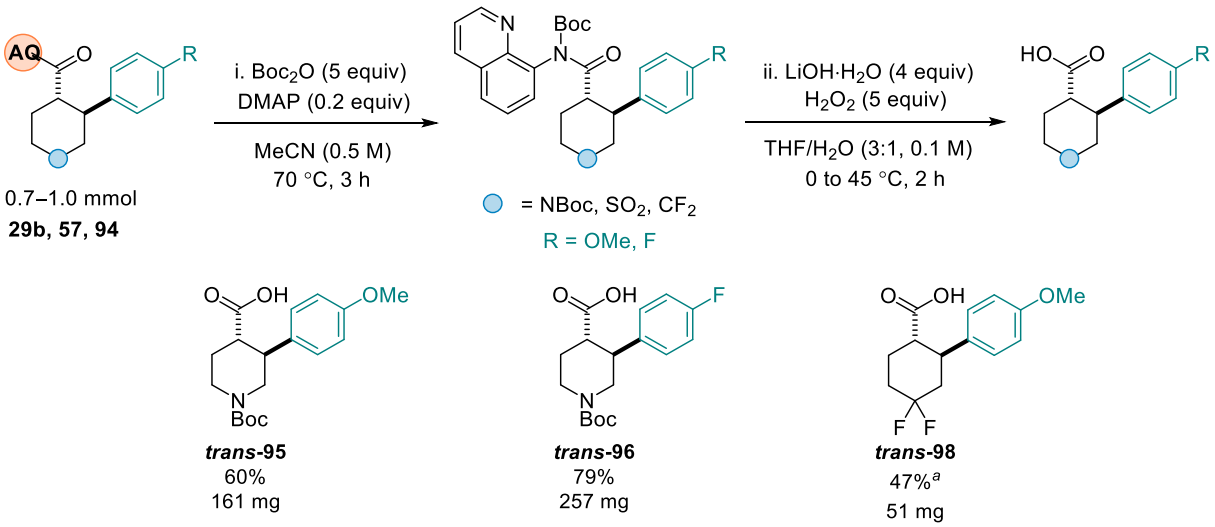
2.2.5.3 Synthesis of Carboxylic Acid Derivatives

The aminoquinoline directing group could be removed under basic hydrolytic conditions similar to those employed before in the deprotection of 2,3-disubstituted 5- and 6-membered *N*-heterocycles. In all cases, Boc protection of the aminoquinoline amide was performed in a sealed vial using 5 equivalents Boc_2O and substoichiometric DMAP, proceeding in high conversions (>90% by crude NMR). The crude residue was telescoped to the hydrolysis step in the presence of LiOOH formed *in situ* from $LiOH·H_2O$ and H_2O_2.

Fine-tuning the equivalents of base and peroxide, as well as increasing the ratio of THF enhanced solubility and reactivity, leading to up to 79% yield of carboxylic acids on 0.7–1.0 mmol scale. C(4) carboxylic acids were unveiled on the c*is*-configured arylated piperidine, 6-membered cyclic sulfone and difluorocyclohexane motifs without any epimerisation (***cis*-95**-***cis*-98**, Scheme 2.35).



Scheme 2.35 *cis* Carboxylic acids synthesised on a range of heterocycles by AQ activation and basic hydrolysis. [a]Synthesised by Dr. Natalia Larionova. [b]$LiOH·H_2O$ (8 equiv), H_2O_2 (10 equiv).

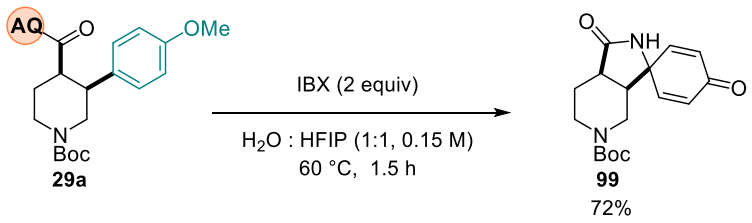


Scheme 2.36 *trans* Carboxylic acids synthesised on a range of heterocycles by AQ activation and basic hydrolysis. [a]$LiOH·H_2O$ (8 equiv), H_2O_2 (10 equiv).

Competing Boc deprotection of the activated amide was observed for the difluorocyclohexane substrate, with a significantly lower propensity towards AQ deprotection. Presumably, the *gem*-difluoro motif locks the 6-membered ring in a conformation that hinders nucleophilic attack on the C(4) carbonyl from a steric perspective. By doubling the equivalents of base and peroxide, ***cis*-98** was isolated in 20% yield, whereas *trans*-configured heterocycles generally afforded higher yields in the hydrolysis step (***trans*-95**, ***trans*-98**) compared to the opposite diastereomers (Scheme 2.36). Again, operating on difluorocyclohexane led to a 47% yield of the corresponding ***trans*-99** acid even in the presence of higher reagent loadings, though the overall reactivity was significantly higher than in the case of the *cis* analogue.

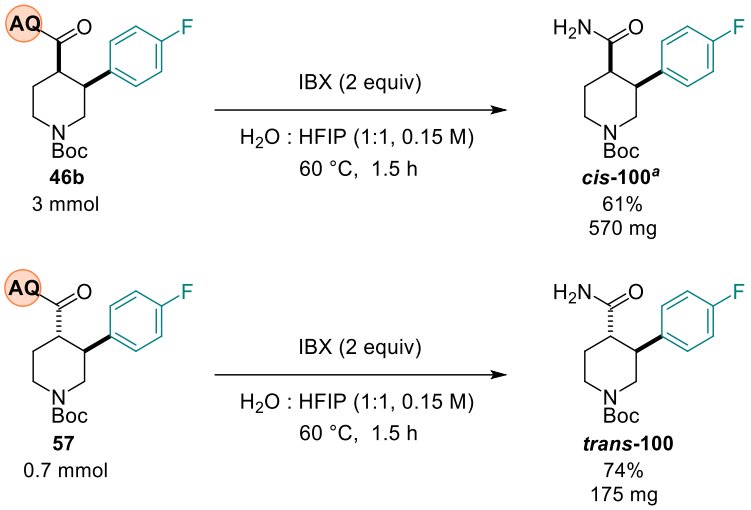
2.2.5.4 Synthesis of Amide and Nitrile Derivatives

To access primary amides, an IBX-mediated oxidative cleavage of the aminoquinoline group was investigated.[230,231] Unfortunately, the 3-methoxyphenyl piperidine substrate **29a** did not lead to the formation of the desired product, as identified by the absence of the -OMe singlet in the ^{1}H NMR of the crude reaction mixture. Instead, based on previous group observations and reports by Chen,[231,232] spirocyclic **99** was hypothesised to have formed (Scheme 2.37). This was suggested to arise *via* overoxidation of the electron-rich *p*-methoxyphenyl moiety, which undergoes cyclisation with the C(4) amide unveiled by initial aminoquinoline cleavage. A similar phenomenon was observed by Chen upon deprotection of an aminoquinoline amide bearing a β-*p*-methoxyphenyl substituent.[231] However, given the higher degree of rotational freedom of the linear alkyl substrate employed, the spirocycle formed only as a minor side-product in this case, besides the desired amide. Additionally, hypervalent iodine (III) species have been known to promote spirocyclisations between secondary amides and 4-methoxyaryl groups, the mechanism believed to occur *via* either a nitrenium or radical cation intermediate.[233] It was rationalised that a *trans* relative stereochemistry would disfavour communication between the 3,4 substituents, preventing cyclisation. Nevertheless, the absence of any primary amide and/or *p*-methoxyaryl groups was still evident in the case of the corresponding *trans*-configured substrate by NMR analysis of the crude reaction mixture.



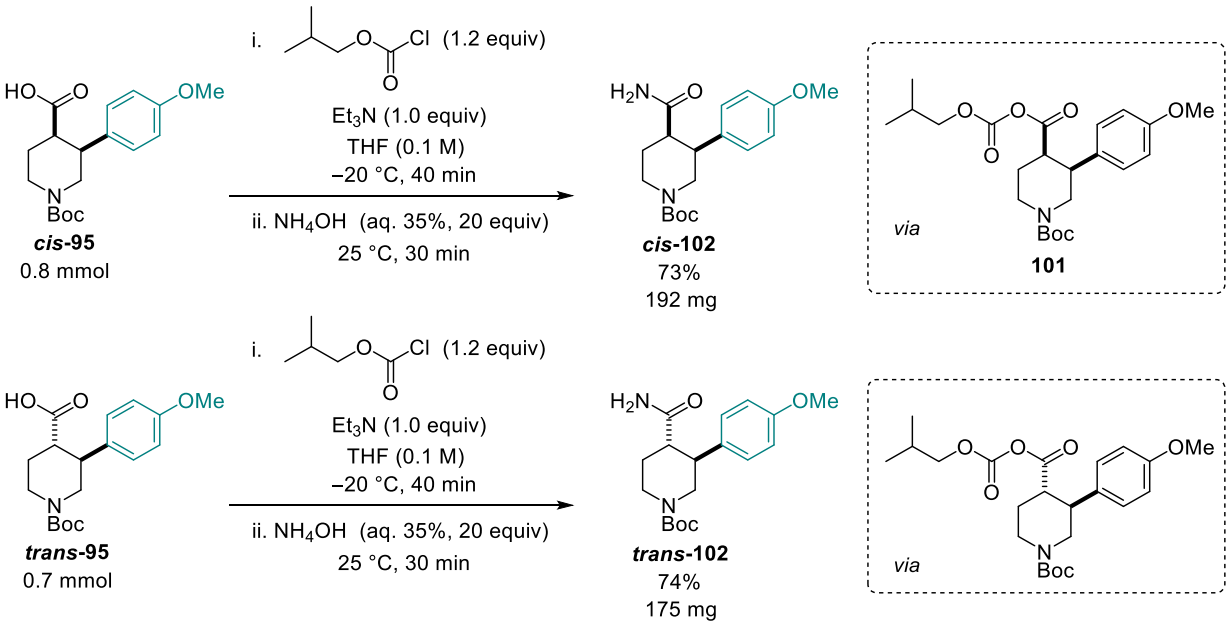
Scheme 2.37 Unsuccessful IBX-mediated AQ deprotection, resulting in formation of a spirocyclic lactam.

Pleasingly, the 3-fluorophenyl substrates exhibited the desired reactivity under the IBX conditions, with the aryl substituent now deactivated towards oxidation. Starting from *cis* or *trans*-arylated piperidines **46b** or **57**, amides ***cis*-100** and ***trans*-100** could be unveiled in 61 and 74% yields, respectively (Scheme 2.38).



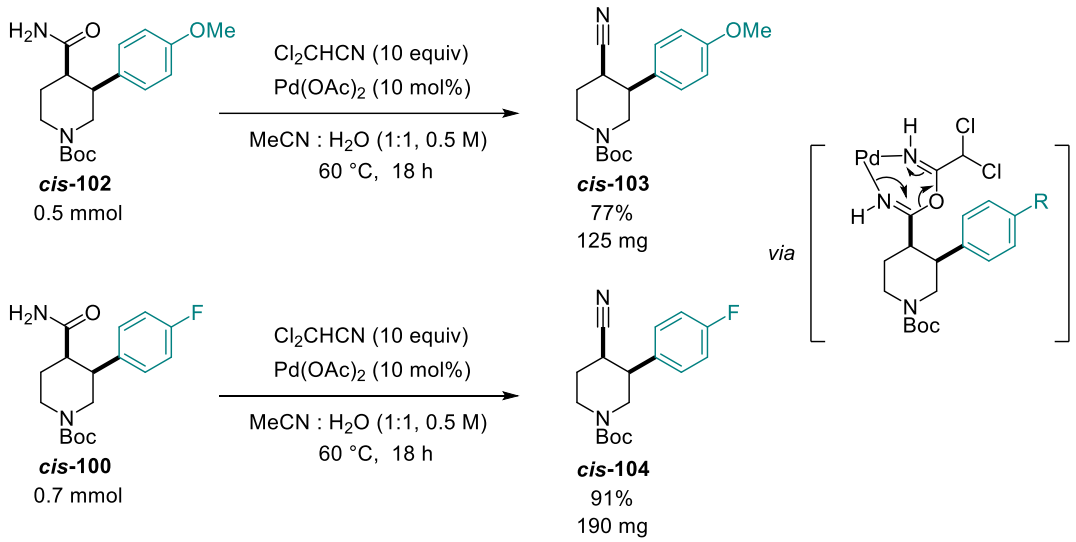
Scheme 2.38 IBX-mediated oxidative AQ removal in the presence of a C(3) *p*-fluorophenyl substituent. [a]Synthesised by Dr. Natalia Larionova.

For the unsuccessful 3-methoxyphenyl piperidine substrates, alternative pathways were studied, such as converting previously synthesised carboxylic acids to the corresponding amides. Inspired by a one-pot 2-step protocol reported by O'Brien and coworkers,[223] carboxylic acid ***cis*-95** was first subjected to condensation with isobutyl chloroformate to form carbonic anhydride **101**. Upon subsequent addition of aqueous ammonia, nucleophilic attack at the least hindered carbonyl centre was promoted in order to afford C(4) amide ***cis*-102** in an excellent 73% yield. (Scheme 2.39). Small percentages (<15%) of C(4) carboxylic acid and isobutyl carbamate side-products were observed, as result of alternative attack of ammonia at the carbonate C=O. Finally, the same one-pot conditions were successful in generating amide ***trans*-102** in 74% yield from ***trans*-95**.



Scheme 2.39 Alternative amide synthesis from carboxylic acids *via* nucleophilic attack of an asymmetric carbonic anhydride.

Adapting a procedure by Naka,[234] primary *cis*-amides were dehydrated to C(4) nitrile derivatives ***cis*-103** and ***cis*-104** (Scheme 2.40). Dichloroacetonitrile was a key reagent, since this selectively associates with the amide carbonyl in the presence of Pd catalyst and acts as water acceptor in an exothermic fashion, by generation of a thermodynamically more stable co-product. In contrast to Naka's original procedure in which $Pd(TFA)_2$ was empirically found to give the highest nitrile product yield, $Pd(OAc)_2$ performed best on the piperidine C(4) amide substrates, affording ***cis*-104** in >90% isolated yield from the corresponding C(4) piperidine amide ***cis*-100.** Overall this strategy benefits from operational simplicity and good functional group tolerance.

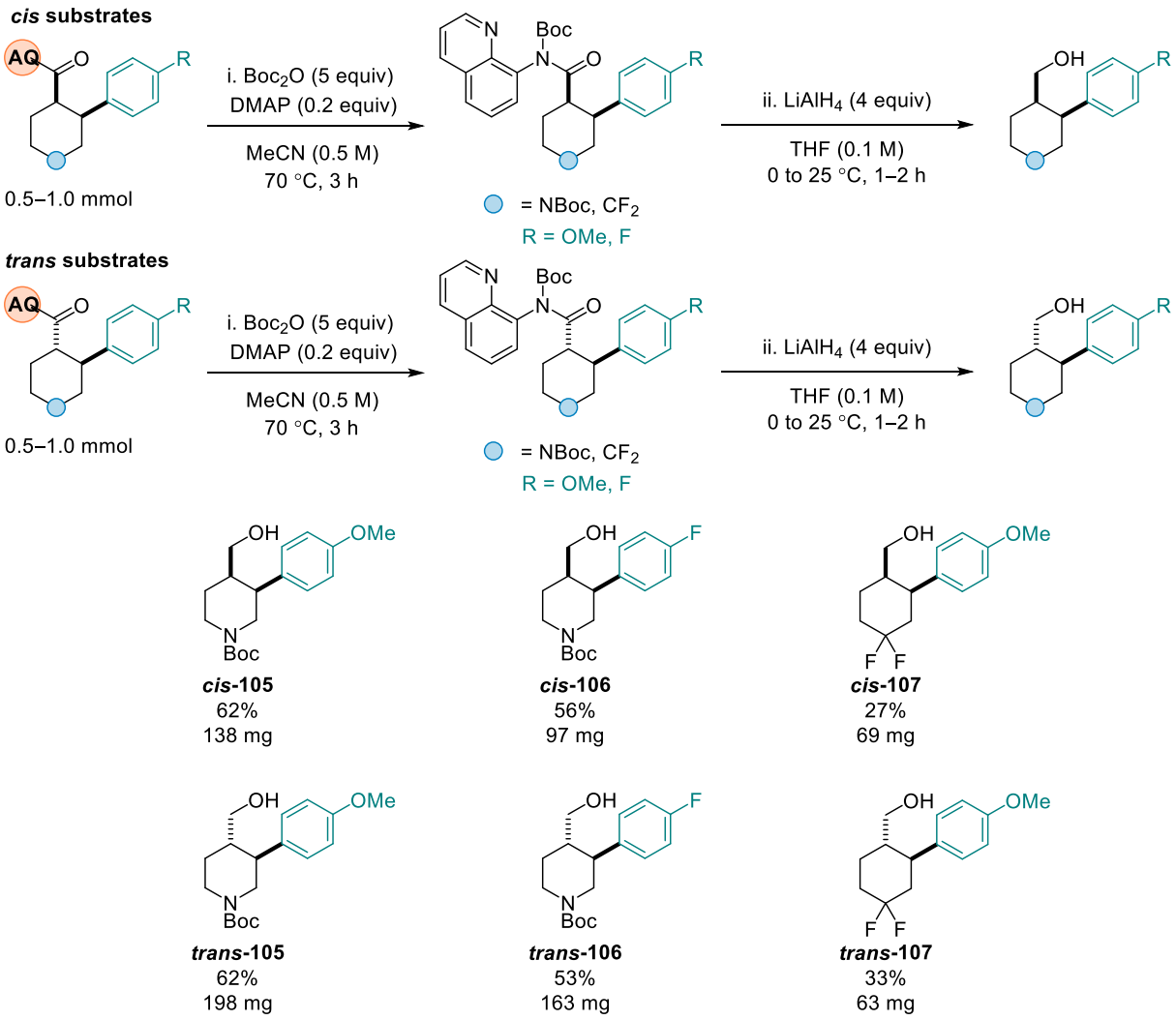


Scheme 2.40 Nitrile synthesis by Pd-catalysed amide dehydration using dichloroacetonitrile water acceptor.

2.2.5.5 Synthesis of Alcohol Derivatives

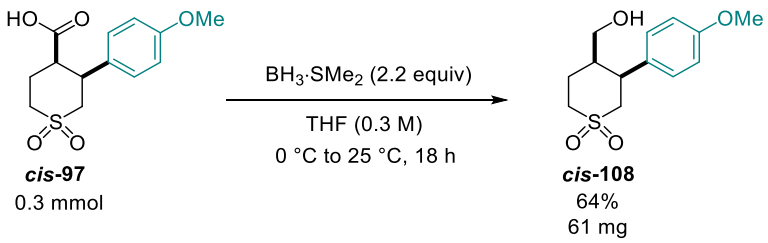
Similar to a group reported protocol on 3,4-disubstituted pyrrolidines, Boc-activated aminoquinoline amides could also be reduced with $LiAlH_4$ to unveil the alcohol functionality.

The 2-step telescoped procedure was employed, this time with nucleophilic attack by hydride in the last step, affording *cis* or *trans* primary alcohols in yields ranging from 27-62% (Scheme 2.41). Notably, no epimerisation of the *cis* configured substrates was seen. Again a lower reactivity was observed in the case of difluorocyclohexane, most likely based on similar steric grounds as before.



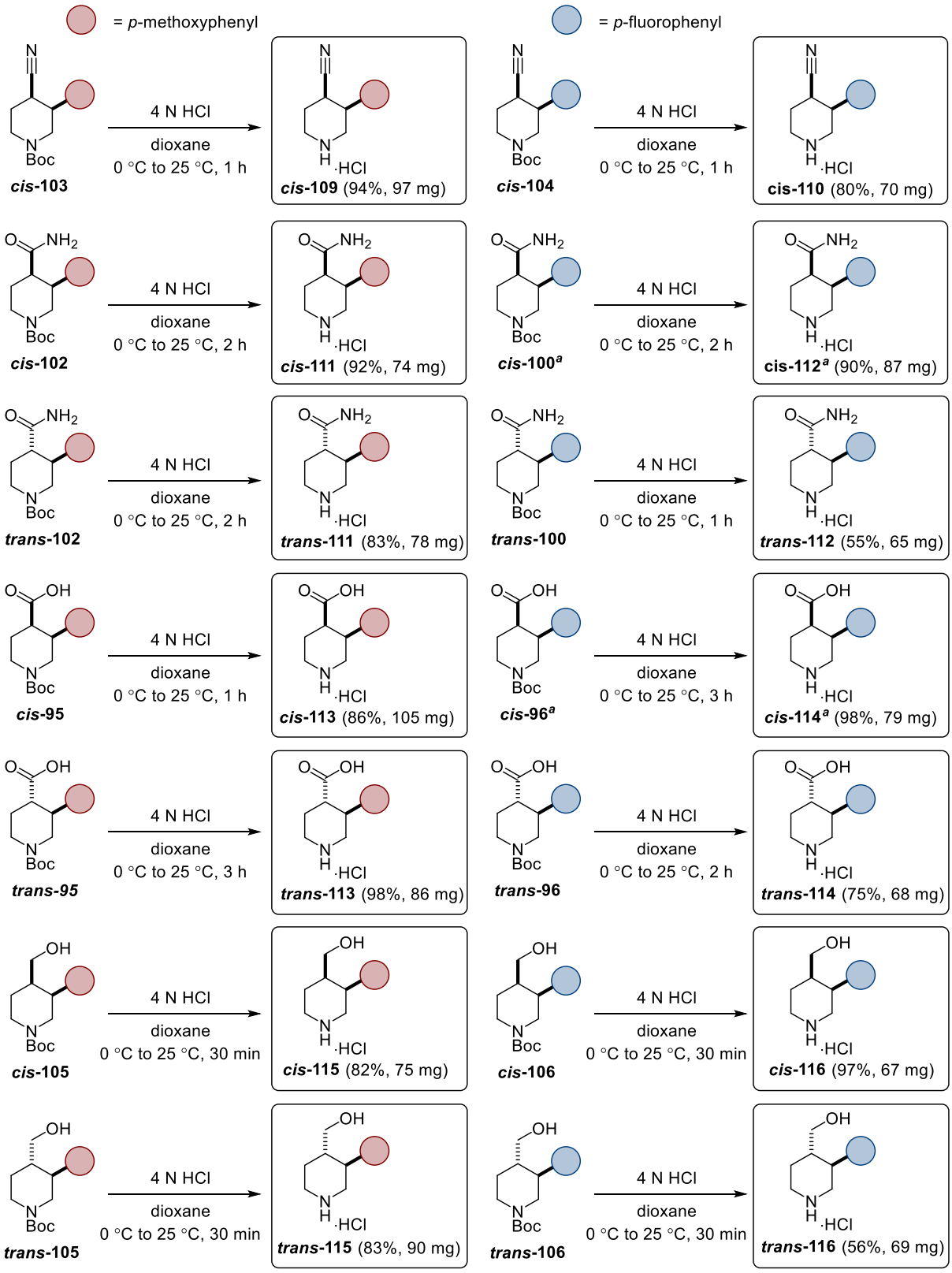
Scheme 2.41 A telescoped AQ activation/reductive removal for the synthesis of *cis* and *trans* alcohols.

Primary alcohols could alternatively be accessed by $BH_3{\cdot}SMe_2$ reduction of the corresponding carboxylic acids, providing opportunities to diversify the fragment library when functionalities sensitive to $LiAlH_4$ reduction may be present in the molecule. The 6-membered sulfone ***cis*-97** bearing a C(4) carboxylic acid could be easily reduced under these mild conditions to alcohol ***cis*-108** in 64% yield (Scheme 2.42).



Scheme 2.42 Alternative $BH_3{\cdot}SMe_2$ reduction of carboxylic acids to alcohols.

2.2.5.6 Boc Deprotection of Piperidine Derivatives



Scheme 2.43 Boc deprotection for generating 3,4-disubstituted piperidine fragments with a C(4) polar functionality. [a]Compounds synthesised by Dr. Natalia Larionova.

All the final piperidine fragments were obtained by Boc-deprotection using 4 N HCl in dioxane, being isolated as the corresponding hydrochloride salts (Scheme 2.43). Desired products were obtained in high yields, up to 98%. In all cases, the HCl salt completely precipitated out of solution within 1-3 h of stirring under ambient temperature conditions, with the resulting precipitates filtrated and washed with ice-cold Et_2O to afford pure fragments without the need for further purification. A slightly lower yield of only 35% was initially observed in the deprotection of ***trans*-106**. This was possibly due to protonation/alcohol elimination under the prolonged exposure to acidic conditions, hence reducing the reaction time from 2 h to 30 min increased the yield of ***trans*-116** to 55%. On the other hand amide ***trans*-112** exhibited hygroscopic properties during filtration, resulting in slow formation of small semi-liquid droplets that associated with or passed through the filter particles. This was suggested to have contributed to the slightly lower isolated yield of 55%.

2.2.6 Fragment Library Overview and Property Analysis

2.2.6.1 General Overview and Physicochemical Property Analysis

Using the C(sp^3)–H functionalisation strategy, a collection of 45 hetero- and carbocyclic fragments with a variety of disubstitution patterns and binding elements was assembled in collaboration with Dr. Daniele Antermite and Dr. Natalia Larionova.

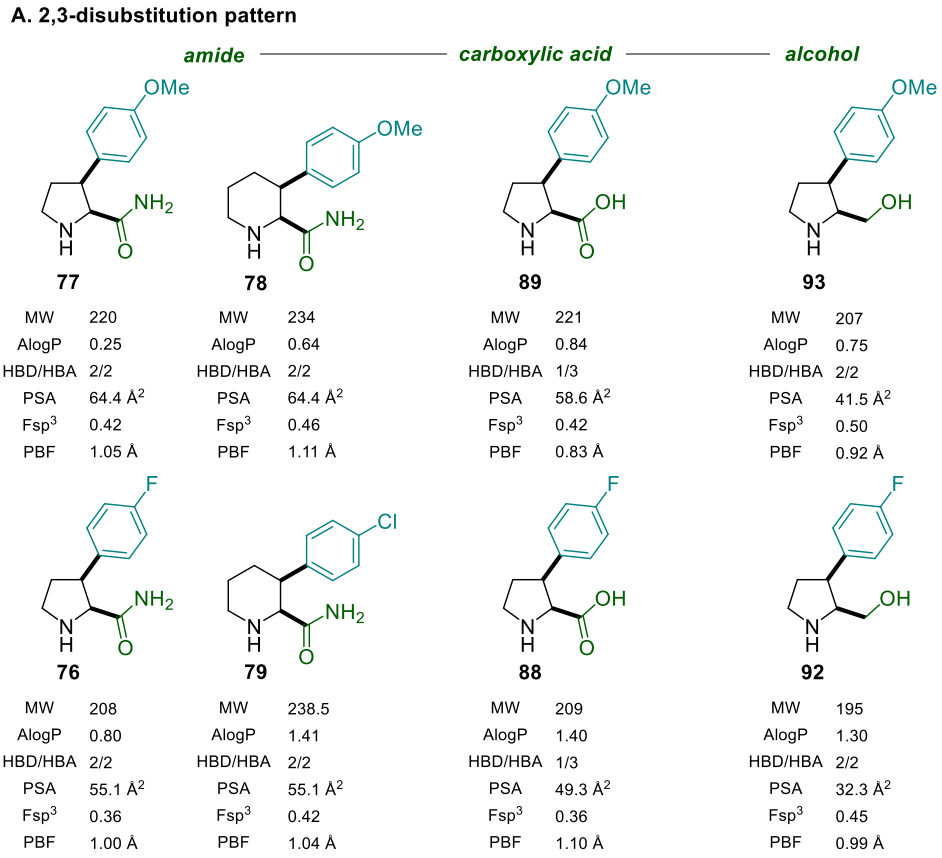


Figure 2.14 Overview of the synthesised fragments bearing the 2,3-disubstitution pattern. Salts omitted for the purpose of analysis.

The author of this thesis has synthesised a total of 26 fragments bearing either the 2,3- or the 4,3-disubstitution pattern, together with developing the C(3) arylation strategy with a C(4) directing group (Section 2.1), as well as all the divergent aminoquinoline deprotection strategies presented in Section 2.2. A set of 17 fragments bearing the 3,4-disubstitution pattern have been independently generated by Dr. Daniele Antermite, together with related arylation and directing group deprotection methodologies, and are summarised in Figure 2.15. Finally, two of the fragments on the 4,3-disubstitution pattern (***cis*-112** and ***cis*-114**) have been synthesised by Dr. Natalia Larionova using methodology developed by the author of this thesis and are acknowledged in Figure 2.16.

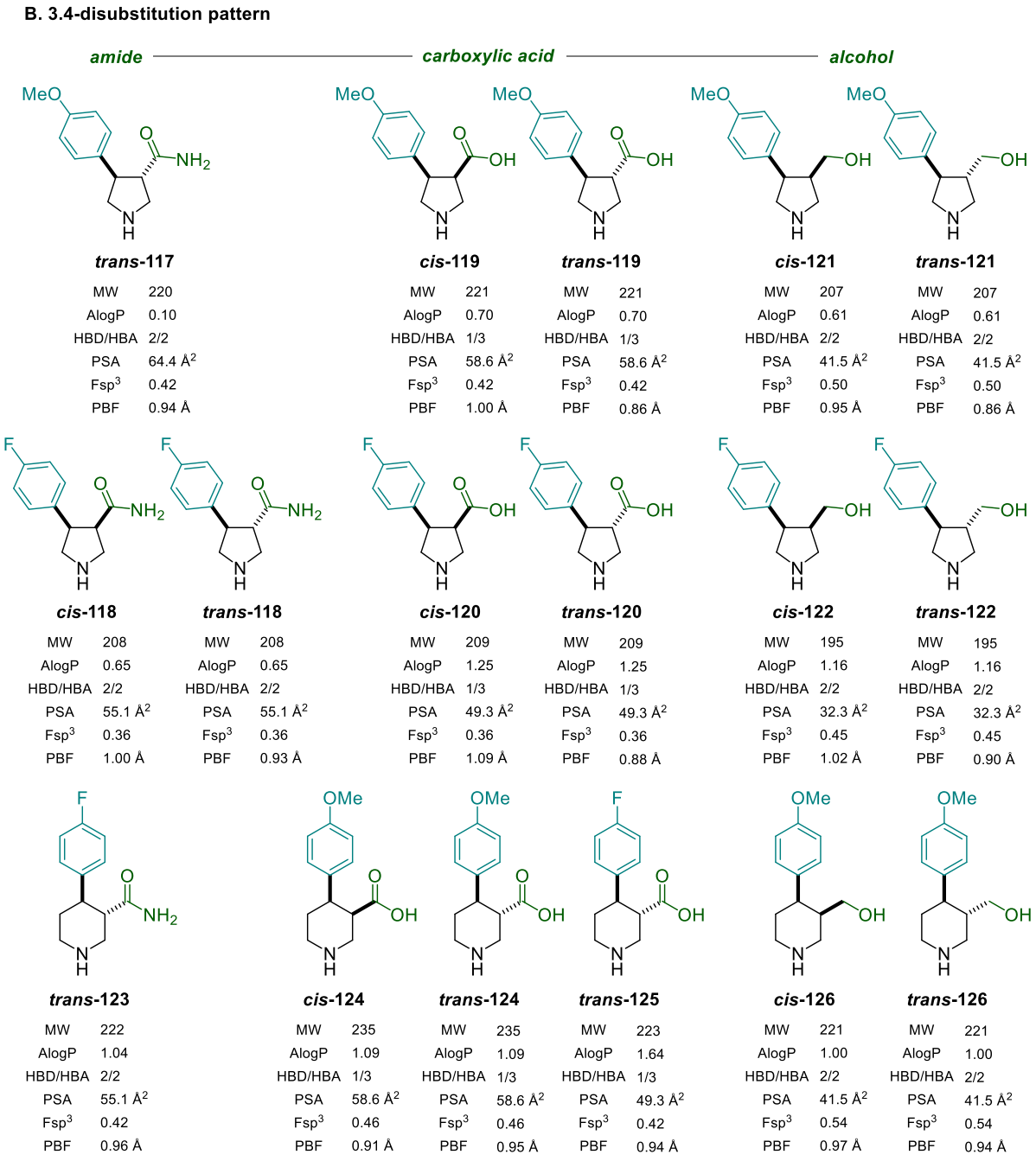
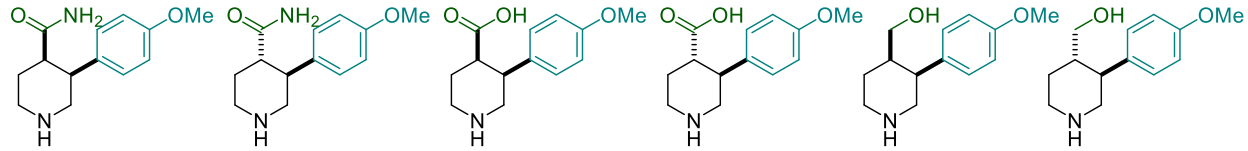


Figure 2.15 Overview of the synthesised fragments bearing the 3,4-disubstitution pattern. All compounds in this figure have been synthesised by Dr. Daniele Antermite. Salts omitted for the purpose of analysis.

C. 4.3-disubstitution pattern

amide — ***carboxylic acid*** — ***alcohol***



***cis*-111**

MW	234
AlogP	0.49
HBD/HB	2/2
PSA	64.4 Å^2
Fsp^3	0.46
PBF	0.97 Å

***trans*-111**

MW	234
AlogP	0.49
HBD/HBA	2/2
PSA	64.4 Å^2
Fsp^3	0.46
PBF	0.85 Å

***cis*-113**

MW	235
AlogP	1.09
HBD/HBA	1/3
PSA	58.6 Å^2
Fsp^3	0.46
PBF	0.89 Å

***trans*-113**

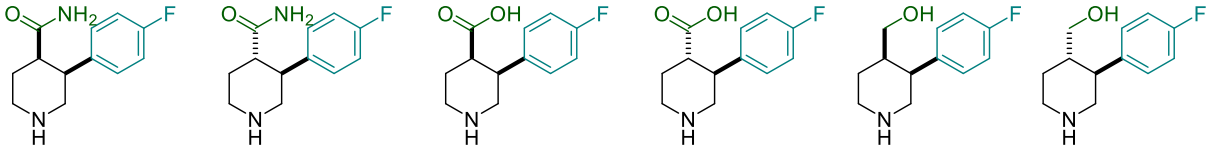
MW	235
AlogP	1.09
HBD/HBA	1/3
PSA	58.6 Å^2
Fsp^3	0.46
PBF	0.93 Å

***cis*-115**

MW	221
AlogP	1.00
HBD/HBA	2/2
PSA	41.5 Å^2
Fsp^3	0.54
PBF	0.94 Å

***trans*-115**

MW	221
AlogP	1.00
HBD/HBA	2/2
PSA	41.5 Å^2
Fsp^3	0.54
PBF	0.92 Å



***cis*-112**[a]

MW	222
AlogP	1.04
HBD/H	2/2
TPSA	55.1 Å^2
Fsp^3	0.42
PBF	1.00 Å

***trans*-112**

MW	222
AlogP	1.04
HBD/HBA	2/2
PSA	55.1 Å^2
Fsp^3	0.42
PBF	0.88 Å

***cis*-114**[a]

MW	223
AlogP	1.64
HBD/HBA	1/3
PSA	49.3 Å^2
Fsp^3	0.42
PBF	1.07 Å

***trans*-114**

MW	223
AlogP	1.64
HBD/HBA	1/3
PSA	49.3 Å^2
Fsp^3	0.42
PBF	0.89 Å

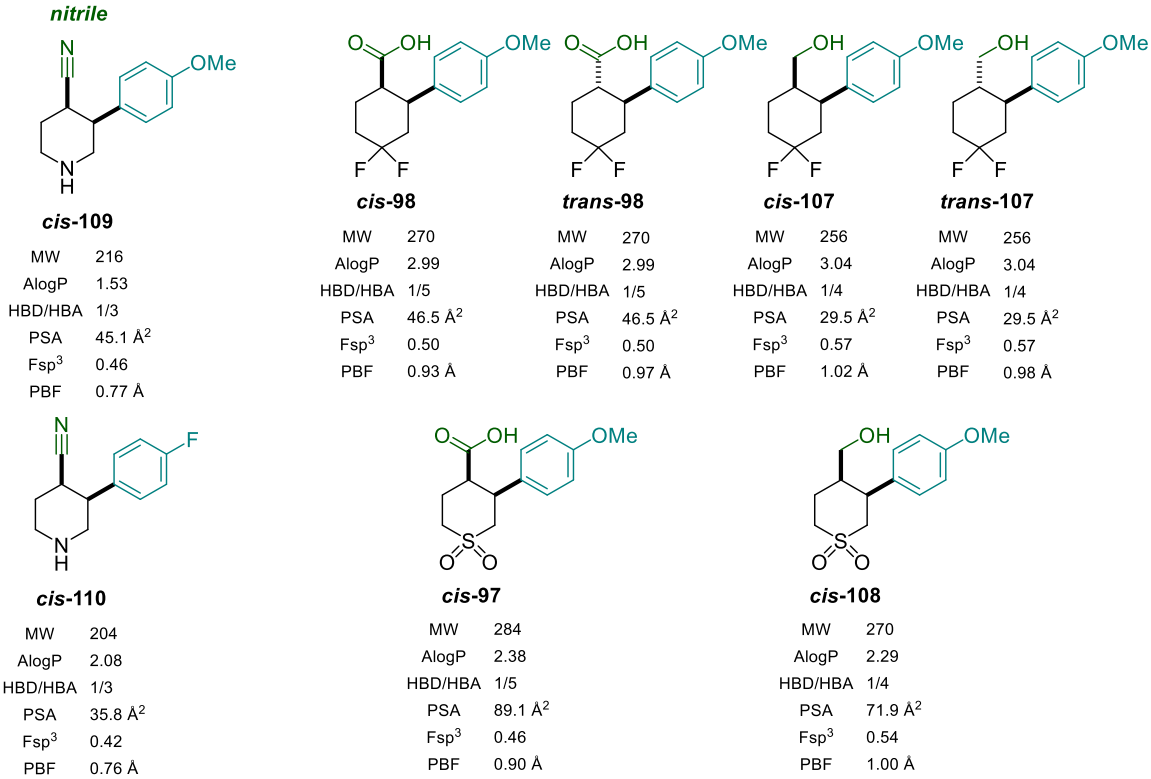
***cis*-116**

MW	209
AlogP	2.15
HBD/HBA	2/2
PSA	32.3 Å^2
Fsp^3	0.50
PBF	1.01 Å

***trans*-116**

MW	209
AlogP	2.15
HBD/HBA	2/2
PSA	32.3 Å^2
Fsp^3	0.50
PBF	0.95 Å

nitrile



***cis*-109**

MW	216
AlogP	1.53
HBD/HBA	1/3
PSA	45.1 Å^2
Fsp^3	0.46
PBF	0.77 Å

***cis*-98**

MW	270
AlogP	2.99
HBD/HBA	1/5
PSA	46.5 Å^2
Fsp^3	0.50
PBF	0.93 Å

***trans*-98**

MW	270
AlogP	2.99
HBD/HBA	1/5
PSA	46.5 Å^2
Fsp^3	0.50
PBF	0.97 Å

***cis*-107**

MW	256
AlogP	3.04
HBD/HBA	1/4
PSA	29.5 Å^2
Fsp^3	0.57
PBF	1.02 Å

***trans*-107**

MW	256
AlogP	3.04
HBD/HBA	1/4
PSA	29.5 Å^2
Fsp^3	0.57
PBF	0.98 Å

***cis*-110**

MW	204
AlogP	2.08
HBD/HBA	1/3
PSA	35.8 Å^2
Fsp^3	0.42
PBF	0.76 Å

***cis*-97**

MW	284
AlogP	2.38
HBD/HBA	1/5
PSA	89.1 Å^2
Fsp^3	0.46
PBF	0.90 Å

***cis*-108**

MW	270
AlogP	2.29
HBD/HBA	1/4
PSA	71.9 Å^2
Fsp^3	0.54
PBF	1.00 Å

Figure 2.16 Overview of the synthesised fragments bearing the 4,3-disubstitution pattern.[a]Compounds synthesised by Dr. Natalia Larionova. Salts omitted for the purpose of analysis.

Overall, the collection consists of: (i) 8 pyrrolidine and piperidine fragments bearing the 2,3-disubstitution pattern (Figure 2.14) (ii) 17 pyrrolidine and piperidine fragments bearing the 3,4-disubstitution pattern (Figure 2.15) and (iii) 20 piperidine, 1,1-difluorocyclohexane and tetrahydrothiopyran dioxide fragments bearing the 4,3-disubstitution pattern (Figure 2.16). For the purposes of this analysis, piperidine and pyrrolidine fragments were stripped from their corresponding salt forms.

Key physicochemical descriptors are summarised for each compound and were calculated using SwissADME, a freely available web tool for the analysis of small molecule medicinal chemistry parameters.[235] AlogP was computed using the atomistic method by Wildman and Crippen,[236] whereas the hydrogen bond donor/acceptors were calculated at physiological pH = 7.4, with halogens counted as hydrogen bond acceptors. Also, amide C–N bonds were excluded from the rotatable bond count (NRotB). Compliancy with the 'Rule of 3' was observed in all cases, with alcohols fitting the 'Rule of 2' specifications. The average physicochemical properties across the entire fragment library are also situated well within the Rule of 3 space spanned by the first radar plot in Figure 2.17. Notably, properties such as AlogP, PSA and HBA/HBD are within the 'Rule of 2' space, with a generally low overall lipophilicity observed. To study the potential physicochemical property inflation upon elaboration, the fragments were virtually decorated with up to two substituents using the online Lead-Likeness and Molecular Analysis (LLAMA) platform.[237] This operation implied the addition of a series of medicinally relevant capping groups to common exit vectors such as free carboxylic acids, amides and aryl halides. With the capping groups chosen from the default set of 44 LLAMA reagents (see Appendix 2), their installation followed the allowed reactivity dictated by a predefined LLAMA set of chemical transformations such as cross-coupling, amide formation, acylation and alcohol functionalisation. In this way, a total of 8625 virtual compounds were generated and their average physicochemical properties analysed against the Rule of 5 space in the second radar plot in Figure 2.17.

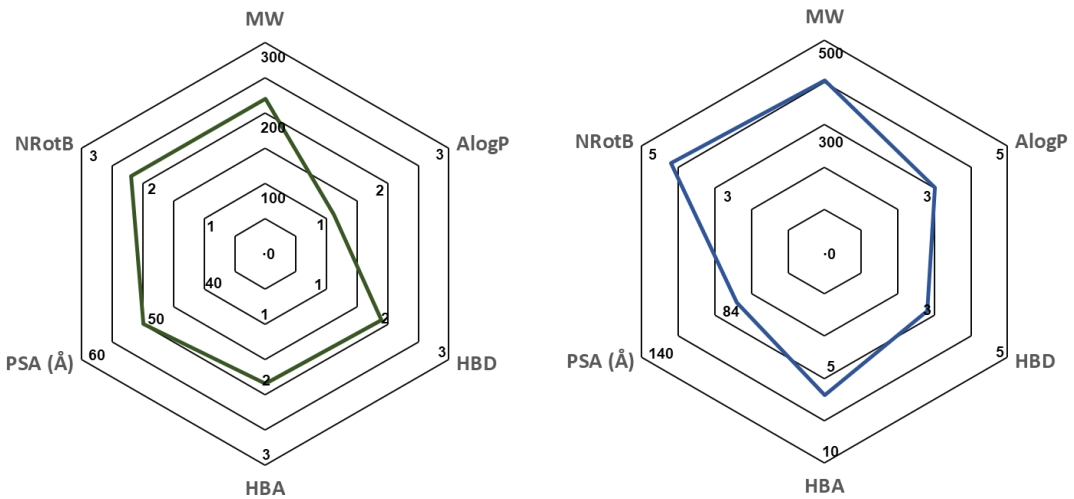


Figure 2.17 Left: Average physicochemical properties across the fragment library, represented in relationship to the upper limits of the Rule of 3. Right: Average physicochemical properties of the virtually decorated fragments represented in relationship to the upper limits of Lipinski's Rule of 5.

Gratifyingly, even with 7502 twice decorated fragments present, excellent Rule of 5 compliancy was seen, with PSA, HBD and AlogP still within the lead-like space. Despite relatively high increases in the average MW (from 220 to 400) and lipopihilicity (from 1.1 to 3 A logP), these stay within desirable limits for drug-like space and would allow room for further structural fine-tuning in a drug discovery program. Moreover, the moderate lipophilicity would likely corelate with a good balance between solubility and permeability, the relatively low AlogP at fragment stage being key to this outcome. The synthesised fragment library would therefore present a sensible starting point for the elaboration of leads and candidates with advantageous physicochemical profiles.

2.2.6.2 Shape Analysis

LLAMA also supports the calculation of the principal moments of inertia of a molecule along the x, y and z axis as a measure of assessing 3-dimensionality. To allow construction of a 2D graph, the values are normalised to NPR1 (= inertia(x)/inertia(z)) and NPR2 (= inertia(y)/inertia(z)). The representation of NPR1 against NPR2 can be translated to a triangular PMI plot, in which the molecular shapes are distributed with respect to a linear, spherical and disc-like reference points represented by acetylene, adamantane and benzene, respectively. Although there is no clear relationship between the location of a compound on the PMI plot and the likelihood of success in a drug discovery programme, the ability to explore uncharted areas such as those away from the disc-rod axis would arguably constitute an advantage in tackling current challenging targets. The synthesised fragments were therefore analysed based on both their individual shapes, as well as for their ability to serve as starting points for elaboration of highly 3-dimensional leads through the generation of virtually decorated libraries.

By contrast to typical screening libraries in which the majority of compounds reside close to the disc-rod axis, all the 45 synthesised fragment were found to be positioned away from this axis, spreading towards the sphere-like apex (Figure 2.18). Interestingly, *cis*-substituted compounds tended to be further away from the disc-rod axis compared to the corresponding *trans* analogues. For instance, 4,3-*cis*-disubstituted piperidine ***cis*-111** is one of the fragments with the highest overall 3D character, whereas its *trans* epimer ***trans*-111** lies closest to the disc-rod axis out of the whole fragment library. Surprisingly, it was found that even enantiomers of the same molecule (**(*S,R*)-111** and **(*R,S*)-111**) do not have the same NPR coordinates – this could be due to different minimum energy conformers identified by LLAMA for each enantiomer, based on variations in computed intramolecular H-bonding interactions. However, the mean PMI coordinates for the whole library (represented by the red cross) was not found to vary significantly when only one set of enantiomers (e.g. (*S,R*) instead of (*R,S*)) were considered.

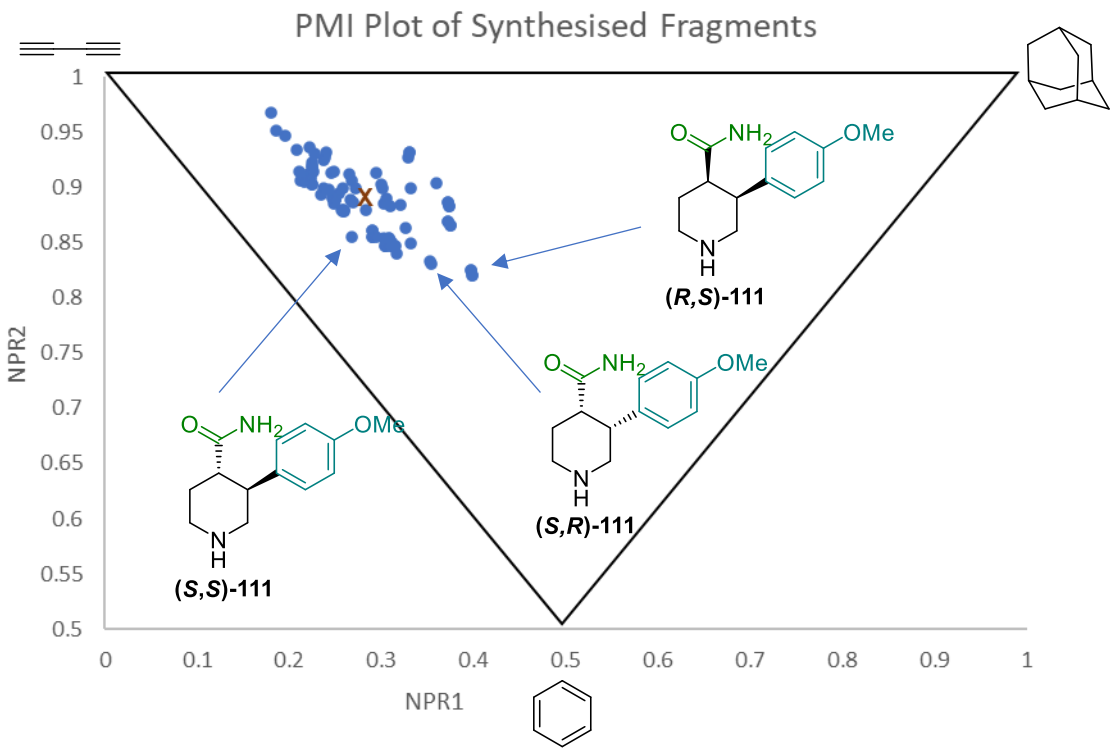


Figure 2.18 PMI plot of the 45 synthesised fragments. Mean PMI coordinates: NPR1 = 0.284 and NPR2 = 0.887 (denoted by X).

On the other hand, the plane of best fit (PBF) has been argued to provide a more accurate representation of 3-dimensionality, with calculations also enabled by LLAMA.[222,238] This involves the theoretical fitting of the molecule to a plane, followed by the determination of the distance from this to the furthest out-of-plane atom. To assess the correlation between the PMI and the PBF values, the previous datapoints of the PMI plot were colour graded from yellow to red according to the amplitude of the computed PBF, with red corresponding to the highest PBF values and, implicitly, to structures envisioned as most 3-dimensional (Figure 2.19). Surprisingly, no clear association was seen between the two, as compounds with PBF > 1 were scattered over various regions of the PMI plot, with more than a quarter accumulated close to the disc-rod axis. Although not focused on 3-dimensionality only as a measure of fragment quality, the outcome prompts the use of a more general shape assessment criteria, stating that a combination of average NPR1 + NPR2 > 1.07 and PBF > 0.6 denotes a high 3D character.[238] With the mean NPR1 + NPR2 = 1.17 and the average PBF = 0.95 across the whole library, a high 3-dimensional character can therefore be inferred. However, the ability to generate topologically diverse leads from these fragments would be of high value in tuning the complementarity of the ligand to the target and will be later assessed in this section.

The effect of substitution pattern upon PMI coordinates was also studied (Figure 2.20). Interestingly, each substitution pattern appeared to swath different areas of chemical space, with a progressive distancing from the rod-sphere axis going from 2,3-disubstitution to 3,4- and 4,3-disubstitutions. This implies the possibility of modulating the molecular shape to be more rod-sphere-like or disc-like depending on the substitution pattern..

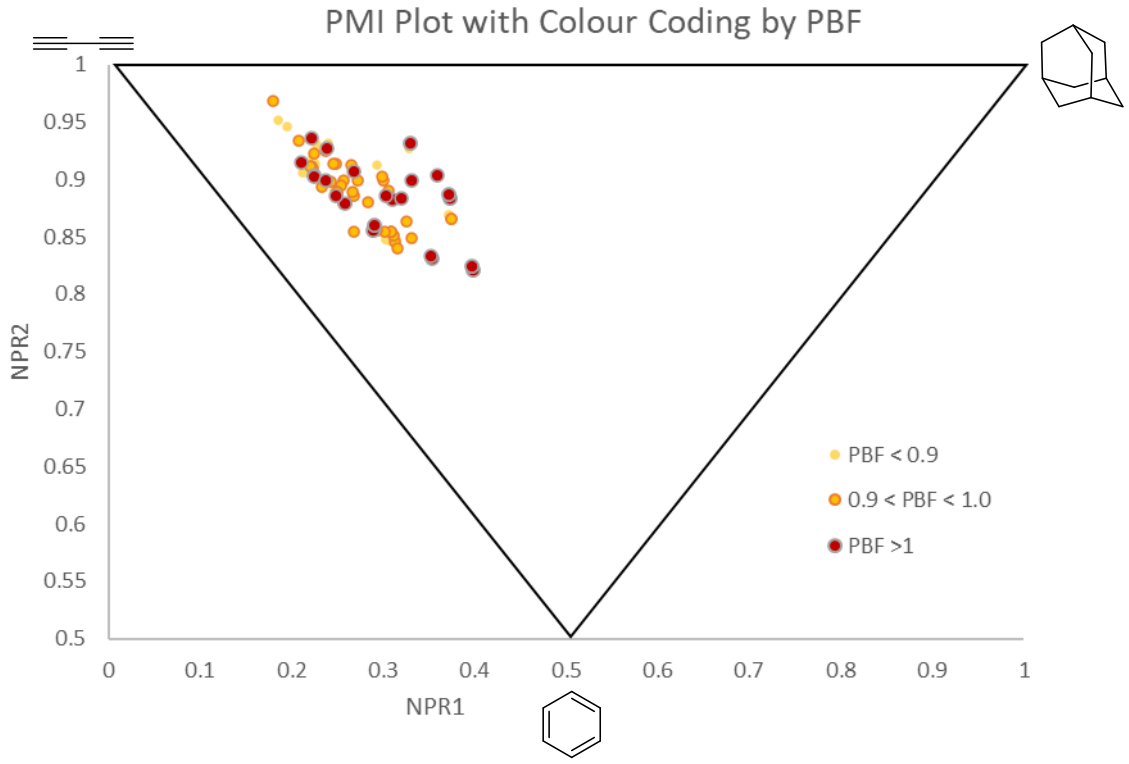


Figure 2.19 PMI plot of the 45 synthesised fragments, with colour coding by individually calculated PBF values.

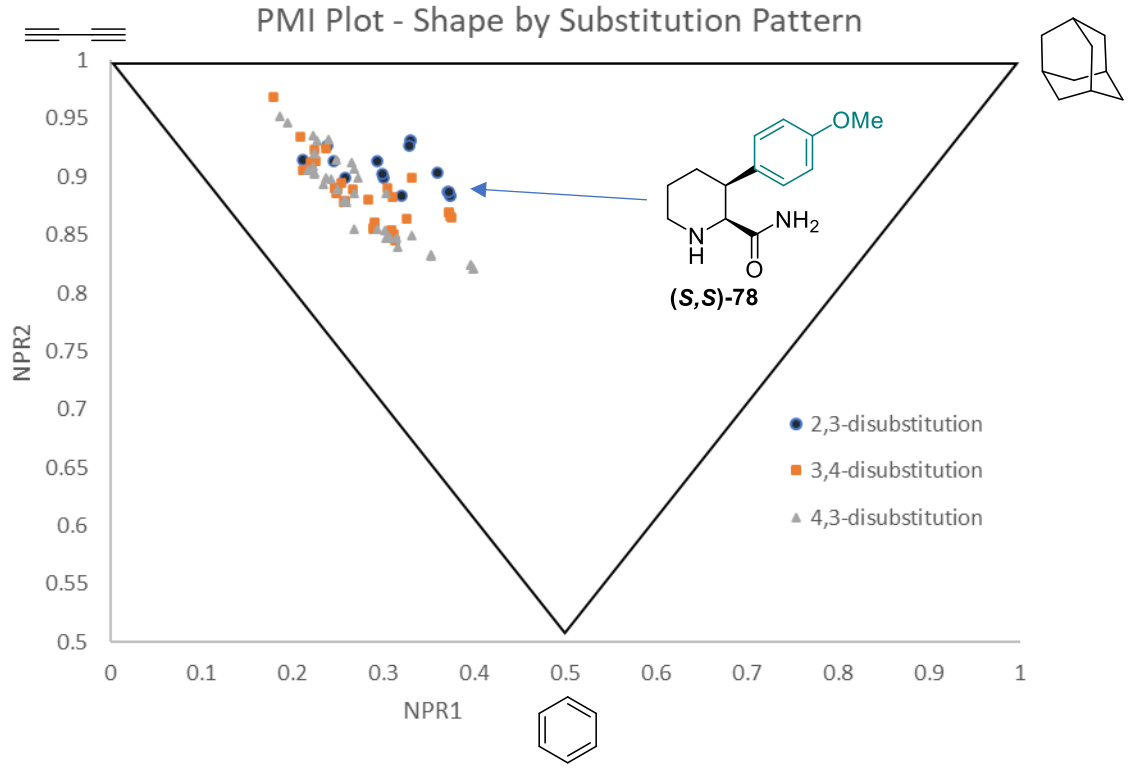


Figure 2.20 PMI plot of the 45 synthesised fragments, with datapoints denoted by substitution pattern.

The 2,3-disubstituted pyrrolidines and piperidines had a horizontal distribution across the triangular PMI plot, with the 6-membered substrates such as **(*S,S*)-78** generally placed furthest away from the disc-rod axis. Importantly, 4 compounds of each substitution pattern were represented in the set of 12 structures tending farthest right on the plot.

Last, but not least, the position of different pharmacophore types on the PMI plot was analysed (Figure 2.21). Whereas a clear pattern could not be identified as in the example above, pyrrolidines and piperidines generally accounted for the most shapely fragments, however, the ability to derive highly 3D leads from cyclic sulfones and *gem*-disubstituted cyclohexanes should not be underestimated.

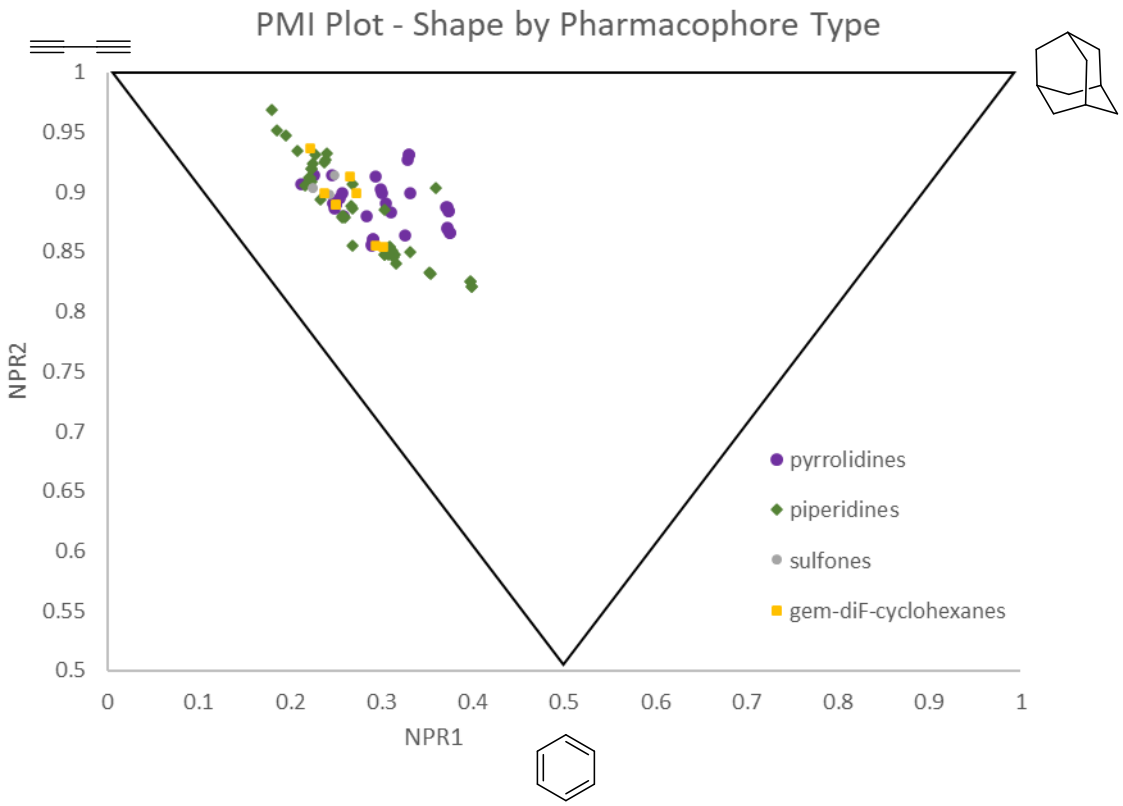


Figure 2.21 PMI plot of the 45 synthesised fragments, with datapoints denoted by pharmacophore type.

Finally, to prove the topological diversity that can be generated from these small and structurally simple compounds, the virtually decorated library generated in LLAMA was analysed from the perspective of shape diversity. Out of the 8625 once- and twice-decorated fragments, only 1505 had the sum NPR1 + NPR2 between 1.023 and 1.07, with 83% (7120) having NPR1 + NPR2 greater than 1.07, which is characteristic of high 3-dimensionality (Figure 2.22). Notably, a few products (<10) exhibited NPR sums of up to 1.59–1.60.

To view the characteristics of lead and drug-like molecules on the PMI plot, a virtual library was generated by randomly selecting a number of decorated compounds from each NPR bin, proportional to % population of the bin and rounded up to the nearest integer. For instance, 11 compounds of the (1.09,1.10] bin were selected as this accounts for 11% of the total decorated products. A total of 125 compounds were included, with the PMI plot of this virtual library of decorated fragments shown in Figure

2.23. The elaborated compounds efficiently sampled a wide variety of topologies, with a significantly increased spread over the area of the PMI plot compared to the parent fragments. Whereas some compounds fall on the disc-rod axis, more than half of the library components are removed from it, with some even displayed closely along the sphere-disc axis.

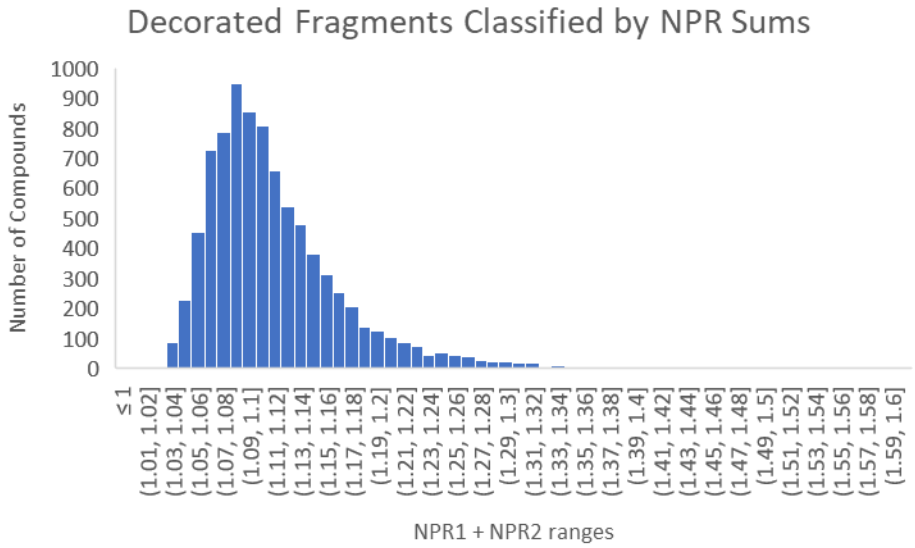


Figure 2.22 Histogram showing the distribution of both once and twice virtually decorated fragments by their corresponding NPR sums. High 3D character seen, with most NPR1 + NPR2 falling between 1.07 and 1.18.

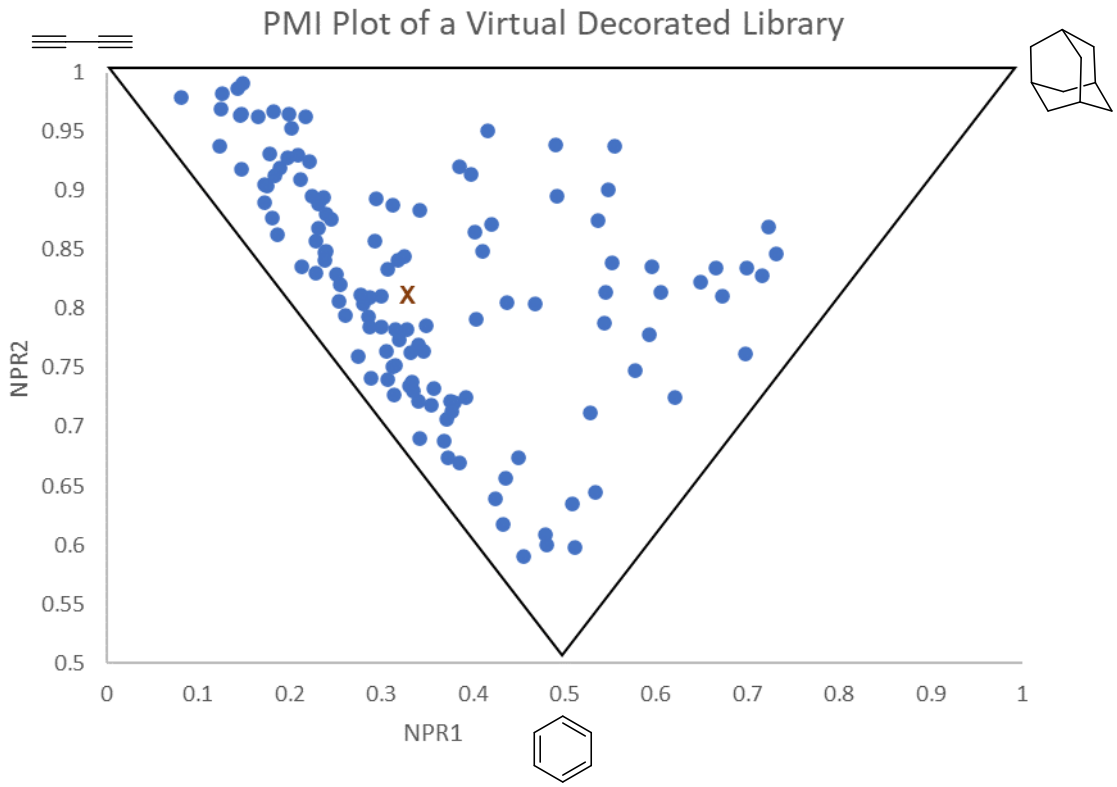


Figure 2.23 PMI plot of a virtual library of 125 once and decorated fragments. Mean PMI coordinates: NPR1 = 0.3501 and NPR2 = 0.8192 (denoted by X).

Finally, the structural novelty of the fragments was assessed against a subset of compounds from the larger ZINC database.The ZINC database comprises of more than 20 million compounds that exhibit ligand-like features from a biological point of view, being representative of the scaffold diversity found in commercial librarires.[239] To enable analysis, LLAMA allowed selecting a random 2% of the "available now" compounds in the ZINC database, as well as identifying the distinct structural assemblies (Murcko frameworks) present in the synthesised library (Table 2.13). Comparison of the Murcko frameworks to those of, or embedded in, the 2% subset of ZINC revealed very few similarities, with overall less than 1000 commercial compounds in a random subset of 400,000 containing either an arylated cyclohexane ring or a C(3) arylated pyrrolidine (entries 1-2). Notably, even fewer possessed a C(3) arylated piperidine, whereas no ZINC compounds in the randomly chosen subset contained a 6-membered cyclic sulfone (entry 5), highlighting the originality and uniqueness of our assembled library.

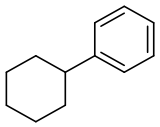
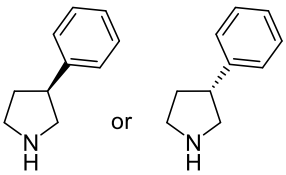
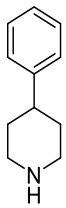
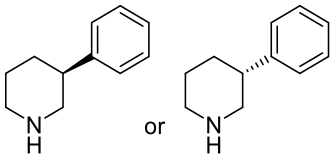
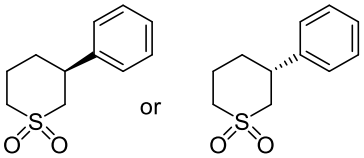
Entry	Murcko Framework for Synthesised Fragment Library	% ZINC compounds with the same or embedded framework
1		0.26
2		0.23
3		0.16
4		0.05
5		0.00

Table 2.13 Overview of the distinct Murcko frameworks in this fragment library and their representation in the ZINC database, from highest to lowest occurrence.

2.2.7 Conclusions

To conclude, a fragment library containing 5- and 6-membered saturated hetero- and carbocycles with a range of disubstitution patterns and binding elements was successfully assembled by Pd-catalysed directed C(sp^3)–H functionalisation.

Starting from inexpensive commercially available pharmacophores, 45 fragments were synthesised in only up to 4 steps each, involving highly regio- and stereoselective aminoquinoline directed arylations on intact rings, followed by derivatisation of this auxiliary to either alcohol, carboxylic acid, amide or nitrile polar functionalities. The arylation products were isolated as single *cis* diastereomers, with epimerisation to corresponding *trans* isomers resulting in a total of 5 different vicinal disubstitution patterns being overall exemplified (*cis*-2,3-, *cis*-3,4-, *trans*-3,4-, *cis*-4,3- and *trans*-4,3-disubstitution). Each fragment was generated in at least 50 mg quantity and contained 3 binding elements: an aryl substituent, a polar functional group and an endo- or exocyclic heteroatom. The nature of binding elements and their diverse spatial distribution sets this library apart from other reported sp^3 rich collections. Moreover, the strategies employed for fragment library construction would have applicability in further probing C(sp^3)–H vectors of choice in further elaboration. The library fits within the ideal fragment-like space in terms of physicochemical properties, with virtual elaboration in LLAMA proving the suitability of fragments as starting points for the elaboration of compounds within desirable lead and/or drug-like space. Despite their small size, the fragments possess a good degree of 3-dimensionality, with distinct topologies dependent on the substitution pattern. More importantly, these allow for elaboration of highly shape-diverse compounds, as illustrated by the enumeration and PMI analysis of a virtual library of 125 once- and twice-decorated fragments.

Most importantly, all the above characteristics were achieved through a fragment design that is simple, yet charting significantly unexplored areas of chemical space by comparison to commercial collections represented within the ZINC database. The novelty and simplicity of design, as well as the excellent physicochemical properties and synthetic tractability are expected to position these fragments for success in screening stages and beyond.

2.3 Synthesis of Building Blocks for DNA-Encoded Libraries (DEL)

2.3.1 Strategies for Construction of DEL Building Blocks

As illustrated in the *Introduction*, building blocks for DNA encoded libraries are small molecules with suitable functionalisation handles for both attachment of a DNA headpiece, as well as further elaboration. DEL libraries are providing a platform for more facile generation of a higher number of compounds than ever before by combinatorial chemistry and rapid hit identification by enabling large compound mixtures to be screened at once. Compounds derived from DNA-encoded libraries have been reported to successfully progress through optimisation and clinical stages. One example is the novel soluble epoxide hydrolase (sEH) inhibitor GSK2256294 designed for treatment of COPD, currently the first compound derived from DEL to enter human trials (Figure 2.24).[240]

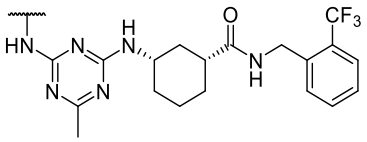


Figure 2.24 GSK2256294, a novel sEH inhibitor and the first DEL-derived compound to enter human clinical trials.

Challenges are however associated with the assembly of DEL libraries, especially with respect to the stability of the DNA tag to reaction conditions used to elaborate parent building blocks.[241] Moreover, elaboration reactions must be compatible with the use of water or DMSO solvents in which the DNA-tagged entities would dissolve. Current well-established on-DNA techniques rely on the presence of specific functionalities on the core scaffold, such as amines, aryl halides carboxylic acids and aldehydes. Efforts are being made to develop novel DNA-compatible methodologies, as well as DNA protecting strategies. [242] Notably, Pfizer developed a photoredox decarboxylative coupling of DNA-tagged Michael acceptors with aminoacids under aqueous conditions, demonstrating a powerful C–C bond formation strategy.[243] More recently, Yu developed a Pd-catalysed protocol under aqueous conditions to enable the C(sp^3)–H functionalisation of small aliphatic molecules with DNA-tagged aryl iodides.[244]

Nevertheless, the identity of the core scaffold is of utmost importance, determining the physicochemical properties of the drug candidates, as well as their overall shapes. Similar to fragments, low molecular weight building blocks with a high sp^3 character and a variety of synthetically accessible diversification handles would be optimal starting points for DEL construction.[245] Importantly, the number of synthetic handles that can be probed in an orthogonal fashion would determine the type of libraries and molecular architectures that can be generated.[246] For instance, a bifunctional scaffold would use one handle to attach the DNA headpiece, whereas the other would be available for elaboration in a linear fashion (Figure 2.25A). Conversely, building blocks with at least 3 points of diversification would enable development of branched libraries, leading to geometries that could probe a wider range of binding modes with a target (Figure 2.25B).

However, it is estimated that less than 2.3% of the commercially available building blocks are at least trifunctionalised, with an increasing demand for small molecules that meet this requirement, and subsequently increase coverage of chemical space.[35] Furthermore, with hits needed to be synthesised off-DNA to confirm their biological activity, a good synthetic tractability of each building block needs to be ensured.

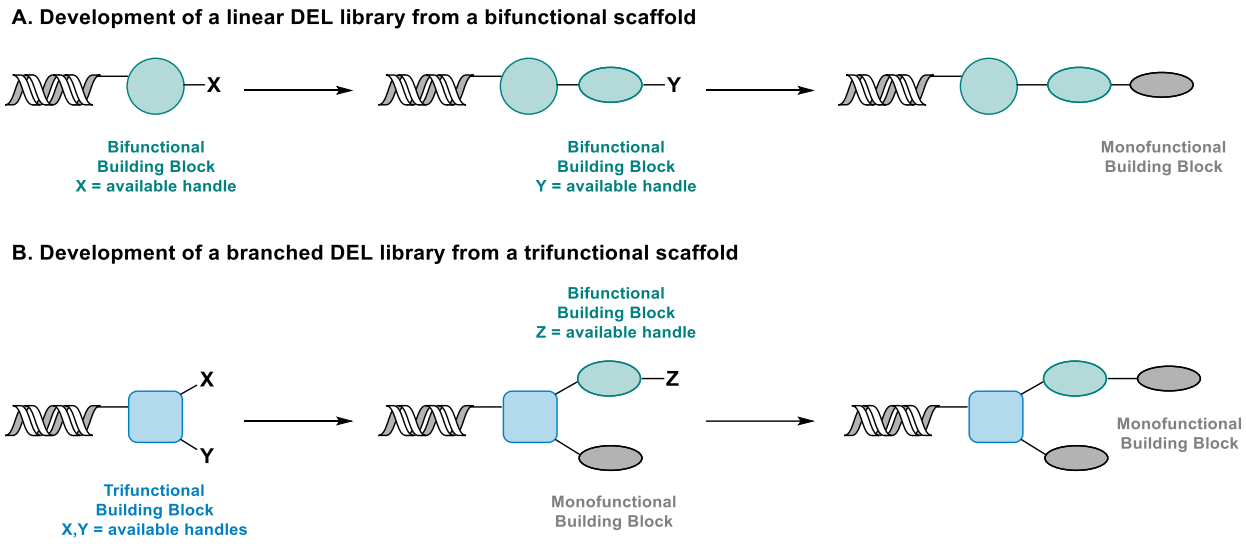


Figure 2.25 Generation of linear of branched DEL compounds, starting from either bifunctional or trifunctional scaffolds, respectively.

Recognising the potential of C(sp^3)–H functionalisation in enhancing the structural features of building blocks, Schreiber and coworkers reported the synthesis and use of 2,3-disubstituted azetidines and pyrrolidines for the generation of DEL libraries (Figure 2.26).[247] Employing previously developed chemistry,[248] off-DNA arylation was performed at C(3) on *N*-TFA protected 4 and 5-membered rings, as directed by the C(2) aminoquinoline amide directing group. Notably, starting from *R*- or *S*-enantiomerically pure aminoacids, either of the stereodefined *cis* isomers could be isolated, with **(*R,R*)-127** and **(*R,R*)-128** shown as example products below. TFA deprotection in the same pot as the arylation led to free amines, providing relief of steric hindrance for further manipulations such as C(2) epimerisation and/or aminoquinoline deprotection to carboxylic acids **(*R,R*)-** and **(*R,S*)-129**, and **(*R,R*)-** and **(*R,S*)-130**. Overall, the full matrix of all the possible stereoisomers around the vicinal C(2)-C(3) centres for both the azetidine and pyrrolidine scaffolds was generated. Importantly, these building blocks were trifunctional, with the C(2) carboxylic acid used as a DNA headpiece attachment point and the ring heteroatom and aryl halide available for elaboration of a DEL library in a branched fashion. The synthesised core scaffolds were ultimately characterised by the presence of 3 sources of diversity, arising from: (i) the choice of stereodefined substitution at C(2)/C(3); (ii) the endocyclic nitrogen acting as synthetic handle and (iii) the aryl halide acting as synthetic handle. After DNA attachment, two split-pool cycles were performed, consisting of *N*-capping reactions by reductive amination/sulfonylation, followed by Suzuki couplings on the aryl iodide. An equal number of azetidine and pyrrolidine compounds were generated, totalling to 107,616 for the DEL library. With excellent DNA barcode

validation observed, screening the library against interactions with a carbonic anhydrase resulted in the correct identification of up to 6 highly potent azetidine hits, highlighting the success of the building block design employed. Moreover, highly stereoselective C(sp^3)–H functionalisation was key to accessing this design even before DNA-attachment, resulting in the generation of a DEL library with a structural complexity even resembling that of compounds derived from DOS approaches.

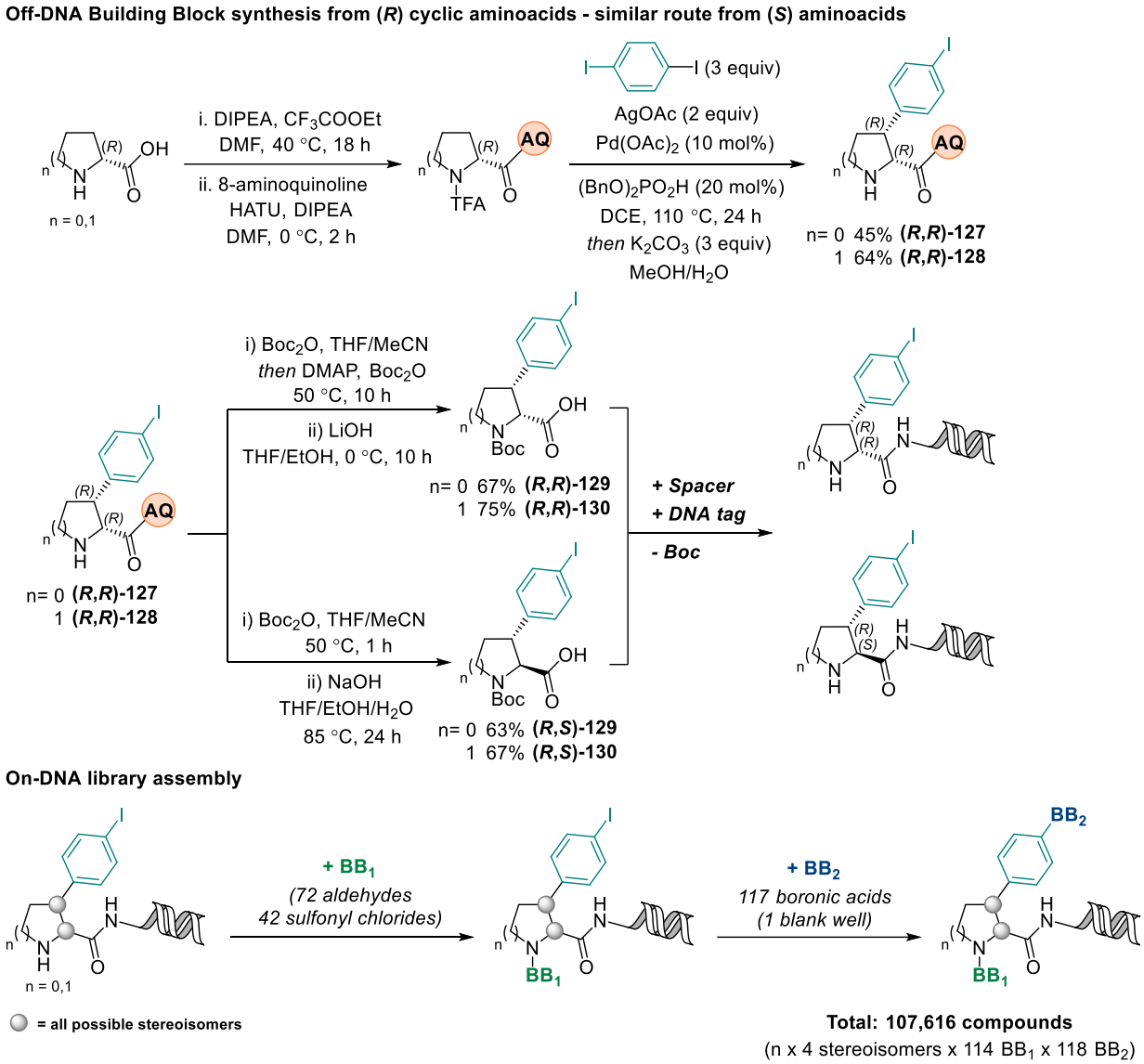


Figure 2.26 Synthesis of DOS-DEL-1 library by Schreiber and coworkers starting from enantiopure 4- and 5-membered cyclic aminoacids,

2.3.2 Project Aims

This project aims to increase the diversity of DEL libraries by enabling access to underexplored core scaffolds and building blocks that present up to 4 diversification points (tetrafunctional) in a variety of spatial orientations. In this respect, small saturated heterocycles present advantageous opportunities as starting points, since the ring heteroatom can be used itself as a synthetic handle, whereas

attachment of functionalities to the cyclic core would result in low molecular weight products with high sp^3 and 3-dimensional character.

Taking advantage of the previous highly stereoselective C(sp^3)–H functionalisation with a C(4) directing group,[166] the decoration of 6-membered heterocycles with bespoke substituents was planned, aiming to ensure the availability of a wide range of synthetic handles to be later exploited by DNA-compatible chemistry. Importantly, the ability to revert to the parent C(4) carboxylic acid was expected to provide the handle for DNA tag attachment in all cases. Three building block designs were envisaged, two trifunctional and one tetrafunctional, as illustrated in Figure 2.27. Firstly, installing aryl bromides at C(3) on *N*-Boc piperidines followed by aminoquinoline deprotection would results in carboxylic acids of design **131**, which would enable on-DNA cross-couplings and *N*-capping reactions. Alternatively, aiming to increase representation of pharmacophores such as tetrahydropyrans and 6-membered cyclic sulfones, these would be arylated with a trifunctional aryl iodide bearing 2 orthogonal diversification handles, a halide and a Boc-protected aniline, resulting in trifunctional building blocks of type **132**. Finally, installing the same *N*-Boc trifunctional aniline on *N*-Ac protected piperidines would allow for orthogonal deprotection of the two nitrogen atoms, affording tetrafunctional building blocks of type **133**, which would be expanded from either of the aryl handles or from the ring heteroatom. Stereochemical diversity of the library would be enhanced by targeting building blocks in both the single *cis* and single *trans* diastereomeric form, with arylation-epimerisation strategies expected to enable accessing the latter.

Last, but not least, given the robustness and proven scalability of the C(sp^3)–H functionalisation methodology to up to 4 mmol scale, each building block will be synthesised in at least 100 mg quantity to prove the synthetic tractability of this methodology.

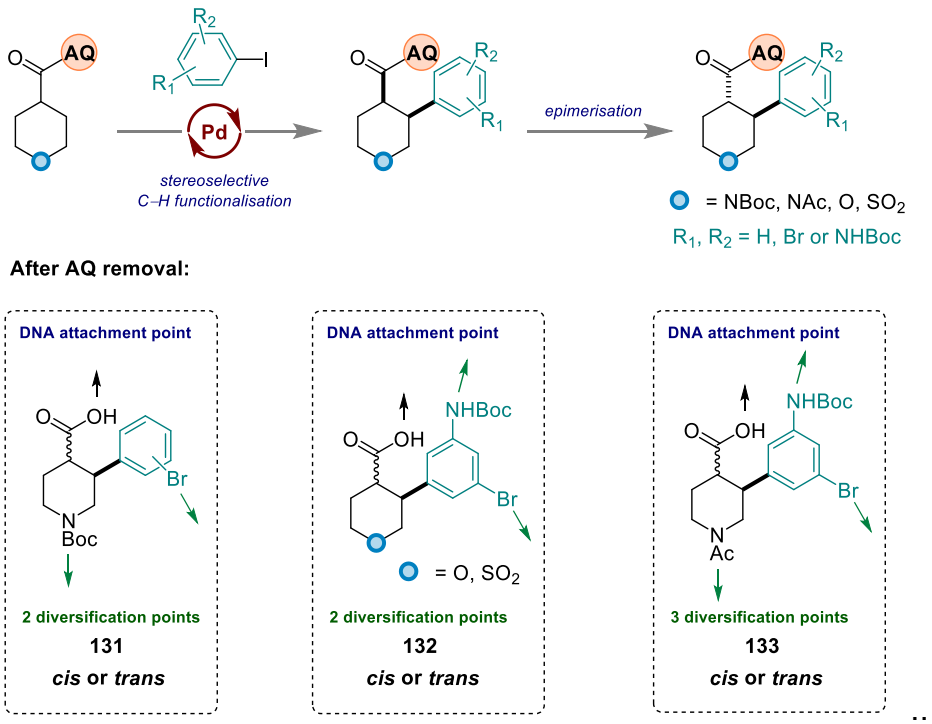


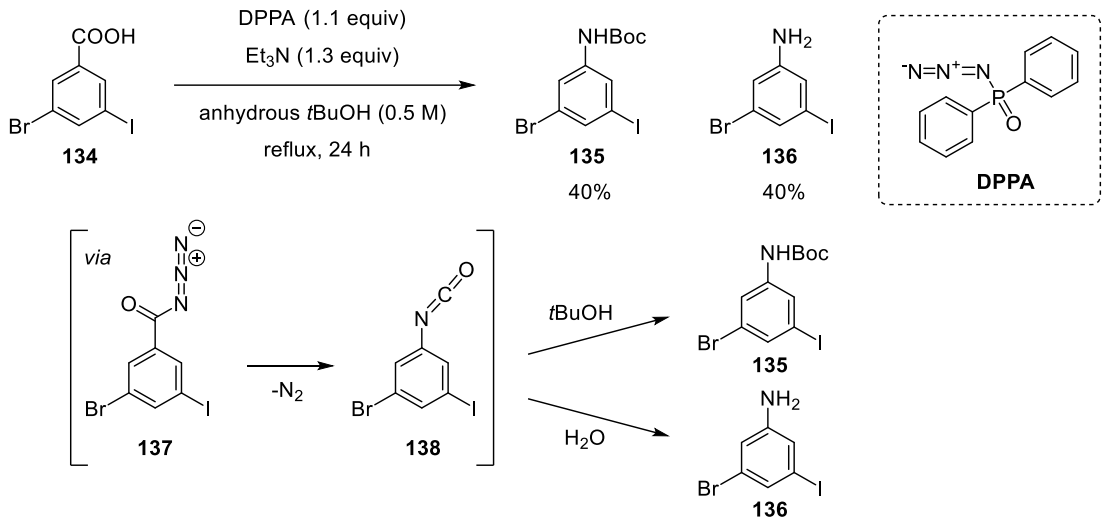
Figure 2.27 Targeted design and synthesis of tri- and tetrafunctional heterocyclic building blocks for DEL elaboration.

2.3.3 Synthesis of Arylated Precursors

2.3.3.1 Large Scale Synthesis of a Bespoke Trifunctional Aryl Iodide

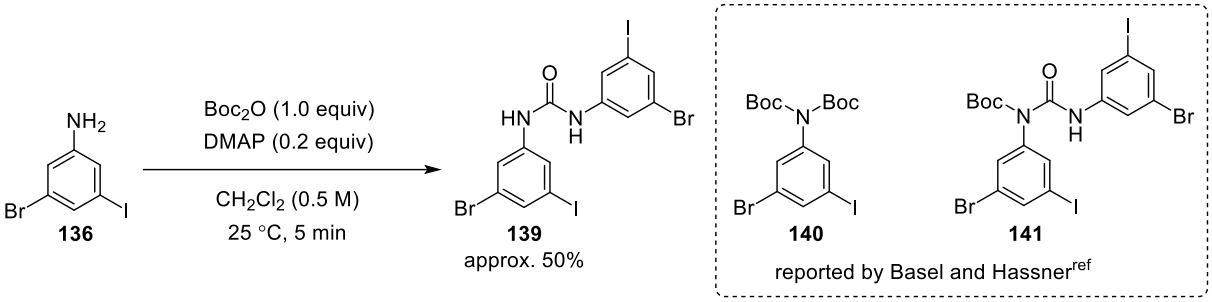
To access novel DEL building blocks with a variety of diversification handles, the functionalisation of saturated heterocycles with the trifunctional *tert*-butyl (3-bromo-5-iodophenyl)carbamate **135** was targeted. This aryl iodide would possess 2 handles for further elaboration, the Boc protected aniline, as well as the bromide, both of which could be exploited in an orthogonal fashion using chemistry compatible with the DNA, such as Boc deprotection/*N*-cappings and/or Suzuki couplings.

With **135** not commercially available, a one-step synthesis was designed starting from the inexpensive 3-bromo-5-iodobenzoic acid **134** (Scheme 2.44). Adapting a procedure by Kumar et al,[249] **134** was converted into acyl azide intermediate **137** in the presence of diphenylphosphoryl azide (DPPA) and triethylamine. A same-pot Curtius rearrangement was expected, with the resulting isocyanate trapped by the solvent (*t*BuOH) to afford the NHBoc aniline **135**. Despite formation of the desired product in 40% yield, the free aniline side-product **136** was observed in a similarly high yield, originating from trapping of isocyanate **138** with water. The latter could be separated by filtration, based on its insolubility in CH_2Cl_2 compared to desired **135**. However, attempts to mono-Boc protect **136** in the presence of 1 equivalent of Boc_2O and substoichiometric DMAP afforded a complex mixture of inseparable products, with 1,3-bis(3-bromo-5-iodophenyl)urea **139** being identified as major by ^{1}H NMR (Scheme 2.45).



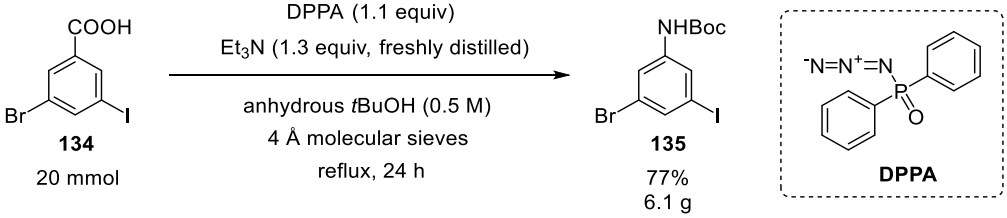
Scheme 2.44 Synthesis of a trifunctional aniline *via* Curtius rearrangement. Isocyanate intermediate trapping by either *t*BuOH or H_2O explains formation of either the Boc-protected or the free aniline, respectively.

Although an unexpected outcome, this confirmed early observations by Basel and Hassner in the Boc protection of aromatic amines and alcohols, who reported also the formation of di-Boc protected aniline **140** and the Boc-protected urea **141** by-products in this same reaction.[250]



Scheme 2.45 Boc protection attempt on the free aniline product. **139** identified by ^{1}H NMR, with **140** and **141** suggested as side-products based on literature reports.[247]

To maximise atom efficiency, adventitious sources of moisture were minimised. Using freshly distilled Et_3N and 4 Å molecular sieves, NHBoc aniline **135** could now be isolated in 70% yield starting from 4 mmol of acid **134**. Scaling up even further to 20 mmol, over 6 g of desired trifunctional **135** was generated in one step, providing a facile and rapid way to access this valuable coupling partner in sufficient quantities for subsequent large-scale arylations (Scheme 2.46).

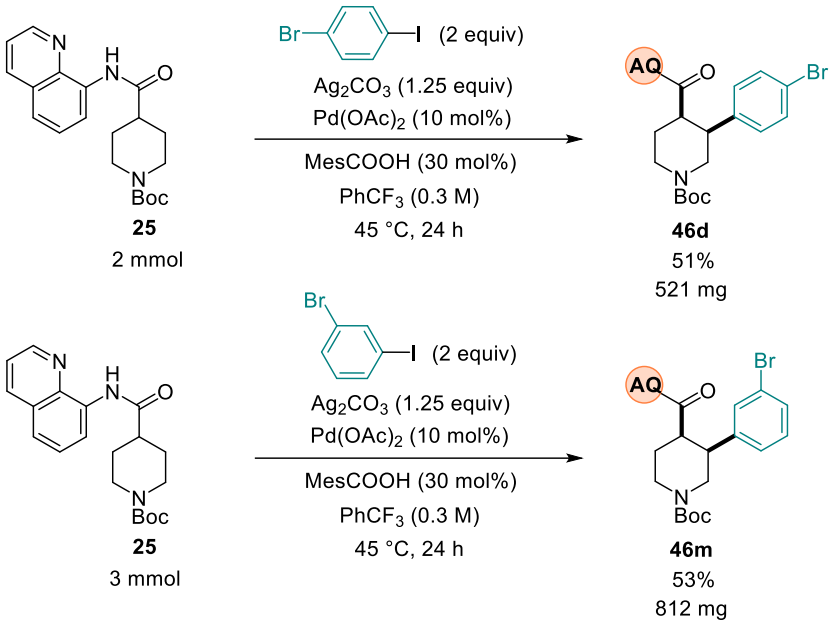


Scheme 2.46 Optimised procedure and multigram synthesis of trifunctional aryl iodide **135**.

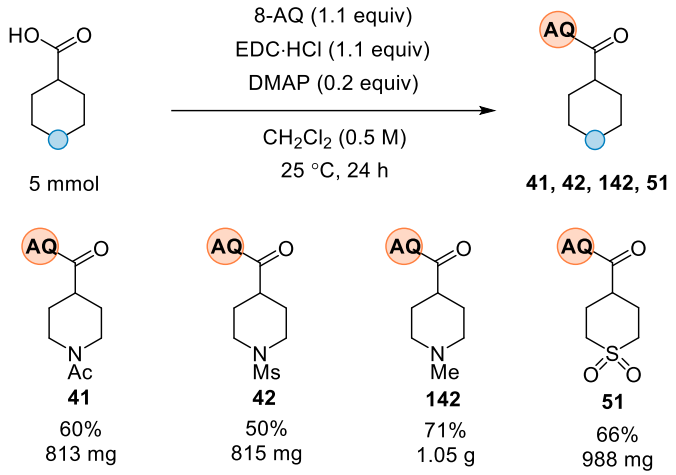
2.3.3.2 Large Scale C(3) Arylation of 6-Membered Heterocycles

Using the previous *cis* selective methodology,[168] 6-membered heterocycles with a C(4) aminoquinoline amide directing group were functionalised at C(3) with arenes bearing one or two diversification points for DEL elaboration.

Firstly, two regioisomeric aryl bromides were successfully installed on *N*-Boc piperidine in 51-53% yields on a 2-3 mmol scale, affording DEL precursors **46d** and **46m** in 500-800 mg quantities (Scheme 2.47). With the previously synthesised trifunctional aniline **135**, C(3) arylation of a variety of 6-membered heterocycles was targeted. Besides available amides from recent studies, the aminoquinoline directing group was installed on commercially available *N*- and *S*- saturated rings bearing a C(4) carboxylic acid functionality. Amide couplings proceeded in good to excellent yields using EDC·HCl and catalytic DMAP to give products **41, 42**, **142** and **51** (Scheme 2.48). A lower yield was observed for *N*-Ms protected piperidine, attributed to mass losses during purification due to the marked insolubility of **42** in common organic solvents.

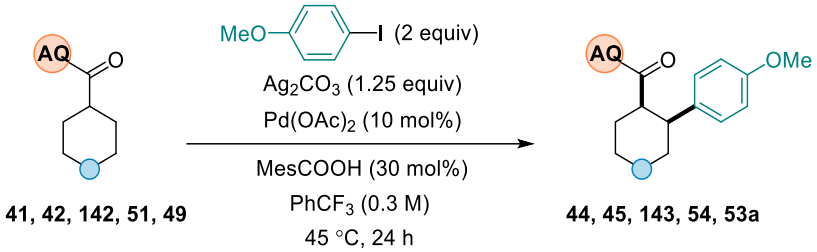


Scheme 2.47 Scale-up installation of regioisomeric bromoaryls on *N*Boc piperidine. Reactions in a sealed microwave vial, under Ar.



Scheme 2.48 Aminoquinoline installation on 6-membered saturated heterocycles.

The reactivity of the entire series of amides was initially studied in the C(3) *cis*-arylation with 4-iodoanisole under standard conditions (Table 2.14). Notably, unreacted *N*-Me piperidine **142** was recovered almost quantitatively (entry 3), whereas *N*-Ac piperidine **41** and THP amide **49** afforded the highest mono-*cis*-functionalisation yields (entries 1, 5). Interestingly, **41** promoted di-*cis*-*cis* arylation, in a yield comparable to the corresponding mono-*cis* product **44** (36% vs 46%, respectively, entry 1). Overall, the THP system performed the best in terms of both reactivity and selectivity, affording 57% **53a**. Both the *N*-Ms protected piperidine and the cyclic sulfone exclusively generated mono-*cis* products **45** and **54** respectively, each in 25% yield (entries 2, 4). However, a low mass recovery was observed for *N*-Ms piperidine, hence **45** was removed from the list of targeted DEL precursors. Conversely, the reactivity of the sulfone was later enhanced by higher temperatures/longer reaction time.

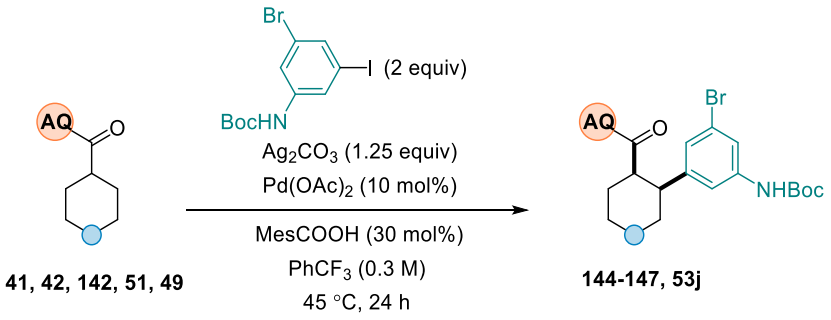


41, 42, 142, 51, 49 — 44, 45, 143, 54, 53a

Entry	○	yield (%)[a]					
		mono-*cis* (%)	mono-*trans* %	di-*cis*-*cis* %	di-*cis*-*trans* %	RSM %	Total %
1	NAc	**44** (43)	-	36	-	10	89
2	NMs	**45** (25)	-	-	-	26	51
3	NMe	**143** (0)	-	-	-	92	92
4	SO_2	**54** (25)	-	-	-	70	95
5[b]	O	**53a** (57)	6	-	7	27	97

Table 2.14 Assessing reactivity of various 6-membered heterocycles in the C(3) arylation with 4-iodobenzene. Reactions on 0.2 mmol scale. [a]^{1}H NMR yields calculated using 1,3,5-trimethoxybenzene as an internal standard. [b]3.0 equiv ArI, 1.5 equiv Ag_2CO_3 and T = 50 °C..

A next set of arylation trials were conducted in the presence of the trifunctional aniline (Table 2.15). *N*-Ac piperidine **41** was the best performing substrate, leading to 53% ^{1}H NMR yield of **144** and only 15% diarylation compared to the former case above, presumably due to the increased steric demand of the multisubstituted aryl iodide (entry 1). Again, lower recovery was observed with *N*-Ms piperidine **42**, albeit a 34% yield of the *cis*-arylated product **145** was obtained (entry 2). As with 4-iodoanisole, *N*-Me piperidine 1**42** did not undergo any reaction (entry 3). As before, cyclic sulfone **51** afforded 27% **147** and no other arylated side-products (entry 4). Gratifyingly, this yield could be improved to 59% by employing additional equivalents of aryl iodide and base and increasing the temperature to 75 °C (entry 5). A significantly lower mono-functionalisation yield was observed this time for the THP substrate **49** (25% of **53j** cf. previously 57%), due to an increased tendency in this case towards diarylation with the trifunctional aryl iodide (entry 6).

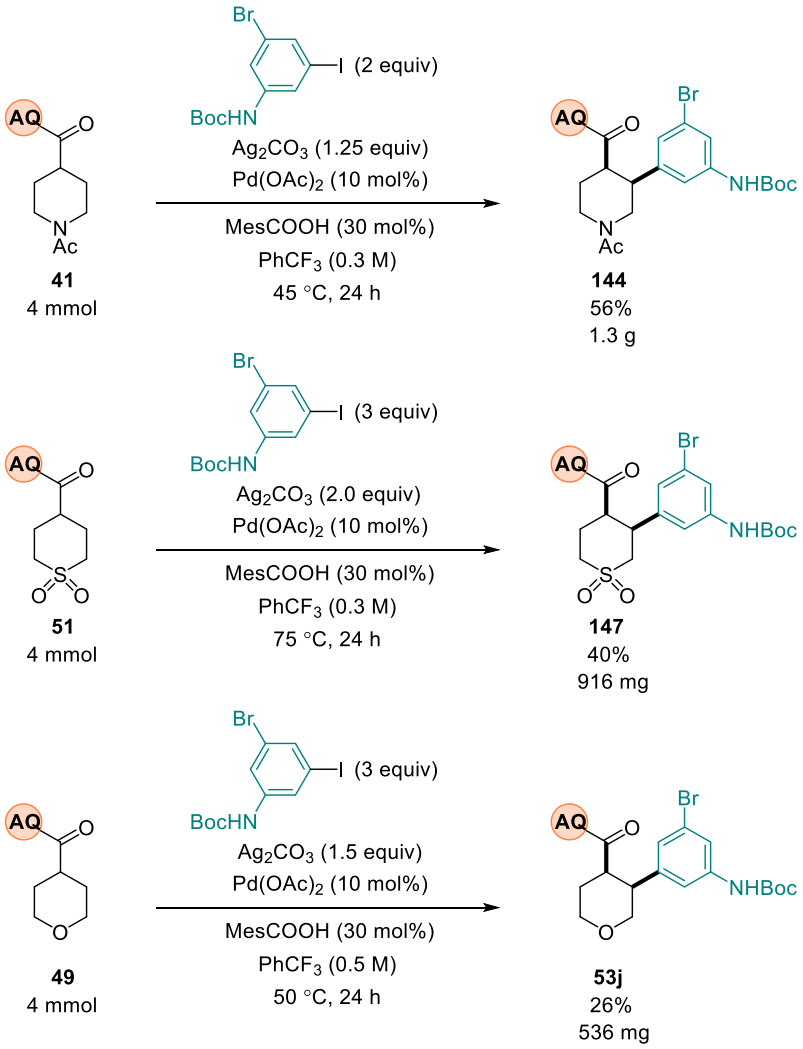


41, 42, 142, 51, 49 → **144-147, 53j**

Entry	○	yield (%)[a]					
		mono-*cis* (%)	**mono-*trans* %**	**di-*cis*-*cis* %**	**di-*cis*-*trans* %**	**RSM %**	**Total %**
1	NAc	**144** (53)	2	15	-	25	95
2	NMs	**145** (34)	-	-	-	45	79
3	NMe	**146** (0)	-	-	-	100	100
4	SO_2	**147** (27)	-	-	-	55	82
5[b]	SO_2	**147** (59)	12	-	-	12	83
5[c]	O	**53j** (25)	2	15	12	38	92

Table 2.15 Assessing reactivity of various 6-membered heterocycles in the C(3) arylation with a trifunctional aryl iodide. Reactions on 0.2 mmol scale. [a]^{1}H NMR yields calculated using 1,3,5-trimethoxybenzene as an internal standard. [b]3.0 equiv ArI, 2.0 equiv Ag_2CO_3 and T = 75 °C. [c]3.0 equiv ArI, 1.5 equiv Ag_2CO_3 and T = 50 °C.

The three best performing heterocycles (**41**, **51** and **49**) were subjected to C(3) arylation on 4 mmol scale in the presence of the trifunctional aniline. Applying the best-found conditions for each substrate led to 26-56% isolated yields of *cis*-functionalised **144**, **147** and **53j**, respectively, corresponding to quantities between 500 mg–1.3 g of building block precursors (Scheme 2.49). Conversions of **41** and **49** were consistent with the 0.2 mmol trial reactions (Table 2.15, entries 1 and 5), whereas a small decrease in reactivity was seen for sulfone **51**.

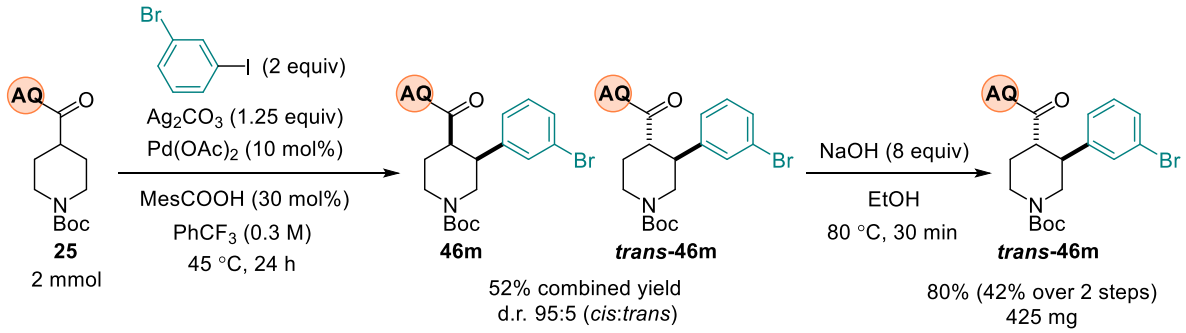


Scheme 2.49 Scale-up C(3) arylation of *N*-Ac piperidine, tetrahydrothipyran dioxide and THP using *tert*-butyl (3-bromo-5-iodophenyl)carbamate.

2.3.3.3 Accessing *trans* Diastereomers

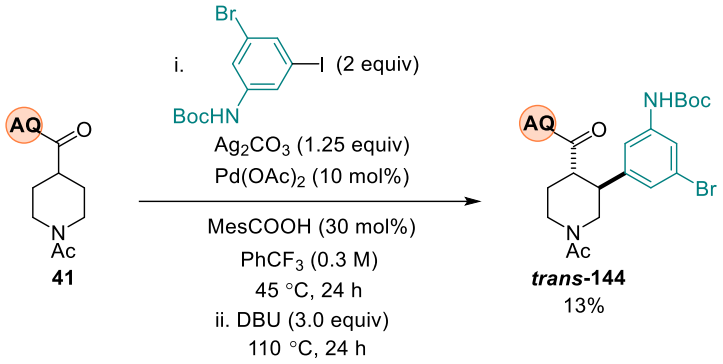
Epimerisation strategies were developed to enable conversion of previously synthesised 3,4-disubstituted heterocycles (**46d, 46m, 144, 147** and **53j**) to corresponding single *trans* diastereomers on the larger scale (>1 mmol).

The one-pot arylation-epimerisation procedure was already proven to allow access to *p*-bromoarylated epimer **61** in 53% yield (see Section 2.1.4, Scheme 2.17). For the *m*-brominated species, **46m** and the corresponding *trans* side product ***trans*-46m** were deliberately isolated as a mixture in 52% combined yield (95:5 d.r. *cis*:*trans*). Treating this mixture with excess NaOH at 80 °C gave conversion to ***trans*-46m** in 42% yield over two steps (Scheme 2.50). Notably, no hydrolysis of the aminoquinoline amide could be observed under the highly basic conditions.



Scheme 2.50 C(4) epimerisation to generate the *trans* isomers of bromoarylated *N*Boc piperidines.

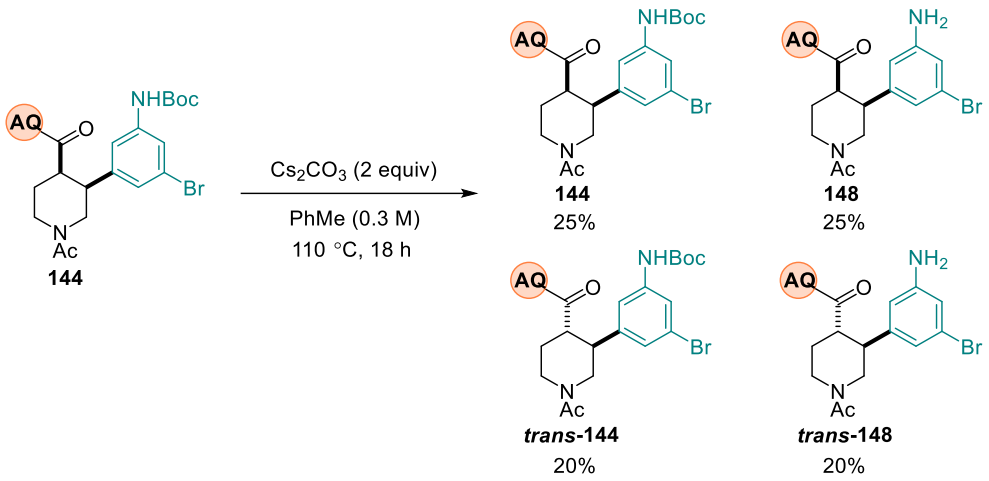
Moving to the *N*-Ac protected piperidine **41**, the DBU-mediated epimerisation posed challenges due to the lability of the aniline Boc protecting group. Upon treatment with 3 equiv DBU and heating to 110 °C, a dense and highly insoluble precipitate formed, comprising of the free aniline and a mixture of unidentified amides. The organic filtrate was found to contain only the desired ***trans*-144**, albeit in only 13% yield (Scheme 2.51).



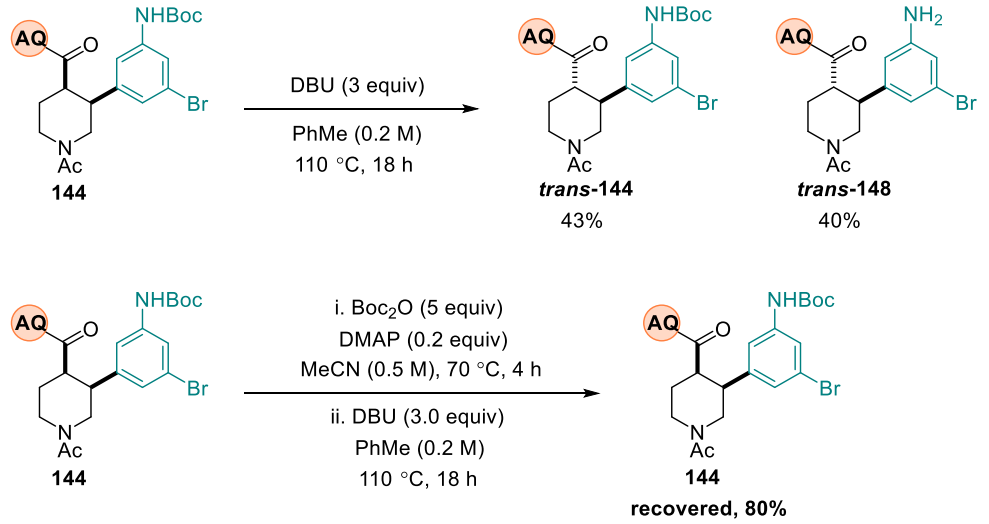
Scheme 2.51 One-pot arylation-epimerisation in the presence of a trifunctional arylating agent.

Alternatively, a stepwise approach to the *trans* epimer was attempted, with the isolated *cis*-arylated piperidine **144** being subjected to a range of basic conditions. Treatment with Cs_2CO_3 at 110 °C overnight promoted epimerisation in a 40% overall yield, however, *trans* products bearing either the protected (***trans*-144**) or the deprotected aniline (***trans*-148**) were formed to similar extents (Scheme 2.52). Boc removal from the *cis* starting material was also observed in 25% yield to give **148**, with NMR monitoring revealing a faster initial formation of **148** compared to the two *trans* products. Despite the high temperature, unreacted **41** was still present in approximately 25%, accounting for the mass balance. Unfortunately, varying the reaction time or temperature was not found to improve the conversion or prevent Boc deprotection. Running the reaction in the presence of K_2CO_3 in methanol at reflux led to decreased epimerisation and enhanced Boc deprotection, affording **148** as major product in 40%, with ***trans*-144** and ***trans*-148** each observed in <10% yield. Boc reprotection of the free aniline was not further investigated at this point due to the challenges previously encountered on 5-bromo-3-iodoaniline (see Scheme 2.45). Employing a stronger base such as NaOH was detrimental, leading to advanced starting material decomposition. However, when subjecting **144** to DBU-mediated epimerisation in a discrete step, isomers ***trans*-144** and ***trans*-148** formed in equal amounts and as sole products, in a combined 83% yield (Scheme 2.53). Attempting to increase the rate of epimerisation

compared to Boc cleavage, amide pre-activation was performed by treatment with Boc_2O. Unfortunately, the desired reactivity could not be promoted, with starting **144** recovered in a significant amount through amide deprotection (Scheme 2.53). At this point it was decided to employ a stepwise arylation epimerisation for generating the *trans N*-Ac piperidine building block (see Section 2.3.5).

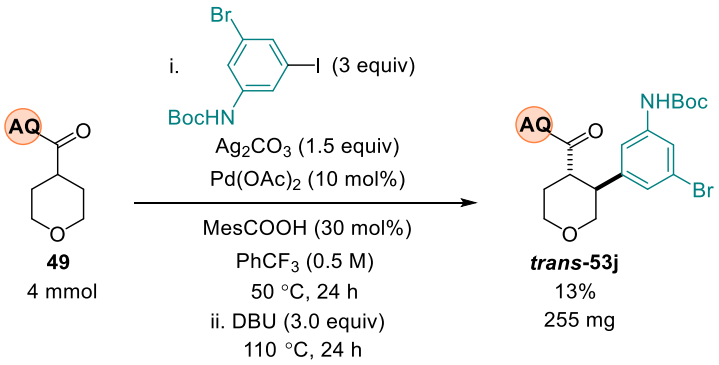


Scheme 2.52 Cs_2CO_3 mediated epimerisation of *cis* **144**. Yields determined by ^1H NMR of the precipitate (**148** and ***trans*-148**) and organic filtrate (**144** and ***trans*-144**).



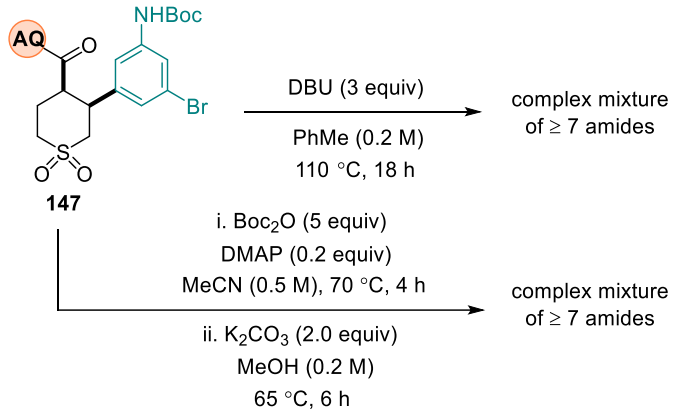
Scheme 2.53 DBU epimerisation of **144** in a discrete step, including attempt at amide pre-activation.

On the other hand, the one-pot arylation epimerisation was successful for isolating a useful quantity of the *trans*-arylated THP substrate **trans-53j** on the large scale, albeit in only 13% yield (Scheme 2.54). A dense insoluble precipitate formed, characteristic of aniline deprotection, which prevented efficient stirring, as well as filtration of the crude reaction mixture through Celite. Due to consumption of available **53j** previous stepwise arylation-epimerisation approaches were not investigated, however, later findings revealed the possibility of switching the diastereoselectivity of the arylation itself towards *trans*-arylation, by employing a BINOL additive (see Section 2.4.3).



Scheme 2.54 One-pot arylation-epimerisation of the THP ring using a trifunctional arylating agent.

Finally, DBU epimerisation of cyclic sulfone **147** was attempted, this unfortunately leading to a complex mixture containing at least 7 distinct amide peaks by ^{1}H NMR. Amide pre-activation by Boc protection, followed by epimerisation in the presence of only 2 equivalents of K_2CO_3 was still unsuccessful, giving a similar outcome (Scheme 2.55). Presumably, deprotonation at sites other than C(4), especially due to the generally high acidity of phenyl-substituted alkyl sulfones,[251] results in formation of unstable vinyl sulfones, as well as ring opening and/or fragmentation. Again, a diastereoswitchable arylation protocol was envisaged as a solution, since *trans* isomers would be generated under less basic conditions (Section 2.4.3).



Scheme 2.55 Unsuccessful epimerisation attempt on the 6-membered cyclic sulfone.

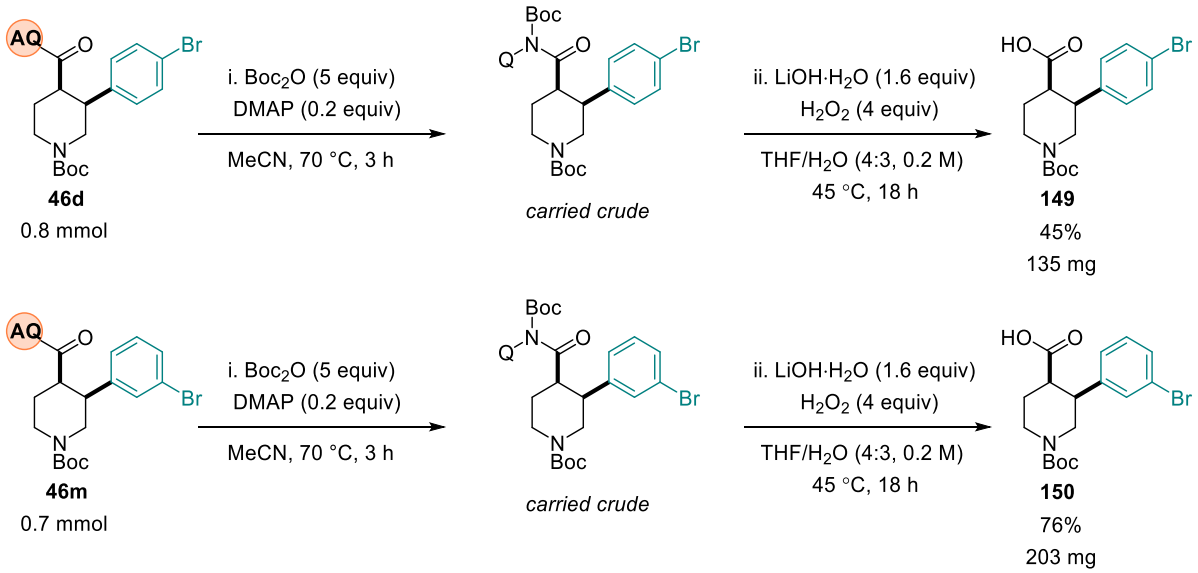
2.3.4 Synthesis of Trifunctional DEL Building Blocks

2.3.4.1 N-Boc Piperidine Building Blocks

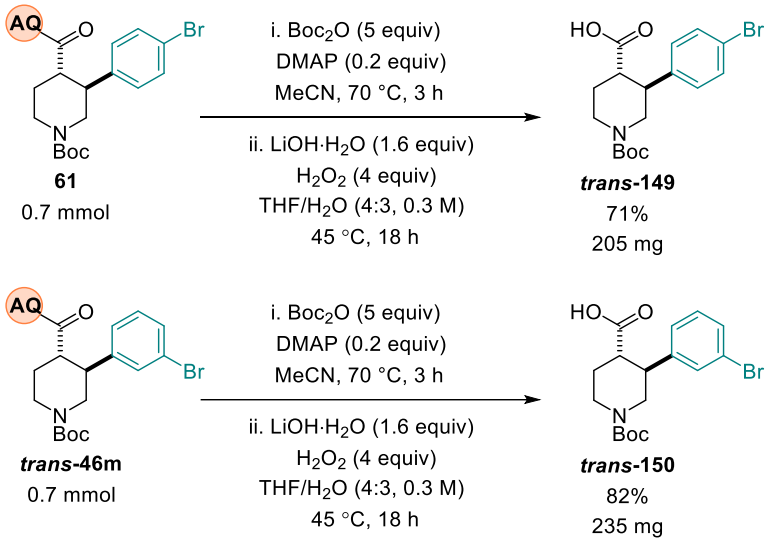
The aminoquinoline auxiliary was removed from piperidines **46d** and **46m** to unveil the parent C(4) carboxylic acids, which would serve as handle for attachment of building blocks to DNA headpieces. Following the same conditions as in the case of carboxylic acid fragment synthesis, amide activation and LiOOH mediated deprotection occurred smoothly on 0.7-0.8 mmol scale to afford *cis* carboxylic acids **149** and **150**, respectively, in good to excellent yields and in over 100 mg quantities (Scheme 2.56). In both cases, the crude Boc-protected amides were carried to the subsequent step, whilst acids could be isolated by acid-base work-up, without the need for chromatographic purification. A rather

modest 45% yield was observed for *p*-bromo substituted **149**, presumably due to off-site nucleophilic attack at the carbamate to regenerate **46d**, which accounted for the mass balance. On the other hand, the *m*-bromo substituted analogue appeared to increase steric hindrance at the carbamate, favouring desired attack at the C(4) carbonyl instead, and leading to acid **150** in 76% yield.

The *trans* isomers **61** and ***trans*-46m** were similarly deprotected to the corresponding acids ***trans*-149** and ***trans*-150**, respectively. With substituents on opposite faces of the ring, nucleophilic attack at the desired carbonyl centre was facilitated, affording yields above 70% in both cases (Scheme 2.57).



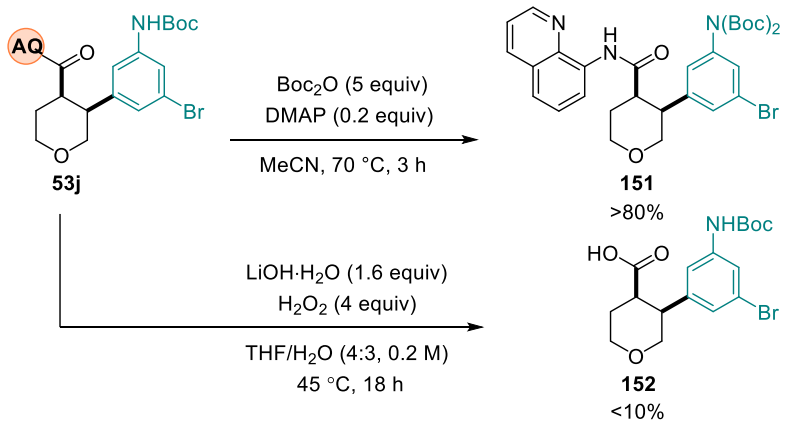
Scheme 2.56 Synthesis of bromoarylated *cis* carboxylic acids. Reactions in sealed microwave vials, under Ar.



Scheme 2.57 Synthesis of bromoarylated *trans* carboxylic acids. Reactions in sealed microwave vials, under Ar.

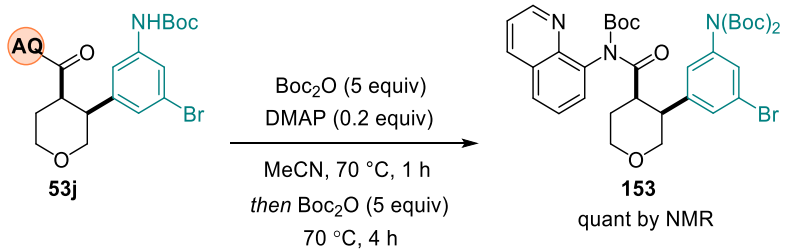
2.3.4.2 Tetrahydropyran and Cyclic Sulfone Building Blocks

Substrates bearing the trifunctional aryl were subjected to aminoquinoline deprotection to the corresponding carboxylic acids. Starting with THP substrate **53j**, amide Boc protection was performed under the same conditions as in the previous section (Scheme 2.58). However, after 3 h, ^{1}H NMR of the crude reaction mixture indicated the presence of only one *tert*-butyl environment (C(C*H*$_3$)$_3$) at δ = 1.65 ppm with an integration of 18 H in reference to any of the 3 distinct aromatic signals (HC$_{Ar}$). This suggested formation of the di-Boc protected aniline **151**, with the NHBoc amine moiety showing a markedly higher reactivity towards a second protection compared to the amide. Meanwhile, subjecting the non-activated amide **53j** directly to LiOOH treatment afforded only trace amounts (<10%) of desired carboxylic acid **152**.



Scheme 2.58 Boc protection at the more reactive NHBoc aniline instead of the desired amide. Attempted basic hydrolysis of the non-activated amide.

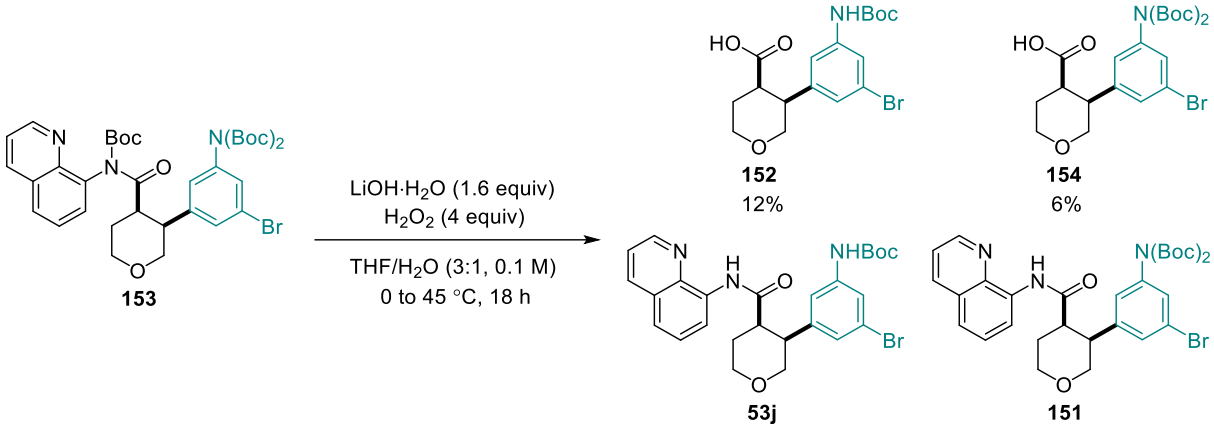
To overcome the lower reactivity at the desired centre, full Boc protection of both the aniline and the amide was promoted by a second addition of another 5 equivalents of Boc$_2$O after 1 h, followed by heating back to 70 °C for 4 h (Scheme 2.59). Two *tert*-butyl environments were now observed in the ^{1}H NMR at δ = 1.70 ppm and δ = 1.18 ppm with a relatively integration of 2:1, respectively, supporting formation of the protected amide. The complete disappearance of the characteristic amide peak also supported the conversion of **53j** to tri-Boc protected **153**, with the crude product of satisfactory purity for subjection to hydrolysis.



Scheme 2.59 Full Boc protection of THP substrate **53j**.

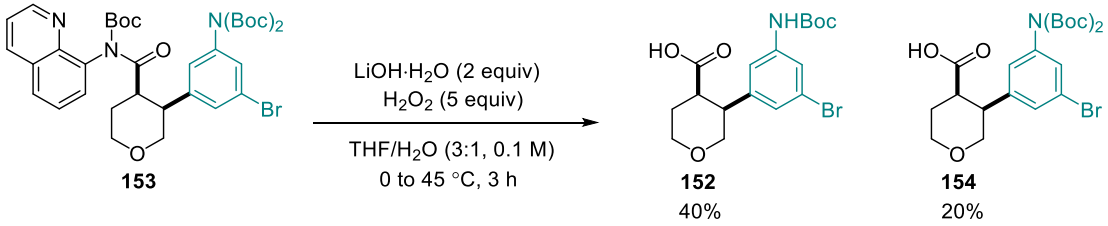
The LiOOH conditions were adjusted to allow solubilising **153**, by increasing the proportion of THF in the solvent mixture to a 3:1 THF:H$_2$O ratio, as well as employing a 0.1 M substrate concentration. Using

the same equivalents of LiOH and H_2O_2 as before, aminoquinoline deprotection occurred in an overall 18% yield (Scheme 2.60). Interestingly, carboxylic acids bearing either the NHBoc or the $N(Boc)_2$ aniline were observed (**152**, **154**), the basic conditions favouring mono-Boc deprotection to give acid **152** in a higher yield than **154**. **53j** and **151** accounted for the mass balance, formed by amide and/or aniline Boc deprotection of **153**.



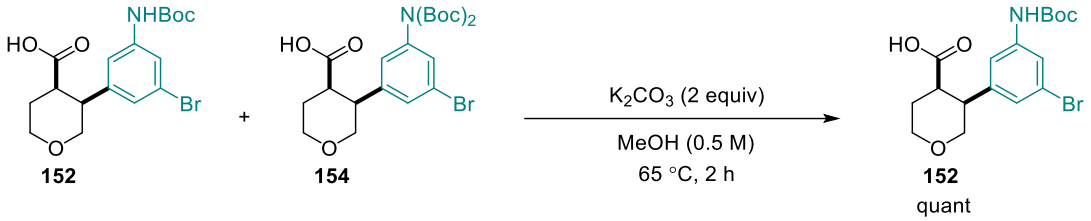
Scheme 2.60 Basic LiOOH conditions leading to partial aminoquinoline amide hydrolysis, as well as concomitant mono-Boc deprotection outcomes.

It was suspected that insufficient *in-situ* quantities of LiOOH were responsible for the low conversion to acids, with LiOH presumed to promote the competing amide Boc deprotection. To probe this, the equivalents of both $LiOH{\cdot}H_2O$ and H_2O_2 were slightly increased to 2 and 5, respectively, whilst maintaining the same 1:2.5 ratio, respectively. Gratifyingly, this greatly enhanced AQ deprotection, with acids **152** and **154** formed now in an overall 60% yield (Scheme 2.61).



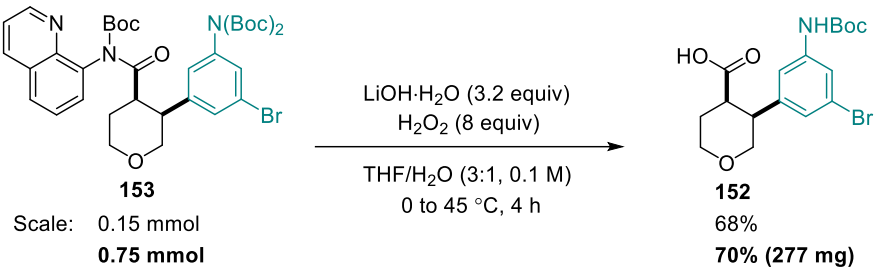
Scheme 2.61 Improved conditions for hydrolysis of the activated aminoquinoline amide **153** to carboxylic acids. Mixture isolated by acid-base work-up, with yields estimated by ^{1}H NMR based on relative integration of *tert*-butyl signals.

Converting the mixture of acids to a single chemical entity was highly desirable. Although converting the mixture to **154** by Boc protection appeared feasible, treatment with 1 equiv of Boc_2O with respect to the amount of mono-Boc protected **152** quickly formed a complex mixture of urea products at ambient temperature, reminiscent of the outcomes of trifunctional aniline **136** protection (see Section 2.3.3.1). Conversely, treatment with K_2CO_3 in MeOH under reflux enabled converging the mixture to **152** in a quantitative fashion, by selective mono-Boc deprotection of **154** (Scheme 2.62).



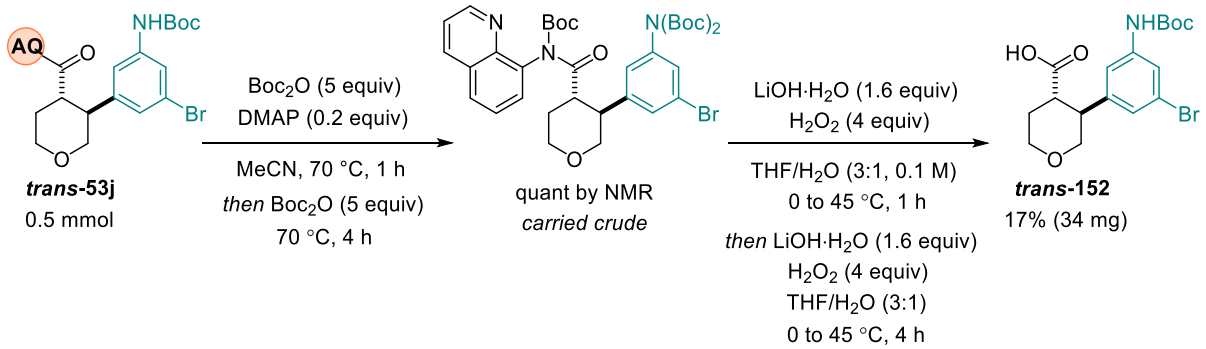
Scheme 2.62 Aniline mono-Boc deprotection with K_2CO_3 and conversion to single acid **152**.

Whereas this addressed the incomplete Boc deprotection in the previous step, the potential for effecting this transformation in the same step with AQ hydrolysis was explored. Doubling the amounts of LiOH·H_2O and H_2O_2 compared to Scheme 2.61, **152** could be directly isolated in an excellent 68% yield, with excess LiOOH fully cleaving one of the aniline Boc groups besides enhancing aminoquinoline removal (Scheme 2.63). These conditions provided a rapid and step-efficient entry to building block **152** in over 270 mg quantity on 0.75 mmol scale.



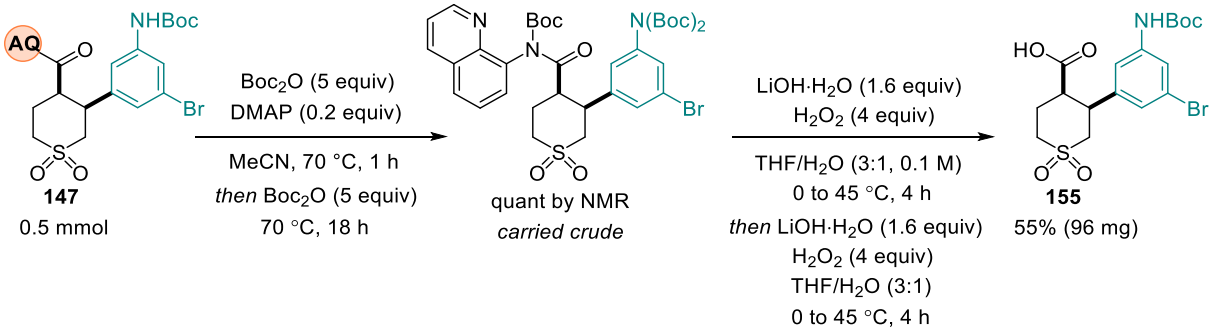
Scheme 2.63 Optimised AQ deprotection, enabling same-step aniline mono-Boc deprotection.

Next, AQ deprotection on the *trans*-arylated THP ***trans*-53j** was attempted under the previously optimised conditions, with the initial di-Boc protection occurring quantitatively by NMR. Unfortunately, only 17% yield of acid ***trans*-152** could be isolated, with starting ***trans*-53j** accounting for the mass balance. Presumably, the *trans* conformation of the 6-membered ring disfavours attack of LiOOH at the C(4) carbonyl centre, leading to cleavage of the amide Boc group instead. Despite portionwise addition of reagents in the hydrolysis step, no improvement in the yield of ***trans*-152** could be observed (Scheme 2.64).



Scheme 2.64 Boc activation and AQ deprotection on THP ***trans*-53j**, with portion wise addition of hydrolysis reagents.

The AQ removal conditions optimised for *cis*-THP **53j** were not successful on the sulfone substrate either, leading to advanced decomposition of starting **147** and only 10% yield of acid bearing mono-Boc aniline protection. Following a 18 h reaction time for ensuring full Boc protection in the first step, gradual addition of LiOH·H_2O and H_2O_2 in 2 equal portions led in this case to a major boost in yield to 55% over the 2-step sequence (**155**, Scheme 2.65).

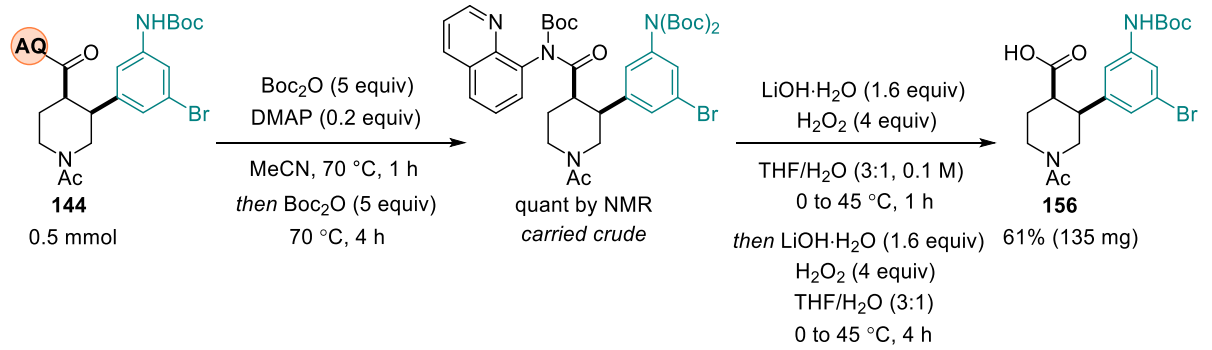


Scheme 2.65 Boc activation and AQ deprotection on sulfone **147**, with portion wise addition of hydrolysis reagents.

2.3.5 Synthesis of Tetrafunctional DEL Building Blocks

The successful functionalisation of *N*-Ac piperidine with trifunctional NHBoc aniline **135** opened opportunities for the synthesis of DEL building blocks with 3 diversification points, with an additional elaboration handle on the ring heteroatom besides the two existent on the arene.

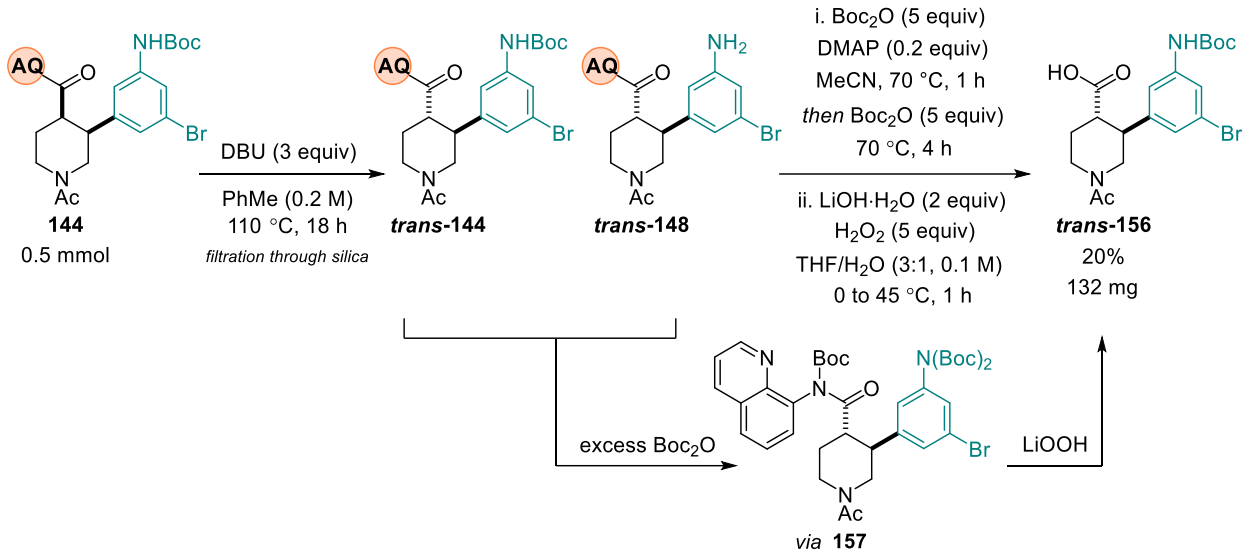
Boc activation of aminoquinoline amide, followed by amide hydrolysis proceeded smoothly on *N*-Ac protected piperidine **144**, affording over 100 mg of acid **156** in 61% yield over the telescoped steps (Scheme 2.66). As in the case of the cyclic sulfone, preferential removal of aminoquinoline over amide Boc deprotection was enabled by addition of LiOH·H_2O and H_2O_2 in 2 equal portions, up to a total of 3.2 and 8 equivalents, respectively.



Scheme 2.66 Boc activation and AQ deprotection on *cis N*-Ac piperidine **144**, with portionwise addition of hydrolysis reagents.

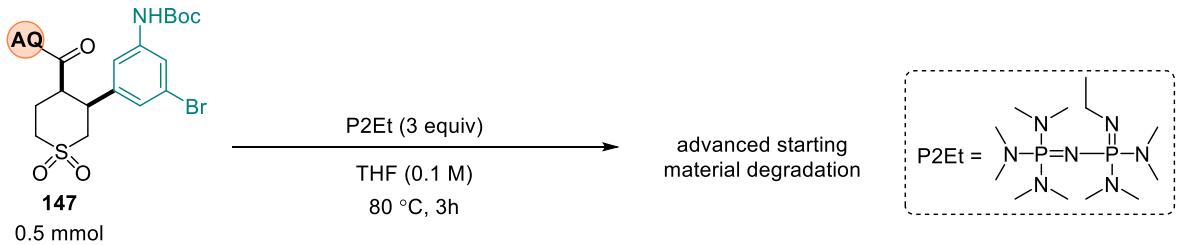
Finally, a strategy was devised to also allow deriving the corresponding *trans* carboxylic acid from **144**. Previous studies have demonstrated that DBU epimerisation of **144** in a discrete step is the most viable route towards accessing the *trans* epimer, albeit with competing aniline Boc deprotection (Section 2.3.3.3). Moreover, further deprotection of desired ***trans*-144** was found to occur on silica during

purification, given the presence of excess DBU. Interestingly, subjecting the crude mixture of *trans* epimers to the amide activation step after a short filtration through a plug of silica resulted in global Boc protection at all available sites on ***trans*-144** and ***trans*-148**, converging to the formation of single intermediate **157**. Conveniently, this intermediate could be carried directly to the LiOOH hydrolysis step to unveil the C(4) carboxylic acid, as well as simultaneously mono-deprotect the aniline. Due to a higher perceived lability of the aniline Boc group under basic conditions, lower loadings of $LiOH{\cdot}H_2O$ and H_2O_2 were employed as a precaution. ***Trans*-156** was isolated in 20% yield after acid-base work-up as the only carboxylic acid product (Scheme 2.67). Notably this was achieved *via* a 3-step telescoped process from **144** consisting of epimerisation – amide activation – AQ hydrolysis, requiring no chromatographic separations.



Scheme 2.67 Telescoped epimerisation – amide activation – AQ hydrolysis procedure for the synthesis of a *trans* carboxylic acid directly from *cis*-arylated piperidine **144**.

Unfortunately, application of the 3-step telescoped epimerisation-deprotection procedure on *cis*-arylated 6-membered cyclic sulfones proved unsuccessful, leading to no evidence of acid formation. DBU-mediated epimerisation was unsuccessful in this case, affording only trace amounts of *trans* isomer and almost complete recovery of unreacted starting material. Epimerisation in the presence of a phosphazene base (P_2Et) was attempted – however, this also led to significant degradation of sulfone, as previously experienced with other bases (Scheme 2.68). Section 2.4 will describe an alternative route to accessing *trans* isomers by switching the diastereoselectivity of the C(3) arylation reaction.



Scheme 2.68 Attempted epimerisation of **147** in the presence of a phosphazene base.

2.3.6 DEL Building Block Library Overview and Conclusions

A total of 9 building blocks for the elaboration of DNA-encoded libraries were synthesised in only 3 steps each from common feedstocks, showcasing underrepresented trifunctional and even tetrafunctional scaffolds. Taking advantage of the favourable physicochemical properties of 6-membered saturated heterocycles, C(sp^3)–H functionalisation was employed as a strategy for installing desired structural features to generate the 3 designs summarised in Figure 2.28.

The highly *cis* stereoselective C(3) functionalisation in the presence of a C(4) aminoquinoline directing group was now demonstrated on the large scale in the presence of more sterically demanding coupling partners, such as a di-*meta*-substituted arene, for which a facile multigram synthesis has also been reported.

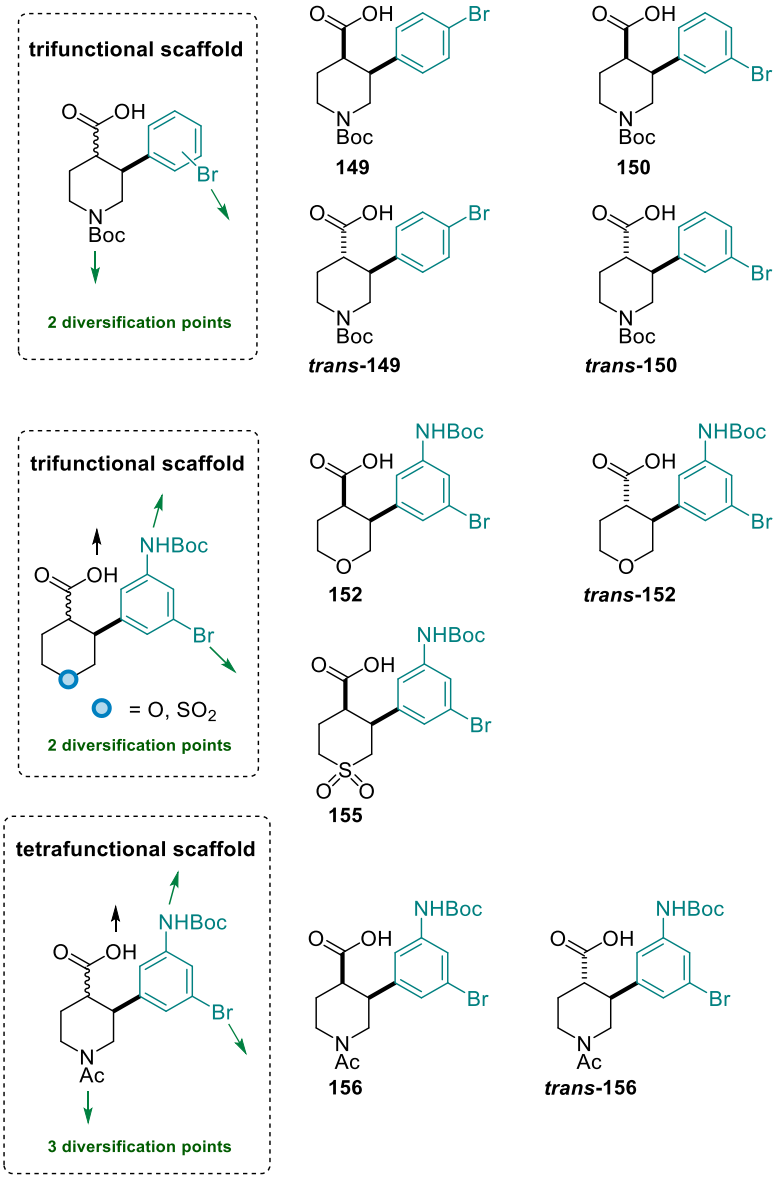


Figure 2.28 Summary of synthesised heterocyclic scaffolds for DEL library elaboration.

Compared to mono-brominated aryl iodides, this substituent posed significant challenges in the epimerisation of *cis* products to corresponding *trans* diastereomers, however, solutions were proposed according on the structural particularities of the substrate. In all cases, methods were successfully developed for aminoquinoline removal to the corresponding C(4) carboxylic acids, which would act as points for DNA attachment. At least 2 other points of diversification were present on each building block, either from the endocyclic heteroatom or the C(3) aryl, to enable construction of large DEL libraries in highly branched fashions. Overall, the range of pharmacophores and diversification handles, as well as the different stereochemical configurations would enhance the quality and shape-diversity of the drug-like compounds produced through split-pool iterations, despite limitations with regards to DNA-compatible chemistry. Moreover, all piperidines were accessed in at least 100 mg quantities, with at least 30 mg of the other O and/or SO_2 substrates, demonstrating availability of synthetic tools for off-DNA synthesis of potential hits in useful quantities.

.

2.4 Enantioselective C(sp^3)–H Functionalisation of Piperidines Bearing a C4 Directing Group

2.4.1 A Chiral Ligand Strategy

Biological homochirality is one of the fundamental hallmarks of life.[252] Enantiomerically pure molecules are omnipresent in nature, either as building blocks or as products of biological pathways. Scientists have always been fascinated by and sought to explain the origin of single-handedness in the biological world – an aspect closely related to the origin of life itself.

The phenomenon of chirality in nature has major implications in the discovery of new drugs, since proteins in the human body would recognise ligands in an enantioselective fashion. The two enantiomers of a racemic drug could therefore have significantly different profiles in terms of biological activity, toxicology, pharmacokinetics and metabolism, hence requirements are in place to ensure a good understanding of the individual effects of each isomer,[253] as well the potential for *in-vivo* interconversion between the two.[254] Up until 2002, 88% of the available chiral drugs were marketed as racemates. [255] However, in 2015, 44 of the 45 approved chiral drugs were formulated as single enantiomers, suggesting a clinical advantage of single stereoisomer drugs and increased efforts towards accessing them.[256] Depending on the structural particularities of a molecule, separation of individual enantiomers out of a racemic mixture can be time-consuming.[257] Alternatively, desired enantiomeric forms can be derived from the chiral pool or by resolution of racemates. Asymmetric synthesis provides opportunities for *de novo* assembly of a wide variety of compound classes in enantiomerically pure forms.[258] However, as illustrated below, methodologies are limited for the derivatisation of common pharmacophores such as saturated heterocycles in an enantioselective fashion, or require the use of expensive chiral catalysts.[271] The importance of accessing highly 3-dimensional molecules in single enantiomeric forms has increasingly been recognised in the context of modern drug discovery, especially in combinatorial chemistry approaches that would allow a quick and rigorous exploration of chemical and chiral space.[68] Moreover, having the synthetic tools to fine-tune the absolute configuration of stereogenic centres of a hit would tremendously improve the ability to synthesise improved drugs in the future.

Pd-catalysed asymmetric functionalisations have been achieved on a series of sp^3 substrates by judicious choice of directing groups and chiral ligands (Sections 2.4.1.2 and 2.4.1.3).

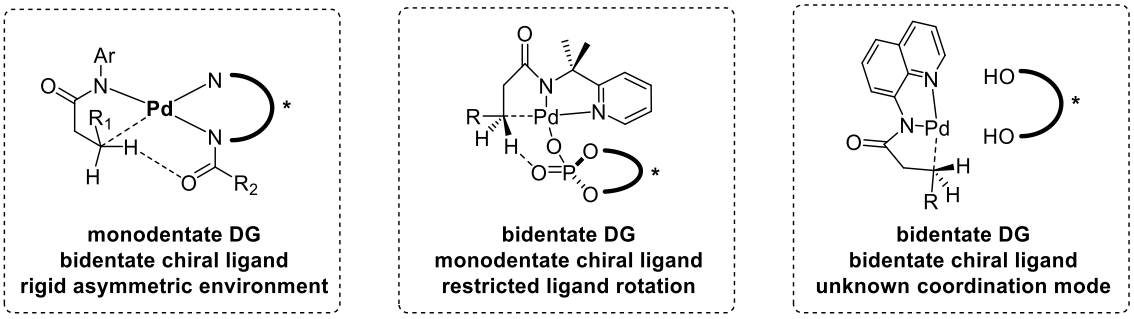


Figure 2.29 Overview of the chiral ligand strategies employed in enantioselective C(sp^3)–H functionalisation.

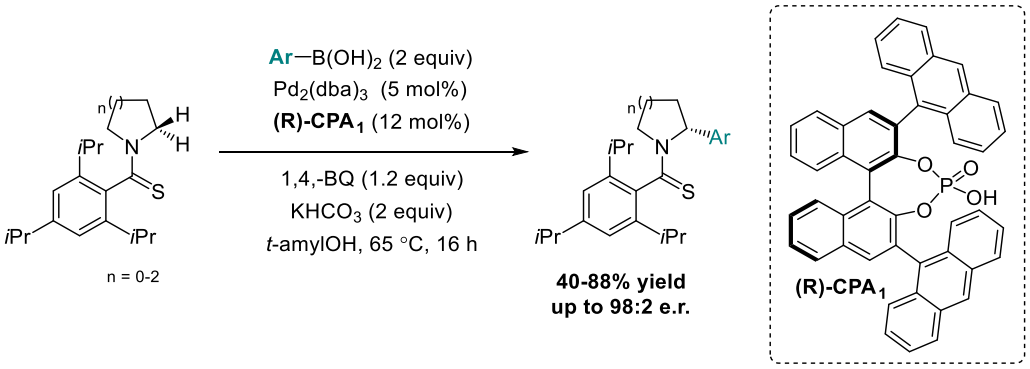
Based on the available Pd coordination sites, the following scenarios have been described, as illustrated in Figure 2.29: i. monodentate directing group and bidentate ligand – generating a rigid asymmetric

environment; ii. bidentate directing group and monodentate ligand – with options of tuning the directing group to prevent free ligand rotation and iii. Bidentate directing group and bidentate ligand – with model of coordination unknown.

2.4.1.1 Reported Use of Monodentate Directing Groups and Chiral Ligands

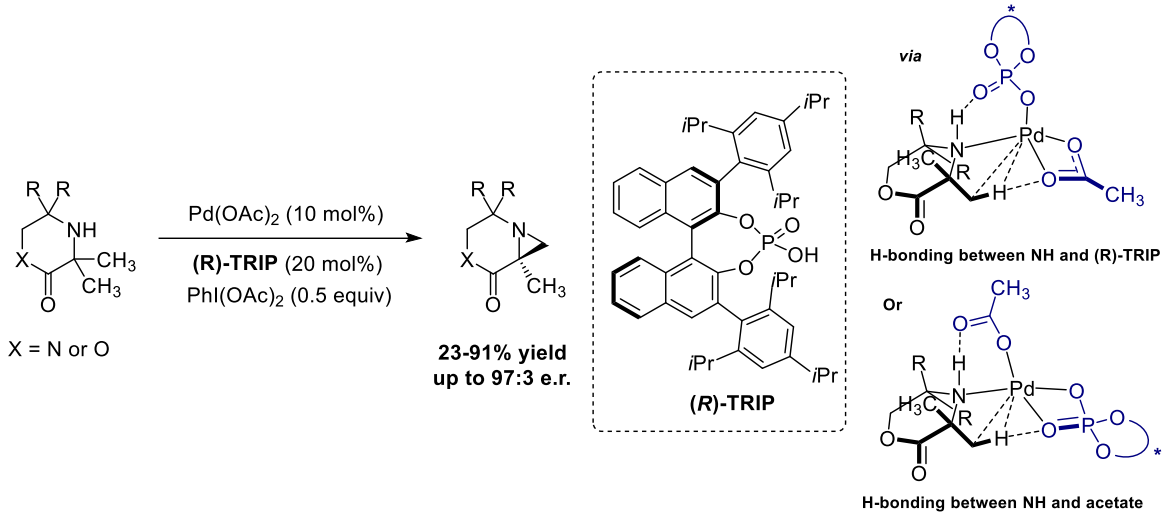
With monodentate directing groups, multiple coordination sites are available on Pd at various points during the catalytic cycle. This allows for bidentate coordination of chiral ligands, which generates a more rigid conformation of the resulting complex, creating a strongly asymmetric environment.

In 2017, Yu and coworkers addressed a longstanding challenge of achieving the enantioselective α-C-H functionalisation of saturated 4, 5 and 6-membered *N* heterocycles using a monodentate thioamide directing group and chiral phosphoric acid ligands (Scheme 2.69).[259] Up until this point, asymmetric functionalisation at these positions could be achieved by enantioselective lithiation and subsequent trapping with electrophiles, requiring however stoichiometric amounts of reagents and having a limited *N*-heterocycle scope.[260,261] In Yu's approach, a Pd(0)/Pd(II) mechanism is in operation and $Pd_2(dba)_3$ is used as catalyst due to the lack of anionic ligands which could potentially enhance background functionalisation in a non-enantioselective fashion. Although the enantioinduction mechanism is not fully understood, **(*R*)-CPA$_1$** ligand bearing bulky 3,3'-anthracenyl substituents affords excellent e.r. values in the presence of a range of aryl boronic acid partners. The methodology is also applicable to the functionalisation of linear alkyl amines.



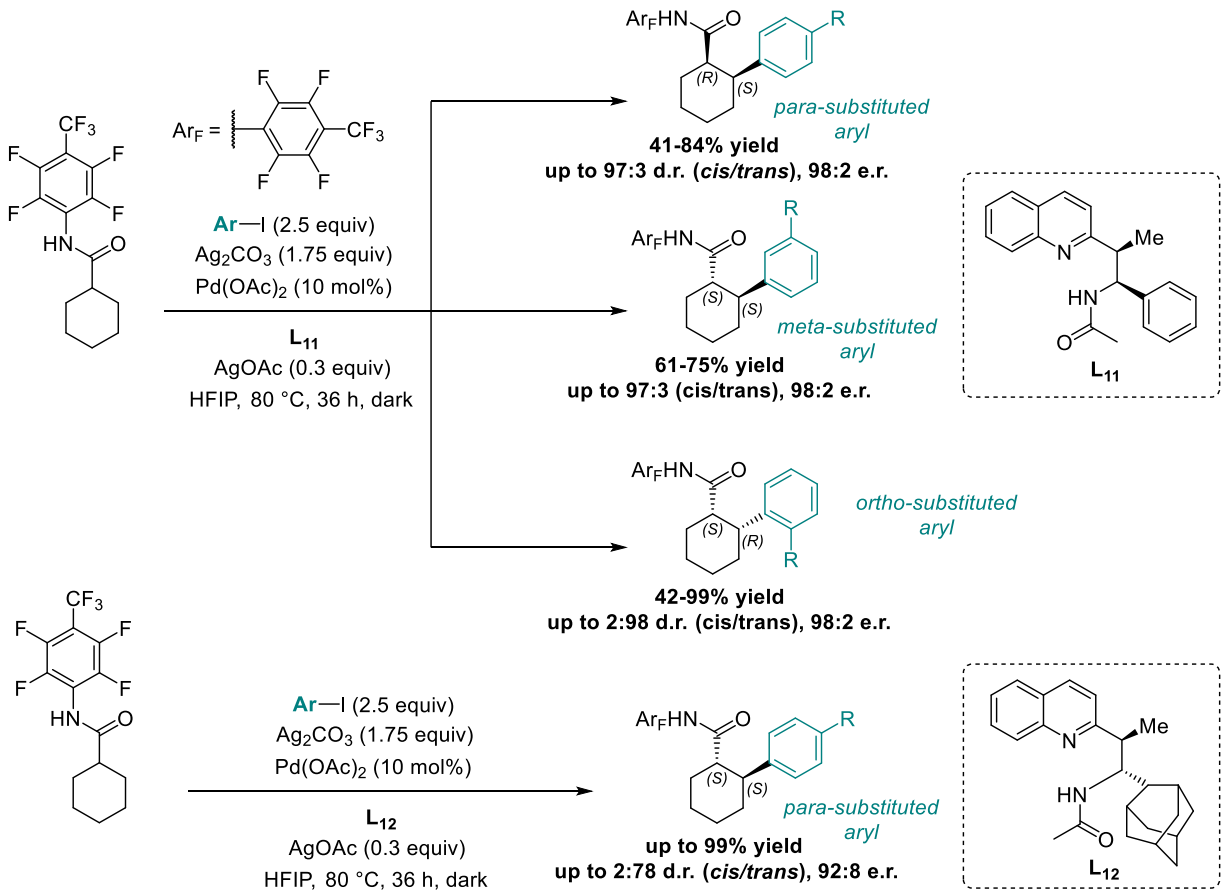
Scheme 2.69 Asymmetric thioamide-directed α-C-H functionalisation of saturated *N* heterocycles.

Weakly coordinating native functionalities such as amines have been used to direct enantioselective C-H activation on methyl C(sp^3)–H bonds, which have lower bond energies compared to methylene. Gaunt and coworkers have reported the intramolecular enantioselective functionalisation between an aliphatic secondary amine and a neighbouring α-methyl group, resulting in aziridine formation (Scheme 2.70).[262] An **(*R*)-TRIP** ligand was used to impart enantioselectivity, whereas PIDA modulated the concentration of acetate which would have otherwise negatively impacted the e.r. Hydrogen-bond control in the C–H cleavage step is thought to account for the observed stereoselectivity, with participation of a Pd(II) complex coordinated to one acetate and one TRIP ligand. A possible pathway could involve H-bonding between NH and the chiral ligand, allowing cleavage of an enantiotopic C–H to be mediated by the acetate ligand. A second possibility would see the acetate interacting with the NH through H-bonding, allowing an enantioselective CMD mediated by the TRIP ligand.



Scheme 2.70 Enantioselective cyclisation by intramolecular C(sp^3)-H amination of methylene mediated by (R)-TRIP.

Highly relevant to this project, Yu reported in 2019 the first example of enantioselective functionalisation on cyclic saturated substrates.[263] Using a perfluorinated tolylamide directing group and bespoke APAQ (acetyl-protected aminoethyl quinoline) ligands, monoarylation of the unbiased cyclohexane ring could be achieved with high regio-, diastereo- and enantioselectivity (Scheme 2.71).

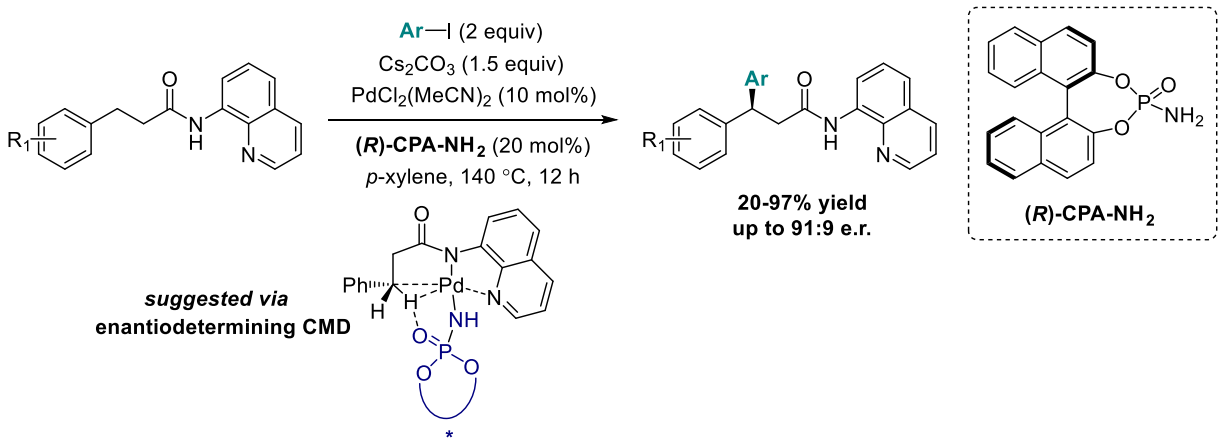


Scheme 2.71 Enantio- and diastereoswitchable C(sp^3)-H mono-functionalisation of cyclohexane.

Interestingly, the steric demands of the aryl were found to influence the stereochemical outcome, with *p*-, *m*- and *o*-substituted aromatics each leading to a different major enantiomer. Also, while *p*- and *o*-substituted aryls afforded *cis* isomers, the *trans* diastereomer was formed with *m*-substituted coupling partners. This could point to a stereodetermining oxidative addition, in which the aryl occupies the least hindered space in coordinating to the Pd(IV) complex. The ligand could also dictate specific enantio- and diastereoselectivity, with **L_{11}** affording the *cis* (*R,S*) enantiomer and **L_{12}** giving the *trans*-(*S,S*) enantiomer in the presence of *p*-substituted aryl iodides.

2.4.1.2 Reported Use of Bidentate Directing Groups and Chiral Ligands

Bidentate directing groups have by far the most widespread use in directing functionalisation of unbiased methylene groups. Pioneering work by Duan first reported the enantioselective Pd-catalysed C(sp^3)–H functionalisation in the presence of the aminoquinoline amide directing group.[264] Using a chiral phosphoric amide ligand, e.r. values of up to 91:9 were achieved in the arylation of linear substrates at activated benzylic positions (Scheme 2.72). The active palladium species involved in C–H activation was suggested to display the bidentate aminoquinoline and the monodentate phosphoric amide ligands coordinated through the nitrogen atoms, the latter inducing enantioselectivity in the CMD step through its chiral backbone. With phosphoric acids not as efficient in accelerating the reaction rate, it was hypothesised that the higher basicity of the P=O bond in **(*R*)-CPA-NH_2** enhanced the rate-determining C–H cleavage step.



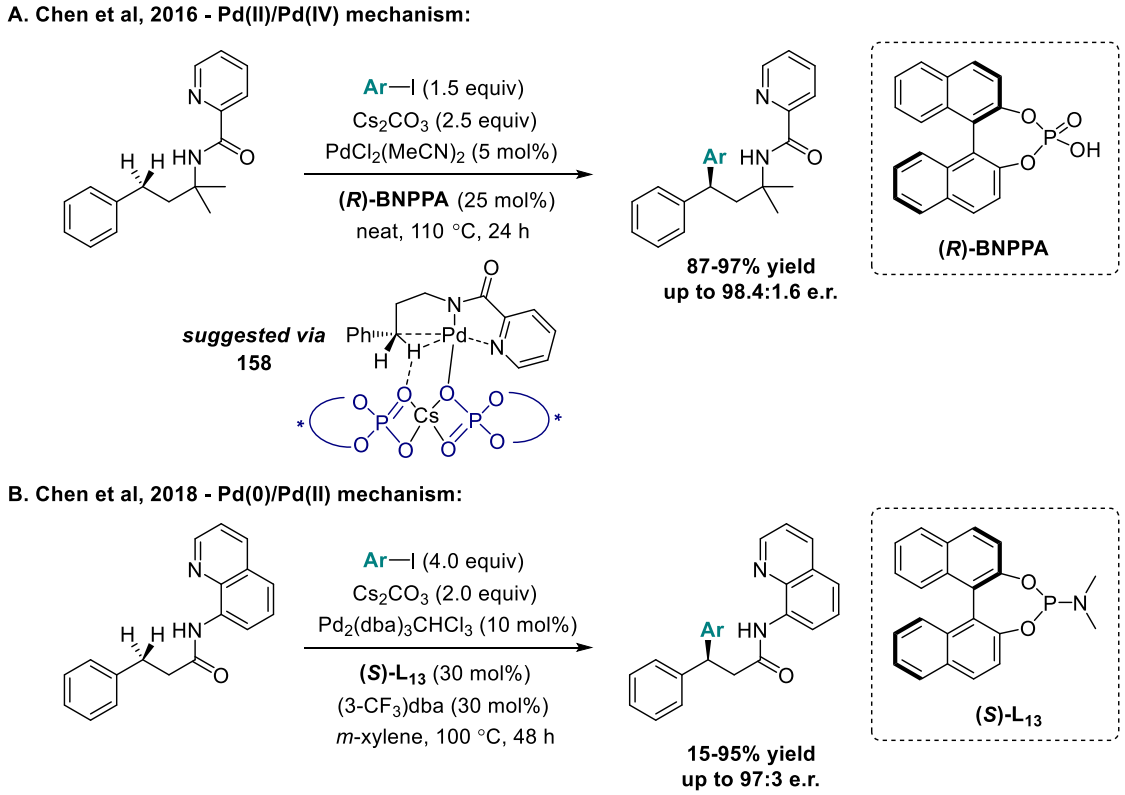
Scheme 2.72 Enantioselective C(sp^3)–H arylation at benzylic positions using a chiral phosphoric amide.

The procedure led to poor enantioselectivity when applied to the functionalisation of unactivated and/or unbiased methylene groups in linear alkanes. Reasons for this could include the unrestricted rotation of the mono-coordinated chiral ligand in the pre-CMD transition state,[265] as well as background C–H activation promoted by the aminoquinoline auxiliary alone.[266,126]

In 2016, Chen and co-workers developed a similar protocol on linear saturated chains, this time aimed at the enantioselective functionalisation of benzylic positions situated γ to a picolinamide directing group (Scheme 2.73A).[267] The use of **(*R*)-BNPPA** and Cs_2CO_3 as base were essential for achieving high levels of enantioinduction, with up to 98.4:1.6 e.r. seen. Moreover, further mechanistic studies were conducted, aimed at determining the variation in the *ee* of desired product as a function of the chiral ligand *ee*.

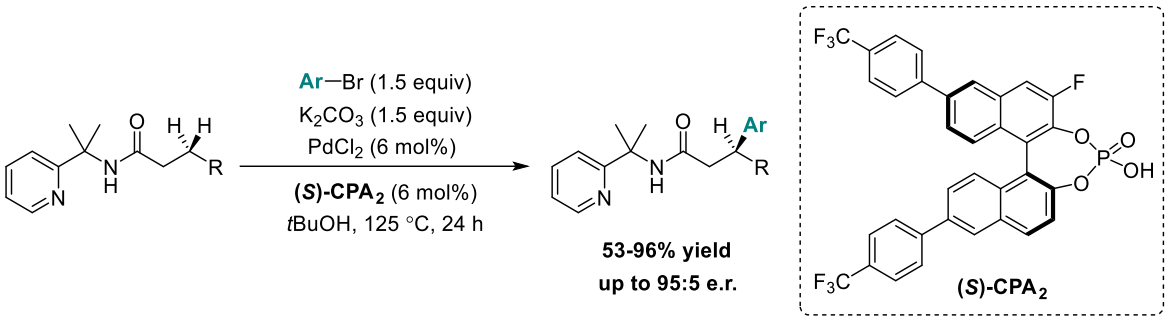
Crucially, the non-linear relationship found invalidated previous assumptions that a single molecule of chiral ligand is involved in the enantiodetermining step.[264] It was hence suggested that the essential role of Cs^+ might consist in the formation of phosphoric acid clusters, due to its size and ability to coordinate to multiple anions. Coordination of two molecules of **(*R*)-BNPPA** to Cs^+ could result in scenario **158** whereby one acid communicates with Pd, whilst the other acid induces an enantioselective C–H abstraction. In 2018, Houk reported a detailed computational investigation of the reaction mechanism which denied the involvement of **158** in the catalytic cycle.[268] The model accounting for the experimentally observed enantioselectivity was found to display a single chiral phosphoric acid molecule coordinated to Pd in monodentate fashion, with the P=O bond involved in an enantioinductive C-H abstraction. Key to the observed enantioselectivity were the stabilising edge-to-face aryl-aryl interactions between the ligand and the pre-existent phenyl on the substrate, during the transition state leading to C–H activation. The Cs cation, as well as potential ligand clusters bound by it were therefore suggested to have off-catalytic roles.

Also in 2018, Chen developed an unprecedented aminoquinoline-directed functionalisation proceeding through a Pd(0)/Pd(II) manifold (Scheme 2.73B).[269] In this case, oxidative addition precedes C–H abstraction, with the resulting Pd(II) complex stabilised by the phosphoramidite ligand **(*S*)-L_{13}**. Consequently, a chiral environment is ensured throughout the following catalytic steps, with the competing Pd(II)/Pd(IV) process which would erode enantioselectivity inhibited by addition of excess dba ligand. DFT calculations supported in this case an enantiodetermining C–H activation in which both phosphoramidite **(*S*)-L_{13}** and Cs_2CO_3 are involved.



Scheme 2.73 Enantioselective C(sp^3)–H arylation: (A) at activated γ positions with a picolinamide directing group. (B) through a Pd(0)/Pd(II) manifold using an aminoquinoline directing group and a phosphoramidite ligand.

Shi employed the 2-pyridinylisopropyl (PIP) directing group (Scheme 2.74).[270] The *gem*-dimethyl moiety on the PIP backbone was argued to lock the chiral phosphoric acid ligand on Pd in a more rigid conformation, leading to high levels of enantioinduction. Indeed, using the non-C_2-symmetrical phosphoric acid ligand **(*S*)-CPA$_2$**, arylation of unbiased methylene C–H bonds could be promoted in high yields and consistent e.r. values, even when using aryl bromide coupling partners. As expected, modifications of the directing group backbone to reduce the steric hindrance negatively impacted the yield and stereochemical outcome. Lastly, KIE studies revealed the C–H activation as being rate-determining, whilst a linear relationship was found between the *ee* of **(*S*)-CPA$_2$** and the *ee* of arylated product. By contrast to the picolinamide-directed functionalisation, a single ligand seemed to contribute to determining e.r. in this case, though no mechanistic studies aimed at elucidating the stereodetermining step were reported.

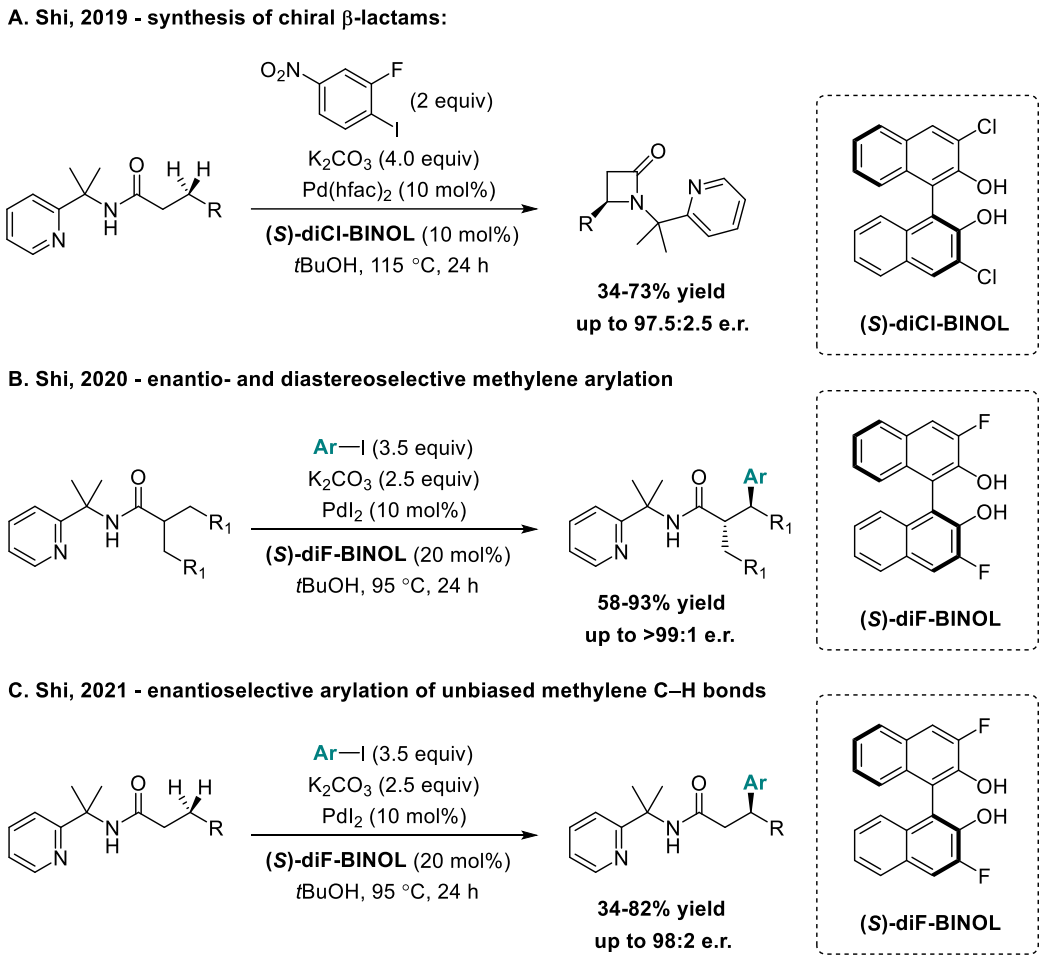


Scheme 2.74 Enantioselective C(sp^3)–H arylation of linear alkyl substrates at unactivated methylene position using a PIP directing group.

Despite the limited number of coordination sites on Pd in the pre-transition intermediate leading to C–H activation, strongly coordinating bidentate ligands have been successfully used in conjunction with bidentate directing groups to promote a desymmetrising C–H functionalisation,[271] though the mechanism of enantioinduction is currently unknown.

Shi first reported the first use of a chiral BINOL ligand to achieve the enantioselective alkynylation of linear alkenes, as directed by the PIP auxiliary.[272] To prevent a background non-enantioselective CMD accelerated by anionic ligands such as acetate, a PdI_2 catalyst was used, whereas a 3,3'-difluoro-substituted BINOL was found to induce the highest e.r., arguably due to increased acidity of the hydroxyl groups. Further developments allowed an intramolecular amination of linear aliphatic PIP carboxamides to form β-lactams.[273] **(*S*)-diCl-BINOL** was used as ligand, together with an electron deficient aryl iodide to act as oxidant and hinder intermolecular cross-coupling (Scheme 2.75A).

Later on, Shi demonstrated excellent diastereo- and enantiocontrol in the arylation of symmetrical dialkyl substrates, which pose significant challenges due to their high rotational freedom (Scheme 2.75B).[274] Using a PIP directing group and **(*S*)-diF-BINOL**, two contiguous stereocentres could be defined in one step, with a second functionalisation possible in order to set 3 contiguous stereogenic centres. Finally, a similar transformation to the one illustrated in Scheme 2.74 could be demonstrated by the same group in the presence of a BINOL ligand instead of a phosphoric acid (Scheme 2.75C).[275]



Scheme 2.75 Enantioselective C(sp^3)–H functionalisations in the presence of bidentate directing groups and bidentate BINOL ligands.

This methodology has later been expanded to allow methylene functionalisation with pre-existent substituents in an intramolecular fashion to synthesise chiral benzo-fused analogues.[276,277]

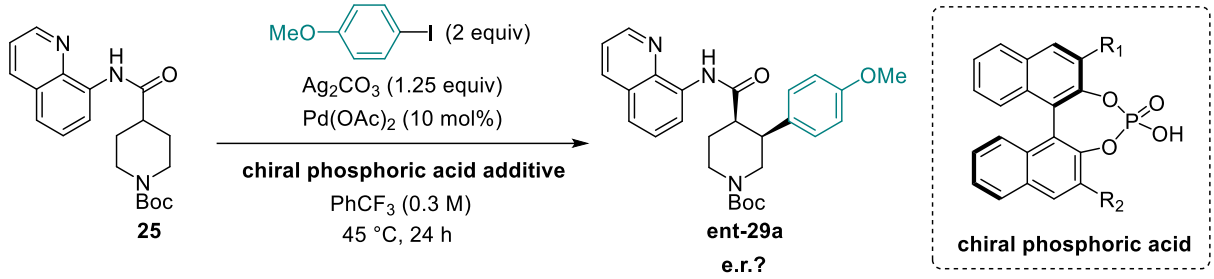
2.4.2 Project Aims

With piperidines being privileged motifs in medicinal chemistry, and inspired by earlier success in the highly selective functionalisation of these cores to isolate single diastereomeric products (either *cis* or *trans*), the development of an asymmetric variant was now aimed for. Crucially, enantioselective C–H functionalisation reactions of saturated heterocycles at positions remote from the heteroatom are not yet known.

With tools available for the deprotection of C(4) aminoquinoline amides, maintaining the same directing group was initially targeted. Starting with the available *N*-Boc substrate **25** from previous studies, enantioselectivity was aimed to be imparted to the expected *cis*-arylated piperidine by use of a commercially available chiral phosphoric acid as additive (Scheme 2.76).

A screen of chiral phosphoric acids would first be conducted, seeking to observe enhancement in enantioselectivity based on participation of the phosphate in concerted metalation-deprotonation and/or continuation of the catalytic cycle with this as a ligand on Pd, preserving an asymmetric environment

during any stereodetermining step. Moreover, a high yield may also be attainable, with some ligands known for enhancing the C–H abstraction process by providing a lower energy pathway alternative.[114,278] A series of Pd sources may also be trialled, focusing on catalysts that do not already possess ligands able to participate in the CMD, in order to maximise participation of the chiral phosphate. Alternatively, an asymmetric functionalisation may be developed *via* any of the other strategies previously discussed in this chapter, through combinations of either bidentate auxiliaries with bidentate ligands or monodentate ligands with bidentate auxiliaries. Finally, a mechanistic explanation of the enantioinduction event would be sought, together with the demonstration of a wide aryl iodide and heterocycle scope and removal of the C(4) auxiliary with retention of configuration at the stereodefined C(3) and C(4) centres formed in this reaction.

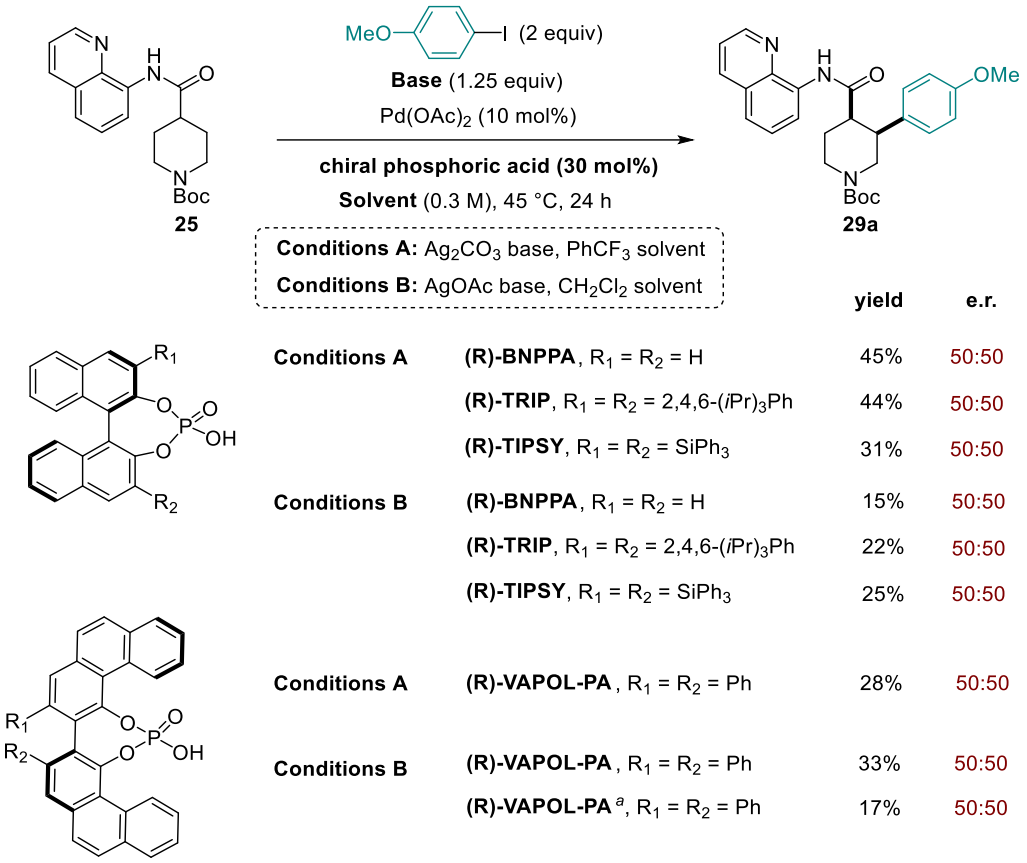


Scheme 2.76 Initial plan for achieving a *cis* enantioselective C(3)–H functionalisation in the presence of a chiral phosphoric acid and a C(4) aminoquinoline amide directing group.

2.4.3 Methodology Development

2.4.3.1 Exploring Chiral Phosphoric Acid (CPA) Ligands

A range of **(*R*)-** and **(*S*)-BINOL** derived phosphoric acids were screened as additives under the standard reaction conditions,[168] using *N*-Boc piperidine **25** with *p*-methoxyphenyl iodide as the coupling partner (Scheme 2.77). With an unsubstituted binaphthyl core, **(*R*)-BNPPA** gave the highest product yield (45%) – interestingly this was mirrored by **(*R*)-TRIP** despite its 3,3' substitution with bulky phenyl groups. Similar yields were obtained with the opposite enantiomers, **(*S*)-BNPPA** and **(*S*)-TRIP**, however, no enantioselectivity was observed in these cases either. On the other hand, the presence of 3,3' substituents linked through Si in **(*R*)-TIPSY**, as well as the polyaromatic core in **(*R*)-VAPOL-PA** appeared detrimental to reactivity. Nevertheless, lower levels of mono-*cis* arylation were observed in all cases compared to the racemic variant using MesCOOH, which afforded yields up to 70% (see Section 2.1.1.3). Despite exclusive formation of the mono-*cis* arylated piperidine in all cases, none of the trialled acids were capable of inducing enantioselectivity, with racemic products isolated.

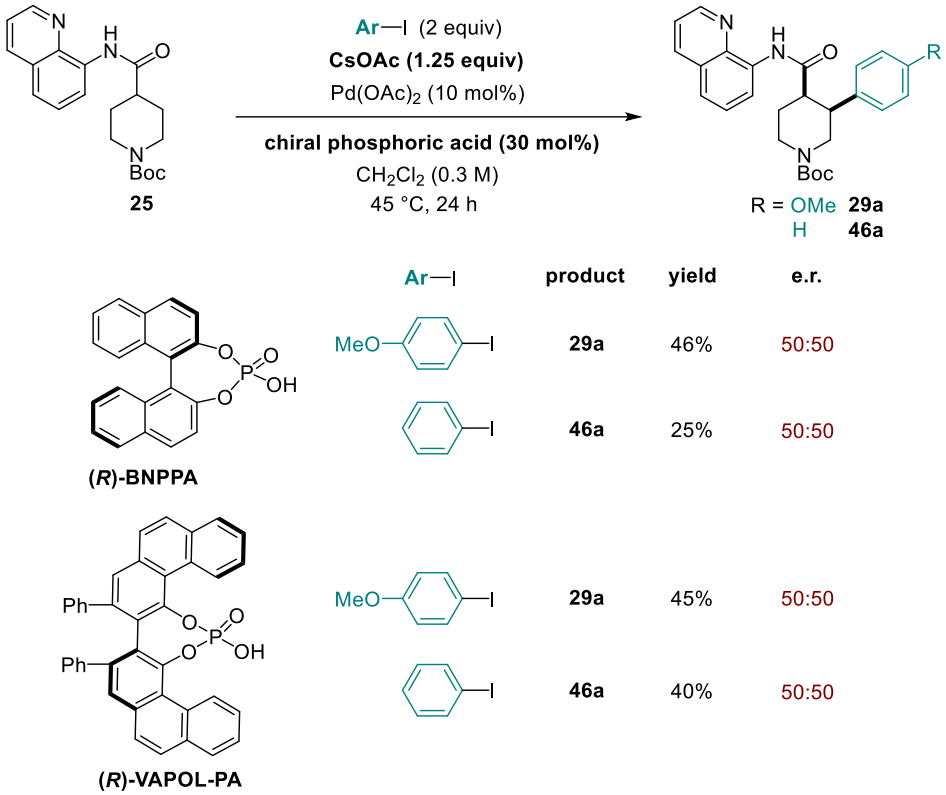


Scheme 2.77 Chiral phosphoric acid (CPA) additive screen under the standard reaction conditions. Isolated yields shown. [a] Conducted at 25 °C.

The lack of enantioselectivity was ascribed to a competition between the carbonate, acetate and phosphate ligands in coordinating to the metal centre.[272] To minimise potential background processes, silver carbonate was replaced by silver acetate in order to match the Pd catalyst counterion. Moreover, aromatic solvents have been speculated to disrupt π-π interactions conducive to enantioinduction in C-H functionalisation, such as the stacking between chiral ligand and aromatic motifs on the substrate.[267,268] To prevent this, trifluorotoluene was also replaced by dichloromethane. The chiral phosphoric acids from above were screened again under Conditions B, however, no enantioinduction was observed (Scheme 2.77). However, higher yields were seen, with **(*R*)-VAPOL-PA** affording 33% mono-*cis* arylation at 45 °C. The **(*R*)-VAPOL-PA** mediated reaction was repeated at 25 °C to study the possibility of controlling enantioselectivity at lower temperatures. Unfortunately, the racemic *cis* product was again generated.

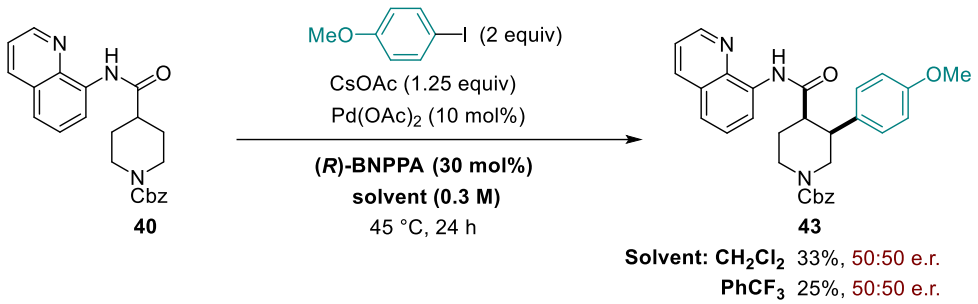
Seeking to explore alternative bases, CsOAc was one of the most promising choices due to the higher coordination number of the Cs^+ cation. Multi-ligated species may be able to increase enantiocontrol by enhancing arene-arene interactions or aiding off-cycle ligand association.[267,268] With CsOAc as base, **(*R*)-BNPPA** and **(*R*)-VAPOL-PA** were screened again, this time also varying the electronics of the coupling partner (Scheme 2.78). Whereas the enantiodetermining step is unknown at this stage, the electron-rich *p*-methoxyphenyl iodide may enhance formation of both *cis* enantiomers at similar rates. To counteract this, for each chiral additive, reactions were run in parallel using iodobenzene as

electrophile. Unfortunately, even after minimising the electronic bias on the aryl group, no enantioselectivity was observed, despite formation of **29a** and **46a** in moderate to good yields.



Scheme 2.78 Chiral phosphoric acid (CPA) additive screen using CsOAc base and varying the aryl coupling partner. Isolated yields shown.

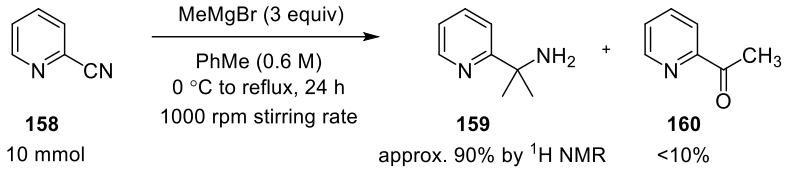
Finally, it was envisaged that the lack of suitable stereochemical communication between the piperidine substrate and the chiral ligand might explain the lack of selectivity. To promote new aryl-aryl stacking interactions between the two, piperidine **40** bearing an *N*-Cbz protecting group was subjected to the CsOAc-mediated conditions in the presence of **(*R*)-BNPPA** (Scheme 2.79). Again, even with reverting back to the use of trifluorotoluene as solvent, no interactions conducive to enantioinduction occurred.



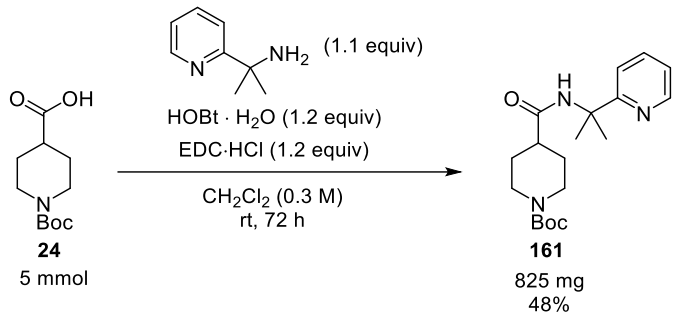
Scheme 2.79 Increasing aromatic features on the substrate - trialling *N*-Cbz protected piperidine under the **(*R*)-BNPPA** mediated reaction conditions. Isolated yields shown.

2.4.3.2 A 2-(Pyridin-2-yl)isopropyl Amine (PIP) Directing Group

In reports by Shi, greater enantiocontrol was achieved when substrates possessed steric features that restrict the rotational freedom of metal-coordinated chiral phosphoric acids, such as the *gem*-dimethyl moiety on the PIP directing group (see Section 2.4.1.2).[270] Some of the previous screens were therefore repeated in the presence of the PIP directing group instead of aminoquinoline (Scheme 2.82). Additionally, this new directing group exhibited a higher degree of 3-dimensionality, with rotation of the pyridyl moiety possible in order to potentially enhance π-π interactions with other aromatic components. Firstly, the PIP directing group **159** was synthesised on 10 mmol scale by a double Grignard addition to 2-cyanopyridine **158** (Scheme 2.80).[169] A high stirring rate (1000 rpm) during the dropwise addition of the Grignard reagent was essential to obtaining the desired amine in excellent yield, while minimising the formation of ketone side-product **160** by hydrolysis of the corresponding imine intermediate. With only **159** participating in the subsequent amide coupling, the crude mixture was used in the directing group installation stage, which afforded 48% yield of *N*-Boc piperidine **161** (Scheme 2.81).



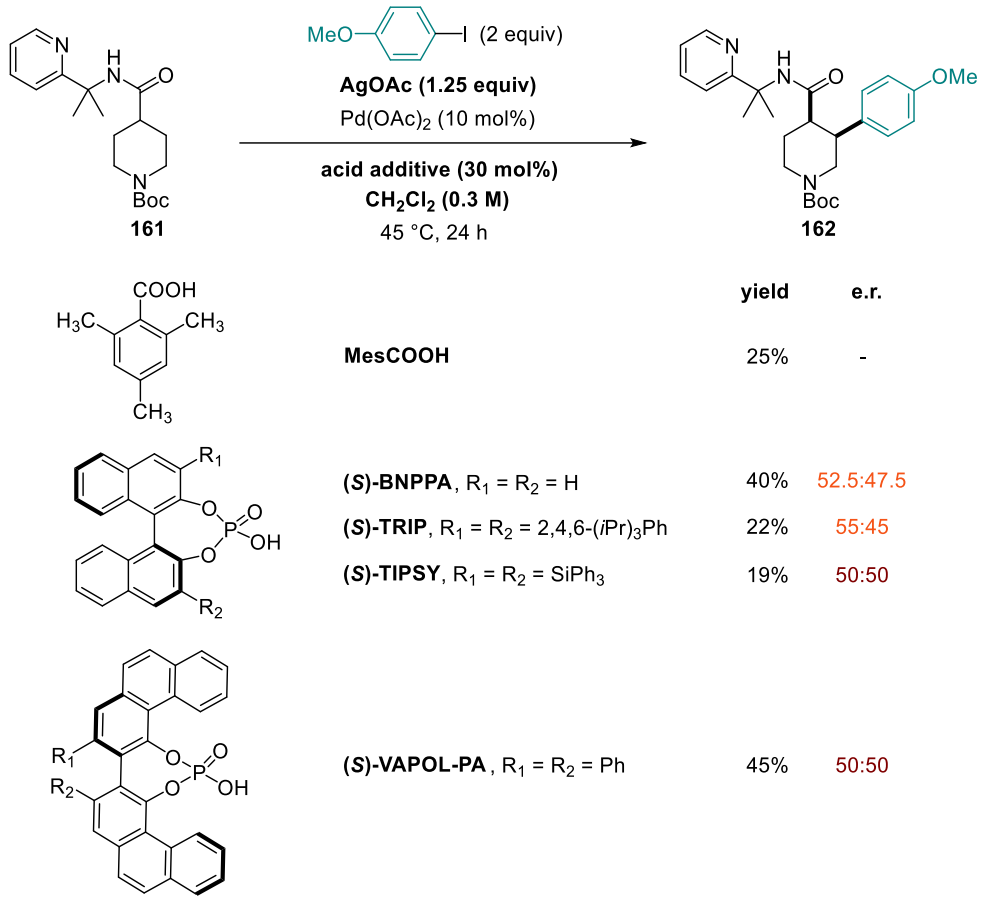
Scheme 2.80 Synthesis of the PIP directing group by double Grignard addition to 2-cyanopyridine.



Scheme 2.81 Installation of the PIP directing group by amide coupling with the piperidine C(4) carboxylic acid.

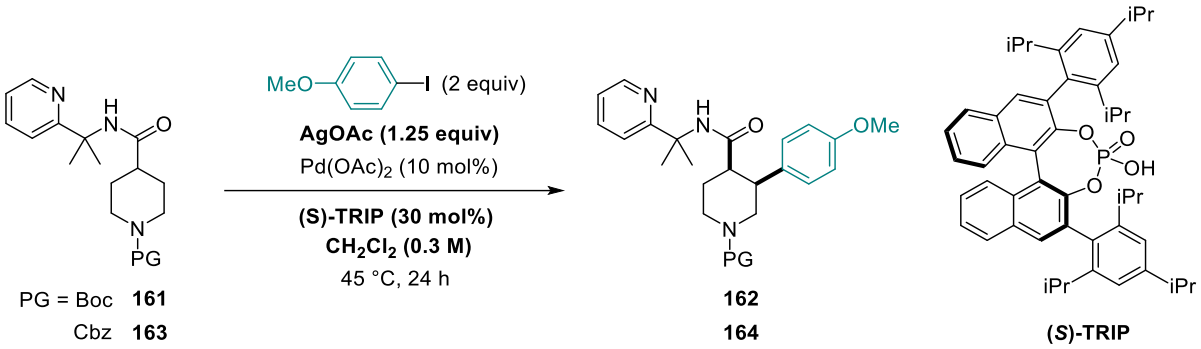
The PIP-containing substrate **161** was subjected to arylation under the modified conditions using AgOAc base and CH_2Cl_2 solvent (Scheme 2.82). (*S*)-Configured phosphoric acids were screened, with the reactivity outcomes compared against the MesCOOH mediated reaction. With **162** being the only arylated piperidine isolated in all cases, assessing its yield by ^{1}H NMR analysis of the crude reaction mixture by was complicated by peak broadening. This is most likely due to H-bonding interactions promoted by the PIP directing group, which were found to occur regardless of the range of NMR solvents trialled ($CDCl_3$, methanol-d_4, acetone-d_6). Instead, isolated yields of **162** were reported in all cases. **(*S*)-BNPPA** afforded **162** in 40% yield, this time with a small bias observed in e.r. (52.5:47.5). Moreover, compared to the racemic variant in presence of MesCOOH a significant involvement of the chiral ligand in the catalytic cycle was evident through an observed improvement in yield. However, ligands with bulky 3,3' biaryl substituents such as **(*S*)-TRIP** and **(*S*)-TIPSY** seemed to inhibit the formation of **162** compared to the MesCOOH-mediated racemic variant. Nevertheless, **(*S*)-TRIP** led to the highest e.r. observed so

far (55:45), suggesting that the enantiodetermiming step is different from the rate-determining step, since the latter seems to be negatively impacted by this ligand as reflected by the yield. Finally, **(*S*)-VAPOL-PA** significantly enhanced the yield of **162** to up to 45%, though no enantioinduction was observed.



Scheme 2.82 Additive screen in the presence of the PIP directing group. Isolated yields shown.

With **(*S*)-TRIP** as the additive of choice, further modifications to the reaction conditions were investigated to improve the observed e.r. (Table 2.16). Firstly, a marked difference in reactivity was observed between the *N*-Boc protected **161** and *N*-Cbz piperidine **163**, the latter undergoing no transformation under the functionalisation conditions (entry 2). With **161** as model substrate, reducing the temperature to 25 °C led to a decrease in the yield of **162**, but identical levels of enantioinduction (entry 3). Trialling other bases commonly used in enantioselective C(sp^3)–H functionalisations [270,272-277] led to either very low conversion in the case of CsOAc, or racemic product in the case of K_2CO_3 (entries 4-5). Finally, running the reaction in polar protic solvents [270,272-277] was again unsuccessful in promoting any arylation (entry 6). With no highly enantioselective conditions found, screening stronger coordinating bidentate chiral ligands was next considered.



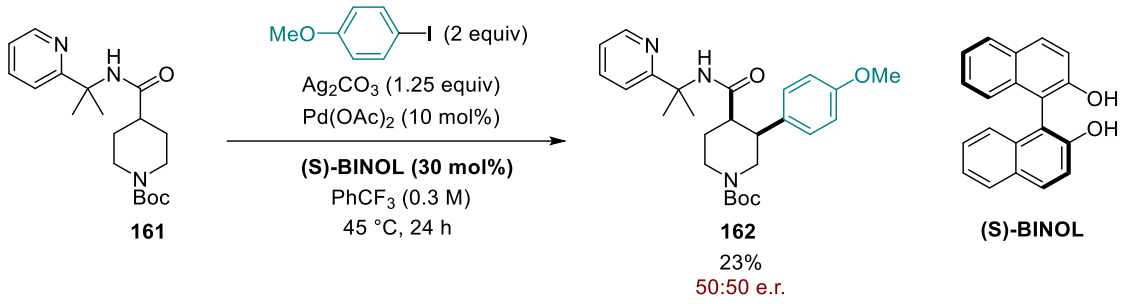
Entry	Substrate	Changes to conditions	mono-*cis* (yield %)[a]	mono-*cis* e.r.
1	**161**	None	**162** (22)	55:45
2	**163**	None	**164** (0)	-
3	**161**	25 °C instead of 45 °C	**162** (13)	55:45
4	**161**	CsOAc instead of AgOAc	**162** (<5[b])	n/a
5	**161**	K_2CO_3 instead of AgOAc	**162** (14)	50:50
6	**161**	*t*-amylOH instead of CH_2Cl_2	**162** (0)	-

Table 2.16 Studying the effect upon the e.r. of the mono-*cis* arylated product with changes in the reaction conditions. Reactions on 0.4 mmol scale. [a] Isolated yield. [b] Yield determined by ^{1}H NMR using 1,3,5-trimethoxybenzene as internal standard – e.r. ratio not determined due to the low conversion.

2.4.3.3 Exploring Bidentate BINOL Ligands

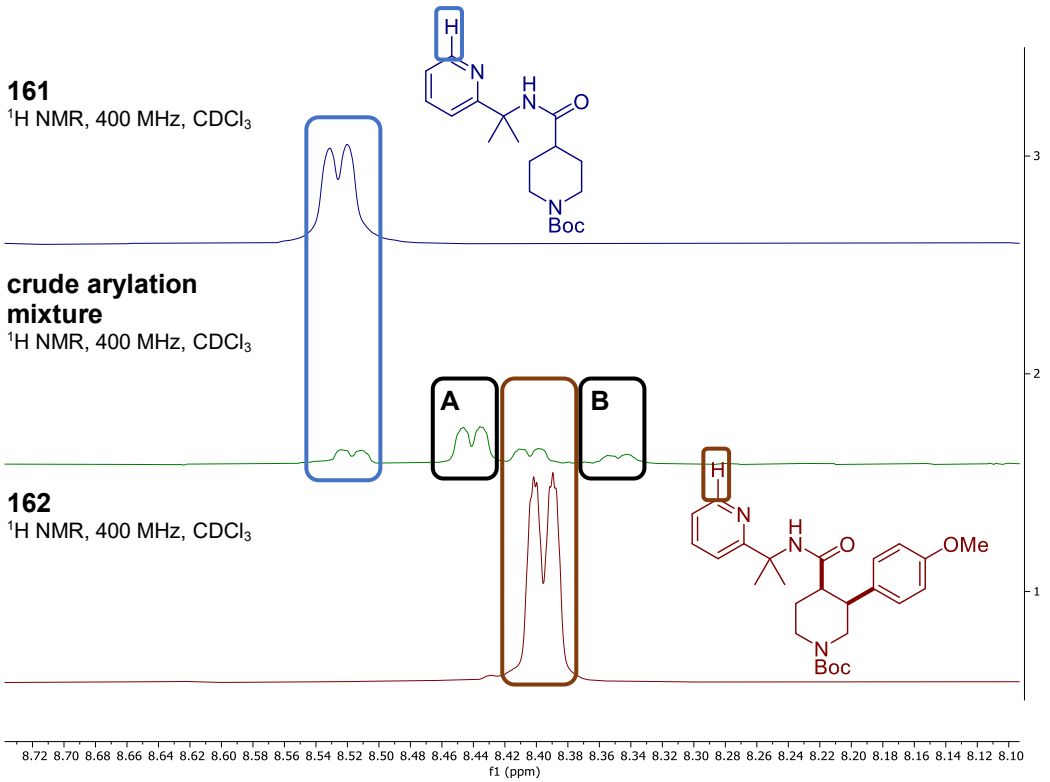
Inspired by the series of protocols developed by Shi, [272-277] the effect of a BINOL additive on the functionalisation of piperidine amide **161** was investigated under previously reported diastereoselective conditions (See Section 2.1.2).[168] Using **(*S*)-BINOL**, mono-*cis* **162** was formed as the only product in 23% yield, however, no evidence of chiral ligand involvement in enhancing enantioselectivity was seen (Scheme 2.83).

Next, commercially available BINOL ligands were screened, this time matching the set of conditions reported by Shi in the functionalisation of symmetrical alkanes, which overcame similar selectivity issues as the ones posed by our substrate.[274] Compared to the use of phosphoric acid additives, less extensive H-bonding interaction now facilitated the analysis of the crude reaction mixtures by ^{1}H NMR. Although **162** is the only isolated product in all cases, spectroscopic evidence supports the formation of additional products.



Scheme 2.83 Trialling (*S*)-BINOL ligand under the previously optimised diastereoselective conditions.

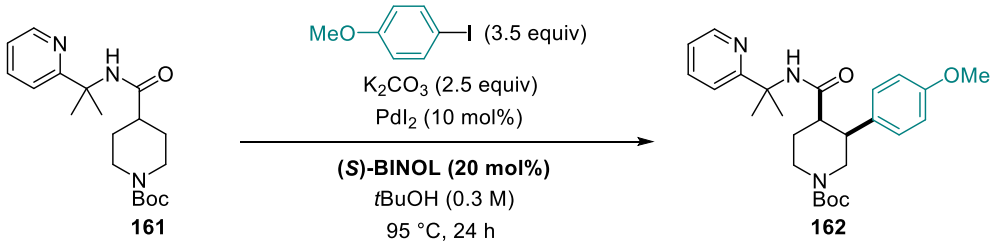
This is best illustrated by the crude mixture of the **(*S*)-BINOL** mediated reaction, which exhibits 4 distinct sets of doublets in the 8.3–8.7 ppm region. Two doublets were identified as originating from the starting material (8.52 ppm) and the *cis*-arylated product (8.41 ppm), respectively, each corresponding to the C(2) proton on the pyridine moiety (Figure 2.29). Given the similarities in chemical shifts and the elevated reaction temperature, the 2 other signals likely correspond to products of PIP-directed functionalisation such as the *trans*, *cis-trans* or *cis-cis* arylated piperidines. Interestingly, unknown product **A** seems to form as major instead of **162**, however, separation of unknown components **A** and **B** was unsuccessful by standard chromatographic methods.

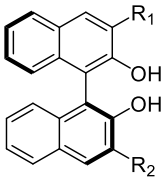
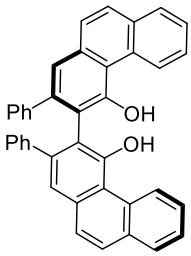
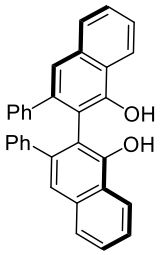
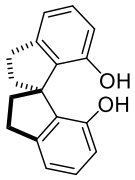


162 (%)	Unknown product A (%)	Unknown product B (%)	RSM (%)	Total recovery (%)
19	37	14	23	93

Figure 2.29 ^{1}H NMR analysis of the crude reaction mixture after functionalisation, by comparison to the starting material (top) and isolated product **162** (bottom). Yields calculated by ^{1}H NMR using 1,3,5-trimethoxybenzene as internal standard.

Surprisingly, out of the ligands trialled, only **(*S*)-BINOL** led to a noticeable improvement in the e.r. of isolated **162** (65.5:34.5, equivalent to 31% *ee*) (Scheme 2.84). BINOL ligands with substituted biaryl scaffolds, as well as extended π systems of various architectures such as **(*S*)-VAPOL** and **(*S*)-VANOL** led only to racemic mixtures. Additionally, even the more 3-dimensional **(*S*)-SPINOL** backbone was still not successful in inducing the desired stereoselectivity, despite increasing the yield of **162** to 48%.

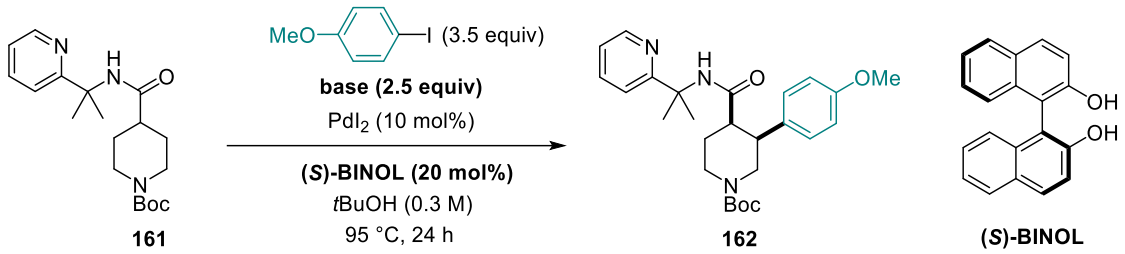


		yield	e.r.
	**(*S*)-BINOL**, $R_1 = R_2 = H$	12%	65.5:34.5
	(*S*)-diBr-BINOL, $R_1 = R_2 = Br$	0%[a]	-
	(*S*)-diPh-BINOL, $R_1 = R_2 = Ph$	14%	50:50
	**(*S*)-VAPOL**	19%	50:50
	**(*S*)-VANOL**	22%	50:50
	**(*S*)-SPINOL**	48%	50:50

Scheme 2.84 Screen of BINOL ligands on the PIP-containing piperidine under conditions adapted from Shi. Reactions on 0.2 mmol scale. Isolated yields shown. [a]Dense precipitate formed – no evidence of **162** presence by ^{1}H NMR.

Using the hit conditions in the presence of **(*S*)-BINOL**, a set of different bases were screened to identify further potential avenues for enantioselectivity optimisation (Table 2.17). Out of the carbonate bases trialled (entries 1-3), only K_2CO_3 induced a bias in e.r., suggesting a potential role played by the K^+ cation in achieving enantioselectivity, such as the ability to pre-coordinate multiple BINOL molecules in

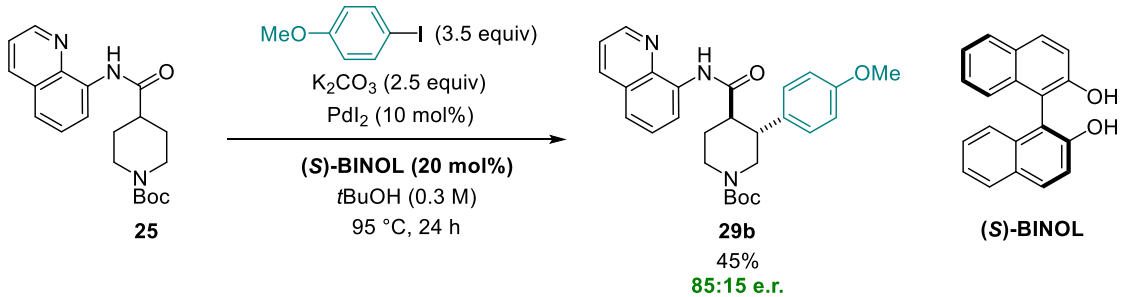
a chelating fashion.[279,280] Acetate bases were unsuccessful in impacting the e.r., with Cs bases promoting only very low conversions (entries 4-5).



Entry	Base	162 yield (%)[a]	162 e.r.
1	K_2CO_3	12	65.5:34.5
2	Ag_2CO_3	25	50:50
3	Cs_2CO_3	<5[b]	n/a
4	AgOAc	15	50:50
5	CsOAc	<5[b]	n/a

Table 2.17 Base screen under the hit conditions using (S)-BINOL. Reactions on 0.2 mmol scale. [a]Isolated yields shown. [b]Yield determined by ^{1}H NMR using 1,3,5-trimethoxybenzene as internal standard – e.r. ratio not determined due to the low conversion.

Notably, despite the PIP auxiliary arguably restricting the rotation of weaker coordinating phosphate ligands,[270] the rationale for its use in conjunction with BINOL ligands is not as well documented. With only reduced yields of **162** and moderate e.r. values in the presence of the PIP directing group, it was decided to reinvestigate the performance of aminoquinoline amide **25** under the above conditions (Scheme 2.85). Surprisingly, exclusive formation of *trans* isomer ***29b*** was now observed in 45% yield, despite the typical *cis* stereoselectivity in the absence of BINOL ligands. Pleasingly, the reversal in stereoselectivity was also accompanied by a significant improvement in e.r., now determined as 85:15 (70% *ee*) in the favour of ***29b***, which will from now on denote one of the possible *trans* enantiomers.

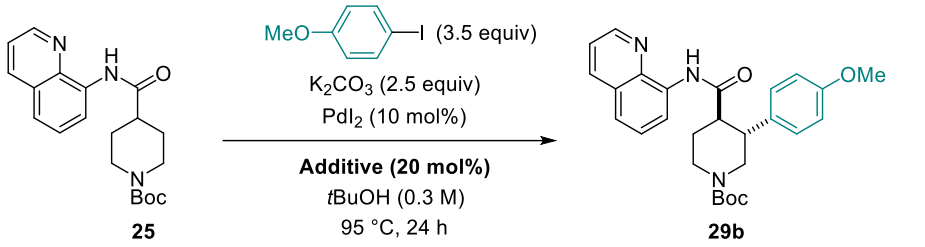


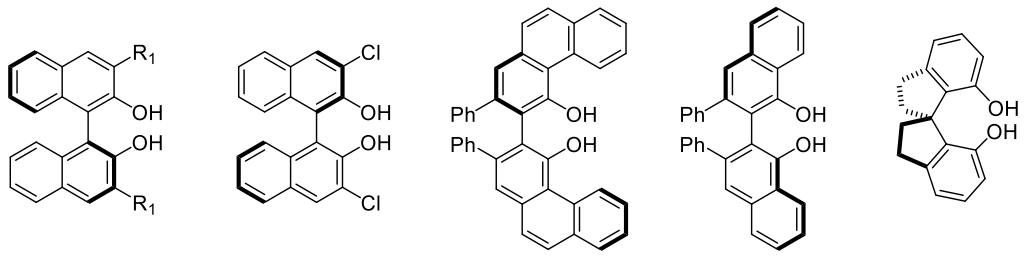
Scheme 2.85 Using the aminoquinoline directing group under the BINOL-mediated conditions. Reversal in diastereoselectivity and high improvement in e.r. observed.

2.4.3.4 Reaction Optimisation

With a boost in enantioselectivity under the aminoquinoline-directed conditions, further optimisation was carried out to improve the yield and e.r. of **29b**. In all cases and unless otherwise stated, optimisation reactions were carried out on 0.1 mmol scale, with yields determined by ^{1}H NMR of the crude reaction mixture using 1,3,5-trimethoxybenzene as internal standard. For e.r. determination, a pure fraction of **29b** was isolated by preparative TLC and analysed by HPLC unless otherwise noted.

Firstly, a range of BINOL-type additives were screened, affording good to excellent *trans* selectivities (Table 2.18). Depending on the 3,3' substitution, various outcomes were observed, with phenyl substituents leading to a marked drop in diastereoselectivity and formation of both **29b** and the corresponding *cis* isomer **29a** in comparable yields (entry 2). Interestingly, out of these, only **29b** was formed as a non-racemic mixture, albeit in modest e.r. (56:44). Pleasingly, **(*S*)-diBr-BINOL** afforded **29b** in an excellent 91:9 e.r., with only trace amounts of diarylation. Other 3,3'-dihalogenated BINOL cores were not commercially available or easily accessible, however, **(*R*)-diCl-BINOL** was kindly provided by Dr. Tsz Kan Ma from Imperial College (entry 3). Compared to the most similar (*S*)-configured ligand **(*S*)-diBr-BINOL**, a similar level of enantioinduction was observed with this (*R*)-configured ligand, this time in the favour of the opposite enantiomer, proving that inversion of enantioselectivity is possible as a function of ligand stereochemistry. **(*S*)-VAPOL**, **(*S*)-VANOL** and **(*S*)-SPINOL** each led to racemic **29b**, the former affording only 8% yield (entries 4-7).





R_1 = H (*S*)-BINOL
R_1 = Ph (*S*)-diPh-BINOL
R_1 = Br (*S*)-diBr-BINOL

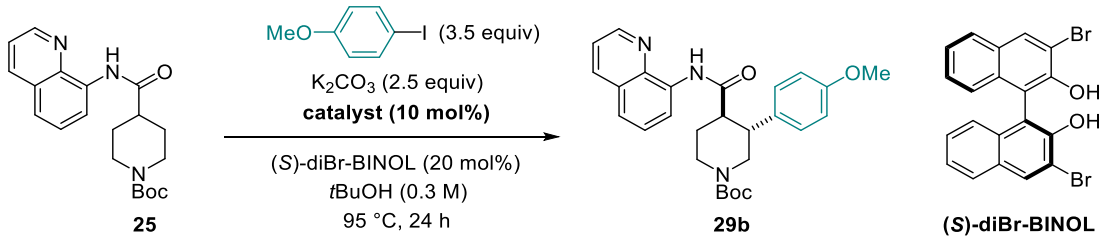
(*R*)-diCl-BINOL[a] (*S*)-VAPOL (*S*)-VANOL (*S*)-SPINOL

Entry	Additive	29b yield (%)	29b e.r.	Side-product(s) (yield), e.r.
1	**(*S*)-BINOL**	50	85:15	-
2	**(*S*)-diPh-BINOL**	30	56:44	mono-*cis* **29a** (27%), 50:50

3	**(*S*)-diBr-BINOL**	29	91:9	di-*cis*-*trans* **29c** (<5%), n/a
4	**(*R*)-diCl-BINOL**	28	11:89	di-*cis*-*trans* **29c** (<5%), n/a
5	**(*S*)-VAPOL**	8	50:50	-
6	**(*S*)-VANOL**	30	50:50	-
7	**(*S*)-SPINOL**	43	50:50	-

Table 2.18 Screen of BINOL additives under the aminoquinoline-directed functionalisation conditions.[a] BINOL ligand prepared by Dr. Tsz Kan Ma.

The source of Pd(II) may influence selectivity, with ligands such as acetate being able to promote background CMD in the absence of any assistance from the chiral ligand.[266, 272, 278] To favour BINOL coordination to the metal catalyst and formation of a chiral complex, halogenated Pd(II) species were initially trialled (Table 2.19, entries 1-4). Good to excellent enantiomeric ratios were observed with PdI_2 and $PdBr_2$, however $PdCl_2$ failed to produce a useful amount of product. Surprisingly, switching to $PdCl_2(MeCN)_2$ to enhance catalyst solubility in *t*BuOH resulted in the highest observed yield of **29b** so far, as well as excellent e.r. (94:6, entry 4). Similarly high enantioinduction was observed with $Pd(OAc)_2$, though lower yields, together with background *cis* arylation were observed (entry 5). $Pd(hfac)_2$ led to good e.r. and yield, though lower overall performance compared to $PdCl_2(MeCN)_2$ (entry 6).



25 **29b** **(*S*)-diBr-BINOL**

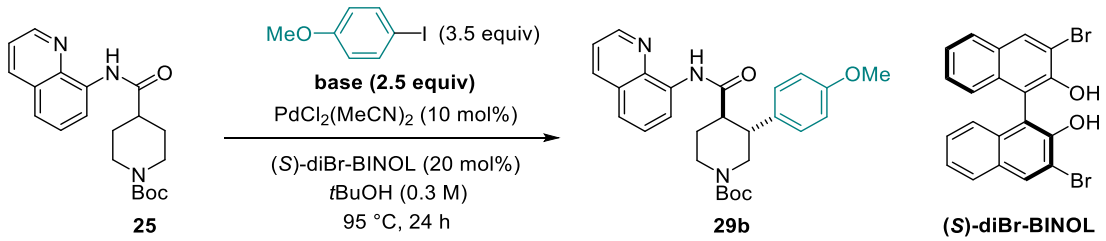
Entry	Catalyst	29b yield (%)	29b e.r.	Side-product(s) (yield), e.r.
1	PdI_2	29	91:9	-
2	$PdBr_2$	17	87:13	-
3	$PdCl_2$	<5	n/a	-
4	$PdCl_2(MeCN)_2$	53	94:6	-
5	$Pd(OAc)_2$	33	94.5:5.5	mono-*cis* **29a** (<5%), n/a
6	$Pd(hfac)_2$	32	90:10	-

Table 2.19 Screen of Pd catalysts using **(*S*)-diBr-BINOL** additive.

With $PdCl_2(MeCN)_2$ as the catalyst of choice, a series of bases were screened, starting with carbonates of group 1 metals (Table 2.20, entries 1-4). Interestingly, none of these gave comparable performance

to K_2CO_3. Bases with smaller cations (Li_2CO_3 and Na_2CO_3) were inefficient in promoting the functionalisation, whereas Cs_2CO_3 led to low yield and e.r. Moreover, transition metal carbonates such as Ag_2CO_3 led to complete erosion of enantioselectivity (entry 5). This suggests the essential role played by the K^+ cation in ensuring high levels of enantioinduction. Presumably, K^+ could be suitably sized to promote chelation of multiple BINOL molecules in a cage-type fashion, leading to an asymmetric binaphthalenolate complex that could bias the e.r. through either on or off-catalytic cycle involvement (*vide infra*).

To further investigate the effects of the negative counterion, a range of potassium bases were screened (entries 6-10). The nature of the counterion was found to significantly impact the product distribution, with side-products of arylation being formed in varying amounts with the phosphate, bicarbonate, pivalate and acetate bases (entries 6-8 and 10). This is suggestive of different deprotonation mechanisms in operation depending on the counterion. For instance, an inner-sphere CMD might lead to different selectivity outcomes compared to an outer-sphere process.[122,278,281]

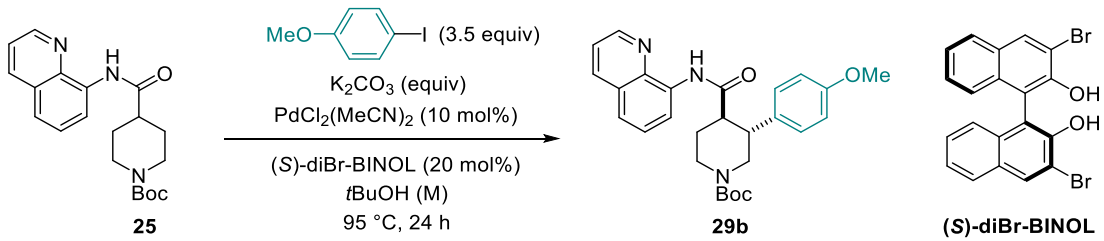


Entry	Base	29b yield (%)	29b e.r.	Side-product(s) (yield), e.r.
1	Li_2CO_3	<5	n/a	-
2	Na_2CO_3	<5	n/a	-
3	K_2CO_3	53	94:6	-
4	Cs_2CO_3	20	59:41	
5	Ag_2CO_3	25	50:50	
6	K_3PO_4	43	86:14	mono-*cis* (15%), 57:43
7	$KHCO_3$	40	82:18	mono-*cis* (37%), 58:42 *cis-trans* (14%), n/a
8	KOPiv	12	50:50	mono-*cis* (55%), 58:42 *cis-trans* (15%), n/a
9	KO*t*Bu	0	-	
10	KOAc	<5	n/a	mono-*cis* (25%), 50:50
11	CsOAc	20	57.5:42.5	-
12	AgOAc	15	55:45	-

Table 2.20 Base screen using $PdCl_2(MeCN)_2$ catalyst and (*S*)-diBr-BINOL additive.

Compared to carbonate, the phosphate and bicarbonate bases afforded a decreased yield and e.r. of ***en*-29b**. The pivalate and acetate preferentially promoted *cis* instead of *trans* functionalisation in up to 55% yield, however, as in all other cases, low or no enantioinduction was associated with the formation of the mono-*cis* arylated piperidine. Presumably, this is due to minimal or no involvement of BINOL in the *cis*-functionalisation pathway. Finally, $KHCO_3$ and KOPiv also promoted diarylation, whereas KO*t*Bu fully inhibited functionalisation, most likely due to favouring deprotonation of **25** instead (entry 9).

Given the selectivity of the K_2CO_3 mediated reaction, it was envisaged that running the reaction at higher concentrations would aid further increasing the yield of **29b**, whilst maintaining a desirable product distribution. Pleasingly, increasing the concentration from 0.3 M to 1 M in the presence of 2.5 equivalents of base led to 81% yield of **29b**, as well as an improvement in e.r. (Table 2.21, entries 1-2). An excellent selectivity was maintained, with only trace amounts of mono-*cis* and *cis-trans* side-products seen. Decreasing the high base loading to only 1.5 equivalents was possible, affording an even higher yield of **29b** (entry 3). Further increasing the concentration to 1.5 M led to a small drop in e.r, but a more significant decrease in yield to only 45%, most likely due to inefficient stirring of the dense heterogenous mixture in the absence of suitable solvent volumes.



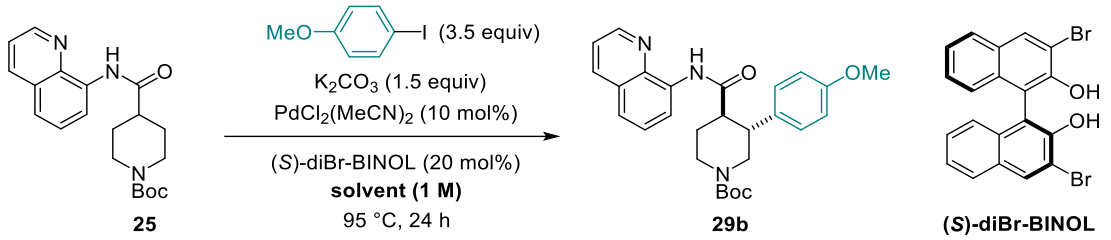
25 **29b** **(*S*)-diBr-BINOL**

Entry	Base equiv	Conc (M)	29b yield (%)	29b e.r.	Side-product(s) (yield), e.r.
1	2.5	0.3	53	94:6	-
2	2.5	1	81	97.5:2.5	mono-*cis* (<5%), n/a *cis-trans* (<5%), n/a
3	1.5	1	85	96.5:3.5	mono-*cis* (<5%), n/a *cis-trans* (<5%), n/a
4	1.5	1.5	45	95:5	mono-*cis* (<5%), n/a *cis-trans* (<5%), n/a

Table 2.21 Base equivalents and concentration screen.

Next, a solvent screen was performed, with alcohols generally found to perform best in terms of yield and e.r. (Table 2.22, entries 1-3). Based on miscibility, solvent mixtures of *t*BuOH and PhMe were also examined, since the aromatic component could aid enhance π-π interactions conducive to enantioinduction. As expected, small percentages of PhMe in *t*BuOH (20%) led to a slight increase in e.r. (entry 4) Increasing the amount of PhMe negatively impacted the yield and e.r. and progressively steered the reactivity towards *cis* arylation, with PhMe alone affording the *cis* product preferentially in modest e.r. (entry 7). Enantio- and diastereoselectivity could potentially be explained by a π-π stacking

model between BINOL and aminoquinoline, since aromatic solvents lead to such a marked difference in stereoselectivity, most likely by disrupting interactions between these elements. Finally, the reaction in dioxane led to excellent e.r, but low yield, whereas using CH_2Cl_2 at lower temperatures failed to form any product (entries 8-9).

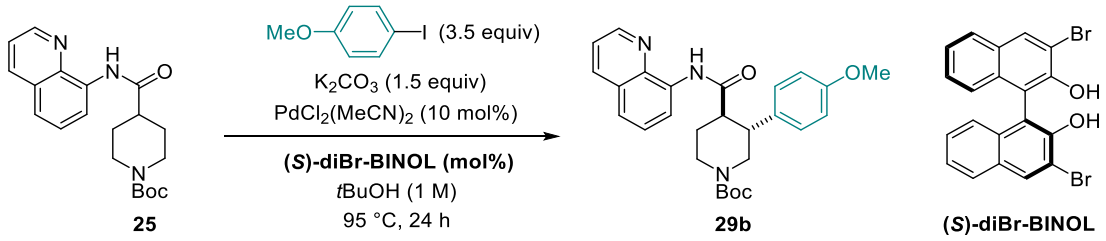


25 **29b** **(*S*)-diBr-BINOL**

Entry	Solvent	29b yield (%)	29b e.r.	Side-product(s) (yield), e.r.
1	*t*BuOH	85	96.5:3.5	-
2	*t*-amylOH	78	93:7	-
3	trifluoroethanol	52	77:33	-
4	*t*BuOH/PhMe (8:2)	83	97.5:2.5	mono-*cis* (<5%), n/a *cis-trans* (<5%), n/a
5	*t*BuOH/PhMe (6:4)	67	95:5	mono-*cis* (<5%), n/a *cis-trans* (<5%), n/a
6	*t*BuOH/PhMe (3:7)	30	83:17	mono-*cis* (25%), 55:45
7	PhMe	17	58:42	mono-*cis* (34%), 55:45
8	dioxane	34	94:6	
9[a]	CH_2Cl_2	0	-	

Table 2.22 Solvent screen under the pre-optimised conditions.[a]Reaction conducted at 45 °C.

Last but not least, the **(*S*)-diBr-BINOL** loading was examined, with higher quantities of chiral ligand found to lead to higher enantioselectivity (Table 2.23). Using only 10 mol% ligand led to lower yield of **29b** at the expense of *cis* arylation, as well as a modest e.r. Increasing to 30 mol% was judged as optimum, leading to the highest observed e.r. (98:2), as well as excellent diastereoselectivity and over 80% yield of desired **29b** (entry 3). Moreover, this was considered to achieve a good balance between the quantity of chiral ligand required and the enantioselectivity and yield outcomes.



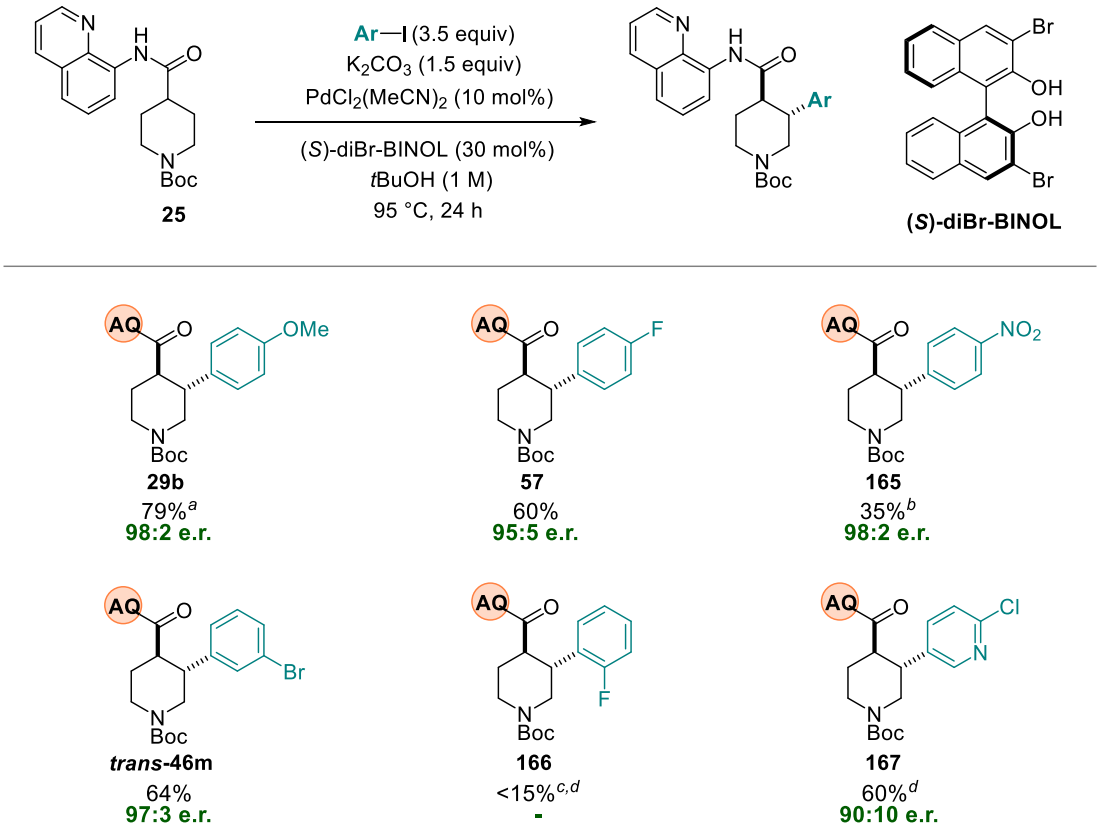
Entry	(*S*)-diBr-BINOL mol%	29b yield (%)	29b e.r.	Side-product(s) (yield), e.r.
1	10	39	88:22	mono-*cis* (16%), 55:45
2	20	85	97:3	mono-*cis* (<5%), n/a *cis*-*trans* (<5%), n/a
3	30	83 (79)	98:2	mono-*cis* (<5%), n/a *cis*-*trans* (<5%), n/a

Table 2.23 BINOL loading screen and final optimised conditions. Isolated yield in parentheses.

2.4.4 Reaction Scope

With the optimised conditions, the reaction scope with respect to the aryl iodide was investigated. To assess the performance and limitations of the methodology, an initial set of coupling partners was selected to represent a range of electronic and steric features. All *trans*-arylated products were formed in excellent enantiomeric ratios (e.r. > 90:10) and in generally higher yields compared to the *cis*-functionalised products afforded by the previous diastereoselective protocol (Scheme 2.86).

The electron-rich 4-iodoanisole gave the highest isolated yield (79%) and e.r. (98:2, **29b**). Pleasingly, similar levels of enantioinduction were maintained upon scaling the reaction up to 1 mmol (97:3 e.r.). However, uniform stirring of the solid reagents was difficult to achieve given the high concentration, resulting in only a 45% isolated yield of **29b**, with unreacted starting material accounting for the mass balance. *p*-Fluorophenyl iodide afforded **57** in 60% yield, as well as 95:5 e.r. Electron-poor *p*-nitro-substituted, as well as *meta*-Br-substituted arenes both gave good yields and similarly high e.r. values (**165** and ***trans*-46m**, 98:2 and 97:3 e.r., respectively). In the former case, stirring of the heterogenous mixture was again challenging despite decreasing concentration, leading to 35% yield. Gratifyingly, the more sterically demanding 2-fluoroiodobenzene could be installed, although the desired product was inseparable from the starting amide by standard chromatographic procedures (**166**). Finally, despite heteroaryls being notoriously challenging coupling partners in C(sp^3)–H functionalisations, 2-chloropyridine could now be installed in a markedly improved 60% yield compared to the racemic MesCOOH-mediated variant of the reaction (**167**). Furthermore, only a slight decrease in e.r. was seen in this case, presumably due to competition between pyridine, carbonate and BINOL for coordination to Pd in the enantioinductive step.



Scheme 2.86 Final optimised conditions and initial reaction scope with respect to the aryl iodide. Reactions on 0.2 mmol scale. [a]Reaction also carried out on 1 mmol scale, affording 45% **29b** (97:3 e.r.) [b] 0.5 M concentration [c] Product could not be isolated [d] Yield determined by ^{1}H NMR using 1,3,5-trimethoxybenzene as internal standard, mass losses occurred during purification (35% final isolated yield).

2.4.5 Mechanistic Considerations

A set of experiments were performed to further understand the factors contributing to enantioinduction. The reaction profile was firstly analysed, to allow exploring variations in product distribution, as well as in the enantioselectivity of **29b** with time (Figure 2.30). Pleasingly, a steep linear increase in the yield of **29b** is seen for the first 12 h, reaching a plateau at around 80% between 16 h and 24 h. This supports the optimal reaction time of 24 h, since a peak in product formation is achieved at this point. The *cis*- and *cis-trans* arylated side-products **29a** and **29c,** respectively, start to form only after 5 h. The amount of *cis*-arylated product slightly decreases beyond 12 h, concomitantly with a slight increase in *cis-trans* arylation, suggesting the origin of the latter from a second arylation of **29a**. However, low levels of side-product formation (<10% combined yield) are maintained over the course of 24 h, with unreacted starting material accounting for the mass balance at any point.

Interestingly, the level of enantioinduction is invariable with time, with **29*b*** forming from the outset in 96% *ee* (corresponding to 98:2 e.r.). This could indicate an irreversible enantiodetermining step taking place in the early stages of the catalytic cycle, such as the C–H activation.

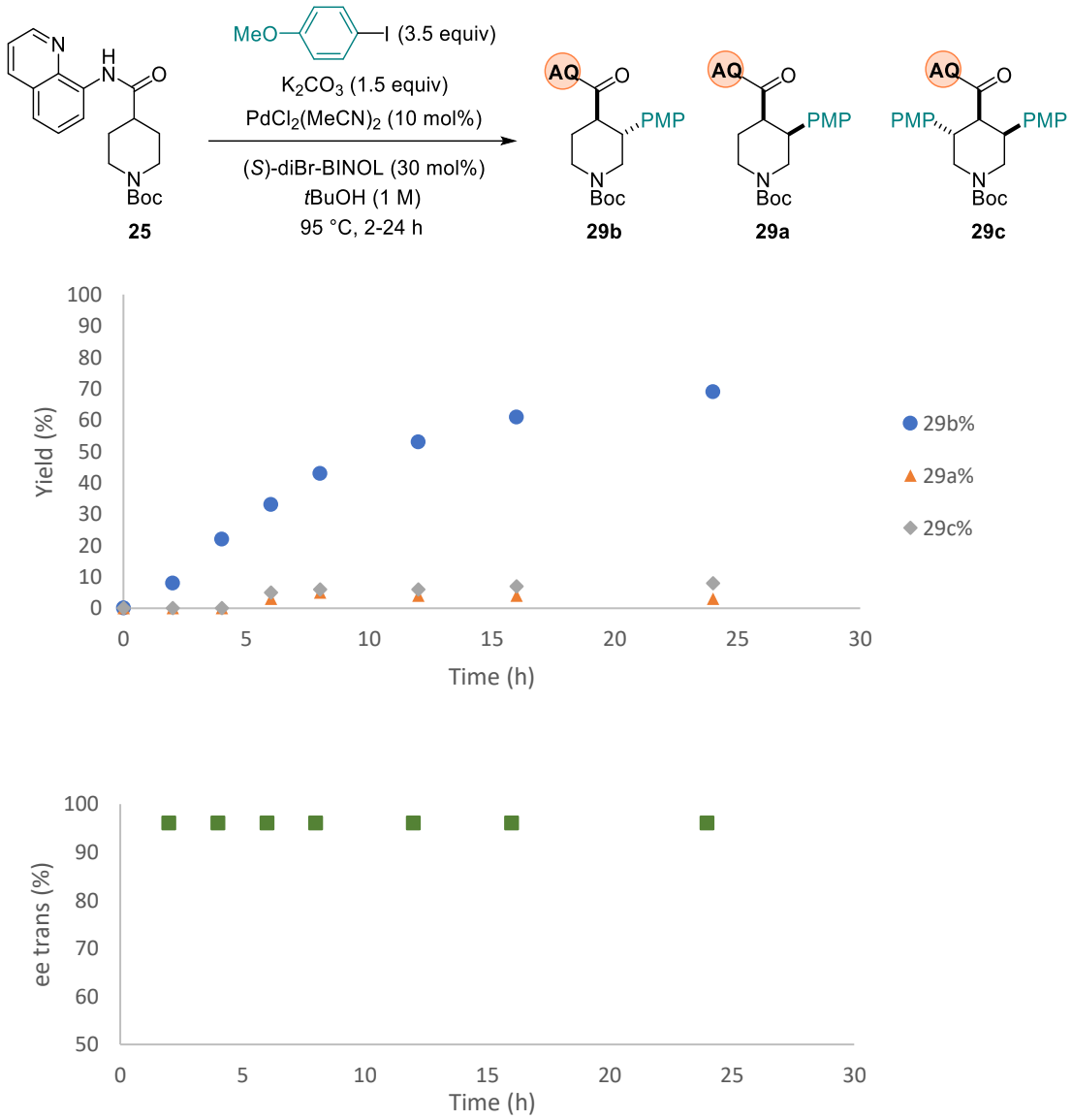
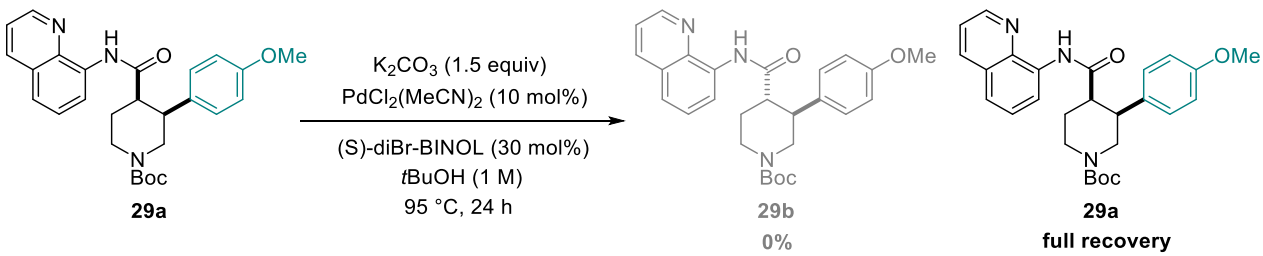


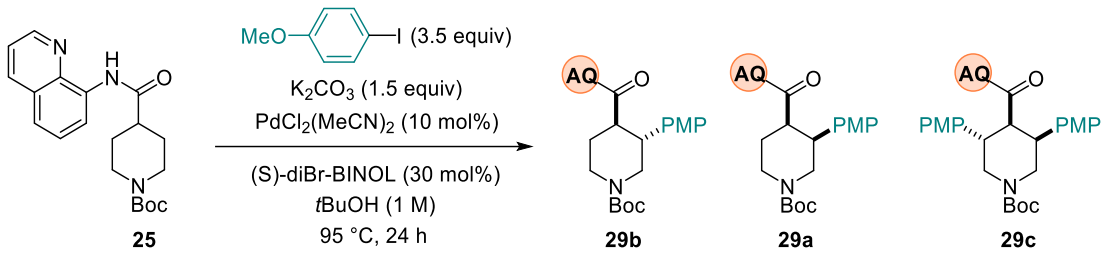
Figure 2.30 Reaction profile for the pre-optimised conditions shown. Variation in yield of products, as well as *ee* of **29b** studied over 24 h. *ee* values used for the purposes of this plot.

The absence of *cis*-arylated product in the first 5 hours seems to imply formation of **29b** *via* a *trans* C–H activation pathway rather than epimerisation of the diastereoisomer. To verify this, the *cis* configured **29a** was resubjected to the reaction conditions in the absence of aryl iodide and no epimerisation was observed (Scheme 2.87).



Scheme 2.87 Probing epimerisation of **29a** under the optimised reaction conditions.

With the factors determining the stereochemical outcome unknown, a series of control experiments were run (Table 2.24). As expected, full starting material recovery was observed when running the reaction either in the absence of aryl iodide, K_2CO_3 or Pd catalyst (entries 2-4). However, running the reaction in the absence of **(*S*)-diBr-BINOL** almost completely shut down the *trans* arylation pathway, generating 33% of racemic *cis* isomer **29a**, as well as significant diarylation (entry 5). It follows from here that besides enantiocontrol, **(*S*)-diBr-BINOL** also plays an essential role in achieving diastereocontrol towards *trans* arylation.

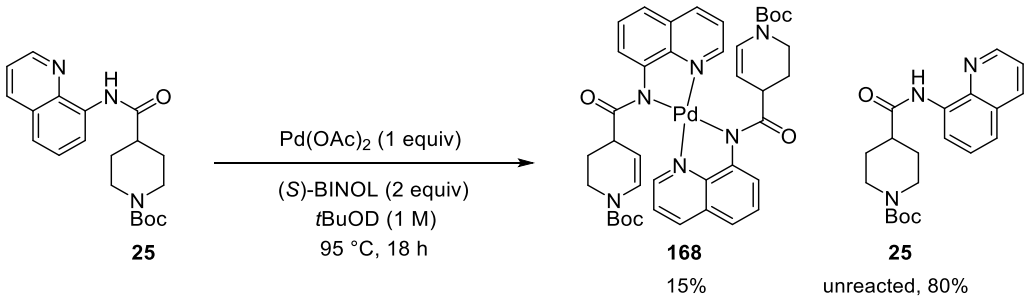


Entry	Modifications to conditions	Observations
1	None	83% **29b** (98:2 e.r.) <5% **29a** <5% **29c**
2	No aryl iodide	**25** fully recovered
3	No K_2CO_3	**25** fully recovered
4	No $PdCl_2(MeCN)_2$	**25** fully recovered
5	No (S)-diBr-BINOL	33% **29a** (50:50 e.r.) 15% **29c** 7% **29b** (50:50 e.r.)

Table 2.24 Control experiments to confirm factor(s) essential to reactivity and stereochemical control.

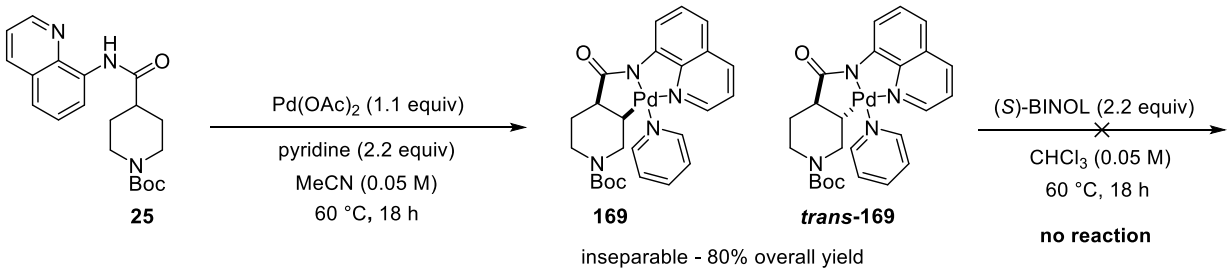
To investigate the origin of *trans* arylation in the presence of a BINOL additive, deuteration studies were performed (Scheme 2.88). Substrate **25** was reacted at 95 °C with a stoichiometric amount of Pd(II) catalyst and **(*S*)-BINOL**, opting for an excess of the ligand with respect to Pd (1:2 ratio, respectively) to reflect the usual reaction environment. A stable palladacycle coordinated to aminoquinoline and/or BINOL, or C(3) deuteration in the presence of *t*BuOD solvent were anticipated, with the stereoselectivities of their formation expected to facilitate a mechanistic interpretation. Instead, the only isolated Pd complex appeared to exhibit two alkene proton environments by ^{1}H NMR. The 1:1 integration, together with the coupling between these protons (J = 6.0 Hz) and their chemical shifts (δ = 8.82 ppm and δ = 4.99 ppm) were indicative of the presence of a CH=CH moiety next to the ring heteroatom, most likely generated *via* β-hydride elimination from the corresponding 5,6-fused Pd-cycle. However, the lack of other stabilising ligands in this complex led as judged by NMR to assigning its identity as dimer **168**, in which Pd^{II} is coordinated by 2 AQ groups.

A large percentage of **25** was recovered unreacted (80%), whereas performing the same reaction in the presence of 2 equivalents of K_2CO_3 still led to no observed deuteration.



Scheme 2.88 Attempted palladacycle formation in the presence of aminoquinoline and BINOL ligands. β-hydride elimination observed.

To prevent β-hydride elimination, the palladacycle formation was attempted in the presence of pyridine as a σ-donor ligand (Scheme 2.89). Despite complicated by rotamer interconversion, ^{1}H NMR analysis suggested the formation of 2 new compounds which were inseparable from each other by standard purification procedures, but could be isolated as a mixture. Gratifyingly, mass spec analysis confirmed that the isolated products matched the molecular weight expected for the pyridine-stabilised palladacycle. These were consequently assigned as the corresponding *cis* and *trans* diastereomers **169** and ***trans*-169**, their combined calculated yield being 80%. With palladacycle formation thought to be reversible, displacement of pyridine by BINOL was expected to lead to the thermodynamically preferred configuration of the palladacycle (*cis* or *trans*) that is potentially involved in the enantioselective transformation. Unfortunately, ligand displacement proved unsuccessful, with coordination of pyridine to Pd favoured over BINOL coordination.



Scheme 2.89 Palladacycle formation in the presence of pyridine as stabilising ligand. Unsuccessful attempt at displacing pyridine by (S)-BINOL.

The unsuccessful isolation of the relevant palladacycle could be due to the assumption that a single BINOL molecule is closely coordinated to Pd throughout the catalytic cycle and contributing to enantioinduction. More than often, multiple BINOL ligands contribute to determining enantioselectivity, though mechanistic explanations for this are limited.

Further insights into the involvement of **(*S*)-diBr-BINOL** in the reaction were gained by studying the relationship between the *ee* of **29b** against the *ee* of ligand (Figure 2.31). An overall non-linear effect was found, with a negative linear correlation seen at low BINOL enantiopurities and a positive linear correlation beyond 40% *ee* of BINOL. This could suggest a delayed onset of enantioinduction due to inital formation of a BINOL multimer complex which temporarily restricts the active ligand available.

Once the active form of the ligand is formed or released, enhanced enantioinduction takes place. However, as previously seen by Chen and Houk,[267,268] conclusions can not be drawn solely on the basis of this plot with regards to the on- or off-catalytic cycle involvement of a BINOL multimer.

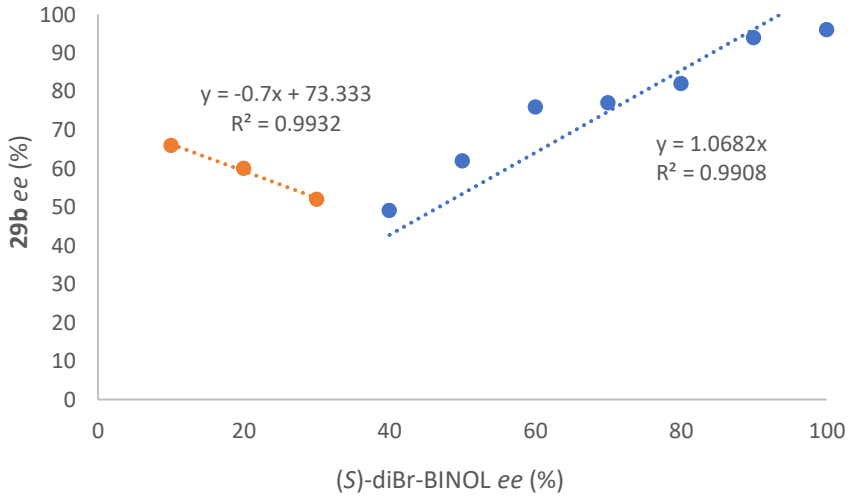


Figure 2.31 Plot of the relationship between the *ee* of product **29b** against the *ee* of (S)-diBr-BINOL used. Reactions carried out on 0.1 mmol scale, with samples of **29b** isolated by preparative TLC for HPLC analysis.

Mechanistic speculations can be made, in particular with regards to the specificity of the reaction for the use of K_2CO_3. K^+ has previously been involved in enantioselective transformations using polyether-linked BINOLs, as reported by Song.[282] The crown-type ether structure chelated the suitably sized cation, efficiently solvating the potassium base. Moreover, X-ray studies discovered stabilising interactions of K^+ with the 3,3' carbon-halogen bonds on the binaphthyl core in structure **170**, which were essential for high levels of enantioinduction (Figure 2.32).[280] The resulting counterion (in this case F^-) was delivered from a chiral environment, hence acting as a "chiral" base in promoting desilylation of TIPS-protected alcohols.

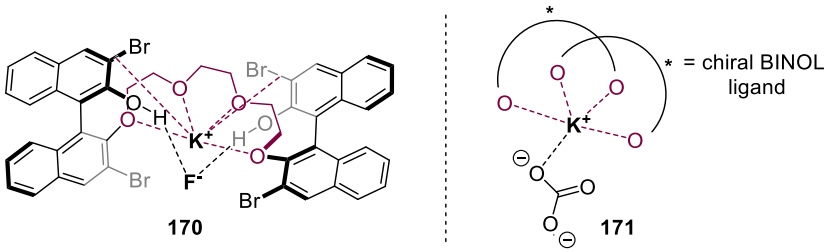


Figure 2.32 Right:Structure of a chiral complex between KF and polyether-linked BINOLs isolated by Song. Left: Schematic cation-binding model proposed for generating a "chiral" carbonate anion.

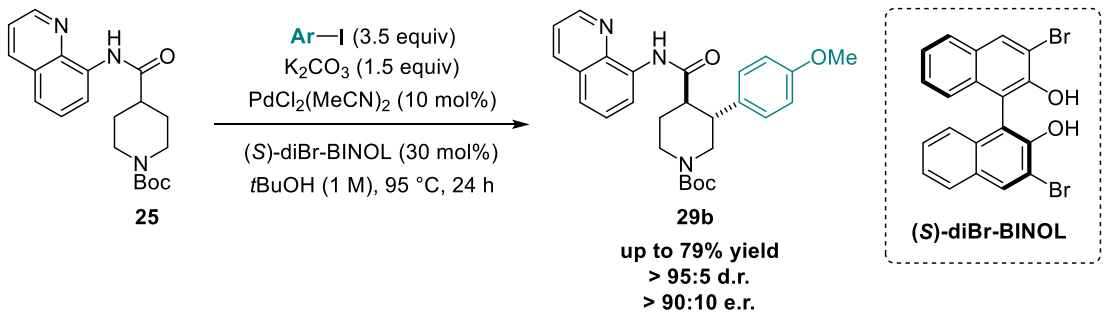
A trimeric BINOL complex such as illustrated by **171** could be in operation in our case, solubilising K_2CO_3 by chelation to the potassium cation. With a surrounding asymmetric environment, a "chiral" carbonate anion would promote C–H activation diastereo- and enantioselectively either by inner or outer sphere CMD. Alternatively, the multimer might participate itself in C–H abstraction through a BINOL O^- anion. The aminoquinoline scaffold could also be promoting attractive or repulsive interactions with the BINOL backbone that are key to the observed outcome. This is evidenced by lower e.r. and d.r. values for the

trans isomer in the presence of the less aromatic PIP directing group (see Section 2.4.1.4). However, despite the emerging BINOL-mediated enantioselective C(sp^3)–H functionalisations, mechanistic investigations are limited, with the enantiodetermining step unknown in all cases.[271-277] As seen with our substrate, isolation of BINOL-coordinated metal complexes remains a challenge in assessing the structures of active intermediates.

2.4.6 Conclusion

In summary, unbiased saturated heterocycles could be arylated at C(3) in a highly regio- diastereo- and enantioselective fashion using an aminoquinoline directing group and a chiral BINOL additive (Scheme 2.90). Using (*S*)-diBr-BINOL and $PdCl_2(MeCN)_2$ catalyst, excellent e.r. values of up to 98:2 were achieved, with consistent enantioselectivities observed across a range of electronically and structurally different aryl iodides. High yields and diastereoselectivities were seen for the formation of *trans* arylated product **29b**, with the *cis*-arylated product formed preferentially in the absence of a BINOL additive. This constitutes the first example of enantioselective C(sp^3)–H functionalisation of saturated heterocycles at remote positions from the heteroatom, opening unprecedented opportunities in medicinal chemistry for accessing enantiomerically pure drugs and drug analogues.

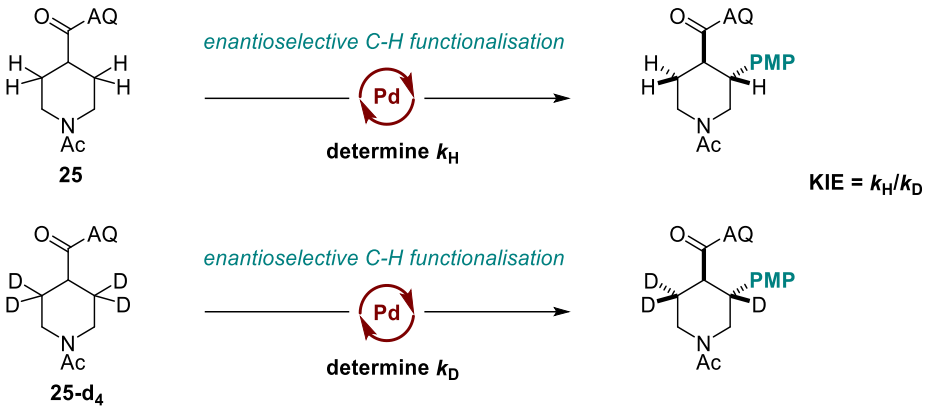
Early mechanistic investigations revealed a possible accumulation of BINOL ligands which was rationalised to be coordinated to K^+ in a chelate fashion. The steric bulk of this complex could be contributing to inverting the diastereoselectivity to favour *trans* instead of *cis* arylation, as observed. However, there is currently a lack of suitable tools to allow mechanistic investigations into stereodetermining step(s), together with the significant challenge in isolating complexes associated with key pre-transition states.



Scheme 2.90 The first enantioselective C(sp^3)–H functionalisation of piperidines at positions remote from heteroatom.

Unfortunately, attempts at crystallising **29b** or its corresponding HCl salt post Boc-deprotection has proven unsuccessful in the available timeframe. However, further efforts would be directed at elucidating the absolute stereochemical configuration of **29b** by X-ray diffraction, since thiscould prove valuable in rationalising the pathways leading to its formation. Additionally, experimental identification of the rate-limiting step would aid future computational studies by providing the highest energy-reference point in the catalytic cycle. The kinetic isotope effect (KIE) in the C–H abstraction step could be studied by comparing the initial rates of reaction between substrate **25** and the corresponding β-deuterium labelled

25-d$_4$ (Scheme 2.91). An *N*-Ac protecting group would be employed on the piperidine ring due to its higher stability, especially in acidic environments.



Scheme 2.91 Determining the KIE for the C–H activation step.

On the other hand, a polyether-linked BINOL complex similar to the one used by Song could be employed to chelate K^+.[282] If similar levels of enantioinduction are seen compared to the **(*S*)-diBr-BINOL** mediated reaction, accumulation of BINOL into a multimer would be supported, as well as involvement of a "chiral" carbonate ligand in deprotonation. Conversely, the effects of a BINOL-ligated Pd species in the reaction could be probed by synthesising the Pd((*S*)-diBr-BINOL)$_2$(MeCN)$_2$ complex, since well-defined Pd biphenanthrol complexes stabilised by MeCN are known.[283] This could be used as a Pd source or in various loadings alongside $PdCl_2(MeCN)_2$ to observe changes in the reaction enantioselectivity.

It is hoped that the information extracted from the above experiments above would allow different coordination models between the substrate and the element imparting asymmetry to be proposed, Computational calculations could then be conducted to individually assess the ability of these models to reproduce the experimentally observed e.r. and d.r. values.

Finally, there are extensive opportunities for expanding the reaction scope, both with respect to the coupling partner and the cyclic substrate. Future prospects would see this methodology applied to *O*- and *S*-based 6-membered rings, as well as to saturated heterocycles of different sizes. Furthermore, the ability to reproduce previously reported directed functionalisations on saturated heterocycles in a highly enantioselective fashion, would be of enormous synthetic value.

3 Conclusions and Future Work

Advances in C(sp^3)–H functionalisation are reshaping the way organic and medicinal chemists think about the synthesis of desired molecules, by allowing selective elaboration of common feedstocks along less explored C–H vectors. With C–H bonds being ubiquitous, these tools also promise a rapid, broad and comprehensive exploration of the chemical space associated with any scaffolds of interest.

This thesis has demonstrated the development of methodologies for the regio- and stereoselective C(3) functionalisation of 6-membered saturated hetero- and carbocycles in the presence of a C(4) directing group. With access to novel 3,4-disubstitution patterns unlocked in only two steps from commercially available carboxylic acid, these tools contribute towards the wider vision of enabling any C–H bond of choice in common pharmacophores to be used as a functional handle for the construction and tailoring of medicinally relevant molecules to biological targets.

Firstly, the identification of aminoquinoline as a suitable bidentate directing group, followed by an OFAT and a DoE-driven optimisation approach enabled the selectivity issues posed by the chosen system, which possessed four equivalent C(3) C–H sites, to be overcome (Figure 3.1A). Excellent >85:15 selectivity for the single *cis* diastereomer was achieved for *N*, *O* and *S*-heterocycles, as well as for carbocycles, with high isolated product yields. Moreover, a facile one-pot arylation-epimerisation procedure provided access to single *trans* diastereomers, thereby enabling entry to a wider stereochemical diversity at will. Temperatures below 50 °C were employed, this being the first example of saturated heterocycle functionalisation at an unactivated position to not require temperatures in excess of 100 °C. Electron-rich and electron-poor aryls were tolerated, as well as heteroaryls and one example of a vinyl iodide.

Next, strategies for divergent removal of the aminoquinoline auxiliary were successfully developed, unveiling free polar functional groups at C(4) such as alcohols, carboxylic acids, amides and nitriles (Figure 3.1B). After deprotection of the ring heteroatom, the isolated molecules represented shape-diverse fragments with favourable physicochemical properties for FBDD screening. These were incorporated into a fragment library of 45 compounds constructed around a design which featured the presence of 3 different binding elements: an aryl, a polar functionality and the core heteroatom. This library spanned a diverse spatial distribution of binding elements, containing 5 stereodefined vicinal disubstitution patterns, with each member synthesised in at least 50 mg and in only maximum 4 steps from commercial materials. Moreover, virtual fragment decoration in LLAMA demonstrated the potential to derive highly 3-dimensional lead-like compounds that can uniformly sample the available chemical space whilst maintaining desirable physicochemical profiles.

The synthetic potential of the methodology was also demonstrated in the synthesis of novel building blocks for DNA-encoded libraries. For this, aryl coupling partners with orthogonal functional handles were successfully installed, affording tri- and even tetrafunctional blocks that are currently scarce in commercial collections catering for this type of screening approach. Following methodology development in terms of epimerisation and directing group deprotection, the molecules could be made

available as either *cis* or *trans* single diastereomers in order to allow a comprehensive exploration of the stereochemical space around each scaffold.

Finally, the first example of catalytic enantioselective C(sp^3)–H functionalisation at an unactivated position on a saturated heterocycles has been demonstrated (Figure 3.1C). Employing a BINOL-derived ligand in conjunction with the C(4) bidentate aminoquinoline group resulted in overriding both the diastereo- and enantioselectivity issues associated with the unbiased piperidine substrate used and setting the absolute stereochemistry at the adjacent C(3) and C(4) centres in one step. In this case, the formation of *trans*-configured enantiomers was observed in high yields (up to 79%), diastereoselectivities (d.r. > 95:5) and enantiopurities (90:10 < e.r. < 98:2), with excellent compatibility seen with an initial set of aryl iodides trialled.

It is hoped that the methodologies developed in this thesis would complement existing strategies in the medicinal chemistry toolkit and help contribute towards drug discovery programs by enabling diversification of screening libraries, elaboration of leads by functionalisation along previously inaccessible vectors, as well as synthesis of certain pharmacophores in enantiomerically pure forms.

Future work would see the elucidation of the coordination mode of the BINOL ligand that is conducive to the observed high enantioselectivity for the *trans* isomer. However, this remains an unaddressed challenge so far, as reports that describe other enantioselective C(sp^3)-H functionalisations in the presence of two strongly coordinating bidentate groups have been unable to explain the underlying mechanism.[272-275,277] Since full coordination of both aminoquinoline and the BINOL derivative would occupy all the 4 available sites on Pd, it remains likely that at least one ligand binds in a monodentate fashion prior to C–H insertion. Presumably, running the reaction whilst sequentially blocking in turn each of the *N* or *O* heteroatoms on the ligand/directing group would enable detection of the group that does not require full coordination to the metal centre in order for desymmetrisation to take place. Additionally, this would lead to a more informed choice of mechanistic investigation experiments to elucidate the enantiodetermining step.

Current limitations exist in the area of transition metal catalysed functionalisation of unactivated C–H bonds, such as the use of strongly coordinating directing groups that often pose deprotection challenges. The development of similar highly stereoselective methodologies compatible with a weakly coordinating monodentate directing group and/or with native or retainable polar functional handles such as carboxylic acids and/or sulfonamides would be extremely advantageous,[284,285] eliminating the need for directing group installation/removal (Figure 3.2).

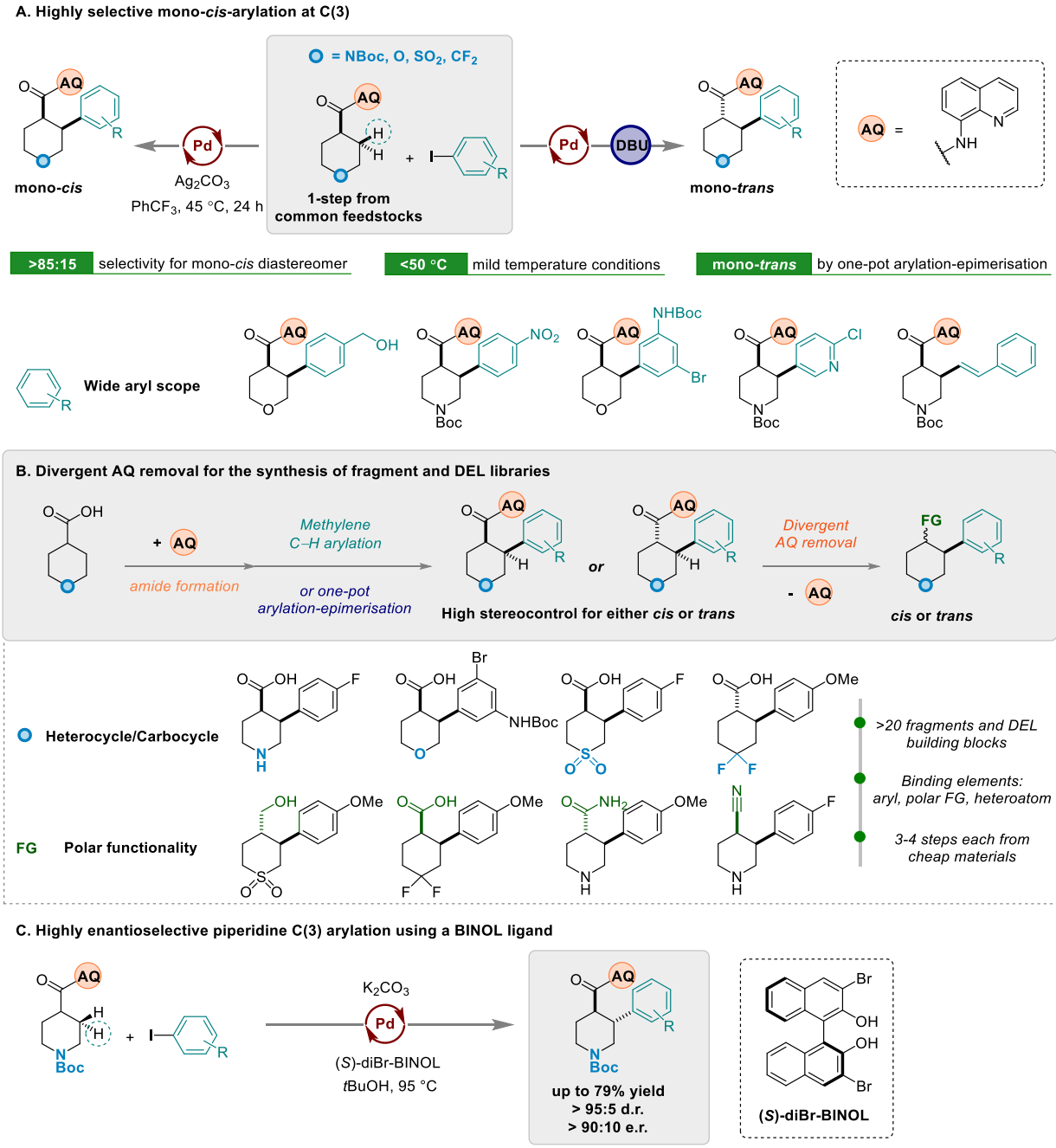


Figure 3.1 Overview of the key methodologies developed as part of this thesis.

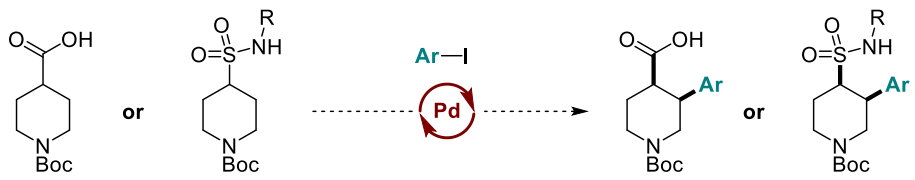


Figure 3.2 Future work – C(3) arylation of 6-membered saturated rings with a retainable, weakly coordinating C(4) polar group. R = (hetero)aromatic.

4 Experimental Details and Characterisation Data

4.1 General Experimental Considerations

All non-aqueous reactions were carried out under an inert atmosphere (argon) with flame-dried glassware using standard techniques, unless otherwise specified. Anhydrous solvents were obtained by filtration through drying columns (MeCN) or used as supplied (α,α,α-trifluorotoluene – Sigma product number: 547948 and THF – Fisher product number: 11924899). Reactions in sealed tubes were run using Biotage microwave vials (2–5 mL or 10–20 mL recommended volumes). Aluminum caps equipped with molded butyl/PTFE septa were used for reactions in α,α,α-trifluorotoluene. Simple butyl septa were used for reactions in MeCN or alcoholic solvents.

Chromatographic purification was performed either manually using 230–400 mesh silica, with the indicated solvent system according to standard techniques or using an automated flash chromatography Biotage® Selekt system with Biotage® Sfaar® HC cartridges (50-100 g) under the indicated conditions. Analytical thin-layer chromatography (TLC) was performed on precoated, glass-backed silica gel plates. Visualization of the developed chromatogram was performed by UV absorbance (254 nm) and/or stained with a potassium permanganate solution or ninhydrin solution in ethanol.

IR spectra were recorded as solids or neat liquids on an Agilent Cary 630 FTIR spectrometer and are reported in wavenumbers (cm^{-1}) to the nearest integer.

Nuclear magnetic resonance spectra were recorded on 400 or 500 MHz spectrometers. The frequency used to record the NMR spectra is given in each assignment and spectrum (^{1}H NMR at 400 or 500 MHz; ^{13}C NMR at 101 MHz or 126 MHz; ^{19}F NMR at 377 or 471 MHz). Chemical shifts for ^{1}H NMR spectra were recorded in parts per million from tetramethylsilane with the residual protonated solvent resonance as the internal standard ($CDCl_3$: δ 7.27 ppm, DMSO-d_6: δ 2.50 ppm, CD_3OD: δ 3.31 ppm, CD_3CN: δ 1.93 ppm, toluene-d_8: δ 2.07 ppm for CD_3, 7.08 ppm for *m*-DC_{Ar}, 6.96–7.00 ppm for *p*-DC_{Ar} and *o*-DC_{Ar}). Data was reported as follows: chemical shift (multiplicity [s = singlet, d = doublet, t = triplet, m = multiplet and br = broad], coupling constant, integration and assignment). *J* values are reported in Hz. All multiplet signals were quoted over a chemical shift range. ^{13}C NMR spectra were recorded with complete proton decoupling. Chemical shifts were reported in parts per million from tetramethylsilane with the solvent resonance as the internal standard ($^{13}CDCl_3$: δ 77.0 ppm, $(^{13}CD_3)_2SO$: δ 39.5 ppm, $^{13}CD_3OD$: δ 49.0 ppm, $^{13}CD_3{}^{13}CN$: δ 1.3 ppm for $^{13}CD_3$, $^{13}CD_3{}^{13}C_6D_5$: δ 20.4 ppm for $^{13}CD_3$, 137.5 ppm for *ipso*-$^{13}C_{Ar}$). Assignments of ^{1}H and ^{13}C spectra, as well as *cis*- or *trans*-configuration, were based upon the analysis of δ and *J* values, as well as DEPT, COSY, HMBC, HSQC and NOESY experiments where appropriate. ^{19}F NMR spectra were recorded with proton decoupling unless otherwise stated. ^{19}F NMR spectra are indirectly referenced to $CFCl_3$, automatically via direct measurement of the absolute frequency of the deuterium lock signal by the spectrometer hardware.
All *tert*-butyloxycarbonyl (Boc) containing compounds appeared as a mixture of rotamers in the NMR spectra at rt. In most cases, NMR experiments at 373 K were carried out in order to assign the signals.

The high resolution mass spectrometry (HRMS) analyses were performed using electrospray ion source (ESI) or atmospheric pressure chemical ionization (APCI) using an atmospheric solids analysis probe (ASAP). ESI was performed using a Waters LCT Premier equipped with an ESI source operated either in positive or negative ion mode. The software used was MassLynx 4.1, this software does not account for the electron and all the calibrations/references are calculated accordingly, *i.e.* $[M+H]^+$ is detected and the mass is calibrated to output [M+H]. APCI was performed using an Orbitrap XL or Xevo G2S using an ASAP to insert samples into the APCI source. The sample was introduced at ambient temperature and the temperature increased until the sample vaporized.

All melting points were determined in open glass capillaries and are uncorrected.

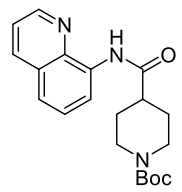
Reagents: Commercial reagents were used as supplied or purified by standard techniques where necessary. $Pd(OAc)_2$ was purchased from Fluorochem Ltd and used as supplied (purity >98%). 8-Aminoquinoline was purchased from TCI Chemicals and used as supplied. Ag_2CO_3 and K_2CO_3 (powder, 325 mesh) were purchased from Sigma-Aldrich, with K_2CO_3 flame-dried as part of the reaction set-up. 2-Iodoxybenzoic acid (IBX) was purchased as a mixture of the title compound (30 wt.% or 45 wt.%) and isophthalic acid and benzoic acid stabilisers, with the mixture used as supplied without any further purification.

HPLC analyses were carried out on an Agilent 1260 Infinity Series system, employing Daicel Chiracel columns, under the specified conditions.

4.2 Compounds for Chapter 2.1

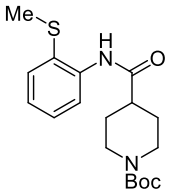
4.2.1 Directing Group Screen

***tert*-Butyl 4-(quinolin-8-yl-carbamoyl)piperidine-1-carboxylate (25)**



4-DMAP (49 mg, 0.40 mmol, 0.2 equiv) and EDC·HCl (460 mg, 2.40 mmol, 1.2 equiv) were added to a solution of *N*-Boc-piperidine-4-carboxylic acid (458 mg, 2.00 mmol, 1.0 equiv) and 8-aminoquinoline (346 mg, 2.40 mmol, 1.2 equiv) in CH_2Cl_2 (15 mL). After stirring at rt for 24 h, the reaction was diluted with CH_2Cl_2 (20 mL), then sat. aq. $NaHCO_3$ (30 mL) was added and the aqueous layer extracted with CH_2Cl_2 (3 x 20 mL). The combined organic extracts were dried over Na_2SO_4, filtered, and the solvent removed under reduced pressure. Purification of the residue by flash column chromatography (20% to 60% EtOAc/hexane) afforded amide **25** as a white solid (448 mg, 1.26 mmol, 63%). R_f 0.38 (35% EtOAc/hexane); mp = 120–123 °C (from EtOAc); IR (film)/cm^{-1} 3366 (NH br), 2929, 2983, 1692 (C=O), 1681 (C=O), 1528, 1409, 1297, 1163, 940; ^{1}H NMR (400 MHz, $CDCl_3$) δ 9.94 (br s, 1 H, NH), 8.86–8.72 (m, 2 H, 2 × HC_{Ar}), 8.16 (dd, *J* = 8.2, 1.7 Hz, 1 H, HC_{Ar}), 7.58–7.40 (m, 3 H, 3 × HC_{Ar}), 4.23 (br s, 2 H, 2 × NC*H*HCH_2), 2.89–2.82 (m, 2 H, 2 × NCH*H*CH_2), 2.70–2.54 (m, 1 H, CH(C=O)), 2.12–1.95 (m, 2 H, 2 × NCH_2CHH), 1.94–1.76 (m, 2 H, 2 × NCH_2CHH), 1.48 (s, 9 H, $C(CH_3)_3$); ^{13}C NMR (101 MHz, $CDCl_3$) δ 172.9 (C=O amide), 154.7 (C=O carbamate), 148.1 (C_{Ar}), 138.3 (C_{Ar} quat), 136.3 (C_{Ar}), 134.2 (C_{Ar} quat), 127.9 (C_{Ar} quat), 127.3 (C_{Ar}), 121.6 (C_{Ar}), 121.5 (C_{Ar}), 116.4 (C_{Ar}), 79.6 ($C(CH_3)_3$), 44.6 (2 × NCH_2CH_2), 43.2 (*C*H(C=O)), 28.6 (2 × NCH_2CH_2), 28.4 ($C(CH_3)_3$); HRMS (ESI) *m/z* Calculated for $C_{20}H_{26}N_3O_3$ [M+H] 356.1976; Found 356.1974.

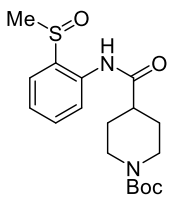
***tert*-Butyl 4-((2-(methylthio)phenyl)carbamoyl)piperidine-1-carboxylate (26)**



4-DMAP (203 mg, 1.60 mmol, 0.2 equiv) and EDC·HCl (1.69 g, 8.80 mmol, 1.1 equiv) were added to a solution of *N*-Boc-piperidine-4-carboxylic acid (1.83 g, 8.00 mmol, 1.0 equiv) and 2-(methylthio)aniline (0.97 mL, 8.80 mmol, 1.1 equiv) in CH_2Cl_2 (16 mL). After stirring for 24 h at rt, the reaction was diluted with CH_2Cl_2 (10 mL), then sat. aq. $NaHCO_3$ (30 mL) was added and the aqueous layer extracted with CH_2Cl_2 (3 x 20 mL). The combined organic extracts were dried over Na_2SO_4 and filtered. The solvent was removed under reduced pressure. Purification of the residue by flash column chromatography (5% to 20% EtOAc/pentane) afforded amide **26** as a white solid (1.96 g, 5.60 mmol, 72%). R_f 0.35 (20% EtOAc/pentane); mp = 110–113 °C (from EtOAc); IR (film)/cm^{-1} 3224 (NH br), 2974, 2930, 2848, 1689 (C=O), 1658 (C=O), 1472, 1420, 1234, 1160, 1121, 1081, 1037, 738; ^{1}H NMR (400 MHz, $CDCl_3$) δ 8.43 (br s, 1 H, NH), 8.33 (d, *J* = 8.3 Hz, 1 H, HC_{Ar}), 7.49 (d, *J* = 8.2 Hz, 1 H, HC_{Ar}), 7.32 (t, *J* = 8.3 Hz, 1 H, HC_{Ar}), 7.07 (t, *J* = 8.2 Hz, 1 H, HC_{Ar}), 4.21 (br s, 2 H, 2 × NC*H*HCH_2), 2.84 (t, *J* = 13.5 Hz, 2 H, 2 × NCH*H*CH_2), 2.50 (tt, *J* = 12.0, 3.8 Hz, 1 H, CH(C=O)), 2.39 (s, 3 H, SCH_3), 1.98 (br d, 2 H, *J* = 13.0 Hz, 2 × NCH_2CHH), 1.76 (qd, *J* = 12.0, 4.3 Hz, 2 H, 2 × NCH_2CHH), 1.48 (s, 9 H, $C(CH_3)_3$); ^{13}C NMR (101 MHz, $CDCl_3$) δ 172.5 (C=O amide), 154.6 (C=O carbamate), 138.0 (C_{Ar} quat), 132.8 (C_{Ar}), 128.9 (C_{Ar}), 125.3 (C_{Ar} quat), 124.4 (C_{Ar}), 120.6 (C_{Ar}), 79.6 ($C(CH_3)_3$), 44.4 (*C*H(C=O)), 43.2 (2 × NCH_2CH_2), 28.6 (2

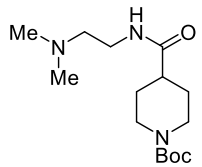
× NCH_2CH_2), 28.4 (SCH_3), 18.9 ($C(CH_3)_3$); HRMS (ESI) *m/z* Calculated for $C_{18}H_{27}SN_2O_3$ [M+H] 351.1752; Found 351.1742.

***tert*-Butyl 4-((2-(methylsulfinyl)phenyl)carbamoyl)piperidine-1-carboxylate (27)**



3-Chloroperoxybenzoic acid (480 mg, 2.76 mmol, 1.2 equiv) was added to a solution of **26** (805 mg, 2.30 mmol, 1.0 equiv) in CH_2Cl_2 (46 mL) at rt. The resulting mixture was stirred until TLC showed reaction completion (approx. 8 h) and then quenched with sat. aq. $NaHCO_3$ (20 mL). The organic layer was separated, washed with sat. aq. $NaHCO_3$ (3 x 25 mL), brine (2 x 25 mL), dried over Na_2SO_4 and filtered. The solvent was removed under reduced pressure. Purification of the residue by flash column chromatography (15% to 50% EtOAc/pentane) afforded sulfoxide **27** as a white crystalline solid (345 mg, 0.55 mmol, 63%). R_f 0.29 (30% EtOAc/pentane); mp = 131–133 °C (from EtOAc); IR (film)/cm^{-1} 3235 (NH br), 2974, 2844, 1692 (C=O), 1659 (C=O), 1532, 1416 (S=O), 1170, 1118, 1043, 961, 757; ^{1}H NMR (400 MHz, $CDCl_3$) δ 10.67 (br s, 1 H, NH), 8.45 (d, *J* = 8.0 Hz, 1 H, HC_{Ar}), 7.44 (t, *J* = 7.5 Hz, 1 H, HC_{Ar}), 7.24 (dd, *J* = 7.5, 1.5 Hz, 1 H, HC_{Ar}), 7.09 (t, *J* = 7.5 Hz, 1 H, HC_{Ar}), 4.23–4.04 (br m, 2 H, 2 × NC*H*HCH_2), 2.87 (s, 3 H, SCH_3), 2.75 (t, *J* = 13.0 Hz, 2 H, 2 × NCH*H*CH_2), 2.43 (tt, *J* = 12.0, 3.5 Hz, 1 H, CH(C=O)), 1.91 (br d, *J* = 11.0 Hz, 2 H, 2 × NCH_2C*H*H), 1.78–1.62 (m, 2 H, 2 × NCH_2CH*H*), 1.43 (s, 9 H, $C(CH_3)_3$); ^{13}C NMR (101 MHz, $CDCl_3$) δ 173.2 (C=O amide), 154.5 (C=O carbamate), 140.3 (C_{Ar} quat), 132.5 (C_{Ar} quat), 127.3 (C_{Ar}), 125.6 (C_{Ar}), 123.5 (C_{Ar}), 122.9 (C_{Ar}), 79.5 (*C*$(CH_3)_3$), 44.2 (2 × N*C*H_2CH_2), 43.3 (2 × NCH_2*C*H_2), 40.8 (*C*H(C=O)), 28.3 (C(*C*$H_3)_3$ and SCH_3); HRMS (ESI) *m/z* Calculated for $C_{18}H_{27}SN_2O_4$ [M+H] 351.1752 ; Found 351.1742.

***tert*-Butyl 4-((2-(dimethylamino)ethyl)carbamoyl)piperidine-1-carboxylate (28)**

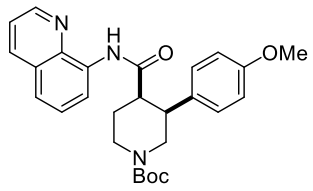


N,*N*-Diisopropylethylamine (1.1 mL, 6.00 mmol, 3.0 equiv) and HATU (760 mg, 2.00 mmol, 1.0 equiv) were added to a solution of *N*-Boc-piperidine-4-carboxylic acid (458 mg, 2.00 mmol, 1.0 equiv) and *N*,*N'*-dimethylethylenediamine (0.24 mL, 2.20 mmol, 1.1 equiv) in DMF (5 mL) After stirring at rt for 24 h, the reaction was diluted with EtOAc (20 mL), then sat. aq. $NaHCO_3$ (30 mL) was added and the aqueous layer was extracted with EtOAc (3 x 20 mL). The combined organic extracts were washed with brine (30 mL), dried over Na_2SO_4 and filtered. The solvent was removed under reduced pressure. Purification of the residue by flash column chromatography (5% to 15% MeOH/pentane) afforded amide **28** as a colorless dense oil (116 mg, 0.30 mmol, 13%). R_f 0.10 (15% MeOH/CH_2Cl_2); IR (film)/cm^{-1} 3392 (NH br), 2944, 2862, 2781, 1685 (C=O), 1680 (C=O), 1531, 1428, 1338, 1170, 910, 730; ^{1}H NMR (400 MHz, $CDCl_3$) δ 6.37 (br s, 1 H, NH), 4.19–4.10 (m, 2 H, 2 × NC*H*HCH_2), 3.41–3.31 (m, 2 H, NHC*H*$_2$), 2.79–2.73 (m, 2 H, 2 × NCH*H*CH_2), 2.54 (t, *J* = 5.8 Hz, 2 H, $(CH_3)_2$NC*H*$_2$), 2.34 (s, 6 H, N(C*H*$_3)_2$), 2.27 (tt, *J* = 11.6, 3.7 Hz, 1 H, CH(C=O)), 1.82 (app d, *J* = 12.7 Hz, 2 H, 2 × NCH_2C*H*H), 1.71–1.56 (m, 2 H, 2 × NCH_2CH*H*), 1.46 (s, 9 H, C(C*H*$_3)_3$); ^{13}C NMR (101 MHz, $CDCl_3$) δ 174.4 (C=O amide), 154.6 (C=O carbamate), 79.5 (*C*$(CH)_3$), 57.7 ($(CH_3)_2$N*C*H_2), 45.1 (N$(CH_3)_2$), 43.2 (2 × N*C*H_2CH_2CH), 36.5 (NH*C*H_2CH_2), 35.4 (*C*H(C=O)), 28.8 (2 × NCH_2*C*H_2CH), 28.4 (C(*C*$H_3)_3$); HRMS (ESI) *m/z* Calculated for $C_{15}H_{30}N_3O_3$ [M+H] 385.2850 ; Found 385.2849.

General Screening Procedure for Generating *N*-Boc Piperidine Arylated Products 29a-d, 30b

A microwave vial was charged with K_2CO_3 (138 mg, 1.00 mmol, 2.0 equiv), flame-dried, and allowed to cool under argon. Either starting amide **25-28** (0.50 mmol, 1.0 equiv), then 4-iodoanisole (351 mg, 1.50 mmol, 3.0 equiv), PivOH (16 mg, 0.15 mmol, 0.3 equiv) and $Pd(OAc)_2$ (5.60 mg, 25.0 μmol, 5 mol %) were added sequentially. The reaction vessel was sealed and purged with argon, then $PhCF_3$ (2.5 mL, 0.2 M) was added by syringe. The reaction tube was then placed in a preheated oil bath and stirred at 110 ºC for 24 h. The reaction mixture was then allowed to cool to rt and EtOAc (10 mL) was added. The mixture was filtered through a pad of Celite, eluting with further EtOAc (2 × 10 mL). The solvent was removed under reduced pressure, and the crude material purified by flash column chromatography (10% to 20% acetone/pentane) to afford the products below (in their elution order). Et_2O (5 mL), followed by pentane (5 mL) were added to each of the resulting products, with the resulting suspension concentrated under reduced pressure. This procedure was repeated three times to eliminate residual solvent and afford desired arylated piperidines

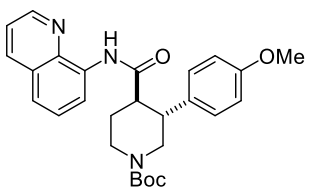
***tert*-Butyl-*cis*-(±)-3-(4-methoxyphenyl)-4-(quinolin-8-ylcarbamoyl)piperidine-1-carboxylate (29a)**



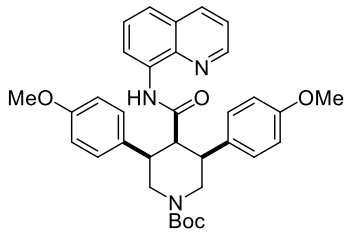
Prepared according to the **General Screening Procedure** above using amide **25** (178 mg). Product **29a** was isolated as a white solid (40 mg, 0.09 mmol, 18%). R_f 0.34 (20% acetone/pentane); mp = 135–137 °C (from Et_2O/pentane); IR (film)/cm^{-1} 3348 (NH br), 2933, 2974, 1681 (C=O), 1528, 1483, 1423, 1245 (C–O), 1163 (C–O), 910, 828, 731; ^{1}H NMR (500 MHz, DMSO-d_6, 373 K) δ 9.62 (br s, 1 H, NH), 8.80 (dd, *J* = 4.2, 1.7 Hz, 1 H, HC_{Ar}), 8.46 (dd, *J* = 7.7, 1.4 Hz, 1 H, HC_{Ar}), 8.31 (dd, *J* = 7.7, 1.5 Hz, 1 H, HC_{Ar}), 7.58 (dd, *J* = 8.3, 1.3 Hz, 1 H, HC_{Ar}), 7.55 (dd, *J* = 8.3, 4.2 Hz, 1 H, HC_{Ar}), 7.50 (t, *J* = 7.9 Hz, 1 H, HC_{Ar}), 7.22–7.17 (m, 2 H, 2 × HC_{Ar}), 6.72–6.66 (m, 2 H, 2 × HC_{Ar}), 4.00 (dd, *J* = 13.0, 8.1 Hz, 1 H, NC*H*HCHAr), 3.82 (ddd, *J* = 12.9, 8.6, 3.8 Hz, 1 H, NC*H*HCH$_2$), 3.73 (dd, *J* = 13.0, 4.1 Hz, 1 H, NCH*H*CHAr), 3.58 (s, 3 H, OCH_3), 3.54 (ddd, *J* = 12.7, 7.0, 4.7 Hz, 1 H, NCH*H*CH$_2$), 3.31 (ddd, *J* = 6.3, 4.7, 4.5 Hz, 1 H, CH(C=O)), 3.23 (ddd, *J* = 8.7, 6.7, 4.1 Hz, 1 H, CHAr), 2.05 (ddt, *J* = 13.1, 6.5, 3.8 Hz, 1 H, NCH$_2$C*H*H), 1.90 (ddt, *J* = 13.3, 8.6, 4.6 Hz, 1 H, NCH$_2$CH*H*), 1.43 (s, 9 H, C(CH_3)$_3$); ^{13}C NMR (126 MHz, DMSO-d_6, 373 K) δ 171.4 (C=O amide), 157.6 (C_{Ar} quat), 153.7 (C=O carbamate), 147.9 (C_{Ar}), 137.6 (C_{Ar} quat), 135.7 (C_{Ar}), 133.7 (C_{Ar} quat), 132.6 (C_{Ar} quat), 128.3 (2 × C_{Ar}), 127.2 (C_{Ar} quat), 126.2 (C_{Ar}), 121.3 (C_{Ar}), 121.0 (C_{Ar}), 115.9 (C_{Ar}), 113.2 (2 × C_{Ar}), 78.2 (*C*(CH_3)$_3$), 54.4 (OCH_3), 45.43 (N*C*H$_2$CHAr), 45.36 (*C*H(C=O)), 41.4 (CHAr), 40.5 (N*C*H$_2$CH$_2$), 27.7 (C(*C*H$_3$)$_3$), 25.6 (NCH$_2$*C*H$_2$); HRMS (ESI) *m/z* Calculated for $C_{27}H_{32}N_3O_4$ [M+H] 462.2393; Found 462.2388.

***tert*-Butyl-*trans*-(±)-3-(4-methoxyphenyl)-4-(quinolin-8-ylcarbamoyl)piperidine-1-carboxylate (29b) and *tert*-Butyl-*cis, cis*-(±)-3,5-bis(4-methoxyphenyl)-4-(quinolin-8-ylcarbamoyl)piperidine-1-carboxylate (29d)**

The above **General Screening Procedure** also afforded a mixture of *trans*- and *di-cis-cis* arylated piperidines **29b** and **29d** in an approx. 4:1 ratio, respectively. R_f 0.30 (20% acetone/pentane); A second purification by column chromatography (10% Et_2O in CH_2Cl_2) allowed the separation of the individual products **29b** and **29d**, as follows:

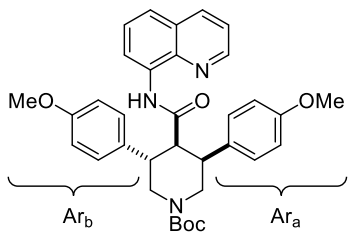


***trans* 29b**: isolated as a white powder (59 mg, 0.13 mmol, 26%). R_f 0.37 (10% Et_2O/CH_2Cl_2); mp = 99–101 °C (from Et_2O/pentane); IR (film)/cm^{-1} 3347 (NH br), 3045, 2931, 2858, 2837, 1663 (C=O), 1526, 1485, 1422, 1366, 1245, 1157, 926, 732; ^{1}H NMR (400 MHz, DMSO-*d*$_6$, 373 K) δ 9.71 (br s, 1 H, NH), 8.86 (dd, *J* = 4.2, 1.7 Hz, 1 H, HC_{Ar}), 8.43 (dd, *J* = 7.7, 1.4 Hz, 1 H, HC_{Ar}), 8.34–8.28 (m, 1 H, HC_{Ar}), 7.57 (ddd, *J* = 8.3, 2.8, 1.5 Hz, 2 H, 2 × HC_{Ar}), 7.46 (dd, *J* = 7.9, 7.8 Hz, 1 H, HC_{Ar}), 7.33–7.23 (m, 2 H, 2 × HC_{Ar}), 6.83–6.74 (m, 2 H, 2 × HC_{Ar}), 4.13 (ddd, *J* = 11.0, 4.3, 2.2 Hz, 1 H, NC*H*HCH_2), 4.00 (dd, *J* = 10.1, 8.8 Hz, 1 H, NC*H*HCHAr), 3.62 (s, 3 H, OCH_3), 3.22 (td, *J* = 11.4, 3.7 Hz, 1 H, CH(C=O)), 3.02–2.99 (m, 1 H, NCH*H*CH_2), 2.95–2.85 (m, 2 H, NCH*H*CHAr and CHAr), 2.04 (dq, *J* = 13.2, 3.2 Hz, 1 H, NCH_2CHH), 1.81–1.64 (m, 1 H, NCH_2CH*H*), 1.46 (s, 9 H, $C(CH_3)_3$); ^{13}C NMR (101 MHz, DMSO-*d*$_6$, 373 K) δ 171.6 (C=O amide), 157.8 (C_{Ar} quat), 153.5 (C=O carbamate), 148.0 (C_{Ar}), 137.6 (C_{Ar} quat), 135.8 (C_{Ar}), 133.8 (C_{Ar} quat), 132.7 (C_{Ar} quat), 128.0 (2 × C_{Ar}), 127.2 (C_{Ar} quat), 126.2 (C_{Ar}), 121.4 (C_{Ar}), 121.1 (C_{Ar}), 115.8 (C_{Ar}), 113.6 (2 × C_{Ar}), 78.4 (*C*$(CH_3)_3$), 54.5 (OCH_3), 49.3 (N*C*H_2CHAr), 49.1 (*C*H(C=O)), 43.6 (CHAr), 42.6 (N*C*H_2CH_2), 28.8 (NCH_2*C*H_2) 27.7 (C(*C*$H_3)_3$); HRMS (ESI) *m/z* Calculated for $C_{27}H_{32}N_3O_4$ [M+H] 462.2393; Found 462.2396.



di-*cis*-*cis* 29d: isolated as a yellow gum (68 mg, 0.12 mmol, 24%). R_f 0.55 (10% Et_2O/CH_2Cl_2); IR (film)/cm^{-1} 3352 (NH br), 2999, 2973, 2932, 1679 (C=O), 1523, 1485, 1424, 1245, 1169, 1116, 1034, 826, 792; ^{1}H NMR (400 MHz, DMSO-*d*$_6$, 373 K) δ 8.90 (br s, 1 H, NH), 8.60 (dd, *J* = 4.2, 1.7 Hz, 1 H, HC_{Ar}), 8.35 (dd, *J* = 7.6, 1.4 Hz, 1 H, HC_{Ar}), 8.25–8.19 (m, 1 H, HC_{Ar}), 7.53–7.40 (m, 3 H, 3 × HC_{Ar}), 7.26–7.19 (m, 4 H, 4 × HC_{Ar}), 6.72–6.65 (m, 4 H, 4 × HC_{Ar}), 4.11–3.95 (m, 4 H, 2 × NC*H*$_2$CH), 3.52 (s, 6 H, 2 × OCH_3), 3.44 (t, *J* = 4.7 Hz, 1 H, CH(C=O)), 3.23 (dt, *J* = 11.6, 4.7 Hz, 2 H, 2 × CHAr), 1.46 (s, 9 H, C(C*H*$_3)_3$); ^{13}C NMR (101 MHz, DMSO-*d*$_6$, 373 K) δ 170.2 (C=O amide), 157.7 (2 × C_{Ar} quat), 154.0 (C=O carbamate), 147.6 (C_{Ar}), 137.1 (C_{Ar} quat), 135.5 (C_{Ar}), 133.2 (C_{Ar} quat), 132.4 (2 × C_{Ar} quat), 127.7 (4 × C_{Ar}), 126.9 (C_{Ar} quat), 126.1 (C_{Ar}), 121.1 (C_{Ar}), 121.0 (C_{Ar}), 115.4 (C_{Ar}), 113.4 (4 × C_{Ar}), 78.4 (*C*$(CH_3)_3$), 54.4 (2 × OCH_3), 53.1 (*C*H(C=O)), 43.3 (2 × CHAr), 42.9 (2 × N*C*H_2CH), 27.7 (C(*C*$H_3)_3$); HRMS (ESI) *m/z* Calculated for $C_{34}H_{38}N_3O_5$ [M+H] 568.2811; Found 568.2814.

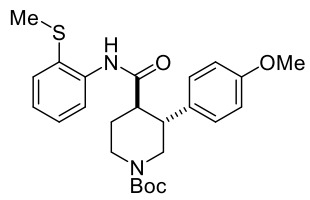
tert-Butyl-_cis,trans_-(±)-3,5-bis(4-methoxyphenyl)-4-(quinolin-8-ylcarbamoyl)piperidine-1-carboxylate (29c)



Prepared according to the **General Screening Procedure** above. Product **29c** was isolated as a colourless oil (27 mg, 0.05 mmol, 10%). R_f 0.18 (20% acetone/pentane); IR (film)/cm^{-1} 3340 (NH br), 2997, 2970, 2926, 2833, 1676 (C=O), 1512, 1482, 1423, 1246, 1157, 1035, 910, 827, 730; ^{1}H NMR (500 MHz, DMSO-*d*$_6$, 373 K) δ 9.69 (br s, 1 H, NH), 8.84 (dd, *J* = 4.2, 1.7 Hz, 1 H, HC_{Ar}), 8.29 (ddd, *J* = 8.3, 1.7, 0.4 Hz, 1 H, HC_{Ar}), 8.23 (dd, *J* = 7.7, 1.3 Hz, 1 H, HC_{Ar}), 7.58–7.51 (m, 2 H, 2 × HC_{Ar}), 7.40 (t, *J* = 8.0 Hz, 1 H, HC_{Ar}), 7.37–7.31 (m, 2 H, 2 × HC_{Ar}), 7.23–7.15 (m, 2 H, 2 × HC_{Ar}), 6.87–6.80 (m, 2 H, 2 × HC_{Ar}), 6.69–

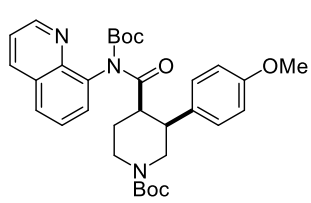
6.63 (m, 2 H, 2 × HC_{Ar}), 4.26–4.14 (m, 2 H, NC*H*HCHAr$_b$ and NC*H*HCHAr$_a$), 3.69 (s, 3 H, OCH_3), 3.67 (dd, *J* = 10.6, 5.4 Hz, 1 H, CH(C=O)), 3.59 (s, 3 H, OCH_3), 3.56 (dd, *J* = 9.6, 3.3 Hz, 1 H, NCH*H*CHAr$_a$) 3.51 (ddd, *J* = 5.4, 4.1, 3.9 Hz, 1 H, CHAr$_a$), 3.45 (td, *J* = 10.6, 4.6 Hz, 1 H, CHAr$_b$), 3.13 (dd, *J* = 13.1, 10.6 Hz, 1 H, NCH*H*CHAr$_b$), 1.41 (s, 9 H, C(C*H*$_3$)$_3$); ^{13}C NMR (126 MHz, DMSO-*d*$_6$, 373 K) δ 169.7 (C=O amide), 157.7 (C=O carbamate), 157.6 (C_{Ar} quat), 153.4 (C_{Ar} quat), 147.9 (C_{Ar}), 137.6 (C_{Ar} quat), 135.7 (C_{Ar}), 133.8 (C_{Ar} quat), 133.3 (C_{Ar} quat), 132.5 (C_{Ar} quat), 128.9 (2 × C_{Ar}), 128.1 (2 × C_{Ar}), 127.2 (C_{Ar} quat), 126.1 (C_{Ar}), 121.2 (C_{Ar}), 120.8 (C_{Ar}), 115.6 (C_{Ar}), 113.5 (2 × C_{Ar}), 113.0 (2 × C_{Ar}), 78.5 (*C*(CH$_3$)$_3$), 54.6 (OCH_3), 54.4 (OCH_3), 52.0 (*C*H(C=O)), 48.3 (N*C*H$_2$CHAr$_b$), 46.9 (N*C*H$_2$CHAr$_a$), 40.5 (CHAr$_a$), 38.1 (CHAr$_b$), 27.6 (C(*C*H$_3$)$_3$); HRMS (ESI) *m/z* Calculated for $C_{34}H_{38}N_3O_5$ [M+H] 568.2811; Found 568.2821.

tert-Butyl-_trans_-(±)-3-(4-methoxyphenyl)-4-((2-(methylthio)phenyl)carbamoyl)piperidine-1-carboxylate (30b)



Prepared according to the **General Screening Procedure** above using amide **26** (175 mg). Product **30b** was isolated as a white crystalline solid (57 mg, 0.13 mmol, 25%). R_f 0.29 (15% acetone/pentane); mp = 109–110 °C (from Et_2O/pentane); IR (film)/cm^{-1} 3205 (NH br), 2974, 2922, 2836, 1685 (C=O), 1658 (C=O), 1513, 1420, 1245 (C–O), 1155 (C–O), 1032, 827, 746; ^{1}H NMR (400 MHz, toluene-d$_8$, 373 K) δ 8.34 (d, *J* = 9.2 Hz, 1 H, HC_{Ar}), 7.77 (br s, 1 H, NH), 7.10 (dd, *J* = 7.8, 1.5 Hz, 1 H, HC_{Ar}), 7.05–6.99 (m, 1 H, HC_{Ar}), 6.90 (d, *J* = 7.4 Hz, 2 H, 2 × HC_{Ar}), 6.61 (t, *J* = 9.0 Hz, 1 H, HC_{Ar}), 6.56 (d, *J* = 7.4 Hz, 2 H, 2 × HC_{Ar}), 4.19–4.11 (m, 2 H, NC*H*HCHAr and NC*H*HCH$_2$), 3.24 (s, 3 H, OCH_3), 2.97 (td, *J* = 11.7, 4.2 Hz, 1 H, CHAr), 2.57 (dd, *J* = 13.0, 11.7 Hz, 1 H, NCH*H*CHAr), 2.52 (td, *J* = 11.3, 3.9 Hz, 1 H, NCH*H*CH$_2$), 2.24 (td, *J* = 13.2, 3.1 Hz, 1 H, CH(C=O)), 1.92 (qd, *J* = 11.7, 4.0 Hz, 1 H, NCH$_2$C*H*H), 1.73 (s, 3 H, SCH_3), 1.70–1.60 (m, 1 H, NCH$_2$CH*H*), 1.38 (s, 9 H, C(CH$_3$)$_3$); ^{13}C NMR (101 MHz, toluene-*d*$_8$, 373 K) δ 171.4 (C=O amide), 159.7 (C_{Ar} quat), 154.8 (C=O carbamate), 139.8 (C_{Ar} quat), 133.9 (C_{Ar} quat), 133.5 (C_{Ar}), 129.9 (C_{Ar}), 129.2 (2 × C_{Ar}), 124.2 (C_{Ar}), 124.1 (C_{Ar} quat), 121.5 (C_{Ar}), 115.1 (2 × C_{Ar}), 79.5 (*C*(CH$_3$)$_3$), 55.0 (OCH_3), 52.6 (*C*H(C=O)), 50.7 (N*C*H$_2$CHAr), 45.2 (CHAr), 44.0 (N*C*H$_2$CH$_2$), 29.9 (NCH$_2$*C*H$_2$), 28.8 (C(*C*H$_3$)$_3$), 18.9 (SCH_3); HRMS (ESI) *m/z* Calculated for [M+H] 457.2175; Found 457.2161.

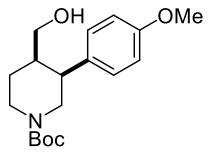
tert-Butyl-_cis_-(±)-4-((_tert_-butoxycarbonyl)(quinolin-8-yl)carbamoyl)-3-(4-methoxyphenyl) piperidine-1-carboxylate (33)



A flame-dried microwave vial was charged with amide **29a** (93 mg, 0.2 mmol, 1.0 equiv), followed by *di-tert*-butyl dicarbonate (Boc_2O, 218 mg, 1.0 mmol, 5.0 equiv) and 4-(dimethylamino)pyridine (DMAP, 49 mg, 0.40 mmol, 2.0 equiv). The reaction vessel was purged with argon, then dry MeCN (450 μL, 0.5 M) was added. The reaction tube was sealed, then heated to 70 °C slowly in an oil bath under an Ar atmosphere. After 18 h, the reaction mixture was then allowed to cool to rt and sat. aq. NH_4Cl (5 mL) was added, followed by CH_2Cl_2 (5 mL). The phases were separated and the aqueous layer was extracted with CH_2Cl_2 (3 × 5 mL). The combined organic layers were dried over Na_2SO_4, filtered, and the solvent was removed under reduced pressure. The crude

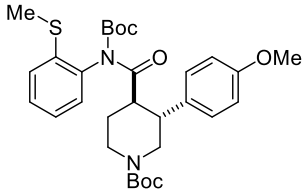
material was purified by flash column chromatography (15% EtOAc/pentane) to give the product **33** as an orange oil (96 mg, 0.19 mmol, 93%). R_f 0.22 (15% EtOAc/pentane); IR (film)/cm^{-1} 2974, 1733 (C=O), 1694 (C=O), 1513, 1423, 1394, 1293, 1248, 1156, 1121, 1036, 829, 791, 765, 697; ^{1}H NMR (400 MHz, acetonitrile-*d*$_3$) δ 8.85 (dd, *J* = 4.3, 1.7 Hz, 1 H, HC_{Ar}), 8.31 (dd, *J* = 8.3, 1.7 Hz, 1 H, HC_{Ar}), 7.89 (dd, *J* = 8.3, 1.3 Hz, 1 H, HC_{Ar}), 7.55–7.44 (m, 2 H, 2 × HC_{Ar}), 7.34–7.24 (m, 2 H, 2 × HC_{Ar}), 6.93 (d, *J* = 8.2 Hz, 2 H, 2 × HC_{Ar}), 6.79 (br s, 1 H, HC_{Ar}), 4.34 (br s, 1 H, NC*H*HCHAr), 4.03 (br s, 1 H, NC*H*HCH$_2$), 3.82 (s, 3 H, OCH_3), 3.70 (dd, *J* = 13.1, 4.3 Hz, 2 H, NCH*H*CH$_2$ and NCH*H*CHAr), 3.55 (ddd, *J* = 12.9, 7.3, 4.0 Hz, 1 H, CH(C=O)), 3.34 (dt, *J* = 7.4, 4.6 Hz, 1 H, CHAr), 2.20 (br s, 1 H, NCH$_2$C*H*H), 1.89–1.78 (m, 1 H, NCH$_2$CH*H*), 1.47 (s, 3 H, SCH_3), 1.43 (s, 9 H, $C(CH_3)_3$), 1.21 (s, 9 H, $C(CH_3)_3$); ^{13}C NMR (101 MHz, acetonitrile-*d*$_3$) δ 177.6 (C=O amide), 158.6 (C_{Ar} quat), 154.6 (C=O carbamate), 152.8 (C=O carbamate), 150.4 (C_{Ar}), 144.0 (C_{Ar} quat), 137.0 (C_{Ar}), 136.2 (C_{Ar} quat), 133.3 (C_{Ar} quat), 129.6 (2 × C_{Ar}), 128.7 (C_{Ar} quat), 127.7 (C_{Ar}), 126.0 (C_{Ar}), 121.8 (C_{Ar}), 117.4 (C_{Ar}), 113.5 (2 × C_{Ar}), 82.5 (*C*$(CH_3)_3$), 79.0 (*C*$(CH_3)_3$), 54.9 (OCH_3), 44.6 (N*C*H$_2$CHAr), 41.4 (*C*H(C=O)), 40.6 (N*C*H$_2$CH$_2$), 27.6 (CHAr), 26.6 (NCH$_2$*C*H$_2$), 25.7 (2 × C(*C*H$_3$)$_3$).

***tert*-Butyl-*cis*-(±)4-(hydroxymethyl)-3-(4-methoxyphenyl)piperidine-1-carboxylate (34)**



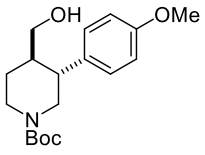
A solution of Boc-protected amide **33** (26 mg, 0.05 mmol, 1.0 equiv) in dry THF (300 μL) was added dropwise to a suspension of $LiAlH_4$ (7.0 mg, 0.19 mmol, 4.0 equiv) in dry THF (200 μL) at 0 °C under an argon atmosphere. The mixture was stirred at room temperature for 6 h and then quenched by slow addition of sat. aq. NH_4Cl (2 mL). After stirring for 30 min at rt, EtOAc (5 mL) was added and the phases were separated. The aqueous layer was extracted with EtOAc (3 × 5 mL) and the combined organic layers were dried over Na_2SO_4, filtered and the solvent removed under reduced pressure. Purification of the residue by flash column chromatography (5% to 20% grading acetone/pentane) afforded primary alcohol **34** as a colourless oil (7.7 mg, 0.024 mmol, 48%). R_f 0.45 (20% acetone/pentane); IR (film)/cm^{-1} 3442 (OH br), 2974, 2930, 1689 (C=O), 1511, 1430, 1366, 1249, 1161, 1036, 829; ^{1}H NMR (500 MHz, DMSO-*d*$_6$, 373 K) δ 7.16 (dd, *J* = 8.9, 0.5 Hz, 2 H, 2 × HC_{Ar}), 6.83 (d, *J* = 8.8 Hz, 2 H, 2 × HC_{Ar}), 3.97 (t, *J* = 5.0 Hz, 1 H, OH), 3.82–3.75 (m, 2 H, NC*H*HCHAr and NC*H*HCH$_2$), 3.75 (s, 3 H, OCH_3), 3.40 (dd, *J* = 13.2, 4.2 Hz, 1 H, NCH*H*CH$_2$), 3.23–3.16 (m, 2 H, C*H*HOH and NCH*H*CHAr), 3.11 (ddd, *J* = 10.7, 6.1, 4.9 Hz, 1 H, CH*H*OH), 2.99–2.94 (m, 1 H, CHAr, *superimposed onto H$_2$O peak*), 2.01–1.94 (m, 1 H, C*H*CH$_2$OH), 1.62–1.53 (m, 2 H, NCH$_2$C*H*$_2$), 1.40 (s, 9 H, $C(CH_3)_3$); ^{13}C NMR (126 MHz, DMSO-*d*$_6$, 373 K) δ 157.4 (C_{Ar} quat), 153.7 (C=O carbamate), 133.3 (C_{Ar} quat), 128.8 (2 × C_{Ar}), 113.1 (2 × C_{Ar}), 78.0 (*C*$(CH_3)_3$), 60.8 (CH_2OH), 54.6 (OCH_3), 46.4 (N*C*H$_2$CHAr), 41.3 (N*C*H$_2$CH$_2$), 40.6 (CHAr), 40.0 (*C*HCH$_2$OH), 27.7 (C(*C*H$_3$)$_3$), 23.9 (NCH$_2$*C*H$_2$); HRMS (ESI) *m/z* Calculated for $C_{18}H_{28}NO_4$ [M+H] 322.2018; Found 322.2023.

tert-Butyl-_trans_-(±)-4-((_tert_-butoxycarbonyl)(2-(methylthio)phenyl)carbamoyl)-3-(4-methoxyphenyl) piperidine-1-carboxylate (35)



A flame-dried microwave vial was charged with amide **30b** (35 mg, 0.08 mmol, 1.0 equiv), followed by di-*tert*-butyl dicarbonate (Boc_2O, 139 mg, 0.64 mmol, 8.0 equiv) and 4-(dimethylamino)pyridine (DMAP, 36 mg, 0.30 mmol, 4.0 equiv). The reaction vessel was purged with argon, then dry MeCN (1 mL) was added. The reaction tube was then heated to 70 °C slowly in an oil bath, with a reflux condenser attached and under an Ar atmosphere. After 18 h, the reaction mixture was then allowed to cool to rt and sat. aq. NH_4Cl (5 mL) was added, followed by CH_2Cl_2 (5 mL). The phases were separated and the aqueous layer was extracted with CH_2Cl_2 (3 × 5 mL). The combined organic layers were dried over Na_2SO_4, filtered, and the solvent was removed under reduced pressure. The crude material was purified by flash column chromatography (15% EtOAc/pentane) to give the pure product **35** as a colourless oil (39 mg, 0.07 mmol, 91%). R_f 0.20 (15% EtOAc/pentane); IR (film)/cm^{-1} 2929, 1737 (C=O), 1696 (C=O), 1368, 1293, 1245, 1156, 1103; ^{1}H NMR (400 MHz, toluene-d_8, 298 K) δ 7.10 (br s, 4 H, 4 × HC_{Ar}), 7.00 (br s, 1 H, HC_{Ar}), 6.96 (br s, 1 H, HC_{Ar}), 6.91–6.80 (m, 3 H, 3 x HC_{Ar}), 6.77–6.60 (m, 4 H, 4 x HC_{Ar}), 6.09 (d, *J* = 7.0 Hz, 1 H, HC_{Ar}), 4.68–4.49 (m, 1 H, NC*H*HCHAr), 4.51–4.34 (m, 2 H, NCH*H*CHAr and NC*H*HCH_2), 4.32 (td, *J* = 11.2, 3.4, 1 H, NCH*H*CH_2), 3.30 (s, 3 H, OCH_3), 3.22 (td, *J* = 11.2, 3.4 Hz, 1 H, CHAr), 2.80 (br s, 1 H, CH(C=O)), 2.40 (d, *J* = 14.5, 1 H, NCH_2C*H*H), 1.97 (d, *J* = 8.7, 1 H, NCH_2CH*H*), 1.88 (s, 3 H, SCH_3), 1.42 (s, 9 H, $C(CH_3)_3$), 1.21 (s, 9 H, $C(CH_3)_3$); ^{13}C NMR (101 MHz, toluene-d_8, 298 K) δ 175.8 (C=O amide), 158.8 (C_{Ar} quat), 154.0 (C=O carbamate), 152.3 (C=O carbamate), 138.1 (C_{Ar} quat), 137.3 (C_{Ar} quat), 133.4 (C_{Ar}), 129.3 (2 × C_{Ar}), 129.0 (C_{Ar}), 128.9 (C_{Ar}), 127.1 (C_{Ar} quat), 125.5 (C_{Ar}), 113.8 (2 × C_{Ar}), 81.8 (*C*$(CH_3)_3$), 78.6 (*C*$(CH_3)_3$), 54.2 (OCH_3), 48.6 (*C*H(C=O)), 48.0 (N*C*H_2CHAr), 45.4 (CHAr), 43.7 (N*C*H_2CH_2), 29.2 (NCH_2*C*H_2), 28.0 (C(*C*$H_3)_3$), 27.2 (C(*C*$H_3)_3$), 15.1 (SCH_3).

tert-Butyl-_trans_-(±)-4-(hydroxymethyl)-3-(4-methoxyphenyl)piperidine-1-carboxylate (36)

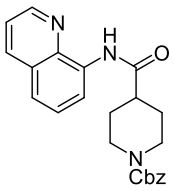


A solution of Boc-protected amide **35** (26 mg, 0.05 mmol, 1.0 equiv) in dry THF (300 μL) was added dropwise to a suspension of $LiAlH_4$ (7.0 mg, 0.19 mmol, 4.0 equiv) in dry THF (200 μL) at 0 °C under an argon atmosphere. The mixture was stirred at room temperature for 1 h and then quenched by slow addition of sat. aq. NH_4Cl (2 mL). After stirring at rt for 30 min, EtOAc (5 mL) was added and the phases were separated. The aqueous layer was extracted with EtOAc (3 × 5 mL) and the combined organic layers were dried over Na_2SO_4, filtered and the solvent removed under reduced pressure. Purification of the residue by flash column chromatography (5% to 20% grading acetone/pentane) afforded primary alcohol **36** as a white solid (10.4 mg, 0.03 mmol, 65%). R_f 0.34 (20% acetone/pentane); mp = 55–57 °C (from Et_2O/pentane); IR (film)/cm^{-1} 3443 (OH br), 2997, 2971, 2908, 1668 (C=O), 1511, 1422, 1364, 1245, 1164, 1131, 1035, 828, 732; ^{1}H NMR (400 MHz, DMSO-d_6, 373 K) δ 7.17–7.11 (m, 2 H, 2 × HC_{Ar}), 6.90–6.85 (m, 2 H, 2 × HC_{Ar}), 4.05 (ddt, *J* = 13.1, 4.5, 2.3 Hz, 1 H, NC*H*HCH_2), 3.87 (ddd, J = 12.9, 4.4, 1.8 Hz, 1 H, NC*H*HCHAr), 3.75 (s, 3 H, OCH_3), 3.22 (dt, *J* = 10.9, 3.2 Hz, 1 H, C*H*HOH), 3.07–3.05 (m, 1 H, CH*H*OH), 2.83 (td, *J* = 12.9, 2.9 Hz, 1 H, NCH*H*CH_2), 2.76 (dd, *J* = 13.0, 11.6 Hz, 1 H, NCH*H*CHAr), 2.39 (td, *J* =

11.3, 4.4 Hz, 1 H, CHAr), 1.92–1.84 (m, 1 H, NCH_2CHH), 1.79 (dtq, *J* = 10.9, 7.2, 3.5 Hz, 1 H, $CHCH_2OH$), 1.41 (s, 9 H, $C(CH_3)_3$), 1.38–1.25 (m, 1 H, NCH_2CHH); ^{13}C NMR (101 MHz, DMSO-d_6, 373 K) δ 157.7 (C_{Ar} quat), 153.6 (C=O carbamate), 133.6 (C_{Ar} quat), 128.1 (2 × C_{Ar}), 113.7 (2 × C_{Ar}), 78.2 ($C(CH_3)_3$), 62.6 (CH_2OH), 54.8 (OCH_3), 49.9 (NCH_2CHAr), 43.34 (NCH_2CH_2), 43.27 (*C*HAr), 42.6 ($CHCH_2OH$), 28.0 (NCH_2CH_2), 27.8 ($C(CH_3)_3$); HRMS (ESI) *m/z* Calculated for $C_{18}H_{28}NO_4$ [M+H] 322.2018; Found 322.2025.

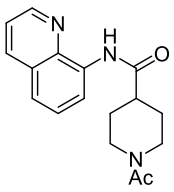
4.2.2 Scope of *N*-Protecting Group and Aryl Iodide

Benzyl 4-(quinolin-8-ylcarbamoyl)piperidine-1-carboxylate (40)



4-DMAP (127 mg, 1.00 mmol, 0.2 equiv) and EDC·HCl (1.05 g, 5.50 mmol, 1.1 equiv) were added to a solution of *N*-Cbz-piperidine-4-carboxylic acid (1.32 g, 5.00 mmol, 1.0 equiv) and 8-aminoquinoline (792 mg, 5.50 mmol, 1.1 equiv) in CH_2Cl_2 (10 mL). After stirring at rt for 24 h, the reaction was diluted with CH_2Cl_2 (10 mL), then sat. aq. $NaHCO_3$ (20 mL) was added and the aqueous layer extracted with CH_2Cl_2 (3 x 15 mL). The combined organic extracts were dried over Na_2SO_4, filtered, and the solvent removed under reduced pressure. Purification of the residue by flash column chromatography (20% to 50% EtOAc/pentane) afforded amide **40** as a white amorphous solid (1.52 g, 3.92 mmol, 78%). R_f 0.47 (40% EtOAc/pentane); mp = 138–140 °C (from EtOAc/pentane); IR (film)/cm^{-1} 3337 (NH), 3049, 2947, 2919, 1686 (C=O), 1670 (C=O), 1529, 1421, 1226, 1160, 1057, 946, 757, 671; ^1H NMR (400 MHz, $CDCl_3$) δ 9.95 (br s, 1 H, NH), 8.86–8.72 (m, 2 H, 2 × HC_{Ar}), 8.16 (dd, *J* = 8.3, 1.7 Hz, 1 H, HC_{Ar}), 7.57–7.49 (m, 2 H, 2 × HC_{Ar}), 7.46 (dd, *J* = 8.3, 4.2 Hz, 1 H, HC_{Ar}), 7.41–7.29 (m, 5 H, 5 × HC_{Ar}), 5.17 (s, 2 H, CH_2Ph), 4.42–4.32 (m, 2 H, 2 × $NCHHCH_2$), 3.01–2.89 (m, 2 H, 2 × $NCHHCH_2$), 2.66 (tt, *J* = 11.5, 3.8 Hz, 1 H, CH(C=O)), 2.15–1.97 (m, 2 H, 2 × NCH_2CHH), 1.94–1.80 (m, 2 H, 2 × NCH_2CHH); ^{13}C NMR (101 MHz, $CDCl_3$) δ 172.7 (C=O amide), 155.1 (C=O carbamate), 148.1 (C_{Ar}), 138.3 (C_{Ar} quat), 136.7 (C_{Ar} quat), 136.3 (C_{Ar}), 134.2 (C_{Ar} quat), 128.4 (2 × C_{Ar}), 127.9 (C_{Ar}), 127.83 (2 × C_{Ar}), 127.80 (C_{Ar} quat), 127.3 (C_{Ar}), 121.6 (C_{Ar}), 121.5 (C_{Ar}), 116.4 (C_{Ar}), 67.1 (NCO_2CH_2), 44.4 (2 × NCH_2CH_2), 43.4 (*C*H(C=O)), 28.5 (2 × NCH_2CH_2); HRMS (ESI) *m/z* Calculated for $C_{23}H_{24}N_3O_3$ [M+H] 390.1818; Found 390.1830.

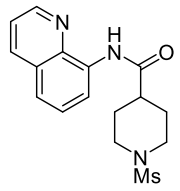
1-Acetyl-*N*-(quinolin-8-yl)piperidine-4-carboxamide (41)



4-DMAP (254 mg, 2.00 mmol, 0.2 equiv) and EDC·HCl (2.10 g, 11.00 mmol, 1.1 equiv) were added to a solution of *N*-Ac-piperidine-4-carboxylic acid (1.70 g, 10.00 mmol, 1.0 equiv) and 8-aminoquinoline (1.60 g, 11.00 mmol, 1.1 equiv) in CH_2Cl_2 (20 mL). After stirring at rt for 24 h, the reaction was diluted with CH_2Cl_2 (10 mL), then sat. aq. $NaHCO_3$ (20 mL) was added and the aqueous layer extracted with CH_2Cl_2 (3 x 15 mL). The combined organic extracts were dried over Na_2SO_4, filtered, and the solvent removed under reduced pressure. Purification of the residue by flash column chromatography (40% to 60% acetone/pentane) afforded amide **41** as a white amorphous solid (2.12 g, 7.10 mmol, 71%). R_f 0.22 (50% acetone/pentane); mp = 168–171 °C (from acetone/pentane); IR (film)/cm^{-1} 3355 (NH br), 3012, 2930, 2855, 1674 (C=O), 1521 (C=O), 1484, 1323, 1297, 1156, 932, 831, 764; ^1H NMR (400 MHz, $CDCl_3$) δ 9.95 (br s, 1 H, NH), 8.80 (dd, *J* = 4.3, 1.7 Hz, 1 H, HC_{Ar}), 8.75 (dd, *J* = 6.7, 2.3 Hz, 1 H, HC_{Ar}), 8.17 (dd,

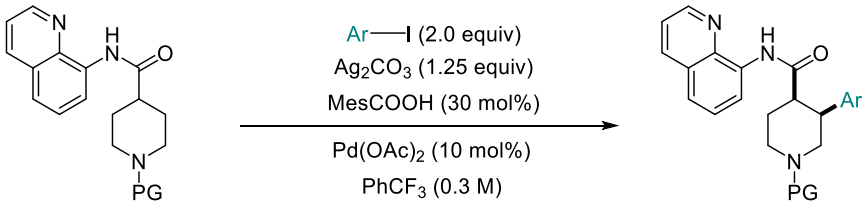
J = 8.3, 1.7 Hz, 1 H, HC_{Ar}), 7.56–7.49 (m, 2 H, 2 × HC_{Ar}), 7.46 (dd, *J* = 8.3, 4.3 Hz, 1 H, HC_{Ar}), 4.77–4.59 (m, 1 H, NC*H*HCH_2), 4.04–3.89 (m, 1 H, NCH*H*CH_2), 3.19 (ddd, *J* = 13.6, 12.0, 2.8 Hz, 1 H, NC*H*HCH_2), 2.84–2.65 (m, 2 H, NCH*H*CH_2 and HC(C=O)), 2.13 (s, 3 H, CH_3), 2.11–2.04 (m, 2 H , 2 × NCH_2CHH), 1.85 (dddd, *J* = 25.1, 13.4, 11.7, 4.3 Hz, 2 H, 2 × NCH_2CHH); ^{13}C NMR (101 MHz, $CDCl_3$) δ 172.5 (C=O amide), 168.9 (C=O acetyl), 148.1 (C_{Ar}), 138.2 (C_{Ar} quat), 136.5 (C_{Ar}), 134.1 (C_{Ar} quat), 127.9 (C_{Ar} quat), 127.4 (C_{Ar}), 121.7 (C_{Ar}), 121.6 (C_{Ar}), 116.6 (C_{Ar}), 45.8 (NCH_2CH_2), 44.4 (*C*H(C=O)), 40.9 (NCH_2CH_2), 29.0 (NCH_2CH_2), 28.6 (NCH_2CH_2), 21.5 ($COCH_3$); HRMS (ESI) *m/z* Calculated for $C_{17}H_{20}N_3O_2$ [M+H] 297.1477; Found 297.1470. *Note: the difference in chemical shift between protons and carbons that are expected to be chemically equivalent is most likely caused by the presence of the molecule as a single rotamer on a longer timescale compared to the ^{1}H and ^{13}C NMR relaxation times. The stable rotameric structure arises from a restricted rotation around the N-Ac single bond.*

1-(Methylsulfonyl)-*N*-(quinolin-8-yl)piperidine-4-carboxamide (42)



4-DMAP (127 mg, 1.00 mmol, 0.2 equiv) and EDC·HCl (1.05 g, 5.50 mmol, 1.1 equiv) were added to a solution of *N*-Ms-piperidine-4-carboxylic acid (1.04 g, 5.00 mmol, 1.0 equiv) and 8-aminoquinoline (792 mg, 5.50 mmol, 1.1 equiv) in CH_2Cl_2 (10 mL). After stirring at rt for 24 h, the reaction was diluted with CH_2Cl_2 (10 mL), then sat. aq. $NaHCO_3$ (20 mL) was added and the aqueous layer extracted with CH_2Cl_2 (3 x 10 mL). The combined organic extracts were dried over Na_2SO_4, filtered, and the solvent removed under reduced pressure. Purification of the residue by flash column chromatography (40% acetone/pentane) afforded amide **42** as a pale pink crystalline solid (833 mg, 2.50 mmol, 50%). R_f 0.44 (40% acetone/pentane); mp not observed up to 270 °C (from acetone/pentane); IR (film)/cm^{-1} 3347 (NH), 3049, 2929, 2851, 1681 (C=O), 1524, 1483, 1323 (S=O sulfone), 1151 (S=O sulfone), 932, 827; ^{1}H NMR (400 MHz, $CDCl_3$) δ 10.00 (br s, 1 H, NH), 8.88–8.70 (m, 2 H, 2 × HC_{Ar}), 8.20 (dd, *J* = 8.2, 1.7 Hz, 1 H, HC_{Ar}), 7.61–7.45 (m, 3 H, 3 × HC_{Ar}), 3.97–3.81 (m, 2 H, 2 × NC*H*HCH_2), 2.94 (ddd, *J* = 12.1, 10.8, 3.0 Hz, 2 H, 2 × NCH*H*CH_2), 2.84 (s, 3 H, CH_3), 2.67 (tt, *J* = 10.6, 4.0 Hz, 1 H, HC(C=O)), 2.23–2.16 (m, 2 H, 2 × NCH_2CHH), 2.15–1.99 (m, 2 H, 2 × NCH_2CHH); ^{13}C NMR (101 MHz, $CDCl_3$) δ 172.2 (C=O amide), 148.2 (C_{Ar}), 138.3 (C_{Ar} quat), 136.6 (C_{Ar}), 134.0 (C_{Ar} quat), 128.0 (C_{Ar} quat), 127.4 (C_{Ar}), 121.8 (C_{Ar}), 121.7 (C_{Ar}), 116.7 (C_{Ar}), 45.2 (2 × NCH_2CH_2), 43.3 (*C*H(C=O)), 35.2 (CH_3), 28.4 (2 × NCH_2CH_2); HRMS (ESI) *m/z* Calculated for $C_{16}H_{20}N_3O_3S$ [M+H] 333.1147; Found 333.1142.

General Procedure A for C–H arylation of *N*-Protected Piperidines 25 and 40-42

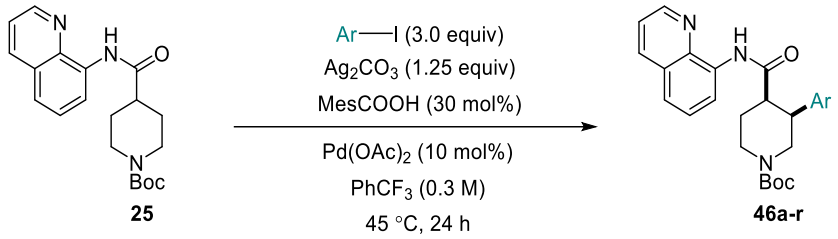


25, 40-42 PG = Boc, Cbz, Ac, Ms — **29a, 43-45**

A flame-dried microwave vial was charged with either of the amides **25** or **40-42** (0.40 mmol, 1.0 equiv). The requisite aryl iodide (0.80 mmol, 2.0 equiv), Ag_2CO_3 (138 mg, 0.50 mmol, 1.25 equiv), 2,4,6-

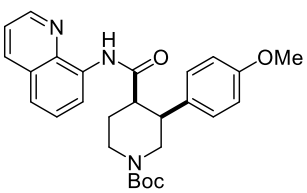
trimethylbenzoic acid (MesCOOH, 20 mg, 0.12 mmol, 0.3 equiv) and $Pd(OAc)_2$ (9 mg, 0.04 mmol, 0.1 equiv) were added sequentially. The reaction vessel was sealed and purged with argon, then $PhCF_3$ (1.34 mL, 0.3 M) was added by syringe. The reaction tube was placed in a preheated oil bath and stirred at 45 °C for 24 h. The reaction mixture was then allowed to cool to rt, diluted with EtOAc (5 mL) and filtered through a pad of Celite, eluting with further EtOAc (2 × 10 mL). The solvent was removed under reduced pressure and the crude material purified by flash column chromatography under the specified conditions. Et_2O (5 mL), followed by pentane (5 mL) were added to the resulting *cis*-3-arylated piperidine, with the resulting suspension concentrated under reduced pressure. This procedure was repeated three times to eliminate residual solvent and afford desired arylated piperidines.

General Procedure B for C–H arylation of *N*-Boc Protected Piperidines



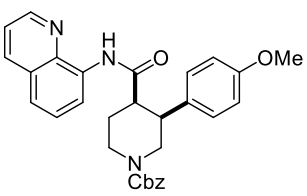
A flame-dried microwave vial was charged with amide **25** (142 mg, 0.40 mmol, 1.0 equiv). The requisite aryl iodide (1.20 mmol, 3.0 equiv), Ag_2CO_3 (138 mg, 0.50 mmol, 1.25 equiv), 2,4,6-trimethylbenzoic acid (MesCOOH, 20 mg, 0.12 mmol, 0.3 equiv) and $Pd(OAc)_2$ (9 mg, 0.04 mmol, 0.1 equiv) were added sequentially. The reaction vessel was sealed and purged with argon, then $PhCF_3$ (1.34 mL, 0.3 M) was added by syringe. The reaction tube was placed in a preheated oil bath and stirred at 45 °C for 24 h. The reaction mixture was then allowed to cool to rt, diluted with EtOAc (5 mL) and filtered through a pad of Celite, eluting with further EtOAc (2 × 10 mL). The solvent was removed under reduced pressure and the crude material purified by flash column chromatography under the specified conditions. Et_2O (5 mL), followed by pentane (5 mL) were added to the resulting *cis*-3-arylated piperidine, with the resulting suspension concentrated under reduced pressure. This procedure was repeated three times to eliminate residual solvent and afford desired arylated piperidines.

***tert*-Butyl-*cis*-(±)-3-(4-methoxyphenyl)-4-(quinolin-8-ylcarbamoyl)piperidine-1-carboxylate (29a)**



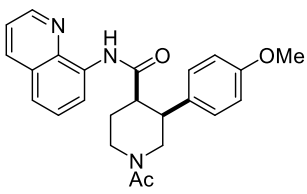
Prepared according to **General Procedure A** using amide **25** (142 mg) and 4-iodoanisole (187 mg). Purification by flash column chromatography (15% to 25% acetone/pentane) afforded arylated piperidine **29a** as a white solid (125 mg, 0.27 mmol, 68%). All characterisation information in full agreement with data previously reported for **29a** (page 164).

Benzyl-*cis*-(±)-3-(4-methoxyphenyl)-4-(quinolin-8-ylcarbamoyl)piperidine-1-carboxylate (43)



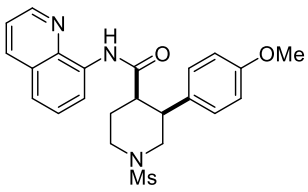
Prepared according to **General Procedure A** using amide **40** (156 mg) and 4-iodoanisole (187 mg). Purification by flash column chromatography (5% to 10% Et_2O/CH_2Cl_2) afforded an inseparable mixture of arylated piperidine **43** and starting material **40** in approximately a 7:1 ratio, respectively. (210 mg, 67% combined yield). R_f 0.40 (10% Et_2O/CH_2Cl_2); IR (film)/cm^{-1} 3341 (NH), 2948, 2833, 1678 (C=O), 1516, 1481, 1422, 1239, 1112, 1033, 827, 730; ^{1}H NMR (400 MHz, DMSO-*d*$_6$, 373 K, major product **43**) δ 9.63 (br s, 1 H, NH), 8.80 (dd, *J* = 4.2, 1.7 Hz, 1 H, HC_{Ar}), 8.45 (dd, *J* = 7.6, 1.4 Hz, 1 H, HC_{Ar}), 8.31 (dd, *J* = 8.3, 1.7 Hz, 1 H, HC_{Ar}), 7.61–7.54 (m, 2 H, 2 × HC_{Ar}), 7.50 (t, *J* = 7.9 Hz, 1 H, HC_{Ar}), 7.39–7.29 (m, 5 H, 5 × HC_{Ar}), 7.22–7.12 (m, 2 H, 2 × HC_{Ar}), 6.74–6.61 (m, 2 H, 2 × HC_{Ar}), 5.12 (s, 2 H, O*C*H_2Ph), 4.07 (dd, *J* = 12.9, 8.5 Hz, 1 H, NC*H*HCHAr), 3.96–3.79 (m, 2 H, NC*H*HCH_2 and NCH*H*CHAr), 3.66 (ddd, *J* = 13.1, 6.5, 4.7 Hz, 1 H, NCH*H*CH_2), 3.58 (s, 3 H, OCH_3), 3.34 (dt, *J* = 6.1, 4.8 Hz, 1 H, CH(C=O)), 3.26 (dt, *J* = 8.8, 4.5 Hz, 1 H, CHAr), 2.07 (dtd, *J* = 13.6, 6.2, 3.9 Hz, 1 H, NCH_2C*H*H), 1.93 (ddt, *J* = 13.6, 9.0, 4.6 Hz, 1 H, NCH_2CH*H*); ^{13}C NMR (101 MHz, DMSO-*d*$_6$, 373 K, major product **43**) δ 171.4 (C=O amide), 157.6 (C_{Ar} quat), 154.4 (C=O carbamate), 148.0 (C_{Ar}), 137.7 (C_{Ar} quat), 136.7 (C_{Ar} quat), 135.8 (C_{Ar}), 133.7 (C_{Ar} quat), 132.4 (C_{Ar} quat), 128.2 (2 × C_{Ar}), 127.8 (2 × C_{Ar}), 127.2 (C_{Ar} quat), 127.1 (C_{Ar}), 126.9 (2 × C_{Ar}), 126.2 (C_{Ar}), 121.3 (C_{Ar}), 121.1 (C_{Ar}), 116.0 (C_{Ar}), 113.3 (2 × C_{Ar}), 65.8 (O*C*H_2Ph), 54.5 (OCH_3), 45.5 (N*C*H_2CHAr), 45.2 (*C*H(C=O)), 41.4 (*C*HAr), 40.7 (N*C*H_2CH_2), 25.6 (NCH_2*C*H_2); HRMS (ESI) *m/z* Calculated for $C_{30}H_{30}N_3O_3$ [M+H] 496.2236; Found 496.2231.

***cis*-(±)-1-Acetyl-3-(4-methoxyphenyl)-*N*-(quinolin-8-yl)piperidine-4-carboxamide (44)**



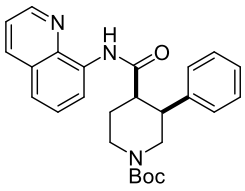
Prepared according to **General Procedure A** using amide **41** (161 mg) and 4-iodoanisole (187 mg). Purification by flash column chromatography (20% to 40% acetone/pentane) afforded arylated piperidine **44** as a yellow gum (89 mg, 0.18 mmol, 44%). R_f 0.39 (35% acetone/pentane); IR (film)/cm^{-1} 3340 (NH), 2998, 2928, 2833, 1676 (C=O), 1623 (C=O), 1518, 1482, 1423, 1377, 1245, 828, 791, 730; ^{1}H NMR (500 MHz, DMSO-*d*$_6$, 373 K) δ 9.61 (br s, 1 H, NH), 8.80 (dd, *J* = 4.2, 1.7 Hz, 1 H, HC_{Ar}), 8.46 (dd, *J* = 7.6, 1.4 Hz, 1 H, HC_{Ar}), 8.31 (ddd, *J* = 8.3, 1.7, 0.4 Hz, 1 H, HC_{Ar}), 7.61–7.53 (m, 2 H, 2 × HC_{Ar}), 7.53–7.47 (m, 1 H, HC_{Ar}), 7.24–7.16 (m, 2 H, 2 × HC_{Ar}), 6.73–6.68 (m, 2 H, 2 × HC_{Ar}), 4.02 (br s, 1 H, NC*H*HCHAr), 3.89 (ddd, *J* = 12.9, 8.9, 3.8 Hz, 1 H, NC*H*HCH_2), 3.68 (d, *J* = 11.3 Hz, 1 H, NCH*H*CH_2), 3.58 (s, 3 H, OCH_3), 3.36 (dt, *J* = 6.0, 4.9 Hz, 1 H, CH(C=O)), 3.25 (br s, 1 H, CHAr), 2.13–2.08 (m, 1 H, NCH_2C*H*H), 2.05–1.89 (m, 4 H, NCH_2CH*H* and NCO_2CH_3); NCH*H*CHAr not observed; ^{13}C NMR (126 MHz, DMSO-*d*$_6$, 373 K) δ 171.4 (C=O aminoquinoline amide), 167.9 (C=O acetyl), 157.6 (C_{Ar} quat), 147.9 (C_{Ar}), 137.7 (C_{Ar} quat), 135.8 (2 × C_{Ar}), 133.7 (C_{Ar} quat), 132.5 (C_{Ar} quat), 128.2 (C_{Ar}), 127.2 (C_{Ar} quat), 126.2 (C_{Ar}), 121.3 (C_{Ar}), 121.0 (C_{Ar}), 115.9 (C_{Ar}), 113.3 (2 × C_{Ar}), 54.5 (OCH_3), 45.2 (*C*H(C=O)), 41.7 (CHAr), 26.5 (NCH_2*C*H_2), 20.5 (NCO_2*C*H_3); Note: N*C*H_2CHAr and N*C*H_2CH_2 not observed. Chemical shift of NCH_2*C*H_2 assigned based on the HSQC correlation observed with the corresponding NCH_2C*H*$_2$ protons; HRMS (ESI) *m/z* Calculated for $C_{24}H_{26}N_3O_3$ [M+H] 404.1974; Found 404.1971.

***cis*-(±)-3-(4-Methoxyphenyl)-1-(methylsulfonyl)-*N*-(quinolin-8-yl)piperidine-4-carboxamide (45)**



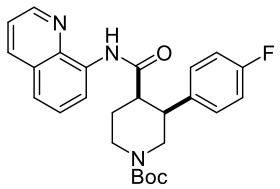
Prepared according to **General Procedure A** using amide **42** (133 mg) and 4-iodoanisole (187 mg). Purification by flash column chromatography (10% to 30% acetone/pentane) afforded arylated piperidine **45** as a pale yellow gum (42 mg, 0.10 mmol, 26%). R_f 0.47 (35% acetone/pentane); IR (film)/cm^{-1} 3340 (NH br), 3046, 2950, 2921, 2848, 1680 (C=O), 1525 (S=O), 1484, 1324, 1153, 965, 933, 911; ^{1}H NMR (400 MHz, $CDCl_3$, 298 K) δ 9.40 (br s, 1 H, NH), 8.64 (dd, *J* = 4.2, 1.7 Hz, 1 H, HC_{Ar}), 8.61 (dd, *J* = 6.2, 2.8 Hz, 1 H, HC_{Ar}), 8.12 (dd, *J* = 8.3, 1.7 Hz, 1 H, HC_{Ar}), 7.53–7.46 (m, 2 H, 2 × HC_{Ar}), 7.41 (dd, *J* = 8.3, 4.2 Hz, 1 H, HC_{Ar}), 7.24–7.17 (m, 2 H, 2 × HC_{Ar}), 6.71–6.64 (m, 2 H, 2 × HC_{Ar}), 3.90 (t, *J* = 11.0 Hz, 1 H, NC*H*HCHAr), 3.78–3.73 (m, 1 H, NCH*H*CHAr), 3.73–3.63 (m, 2 H, NCH_2CH$_2$), 3.58 (s, 3 H, OCH_3), 3.35 (dt, *J* = 10.2, 4.5 Hz, 1 H, CHAr), 3.08 (q, *J* = 4.4 Hz, 1 H, CH(C=O)), 2.89 (s, 3 H, SCH_3), 2.34–2.16 (m, 2 H, NCH$_2$CH_2); ^{13}C NMR (101 MHz, $CDCl_3$, 298 K) δ 172.1 (C=O amide), 158.6 (C_{Ar} quat), 148.0 (C_{Ar}), 138.2 (C_{Ar} quat), 136.2 (C_{Ar}), 133.9 (C_{Ar} quat), 131.9 (C_{Ar} quat), 128.6 (2 × C_{Ar}), 127.8 (C_{Ar} quat), 127.1 (C_{Ar}), 121.7 (C_{Ar}), 121.5 (C_{Ar}), 116.3 (C_{Ar}), 114.0 (2 × C_{Ar}), 55.0 (OCH_3), 46.6 (N*C*H$_2$CHAr), 46.1 (*C*H(C=O)), 43.5 (CHAr), 42.4 (N*C*H$_2$CH$_2$), 34.3 (SCH_3), 28.1 (NCH$_2$*C*H$_2$); HRMS (ESI) ***m/z*** Calculated for $C_{23}H_{26}N_3O_4S$ [M+H] 440.1644; Found 440.1637.

***tert*-Butyl-*cis*-(±)-3-phenyl-4-(quinolin-8-ylcarbamoyl)piperidine-1-carboxylate (46a)**



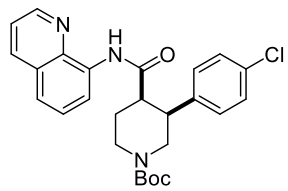
Prepared according to **General Procedure A** using amide **25** (142 mg) and iodobenzene (177 mg). Purification by flash column chromatography (5% to 10% Et_2O/CH_2Cl_2) afforded arylated piperidine **46a** as a pale yellow foam (91 mg, 0.21 mmol, 53%). R_f 0.48 (10% Et_2O/CH_2Cl_2); mp = 98–100 °C (from Et_2O/pentane); IR (film)/cm^{-1} 3343 (NH br), 2999, 2970, 2922, 1673 (C=O), 1520, 1481, 1419, 1364, 1322, 1239, 1158, 1110, 910, 825, 792, 760; ^{1}H NMR (400 MHz, DMSO-*d*$_6$, 373 K) δ 9.66 (br s, 1 H, NH), 8.81 (dd, *J* = 4.2, 1.7 Hz, 1 H, HC_{Ar}), 8.44 (dd, *J* = 7.6, 1.4 Hz, 1 H, HC_{Ar}), 8.31 (dd, *J* = 8.3, 1.7 Hz, 1 H, HC_{Ar}), 7.62–7.52 (m, 2 H, 2 × HC_{Ar}), 7.52–7.46 (m, 1 H, HC_{Ar}), 7.32–7.26 (m, 2 H, 2 × HC_{Ar}), 7.14 (ddd, *J* = 7.7, 6.9, 1.2 Hz, 2 H, 2 × HC_{Ar}), 7.09–7.02 (m, 1 H, HC_{Ar}), 4.07 (dd, *J* = 13.0, 8.1 Hz, 1 H, NC*H*HCHAr), 3.87–3.74 (m, 2 H, NC*H*HCH$_2$ and NCH*H*CHAr), 3.55 (ddd, *J* = 13.2, 6.5, 4.3 Hz, 1 H, NCH*H*CH$_2$), 3.37 (dt, *J* = 6.5, 4.8 Hz, 1 H, CH(C=O)), 3.28 (dt, *J* = 8.7, 4.5 Hz, 1 H, CHPh), 2.14–2.02 (m, 1 H, NCH$_2$C*H*H), 1.92 (td, *J* = 8.8, 4.3 Hz, 1 H, NCH$_2$CH*H*), 1.42 (s, 9 H, C(CH$_3$)$_3$); ^{13}C NMR (101 MHz, DMSO-*d*$_6$, 373 K) δ 171.3 (C=O amide), 153.7 (C=O carbamate), 148.0 (C_{Ar}), 140.6 (C_{Ar} quat), 137.7 (C_{Ar} quat), 135.8 (C_{Ar}), 133.7 (C_{Ar} quat), 127.4 (2 × C_{Ar}), 127.3 (2 × C_{Ar}), 127.2 (C_{Ar} quat), 126.2 (C_{Ar}), 125.8 (C_{Ar}), 121.3 (C_{Ar}), 121.1 (C_{Ar}), 115.9 (C_{Ar}), 78.2 (*C*(CH$_3$)$_3$), 45.24 (N*C*H$_2$CHAr), 45.15 (*C*H(C=O)), 42.1 (*C*HAr), 40.5 (N*C*H$_2$CH$_2$), 27.7 (C(*C*H$_3$)$_3$), 25.6 (NCH$_2$*C*H$_2$); HRMS (ESI) ***m/z*** Calculated for $C_{26}H_{30}N_3O_3$ [M+H] 432.2287; Found 432.2292.

***tert*-Butyl-*cis*-(±)-3-(4-fluorophenyl)-4-(quinolin-8-ylcarbamoyl)piperidine-1-carboxylate (46b)**



Prepared according to **General Procedure A** using amide **25** (142 mg) and 4-fluoroiodobenzene (178 mg). Purification by sequential flash column chromatography (5% to 8% Et_2O/CH_2Cl_2, followed by 20% acetone/pentane) afforded arylated piperidine **46b** as a yellow foamy solid (98 mg, 0.22 mmol, 56%). R_f 0.47 (10% Et_2O/CH_2Cl_2); mp = 68–70 °C (from Et_2O/pentane); IR (film)/cm^{-1} 3342 (NH br), 3001, 2972, 2924, 1675 (C=O), 1521 (C=O), 1481, 1420, 1365, 1226, 1158, 1111, 906, 826, 728; ^{1}H NMR (400 MHz, DMSO-*d*$_6$, 373 K) δ 9.64 (br s, 1 H, NH), 8.81 (dd, *J* = 4.2, 1.7 Hz, 1 H, HC_{Ar}), 8.42 (dd, *J* = 7.6, 1.3 Hz, 1 H, HC_{Ar}), 8.31 (ddd, *J* = 8.3, 1.7, 0.4 Hz, 1 H, HC_{Ar}), 7.61–7.53 (m, 2 H, 2 × HC_{Ar}), 7.49 (t, *J* = 7.9 Hz, 1 H, HC_{Ar}), 7.34–7.27 (m, 2 H, 2 × HC_{Ar}), 6.96–6.89 (m, 2 H, 2 × HC_{Ar}), 4.01 (dd, *J* = 13.0, 8.0 Hz, 1 H, NC*H*HCHAr), 3.81 (ddd, *J* = 12.7, 8.5, 3.9 Hz, 1 H, NC*H*HCH$_2$), 3.73 (dd, *J* = 13.0, 4.1 Hz, 1 H, NCH*H*CHAr), 3.53 (ddd, *J* = 13.1, 6.7, 4.3 Hz, 1 H, NCH*H*CH$_2$), 3.35 (dt, *J* = 6.6, 4.8 Hz, 1 H, CH(C=O)), 3.29 (dt, *J* = 8.6, 4.5 Hz, 1 H, CHAr), 2.05 (dtd, *J* = 13.5, 6.6, 3.8 Hz, 1 H, NCH$_2$C*H*H), 1.90 (ddt, *J* = 13.3, 8.8, 4.5 Hz, 1 H, NCH$_2$CH*H*), 1.42 (s, 9 H, C(C*H*$_3$)$_3$); ^{13}C NMR (126 MHz, DMSO-*d*$_6$, 373 K) δ 171.2 (C=O amide), 160.6 (d, J_{CF} = 246.7 Hz, FC$_{Ar}$ quat), 153.7 (C=O carbamate), 148.0 (C_{Ar}), 137.7 (C_{Ar} quat), 136.7 (d, J_{CF} = 3.4 Hz, F-*p*-C_{Ar} quat), 135.8 (C_{Ar}), 133.6 (C_{Ar} quat), 129.1 (d, J_{CF} = 8.1 Hz, 2 × F-*m*-C_{Ar}), 127.2 (C_{Ar} quat), 126.2 (C_{Ar}), 121.3 (C_{Ar}), 121.1 (C_{Ar}), 116.0 (C_{Ar}), 114.1 (d, J_{CF} = 21.0 Hz, 2 × F-*o*-C_{Ar}), 78.3 (*C*(CH$_3$)$_3$), 45.3 (N*C*H$_2$CHAr), 45.1 (*C*H(C=O)), 41.3 (*C*HAr), 40.5 (N*C*H$_2$CH$_2$), 27.6 (C(*C*H$_3$)$_3$), 25.5 (NCH$_2$*C*H$_2$); ^{19}F{^{1}H} NMR (471 MHz, DMSO-*d*$_6$, 373 K) δ –116.69 (s); HRMS (ESI) *m/z* Calculated for $C_{26}H_{29}FN_3O_3$ [M+H] 450.2193; Found 450.2191.

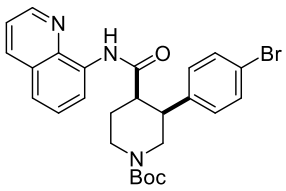
***tert*-Butyl-*cis*-(±)-3-(4-chlorophenyl)-4-(quinolin-8-ylcarbamoyl)piperidine-1-carboxylate (46c)**



Prepared according to **General Procedure A** using amide **25** (142 mg) and 1-chloro-4-iodobenzene (192 mg). Purification by sequential flash column chromatography (5% to 8% Et_2O/CH_2Cl_2, followed by 20% acetone/pentane) afforded arylated piperidine **46c** as a pale yellow solid (110 mg, 0.25 mmol, 50%). R_f 0.39 (10% Et_2O/CH_2Cl_2); mp = 109–111°C (from Et_2O/pentane); IR (film)/cm^{-1} 3275 (NH br), 2967, 2926, 2906, 1675 (C=O), 1521 (C=O), 1479, 1420, 1240, 1160, 1113, 1007, 823, 795, 752; ^{1}H NMR (400 MHz, DMSO-*d*$_6$, 373 K) δ 9.66 (br s, 1 H, NH), 8.82 (dd, *J* = 4.2, 1.7 Hz, 1 H, HC_{Ar}), 8.42 (dd, *J* = 7.6, 1.3 Hz, 1 H, HC_{Ar}), 8.32 (dd, *J* = 8.2, 1.7 Hz, 1 H, HC_{Ar}), 7.61–7.53 (m, 2 H, 2 × HC_{Ar}), 7.50 (t, *J* = 7.9 Hz, 1 H, HC_{Ar}), 7.33–7.27 (m, 2 H, 2 × HC_{Ar}), 7.20–7.14 (m, 2 H, 2 × HC_{Ar}), 4.02 (dd, *J* = 13.0, 8.0 Hz, 1 H, NC*H*HCHAr), 3.82 (ddd, *J* = 12.7, 8.4, 3.9 Hz, 1 H, NC*H*HCH$_2$), 3.74 (dd, *J* = 13.0, 4.1 Hz, 1 H, NCH*H*CHAr), 3.53 (ddd, *J* = 13.1, 6.7, 4.3 Hz, 1 H, NCH*H*CH$_2$), 3.38 (dt, *J* = 6.6, 4.8 Hz, 1 H, CH(C=O)), 3.30 (dt, *J* = 8.6, 4.4 Hz, 1 H, C*H*Ar), 2.06 (ddt, *J* = 13.5, 6.7, 3.3 Hz, 1 H, NCH$_2$C*H*H), 1.91 (ddt, *J* = 13.3, 8.7, 4.5 Hz, 1 H, NCH$_2$CH*H*), 1.42 (s, 9 H, C(C*H*$_3$)$_3$); ^{13}C NMR (101 MHz, DMSO-*d*$_6$, 373 K) δ 171.1 (C=O amide), 153.7 (C=O carbamate), 148.0 (C_{Ar}), 139.6 (C_{Ar} quat), 137.7 (C_{Ar} quat), 135.8 (C_{Ar}), 133.6 (C_{Ar} quat), 130.8 (C_{Ar} quat), 129.1 (2 × C_{Ar}), 127.4 (2 × C_{Ar}), 127.2 (C_{Ar} quat), 126.2 (C_{Ar}), 121.3 (C_{Ar}), 121.2 (C_{Ar}), 116.1 (C_{Ar}), 78.3 (*C*(CH$_3$)$_3$), 45.1 (N*C*H$_2$CHAr), 45.0

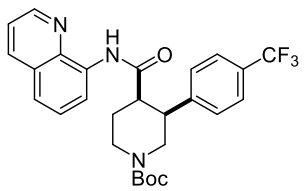
(*C*H(C=O)), 41.4 (*C*HAr), 40.5 (N*C*H$_2$CH$_2$), 27.6 (C(*C*H$_3$)$_3$), 25.4 (NCH$_2$*C*H$_2$); HRMS (ESI) *m/z* Calculated for $C_{26}H_{29}{}^{35}ClN_3O_3$ [M+H] 466.1897; Found 466.1901.

tert-Butyl-_cis_-(±)-3-(4-bromophenyl)-4-(quinolin-8-ylcarbamoyl)piperidine-1-carboxylate (46d)



Prepared according to **General Procedure A** using amide **25** (142 mg) and 4-bromo-1-iodobenzene (227 mg). Purification by flash column chromatography (2% to 5% Et$_2$O/CH$_2$Cl$_2$) afforded arylated piperidine **46d** as a light pink crystalline solid (139 mg, 0.28 mmol, 55%). R_f 0.51 (5% Et$_2$O/CH$_2$Cl$_2$); mp = 134–135 °C (from Et$_2$O/pentane); IR (film)/cm^{-1} 3288 (NH), 3042, 2971, 2930, 1681 (C=O), 1525 (C=O), 1484, 1424, 1323, 1290, 1241, 1163, 1115, 1010, 932, 824, 753; ^{1}H NMR (400 MHz, DMSO-*d*$_6$, 373 K) δ 9.66 (br s, 1 H, NH), 8.82 (dd, *J* = 4.2, 1.7 Hz, 1 H, HC$_{Ar}$), 8.42 (dd, *J* = 7.6, 1.4 Hz, 1 H, HC$_{Ar}$), 8.32 (ddd, *J* = 8.3, 1.7, 0.4 Hz, 1 H, HC$_{Ar}$), 7.63–7.54 (m, 2 H, 2 × HC$_{Ar}$), 7.53–7.47 (m, 1 H, HC$_{Ar}$), 7.35–7.28 (m, 2 H, 2 × HC$_{Ar}$), 7.27–7.19 (m, 2 H, 2 × HC$_{Ar}$), 4.01 (dd, *J* = 13.0, 8.0 Hz, 1 H, NC*H*HCHAr), 3.82 (ddd, *J* = 12.7, 8.3, 3.9 Hz, 1 H, NC*H*HCH$_2$), 3.73 (dd, *J* = 13.0, 4.1 Hz, 1 H, NCH*H*CHAr), 3.59–3.50 (m, 1 H, NCH*H*CH$_2$), 3.38 (dt, *J* = 6.7, 4.8 Hz, 1 H, CH(C=O)), 3.28 (dt, *J* = 8.6, 4.4 Hz, 1 H, CHAr), 2.06 (dtd, *J* = 13.6, 6.7, 3.9 Hz, 1 H, NCH$_2$C*H*H), 1.92 (ddt, *J* = 13.3, 8.7, 4.5 Hz, 1 H, NCH$_2$CH*H*), 1.42 (s, 9 H, C(CH$_3$)$_3$); ^{13}C NMR (101 MHz, DMSO-*d*$_6$, 373 K) δ 171.1 (C=O amide), 153.7 (C=O carbamate), 148.1 (C$_{Ar}$), 140.1 (C$_{Ar}$ quat), 137.7 (C$_{Ar}$ quat), 135.8 (C$_{Ar}$), 133.6 (C$_{Ar}$ quat), 130.3 (2 × C$_{Ar}$), 129.5 (2 × C$_{Ar}$), 127.2 (C$_{Ar}$ quat), 126.2 (C$_{Ar}$), 121.3 (C$_{Ar}$), 121.2 (C$_{Ar}$), 119.2 (C$_{Ar}$ quat), 116.1 (C$_{Ar}$), 78.3 (*C*(CH$_3$)$_3$), 45.1 (N*C*H$_2$CHAr), 44.9 (*C*H(C=O)), 41.4 (*C*HAr), 40.5 (N*C*H$_2$CH$_2$), 27.6 (C(*C*H$_3$)$_3$), 25.4 (NCH$_2$*C*H$_2$); HRMS (ESI) *m/z* Calculated for $C_{26}H_{29}{}^{79}BrN_3O_3$ [M+H] 510.1392; Found 510.1394.

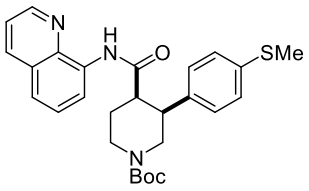
tert-Butyl-_cis_-(±)-4-(quinolin-8-ylcarbamoyl)-3-(4-(trifluoromethyl)phenyl)piperidine-1-carboxylate (46e)



Prepared according to **General Procedure A** using amide **25** (142 mg) and 1-iodo-4-(trifluoromethyl)benzene (272 mg). Purification by flash column chromatography (5% to 8% Et$_2$O/CH$_2$Cl$_2$) afforded arylated piperidine **46e** as a pale yellow solid (116 mg, 0.23 mmol, 58%). R_f 0.46 (10% Et$_2$O/CH$_2$Cl$_2$); mp = 146–148 °C (from Et$_2$O/Pentane); IR (film)/cm^{-1} 3283 (NH), 2980, 2930, 1675 (C=O), 1524 (C=O), 1422, 1320, 1287, 1241, 1162 (C–F), 1119 (C–F), 1061, 824, 752; ^{1}H NMR (400 MHz, DMSO-*d*$_6$, 373 K) δ 9.67 (br s, 1 H, NH), 8.79 (dd, *J* = 4.2, 1.7 Hz, 1 H, HC$_{Ar}$), 8.41 (dd, *J* = 7.7, 1.4 Hz, 1 H, HC$_{Ar}$), 8.34–8.29 (m, 1 H, HC$_{Ar}$), 7.62–7.51 (m, 3 H, 3 × HC$_{Ar}$), 7.51–7.45 (m, 4 H, 4 × HC$_{Ar}$), 4.07 (dd, *J* = 13.1, 7.7 Hz, 1 H, NC*H*HCHAr), 3.84 (ddd, *J* = 12.6, 8.3, 3.9 Hz, 1 H, NC*H*HCH$_2$), 3.78 (dd, *J* = 13.0, 4.0 Hz, 1 H, NCH*H*CHAr), 3.55 (ddd, *J* = 13.1, 6.7, 4.2 Hz, 1 H, NCH*H*CH$_2$), 3.47–3.37 (m, 2 H, CH(C=O) and CHAr), 2.09 (dtd, *J* = 13.5, 6.6, 3.9 Hz, 1 H, NCH$_2$C*H*H), 1.95 (ddt, *J* = 13.3, 8.8, 4.5 Hz, 1 H, NCH$_2$CH*H*), 1.41 (s, 9 H, C(C*H*$_3$)$_3$); ^{13}C NMR (101 MHz, DMSO-*d*$_6$, 373 K) δ 171.0 (C=O amide), 153.6 (C=O carbamate), 148.0 (C$_{Ar}$), 145.5 (C$_{Ar}$ quat), 137.7 (C$_{Ar}$ quat), 135.8 (C$_{Ar}$), 133.5 (C$_{Ar}$ quat), 128.2 (2 × C$_{Ar}$), 126.9 (q, J_{CF} = 30.0 Hz, F$_3$CC$_{Ar}$ quat), 126.1 (C$_{Ar}$), 124.2 (q, J_{CF} = 3.9 Hz, 2 × C$_{Ar}$), 123.6 (q, J_{CF} = 271.9 Hz, CF$_3$ quat), 121.3 (C$_{Ar}$), 121.2 (C$_{Ar}$), 116.1 (C$_{Ar}$), 78.4

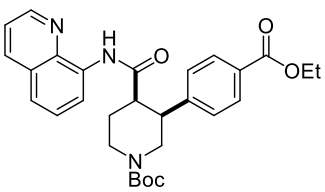
($C(CH_3)_3$), 45.0 (NCH_2CHAr), 44.9 ($CH(C=O)$), 41.8 ($CHAr$), 40.6 (NCH_2CH_2), 27.6 ($C(CH_3)_3$), 25.5 (NCH_2CH_2); $^{19}F\{^1H\}$ NMR (376 MHz, DMSO-d_6) δ –61.22 (s); HRMS (ESI) *m/z* Calculated for $C_{27}H_{29}F_3N_3O_3$ [M+H] 500.2161; Found 500.2150.

tert-Butyl-*cis*-(±)-3-(4-(methylthio)phenyl)-4-(quinolin-8-ylcarbamoyl)piperidine-1-carboxylate (46f)



Prepared according to **General Procedure A** using amide **25** (142 mg) and 4-iodothioanisole (200 mg). Purification by flash column chromatography (5% to 8% Et_2O/CH_2Cl_2) afforded arylated piperidine **46f** as a white solid (91 mg, 0.19 mmol, 48%). R_f 0.35 (10% Et_2O/CH_2Cl_2); mp = 167–169 °C (from Et_2O/pentane); IR (film)/cm^{-1} 3341 (NH br), 2999, 2971, 2919, 1676 (C=O), 1522 (C=O), 1482, 1421, 1365, 1322, 1241, 1162, 1384, 917, 823, 791, 730; ^1H NMR (500 MHz, DMSO-d_6, 373 K) δ 9.65 (s, 1 H, NH), 8.81 (dd, *J* = 4.2, 1.7 Hz, 1 H, HC_{Ar}), 8.45 (dd, *J* = 7.7, 1.4 Hz, 1 H, HC_{Ar}), 8.31 (ddd, *J* = 8.3, 1.7, 0.4 Hz, 1 H, HC_{Ar}), 7.62–7.54 (m, 2 H, 2 × HC_{Ar}), 7.52–7.47 (m, 1 H, HC_{Ar}), 7.25–7.20 (m, 2 H, 2 × HC_{Ar}), 7.08–7.03 (m, 2 H, 2 × HC_{Ar}), 4.01 (dd, *J* = 13.0, 8.1 Hz, 1 H, NC*H*HCHAr), 3.82 (ddd, *J* = 12.7, 8.5, 3.8 Hz, 1 H, NC*H*HCH_2), 3.74 (dd, *J* = 13.0, 4.1 Hz, 1 H, NCH*H*CHAr), 3.58–3.49 (m, 1 H, NCH*H*CH_2), 3.35 (dt, *J* = 6.6, 4.8 Hz, 1 H, CH(C=O)), 3.26 (dt, *J* = 8.6, 4.4 Hz, 1 H, CHAr), 2.28 (s, 3 H, SCH_3), 2.05 (ddt, *J* = 13.4, 6.6, 3.4 Hz, 1 H, NCH_2CHH), 1.91 (ddd, *J* = 13.6, 8.8, 4.4 Hz, 1 H, NCH_2CHH), 1.42 (s, 9 H, $C(CH_3)_3$); ^{13}C NMR (126 MHz, DMSO-d_6, 373 K) δ 171.2 (C=O amide), 153.7 (C=O carbamate), 148.0 (C_{Ar}), 137.7 (C_{Ar} quat), 137.6 (C_{Ar} quat), 135.7 (C_{Ar}), 135.5 (C_{Ar} quat), 133.7 (C_{Ar} quat), 127.9 (2 × C_{Ar}), 127.2 (C_{Ar} quat), 126.2 (C_{Ar}), 126.0 (2 × C_{Ar}), 121.3 (C_{Ar}), 121.1 (C_{Ar}), 115.9 (C_{Ar}), 78.2 ($C(CH_3)_3$), 45.2 (NCH_2CHAr), 45.1 ($CH(C=O)$), 41.6 ($CHAr$), 40.5 (NCH_2CH_2), 27.7 ($C(CH_3)_3$), 25.5 (NCH_2CH_2), 14.7 (SCH_3); HRMS (ESI) *m/z* Calculated for $C_{27}H_{32}N_3O_3S$ [M+H] 478.2164; Found 478.2149.

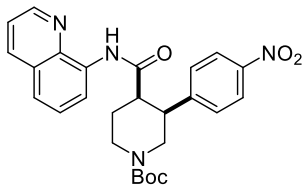
tert-Butyl-*cis*-(±)-3-(4-(ethoxycarbonyl)phenyl)-4-(quinolin-8-ylcarbamoyl)piperidine-1-carboxylate (46g)



Prepared according to **General Procedure A** using amide **25** (142 mg) and ethyl-4-iodobenzoate (220 mg). Purification by sequential flash column chromatography (5% to 8% Et_2O/CH_2Cl_2, followed by 15% to 20% acetone/pentane) afforded arylated piperidine **46g** as a white solid (75 mg, 0.15 mmol, 37%). R_f 0.49 (10% Et_2O/CH_2Cl_2); mp = 172–174 °C (from Et_2O/pentane); IR (film)/cm^{-1} 3341 (NH br), 2973, 2927, 1711 (C=O), 1680 (C=O), 1523, 1482, 1420, 1365, 1276, 1162, 1107, 826, 791; ^1H NMR (400 MHz, DMSO-d_6, 373 K) δ 9.63 (br s, 1 H, NH), 8.77 (dd, *J* = 4.2, 1.7 Hz, 1 H, HC_{Ar}), 8.41 (dd, *J* = 7.6, 1.4 Hz, 1 H, HC_{Ar}), 8.30 (dd, *J* = 8.3, 1.7 Hz, 1 H, HC_{Ar}), 7.75–7.69 (m, 2 H, 2 × HC_{Ar}), 7.58 (dd, *J* = 8.3, 1.4 Hz, 1 H, HC_{Ar}), 7.54 (dd, *J* = 8.3, 4.2 Hz, 1 H, HC_{Ar}), 7.49 (t, *J* = 8.0 Hz, 1 H, HC_{Ar}), 7.45–7.38 (m, 2 H, 2 × HC_{Ar}), 4.23 (q, *J* = 7.1 Hz, 2 H, $CO_2CH_2CH_3$), 4.06 (dd, *J* = 13.0, 7.9 Hz, 1 H, NC*H*HCHAr), 3.89–3.74 (m, 2 H, NC*H*HCH_2 and NCH*H*CHAr), 3.56 (ddd, *J* = 13.1, 6.5, 4.3 Hz, 1 H, NCH*H*CH_2), 3.47–3.34 (m, 2 H, CH(C=O) and CHAr), 2.08 (ddq, *J* = 13.2, 6.5, 3.9, 3.2 Hz, 1 H, NCH_2CHH), 1.93 (ddt, *J* = 13.3, 8.8, 4.5 Hz, 1 H, NCH_2CHH), 1.42 (s, 9 H,

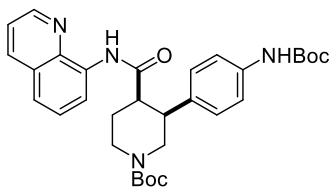
C(C*H*$_3$)$_3$), 1.24 (t, *J* = 7.0 Hz, 3 H, $CO_2CH_2CH_3$); ^{13}C NMR (101 MHz, DMSO-*d*$_6$, 373 K) δ 171.0 (C=O amide), 165.0 (C=O ester), 153.7 (C=O carbamate), 148.0 (C_{Ar}), 146.1 (C_{Ar} quat), 137.7 (C_{Ar} quat), 135.8 (C_{Ar}), 133.6 (C_{Ar} quat), 128.2 (C_{Ar}), 128.0 (2 × C_{Ar}), 127.6 (C_{Ar} quat), 127.2 (2 × C_{Ar}), 126.2 (C_{Ar} quat), 121.3 (C_{Ar}), 121.2 (C_{Ar}), 116.1 (C_{Ar}), 78.4 (*C*(CH$_3$)$_3$), 59.8 ($CO_2CH_2CH_3$), 45.0 (N*C*H$_2$CHAr), 44.9 (*C*H(C=O)), 42.0 (N*C*H$_2$CH$_2$), 40.5 (*C*HAr), 27.6 (*C*(CH$_3$)$_3$), 25.6 (NCH$_2$*C*H$_2$), 13.5 ($CO_2CH_2CH_3$); HRMS (ESI) *m/z* Calculated for $C_{29}H_{34}N_3O_5$ [M+H] 504.2498; Found 504.2494.

tert-Butyl-_cis_-(±)-3-(4-nitrophenyl)-4-(quinolin-8-ylcarbamoyl)piperidine-1-carboxylate (46h)



Prepared according to **General Procedure A** using amide **25** (142 mg) and 1-iodo-4-nitrobenzene (200 mg). Purification by flash column chromatography (5% to 8% Et_2O/CH_2Cl_2) afforded arylated piperidine **46h** as a pale orange solid (85 mg, 0.18 mmol, 45%). R_f 0.45 (10% Et_2O/CH_2Cl_2); mp = 165–166 °C (from Et_2O/pentane); IR (film)/cm^{-1} 3338 (NH br) 3001, 2972, 2926, 1676 (C=O), 1518 (N–O), 1482, 1421, 1344 (N–O), 1322, 1161, 909, 730; ^{1}H NMR (400 MHz, DMSO-*d*$_6$, 373 K) δ 9.68 (br s, 1 H, NH), 8.78 (dd, *J* = 4.2, 1.7 Hz, 1 H, HC_{Ar}), 8.40 (dd, *J* = 7.7, 1.4 Hz, 1 H, HC_{Ar}), 8.31 (dd, *J* = 8.3, 1.7 Hz, 1 H, HC_{Ar}), 8.02–7.96 (m, 2 H, 2 × HC_{Ar}), 7.62–7.47 (m, 5 H, 5 × HC_{Ar}), 4.07 (dd, *J* = 13.1, 7.5 Hz, 1 H, NC*H*HCHAr), 3.82 (tq, = 11.6, 3.8 Hz, 2 H, NCH*H*CHAr and NC*H*HCH$_2$), 3.63–3.52 (m, 1 H, NCH*H*CH$_2$), 3.52–3.43 (m, 2 H, CH(C=O) and CHAr), 2.14–2.06 (m, 1 H, NCH$_2$C*H*H), 2.01–1.91 (m, 1 H, NCH$_2$CH*H*), 1.42 (s, 9 H, C(C*H*$_3$)$_3$); ^{13}C NMR (101 MHz, DMSO-*d*$_6$, 373 K) δ 170.9 (C=O amide), 153.6 (C=O carbamate), 148.8 (C_{Ar} quat), 148.0 (C_{Ar}), 146.0 (C_{Ar} quat), 137.8 (C_{Ar} quat), 135.8 (C_{Ar}), 133.5 (C_{Ar} quat), 128.7 (2 × C_{Ar}), 127.2 (C_{Ar} quat), 126.2 (C_{Ar}), 122.3 (2 × C_{Ar}), 121.34 (C_{Ar}), 121.30 (C_{Ar}), 116.3 (C_{Ar}), 78.5 (*C*(CH$_3$)$_3$), 44.8 (N*C*H$_2$CHAr and *C*H(C=O)), 41.8 (*C*HAr), 40.5 (N*C*H$_2$CH$_2$), 27.6 (C(*C*H$_3$)$_3$), 25.5 (NCH$_2$*C*H$_2$); HRMS (ESI) *m/z* Calculated for $C_{26}H_{29}N_4O_5$ [M+H] 477.2138; Found 477.2137.

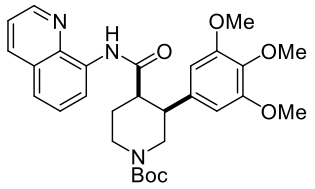
tert-Butyl-_cis_-(±)-3-(4-((_tert_-butoxycarbonyl)amino)phenyl)-4-(quinolin-8-ylcarbamoyl)piperidine-1-carboxylate (46i)



Prepared according to **General Procedure A** using amide **25** (142 mg) and *tert*-butyl (4-iodophenyl)carbamate (255 mg). Purification by flash column chromatography (5% to 8% Et_2O/CH_2Cl_2) afforded arylated piperidine **46i** as a white powder (104 mg, 0.19 mmol, 48%). R_f 0.37 (10% Et_2O/CH_2Cl_2); mp = 183–185 °C (from Et_2O/Pentane); IR (film)/cm^{-1} 3345 (NH), 3328 (NH br), 3000, 2973, 2926, 1680 (C=O), 1672 (C=O), 1522 (C=O), 1482, 1418, 1365, 1237, 1157, 1051, 908, 827, 729; ^{1}H NMR (500 MHz, DMSO-*d*$_6$, 373 K) δ 9.64 (br s, 1 H, NH amide), 8.81 (dd, *J* = 4.2, 1.7 Hz, 1 H, HC_{Ar}), 8.67 (s, 1 H, ArN*H*Boc), 8.45 (dd, *J* = 7.6, 1.4 Hz, 1 H, HC_{Ar}), 8.34–8.29 (m, 1 H, HC_{Ar}), 7.58 (dd, *J* = 8.3, 1.3 Hz, 1 H, HC_{Ar}), 7.54 (dd, *J* = 8.3, 4.2 Hz, 1 H, HC_{Ar}), 7.52–7.48 (m, 1 H, HC_{Ar}), 7.23–7.20 (m, 2 H, 2 × HC_{Ar}), 7.17–7.13 (m, 2 H, 2 × HC_{Ar}), 4.01 (dd, *J* = 13.0, 8.1 Hz, 1 H, NC*H*HCHAr), 3.82 (ddd, *J* = 12.7, 8.4, 3.8 Hz, 1 H, NC*H*HCH$_2$), 3.72 (dd, *J* = 13.0, 4.1 Hz, 1 H, NCH*H*CHAr), 3.52 (ddd, *J* = 13.0, 6.7, 4.3 Hz, 1 H, NCH*H*CH$_2$), 3.31 (dt, *J* = 6.6, 4.8 Hz, 1 H, CH(C=O)), 3.22 (dt, *J* = 8.6, 4.5 Hz, 1 H, CHAr), 2.04 (ddt, *J* = 13.5, 6.7, 3.3 Hz, 1 H, NCH$_2$C*H*H), 1.90 (tt, *J* = 8.8,

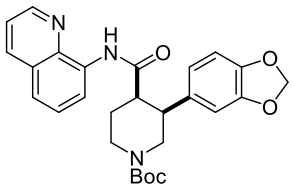
4.4 Hz, 1 H, $NCH_2CH\mathit{H}$), 1.49–1.39 (m, 18 H, 2 × $C(C\mathit{H}_3)_3$); ^{13}C NMR (126 MHz, DMSO-d_6, 373 K) δ 171.3 (C=O amide), 153.7 (C=O carbamate), 152.2 (C=O carbamate), 148.0 (C_{Ar}), 137.7 (C_{Ar} quat), 137.4 (C_{Ar} quat), 135.7 (C_{Ar}), 134.2 (C_{Ar} quat), 133.7 (C_{Ar} quat), 127.4 (2 × C_{Ar}), 127.2 (C_{Ar} quat), 126.2 (C_{Ar}), 121.2 (C_{Ar}), 121.0 (C_{Ar}), 117.7 (2 × C_{Ar}), 115.9 (C_{Ar}), 78.3 ($C(\mathit{C}H_3)_3$), 78.2 ($C(\mathit{C}H_3)_3$), 45.4 (NCH_2CHAr), 45.3 ($\mathit{C}H(C=O)$), 41.5 ($\mathit{C}HAr$), 40.5 (NCH_2CH_2), 27.7 (2 × $C(\mathit{C}H_3)_3$), 25.5 ($NCH_2\mathit{C}H_2$); HRMS (ESI) ***m/z*** Calculated for $C_{31}H_{39}N_4O_5$ [M+H] 547.2920; Found 547.2911.

***tert*-Butyl-*cis*-(±)-4-(quinolin-8-ylcarbamoyl)-3-(3,4,5-trimethoxyphenyl)piperidine-1-carboxylate (46j)**



Prepared according to **General Procedure A** using amide **25** (142 mg) and 3,4,5-trimethoxyiodobenzene (235 mg). Purification by flash column chromatography (15% to 22% acetone/pentane) afforded arylated piperidine **46i** as a white solid (125 mg, 0.24 mmol, 60%). R_f 0.36 (25% acetone/pentane); mp = 85–88 °C (from Et_2O/pentane); IR (film)/cm^{-1} 3341 (NH br), 2967, 2930, 2835, 1679 (C=O), 1586 (C=O), 1524, 1483, 1457, 1421, 1325, 1238, 1164, 1124, 731; ^1H NMR (400 MHz, DMSO-d_6, 373 K) δ 9.62 (br s, 1 H, NH), 8.79 (dd, *J* = 4.2, 1.7 Hz, 1 H, HC_{Ar}), 8.50 (dd, *J* = 7.6, 1.4 Hz, 1 H, H_{Ar}), 8.31 (ddd, *J* = 8.3, 1.7, 0.4 Hz, 1 H, HC_{Ar}), 7.64–7.45 (m, 3 H, 3 × HC_{Ar}), 6.56 (2 x s, 2 H, 2 × HC_{Ar}), 3.97 (dd, *J* = 13.0, 8.1 Hz, 1 H, $NC\mathit{H}HCHAr$), 3.88 (ddd, *J* = 12.7, 8.6, 3.9 Hz, 1 H, $NC\mathit{H}HCH_2$), 3.77–3.69 (m, 1 H, $NCH\mathit{H}CHAr$), 3.57–3.54 (m, 1 H, $NCH\mathit{H}CH_2$), 3.53 (s, 6 H, 2 × OCH_3), 3.38 (s, 3 H, OCH_3), 3.32 (dt, *J* = 6.4, 4.6 Hz, 1 H, CH(C=O)), 3.27–3.22 (m, 1 H, CHAr), 2.05 (ddt, *J* = 13.3, 6.5, 3.3 Hz, 1 H, $NCH_2C\mathit{H}H$), 1.89 (tt, *J* = 8.8, 4.4 Hz, 1 H, $NCH_2CH\mathit{H}$), 1.44 (s, 9 H, $C(C\mathit{H}_3)_3$); ^{13}C NMR (101 MHz, DMSO-d_6, 373 K) δ 171.4 (C=O amide), 153.8 (C=O carbamate), 152.2 (C_{Ar} quat), 148.0 (C_{Ar}), 137.6 (C_{Ar} quat), 136.9 (C_{Ar} quat), 135.9 (C_{Ar} quat), 135.8 (C_{Ar}), 133.7 (2 × C_{Ar} quat), 127.4 (C_{Ar}), 127.2 (C_{Ar} quat), 126.2 (C_{Ar}), 121.3 (C_{Ar}), 121.0 (C_{Ar}), 115.6 (C_{Ar}), 106.1 (2 × C_{Ar}), 78.3 ($\mathit{C}(CH_3)_3$), 59.1 (OCH_3), 55.4 (2 × OCH_3), 45.4 ($\mathit{C}H(C=O)$), 45.1 (NCH_2CHAr), 42.0 ($\mathit{C}HAr$), 40.6 (NCH_2CH_2), 27.7 ($C(\mathit{C}H_3)_3$), 25.3 ($NCH_2\mathit{C}H_2$); HRMS (ESI) ***m/z*** Calculated for $C_{29}H_{36}N_3O_6$ [M+H] 522.2604; Found 522.2614.

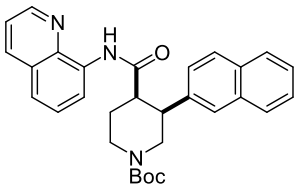
***tert*-Butyl-*cis*-(±)-3-(benzo[*d*][1,3]dioxol-5-yl)-4-(quinolin-8-ylcarbamoyl)piperidine-1-carboxylate (46k)**



Prepared according to **General Procedure A** using amide **25** (142 mg) and 5-iodobenzo[*d*][1,3]dioxole (199 mg). Purification by flash column chromatography (10% to 18% acetone/pentane) afforded arylated piperidine **46k** as a light pink crystalline solid (137 mg, 0.29 mmol, 72%). R_f 0.40 (18% acetone/pentane); mp = 128–130 °C (from Et_2O/Pentane); IR (film)/cm^{-1} 3339 (NH br), 3000, 2990, 2922, 1675 (C=O), 1522 (C=O), 1482, 1420, 1365 1323, 1232, 1161, 1124, 1038, 928, 910, 824, 730; ^1H NMR (400 MHz, DMSO-d_6, 373 K) δ 9.62 (br s, 1 H, NH), 8.82 (dd, *J* = 4.2, 1.7 Hz, 1 H, HC_{Ar}), 8.46 (dd, *J* = 7.6, 1.4 Hz, 1 H, HC_{Ar}), 8.32 (dd, *J* = 8.3, 1.7 Hz, 1 H, HC_{Ar}), 7.62–7.54 (m, 2 H, 2 × HC_{Ar}), 7.55–7.47 (m, 1 H, HC_{Ar}), 6.86–6.80 (m, 1 H, HC_{Ar}), 6.72 (ddd, *J* = 8.0, 1.8, 0.6 Hz, 1 H, HC_{Ar}), 6.62 (d, *J* = 7.9 Hz, 1 H, HC_{Ar}), 5.78 (d, *J* = 15.0 Hz, 1 H, $OC\mathit{H}HO$), 5.77 (d, *J* = 15.0 Hz, 1

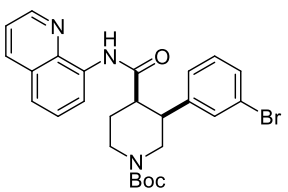
H, OCH*H*O), 3.95 (dd, *J* = 13.0, 8.3 Hz, 1 H, NC*H*HCHAr), 3.81 (ddd, *J* = 12.8, 8.7, 3.8 Hz, 1 H, NC*H*HCH$_2$), 3.72 (dd, *J* = 13.0, 4.1 Hz, 1 H, NCH*H*CHAr), 3.58–3.50 (m, 1 H, NCH*H*CH$_2$), 3.31 (dt, *J* = 6.4, 4.8 Hz, 1 H, CH(C=O)), 3.21 (dt, *J* = 8.7, 4.5 Hz, 1 H, CHAr), 2.04 (ddt, *J* = 13.1, 6.4, 3.2 Hz, 1 H, NCH$_2$C*H*H), 1.89 (tt, *J* = 9.0, 4.5 Hz, 1 H, NCH$_2$CH*H*), 1.43 (s, 9 H, C(C*H*$_3$)$_3$); ^{13}C NMR (101 MHz, DMSO-*d*$_6$, 373 K) δ 171.3 (C=O amide), 153.7 (C=O carbamate), 148.0 (C$_{Ar}$), 146.6 (C$_{Ar}$ quat), 145.3 (C$_{Ar}$ quat), 137.7 (C$_{Ar}$ quat), 135.8 (C$_{Ar}$), 134.4 (C$_{Ar}$ quat), 133.7 (C$_{Ar}$ quat), 127.2 (C$_{Ar}$ quat), 126.2 (C$_{Ar}$), 121.3 (C$_{Ar}$), 121.1 (C$_{Ar}$), 120.4 (C$_{Ar}$), 115.9 (C$_{Ar}$), 107.8 (C$_{Ar}$), 107.2 (C$_{Ar}$), 100.0 (O*C*H$_2$O), 78.2 (*C*(CH$_3$)$_3$), 45.4 (*C*H(C=O)), 45.3 (N*C*H$_2$CHAr), 41.8 (*C*HAr), 40.5 (N*C*H$_2$CH$_2$), 27.7 (C(*C*H$_3$)$_3$), 25.6 (NCH$_2$*C*H$_2$); HRMS (ESI) *m/z* Calculated for $C_{27}H_{30}N_3O_5$ [M+H] 476.2185; Found 476.2178.

tert-Butyl-_cis_-(±)-3-(naphthalen-2-yl)-4-(quinolin-8-ylcarbamoyl)piperidine-1-carboxylate (46l)



Prepared according to **General Procedure A** using amide **25** (142 mg) and 2-iodonaphthalene (203 mg). Purification by sequential flash column chromatography (5% to 8% Et$_2$O/CH$_2$Cl$_2$, followed by 20% acetone/pentane) afforded arylated piperidine **46l** as a pale green powder (135 mg, 0.28 mmol, 70%). R$_f$ 0.51 (10% Et$_2$O/CH$_2$Cl$_2$); mp = 165–166 °C (from Et$_2$O/pentane); IR (film)/cm^{-1} 3343 (NH br), 3048, 3000, 2969, 2923, 1682 (C=O), 1523 (C=O), 1482, 1421, 1364, 1323, 1162, 822, 790, 753; ^{1}H NMR (400 MHz, DMSO-*d*$_6$, 373 K) δ 9.64 (br s, 1 H, NH), 8.59 (dd, *J* = 4.2, 1.7 Hz, 1 H, HC$_{Ar}$), 8.40 (dd, *J* = 7.6, 1.4 Hz, 1 H ,HC$_{Ar}$), 8.29–8.22 (m, 1 H, HC$_{Ar}$), 7.81–7.76 (m, 1 H, HC$_{Ar}$), 7.72–7.61 (m, 3 H, 3 × HC$_{Ar}$), 7.54 (dd, *J* = 8.3, 1.4 Hz, 1 H, HC$_{Ar}$), 7.50–7.42 (m, 3 H, 3 × HC$_{Ar}$), 7.39–7.32 (m, 2 H, 2 × HC$_{Ar}$), 4.16 (dd, *J* = 13.0, 7.4 Hz, 1 H, NC*H*HCHAr), 3.94–3.83 (m, 2 H, NC*H*HCH$_2$ and NCH*H*CHAr), 3.59 (ddd, *J* = 13.1, 6.7, 4.4 Hz, 1 H, NCH*H*CH$_2$), 3.52–3.44 (m, 2 H, CH(C=O) and CHAr), 2.13 (ddd, *J* = 13.1, 6.7, 3.7 Hz, 1 H, NCH$_2$C*H*H), 1.97 (td, *J* = 8.9, 4.3 Hz, 1 H, NCH$_2$CH*H*), 1.42 (s, 9 H, C(C*H*$_3$)$_3$); ^{13}C NMR (101 MHz, DMSO-*d*$_6$, 373 K) δ 171.3 (C=O amide), 153.7 (C=O carbamate), 147.8 (C$_{Ar}$), 138.2 (C$_{Ar}$ quat), 137.6 (C$_{Ar}$ quat), 135.6 (C$_{Ar}$), 133.6 (C$_{Ar}$ quat), 132.5 (C$_{Ar}$ quat), 131.5 (C$_{Ar}$ quat), 127.1 (C$_{Ar}$ quat), 126.84 (C$_{Ar}$), 126.82 (C$_{Ar}$), 126.6 (C$_{Ar}$), 126.1 (C$_{Ar}$), 126.0 (C$_{Ar}$), 125.7 (C$_{Ar}$), 125.2 (C$_{Ar}$), 124.8 (C$_{Ar}$), 121.2 (C$_{Ar}$), 121.1 (C$_{Ar}$), 116.0 (C$_{Ar}$), 78.3 (*C*(CH$_3$)$_3$), 45.32 (N*C*H$_2$CHAr), 45.27 (*C*H(C=O)), 42.1 (*C*HAr), 40.7 (N*C*H$_2$CH$_2$), 27.7 (C(*C*H$_3$)$_3$), 25.6 (NCH$_2$*C*H$_2$); HRMS (ESI) *m/z* Calculated for $C_{30}H_{32}N_3O_3$ [M+H] 482.2444; Found 482.2452.

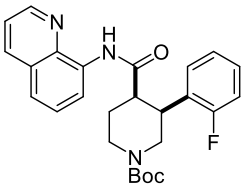
tert-Butyl-_cis_-(±)-3-(3-bromophenyl)-4-(quinolin-8-ylcarbamoyl)piperidine-1-carboxylate (46m)



Prepared according to **General Procedure A** using amide **25** (142 mg) and 3-bromoiodobenzene (227 mg). Purification by flash column chromatography (5% to 8% Et$_2$O/CH$_2$Cl$_2$) afforded arylated piperidine **46m** as a light pink crystalline solid (94 mg, 0.18 mmol, 46%). R$_f$ 0.44 (7% Et$_2$O/CH$_2$Cl$_2$); mp = 138–140 °C (from Et$_2$O/pentane); IR (film)/cm^{-1} 3342 (NH br), 3000, 2970, 2923, 1679 (C=O), 1523 (C=O), 1481, 1421, 1365, 1323, 1241, 1162, 1112, 788, 731; ^{1}H NMR (400 MHz, DMSO-*d*$_6$, 373 K) δ 9.71 (br s, 1 H, NH), 8.84 (dd, *J* = 4.2, 1.7 Hz, 1 H, HC$_{Ar}$), 8.42 (dd, *J* = 7.6, 1.4 Hz, 1 H, HC$_{Ar}$), 8.32 (ddd, *J* = 8.3, 1.7, 0.4 Hz, 1 H, HC$_{Ar}$), 7.67–7.55 (m, 2 H, 2 × HC$_{Ar}$), 7.55–7.45 (m, 2 H, 2 × HC$_{Ar}$), 7.29–7.17 (m, 2 H, 2 × HC$_{Ar}$), 7.08 (t, *J* = 7.8 Hz, 1 H, HC$_{Ar}$), 4.05 (dd, *J* = 13.1, 7.4,

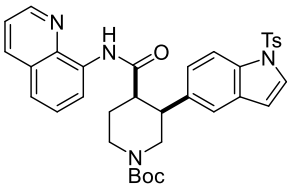
1 H, NC*H*HCHAr), 3.87 (ddd, *J* = 13.4, 7.8, 4.0 Hz, 1 H, NC*H*HCH$_2$), 3.70 (dd, *J* = 13.1, 4.0 Hz, 1 H, NCH*H*CHAr), 3.48 (ddd, *J* = 13.0, 7.2, 4.2 Hz, 1 H, NCH*H*CH$_2$), 3.39 (dt, *J* = 7.1, 4.8 Hz, 1 H, CH(C=O)), 3.33 (dt, *J* = 7.3, 4.4 Hz, 1 H, CHAr), 2.09–1.98 (m, 1 H, NCH$_2$C*H*H), 1.90 (ddt, *J* = 13.8, 7.9, 4.4 Hz, 1 H, NCH$_2$CH*H*), 1.43 (s, 9 H, C(CH$_3$)$_3$); ^{13}C NMR (101 MHz, DMSO-*d*$_6$, 373 K) δ 171.0 (C=O amide), 153.6 (C=O carbamate), 148.0 (C$_{Ar}$), 143.3 (C$_{Ar}$ quat), 137.8 (C$_{Ar}$ quat), 135.8 (C$_{Ar}$), 133.5 (C$_{Ar}$ quat), 130.3 (C$_{Ar}$), 129.4 (C$_{Ar}$), 128.8 (C$_{Ar}$), 127.3 (C$_{Ar}$ quat), 126.4 (C$_{Ar}$), 126.2 (C$_{Ar}$), 121.3 (C$_{Ar}$), 121.2 (C$_{Ar}$), 121.0 (C$_{Ar}$ quat), 116.2 (C$_{Ar}$), 78.4 (*C*(CH$_3$)$_3$), 45.2 (N*C*H$_2$CHAr), 45.0 (*C*H(C=O)), 41.5 (CHAr), 40.6 (N*C*H$_2$CH$_2$), 27.7 (C(*C*H$_3$)$_3$), 25.1 (NCH$_2$*C*H$_2$); HRMS (ESI) *m/z* Calculated for $C_{26}H_{29}{}^{79}BrN_3O_3$ [M+H] 510.1392; Found 510.1381.

tert-Butyl-_cis_-(±)-3-(2-fluorophenyl)-4-(quinolin-8-ylcarbamoyl)piperidine-1-carboxylate (46n)



Prepared according to **General Procedure A** using amide **25** (142 mg) and 2-fluoroiodobenzene (266 mg). Purification by flash column chromatography (5% to 8% Et$_2$O/CH$_2$Cl$_2$) afforded arylated piperidine **46n** as a white solid (47 mg, 0.10 mmol, 26%). R$_f$ 0.42 (10% Et$_2$O/CH$_2$Cl$_2$); mp = 85–88 °C (from Et$_2$O/pentane); IR (film)/cm^{-1} 3339 (NH br), 2968, 2923, 1681 (C=O), 1523 (C=O), 1483, 1420, 1383, 1364, 1240, 1161, 1114, 910, 790, 755; ^{1}H NMR (400 MHz, DMSO-*d*$_6$, 373 K) δ 9.71 (br s, 1 H, NH), 8.81 (dd, *J* = 4.2, 1.7 Hz, 1 H, HC$_{Ar}$), 8.44 (dd, *J* = 7.6, 1.4 Hz, 1 H, HC$_{Ar}$), 8.31 (dd, *J* = 8.3, 1.7 Hz, 1 H, HC$_{Ar}$), 7.61–7.53 (m, 2 H, 2 × HC$_{Ar}$), 7.52–7.46 (m, 1 H, HC$_{Ar}$), 7.37 (td, *J* = 7.8, 1.7 Hz, 1 H, HC$_{Ar}$), 7.12 (dddd, *J* = 8.2, 7.2, 5.4, 1.7 Hz, 1 H, HC$_{Ar}$), 7.06–6.92 (m, 2 H, 2 × HC$_{Ar}$), 4.08 (dd, *J* = 13.0, 8.2 Hz, 1 H, NC*H*HCHAr), 3.83 (ddd, *J* = 12.8, 8.5, 3.9 Hz, 1 H, NC*H*HCH$_2$), 3.73 (dd, *J* = 13.0, 4.1 Hz, 1 H, NCH*H*CHAr), 3.60–3.54 (m, 2 H, NCH*H*CH$_2$ and CHAr), 3.40 (dt, *J* = 6.6, 5.0 Hz, 1 H, CH(C=O)), 2.19–2.06 (m, 1 H, NCH$_2$C*H*H), 1.94 (ddt, *J* = 13.5, 8.5, 4.6 Hz, 1 H, NCH$_2$CH*H*), 1.39 (s, 9 H, C(C*H*$_3$)$_3$); ^{13}C NMR (101 MHz, DMSO-*d*$_6$, 373 K) δ 171.1 (C=O amide), 159.9 (d, *J*$_{CF}$ = 246.7 Hz, F*C*$_{Ar}$ quat), 153.6 (C=O carbamate), 148.0 (C$_{Ar}$), 137.7 (C$_{Ar}$ quat), 135.7 (C$_{Ar}$), 133.7 (C$_{Ar}$ quat), 128.4 (d, *J*$_{CF}$ = 4.1 Hz, F-*m*-C$_{Ar}$), 127.7 (d, *J*$_{CF}$ = 9.0 Hz, F-*m*-C$_{Ar}$), 127.3 (d, *J*$_{CF}$ = 14.5 Hz, F-*o*-C$_{Ar}$ quat), 127.2 (C$_{Ar}$ quat), 126.2 (C$_{Ar}$), 123.3 (d, *J*$_{CF}$ = 3.5 Hz, F-*p*-C$_{Ar}$), 121.3 (C$_{Ar}$), 121.1 (C$_{Ar}$), 116.0 (C$_{Ar}$), 114.3 (d, *J*$_{CF}$ = 22.0 Hz, F-*o*-C$_{Ar}$), 78.3 (*C*(CH$_3$)$_3$), 44.8 (N*C*H$_2$CHAr), 43.8 (*C*H(C=O)), 40.6 (N*C*H$_2$CH$_2$), 34.9 (*C*HAr), 27.6 (C(*C*H$_3$)$_3$), 25.8 (NCH$_2$*C*H$_2$); ^{19}F{^{1}H} NMR (376 MHz, DMSO-*d*$_6$, 373 K) δ –117.25 (s); HRMS (ESI) *m/z* Calculated for $C_{26}H_{29}FN_3O_3$ [M+H] 450.2193; Found 450.2184.

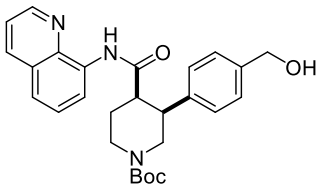
tert-Butyl-_cis_-(±)-4-(quinolin-8-ylcarbamoyl)-3-(1-tosyl-1_H_-indol-5-yl)piperidine-1-carboxylate (46o)



Prepared according to **General Procedure A** using amide **25** (142 mg) and 5-iodo-1-tosyl-1*H*-indole (318 mg). Purification by flash column chromatography (5% to 8% Et$_2$O/CH$_2$Cl$_2$) afforded arylated piperidine **46o** as a white solid in an inseparable 20 : 1 mixture of *cis* and *trans* diastereomers (130 mg, 0.21 mmol, 51%). R$_f$ 0.51 (10% Et$_2$O/CH$_2$Cl$_2$); mp = 136–137 °C (from Et$_2$O/pentane); IR (film)/cm^{-1} 3339 (NH br), 2972, 1674 (C=O), 1521 (C=O), 1481, 1420, 1366, 1166 (S=O), 1125 (S=O), 905, 818, 790, 723, 668, 580; ^{1}H NMR (400 MHz, DMSO-*d*$_6$, 373

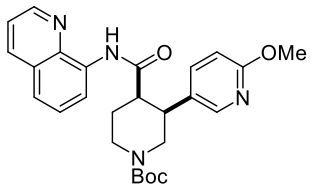
K, major diastereomer **46o**) δ 9.56 (br s, 1 H, NH), 8.63 (dd, *J* = 4.2, 1.7 Hz, 1 H, HC_{Ar}), 8.37 (dd, *J* = 7.7, 1.4 Hz, 1 H, HC_{Ar}), 8.28 (dd, *J* = 8.3, 1.7 Hz, 1 H, HC_{Ar}), 7.73–7.65 (m, 3 H, 3 × HC_{Ar}), 7.59–7.52 (m, 2 H, 2 × HC_{Ar}), 7.51–7.44 (m, 3 H, 3 × HC_{Ar}), 7.28 (dd, *J* = 8.7, 1.9 Hz, 1 H, HC_{Ar}), 7.25–7.19 (m, 2 H, 2 × HC_{Ar}), 6.57 (dd, *J* = 3.7, 0.8 Hz, 1 H, TsNCHC*H*), 4.03 (dd, *J* = 13.0, 7.6 Hz, 1 H, NC*H*HCHAr), 3.84 (ddd, *J* = 12.7, 8.5, 3.9 Hz, 1 H, NCH*H*CH_2), 3.77 (dd, *J* = 12.9, 3.7 Hz, 1 H, NCH*H*CHAr), 3.55 (ddd, *J* = 13.1, 6.8, 4.4 Hz, 1 H, NCH*H*CH_2), 3.43–3.32 (m, 2 H, CH(C=O) and CHAr), 2.27 (s, 3 H, SO_2PhCH_3), 2.08 (ddt, *J* = 12.9, 6.3, 3.3 Hz, 1 H, NCH_2CHH), 1.92 (tt, *J* = 8.8, 4.7 Hz, 1 H, NCH_2CH*H*), 1.37 (s, 9 H, $C(CH_3)_3$); ^{13}C NMR (101 MHz, DMSO-*d*$_6$, 373 K, major diastereomer **46o**) δ 171.3 (C=O amide), 153.7 (C=O carbamate), 147.8 (C_{Ar}), 144.5 (C_{Ar} quat), 137.6 (C_{Ar} quat), 135.8 (C_{Ar} quat), 135.7 (C_{Ar}), 134.4 (C_{Ar} quat), 133.6 (C_{Ar} quat), 132.7 (C_{Ar} quat), 129.9 (C_{Ar} quat), 129.4 (2 × C_{Ar}), 127.2 (C_{Ar} quat), 126.1 (2 × C_{Ar}), 125.8 (2 × C_{Ar}), 124.4 (C_{Ar}), 121.2 (C_{Ar}), 121.1 (C_{Ar}), 120.0 (C_{Ar}), 116.0 (C_{Ar}), 112.1 (C_{Ar}), 108.5 (C_{Ar}), 78.2 (*C*$(CH_3)_3$), 45.5 (N*C*H_2CHAr), 45.3 (*C*H(C=O)), 41.9 (*C*HAr), 40.5 (N*C*H_2CH_2), 27.6 ($C(CH_3)_3$), 25.6 (NCH_2CH_2), 20.3 (SO_2PhCH_3); HRMS (ESI) *m/z* Calculated for $C_{35}H_{37}N_4O_5S$ [M+H] 625.2485; Found 625.2490.

tert-Butyl-_cis_-(±)-3-(4-(hydroxymethyl)phenyl)-4-(quinolin-8-ylcarbamoyl)piperidine-1-carboxylate (46p)



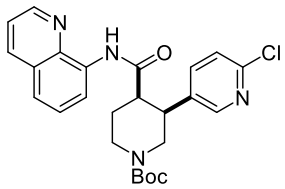
Prepared according to **General Procedure A** using amide **25** (142 mg) and (4-iodophenyl)methanol (188 mg). Purification by flash column chromatography (5% to 20% acetone/pentane) afforded arylated piperidine **46p** as a white solid in an inseparable 12 : 1 mixture of *cis* and *trans* diastereomers (92 mg, 0.20 mmol, 50%). R_f 0.31 (20% acetone/pentane); mp = 89–92 °C (from Et_2O/pentane); IR (film)/cm^{-1} 3412 (OH br), 3343 (NH br), 3002, 2971, 2922, 1674 (C=O), 1524 (C=O), 1482, 1422 (C–O), 1384, 1366, 1322, 1243, 1162, 910, 825, 731; ^{1}H NMR (500 MHz, DMSO-*d*$_6$, 373 K, major diastereomer **46p**) δ 9.69 (br s, 1 H, NH), 8.82 (dd, *J* = 4.2, 1.7 Hz, 1 H, HC_{Ar}), 8.45 (dd, *J* = 7.6, 1.4 Hz, 1 H, HC_{Ar}), 8.31 (dd, *J* = 8.3, 1.7 Hz, 1 H, HC_{Ar}), 7.61–7.53 (m, 2 H, 2 × HC_{Ar}), 7.52–7.47 (m, 1 H, HC_{Ar}), 7.27–7.20 (m, 2 H, 2 × HC_{Ar}), 7.14–7.06 (m, 2 H, 2 × HC_{Ar}), 4.33 (s, 2 H, C*H*$_2$OH), 4.07 (dd, *J* = 13.0, 8.0 Hz, 1 H, NC*H*HCHAr), 3.82 (ddd, *J* = 12.7, 8.4, 3.8 Hz, 1 H, NC*H*HCH_2), 3.74 (dd, *J* = 13.0, 4.1 Hz, 1 H, NCH*H*CHAr), 3.54 (ddd, *J* = 13.1, 6.7, 4.3 Hz, 1 H, NCH*H*CH_2), 3.36 (dt, *J* = 6.6, 4.7 Hz, 1 H, CH(C=O)), 3.27 (dt, *J* = 8.6, 4.5 Hz, 1 H, CHAr), 2.26 (s, 1 H, OH), 2.09–2.02 (m, 1 H, NCH_2CHH), 1.92 (ddd, *J* = 13.6, 8.8, 4.4 Hz, 1 H, NCH_2CH*H*), 1.43 (s, 9 H, $C(CH_3)_3$); ^{13}C NMR (126 MHz, DMSO-*d*$_6$, 373 K, major diastereomer **46p**) δ 171.3 (C=O amide), 153.7 (C=O carbamate), 148.0 (C_{Ar}), 140.2 (C_{Ar} quat), 138.9 (C_{Ar} quat), 137.7 (C_{Ar} quat), 135.8 (C_{Ar}), 133.7 (C_{Ar} quat), 127.4 (C_{Ar}), 127.2 (C_{Ar} quat), 127.0 (C_{Ar}), 126.7 (C_{Ar}), 126.2 (C_{Ar}), 125.6 (C_{Ar}), 121.3 (C_{Ar}), 121.0 (C_{Ar}), 116.0 (C_{Ar}), 78.2 (*C*$(CH_3)_3$), 62.2 (*C*H_2OH), 45.4 (N*C*H_2CHAr), 45.2 (*C*H(C=O)), 41.9 (*C*HAr), 40.5 (N*C*H_2CH_2), 27.7 ($C(CH_3)_3$), 25.6 (NCH_2CH_2); HRMS (ESI) *m/z* Calculated for $C_{27}H_{32}N_3O_4$ [M+H] 462.2393; Found 462.2395.

tert-Butyl-_cis_-(±)-3-(6-methoxypyridin-3-yl)-4-(quinolin-8-ylcarbamoyl)piperidine-1-carboxylate (46q)



Prepared according to **General Procedure B** using 2-methoxy-5-iodopyridine (236 mg). Purification by flash column chromatography (5% to 8% Et_2O/CH_2Cl_2) afforded arylated piperidine **46q** as a white solid (69 mg, 0.15 mmol, 38%). R_f 0.21 (10% Et_2O/CH_2Cl_2); mp = 115–117 °C (from Et_2O/pentane); IR (film)/cm^{-1} 3339 (NH br), 3000, 2971, 2967, 1675 (C=O), 1521 (C=O), 1458, 1420, 1258, 1240, 1158, 1104, 1023, 909, 823, 791, 727; ^{1}H NMR (400 MHz, DMSO-d_6, 373 K) δ 9.74 (br s, 1 H, NH), 8.82 (dt, J = 4.2, 1.5 Hz, 1 H, HC_{Ar}), 8.43 (dt, J = 7.6, 1.3 Hz, 1 H, HC_{Ar}), 8.33 (dt, J = 8.3, 1.5 Hz, 1 H, HC_{Ar}), 8.04 (d, J = 2.6 Hz, 1 H, HC_{Ar}), 7.63–7.54 (m, 3 H, 3 × HC_{Ar}), 7.54–7.47 (m, 1 H, HC_{Ar}), 6.57 (dt, J = 8.7, 0.9 Hz, 1 H, HC_{Ar}), 4.03 (dd, J = 13.0, 7.4 Hz, 1 H, NC*H*HCHAr), 3.86 (ddd, J = 12.6, 7.8, 4.2 Hz, 1 H, NC*H*HCH_2), 3.75–3.65 (m, 4 H, OCH_3 and NCH*H*CHAr), 3.53–3.41 (m, 1 H, NCH*H*CH_2), 3.36 (q, J = 5.6 Hz, 1 H, CH(C=O)), 3.30 (dt, J = 8.4, 4.6 Hz, 1 H, CHAr), 2.10–1.99 (m, 1 H, NCH_2C*H*H), 1.91 (ddt, J = 12.8, 8.0, 4.4 Hz, 1 H, NCH_2CH*H*), 1.42 (s, 9 H, C(C*H*$_3$)$_3$); ^{13}C NMR (101 MHz, DMSO-d_6, 373 K) δ 172.1 (C=O amide), 163.0 (OC_{Ar} quat), 154.7 (C=O carbamate), 149.1 (C_{Ar}), 146.5 (C_{Ar}), 139.1 (C_{Ar}), 138.8 (C_{Ar} quat), 136.8 (C_{Ar}), 134.6 (C_{Ar} quat), 130.0 (C_{Ar} quat), 128.3 (C_{Ar} quat), 127.2 (C_{Ar}), 122.3 (C_{Ar}), 122.2 (C_{Ar}), 117.2 (C_{Ar}), 110.0 (C_{Ar}), 79.3 (*C*$(CH_3)_3$), 53.2 (OCH_3), 46.5 (N*C*H_2CHAr), 46.0 (*C*H(C=O)), 41.7 (N*C*H_2CH_2), 40.0 (*C*HAr), 28.6 (C(*C*$H_3)_3$), 26.0 (NCH_2*C*H_2); HRMS (ESI) *m/z* Calculated for $C_{26}H_{31}N_4O_4$ [M+H] 463.2345; Found 463.2328.

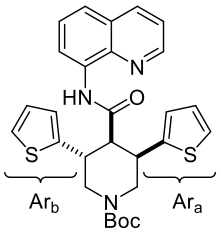
tert-Butyl-_cis_-(±)-3-(6-chloropyridin-3-yl)-4-(quinolin-8-ylcarbamoyl)piperidine-1-carboxylate (46r)



Prepared according to **General Procedure B** using 2-chloro-5-iodopyridine (288 mg). Purification by flash column chromatography (5% to 8% Et_2O/CH_2Cl_2) afforded arylated piperidine **46r** as a white solid (46 mg, 0.10 mmol, 25%) in an inseparable 13 : 1 mixture of *cis* and *trans* diastereomers. R_f 0.24 (10% Et_2O/CH_2Cl_2); mp = 96–98 °C (from Et_2O/pentane); IR (film)/cm^{-1} 3338 (NH br), 2998, 2971, 2924, 1678 (C=O), 1524 (C=O), 1482, 1422, 1366, 1240, 1162, 1108, 910, 837, 731; ^{1}H NMR (500 MHz, DMSO-d_6, 373 K, major diastereomer **46r**) δ 9.80 (br s, 1 H, NH), 8.85 (dd, J = 4.2, 1.7 Hz, 1 H, HC_{Ar}), 8.39 (dd, J = 7.6, 1.3 Hz, 1 H, HC_{Ar}), 8.34 (dd, J = 8.3, 1.7 Hz, 1 H, HC_{Ar}), 8.30 (dt, J = 2.6, 0.6 Hz, 1 H, HC_{Ar}), 7.72 (dd, J = 8.3, 2.6 Hz, 1 H, HC_{Ar}), 7.64–7.61 (m, 1 H, HC_{Ar}), 7.58 (dd, J = 8.3, 4.2 Hz, 1 H, HC_{Ar}), 7.54–7.49 (m, 1 H, HC_{Ar}), 7.26 (d, J = 8.3 Hz, 1 H, HC_{Ar}), 4.07 (dd, J = 13.1, 7.0 Hz, 1 H, NC*H*HCHAr), 3.92–3.83 (m, 1 H, NC*H*HCH_2), 3.69 (dd, J = 13.2, 4.0 Hz, 1 H, NCH*H*CHAr), 3.49–3.39 (m, 3 H, NCH*H*CH_2 , CH(C=O) and CHAr), 2.10–2.00 (m, 1 H, NCH_2C*H*H), 1.93 (ddt, J = 13.9, 7.4, 4.4 Hz, 1 H, NCH_2CH*H*), 1.42 (s, 9 H, C(C*H*$_3$)$_3$); ^{13}C NMR (126 MHz, DMSO-d_6, 373 K, major diastereomer **46r**) δ 170.8 (C=O amide), 153.6 (C=O carbamate), 148.8 (C_{Ar}), 148.1 (C_{Ar} and C_{Ar} quat), 138.4 (C_{Ar}), 137.9 (C_{Ar} quat), 135.8 (C_{Ar}), 135.7 (C_{Ar} quat), 133.5 (C_{Ar} quat), 127.3 (C_{Ar} quat), 126.2 (C_{Ar}), 122.9 (C_{Ar}), 121.4 (C_{Ar}), 121.3 (C_{Ar}), 116.5 (C_{Ar}), 78.5 (*C*$(CH_3)_3$), 45.2 (N*C*H_2CHAr),

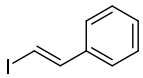
44.7 (*C*H(C=O)), 40.7 (N*C*H$_2$CH$_2$), 38.9 (*C*HAr), 27.6 (C(*C*H$_3$)$_3$), 24.9 (NCH$_2$*C*H$_2$); HRMS (ESI) *m/z* Calculated for $C_{25}H_{28}{}^{35}ClN_4O_3$ [M+H] 467.1850; Found 467.1854.

tert-Butyl-_cis,trans_-(±)-4-(quinolin-8-ylcarbamoyl)-3,5-di(thiophen-2-yl)piperidine-1-carboxylate (47)



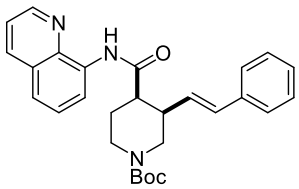
Prepared according to **General Procedure A** using amide **25** (142 mg) and 2-iodothiophene (168 mg). Purification by flash column chromatography (5% to 8% Et$_2$O/CH$_2$Cl$_2$) afforded di-*cis*-*trans*-arylated piperidine **47** as a white crystalline solid (113 mg, 0.22 mmol, 55%). R$_f$ 0.44 (10% Et$_2$O/CH$_2$Cl$_2$); mp = 183–185 °C (from Et$_2$O/pentane); IR (film)/cm^{-1} 3339 (NH br), 2972, 2923, 1682 (C=O), 1523 (C=O), 1481, 1420, 1296, 1154, 909, 730, 696; ^{1}H NMR (400 MHz, DMSO-*d*$_6$, 373 K) δ 9.98 (br s, 1 H, NH), 8.89 (dd, *J* = 4.2, 1.7 Hz, 1 H, HC$_{Ar}$), 8.36–8.26 (m, 2 H, 2 × HC$_{Ar}$), 7.61–7.52 (m, 2 H, 2 × HC$_{Ar}$), 7.44 (t, *J* = 8.0 Hz, 1 H, HC$_{Ar}$), 7.30–7.23 (m, 2 H, 2 × HC$_{Ar}$), 7.07 (dd, *J* = 3.6, 1.2 Hz, 1 H, HC$_{Ar}$), 6.92 (dd, *J* = 5.1, 3.5 Hz, 1 H, HC$_{Ar}$), 6.86–6.80 (m, 2 H, 2 × HC$_{Ar}$), 4.32 (ddd, *J* = 13.2, 4.7, 1.5 Hz, 1 H, NC*H*HCHAr$_b$), 4.18 (ddd, *J* = 13.0, 3.5, 1.5 Hz, 1 H, NC*H*HCHAr$_a$), 3.99 (ddd, *J* = 3.8, 3.8, 3.7 Hz, 1 H, CHAr$_a$), 3.83 (td, *J* = 10.5, 4.7 Hz, 1 H, CHAr$_b$), 3.66 (dd, *J* = 10.6, 4.8 Hz, 1 H, CH(C=O)), 3.54 (dd, *J* = 13.1, 3.7 Hz, 1 H, NCH*H*CHAr$_a$), 3.12 (dd, *J* = 13.2, 10.5 Hz, 1 H, NCH*H*CHAr$_b$), 1.42 (s, 9 H, C(C*H*$_3$)$_3$); ^{13}C NMR (101 MHz, DMSO-*d*$_6$, 373 K) δ 168.9 (C=O amide), 153.3 (C=O carbamate), 148.0 (C$_{Ar}$), 144.1 (C$_{Ar}$ quat), 141.2 (C$_{Ar}$ quat), 137.8 (C$_{Ar}$ quat), 135.8 (C$_{Ar}$), 133.9 (C$_{Ar}$ quat), 127.3 (C$_{Ar}$ quat), 126.2 (C$_{Ar}$), 126.1 (C$_{Ar}$), 125.3 (C$_{Ar}$), 125.2 (C$_{Ar}$), 124.1 (C$_{Ar}$), 124.0 (C$_{Ar}$), 123.3 (C$_{Ar}$), 121.3 (C$_{Ar}$), 121.1 (C$_{Ar}$), 116.2 (C$_{Ar}$), 78.8 (*C*(CH$_3$)$_3$), 53.0 (*C*H(C=O)), 48.9 (N*C*H$_2$CHAr$_b$), 47.6 (N*C*H$_2$CHAr$_a$), 38.0 (*C*HAr$_a$), 34.6 (*C*HAr$_b$), 27.6 (C(*C*H$_3$)$_3$); HRMS (ESI) *m/z* Calculated for $C_{28}H_{30}N_3O_3S_2$ [M+H] 520.1729; Found 520.1718.

[(*E*)–2–Iodoethenyl]benzene (S1)



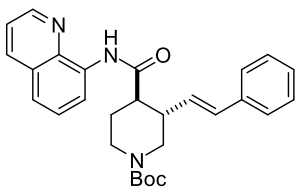
Prepared following a procedure by Charette.[286] Diiodomethane (0.48 mL, 6.00 mmol, 1.5 equiv) was added dropwise to a solution of NaHMDS (1.0 M solution in THF, 12.0 mL, 12.00 mmol, 3.0 equiv) in Et$_2$O (8 mL) at –78 ºC in the dark. After stiring for 30 min, a solution of benzyl bromide (0.48 mL, 4.00 mmol, 1.0 equiv) in THF (3 mL) was added. The reaction was stirred for an additional 2 h at –78 ºC, then allowed to war, to ambient temperature. After another 30 min, DBU (0.6 mL, 4.00 mmol, 1 equiv) was added, then the mixure stirred for 1 h before dilution with Et$_2$O (50 mL). The mixture was filtered through a plug of Celite/silica, then concentrated under reduced pressure. The crude material was purified by flash column chromatography (100% hexane), affording vinyl iodide **S1** as a yellow oil (571 mg, 2.48 mmol, 62%, 98:2 *E*/*Z*). Rf 0.64 (100% hexane); IR (film)/cm^{-1} 3697, 3681, 3057, 3022, 2973, 2923, 2865, 2845, 1595, 1569, 1494, 1444, 1278, 1210, 1169, 1055, 1032, 1012, 944, 792, 726, 688; ^{1}H NMR (400 MHz, CDCl$_3$) δ 7.45 (d, *J* = 14.9 Hz, 1 H, HC=C*H*Ph), 7.38–7.25 (m, 5 H, 5 × HC$_{Ar}$), 6.85 (d, *J* = 14.9 Hz, 1 H, CHI); ^{13}C NMR (101 MHz, CDCl$_3$) δ 144.9 (HC=*C*HPh), 137.6 (C$_{Ar}$ quat), 128.7 (2 × C$_{Ar}$), 128.3 (C$_{Ar}$), 126.0 (2 × C$_{Ar}$), 76.7 (CHI). Characterisation information consistent with data previously reported in literature.[280]

tert-Butyl-_cis_-(±)-4-(quinolin-8-ylcarbamoyl)-3-((_E_)-styryl)piperidine-1-carboxylate (48a)



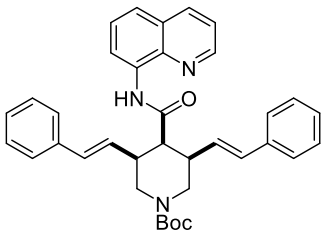
Prepared according to **General Procedure A** using amide **25** (142 mg) and (*E*)-(2-iodovinyl)benzene (185 mg), which was prepared according to a literature procedure by Bull et al.[3] Purification by flash column chromatography (5% to 8% Et_2O/CH_2Cl_2) afforded *cis*-arylated piperidine **48a** as a yellow gum (35 mg, 0.08 mmol, 21%). R_f 0.55 (10% Et_2O/CH_2Cl_2); IR (film)/cm^{-1} 3347 (NH br), 2969, 2920, 2851, 1684 (C=O), 1523, 1482, 1420, 1386, 1364, 1156, 1123, 905, 790, 726; ^{1}H NMR (400 MHz, DMSO-d_6, 373 K) δ 9.96 (br s, 1 H, NH), 8.85 (dd, *J* = 4.2, 1.7 Hz, 1 H, HC_{Ar}), 8.55 (dd, *J* = 7.6, 1.4 Hz, 1 H, HC_{Ar}), 8.32 (dd, *J* = 8.4, 1.7 Hz, 1 H, HC_{Ar}), 7.64–7.47 (m, 3 H, 3 × HC_{Ar}), 7.28–7.22 (m, 2 H, 2 × HC_{Ar}), 7.22–7.14 (m, 2 H, 2 × HC_{Ar}), 7.14–7.07 (m, 1 H, HC_{Ar}), 6.54 (d, *J* = 16.0 Hz, 1 H, HC=C*H*Ph), 6.21 (dd, *J* = 16.0, 8.0 Hz, 1 H, *H*C=CHPh), 4.14–4.03 (m, 2 H, NC*H*HCH(HC=CH) and NC*H*HCH$_2$), 2.96–2.86 (m, 2 H, CH(C=O) and NCH*H*CH$_2$), 2.83 (dd, *J* = 13.2, 11.2 Hz, 1 H, NCH*H*CH(HC=CH))), 2.59 (ddt, *J* = 11.1, 8.0, 4.0 Hz, NCH$_2$C*H*(HC=CH)), 1.98 (dq, *J* = 13.2, 3.1 Hz, 1 H, NCH$_2$C*H*H), 1.78–1.66 (m, 1 H, NCH$_2$CH*H*), 1.47 (s, 9 H, C(C*H*$_3$)$_3$); ^{13}C NMR (101 MHz, DMSO-d_6, 373 K) δ 171.7 (C=O amide), 153.5 (C=O carbamate), 148.1 (C_{Ar}), 137.9 (C_{Ar} quat), 136.5 (C_{Ar} quat), 135.8 (C_{Ar}), 133.8 (C_{Ar} quat), 130.8 (HC=*C*HPh), 129.1 (H*C*=CHPh), 127.7 (2 × C_{Ar}), 127.3 (C_{Ar} quat), 126.6 (C_{Ar}), 126.2 (C_{Ar}), 125.4 (2 × C_{Ar}), 121.34 (C_{Ar}), 121.27 (C_{Ar}), 116.3 (C_{Ar}), 78.4 (*C*(CH$_3$)$_3$), 48.5 (*C*H(C=O)), 47.4 (N*C*H$_2$CH(HC=CH)), 42.4 (N*C*H$_2$CH$_2$), 41.3 (*C*H(HC=CH)), 28.0 (NCH$_2$*C*H$_2$), 27.7 (C(*C*H$_3$)$_3$); HRMS (ESI) ***m/z*** Calculated for $C_{28}H_{32}N_3O_3$ [M+H] 458.2444; Found 458.2435.

tert-Butyl-_trans_-(±)-4-(quinolin-8-ylcarbamoyl)-3-((_E_)-styryl)piperidine-1-carboxylate (48b)



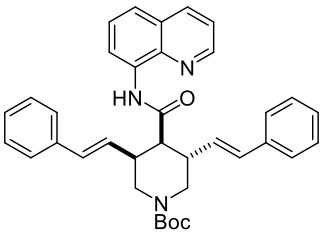
The above reaction also afforded *trans*-arylated piperidine **48b** as a yellow gum (36 mg, 0.08 mmol, 20%). R_f 0.31 (10% Et_2O/CH_2Cl_2); IR (film)/cm^{-1} 3346 (NH br), 3050, 2998, 2970, 2925, 2858, 1680 (C=O), 1522, 1482, 1422, 1386, 1324, 1240, 1160, 753; ^{1}H NMR (400 MHz, DMSO-d_6, 373 K) δ 10.00 (br s, 1 H, NH), 8.85 (dd, *J* = 4.2, 1.7 Hz, 1 H, HC_{Ar}), 8.54 (dt, *J* = 7.6, 1.7 Hz, 1 H, HC_{Ar}), 8.35 (dd, *J* = 8.3, 1.7 Hz, 1 H, HC_{Ar}), 7.66–7.56 (m, 2 H, 2 × HC_{Ar}), 7.56–7.50 (m, 1 H, HC_{Ar}), 7.25–7.10 (m, 5 H, 5 × HC_{Ar}), 6.54 (d, *J* = 16.0 Hz, 1 H, HC=C*H*Ph), 6.27 (dd, *J* = 16.0, 7.9 Hz, 1 H, *H*C=CHPh), 4.09–3.98 (m, 2 H, NC*H*HCH(HC=CH) and NC*H*HCH$_2$), 3.38 (dd, *J* = 13.2, 3.4 Hz, 1 H, NCH*H*CH(HC=CH)), 3.23–3.08 (m, 2 H, NCH*H*CH$_2$ and CH(C=O)), 3.06–3.00 (m, 1 H, NCH$_2$C*H*(HC=CH)), 1.99 (dtd, *J* = 14.5, 10.2, 4.3 Hz, 1 H, NCH$_2$C*H*H), 1.84 (dt, *J* = 13.6, 4.2 Hz, 1 H, NCH$_2$CH*H*), 1.42 (s, 9 H, C(C*H*$_3$)$_3$); ^{13}C NMR (101 MHz, DMSO-d_6, 373 K) δ 171.1 (C=O amide), 153.7 (C=O carbamate), 148.2 (C_{Ar}), 137.9 (C_{Ar} quat), 136.8 (C_{Ar} quat), 135.9 (C_{Ar}), 133.9 (C_{Ar} quat), 130.8 (HC=*C*HPh), 127.8 (2 × C_{Ar}), 127.45 (H*C*=CHPh), 127.36 (C_{Ar} quat), 126.5 (C_{Ar}), 126.3 (C_{Ar}), 125.3 (2 × C_{Ar}), 121.4 (C_{Ar}), 121.2 (C_{Ar}), 116.2 (C_{Ar}), 78.2 (*C*(CH$_3$)$_3$), 47.1 (N*C*H$_2$CH(HC=CH)), 45.7 (*C*H(C=O)), 41.8 (N*C*H$_2$CH$_2$), 39.9 (NCH$_2$*C*H(HC=CH)), 27.6 (C(*C*H$_3$)$_3$), 23.7 (NCH$_2$*C*H$_2$); HRMS (ESI) ***m/z*** Calculated for $C_{28}H_{32}N_3O_3$ [M+H] 458.2448; Found 458.2438.

***tert*-Butyl-*cis,cis*-(±)-4-(quinolin-8-ylcarbamoyl)-3,5-di((*E*)-styryl)piperidine-1-carboxylate (48c)**



The above reaction also afforded *cis*-*cis*-arylated piperidine **48c** as a yellow gum (45 mg, 0.08 mmol, 21%). R_f 0.75 (10% Et_2O/CH_2Cl_2); IR (film)/cm^{-1} 3340 (NH), 3022, 2970, 2924, 1677 (C=O), 1521, 1482, 1419, 1321, 1234, 1165, 1125, 967, 747, 692; ^{1}H NMR (400 MHz, DMSO-d_6, 373 K) δ 9.96 (br s, 1 H, NH), 8.65 (dd, *J* = 4.2, 1.7 Hz, 1 H, HC_{Ar}), 8.49 (dd, *J* = 7.6, 1.4 Hz, 1 H, HC_{Ar}), 8.29 (dd, *J* = 8.3, 1.7 Hz, 1 H, HC_{Ar}), 7.61 (dd, *J* = 8.3, 1.4 Hz, 1 H, HC_{Ar}), 7.53–7.48 (m, 2 H, 2 × HC_{Ar}), 7.28–7.19 (m, 4 H, 4 × HC_{Ar}), 7.19–7.09 (m, 6 H, 6 × HC_{Ar}), 6.65 (d, *J* = 16.1 Hz, 2 H, 2 × HC=C*H*Ph), 6.26 (dd, *J* = 16.1, 7.3 Hz, 2 H, 2 × *H*C=CHPh), 3.94 (dd, *J* = 12.8, 4.6 Hz, 2 H, 2 × NC*H*HCH(HC=CH)), 3.62 (dd, *J* = 12.9, 11.3 Hz, 2 H, 2 × NCH*H*CH(HC=CH)), 3.44 (t, *J* = 4.8 Hz, 1 H, CH(C=O)), 2.89–2.78 (m, 2 H, 2 × NCH_2CH(HC=CH)), 1.47 (s, 9 H, $C(CH_3)_3$); ^{13}C NMR (101 MHz, DMSO-d_6, 373 K) δ 170.3 (C=O amide), 153.9 (C=O carbamate), 148.1 (C_{Ar}), 138.1 (C_{Ar} quat), 136.6 (C_{Ar}), 135.7 (2 × C_{Ar} quat), 133.4 (C_{Ar} quat), 130.6 (C_{Ar}), 128.7 (2 × C_{Ar}), 127.7 (4 × C_{Ar}), 127.3 (C_{Ar} quat), 126.6 (2 × HC=*C*HPh), 126.1 (2 × H*C*=CHPh), 125.4 (4 × C_{Ar}), 121.6 (C_{Ar}), 121.2 (C_{Ar}), 117.0 (C_{Ar}), 78.4 ($C(CH_3)_3$), 48.8 (2 × N*C*H_2CH(HC=CH)), 43.5 (*C*H(C=O)), 40.9 (2 × NCH_2*C*H(HC=CH)), 27.7 ($C(CH_3)_3$); HRMS (ESI) *m/z* Calculated for $C_{36}H_{38}N_3O_3$ [M+H] 560.2913; Found 560.2903.

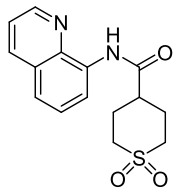
***tert*-Butyl-cis,*trans*-(±)-4-(quinolin-8-ylcarbamoyl)-3,5-di((*E*)-styryl)piperidine-1-carboxylate (48d)**



The above reaction also afforded *cis*-*trans*-arylated piperidine **48d** as a yellow gum (43 mg, 0.08 mmol, 19%). R_f 0.22 (10% Et_2O/CH_2Cl_2); IR (film)/cm^{-1} 3341 (NH br), 3049, 2969, 2921, 1675 (C=O), 1518, 1481, 1420, 1385, 1239, 1154, 1125, 963, 825, 790, 734, 692; ^{1}H NMR (400 MHz, DMSO-d_6, 373 K) δ 10.03 (s, 1 H, NH), 8.84 (dd, *J* = 4.2, 1.7 Hz, 1 H, HC_{Ar}), 8.49 (dd, *J* = 7.7, 1.3 Hz, 1 H, HC_{Ar}), 8.32 (dd, *J* = 8.3, 1.7 Hz, 1 H, HC_{Ar}), 7.64–7.54 (m, 2 H, 2 × HC_{Ar}), 7.48 (t, *J* = 8.0 Hz, 1 H, HC_{Ar}), 7.35–7.29 (m, 2 H, 2 × HC_{Ar}), 7.28–7.19 (m, 6 H, 6 × HC_{Ar}), 7.18–7.14 (m, 2 H, 2 × HC_{Ar}), 6.67 (d, *J* = 16.1 Hz, 1 H, HC=C*H*Ph), 6.49 (d, *J* = 16.0, Hz, 1 H, HC=C*H*Ph), 6.36 (dd, *J* = 16.0, 8.1 Hz, 1 H, *H*C=CHPh), 6.31–6.19 (m, 1 H, *H*C=CHPh), 4.20–4.07 (m, 2 H, 2 × NC*H*HCH(HC=CH)), 3.37 (dd, *J* = 13.1, 3.3 Hz, 1 H, NCH*H*CH(HC=CH)), 3.26 (dd, *J* = 9.8, 4.5 Hz, 1 H, CH(C=O)), 3.09 (dd, *J* = 8.0, 4.1 Hz, 1 H, NCH_2CH(HC=CH)), 3.05–2.99 (m, 2 H, NCH*H*CH(HC=CH) and NCH_2CH(HC=CH)), 1.41 (s, 9 H, $C(CH_3)_3$); ^{13}C NMR (101 MHz, DMSO-d_6, 373 K) δ 171.1 (C=O amide), 154.6 (C=O carbamate), 149.1 (C_{Ar}), 138.9 (C_{Ar} quat), 137.9 (C_{Ar} quat), 137.6 (C_{Ar} quat), 136.8 (C_{Ar}), 134.9 (C_{Ar} quat), 131.9 (C_{Ar}), 131.5 (C_{Ar}), 130.4 (HC=*C*HPh), 128.9 (2 × C_{Ar} and HC=*C*HPh), 128.8 (2 × C_{Ar}), 128.7 (H*C*=CHPh), 128.3 (C_{Ar} quat), 127.6 (H*C*=CHPh), 127.5 (C_{Ar}), 127.2 (C_{Ar}), 126.5 (2 × C_{Ar}), 126.3 (2 × C_{Ar}), 122.3 (C_{Ar}), 122.2 (C_{Ar}), 117.3 (C_{Ar}), 79.4 ($C(CH_3)_3$), 52.6 (*C*H(C=O)), 47.8 (2 × N*C*H_2CH(HC=CH)), 40.6 (NCH_2*C*H(HC=CH)), 37.4 (NCH_2*C*H(HC=CH)), 28.6 ($C(CH_3)_3$); HRMS (ESI) *m/z* Calculated for $C_{36}H_{38}N_3O_3$ [M+H] 560.2913; Found 560.2892.

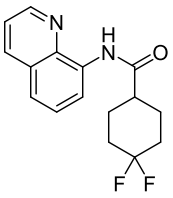
4.2.3 Heterocycle Scope

_N_-(Quinolin-8-yl)tetrahydro-2_H_-thiopyran-4-carboxamide 1,1-dioxide (50)



4-DMAP (508 mg, 4.00 mmol, 0.2 equiv) and EDC·HCl (4.20 g, 22.00 mmol, 1.1 equiv) were added to a solution of tetrahydro-2*H*-thiopyran-4-carboxylic acid 1,1-dioxide (3.56 g, 20.00 mmol, 1.0 equiv) and 8-aminoquinoline (3.20 g, 22.00 mmol, 1.1 equiv) in CH_2Cl_2 (40 mL). After stirring at rt for 24 h, the reaction was diluted with CH_2Cl_2 (20 mL), then sat. aq. $NaHCO_3$ (40 mL) was added and the aqueous layer extracted with CH_2Cl_2 (3 x 30 mL). The combined organic extracts were dried over Na_2SO_4, filtered, and the solvent removed under reduced pressure. Purification of the residue by flash column chromatography (40% to 60% acetone/pentane) afforded amide **50** (3.89 g, 64%) as a dark orange amorphous solid. R_f = 0.41 (40% acetone/pentane); mp = 181–183 °C (from acetone/pentane); IR (film)/cm^{-1} 3336, 3080, 2855, 1674 (C=O), 1480, 1323, 1282 (S=O), 1122 (S=O), 916, 857, 824, 794; ^{1}H NMR (400 MHz, $CDCl_3$) δ 9.98 (br s, 1 H, NH), 8.81 (dd, *J* = 4.2, 1.6 Hz, 1 H, HC_{Ar}), 8.73 (t, *J* = 4.5 Hz, 1 H, HC_{Ar}), 8.19 (dd, *J* = 8.3, 1.7 Hz, 1 H, HC_{Ar}), 7.55 (d, *J* = 4.5 Hz, 2 H, 2 × HC_{Ar}), 7.49 (dd, *J* = 8.2, 4.2 Hz, 1 H, HC_{Ar}), 3.40 (ddd, *J* = 12.0, 7.7, 4.1 Hz, 2 H, 2 × SC*H*HCH_2), 3.09 (ddd, *J* = 13.8, 9.5, 4.0 Hz, 2 H, 2 × SCH*H*CH_2), 2.84 (tt, *J* = 8.1, 3.8 Hz, 1 H, CH(C=O)), 2.73–2.25 (m, 4 H, 2 × SCH_2CH_2); ^{13}C NMR (101 MHz, $CDCl_3$) δ 170.9 (C=O amide), 148.3 (C_{Ar}), 138.3 (C_{Ar} quat), 136.5 (C_{Ar}), 133.8 (C_{Ar} quat), 127.9 (C_{Ar} quat), 127.3 (C_{Ar}), 122.1 (C_{Ar}), 121.8 (C_{Ar}), 116.7 (C_{Ar}), 49.8 (*C*H(C=O)), 41.8 (2 × S*C*H_2CH_2), 27.3 (2 × SCH_2CH_2); HRMS (ESI) *m/z* Calculated for $C_{15}H_{17}N_2O_3S$ [M+H] 304.3640; Found 304.3632.

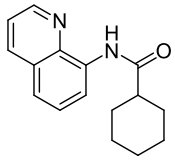
4,4-Difluoro-_N_-(quinolin-8-yl)cyclohexane-1-carboxamide (51)



4-DMAP (508 mg, 4.00 mmol, 0.2 equiv) and EDC·HCl (4.20 g, 22.00 mmol, 1.1 equiv) were added to a solution of 4,4-difluorocyclohexane-1-carboxylic acid (3.30 g, 20.00 mmol, 1.0 equiv) and 8-aminoquinoline (3.17 g, 22.00 mmol, 1.1 equiv) in CH_2Cl_2 (50 mL). After stirring at rt for 24 h, the reaction was diluted with CH_2Cl_2 (30 mL), then sat. aq. $NaHCO_3$ (20 mL) was added and the aqueous layer extracted with CH_2Cl_2 (3 x 50 mL). The combined organic extracts were dried over Na_2SO_4, filtered, and the solvent removed under reduced pressure. Purification of the residue by flash column chromatography (hexane/CH_2Cl_2/Et_2O 9:9:1) afforded amide **51** as a white solid (5.52 g, 19 mmol, 95%). R_f = 0.31 (hexane/CH_2Cl_2/Et_2O 9:9:1); mp = 142–145 °C (from hexane/CH_2Cl_2/Et_2O); IR (film)/cm^{-1} 3348 (NH), 2938, 2871, 1682 (C=O), 1524, 1483, 1377, 1257, 1107, 963, 826; ^{1}H NMR (400 MHz, $CDCl_3$) δ 9.94 (s, 1 H, NH), 8.81 (dd, *J* = 4.2, 1.7 Hz, 1 H, HC_{Ar}), 8.77 (dd, *J* = 6.9, 2.1 Hz, 1 H, HC_{Ar}), 8.18 (dd, *J* = 8.3, 1.7 Hz, 1 H, HC_{Ar}), 7.57–7.50 (m, 2 H, 2 × HC_{Ar}), 7.47 (dd, *J* = 8.3, 4.2 Hz, 1 H, HC_{Ar}), 2.59 (dddd, *J* = 12.2, 10.6, 4.7, 2.7 Hz, 1 H, HC(C=O)), 2.33–2.21 (m, 2 H, 2 × CF_2CHH), 2.21–2.11 (m, 2 H, 2 × CF_2CH_2CHH), 2.11–1.99 (m, 2 H, 2 × CF_2CHH), 1.96–1.78 (m, 2 H, 2 × CF_2CH_2CHH); ^{13}C NMR (101 MHz, $CDCl_3$) δ 172.8 (C=O amide), 148.4 (C_{Ar}), 138.5 (C_{Ar} quat), 136.6 (C_{Ar}), 134.4 (C_{Ar} quat), 128.08 (C_{Ar} quat), 127.6 (C_{Ar}), 122.8 (t, J_{CF} = 241.2 Hz, CF_2), 121.8 (C_{Ar}), 121.8 (C_{Ar}), 116.7 (C_{Ar}), 44.3 (*C*H(C=O)), 33.0 (t, J_{CF} = 24.5 Hz, 2 × CF_2CH_2), 26.1 (t, J_{CF} = 9.0

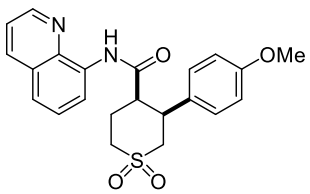
Hz, 2 × $CF_2CH_2CH_2$); $^{19}F\{^1H\}$ NMR (377 MHz, $CDCl_3$) δ –92.90 (d, J_{FF} = 237.5 Hz), –100.55 (d, J_{FF} = 240.5 Hz); HRMS (ESI) *m/z* Calculated for $C_{16}H_{17}N_2OF_2$ [M+H] 291.1309; Found 291.1317.

_N_-(Quinolin-8-yl)cyclohexanecarboxamide (52)



4-DMAP (50 mg, 0.40 mmol, 0.2 equiv) and EDC·HCl (421 mg, 2.20 mmol, 1.1 equiv) were added to a solution of cyclohexanecarboxylic acid (256 mg, 2.00 mmol, 1.0 equiv) and 8-aminoquinoline (316 mg, 2.20 mmol, 1.1 equiv) in CH_2Cl_2 (15 mL). After stirring at rt for 24 h, the reaction was diluted with CH_2Cl_2 (20 mL), then sat. aq. $NaHCO_3$ (30 mL) was added and the aqueous layer extracted with CH_2Cl_2 (3 x 20 mL). The combined organic extracts were dried over Na_2SO_4, filtered, and the solvent removed under reduced pressure. Purification of the residue by flash column chromatography (10% to 20% acetone/pentane) afforded amide **52** as a white solid (462 mg, 1.82 mmol, 91%). R_f 0.46 (30% acetone/pentane); mp = 70–72 °C (from acetone/pentane); IR (film)/cm^{-1} 3355 (NH br), 2929, 2920, 1681 (C=O), 1528, 1409, 1322, 1163, 1119, 940; ^1H NMR (400 MHz, $CDCl_3$) δ 9.89 (br s, 1 H, NH), 8.86–8.77 (m, 2 H, 2 × HC_{Ar}), 8.14 (dd, *J* = 8.3, 1.7 Hz, 1 H, HC_{Ar}), 7.61–7.39 (m, 3 H, 3 × HC_{Ar}), 2.47 (tt, *J* = 11.7, 3.5 Hz, 1 H, CH(C=O)), 2.16–2.03 (m, 2 H, 2 × C*H*HCH(C=O)), 1.96–1.82 (m, 2 H, 2 × CH*H*CH(C=O)), 1.77–1.54 (m, 2 H, 2 × C*H*HCH$_2$CH(C=O)), 1.34 (dddd, *J* = 27.5, 24.4, 12.3, 9.0 Hz, 4 H, C*H*$_2$(CH$_2$)$_2$CH(C=O) and 2 × CH*H*CH$_2$CH(C=O)); ^{13}C NMR (101 MHz, $CDCl_3$) δ 172.9 (C=O amide), 148.6 (C_{Ar}), 137.2 (C_{Ar} quat), 136.7 (C_{Ar}), 133.8 (C_{Ar}), 129.2 (C_{Ar} quat), 127.3 (C_{Ar}), 121.2 (C_{Ar}), 116.5 (C_{Ar} quat), 113.8 (C_{Ar}), 43.2 (*C*H(C=O)), 29.4 (2 × *C*H$_2$CH(C=O)), 24.8 (2 × *C*H$_2$CH$_2$CH(C=O)), 25.3 (*C*H$_2$(CH$_2$)$_2$CH(C=O)); HRMS (ESI) *m/z* Calculated for $C_{16}H_{19}N_2O$ [M+H] 255.3410; Found 255.3408.

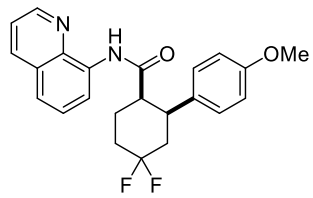
***cis*-(±)-3-(4-Methoxyphenyl)-N-(quinolin-8-yl)tetrahydro-2H-thiopyran-4-carboxamide 1,1-dioxide (54)**



A flame-dried microwave vial was charged with amide **50** (121 mg, 0.40 mmol, 1.0 equiv). Then 4-iodoanisole (280 mg, 1.20 mmol, 3.0 equiv), Ag_2CO_3 (220 mg, 0.80 mmol, 2.0 equiv), MesCOOH (19.7 mg, 0.12 mmol, 0.3 equiv) and $Pd(OAc)_2$ (9 mg, 0.04 mmol, 0.1 equiv) were added sequentially. The reaction vessel was sealed and purged with argon, then $PhCF_3$ (1.34 mL, 0.3 M) was added by syringe. The reaction tube was placed in a preheated oil bath and stirred at 75 °C for 24 h. The reaction mixture was then allowed to cool to rt, diluted with EtOAc (10 mL) and filtered through a pad of Celite, eluting with further EtOAc (2 × 15 mL). The solvent was removed under reduced pressure and the crude material purified by flash column chromatography (40% to 60% acetone/pentane). Et_2O (5 mL), followed by pentane (5 mL) were added to the isolated product, with the resulting suspension concentrated under reduced pressure. This procedure was repeated three times to eliminate residual solvent and afford **54** as a pale pink crystalline solid (55 mg, 0.14 mmol, 34%). R_f 0.31 (40% acetone/pentane); mp = 118–120 °C (from Et_2O/pentane); IR (film)/cm^{-1} 3332 (br NH), 3049, 2930, 2833, 1670 (C=O), 1521, 1379, 1252 (S=O), 1118 (S=O), 1029, 910, 828, 731; ^1H NMR (400 MHz, $CDCl_3$) δ 9.32 (br s, 1 H, NH), 8.67–8.60 (m, 2 H, 2 × HC_{Ar}), 8.12 (dd, *J* = 8.3, 1.7 Hz, 1 H, HC_{Ar}), 7.55–7.49 (m, 2 H, 2 × HC_{Ar}), 7.41 (dd, *J* = 8.3, 4.3 Hz, 1 H, HC_{Ar}), 7.20–7.11 (m, 2 H, 2 × HC_{Ar}), 6.74–

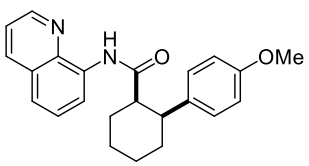
6.66 (m, 2 H, 2 × HC_{Ar}), 4.44 (t, *J* = 13.4 Hz, 1 H, SC*H*HCHAr), 4.05 (td, *J* = 13.7, 4.1 Hz, 1 H, SC*H*HCH$_2$), 3.81 (dt, *J* = 13.4, 3.6 Hz, 1 H, CHAr), 3.58 (s, 3 H, OCH_3), 3.09 (dt, *J* = 13.5, 3.3 Hz, 1 H, SCH*H*CHAr), 3.07–2.99 (m, 2 H, CH(C=O) and SCH*H*CH$_2$), 2.64 (tt, *J* = 13.4, 4.1 Hz, 1 H, SCH$_2$C*H*H), 2.53 (dq, *J* = 14.8, 3.6 Hz, 1 H, SCH$_2$CH*H*); ^{13}C NMR (101 MHz, $CDCl_3$) δ 170.9 (C=O amide), 158.9 (C_{Ar} quat), 148.0 (C_{Ar}), 138.1 (C_{Ar} quat), 136.2 (C_{Ar}), 133.6 (C_{Ar}), 131.7 (C_{Ar} quat), 128.2 (2 × C_{Ar}), 127.8 (C_{Ar} quat), 127.1 (C_{Ar}), 122.1 (C_{Ar}), 121.6 (C_{Ar}), 116.6 (C_{Ar} quat), 114.3 (2 × C_{Ar}), 55.0 (OCH_3), 51.8 (S*C*H$_2$CHAr), 47.0 (S*C*H$_2$CH$_2$), 46.0 (*C*H(C=O)), 43.5 (CHAr), 27.3 (SCH$_2$*C*H$_2$); HRMS (ESI) ***m/z*** Calculated for $C_{22}H_{23}N_2O_4S$ [M+H] 411.1379; Found 411.1382.

cis-(±)-4,4-Difluoro-2-(4-methoxyphenyl)-_N_-(quinolin-8-yl)cyclohexane-1-carboxamide (55)



A flame-dried microwave vial was charged with amide **51** (1.16 g, 4.00 mmol, 1.0 equiv). Then 4-iodoanisole (1.87 g, 8.00 mmol, 2.0 equiv), Ag_2CO_3 (1.38 g, 5.00 mmol, 1.25 equiv), MesCOOH (197 mg, 1.20 mmol, 0.3 equiv) and $Pd(OAc)_2$ (90 mg, 0.40 mmol, 0.1 equiv) were added sequentially. The reaction vessel was sealed and purged with argon, then $PhCF_3$ (13.4 mL) was added by syringe. The reaction tube was placed in a preheated oil bath and stirred at 45 °C for 24 h. The reaction mixture was then allowed to cool to rt, diluted with EtOAc (5 mL) and filtered through a pad of Celite, eluting with further EtOAc (2 × 10 mL). The crude material was purified by flash column chromatography (20% EtOAc/pentane), affording product **55** as an off-white solid (906 mg, 0.23 mmol, 57%). R_f 0.26 (20% EtOAc/hexane); mp = 141–142 °C (from acetone/pentane); IR (film)/cm^{-1} 3345 (NH), 2933, 1676 (C=O), 1522, 1483, 1374, 1245, 1105, 966, 827; ^{1}H NMR (400 MHz, $CDCl_3$) δ 9.22 (s, 1 H, NH), 8.66–8.58 (m, 2 H, 2 × HC_{Ar}), 8.08 (dd, *J* = 8.3, 1.7 Hz, 1 H, HC_{Ar}), 7.52–7.41 (m, 2 H, 2 × HC_{Ar}), 7.37 (dd, *J* = 8.3, 4.2 Hz, 1 H, HC_{Ar}), 7.23–7.15 (m, 2 H, 2 × HC_{Ar}), 6.73–6.65 (m, 2 H, 2 × HC_{Ar}), 3.56 (s, 3 H, OCH_3), 3.38–3.28 (m, 1 H, CHAr), 3.16–2.92 (m, 2 H, CH(C=O) and CF_2C*H*HCHAr), 2.70 (dtt, *J* = 33.2, 13.0, 4.2 Hz, 1 H, CF_2C*H*HCH$_2$), 2.30-2.07 (m, 4 H, CF_2CH*H*CH$_2$, CF_2CH$_2$C*H*$_2$, CF_2CH*H*CH); ^{13}C NMR (101 MHz, $CDCl_3$) δ 172.1 (C=O amide), 158.6 (C_{Ar} quat), 148.0 (C_{Ar}), 138.3 (C_{Ar} quat), 136.2 (C_{Ar}), 134.2 (C_{Ar} quat), 133.5 (C_{Ar} quat), 128.5 (2 × C_{Ar}), 127.9 (C_{Ar} quat), 127.3 (C_{Ar}), 124.5 (dd, J_{CF} = 243.0, 238.1 Hz, CF_2), 121.61 (C_{Ar}), 121.57 (C_{Ar}), 116.4 (C_{Ar}), 114.1 (2 × C_{Ar}), 55.1 (OCH_3), 47.2 (*C*H(C=O)), 42.0 (t, J_{CF} = 10.0 Hz, CHAr), 35.0 (t, J_{CF} = 24.0 Hz, CF_2*C*H$_2$CHAr), 30.0 (t, J_{CF} = 24.1 Hz, CF_2*C*H$_2$CH$_2$), 26.3 (t, J_{CF} = 10.6 Hz, CF_2CH$_2$*C*H$_2$); ^{19}F{^{1}H} NMR (377 MHz, $CDCl_3$) δ –88.29 (d, J_{FF} = 235.9 Hz), –100.76 (d, J_{FF} = 236.0 Hz); HRMS (ESI) m/z Calculated for $C_{23}H_{23}N_2O_2F_2$ [M+H] 397.1728; Found 397.1720.

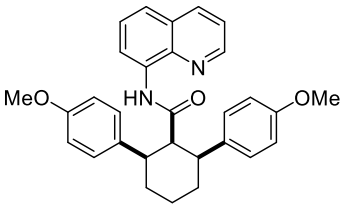
cis-(±)-4,4-Difluoro-2-(4-methoxyphenyl)-_N_-(quinolin-8-yl)cyclohexane-1-carboxamide (56)



A flame-dried microwave vial was charged with amide **52** (116 mg, 0.40 mmol, 1.0 equiv). Then 4-iodoanisole (94 mg, 0.40 mmol, 1.0 equiv), Ag_2CO_3 (138 mg, 0.5 mmol, 1.25 equiv), MesCOOH (20 mg, 0.12 mmol, 0.3 equiv) and $Pd(OAc)_2$ (9 mg, 0.04 mmol, 0.1 equiv) were sequentially added. The reaction vessel was sealed and purged with argon, then $PhCF_3$ (1.34 mL) was added by syringe. The reaction tube was placed in a preheated oil bath and stirred at 45 °C for 48 h. The reaction

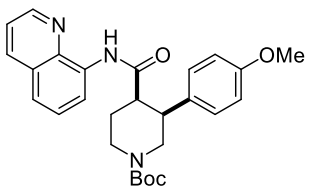
mixture was then allowed to cool to rt, diluted with EtOAc (5 mL) and filtered through a pad of Celite, eluting with further EtOAc (2 × 10 mL). The crude material was purified by flash column chromatography (10% to 20% EtOAc/hexane), affording product **56** as an off-white solid (72 mg, 0.20 mmol, 50%). R_f 0.38 (20% EtOAc/hexane); mp = 135–136 °C (from EtOAc/hexane); IR (film)/cm^{-1} 3354 (NH), 2922, 2855, 1684 (C=O), 1521, 1380, 1325, 1252, 1118, 1036, 828; ^{1}H NMR (400 MHz, $CDCl_3$) δ 9.28 (br s, 1 H, NH), 8.70 (dd, *J* = 7.5, 1.5 Hz, 1 H, HC_{Ar}), 8.65 (dd, *J* = 4.3, 1.7 Hz, 1 H, HC_{Ar}), 8.11 (dd, *J* = 8.3, 1.7 Hz, 1 H, HC_{Ar}), 7.55–7.42 (m, 2 H, 2 × HC_{Ar}), 7.40 (dd, *J* = 8.3, 4.2 Hz, 1 H, HC_{Ar}), 7.31–7.24 (m, 2 H, 2 × HC_{Ar}), 6.75–6.67 (m, 2 H, 2 × HC_{Ar}), 3.61 (s, 3 H, OCH_3), 3.12–2.98 (m, 2 H, CHAr and CH(C=O)), 2.49 (qd, *J* = 12.1, 3.7 Hz, 1 H, C*H*HCHAr), 2.26 (dq, *J* = 13.5, 3.9 Hz, 1 H, C*H*HCH(C=O)), 2.14 (qt, *J* = 12.5, 3.8 Hz, 1 H, C*H*HCH$_2$CHAr), 2.08–1.96 (m, 1 H, CH*H*CHAr), 1.88 (tt, *J* = 13.3, 4.4 Hz, 1 H, CH*H*CH(C=O)), 1.86–1.80 (m, 1 H, C*H*HCH$_2$CH(C=O)), 1.72–1.60 (m, 1 H, CH*H*CH$_2$CHAr), 1.51 (qt, J = 12.4, 3.9 Hz, 1 H, CH*H*CH$_2$CH(C=O)); ^{13}C NMR (101 MHz, $CDCl_3$) δ 173.2 (C=O amide), 157.9 (C_{Ar} quat), 147.7 (C_{Ar}), 136.7 (C_{Ar} quat), 136.1 (C_{Ar}), 134.6 (C_{Ar} quat), 128.6 (2 × C_{Ar}), 127.8 (C_{Ar} quat), 127.3 (C_{Ar}), 121 (C_{Ar}), 121.3 (C_{Ar}), 121.0 (C_{Ar}), 116.2 (C_{Ar} quat), 113.7 (2 × C_{Ar}), 55.0 (OCH_3), 48.9 (*C*H(C=O)), 45.0 (CHAr), 29.7 (*C*H$_2$CH(C=O)), 27.2 (*C*H$_2$CHAr), 26.2 (*C*H$_2$CH$_2$CH(C=O)), 21.8 (*C*H$_2$CH$_2$CHAr); HRMS (ESI) m/z Calculated for $C_{23}H_{25}N_2O_2$ [M+H] 361.4650; Found 361.4645.

***cis*-(±)-4,4-Difluoro-2-(4-methoxyphenyl)-*N*-(quinolin-8-yl)cyclohexane-1-carboxamide (S2)**



The procedure for the synthesis of **56** above also afforded **S2** as a pale-yellow crystalline solid (47 mg, 0.10 mmol, 25%). R_f 0.28 (20% EtOAc/hexane); mp = 184–185 °C (from EtOAc/hexane); IR (film)/cm^{-1} 3355 (NH), 2997, 2930, 2855, 1677 (C=O), 1513, 1379, 1327, 1245, 1178, 1036, 910, 828, 731, 544; ^{1}H NMR (400 MHz, $CDCl_3$) δ 8.70–8.59 (m, 1 H, NH), 8.57–8.45 (m, 2 H, 2 × HC_{Ar}), 8.03 (d, *J* = 8.2 Hz, 1 H, HC_{Ar}), 7.51–7.30 (m, 3 H, 3 × HC_{Ar}), 7.29–7.21 (m, 4 H, 4 × HC_{Ar}), 6.70–6.60 (m, 4 H, 4 × HC_{Ar}), 3.54 (s, 6 H, OCH_3), 3.13 (dt, *J* = 12.4, 3.3 Hz, 2 H, 2 × CHAr), 2.74 (qd, *J* = 12.8, 3.8 Hz, 2 H, 2 × C*H*HCHAr), 2.30–2.19 (m, 1 H, CH(C=O)), 1.86–1.77 (m, 2 H, 2 × CH*H*CHAr), 1.67 (qt, *J* = 13.1, 8.5, 3.9 Hz, 2 H, C*H*$_2$CH$_2$CHAr); ^{13}C NMR (101 MHz, $CDCl_3$) δ 171.3 (C=O amide), 157.9 (2 × C_{Ar} quat), 147.3 (C_{Ar}), 136.4 (2 × C_{Ar} quat), 135.8 (C_{Ar} quat), 134.2 (C_{Ar} quat), 128.7 (C_{Ar} quat), 128.4 (4 × C_{Ar}), 127.5 (C_{Ar}), 127.1 (C_{Ar}), 121.1 (C_{Ar}), 116.1 (C_{Ar}), 113.8 (C_{Ar}), 113.6 (4 × C_{Ar}), 57.4 (*C*H(C=O)), 55.0 (2 × OCH_3), 46.9 (2 × CHAr), 26.7 (2 × *C*H$_2$CHAr), 25.8 (*C*H$_2$CH$_2$CHAr); HRMS (ESI) m/z Calculated for $C_{30}H_{31}N_2O_3$ [M+H] 467.5890; Found 467.5882.

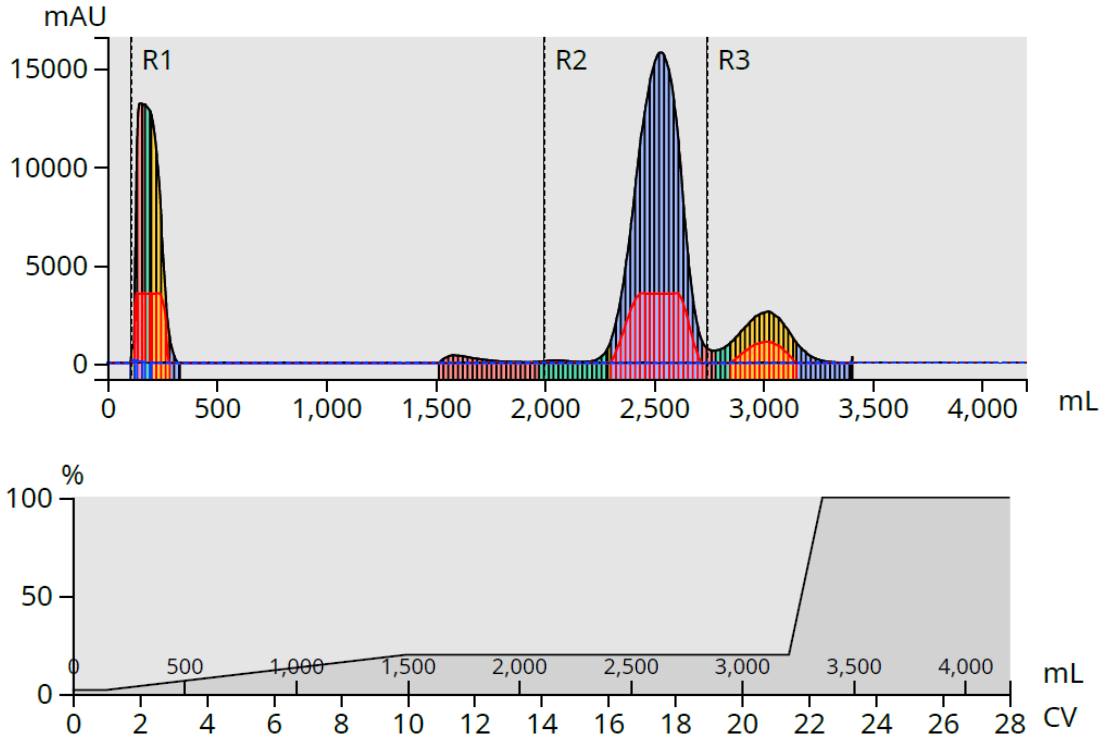
4.2.4 Gram-Scale Arylation of Piperidine Amide 29a



A flask was charged with amide **25** (1.42 g, 4.00 mmol, 1.0 equiv), 4-iodoanisole (1.87 g, 8.00 mmol, 2.0 equiv), Ag_2CO_3 (1.38 g, 5.00 mmol, 1.25 equiv), 2,4,6-trimethylbenzoic acid (MesCOOH, 197 mg, 1.2 mmol, 0.3 equiv) and $Pd(OAc)_2$ (90 mg, 0.4 mmol, 0.1 equiv) in this order. The reaction vessel was covered with a suba seal and purged with argon, then $PhCF_3$ (13.4 mL, 0.3 M) was added by syringe. The flask was placed in a preheated oil bath and stirred at 45 ºC for 18 h under an atmosphere of argon. The mixture was then allowed to cool to rt and EtOAc (20 mL) was added before

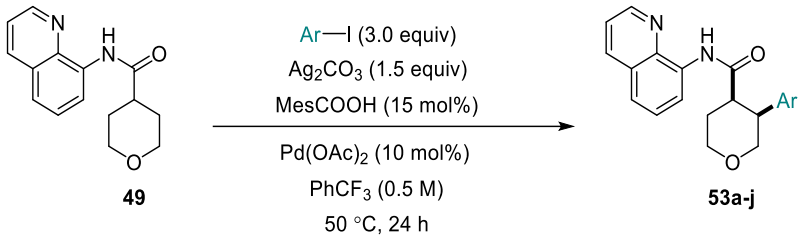
filtering through a pad of Celite, eluting with further EtOAc (2 × 50 mL). The solvent was removed under reduced pressure and the residue purified by automated flash column chromatography (2% to 20% acetone/pentane, see below). The product containing fractions were combined and the solvent was removed under reduced pressure. Et_2O (5 mL) and pentane (10 mL) were added and the solvent was removed under reduced pressure to afford arylated piperidine **29a** as a white solid (1.34 g, 2.91 mmol, 70%). All characterisation information in agreement with data previously reported for **29a**.

Automated Column Conditions: Run on Biotage® Selekt. Column Type: Biotage® Sfär HC 100 g. Flow Rate: 120 mL/min. Sample Mass: 3000 mg. Solvent A: pentane, Solvent B: acetone. UV wavelength detection: λ 200–400 nm. See trace and gradient below. From the left: 1st peak: unreacted aryl iodide. 2nd peak (red): unreacted starting amide **25**. 3rd peak (blue): desired *cis*-arylated product **29a.** 4th peak (yellow): mono-*trans* **29b** and di-*cis*-*cis* arylated **29d** side-products. 5th component (blue tail): di-*cis*-*trans* arylated piperidine side-product **29c**.



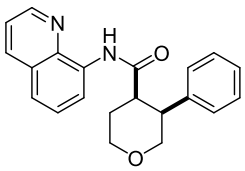
4.2.5 Tetrahydropyran Arylation

General Procedure C for C–H Arylation of Tetrahydropyrans



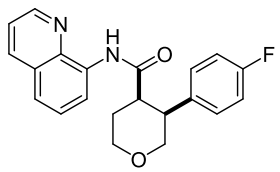
A flame-dried microwave vial was charged with amide **49** (128 mg, 0.50 mmol, 1.0 equiv). The requisite aryl iodide (1.50 mmol, 3.0 equiv), Ag_2CO_3 (206 mg, 0.75 mmol, 1.5 equiv), 2,4,6-trimethylbenzoic acid (MesCOOH, 16.4 mg, 0.08 mmol, 0.15 equiv) and $Pd(OAc)_2$ (11 mg, 0.05 mmol, 0.1 equiv) were added sequentially. The reaction vessel was sealed and purged with argon, then $PhCF_3$ (1 mL, 0.5 M) was added by syringe. The reaction tube was placed in a preheated oil bath and stirred at 50 °C for 24 h. The reaction mixture was then allowed to cool to rt, diluted with EtOAc (5 mL) and filtered through a pad of Celite, eluting with further EtOAc (2 × 10 mL). The solvent was removed under reduced pressure and the crude material purified by flash column chromatography under the specified conditions. Et_2O (5 mL), followed by pentane (5 mL) were added to the isolated product, with the resulting suspension concentrated under reduced pressure. This procedure was repeated three times to eliminate residual solvent and afford desired arylated tetrahydropyrans.

***cis*-(±)-3-Phenyl-N-(quinolin-8-yl)tetrahydro-2H-pyran-4-carboxamide (53b)**



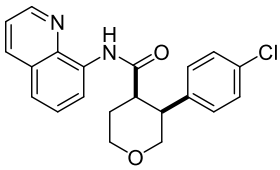
Prepared according to **General Procedure C** using iodobenzene (305 mg). Purification by flash column chromatography (10% Et_2O in CH_2Cl_2) afforded arylated tetrahydropyran **53b** as a pale yellow solid (75 mg, 0.23 mmol, 45%). R_f 0.42 (10% MeCN/CH_2Cl_2); mp = 65–67 °C (from EtO/pentane); IR (film)/cm^{-1} 3349 (br NH), 3029, 2952, 2844, 1683 (C=O), 1523, 1485, 1426, 1325, 1098, 826, 792; ^{1}H NMR (400 MHz, $CDCl_3$, 298 K) δ 9.57 (br s, 1 H, NH), 8.70 (dd, *J* = 4.3, 1.7 Hz, 1 H, HC_{Ar}), 8.64 (dd, *J* = 6.9, 2.2 Hz, 1 H, HC_{Ar}), 8.12 (dd, *J* = 8.3, 1.7 Hz, 1 H, HC_{Ar}), 7.54–7.37 (m, 5 H, 5 × HC_{Ar}), 7.19–7.10 (m, 2 H, 2 × HC_{Ar}), 7.10–7.02 (m, 1 H, HC_{Ar}), 4.47 (dd, *J* = 11.4, 5.4 Hz, 1 H, OC*H*HCHAr), 4.36 (ddd, *J* = 11.4, 6.1, 3.8 Hz, 1 H, OC*H*HCH$_2$), 3.99 (dd, *J* = 11.4, 3.6 Hz, 1 H, OCH*H*CHAr), 3.77 (ddd, *J* = 11.5, 8.1, 3.5 Hz, 1 H, OCH*H*CH$_2$), 3.40 (q, *J* = 4.7 Hz, 1 H, CH(C=O)), 3.20 (dt, *J* = 9.1, 4.6 Hz, 1 H, CHAr), 2.26 (dtd, *J* = 13.6, 8.3, 3.8 Hz, 1 H, OCH$_2$C*H*H), 1.99 (ddt, *J* = 13.9, 10.2, 4.0 Hz, 1 H, OCH$_2$CH*H*); ^{13}C NMR (101 MHz, $CDCl_3$, 298 K) δ 171.6 (C=O amide), 148.0 (C_{Ar}), 140.3 (C_{Ar} quat), 138.3 (C_{Ar} quat), 136.2 (C_{Ar}), 134.1 (C_{Ar} quat), 128.8 (2 × C_{Ar}), 128.2 (2 × C_{Ar}), 127.8 (C_{Ar} quat), 127.3 (C_{Ar}), 126.8 (C_{Ar}), 121.5 (C_{Ar}), 121.4 (C_{Ar}), 116.3 (C_{Ar}), 70.2 (O*C*H$_2$CHAr), 66.0 (O*C*H$_2$CH$_2$), 47.2 (*C*HAr), 43.3 (*C*H(C=O)), 25.7 (OCH$_2$*C*H$_2$); HRMS (ESI) *m/z* Calculated for $C_{21}H_{21}N_2O_2$ [M+H] 333.1603; Found 333.1610.

***cis*-(±)-3-(4-Fluorophenyl)-N-(quinolin-8-yl)tetrahydro-2H-pyran-4-carboxamide (53c)**



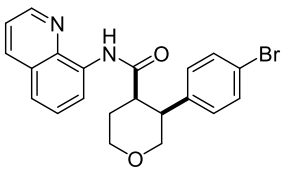
Prepared according to **General Procedure C** using 1-fluoro-4-iodobenzene (332 mg). Purification by flash column chromatography (10% Et_2O/CH_2Cl_2) afforded arylated tetrahydropyran **53c** as a pale yellow solid (62 mg, 0.17 mmol, 33%). R_f 0.25 (10% $MeCN/CH_2Cl_2$); mp = 127–129 °C (from Et_2O/pentane); IR (film)/cm^{-1} 3347 (br NH), 3047, 2960, 2848, 1683 (C=O), 1525, 1485, 1426, 1325, 1224, 1163, 908, 826, 792, 731; ^{1}H NMR (400 MHz, $CDCl_3$, 298 K) δ 9.58 (br s, 1 H, NH), 8.71 (dd, *J* = 4.2, 1.7 Hz, 1 H, HC_{Ar}), 8.63 (dd, *J* = 6.2, 2.8 Hz, 1 H, HC_{Ar}), 8.14 (dd, *J* = 8.3, 1.7 Hz, 1 H, HC_{Ar}), 7.53–7.46 (m, 2 H, 2 × HC_{Ar}), 7.47–7.40 (m, 3 H, 3 × HC_{Ar}), 6.89–6.75 (m, 2 H, 2 × HC_{Ar}), 4.51–4.28 (m, 2 H, OC*H*HCHAr and OC*H*HCH$_2$), 3.97 (dd, *J* = 11.5, 3.5 Hz, 1 H, OCH*H*CHAr), 3.74 (ddd, *J* = 11.8, 8.8, 3.3 Hz, 1 H, OCH*H*CH$_2$), 3.39 (q, *J* = 4.4 Hz, 1 H, CH(C=O)), 3.17 (dt, *J* = 9.3, 4.6 Hz, 1 H, CHAr), 2.24 (ddt, *J* = 13.1, 9.0, 4.5 Hz, 1 H, OCH$_2$C*H*H), 1.96 (dq, *J* = 13.3, 4.0 Hz, 1 H, OCH$_2$CH*H*); ^{13}C NMR (101 MHz, $CDCl_3$, 298 K) δ 171.4 (C=O amide), 161.8 (d, J_{CF} = 246.7 Hz, FC_{Ar} quat), 148.0 (C_{Ar}), 138.3 (C_{Ar} quat), 136.3 (C_{Ar}), 136.0 (d, J_{CF} = 3.4 Hz, F-*p*-C_{Ar} quat), 133.9 (C_{Ar} quat), 130.5 (C_{Ar}), 130.4 (d, J_{CF} = 8.1 Hz, 2 × F-*m*-C_{Ar}), 127.8 (C_{Ar} quat), 127.3 (C_{Ar}), 121.5 (C_{Ar}), 116.4 (C_{Ar}), 114.9 (d, J_{CF} = 21.0 Hz, 2 × F-*o*-C_{Ar}), 70.5 (O*C*H$_2$CHAr), 66.2 (O*C*H$_2$CH$_2$), 47.3 (*C*HAr), 42.4 (*C*H(C=O)), 25.2 (OCH$_2$*C*H$_2$); ^{19}F{^{1}H} NMR (377 MHz, $CDCl_3$, 298 K) δ –116.33 (s); HRMS (ESI) *m/z* Calculated for $C_{21}H_{20}N_2O_2F$ [M+H] 351.1509; Found 351.1495.

***cis*-(±)-3-(4-Chlorophenyl)-N-(quinolin-8-yl)tetrahydro-2H-pyran-4-carboxamide (53d)**



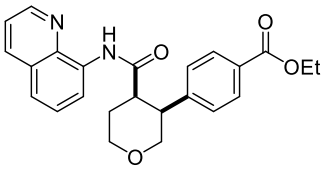
Prepared according to **General Procedure C** using 1-chloro-4-iodobenzene (305 mg). Purification by flash column chromatography (10% $MeCN/CH_2Cl_2$) afforded arylated tetrahydropyran **53d** as a white solid (89 mg, 0.25 mmol, 50%). R_f 0.37 (10% $MeCN/CH_2Cl_2$); mp = 61–63 °C (from Et_2O/pentane); IR (film)/cm^{-1} 3345 (br NH), 2956, 2846, 1683 (C=O), 1525, 1485, 1426, 1325, 1094, 826; ^{1}H NMR (400 MHz, $CDCl_3$, 298 K) δ 9.58 (br s, 1 H, NH), 8.71 (dd, *J* = 4.3, 1.7 Hz, 1 H, HC_{Ar}), 8.62 (dd, *J* = 5.8, 3.2 Hz, 1 H, HC_{Ar}), 8.14 (dd, *J* = 8.3, 1.7 Hz, 1 H, HC_{Ar}), 7.54–7.47 (m, 2 H, 2 × HC_{Ar}), 7.44 (dd, *J* = 8.3, 4.2 Hz, 1 H, HC_{Ar}), 7.42–7.38 (m, 2 H, 2 × HC_{Ar}), 7.12–7.07 (m, 2 H, 2 × HC_{Ar}), 4.45–4.36 (m, 1 H, OC*H*HCHAr), 4.37–4.31 (m, 1 H, OC*H*HCH$_2$), 3.96 (dd, *J* = 11.5, 3.5 Hz, 1 H, OCH*H*CHAr), 3.74 (ddd, *J* = 11.8, 8.8, 3.3 Hz, 1 H, OCH*H*CH$_2$), 3.38 (q, *J* = 4.4 Hz, 1 H, CH(C=O)), 3.18 (dt, *J* = 9.3, 4.6 Hz, 1 H, CHAr), 2.23 (tdd, *J* = 13.2, 8.6, 4.0 Hz, 1 H, OCH$_2$C*H*H), 1.96 (dq, *J* = 13.3, 4.1 Hz, 1 H, OCH$_2$CH*H*); ^{13}C NMR (101 MHz, $CDCl_3$, 298 K) δ 171.2 (C=O amide), 148.1 (C_{Ar}), 138.8 (C_{Ar} quat), 138.3 (C_{Ar} quat), 136.2 (C_{Ar}), 133.9 (C_{Ar} quat), 132.7 (C_{Ar} quat), 130.3 (2 × C_{Ar}), 128.3 (2 × C_{Ar}), 127.8 (C_{Ar} quat), 127.3 (C_{Ar}), 121.6 (2 × C_{Ar}), 116.4 (C_{Ar}), 70.4 (O*C*H$_2$CHAr), 66.2 (O*C*H$_2$CH$_2$), 47.3 (*C*HAr), 42.5 (*C*H(C=O)), 25.2 (OCH$_2$*C*H$_2$); HRMS (ESI) *m/z* Calculated for $C_{21}H_{20}N_2O_2{}^{35}Cl$ [M+H] 367.1213; Found 367.1220.

***cis*-(±)-3-(4-Bromophenyl)-*N*-(quinolin-8-yl)tetrahydro-2H-pyran-4-carboxamide (53e)**



Prepared according to **General Procedure C** using 1-bromo-4-iodobenzene (424 mg). Purification by flash column chromatography (10% Et_2O/CH_2Cl_2) afforded arylated tetrahydropyran **53e** as a yellow amorphous gum (87.6 mg, 0.21 mmol, 43%). R_f 0.38 (10% Et_2O/CH_2Cl_2); IR (film)/cm^{-1} 3343 (NH), 3049, 2952, 2922, 2848, 1677 (C=O), 1521, 1484, 1383, 1323, 1256, 1185, 1126, 1096, 1010, 823, 790, 730, 690; ^{1}H NMR (400 MHz, $CDCl_3$, 298 K) δ 9.58 (br s, 1 H, NH), 8.72 (dd, *J* = 4.2, 1.7 Hz, 1 H, HC_{Ar}), 8.62 (dd, *J* = 5.7, 3.3 Hz, 1 H, HC_{Ar}), 8.15 (dd, *J* = 8.3, 1.7 Hz, 1 H, HC_{Ar}), 7.53–7.48 (m, 2 H, 2 × HC_{Ar}), 7.44 (dd, *J* = 8.3, 4.2 Hz, 1 H, HC_{Ar}), 7.34 (d, *J* = 8.5 Hz, 2 H, 2 × HC_{Ar}), 7.24 (d, *J* = 8.5 Hz, 2 H, 2 × HC_{Ar}), 4.39 (dd, *J* = 11.5, 4.8 Hz, 1 H, OC*H*HCHAr), 4.36–4.30 (m, 1 H, OC*H*HCH$_2$), 3.96 (dd, *J* = 11.5, 3.5 Hz, 1 H, OCH*H*CHAr), 3.74 (ddd, *J* = 11.8, 8.8, 3.3 Hz, 1 H, *OC*H*HC*H$_2$), 3.36 (q, *J* = 4.4 Hz, 1 H, CH(C=O)), 3.18 (dt, *J* = 9.2, 4.6 Hz, 1 H, CHAr), 2.23 (ddt, *J* = 13.3, 9.2, 4.6 Hz, 1 H, OCH$_2$C*H*H), 1.96 (dq, *J* = 13.3, 4.2 Hz, 1H, OCH$_2$CH*H*); ^{13}C NMR (101 MHz, $CDCl_3$, 298 K) δ 171.2 (C=O amide), 148.1 (C_{Ar}), 139.2 (C_{Ar} quat), 138.2 (C_{Ar} quat), 136.2 (C_{Ar}), 133.8 (C_{Ar} quat), 131.2 (2 × C_{Ar}), 130.7 (2 × C_{Ar}), 127.8 (C_{Ar} quat), 127.2 (C_{Ar}), 121.60 (C_{Ar}), 121.57 (C_{Ar}), 120.9 (C_{Ar} quat), 116.4 (C_{Ar}), 70.3 (O*C*H$_2$CHAr), 66.2 (O*C*H$_2$CH$_2$), 47.2 (*C*HAr), 42.5 (*C*H(C=O)), 25.1 (OCH$_2$*C*H$_2$); HRMS (APCI) ***m/z*** Calculated for $C_{21}H_{20}N_2O_2{}^{79}Br^+$ $[M+H]^+$ 411.0703; Found 411.0697.

***cis*-(±)-Ethyl 4-(4-(quinolin-8-ylcarbamoyl)tetrahydro-2H-pyran-3-yl)benzoate (53f)**



Prepared according to **General Procedure C** using ethyl-4-iodobenzoate (413 mg). Purification by flash column chromatography (10% $MeCN/CH_2Cl_2$) afforded an inseparable 8:1 mixture of mono-*cis* arylated tetrahydropyran **53f** and the corresponding di-*cis*-*cis* arylated analogue as a yellow oil (83 mg, 40% combined yield). R_f 0.28 (10% $MeCN/CH_2Cl_2$); IR (film)/cm^{-1} 3347 (br NH), 2956, 2846, 1713 (C=O), 1685 (C=O), 1523, 1485, 1325, 1277, 1183, 1105, 1021, 826, 792, 731;

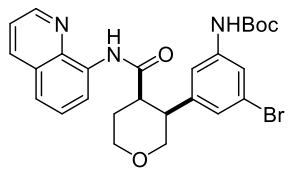
Major mono-cis diastereomer **53f**: ^{1}H NMR (400 MHz, $CDCl_3$, 298 K) δ 9.57 (br s, 1 H, NH), 8.67 (dd, *J* = 4.2, 1.7 Hz, 1 H, HC_{Ar}), 8.61 (dd, *J* = 6.4, 2.6 Hz, 1 H, HC_{Ar}), 8.11 (dd, *J* = 8.2, 1.7 Hz, 1 H, HC_{Ar}), 7.86–7.76 (m, 2 H, 2 × HC_{Ar}), 7.54–7.51 (m, 2 H, 2 × HC_{Ar}), 7.50–7.45 (m, 2 H, 2 × HC_{Ar}), 7.40 (dd, *J* = 8.3, 4.3 Hz, 1 H, HC_{Ar}), 4.45 (dd, *J* = 11.4, 4.8 Hz, 1 H, OC*H*HCHAr), 4.36 (ddd, *J* = 11.5, 5.5, 3.9 Hz, 1 H, OC*H*HCH$_2$), 4.25 (m, 2 H, $CO_2C\mathit{H}_2CH_3$), 3.99 (dd, *J* = 11.5, 3.5 Hz, 1 H, OCH*H*CHAr), 3.76 (ddd, *J* = 11.7, 8.6, 3.3 Hz, 1 H, *OC*H*HC*H$_2$), 3.45 (q, *J* = 4.5 Hz, 1 H, CH(C=O)), 3.22 (dt, *J* = 9.3, 4.6 Hz, 1 H, CHAr), 2.25 (dtd, *J* = 12.9, 8.8, 3.8 Hz, 1 H, OCH$_2$C*H*H), 2.03–1.92 (m, 1 H, OCH$_2$CH*H*), 1.34–1.27 (m, 3 H, $CO_2CH_2C\mathit{H}_3$); ^{13}C NMR (101 MHz, $CDCl_3$, 298 K) δ 171.1 (C=O amide), 166.4 (C=O ester), 148.0 (C_{Ar}), 145.6 (C_{Ar} quat), 138.3 (C_{Ar} quat), 136.2 (C_{Ar}), 133.8 (C_{Ar} quat), 129.8 (C_{Ar} quat), 129.4 (2 × C_{Ar}), 128.9 (2 × C_{Ar}), 127.7 (C_{Ar} quat), 127.2 (C_{Ar}), 121.6 (C_{Ar}), 121.5 (C_{Ar}), 116.4 (C_{Ar}), 70.0 (O*C*H$_2$CHAr), 66.1 (O*C*H$_2$CH$_2$), 60.6 ($CO_2\mathit{C}H_2CH_3$), 47.1 (*C*HAr), 43.1 (*C*H(C=O)), 25.3 (OCH$_2$*C*H$_2$), 14.3 ($CO_2CH_2\mathit{C}H_3$); HRMS (ESI) ***m/z*** Calculated for $C_{24}H_{25}N_2O_4$ $[M+H]$ 405.1814; Found 405.1811.

Cis-cis arylation side-product: ^{1}H NMR (400 MHz, $CDCl_3$, 298 K) δ 8.83 (br s, 1 H, NH), 8.42 (ddq, *J* = 8.8, 4.6, 1.9 Hz, 2 H, 2 × HC_{Ar}), 7.98 (dd, *J* = 8.3, 1.7 Hz, 1 H, HC_{Ar}), 7.93 (t, *J* = 8.3 Hz, 2 H, 2 × HC_{Ar}), 7.26–7.22 (m, 1 H, HC_{Ar}), 4.91 (t, *J* = 11.5 Hz, 2 H, 2 × NC*H*HCHAr), 4.06–4.01 (d, *J* = 4.2 Hz, 2 H, 2 ×

NCH*H*CHAr), 3.59–3.52 (m, 2 H, 2 × CHAr), 3.36 (t, *J* = 4.9 Hz, 1 H, CH(C=O)); ^{13}C NMR (101 MHz, $CDCl_3$, 298 K) δ 169.9 (C=O amide), 166.1 (C=O ester), 147.7 (C_{Ar}), 144.7 (C_{Ar} quat), 137.9 (C_{Ar} quat), 135.8 (C_{Ar}), 133.3 (C_{Ar} quat), 130.0 (C_{Ar} quat), 129.4 (4 × C_{Ar}), 127.8 (4 × C_{Ar}), 126.9 (C_{Ar}), 72.3 (O*C*H_2CHAr), 65.9 (CO_2*C*H_2CH_3), 53.4 (*C*H(C=O)), 45.4 (2 × *C*HAr).

Due to the intrinsically low quantity of the minor trans diastereomer and signal overlap, it was not possible to observe all proton and carbon signals from the minor cis-cis side-product. However, based on previous precedence (see **di-cis-cis 29d) the more shielded amide NH peak at δ = 8.83 ppm (cf 8.90 ppm in **29d**), as well as the CH(C=O) triplet at δ = 3.36 ppm (cf 3.44 ppm in **29d**) are characteristic of a symmetrical arylation product, justifying the assignment.*

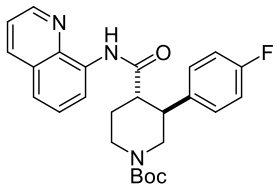
tert-Butyl-_cis_-(±)-(3-bromo-5-4-(quinolin-8-ylcarbamoyl)tetrahydro-2_H_-pyran-3-yl)phenyl) carbamate (53j)



Prepared according to **General Procedure C** using *tert*-butyl (3-bromo-5-iodophenyl)carbamate (597 mg). Purification by flash column chromatography (2% to 15% MeCN/CH_2Cl_2) afforded arylated tetrahydropyran **53j** as a pale yellow crystalline solid (71 mg, 0.13 mmol, 25%). R_f 0.25 (3% MeCN/CH_2Cl_2); mp = 150–153 °C (from Et_2O/pentane); IR (film)/cm^{-1} 3317 (NH br), 2967, 2837, 1722 (C=O), 1677 (C=O), 1599, 1453, 1521, 1424, 1323, 1238, 1156 (C–O), 1092, 828, 790, 690; ^{1}H NMR (400 MHz, $CDCl_3$) δ 9.37 (br s, 1 H, NH amide), 8.65 (dd, *J* = 4.3, 1.6 Hz, 1 H, HC_{Ar}), 8.60 (dd, *J* = 4.9, 4.0 Hz, 1 H, HC_{Ar}), 8.12 (dd, *J* = 8.3, 1.7 Hz, 1 H, HC_{Ar}), 7.53–7.49 (m, 2 H, 2 × HC_{Ar}), 7.42 (dd, *J* = 8.3, 4.2 Hz, 1 H, HC_{Ar}), 7.35 (s, 1 H, HC_{Ar}), 7.10 (t, *J* = 1.8 Hz, 1 H, HC_{Ar}), 7.02 (t, *J* = 1.7 Hz, 1 H, HC_{Ar}), 6.38 (s, 1 H, NHBoc), 4.36 (t, *J* = 13.3 Hz, 1 H, OC*H*HCHAr), 4.04 (td, *J* = 13.4, 4.5 Hz, 1 H, OC*H*HCH_2), 3.78 (dt, *J* = 13.6, 3.5 Hz, 1 H, CHAr), 3.12–2.98 (m, 3 H, OCH*H*CHAr, OCH*H*CH_2, and CH(C=O)), 2.71–2.48 (m, 2 H, OCH_2CH_2), 1.46 (s, 9 H, C(C*H*$_3$)$_3$); ^{13}C NMR (101 MHz, $CDCl_3$) δ 170.4 (C=O amide), 151.9 (C=O carbamate), 148.1 (C_{Ar}), 142.0 (C_{Ar} quat), 140.1 (C_{Ar} quat), 138.1 (C_{Ar} quat), 136.3 (C_{Ar}), 133.2 (C_{Ar} quat), 127.7 (C_{Ar} quat), 127.0 (C_{Ar}), 124.5 (C_{Ar}), 123.2 (C_{Ar} quat), 122.3 (C_{Ar}), 121.7 (C_{Ar}), 120.3 (C_{Ar}), 116.9 (C_{Ar}), 115.4 (C_{Ar}), 81.1 (*C*$(CH_3)_3$), 51.1 (O*C*H_2CHAr), 47.0 (O*C*H_2CH_2), 45.4 (*C*H(C=O)), 43.8 (*C*HAr), 28.2 (C(*C*$H_3)_3$), 27.2 (OCH_2*C*H_2); HRMS (ESI) *m/z* Calculated for $C_{26}H_{29}{}^{79}BrN_3O_4$ [M+H] 526.1341; Found 526.1337.

4.2.6 Diarylation Studies

***tert*-Butyl-*trans*-(±)-3-(4-fluorophenyl)-4-(quinolin-8-ylcarbamoyl)piperidine-1-carboxylate (57)**



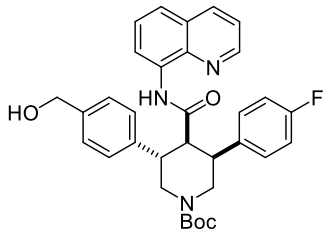
Procedure A: A flame-dried microwave vial was charged with amide **46b** (89 mg, 0.20 mmol, 1.0 equiv). K_2CO_3 (110 mg, 0.40 mmol, 2.0 equiv), pivalic acid (PivOH, 6.2 mg, 0.06 mmol, 0.30 equiv) and $Pd(OAc)_2$ (9.0 mg, 0.04 mmol, 0.1 equiv) were added sequentially. The reaction vessel was sealed and purged with argon, then PhMe (1.34 mL, 0.3 M) was added by syringe. The reaction tube was placed in a preheated oil bath and stirred at 110 °C for 24 h. The reaction mixture was then allowed to cool to rt, diluted with EtOAc (5 mL) and filtered through a pad of Celite, eluting with further EtOAc (2 × 10 mL). The solvent was removed under reduced pressure and the crude material purified by flash column chromatography (10% to 25% acetone/pentane). Et_2O (5 mL), followed by pentane (5 mL) were added to the isolated product, with the resulting suspension concentrated under reduced pressure. This procedure was repeated three times to eliminate residual solvent and afford **57** as a yellow-orange solid (13 mg, 0.03 mmol, 15%). R_f 0.33 (20% acetone/pentane); mp = 134–136 °C (from Et_2O/pentane); IR (film)/cm^{-1} 3342 (NH br), 3041, 2968, 2920, 2853, 1683 (C=O), 1525, 1482, 1420, 1387, 1325, 1234, 1157, 828, 791, 731; ^{1}H NMR (400 MHz, DMSO-d_6, 373 K) δ 9.72 (br s, 1 H, NH), 8.86 (dd, *J* = 4.2, 1.7 Hz, 1 H, HC_{Ar}), 8.41 (dd, *J* = 7.7, 1.4 Hz, 1 H, HC_{Ar}), 8.31 (ddd, *J* = 8.3, 1.7, 0.4 Hz, 1 H, HC_{Ar}), 7.59–7.57 (m, 1 H, HC_{Ar}), 7.57–7.55 (m, 1 H, HC_{Ar}), 7.46 (dd, *J* = 8.2, 7.7 Hz, 1 H, HC_{Ar}), 7.43–7.36 (m, 2 H, 2 × HC_{Ar}), 7.05–6.98 (m, 2 H, 2 × HC_{Ar}), 4.14 (ddt, *J* = 13.3, 4.4, 2.3 Hz, 1 H, NC*H*HCHAr), 4.06–3.98 (m, 1 H, NC*H*HCH_2), 3.32–3.22 (m, 1 H, NCH*H*CHAr), 3.03–2.99 (m, 1 H, NCH*H*CH_2), 2.96–2.93 (m, 2 H, CH(C=O) and CHAr), 2.10–2.01 (m, 1 H, NCH_2C*H*H), 1.74 (tdd, *J* = 12.9, 11.6, 4.5 Hz, 1 H, NCH_2CH*H*), 1.46 (s, 9 H, C(CH_3)$_3$); ^{13}C NMR (101 MHz, DMSO-d_6, 373 K) δ 171.4 (C=O amide), 160.6 (d, J_{CF} = 246.7 Hz, FC_{Ar} quat), 153.5 (C=O carbamate), 148.1 (C_{Ar}), 137.7 (C_{Ar}), 136.8 (d, J_{CF} = 3.4 Hz, F-*p*-C_{Ar} quat), 135.8 (C_{Ar} quat), 133.7 (C_{Ar} quat), 128.9 (d, J_{CF} = 8.1 Hz, 2 × F-*m*-C_{Ar}), 127.2 (C_{Ar} quat), 126.2 (C_{Ar}), 121.4 (C_{Ar}), 121.2 (C_{Ar}), 116.0 (C_{Ar}), 114.5 (d, J_{CF} = 21.0 Hz, 2 × F-*o*-C_{Ar}), 78.5 (*C*$(CH_3)_3$), 49.0 (*C*H(C=O)), 48.9 (N*C*H_2CHAr), 43.7 (CHAr), 42.5 (N*C*H_2CH_2), 28.7 (NCH_2*C*H_2), 27.7 (C(*C*H_3)$_3$); ^{19}F{^{1}H} NMR (376 MHz, DMSO-d_6, 373 K) δ –116.20 (s); HRMS (ESI) *m/z* Calculated for $C_{26}H_{29}N_3O_3F$ [M+H] 450.2193; Found 450.220.

Procedure B: A flame-dried microwave vial was charged with amide **46b** (125 mg, 0.28 mmol, 1.0 equiv) and NaOH (112 mg, 2.80 mmol, 10.0 equiv). The reaction vessel was sealed and purged with Ar, then EtOH (1.2 mL) was added by syringe. The reaction tube was gradually heated to 100 °C in an oil bath, followed by stirring at 100 °C for 30 min. The mixture was then allowed to cool down to rt and evaporated. EtOAc (10 mL) and distilled water (10 mL) were added and the organic phase separated and washed with brine (2 × 5 mL). The organic phase was dried over Na_2SO_4, filtered and concentrated under reduced pressure to afford the *trans*-arylated piperidine **57** as a dark orange solid which did not require further purification (110 mg, 0.25 mmol, 88%). All characterisation information in full agreement with data previously reported in **Procedure A** above.

General Procedure D for Performing a Second Arylation

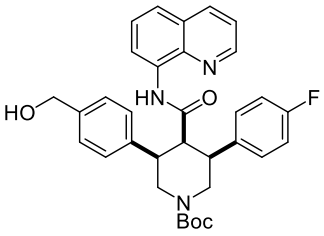
A flame-dried microwave vial was sequentially charged with mono-*cis* arylated amide **46b** or mono-*trans* arylated amide **57** (1.0 equiv), (4-iodophenyl)methanol (2.0 equiv), Ag_2CO_3 (1.25 equiv), MesCOOH (0.3 equiv) and $Pd(OAc)_2$ (0.1 equiv). The reaction vessel was sealed and purged with argon, then $PhCF_3$ (0.3 M) was added by syringe. The reaction tube was placed in a preheated oil bath and stirred at 45 °C for 24 h. The reaction mixture was then allowed to cool to rt, diluted with EtOAc (5 mL) and filtered through a pad of Celite, eluting with further EtOAc (2 × 10 mL). The solvent was removed under reduced pressure and the crude material purified by flash column chromatography (10% to 25% acetone/pentane) to afford the diarylated products from below.

***tert*-Butyl-*trans,cis*-(±)-3-(4-fluorophenyl)-5-(4-(hydroxymethyl)phenyl)-4-(quinolin-8-ylcarbamoyl)piperidine-1-carboxylate (58)**



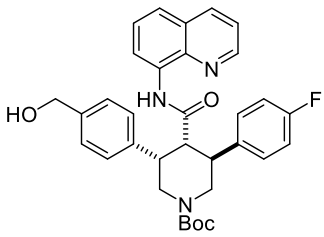
Prepared according to **General Procedure D** using amide **46b** (112 mg, 0.25 mmol), (4-iodophenyl)methanol (117 mg, 0.50 mmol), Ag_2CO_3 (86 mg, 0.27 mmol), MesCOOH (14 mg, 0.07 mmol), $Pd(OAc)_2$ (5.6 mg, 0.03 mmol) and $PhCF_3$ (0.8 mL). **58** was isolated as a yellow powder (27 mg, 0.48 mmol, 19%). R_f 0.21 (20% acetone/pentane); mp = 107–109 °C (from Et_2O/pentane); IR (film)/cm^{-1} 3348 (NH br), 2933, 2974, 1681 (C=O), 1528, 1483, 1423, 1245 (C–O), 1163 (C–O), 910, 828, 731; ^1H NMR (500 MHz, DMSO-d_6, 373 K) δ 9.79 (br s, 1 H, NH), 8.86 (dd, *J* = 4.2, 1.7 Hz, 1 H, HC_{Ar}), 8.33–8.28 (m, 1 H, HC_{Ar}), 8.19 (dd, *J* = 7.7, 1.3 Hz, 1 H, HC_{Ar}), 7.60–7.51 (m, 2 H, 2 × HC_{Ar}), 7.43–7.35 (m, 3 H, 3 × HC_{Ar}), 7.35–7.28 (m, 2 H, 2 × HC_{Ar}), 7.26–7.20 (m, 2 H, 2 × HC_{Ar}), 6.95–6.86 (m, 2 H, 2 × HC_{Ar}), 4.43 (s, 2 H, C*H*$_2$OH), 4.29–4.17 (m, 2 H, NC*H*HCHAr-*p*F and NC*H*HCHAr-*p*CH_2OH), 3.79 (dd, *J* = 10.8, 5.4 Hz, 1 H, CH(C=O)), 3.64–3.56 (m, 2 H, C*H*Ar-*p*F and NCH*H*CHAr-*p*F), 3.50 (ddd, *J* = 10.9, 10.8, 4.7 Hz, 1 H, C*H*Ar-*p*CH_2OH), 3.13 (dd, *J* = 13.1, 10.9 Hz, 1 H, NCH*H*CHAr-*p*CH_2OH), 1.40 (s, 9 H, C(C*H*$_3$)$_3$), 1.19 (s, 1 H, OH); ^{13}C NMR (126 MHz, DMSO-d_6, 373 K) δ 169.5 (C=O amide), 160.6 (d, J_{CF} = 246.7 Hz, FC_{Ar} quat), 153.4 (C=O carbamate), 148.0 (C_{Ar}), 140.5 (C_{Ar} quat), 139.5 (C_{Ar} quat), 137.7 (C_{Ar} quat), 136.7 (d, J_{CF} = 3.4 Hz, F-*p*-C_{Ar} quat), 135.8 (C_{Ar}), 133.7 (C_{Ar} quat), 129.8 (d, J_{CF} = 8.1 Hz, 2 × F-*m*-C_{Ar}), 127.2 (C_{Ar} quat), 126.9 (2 × C_{Ar}), 126.14 (2 × C_{Ar}), 126.09 (C_{Ar}), 121.3 (C_{Ar}), 121.0 (C_{Ar}), 115.8 (C_{Ar}), 113.9 (d, J_{CF} = 21.0 Hz, 2 × F-*o*-C_{Ar}), 78.6 (*C*$(CH_3)_3$), 62.3 (CH_2OH), 51.4 (*C*H(C=O)), 48.3 (N*C*H_2CHAr-*p*F), 46.9 (N*C*H_2CHAr-*p*CH_2OH), 40.6 (*C*HAr-*p*CH_2OH), 38.6 (*C*HAr-*p*F), 27.6 (C(*C*H_3)$_3$); $^{19}F\{^1H\}$ NMR (376 MHz, DMSO-d_6, 373 K) δ –116.73 (s); HRMS (ESI) *m/z* Calculated for $C_{33}H_{35}N_3O_4F$ [M+H] 556.2612; Found 556.2619.

tert-Butyl-_cis,cis_-(±)-3-(4-fluorophenyl)-5-(4-(hydroxymethyl)phenyl)-4-(quinolin-8-ylcarbamoyl)piperidine-1-carboxylate (59)



The above procedure also afforded **59** as a dark yellow gum (21 mg, 0.38 mmol, 15%). R_f 0.29 (20% acetone/pentane); IR (film)/cm^{-1} 3348 (NH br), 2933, 2974, 1681 (C=O), 1528, 1483, 1423, 1245 (C–O), 1163 (C–O), 910, 828, 731; ^{1}H NMR (500 MHz, DMSO-d_6, 373 K) δ 8.94 (br s, 1 H, NH), 8.60 (dd, J = 4.2, 1.7 Hz, 1 H, HC_{Ar}), 8.33 (dd, J = 7.7, 1.4 Hz, 1 H, HC_{Ar}), 8.21 (dd, J = 8.2, 1.7 Hz, 1 H, HC_{Ar}), 7.51 (dd, J = 8.3, 1.3 Hz, 1 H, HC_{Ar}), 7.48–7.42 (m, 2 H, 2 × HC_{Ar}), 7.38–7.32 (m, 2 H, 2 × HC_{Ar}), 7.31–7.25 (m, 2 H, 2 × HC_{Ar}), 7.13–7.08 (m, 2 H, 2 × HC_{Ar}), 6.95–6.85 (m, 2 H, 2 × HC_{Ar}), 4.27 (d, J = 1.0 Hz, 2 H, CH_2OH), 4.11–4.06 (m, 2 H, NCHHCHAr-pCH$_2$OH and NCHHCHAr-pF), 4.03–3.97 (m, 2 H, NCHHCHAr-pCH$_2$OH and NCHHCHAr-pF), 3.55 (t, J = 4.7 Hz, 1 H, CH(C=O)), 3.32 (dt, J = 11.6, 4.7 Hz, 1 H, CHAr-pF), 3.26 (dt, J = 11.1, 5.3 Hz, 1 H, CHAr-pCH$_2$OH), 1.46 (s, 9 H, C(CH_3)$_3$); ^{13}C NMR (126 MHz, DMSO-d_6, 373 K) δ 170.0 (C=O amide), 160.6 (d, J_{CF} = 246.7 Hz, FC_{Ar} quat), 154.0 (C=O carbamate), 147.7 (C_{Ar}), 140.4 (C_{Ar} quat), 138.5 (C_{Ar} quat), 137.2 (C_{Ar} quat), 136.4 (d, J_{CF} = 3.4 Hz, F-p-C_{Ar} quat), 135.5 (C_{Ar}), 133.0 (C_{Ar} quat), 128.5 (d, J_{CF} = 8.1 Hz, 2 × F-m-C_{Ar}), 126.9 (C_{Ar} quat), 126.5 (2 × C_{Ar}), 126.0 (C_{Ar}), 125.9 (2 × C_{Ar}), 121.1 (2 × C_{Ar}), 115.7 (C_{Ar}), 114.3 (d, J_{CF} = 21.0 Hz, 2 × F-o-C_{Ar}), 78.5 (C(CH$_3$)$_3$), 62.2 (CH$_2$OH), 52.5 (CH(C=O)), 43.8 (CHAr-pCH$_2$OH), 43.2 (CHAr-pF), 42.9 (NCH$_2$CHAr-pF), 42.7 (NCH$_2$CHAr-pCH$_2$OH), 27.7 (C(CH$_3$)$_3$); ^{19}F{^{1}H} NMR (376 MHz, DMSO-d_6, 373 K) δ –116.44 (s); HRMS (ESI) ***m/z*** Calculated for $C_{33}H_{35}N_3O_4F$ [M+H] 556.2612; Found 556.2625.

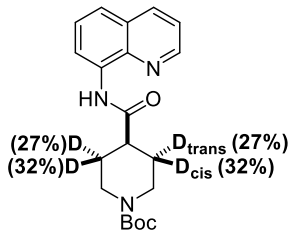
tert-Butyl-_cis,trans_-(±)-3-(4-fluorophenyl)-5-(4-(hydroxymethyl)phenyl)-4-(quinolin-8-ylcarbamoyl)piperidine-1-carboxylate (60)



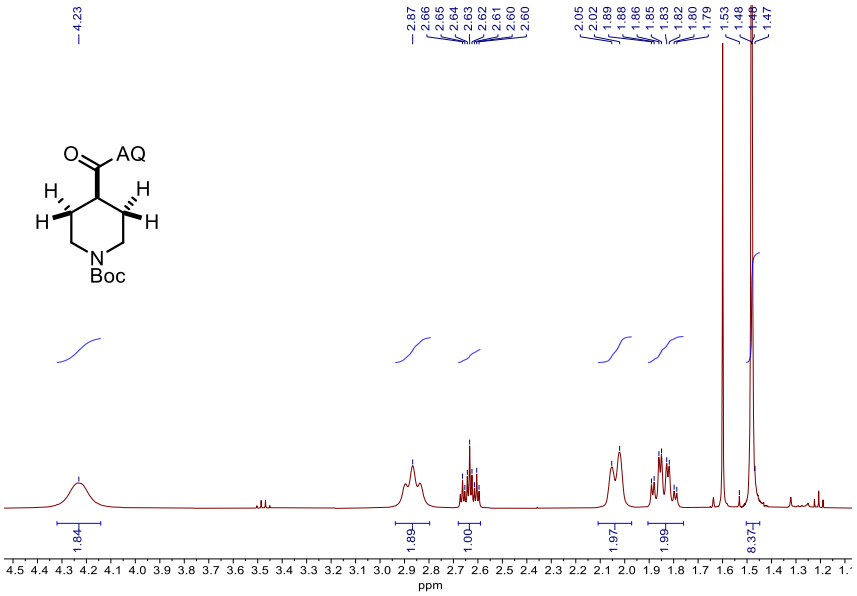
Prepared according to **General Procedure D** using amide **57** (80 mg, 0.17 mmol), (4-iodophenyl)methanol (80 mg, 0.34 mmol), Ag_2CO_3 (58 mg, 0.21 mmol), MesCOOH (8.2 mg, 0.05 mmol), $Pd(OAc)_2$ (3.8 mg, 0.02 mmol) and $PhCF_3$ (0.6 mL). **60** was isolated as an orange gum (32 mg, 0.06 mmol, 34%). R_f 0.24 (20% acetone/pentane); mp = 102–105 °C (from Et_2O/pentane); IR (film)/cm^{-1} 3340 (NH br), 3005, 2974, 2923, 1675 (C=O), 1525, 1483, 1424, 1228, 1158, 908, 828, 730; ^{1}H NMR (500 MHz, DMSO-d_6, 373 K) δ 9.82 (br s, 1 H, NH), 8.86 (dd, J = 4.2, 1.7 Hz, 1 H, HC_{Ar}), 8.33–8.27 (m, 1 H, HC_{Ar}), 8.20 (dd, J = 7.7, 1.3 Hz, 1 H, HC_{Ar}), 7.60–7.52 (m, 2 H, 2 × HC_{Ar}), 7.49–7.44 (m, 2 H, 2 × HC_{Ar}), 7.40 (t, J = 8.0 Hz, 1 H, HC_{Ar}), 7.26–7.20 (m, 2 H, 2 × HC_{Ar}), 7.11–7.03 (m, 4 H, 4 × HC_{Ar}), 4.36 (s, 2 H, CH_2OH), 4.26 (ddd, J = 12.7, 3.5, 1.3 Hz, 1 H, NCHHCHAr-pCH$_2$OH), 4.20 (ddd, J = 13.2, 4.6, 1.3 Hz, 1 H, NCHHCHAr-pCH$_2$OH), 3.79 (dd, J = 10.5, 5.1 Hz, 1 H, CH(C=O)), 3.63–3.56 (m, 2 H, CHAr-pCH$_2$OH and NCHHCHAr-pCH$_2$OH), 3.52 (ddd, J = 10.7, 10.5, 4.6 Hz, 1 H, CHAr-pF), 3.15 (dd, J = 13.1, 10.7 Hz, 1 H, NCHHCHAr-pF), 1.41 (s, 9 H, C(CH_3)$_3$); ^{13}C NMR (126 MHz, DMSO-d_6, 373 K) δ 169.5 (C=O amide), 160.5 (d, J_{CF} = 246.7 Hz, FC_{Ar} quat), 153.4 (C=O carbamate), 148.0 (C_{Ar}), 140.2 (C_{Ar} quat), 138.7 (C_{Ar} quat), 137.7 (C_{Ar} quat), 137.6 (d, J_{CF} = 3.4 Hz, F-p-C_{Ar} quat), 135.7 (C_{Ar}), 133.7 (C_{Ar} quat), 129.0 (d, J_{CF} = 8.1 Hz, 2 × F-m-C_{Ar}), 127.7 (2 × C_{Ar}), 127.2 (C_{Ar} quat), 126.1 (C_{Ar}), 125.5 (2 × C_{Ar}), 121.3 (C_{Ar}), 121.0 (C_{Ar}), 115.9

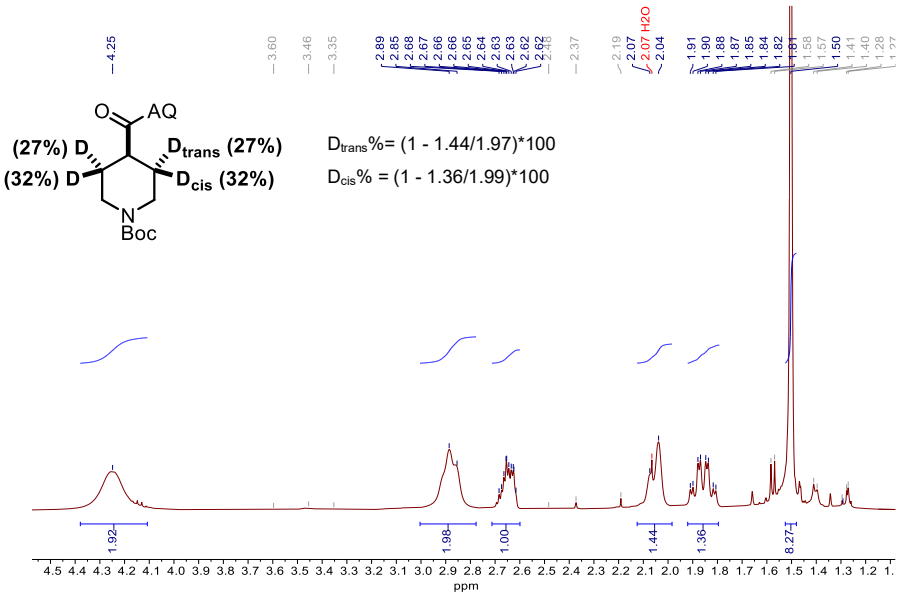
(C_{Ar}), 114.4 (d, J_{CF} = 21.0 Hz, 2 × F-*o*-C_{Ar}), 78.6 ($C(CH_3)_3$), 62.2 (CH_2OH), 51.5 ($CH(C=O)$), 48.1 (NCH_2CHAr-*p*F), 46.8 (NCH_2CHAr-*p*CH_2OH), 41.0 ($CHAr$-*p*CH_2OH), 38.3 ($CHAr$-*p*F), 27.6 ($C(CH_3)_3$); $^{19}F\{^1H\}$ NMR (471 MHz, DMSO-d_6, 373 K) δ –116.52 (s); HRMS (ESI) *m/z* Calculated for $C_{33}H_{35}N_3O_4F$ [M+H] 556.2612; Found 556.2600.

4.2.7 Deuteration Studies



A reaction tube was charged with amide **25** (70 mg, 0.20 mmol, 1.0 equiv), $Pd(OAc)_2$ (4.4 mg, 0.02 mmol, 0.1 equiv), CD_3COOD (0.32 mL, 6.00 mmol, 30.0 equiv) and toluene-d_8 (0.67 mL). The reaction vessel was purged with argon and sealed, then placed in an oil bath (preheated to 45 °C) and stirred for 18 h. The reaction mixture was then diluted with EtOAc (5 mL) and the resulting solution filtered through a pad of Celite, eluting with further EtOAc (2 x 5 mL). The combined organic layers were concentrated under reduced pressure to afford the deuterated product. The deuteration percentages were calculated based on the new relative integration of the *cis*- and *trans*- protons (occurring at 1.85 and 2.04 ppm, respectively) with respect to the α–carbonyl proton (occurring at 2.65 ppm, integral set to 1) in ^{1}H-NMR. Both *cis* and *trans* deuteration (with respect to AQ) occurred at C(3) to similar extents (27%–32%). A control reaction was run following the same procedure in the absence of $Pd(OAc)_2$ – no deuteration occurred in this case.



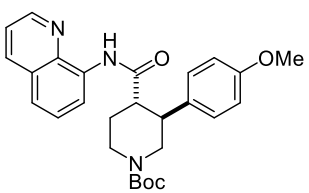


4.2.8 One-Pot Arylation Epimerisation

General Procedure E for One-Pot Arylation Epimerisation

A flame-dried microwave vial (25 mL volume) was charged sequentially with amide **25** (710 mg, 2.00 mmol, 1.0 equiv), the requisite aryl iodide (4.00 mmol, 2.0 equiv), Ag_2CO_3 (690 mg, 2.50 mmol, 1.25 equiv), MesCOOH (99 mg, 0.60 mmol, 0.3 equiv) and $Pd(OAc)_2$ (45.0 mg, 0.20 mmol, 0.1 equiv) in this order. The reaction vessel was sealed and purged with argon, then $PhCF_3$ (6.7 mL, 0.3 M) was added by syringe. The reaction tube was placed in a preheated oil bath and stirred at 45 ºC for 24 h. The reaction mixture was then allowed to cool to rt and 1,8-diazabicyclo[5.4.0]undec-7-ene (DBU, 0.9 mL, 6.00 mmol, 3.0 equiv) was added by syringe. The reaction vessel was then stirred at 110 °C for additional 24 h. The reaction was allowed to cool to rt and EtOAc (20 mL) was added. The resulting mixture was filtered through a pad of Celite, eluting with further EtOAc (2 × 50 mL). The solvent was removed under reduced pressure, and the crude material was purified by flash column chromatography under the specified conditions. Et_2O (5 mL), followed by pentane (5 mL) were added to the isolated product, with the resulting suspension concentrated under reduced pressure. This procedure was repeated three times to eliminate residual solvent and afford desired piperidines.

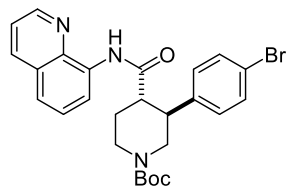
***tert*-Butyl-*trans*-(±)-3-(4-methoxyphenyl)-4-(quinolin-8-ylcarbamoyl)piperidine-1-carboxylate (29b)**



Prepared according to **General Procedure E** using 4-iodoanisole (936 mg).

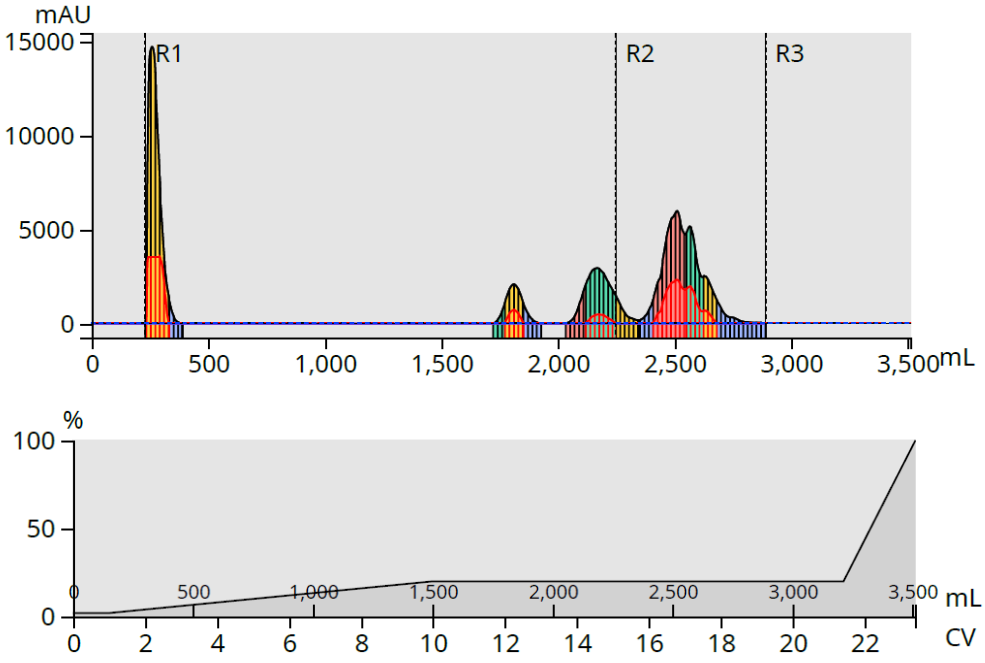
Purification by flash column chromatography (5% to 20% acetone/pentane) afforded a mixture of mono-*trans* arylated piperidine **29b** and di-*cis*-*cis* arylated piperidine **29d**. A second purification by column chromatography (10% Et_2O/CH_2Cl_2) afforded **29b** as a white powder (498 mg, 1.08 mmol, 54%). All characterisation information in agreement with data previously reported for **29b**.

***tert*-Butyl-*trans*-(±)-3-(4-bromophenyl)-4-(quinolin-8-ylcarbamoyl)piperidine-1-carboxylate (61)**



Prepared according to **General Procedure E** using 1-bromo-4-iodobenzene (1.14 g). Purification by automated flash column chromatography (2% to 20% acetone/pentane, see traces below) afforded *trans*-arylated piperidine **61** as a white solid (539 mg, 1.06 mmol, 53%). R_f 0.33 (20% acetone/pentane); mp = 135–138 °C (from Et_2O/pentane); IR (film)/cm^{-1} 3343 (NH br), 3049, 2974, 2930, 2855, 1684 (C=O), 1528 (C=O), 1487, 1424, 1327, 1159, 790, 823, 731; ^{1}H NMR (400 MHz, DMSO-d_6, 373 K) δ 9.73 (br s, 1 H, NH), 8.86 (dd, *J* = 4.2, 1.7 Hz, 1 H, HC_{Ar}), 8.41 (dd, *J* = 7.7, 1.3 Hz, 1 H, HC_{Ar}), 8.34–8.28 (m, 1 H, HC_{Ar}), 7.61–7.55 (m, 2 H, 2 × HC_{Ar}), 7.50–7.43 (m, 1 H, HC_{Ar}), 7.43–7.37 (m, 2 H, 2 × HC_{Ar}), 7.35–7.29 (m, 2 H, 2 × HC_{Ar}), 4.14 (ddt, *J* = 13.2, 4.4, 2.2 Hz, 1 H, NC*H*HCHAr), 4.06–3.98 (m, 1 H, NC*H*HCH$_2$), 3.29 (ddd, *J* = 11.3, 10.0, 2.3 Hz, 1 H, NCH*H*CHAr), 3.03–2.99 (m, 1 H, NCH*H*CH$_2$), 2.97–2.95 (m, 1 H, CH(C=O)), 2.95–2.90 (m, 1 H, CHAr), 2.06 (dq, *J* = 13.2, 3.0 Hz, 1 H, NCH$_2$C*H*H), 1.74 (tdd, *J* = 12.9, 11.6, 4.5 Hz, 1 H, NCH$_2$CH*H*), 1.46 (s, 9 H, C(C*H*$_3$)$_3$); ^{13}C NMR (101 MHz, DMSO-d_6, 373 K) δ 171.3 (C=O amide), 153.5 (C=O carbamate), 148.1 (C_{Ar}), 140.1 (C_{Ar} quat), 137.7 (C_{Ar} quat), 135.8 (C_{Ar}), 133.7 (C_{Ar} quat), 130.8 (2 × C_{Ar}), 129.3 (2 × C_{Ar}), 127.2 (C_{Ar} quat), 126.2 (C_{Ar}), 121.3 (C_{Ar}), 121.2 (C_{Ar}), 119.3 (BrC_{Ar} quat), 116.0 (C_{Ar}), 78.5 (*C*(CH$_3$)$_3$), 48.7 (N*C*H$_2$CHAr), 48.6 (*C*H(C=O)), 43.8 (*C*HAr), 42.5 (N*C*H$_2$CH$_2$), 28.6 (NCH$_2$*C*H$_2$), 27.6 (C(*C*H$_3$)$_3$); HRMS (ESI) *m/z* Calculated for $C_{26}H_{29}{}^{79}BrN_3O_3$ [M+H] 510.1392; Found 510.1412.

Automated Column Conditions: Run on Biotage® Selekt. Column Type: Biotage® Sfär HC 100 g. Flow Rate: 120 mL/min. Sample Mass: 3000 mg. Solvent A: pentane, Solvent B: acetone. UV wavelength detection: λ 200–400 nm. See trace and gradient below. From the left: 1st peak (yellow): unreacted aryl iodide. 2nd peak (yellow): di-arylated side-products. 3rd peak (green): unreacted **46d.** 4th peak: desired *trans*-arylated product **61**.



4.3 Compounds for Chapter 2.2

4.3.1 Aminoquinoline Deprotection on the 2,3-Disubstitution Pattern

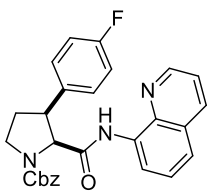
General Procedure F for C(3) Arylation of Pyrrolidines Bearing a C(2) AQ Directing Group

Prepared by adapting a procedure by Bull.[169] A flame-dried microwave vial (25 mL volume) was sequentially charged with the requisite aryl iodide (9.00 mmol, 1.8 equiv), AgOAc (1.50 g, 6.00 mmol, 1.2 equiv), $Pd(OAc)_2$ (56 mg, 0.20 mmol, 0.05 equiv) and *tert*-butyl-2-[(quinolin-8-yl)carbamoyl]pyrrolidine-1-carboxylate (1.88 g, 5.00 mmol, 1.0 equiv) in this order. The reaction vessel was sealed and purged with argon, then placed in a preheated oil bath and stirred at 110 °C for 24 h. The reaction mixture was then allowed to cool to rt and EtOAc (50 mL) was added. The resulting solution was filtered through a pad of Celite, eluting with further EtOAc (2 × 50 mL). The solvent was removed under reduced pressure, and the crude reaction mixture, consisting of an inseparable mixture of 1:1 starting material : product (molar ratio by ^{1}H-NMR spectroscopy) was resubjected to the reaction conditions in a round bottom flask, using the requisite aryl iodide (4.50 mmol, 0.9 equiv), AgOAc (0.75 g, 4.50 mmol, 0.6 equiv) and $Pd(OAc)_2$ (28 mg, 0.13 mmol, 0.03 equiv). After cooling to rt and filtering through Celite using EtOAc (2 x 50 mL) to elute, the reaction mixture was concentrated under reduced pressure. The same reaction was run twice in parallel and the crude mixtures combined before purification. Flash column chromatography of the combined residue under the specified conditions afforded the arylated pyrrolidines from below.

General Procedure G for C(3) Arylation of Piperidines Bearing a C(2) AQ Directing Group

Prepared by adapting a procedure by Bull.[169] A flame-dried microwave vial (25 mL volume) was sequentially charged with benzyl 2-(quinolin-8-ylcarbamoyl)piperidine-1-carboxylate (1.56 g, 4.00 mmol, 1.0 equiv), AgOAc (1.34 g, 8.00 mmol, 2.0 equiv), the requisite aryl iodide (12.00 mmol, 3.0 equiv), $Pd(OAc)_2$ (44.8 mg, 0.20 mmol, 0.05 equiv) and PhMe (1.34 mL) in this order. The reaction vessel was sealed and purged with argon, then placed in a preheated oil bath and stirred at 110 °C for 24 h. The reaction mixture was then allowed to cool to rt and EtOAc (50 mL) was added, before filtering through a pad of Celite, eluting with further EtOAc (2 × 50 mL). The solvent was removed under reduced pressure and the crude reaction mixture was purified by flash column chromatography under the specified conditions to afford the arylated piperidines from below.

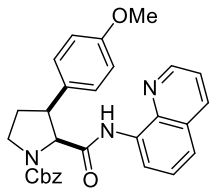
***cis*-(±)-Benzyl-3-(4-fluorophenyl)-2-(quinolin-8-ylcarbamoyl)pyrrolidine-1-carboxylate (67)**



Prepared according to **General Procedure F** using 1-fluoro-4-iodobenzene (1.11 mL, then 0.55 mL). Purification by flash column chromatography (20% to 50% EtOAc/hexane) of the combined residue afforded **67** as a pale yellow solid (3.84 g, 8.80 mmol, 82%).; R_f 0.27 (25% EtOAc/hexane); mp = 148–150 °C; IR (film)/cm^{-1} 3335 (NH br), 2952, 2881, 1690 (C=O), 1604, 1523, 1484, 1407, 1355, 1322, 1222, 1160, 1125, 1101, 990, 826, 791, 735; ^{1}H NMR (400 MHz, $CDCl_3$, mixture of rotamers) δ 9.58 (d, J = 6.8 Hz, 1 H, NH), 8.65 (d, J = 5.3 Hz, 1 H, HC_{Ar}), 8.60–8.47 (m, 1 H, HC_{Ar}), 8.14 (t, J = 8.2 Hz, 1 H, HC_{Ar}), 7.51–7.34 (m, 5 H, 5 × HC_{Ar}), 7.30–7.24 (m, 3 H, 3 × HC_{Ar}), 7.17 (d, J = 7.5 Hz, 1 H, HC_{Ar}), 6.92 (t, J =

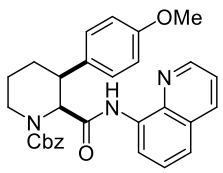
7.5 Hz, 1 H, HC_{Ar}), 6.80 (d, *J* = 8.7 Hz, 2 H, 2 × HC_{Ar}), 5.27–5.09 (m, 2 H, CH_2Ph), 4.75 (d, *J* = 8.4 Hz, 1 H, CH(C=O)), 4.13–4.08 (m, 1 H, NC*H*H), 3.88–3.61 (m, 2 H, NCH*H* and CHAr), 2.77 (q, *J* = 11.7 Hz, 1 H, NCH_2CHH), 2.32–2.22 (m, 1 H, NCH_2CHH); ^{13}C NMR (101 MHz, $CDCl_3$, mixture of rotamers) δ 168.5 (C=O amide), 162.0 (d, J_{CF} = 243.7 Hz, FC_{Ar} quat), 154.5 (C=O carbamate), 148.1 (C_{Ar}), 138.3 (C_{Ar} quat), 136.1 (C_{Ar}), 133.6 (C_{Ar} quat), 132.3 (C_{Ar} quat), 129.6 (d, J_{CF} = 3.0 Hz, F-*p*-C_{Ar} quat), 129.5 (d, J_{CF} = 8.1 Hz, 2 × F-*m*-C_{Ar}), 128.5 (2 × C_{Ar}), 128.0 (C_{Ar} and C_{Ar} quat), 127.7 (2 × C_{Ar}), 127.1 (C_{Ar}), 121.7 (C_{Ar}), 121.5 (C_{Ar}), 116.34 (C_{Ar}), 115.2 (d, J_{CF} = 20.8 Hz, 2 × F-*o*-C_{Ar}), 67.3 (CH_2Ph), 66.3 (*C*H(C=O)), 48.1 and 46.6 (CHAr), 47.2 and 46.3 (NCH_2), 28.8 and 28.1 (NCH_2CH_2); HRMS (ESI) *m/z* Calculated for $C_{28}H_{25}N_3O_3F$ [M+H] 470.1880; Found 470.1863. Characterisation data in agreement with that of a previously isolated sample available in the lab.

cis-(±)-Benzyl-3-(4-methoxyphenyl)-2-(quinolin-8-ylcarbamoyl)pyrrolidine-1-carboxylate (68)



Prepared according to **General Procedure F** using 4-iodoanisole (1.30 g, then 0.75 g). Purification by flash column chromatography (20% to 50% EtOAc/hexane) of the combined residue afforded **68** as an off-white solid (3.50 g, 7.40 mmol, 74%). R_f 0.33 (35% EtOAc/Hexane); mp = 166–167 °C; IR (film)/cm^{-1} 3340 (NH br), 3034, 2952, 2892,1692 (C=O), 1612, 1528, 1489, 1410, 1357, 1325, 1248, 1161, 1035, 982, 825, 795; ^1H NMR (400 MHz, $CDCl_3$, mixture of rotamers) δ 9.52 (br s, 1 H, NH), 8.65 (s, 1 H, HC_{Ar}), 8.53 (d, *J* = 6.2 Hz, 1 H, HC_{Ar}), 8.11 (t, *J* = 10.5 Hz, 1 H, HC_{Ar}), 7.51–7.36 (m, 5 H, 5 × HC_{Ar}), 7.19 (t, *J* = 9.1 Hz, 3 H, 3 × HC_{Ar}), 6.97 (t, *J* = 7.3 Hz, 2 H, 2 × HC_{Ar}), 6.62 (t, *J* = 9.9 Hz, 2 H, 2 × HC_{Ar}), 5.29–5.02 (m, 2 H, CH_2Ph), 4.72 (d, *J* = 8.4 Hz, 1 H, CH(C=O)), 4.13–4.03 (m, 1 H, NC*H*H), 3.82–3.59 (m, 2 H, NCH*H* and CHAr), 3.51 (br s, 3 H, OCH_3) 2.83–2.68 (m, 1 H, NCH_2CHH), 2.28– 2.21 (m, 1 H, NCH_2CHH); ^{13}C NMR (101 MHz, $CDCl_3$, mixture of rotamers) δ 168.8 (C=O amide), 158.7 (C_{Ar} quat), 154.6 (C=O carbamate), 148.0 (C_{Ar}), 138.3 (C_{Ar} quat), 136.8 (C_{Ar} quat), 135.6 (C_{Ar}), 133.8 (C_{Ar} quat), 129.0 (2 × C_{Ar} and C_{Ar} quat), 128.5 (2 × C_{Ar}), 128.1 (C_{Ar} quat), 128.0 (C_{Ar}), 127.6 (2 × C_{Ar}), 127.5 (C_{Ar}), 127.2 (C_{Ar}), 121.4 (C_{Ar}), 116.3 (C_{Ar}), 113.8 (2 × C_{Ar}), 67.1 (CH_2Ph), 66.4 (*C*H(C=O)), 55.0 (OCH_3), 48.2 and 46.7 (CHAr), 47.3 and 46.3 (NCH_2), 28.7 and 28.1 (NCH_2CH_2); HRMS (ESI) *m/z* Calculated for $C_{29}H_{28}N_3O_4$ [M+H] 482.2080; Found 482.2084.

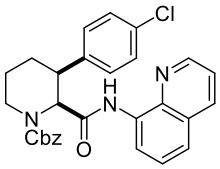
cis-(±)-Benzyl-3-(4-methoxyphenyl)-2-(quinolin-8-ylcarbamoyl)piperidine-1-carboxylate (70)



Prepared according to **General Procedure G** using 4-iodoanisole (1.73 g). Purification by flash column chromatography (15% to 30% EtOAc/hexane) afforded **70** as a white crystalline solid (1.62 g, 3.28 mmol, 82%). R_f 0.17 (20% EtOAc/Hexane); mp = 158–159 °C; IR (film)/cm^{-1} 3330 (br NH), 3034, 2941, 2859, 1684 (C=O), 1521, 1416, 1386, 1323, 1252, 1170, 1036, 970, 827, 790, 731; ^1H NMR (400 MHz, $CDCl_3$, mixture of rotamers) δ 9.40 (br s, 1 H, NH), 8.67–8.50 (m, 2 H, 2 × HC_{Ar}), 8.08 (t, *J* = 9.7 Hz, 1 H, HC_{Ar}), 7.51–7.33 (m, 6 H, 6 × HC_{Ar}), 7.32–7.29 (m, 3 H, 3 × HC_{Ar}), 7.17 (dd, *J* = 6.4, 5.5 Hz, 1 H, HC_{Ar}), 6.71 (d, *J* = 8.1 Hz, 2 H, 2 × HC_{Ar}), 5.27–5.07 (m, 3 H, CH_2Ph and CH(C=O)), 4.34–4.18 (m, 1 H, NC*H*H), 3.79–3.63 (m, 1 H, NCH*H*), 3.57 (s, 3 H, OCH_3), 3.25–3.09 (m, 1 H, CHAr), 2.63–2.46 (m, 1 H, C*H*HCHAr), 2.00–1.89 (m, 2 H, CH*H*CHAr and NCH_2CHH), 1.73 (td, *J* = 12.5, 11.8, 5.9

Hz, 1 H, $NCH_2CH\mathit{H}$); ^{13}C NMR (101 MHz, $CDCl_3$, mixture of rotamers) δ 170.0 (C=O amide), 158.5 (C_{Ar} quat), 154.9 (C=O carbamate), 147.8 (C_{Ar}), 137.1 (C_{Ar} quat), 136.6 (C_{Ar} quat), 136.2 (C_{Ar}), 135.7 (C_{Ar} quat), 133.0 (C_{Ar} quat), 128.9 (2 × C_{Ar} and C_{Ar} quat), 128.5 (2 × C_{Ar}), 127.9 (C_{Ar}), 127.7 (2 × C_{Ar}), 127.0 (C_{Ar}), 121.3 (C_{Ar}), 121.2 (C_{Ar}), 116.3 (C_{Ar}), 114.0 (2 × C_{Ar}), 67.6 (CH_2Ph), 60.7 (*C*H(C=O)), 55.0 (OCH_3), 44.0 (CHAr), 41.4 (NCH_2), 25.6 ($NCH_2\mathit{C}H_2$), 24.2 ($\mathit{C}H_2CHAr$); HRMS (ESI) *m/z* Calculated for $C_{30}H_{30}N_3O_4$ [M+H] 496.2236; Found 496.2221.

cis-(±)-Benzyl-3-(4-chlorophenyl)-2-(quinolin-8-ylcarbamoyl)piperidine-1-carboxylate (71)

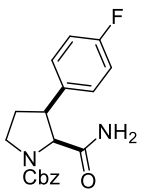


Prepared according to **General Procedure G** using 1-chloro-4-iodobenzene (2.86 g). The reaction was carried out 4 times in parallel, with the crude reaction mixtures combined before purification. Purification by flash column chromatography (15% to 25% EtOAc/hexane) of the combined residue afforded **71** as a yellow crystalline solid (4.66 g, 9.36 mmol, 78%). R_f 0.25 (30% EtOAc/Hexane); mp = 176–178 °C; IR (film)/cm^{-1} 3320 (br NH), 2941, 1687 (C=O), 1525, 1486, 1425, 1346, 1323, 1306, 1257, 1105, 905, 825, 730; ^1H NMR (400 MHz, $CDCl_3$, mixture of rotamers) δ 9.46 (br s, 1 H, NH), 8.72–8.49 (m, 2 H, 2 × HC_{Ar}), 8.10 (ddd, *J* = 11.7, 8.2, 1.7 Hz, 1 H, HC_{Ar}), 7.49–7.45 (m, 2 H, 2 × HC_{Ar}), 7.43–7.35 (m, 4 H, 4 × HC_{Ar}), 7.35–7.27 (m, 3 H, 3 × HC_{Ar}), 7.19–7.15 (m, 3 H, 3 × HC_{Ar}), 5.26 (br s, 2 H, CH_2Ph), 5.23–5.05 (m, 1 H, CH(C=O)), 4.27–4.17 (m, 1 H, NC*H*H), 3.71 (td, *J* = 13.2, 3.4 Hz, 1 H, NCH*H*), 3.25–3.10 (m, 1 H, CHAr), 2.62–2.45 (m, 1 H, C*H*HCHAr), 2.05–1.95 (m, 1 H, $NCH_2C\mathit{H}H$), 1.95–1.83 (m, 1 H, CH*H*CHAr), 1.80–1.64 (m, 1 H, $NCH_2CH\mathit{H}$); ^{13}C NMR (101 MHz, $CDCl_3$, mixture of rotamers) δ 168.4 (C=O amide), 156.5 (C=O carbamate), 148.1 (C_{Ar}), 139.4 (C_{Ar} quat), 138.2 (C_{Ar} quat), 136.5 (C_{Ar} quat), 135.9 (C_{Ar}), 134.0 (C_{Ar} quat), 132.8 (C_{Ar} quat), 129.4 (2 × C_{Ar}), 128.7 (2 × C_{Ar}), 128.5 (2 × C_{Ar}), 128.4 (C_{Ar}), 128.1 (C_{Ar} quat), 128.0 (2 × C_{Ar}), 127.7 (C_{Ar}), 126.9 (C_{Ar}), 121.7 (C_{Ar}), 116.3 (C_{Ar}), 67.7 (*C*H(C=O)), 60.8 and 60.4 (CH_2Ph), 44.3 and 44.1 (CHAr), 41.4 (NCH_2), 25.5 and 25.2 ($NCH_2\mathit{C}H_2$), 24.1 and 24.0 ($\mathit{C}H_2CHAr$); HRMS (ESI) m/z Calculated for $C_{29}H_{27}N_3O_3{}^{35}Cl$ [M+H] 500.1741; Found 500.1727.

General Procedure H for Ozonolysis of AQ to Reveal Free Amides

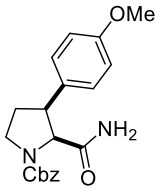
Adapting the literature conditions reported by Maulide,[225] a solution of the C(3) arylated substrate (1.50 mmol, 1.0 equiv) in anhydrous CH_2Cl_2 (15 mL) was cooled to –78 °C and a stream of ozone was passed through until a dark green coloration occurred (approx. 3–4 h). Upon passing a stream of oxygen, decolorisation to pale yellow occurred and the reaction was immediately quenched by addition of dimethylsulfide (DMS, 0.4 mL, 15.00 mmol, 10.0 equiv). The mixture was stirred at rt for 18 h, concentrated under reduced pressure and the residue dissolved in NH_4OH (aq. 28%)/THF (8 mL, 1:1 v/v). After stirring at rt for 20 h, the reaction mixture was diluted with CH_2Cl_2 (15 mL) and washed with sat. aq. NH_4Cl (10 mL). The organic layer was separated and the aqueous layer was extracted with CH_2Cl_2 (3 × 15 mL). The combined organic layers were dried over Na_2SO_4 and the solvent was removed under reduced pressure. The crude material was purified by flash column chromatography under the specified conditions to afford the C(3) amides from below.

***cis*-(±)-Benzyl-2-carbamoyl-3-(4-fluorophenyl)pyrrolidine-1-carboxylate (72)**



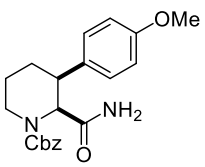
Prepared according to **General Procedure H** using pyrrolidine **67** (705 mg). Purification by flash column chromatography (10% to 40% EtOAc/hexane) afforded amide **72** as a yellow solid (320 mg, 0.90 mmol, 63%). R_f 0.29 (40% EtOAc/hexane); mp = 105–110 °C; IR (film)/cm^{-1} 3332 (br NH), 3194 (br NH), 2952, 2885, 1681 (C=O), 1608, 1513, 1416, 1360, 1226, 1126, 951, 832; ^{1}H NMR (400 MHz, $CDCl_3$, mixture of rotamers) δ 7.38–7.28 (m, 5 H, 5 × HC_{Ar}), 7.27–7.25 (m, 2 H, 2 × HC_{Ar}), 7.05 (dd, *J* = 8.5, 3.1 Hz, 2 H, 2 × HC_{Ar}), 5.57 (br s, 1 H, N*H*H amide), 5.23–5.11 (m, 3 H, NH*H* amide and CH_2Ph), 4.45 (br s, 1 H, CH(C=O)), 3.94 (br t, *J* = 9.7 Hz, 1 H, NC*H*H), 3.71–3.50 (m, 2 H, CHAr and NCH*H*), 2.74 (t, *J* = 13.3 Hz, 1 H, NCH_2CHH), 2.16 (dt, *J* = 11.9, 6.0 Hz, 1 H, NCH_2CHH); ^{13}C NMR (101 MHz, $CDCl_3$) δ 172.0 (C=O amide), 162.1 (d, J_{CF} = 245.8 Hz, FC_{Ar} quat), 154.4 (C=O carbamate), 136.6 (C_{Ar} quat), 132.6 (d, J_{CF} = 3.0 Hz, F-*p*-C_{Ar} quat), 129.7 (d, J_{CF} = 8.1 Hz, 2 × F-*m*-C_{Ar}), 128.5 (2 × C_{Ar}), 128.1 (C_{Ar}), 128.0 (2 × C_{Ar}), 115.5 (d, J_{CF} = 20.0 Hz, 2 × F-*o*-C_{Ar}); 67.3 (CH_2Ph), 64.5 (*C*H(C=O)), 46.5 (CHAr), 46.2 (NCH_2), 28.6 (NCH_2CH_2); ^{19}F{^{1}H} NMR (376 MHz, $CDCl_3$) δ –115.81 (s); HRMS (ESI) ***m/z*** Calculated for $C_{19}H_{20}N_2O_3F$ [M+H] 343.1458; Found 343.1449.

***cis*-(±)-Benzyl-2-carbamoyl-3-(4-methoxyphenyl)pyrrolidine-1-carboxylate (73)**



Prepared according to **General Procedure H** using pyrrolidine **68** (720 mg). Purification by flash column chromatography (10% to 40% EtOAc/hexane) afforded amide **73** as a dense yellow oil (190 mg, 0.50 mmol, 35%). R_f 0.21 (40% EtOAc/Hexane); IR (film/cm^{-1}) 3345 (br NH), 3210 (br NH), 3033, 2958, 2838, 1698 (C=O), 1611, 1518, 1415, 1363, 1250, 1179, 1130, 838, 735; ^{1}H NMR (400 MHz, $CDCl_3$, mixture of rotamers) δ 7.40–7.34 (m, 5 H, 5 × HC_{Ar}), 7.21 (d, *J* = 8.1 Hz, 2 H, 2 × HC_{Ar}), 6.92–6.82 (m, 2 H, 2 × HC_{Ar}), 5.30–5.11 (m, 2 H, CH_2Ph and N*H*H amide), 4.99 (br s, 1 H, NH*H* amide), 4.44–4.30 (m, 1 H, CH(C=O)), 3.92 (br s, 1 H, NC*H*H), 3.79 (s, 3 H, OCH_3), 3.63–3.54 (m, 2 H, CHAr and NCH*H*), 2.65 (br s, 1 H, NCH_2CHH), 2.13 (dt, *J* = 12.4, 6.3 Hz, 1 H, NCH_2CHH); ^{13}C NMR (101 MHz, $CDCl_3$, mixture of rotamers) δ 172.1 (C=O amide), 158.9 (C_{Ar} quat), 155.1 (C=O carbamate), 136.6 (C_{Ar} quat), 129.1 (2 × C_{Ar}), 128.6 (C_{Ar} quat), 128.5 (2 × C_{Ar}), 128.0 (C_{Ar}), 127.9 (2 × C_{Ar}), 113.9 (2 × C_{Ar}), 67.2 (CH_2Ph), 64.7 (*C*H(C=O)), 55.2 (OCH_3), 47.6 and 46.6 (CHAr), 46.2 (NCH_2), 28.6 (NCH_2CH_2); HRMS (ESI) ***m/z*** Calculated for $C_{20}H_{23}N_2O_4$ [M+H] 355.1658; Found 355.1655.

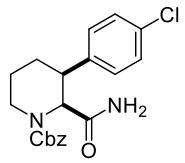
***cis*-(±)-Benzyl-2-carbamoyl-3-(4-methoxyphenyl)piperidine-1-carboxylate (74)**



Prepared according to **General Procedure H** using piperidine **70** (740 mg). Purification by flash column chromatography (10% to 40% EtOAc/hexane) afforded amide **74** as a yellow powder (293 mg, 0.80 mmol, 55%). R_f 0.24 (40% EtOAc/hexane); mp = 145–147 °C; IR (film)/cm^{-1} 3358 (br NH), 3064, 2956, 2836, 1703 (C=O), 1613, 1513, 1416, 1361, 1249, 1185, 1129, 835, 734; ^{1}H NMR (400 MHz, $CDCl_3$, mixture of rotamers) δ 7.53–7.30 (m, 5 H, 5 × HC_{Ar}), 7.31–7.19 (m, 2 H, 2 × HC_{Ar}), 6.97–6.80 (m, 2 H, 2 × HC_{Ar}), 5.40–5.09 (m, 3 H, N*H*H amide and CH_2Ph), 5.09 (br s, 1 H, NH*H* amide), 4.86 (br t, *J* = 5.6, 1 H, CH(C=O)), 4.27–4.06 (m, 1 H, CHAr), 3.81 (s, 3 H, OCH_3), 3.49 (td, *J* = 13.1, 3.3 Hz, 1 H, NC*H*H), 3.02

(ddd, *J* = 13.1, 5.6, 3.5 Hz, 1 H, NCH*H*), 2.57–2.35 (m, 1 H, C*H*HCHAr), 2.05–1.78 (m, 2 H, CH*H*CHAr and NCH_2CHH), 1.63 (tt, *J* = 13.0, 4.3 Hz, 1 H, NCH_2CH*H*); ^{13}C NMR (101 MHz, $CDCl_3$, mixture of rotamers) δ 171.7 (C=O amide), 158.6 (C_{Ar} quat), 156.6 (C=O carbamate), 136.5 (C_{Ar} quat), 133.0 (C_{Ar} quat), 129.1 (2 × C_{Ar}), 128.6 (C_{Ar}), 128.5 (2 × C_{Ar}), 127.9 (2 × C_{Ar}), 113.9 (2 × C_{Ar}), 67.6 (CH_2Ph), 59.4 and 58.6 (*C*H(C=O)), 55.2 (OCH_3), 43.6 and 43.2 (CHAr), 41.1 (NCH_2), 25.5 and 25.2 (*C*H_2CHAr), 24.2 and 23.9 (NCH_2CH_2); HRMS (ESI) *m/z* Calculated for $C_{21}H_{25}N_2O_4$ [M+H] 369.4410; Found 369.4403.

***cis*-(±)-Benzyl-2-carbamoyl-3-(4-chlorophenyl)piperidine-1-carboxylate (75)**

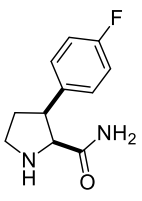


Prepared according to **General Procedure H** using piperidine **71** (750 mg). Purification by flash column chromatography (10% to 30% acetone/pentane) afforded amide **75** as a pale yellow solid (185 mg, 0.50 mmol, 35%). R_f 0.30 (25% acetone/pentane); mp = 120-122 °C; IR (film)/cm^{-1} 3459 (br NH), 3317 (br NH), 2937, 2855, 1674 (C=O), 1602, 1513, 1453, 1360, 1226, 1126, 910, 730; ^1H NMR (400 MHz, $CDCl_3$) δ 7.40–7.31 (m, 5 H, 5 × HC_{Ar}), 7.31–7.22 (m, 4 H, 4 × HC_{Ar}), 5.46 (br s, 1 H, N*H*H amide), 5.33–5.13 (m, 2 H, CH_2Ph), 5.04 (br s, 1 H, NH*H* amide), 4.92–4.71 (m, 1 H, CH(C=O)), 4.25–4.09 (m, 1 H, CHAr), 3.41 (td, *J* = 13.2, 3.2 Hz, 1 H, NC*H*H), 3.00 (ddd, *J* = 13.2, 5.5, 3.5 Hz, 1 H, NCH*H*), 2.60 (qd, *J* = 13.0, 3.7 Hz, 1 H, C*H*HCHAr), 1.91–1.81 (m, 2 H, CH*H*CHAr and NCH_2CHH), 1.64–1.56 (m, 1 H, NCH_2CH*H*); ^{13}C NMR (101 MHz, $CDCl_3$) δ 171.2 (C=O amide), 156.5 (C=O carbamate) 139.5 (C_{Ar} quat), 136.3 (C_{Ar} quat), 132.8 (C_{Ar} quat) 129.6 (2 × C_{Ar}), 128.6 (2 × C_{Ar}), 128.4 (2 × C_{Ar}), 128.2 (C_{Ar}), 127.9 (2 × C_{Ar}), 67.7 (CH_2Ph), 58.0 (*C*H(C=O)), 43.4 (CHAr), 41.0 (NCH_2), 25.3 (*C*H_2CHAr), 23.6 (NCH_2CH_2); HRMS (ESI) *m/z* Calculated for $C_{19}H_{22}{}^{35}ClN_2O$ [M+H-CO_2] 329.1421; Found 329.1426.

General Procedure I for Cbz Deprotection by Hydrogenolysis

Pd/C (10 wt. %) was added to a 5 mL microwave vial containing a solution a solution of the desired Cbz-protected substrate (1.0 equiv) in EtOH (0.2 M). The vial was evacuated and backfilled with Ar three times, followed by evacuation and backfilling with H_2 (balloon). The resulting solution was stirred vigorously at rt for 2 h, then filtered through Celite, washing with EtOH (20 mL). The solvent was removed under reduced pressure to afford the corresponding Cbz deprotected products. In the majority of cases, this gave rise to product of satisfactory purity (>95%), however, flash column chromatography conditions are indicated where further purification has been performed.

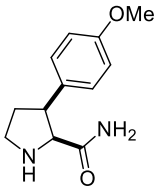
***cis*-(±)-3-(4-Fluorophenyl)pyrrolidine-2-carboxamide (76)**



Prepared according to **General Procedure I** using Pd/C (30 mg) and **72** (110 mg, 0.3 mmol) in EtOH (1.5 mL). Purification by flash column chromatography (0% to 10% MeOH/CH_2Cl_2) afforded **76** as a pale yellow solid (54 mg, 0.26 mmol, 90%). R_f 0.10 (10% MeOH/CH_2Cl_2); mp = 131–134 °C; IR (film)/cm^{-1} 3345 (br NH), 3034, 2960, 1700 (C=O), 1607, 1513, 1416, 1357, 1226, 1130, 909, 834, 737, 730, 700; ^1H NMR (400 MHz, $CDCl_3$) δ 7.23 (dd, *J* = 8.5, 5.4 Hz, 2 H, 2 × HC_{Ar}), 6.98 (t, *J* = 8.5 Hz, 2 H, 2 × HC_{Ar}), 6.62 (br s, 1 H, N*H*H amide), 5.18 (br s, 1 H, NH*H* amide), 3.98 (d, *J* = 8.4 Hz, 1 H, CH(C=O)), 3.64 (ddd, *J* = 8.4, 7.5, 7.4 Hz, 1 H, CHAr), 3.39 (ddd, *J* = 9.7, 7.6, 4.6 Hz, 1 H, NC*H*H), 3.24–3.13 (m, 1 H, NCH*H*), 2.29 (dtd, *J* =

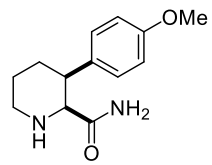
12.6, 7.9, 4.6 Hz, 1 H, NCH_2CHH), 2.07 (dq, *J* = 14.0, 7.3 Hz, 1 H, NCH_2CHH); ^{13}C NMR (101 MHz, $CDCl_3$) δ 175.7 (C=O amide), 164.1 (d, J_{CF} = 242.8 Hz, FC_{Ar} quat), 130.4 (d, J_{CF} = 3.1 Hz, F-*p*-C_{Ar} quat), 128.1 (d, J_{CF} = 8.1 Hz, 2 × F-*m*-C_{Ar}), 115.9 (d, J_{CF} = 20.8 Hz, 2 × F-*o*-C_{Ar}), 64.6 (*C*H(C=O)), 47.7 (CHAr), 43.8 (NCH_2), 32.4 (NCH_2CH_2); $^{19}F\{^1H\}$ NMR (376 MHz, $CDCl_3$) δ –116.53 (s); HRMS (ESI) *m/z* Calculated for $C_{11}H_{14}N_2OF$ [M+H] 209.1090; Found 209.1087.

cis-(±)-3-(4-Methoxyphenyl)pyrrolidine-2-carboxamide (77)



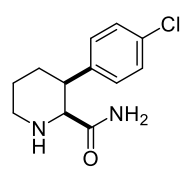
Prepared according to **General Procedure I** using Pd/C (80 mg) and **73** (147 mg, 0.4 mmol) in EtOH (3 mL). Concentration of the filtrate under reduced pressure afforded **77** as a white solid (80 mg, 0.36 mmol, 90%). R_f 0.12 (10% MeOH/CH_2Cl_2); mp = 151–154 °C; IR (film)/cm^{-1} 3425 (br NH), 3325 (br NH), 3183, 2960, 2874, 1670 (C=O), 1513, 1245, 1036, 831; ^1H NMR (400 MHz, $CDCl_3$) δ 7.24–7.15 (m, 2 H, 2 × HC_{Ar}), 6.89–6.79 (m, 2 H, 2 × HC_{Ar}), 6.49 (br s, 1 H, N*H*H amide), 5.03 (br s, 1 H, NH*H* amide), 3.95 (d, *J* = 8.3 Hz, 1 H, CH(C=O)), 3.80 (s, 3 H, OCH_3), 3.62 (dt, *J* = 8.3, 7.7 Hz, 1 H, CHAr), 3.39 (ddd, *J* = 9.7, 7.7, 4.6 Hz, 1 H, NC*H*H), 3.16 (ddd, *J* = 9.7, 8.1, 7.5 Hz, 1 H, NCH*H*), 2.26 (dtd, *J* = 12.6, 7.7, 4.6 Hz, 1 H, NCH_2CHH), 2.08 (dtd, *J* = 12.6, 7.7, 6.6 Hz, 1 H, NCH_2CHH); ^{13}C NMR (101 MHz, $CDCl_3$) δ 175.3 (C=O amide), 158.3 (C_{Ar} quat), 132.9 (C_{Ar} quat), 129.2 (2 × C_{Ar}), 113.5 (2 × C_{Ar}), 66.1 (*C*H(C=O)), 55.2 (OCH_3), 47.2 (CHAr), 46.0 (NCH_2), 32.4 (NCH_2CH_2); HRMS (ESI) *m/z* Calculated for $C_{12}H_{17}N_2O_2$ [M+H] 221.1290; Found 221.1286.

cis-(±)-3-(4-methoxyphenyl)piperidine-2-carboxamide (78)



Prepared according to **General Procedure I** using Pd/C (33 mg) and **74** (130 mg, 0.35 mmol) in EtOH (1.7 mL). Concentration of the filtrate under reduced pressure afforded **78** as a white solid (60 mg, 0.25 mmol, 70%). R_f 0.18 (15% MeOH/CH_2Cl_2); mp = 136–138 °C; IR (film)/cm^{-1} 3459 (br NH), 3317 (br NH), 3198, 1674 (C=O), 1513, 1249, 1182, 1036, 731; ^1H NMR (400 MHz, $CDCl_3$) δ 7.45 (d, *J* = 8.4 Hz, 2 H, 2 × HC_{Ar}), 6.91–6.78 (m, 2 H, 2 × HC_{Ar}), 5.86 (br s, 1 H, N*H*H amide), 5.15 (br s, 1 H, NH*H* amide), 3.80 (s, 3 H, OCH_3), 3.68 (d, *J* = 4.1 Hz, 1 H, CH(C=O)), 3.33–3.24 (m, 2 H, CHAr and NC*H*H), 2.85 (ddd, *J* = 12.8, 9.7, 3.6 Hz, 1 H, NCH*H*), 2.08–1.86 (m, 3 H, CH_2CHAr and NCH_2CHH), 1.53 (dt, *J* = 13.2, 4.5 Hz, 1 H, NCH_2CHH); ^{13}C NMR (101 MHz, $CDCl_3$) δ 175.3 (C=O amide), 158.1 (C_{Ar} quat), 134.3 (C_{Ar} quat), 130.1 (2 × C_{Ar}), 113.6 (2 × C_{Ar}), 63.4 (*C*H(C=O)), 55.2 (OCH_3), 45.6 (CHAr), 41.0 (NCH_2), 29.8 (CH_2CHAr), 22.2 (NCH_2CH_2); HRMS (ESI) *m/z* Calculated for $C_{13}H_{19}N_2O_2$ [M+H] 235.1447; Found 235.1446.

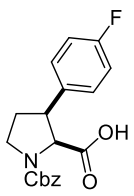
cis-(±)-3-(4-chlorophenyl)piperidine-2-carboxamide (79)



Prepared according to **General Procedure I** using Pd/C (30 mg) and **75** (135 mg, 0.35 mmol) in EtOH (1.5 mL). Purification by flash column chromatography (0% to 10% MeOH/CH_2Cl_2) afforded **79** as a white crystalline solid (73 mg, 0.31 mmol, 75%). R_f 0.10 (10% MeOH/CH_2Cl_2); mp = 131–134 °C; IR (film)/cm^{-1} 3459 (br NH), 3317 (br NH), 3198 (br NH), 2937, 2855, 1674 (C=O), 1602, 1454, 910, 731; ^1H NMR (400 MHz, $CDCl_3$) δ 7.23 (d, *J* = 8.4 Hz, 2 H, 2 × HC_{Ar}), 6.98 (t, *J* = 8.4 Hz, 2 H, 2 × HC_{Ar}), 6.62 (br s, 1 H, N*H*H amide), 5.18 (br

s, 1 H, NH*H* amide), 3.98 (br d, *J* = 8.4 Hz, 1 H, CH(C=O)), 3.64 (dt, *J* = 8.4, 7.5 Hz, 1 H, CHAr), 3.39 (ddd, *J* = 9.7, 7.6, 4.6 Hz, 1 H, NC*H*H), 3.24–3.13 (m, 1 H, NCH*H*), 2.29 (dtd, *J* = 12.6, 7.9, 4.6 Hz, 1 H, NCH_2CHH), 2.07 (dq, *J* = 14.0, 7.3 Hz, 1 H, C*H*HCHAr), 1.98 (br s, 2 H, CH*H*CHAr and NCH_2CHH); ^{13}C NMR (101 MHz, $CDCl_3$) δ 175.2 (C=O amide), 142.3 (C_{Ar} quat), 129.0 (C_{Ar} quat), 128.2 (2 × C_{Ar}), 126.5 (2 × C_{Ar}), 63.3 (*C*H(C=O)), 45.6 (CHAr), 41.8 (NCH_2), 29.6 (*C*H_2CHAr), 22.3 (NCH_2CH_2); HRMS (ESI) *m/z* Calculated for $C_{12}H_{16}{}^{35}ClN_2O$ [M+H] 239.7230; Found 239.7228.

***cis*-(±)-1-((Benzyloxy)carbonyl)-3-(4-fluorophenyl)pyrrolidine-2-carboxylic acid (80)**



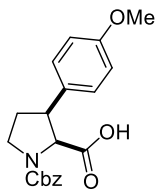
Procedure A, using LiOOH: A microwave vial was charged with amide **72** (471 mg, 1.00 mmol, 1.0 equiv), followed by di-tert-butyl dicarbonate (1.39 g, 5.00 mmol, 5.0 equiv) and 4-DMAP (25.3 mg, 0.20 mmol, 0.2 equiv). The reaction vial was sealed and purged with argon, then MeCN (2 mL) was added by syringe. The reaction tube was then placed in an oil bath and gradually heated to 70 ºC, with stirring at this temperature for 24 h. The reaction mixture was then allowed to cool to rt and sat. sol. NH_4Cl (10 mL) and CH_2Cl_2 (10 mL) were added. The phases were separated and the aqueous layer was extracted with CH_2Cl_2 (3 × 5 mL). The combined organic extracts were dried over Na_2SO_4, filtered and concentrated under reduced pressure. The resulting crude material was filtered through a pad of silica (eluting with 30% EtOAc/hexane) to afford the corresponding Boc-protected amide as a pale orange solid (480 mg), which was carried to the next step without further purification.

A solution of H_2O_2 (30 wt.% in H_2O, 0.3 mL, 3.10 mmol, 4.0 equiv) in THF (0.8 mL) was added to a solution of $LiOH{\cdot}H_2O$ (54.6 mg, 1.30 mmol, 1.6 equiv) in H_2O (1.2 mL) at 0 °C under argon. The resulting mixture was added dropwise to a solution of Boc protected amide obtained in the previous step (440 mg, 0.80 mmol, 1.0 equiv) in THF (2 mL), at 0 °C under argon. The reaction was then stirred at 45 °C for 24 h. Sat. aq. $Na_2S_2O_3$ (5 mL) and EtOAc (10 mL) were added and the reaction mixture was acidified to pH ~ 2 with aq. 1 M HCl. The phases were separated and the aqueous layer was extracted with EtOAc (3 × 10 mL). The combined organic extracts were dried over Na_2SO_4, filtered and the solvent was removed under reduced pressure. Sat. aq. $NaHCO_3$ (approx. 25 mL) was added to the residue and the resulting mixture was washed with EtOAc (2 x 10 mL), discarding the organic layer. The aqueous layer was then acidified to pH ~ 2 with aq. 1 M HCl and extracted with EtOAc (3 x 15 mL). The combined organic extracts were dried over Na_2SO_4, filtered and the solvent removed under reduced pressure to afford acid **80** as a pale yellow solid (212 mg, 0.62 mmol, 62%); R_f 0.18 (20% EtOAc/hexane); mp = 89–91 °C; IR (film/cm^{-1}) 2975 (OH br), 1723 (C=O acid), 1698 (C=O carbamate), 1619, 1516, 1413, 1360, 1245, 1204, 1178, 1112, 1026, 835, 748; ^1H NMR (400 MHz, $CDCl_3$) δ 8.39 (br s, 1 H, COOH), 7.44–7.25 (m, 5 H, 5 × HC_{Ar}), 7.20 (tdd, *J* = 6.6, 5.1, 2.1 Hz, 2 H, 2 × HC_{Ar}), 6.99 (td, *J* = 8.6, 4.2 Hz, 2 H, 2 × HC_{Ar}), 5.24–5.01 (m, 2 H, CH_2Ph), 4.59 (d, *J* = 8.7 Hz, 1 H, CH(C=O)), 3.90 (dd, *J* = 10.4, 8.7 Hz, 1 H, CHAr), 3.70 (tdd, *J* = 13.0, 8.5, 6.1 Hz, 1 H, NC*H*HCH_2), 3.63–3.46 (m, 1 H, NCH*H*CH_2), 2.64–2.41 (m, 1 H, NCH_2CHH), 2.17 (dq, *J* = 12.6, 6.4 Hz, 1 H, NCH_2CHH); ^{13}C NMR (101 MHz, $CDCl_3$, mixture or rotamers) δ 175.5 and 175.1 (COOH), 162.2 (d, J_{CF} = 246.8 Hz, FC_{Ar} quat), 155.0 and 154.2 (C=O carbamate), 136.4 and 136.3 (C_{Ar} quat), 131.7 and 131.6 (d, J_{CF} = 3.3 Hz, F-*p*-C_{Ar} quat), 129.5 and 129.4 (J_{CF} = 7.8 Hz, 2 × F-*m*-C_{Ar}), 128.5 (2 × C_{Ar}), 128.0 (C_{Ar}), 127.6 (2 × C_{Ar}), 115.4 (d, J_{CF} = 20.0 Hz, 2 × F-

o-C_{Ar}), 67.4 and 67.3 (CH_2Ph), 63.8 and 63.5 (*C*H(C=O)), 47.3 (NCH_2), 46.3 and 46.0 (CHAr), 28.5 and 27.5 (*C*H_2CHAr); $^{19}F\{^1H\}$ NMR (376 MHz, $CDCl_3$) δ –114.81 (s); HRMS (ESI) *m/z* Calculated for $C_{19}H_{19}FNO_4$ [M+H] 344.1298; Found 344.1295.

Procedure B, using $NOBF_4$: $NOBF_4$ (51 mg, 0.44 mmol, 2.2 equiv) was added to a solution of free amide **72** (42 mg, 0.20 mmol, 1.0 equiv) in DMF (2 mL) at rt, inducing a colour change from pale yellow to dark green. After stirring at rt for 15 min, the reaction was quenched by dropwise addition of H_2O (1 mL). The reaction mixture was diluted with H_2O (10 mL) and extracted with EtOAc (2 x 10 mL). The combined organics were alternately washed with H_2O (10 mL) and brine (10 mL) twice, then dried over Na_2SO_4 and concentrated under reduced pressure. The residue was purified by flash column chromatography (10 to 30% acetone/pentane) to afford acid **80** as a white powder (46 mg, 0.13 mmol, 67%). All characterisation information in agreement with data previously reported above.

***cis*-(±)-1-((Benzyloxy)carbonyl)-3-(4-methoxyphenyl)pyrrolidine-2-carboxylic acid (84)**

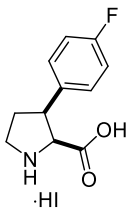


A microwave vial was charged with amide **68** (483 mg, 1.00 mmol, 1.0 equiv), followed by di-tert-butyl dicarbonate (1.39 g, 5.00 mmol, 5.0 equiv) and 4-(dimethylamino)pyridine (DMAP, 25.3 mg, 0.20 mmol, 0.2 equiv). The reaction vial was sealed and purged with argon, then MeCN (2 mL) was added by syringe. The reaction tube was then placed in an oil bath and gradually heated to 70 ºC, with stirring at this temperature for 24 h. The reaction mixture was then allowed to cool to rt and sat. sol. NH_4Cl (10 mL) and CH_2Cl_2 (10 mL) were added. The phases were separated and the aqueous layer was extracted with CH_2Cl_2 (3 × 5 mL). The combined organic extracts were dried over Na_2SO_4, filtered and concentrated under reduced pressure. The resulting crude reaction mixture was filtered through a pad of silica (eluting with 30% EtOAc/hexane) to afford the corresponding Boc-protected amide as a pink crystalline solid (468 mg), which was carried to the next step without further purification.

A solution of H_2O_2 (30 wt.% in H_2O, 0.3 mL, 3.10 mmol, 4.0 equiv) in THF (0.8 mL) was added to a solution of $LiOH{\cdot}H_2O$ (54.6 mg, 1.30 mmol, 1.6 equiv) in H_2O (1.2 mL) at 0 °C. The resulting mixture was added dropwise to a solution of Boc protected amide obtained in the previous step (449 mg, 0.80 mmol, 1.0 equiv) in THF (2 mL), at 0 °C. The reaction was then stirred at 45 °C for 24 h. Sat. aq. $Na_2S_2O_3$ (5 mL) and EtOAc (10 mL) were added and the reaction mixture acidified to pH ~ 2 with aq. 1 M HCl. The phases were separated and the aqueous layer was extracted with EtOAc (3 × 10 mL). The combined organic extracts were dried over Na_2SO_4, filtered and the solvent removed under reduced pressure. Sat. aq. $NaHCO_3$ (approx. 25 mL) was added to the residue and the resulting mixture was washed with EtOAc (2 x 10 mL), discarding the organic layer. The aqueous layer was then acidified to pH ~ 2 with aq. 1 M HCl and extracted with EtOAc (3 x 15 mL). The organics were dried over Na_2SO_4, filtered and the solvent removed under reduced pressure to afford acid **84** as a pale yellow solid (212 mg, 0.60 mmol, 60%); R_f 0.20 (20% EtOAc/Hexane); mp = 110–115 °C; IR (film/cm^{-1}) 2989 (OH br), 1725 (C=O), 1700 (C=O), 1645, 1613, 1518, 1417, 1364, 1247, 1201, 1180, 1117, 1028, 834, 747, 695; ^{1}H-NMR (400 MHz, $CDCl_3$, mixture of rotamers) δ 7.45–7.26 (m, 5 H, 5 × HC_{Ar}), 7.19–7.13 (m, 2 H, 2 × HC_{Ar}), 6.84 (d, *J* = 8.8 Hz, 2 H, 2 × HC_{Ar}), 5.30–5.04 (m, 2 H, CH_2Ph), 4.61 and 4.56 (d, *J* = 8.6 Hz, 1 H, CH(C=O)), 3.93–3.67 (m, 1 H, CHAr), 3.78 (s, 3 H, OCH_3), 3.75–3.61 (m, 1 H, NC*H*H), 3.55 (dt, *J* =

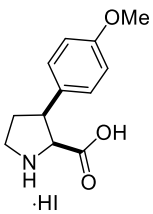
11.2, 8.1 Hz, 1 H, NCH*H*), 2.55 (br q, *J* = 11.6 Hz, 1 H, NCH_2CHH), 2.17 (dq, *J* = 11.6, 5.4 Hz, 1 H, NCH_2CHH); ^{13}C NMR (101 MHz, $CDCl_3$, mixture of rotamers) δ 175.4 and 174.9 (COOH), 159.0 (C_{Ar} quat), 155.0 and 154.2 (C=O carbamate), 136.5 and 136.4 (C_{Ar} quat), 128.9 (C_{Ar} quat), 128.5 (2 × C_{Ar}), 128.1 (2 × C_{Ar}), 128.0 (C_{Ar}), 127.6 (2 × C_{Ar}), 113.9 (2 × C_{Ar}), 67.3 (CH_2Ph), 63.9 and 63.6 (*C*H(C=O)), 55.2 (OCH_3), 47.4 (NCH_2), 46.5 and 46.0 (CHAr), 28.6 and 27.7 (NCH_2CH_2); HRMS (ESI) *m/z* Calculated for $C_{20}H_{22}NO_5$ [M+H] 356.1498; Found 356.1496.

***cis*-(±)-2-Carboxy-3-(4-fluorophenyl)pyrrolidin-1-ium iodide (88)**



Adapting the literature conditions reported by Lyster,[229] TMSI (0.27 mL, 2.00 mmol, 4.0 equiv) was added dropwise over 15 min to a suspension of acid **83** (172 mg, 0.50 mmol, 1.0 equiv) in MeCN (1.8 mL) at –10 °C. The reaction mixture was stirred at –10 °C for 30 min and at –5 °C for a further 1.5 h and then quenched by the addition of MeOH (0.4 mL). The volatiles were removed under reduced pressure. To remove the benzyl iodide by-product, the residue was dissolved in Et_2O (10 mL) and stirred for 10 min, followed by decanting the ethereal layer. This operation was repeated until benzyl iodide was removed (assessed by TLC; R_f of benzyl iodide: 0.90 in 30% EtOAc/hexane). Removal of residual Et_2O solvent under reduced pressure afforded **88** as a dark orange solid (110 mg, 0.30 mmol, 60%, containing 7 mg MeCN (6% by mass) – remaining MeCN could not be removed by available techniques). R_f 0.05 (10% MeOH/CH_2Cl_2); mp = 254–255 °C; IR (film)/cm^{-1} 3377 (br, NH), 2822, 1722 (C=O), 1603, 1450, 1420, 1513, 1371, 1304, 1223, 1107, 839; ^1H NMR (400 MHz, CD_3OD) δ 7.44–7.23 (m, 2 H, 2 × HC_{Ar}), 7.21–7.01 (m, 2 H, 2 × HC_{Ar}), 4.65 (d, *J* = 9.2 Hz, 1 H, CH(C=O)), 4.03 (dt, *J* = 9.2, 8.6 Hz, 1 H, CHAr), 3.76 (ddd, *J* = 11.8, 8.2, 3.8 Hz, 1 H, NC*H*H), 3.48 (ddd, *J* = 11.8, 8.8, 7.4 Hz, 1 H, NCH*H*), 2.57 (dtd, *J* = 13.4, 7.8, 3.8 Hz, 1 H, NCH_2CHH), 2.38 (dtd, *J* = 13.4, 9.3, 8.6 Hz, 1 H, NCH_2CHH); ^{13}C NMR (101 MHz, CD_3OD) δ 168.3 (COOH), 160.3 (d, J_{CF} = 274.1 Hz, FC_{Ar} quat), 133.1 (d, J_{CF} = 3.1 Hz, F-*p*-C_{Ar} quat), 129.8 (d, J_{CF} = 8.1 Hz, 2 × F-*m*-C_{Ar}), 115.1 (d, J_{CF} = 20.8 Hz, 2 × F-*o*-C_{Ar}), 61.6 (*C*H(C=O)), 43.5 (CHAr), 43.3 (NCH_2), 26.9 (NCH_2CH_2); $^{19}F\{^1H\}$ NMR (376 MHz, $CDCl_3$) δ –114.53 (s); HRMS (ESI) *m/z* Calculated for $C_{11}H_{13}FNO_2$ [M+H] 210.0930; Found 210.0925.

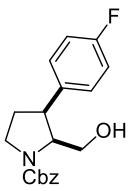
***cis*-(±)-2-Carboxy-3-(4-methoxyphenyl)pyrrolidin-1-ium iodide (89)**



Adapting the literature conditions reported by Lyster,[229] TMSI (0.21 mL, 1.60 mmol, 4.0 equiv) was added dropwise over 15 min to a suspension of acid **84** (137 mg, 0.40 mmol, 1.0 equiv) in MeCN (1.4 mL) at –10 °C. The reaction mixture was stirred at –10 °C for 30 min and at –5 °C for a further 1.5 h and then quenched by the addition of MeOH (0.2 mL). The volatiles were removed under reduced pressure. To remove the benzyl iodide by-product, the residue was dissolved in Et_2O (10 mL) and stirred for 10 min, followed by decanting the ethereal layer. This operation was repeated until benzyl iodide was removed (assessed by TLC; R_f of benzyl iodide: 0.90 in 30% EtOAc/hexane). Removal of residual Et_2O solvent under reduced pressure afforded **89** as an orange crystalline solid (94 mg, 0.28 mmol, 70%). R_f 0.08 (10% MeOH/CH_2Cl_2); mp not observed up to 260 °C; IR (film)/cm^{-1} 3001 (br, OH), 2833, 1610 (C=O), 1513, 1394, 1327, 1249, 1182, 1029, 835; ^1H NMR (400 MHz, CD_3OD) δ 7.23 (d, *J* = 8.8 Hz, 2 H, 2 × HC_{Ar}), 6.89 (d, *J* = 8.8 Hz,

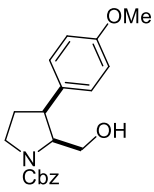
2 H, 2 × HC_{Ar}), 4.64 (d, *J* = 9.1 Hz, 1 H, CH(C=O)), 3.99 (td, *J* = 9.1, 7.8 Hz, 1 H, CHAr), 3.77 (s, 3 H, OCH_3), 3.73 (dt, *J* = 7.9, 4.0 Hz, 1 H, NC*H*HCH_2), 3.50 (ddd, *J* = 11.6, 9.1, 7.9 Hz, 1 H, NCH*H*CH_2), 2.54 (dtd, *J* = 13.3, 7.8, 4.0 Hz, 1 H, NCH_2CHH), 2.42–2.29 (m, 1 H, NCH_2CHH); ^{13}C NMR (101 MHz, CD_3OD) δ 168.5 (COOH), 159.4 (C_{Ar} quat), 129.0 (2 × C_{Ar}), 128.6 (C_{Ar} quat), 113.6 (2 × C_{Ar}), 63.6 (*C*H(C=O)), 54.4 (OCH_3), 45.3 (CHAr), 45.1 (NCH_2), 30.1 (NCH_2CH_2); HRMS (ESI) *m/z* Calculated for $C_{12}H_{16}NO_3$ $[M-I]^+$ 222.1130; Found 222.1125.

***cis*-(±)-Benzyl-3-(4-fluorophenyl)-2-(hydroxymethyl)pyrrolidine-1-carboxylate (90)**



$BH_3{\cdot}SMe_2$ (0.55 mL, 1.10 mmol, 2.2 equiv) was added dropwise to a solution of acid **83** (170 mg, 0.50 mmol, 1.0 equiv) in THF (1.6 mL) at 0 °C. The reaction mixture was stirred at 0 °C for 3 h, then at rt for 18 h. The mixture was then cooled again to 0 °C and quenched by dropwise addition of distilled H_2O (3 mL). After dilution with EtOAc (5 mL), the layers were separated and the organic layer washed with sat. aq. NaCl (10 mL), $NaHCO_3$ (10 mL), H_2O (5 mL) and again with sat. aq. NaCl (5 mL). The organic layer was dried over Na_2SO_4 and concentrated under reduced pressure. The crude product was purified by column chromatography (10% to 35% EtOAc/Hexane) to afford alcohol **90** as a pale yellow oil (113 mg, 0.35 mmol, 70%). R_f 0.66 (35% EtOAc/Hexane); IR (film)/cm^{-1} 3302 (br, OH), 2959, 2835, 1603 (C=O), 1513, 1461, 1409, 1226, 1163, 1059, 839, 805; ^{1}H NMR (400 MHz, DMSO-*d*$_6$) δ 7.42–7.25 (m, 7 H, 7 × HC_{Ar}), 7.12–7.04 (m, 2 H, 2 × HC_{Ar}), 5.19–5.03 (m, 2 H, CH_2Ph), 4.08–3.97 (m, 2 H, CH_2OH), 3.60 (ddd, *J* = 10.5, 9.1, 1.5 Hz, 1 H, C*H*CH_2OH), 3.57–3.43 (m, 2 H, CHAr and NC*H*H), 3.10 (ddd, *J* = 11.3, 5.2, 3.1 Hz, 1 H, NCH*H*), 2.52–2.49 (m, 1 H NCH_2CHH), 2.09–1.99 (m, 1 H, NCH_2CHH); ^{13}C NMR (101 MHz, $CDCl_3$) δ 161.5 (d, J_{CF} = 246.9 Hz, FC_{Ar} quat), 154.8 (C=O carbamate), 136.8 (C_{Ar} quat), 134.4 (d, J_{CF} = 3.0 Hz, F-*p*-C_{Ar} quat), 129.7 (d, J_{CF} = 8.1 Hz, 2 × F-*m*-C_{Ar}), 127.7 (2 × C_{Ar}), 127.0 (C_{Ar}), 126.8 (2 × C_{Ar}), 114.1 (d, J_{CF} = 20.4 Hz, 2 × F-*o*-C_{Ar}), 65.3 (CH_2Ph), 61.4 (*C*HCH_2OH), 59.1 (CH_2OH), 45.2 (NCH_2), 30.0 (CHAr), 27.5 (NCH_2CH_2); ^{19}F{^{1}H} NMR (376 MHz, $CDCl_3$) δ –117.29 (s); HRMS (ESI) *m/z* Calculated for $C_{19}H_{21}FNO_3$ [M+H] 330.1505; Found 330.1501.

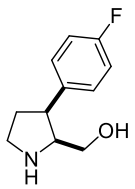
***cis*-(±)-Benzyl-2-(hydroxymethyl)-3-(4-methoxyphenyl)pyrrolidine-1-carboxylate (91)**



$BH_3{\cdot}SMe_2$ (0.6 mL, 1.20 mmol, 2.2 equiv) was added dropwise to a solution of acid **84** (200 mg, 0.56 mmol, 1.0 equiv) in THF (1.7 mL) at 0 °C. The reaction mixture was stirred at 0 °C for 3 h, then at rt for 18 h. The mixture was then cooled again to 0 °C and quenched by dropwise addition of distilled H_2O (3 mL). After dilution with EtOAc (5 mL), the layers were separated and the organic layer washed with sat. aq. NaCl (10 mL), $NaHCO_3$ (10 mL), H_2O (5 mL) and again sat. aq. NaCl (5 mL). The organic layer was dried over Na_2SO_4 and concentrated under reduced pressure. The crude product was purified by column chromatography (10% to 35% EtOAc/hexane) to afford alcohol **91** as a yellow oil (117 mg, 0.34 mmol, 60%). R_f 0.59 (35% EtOAc/hexane); IR (film)/cm^{-1} 3324 (br, OH), 2937, 2837, 1610 (C=O), 1513, 1461, 1409, 1249, 1182, 1036, 835; ^{1}H NMR (400 MHz, $CDCl_3$) δ 7.42–7.36 (m, 5 H, 5 × HC_{Ar}), 7.21 (d, *J* = 8.1 Hz, 2 H, 2 × HC_{Ar}), 6.90 (d, *J* = 8.1 Hz, 2 H, 2 × HC_{Ar}), 5.30–5.11 (m, 2 H, CH_2Ph), 4.30 (t, *J* = 4.0 Hz, 1 H, CH_2OH), 3.82 (s, 3 H, OCH_3), 3.77–3.72 (m, 1 H, C*H*HOH), 3.60–3.50 (m, 2 H, NC*H*H and C*H*CH_2OH), 3.46–3.35

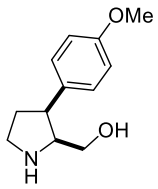
(m, 2 H, CHAr and NCH*H*), 3.27 (t, *J* = 5.5 Hz, 1 H, CH*H*OH), 2.47–2.32 (m, 1 H, NCH_2CHH), 2.16 (dt, *J* = 12.6, 6.5 Hz, 1 H, NCH_2CHH); ^{13}C NMR (101 MHz, $CDCl_3$) δ 158.7 (C_{Ar} quat), 157.5 (C=O carbamate), 136.5 (C_{Ar} quat), 128.9 (2 × C_{Ar}), 128.7 (C_{Ar} quat), 128.6 (2 × C_{Ar}), 128.1 (2 × C_{Ar}), 128.0 (C_{Ar}), 114.1 (2 × C_{Ar}), 67.3 (CH_2Ph), 64.0 ($CHCH_2OH$), 63.1 (CH_2OH), 55.3 (OCH_3), 46.1 (NCH_2), 45.4 (CHAr), 28.4 (NCH_2CH_2); HRMS (ESI) *m/z* Calculated for $C_{20}H_{24}NO_4$ [M+H] 342.1705; Found 342.1699.

cis-(±)-3-(4-Fluorophenyl)pyrrolidin-2-yl)methanol (92)



Prepared according to **General Procedure I** using Pd/C (80 mg) and **90** (113 mg, 0.40 mmol, 1.0 equiv) in EtOH (3 mL). Concentration of the filtrate under reduced pressure afforded **92** as a dense dark yellow oil (67 mg, 0.34 mmol, 85%). R_f 0.12 (10% $MeOH/CH_2Cl_2$); IR (film)/cm^{-1} 3425 (OH br), 2969, 2834, 1513, 1409, 1226, 1163, 1059, 839; ^1H NMR (400 MHz, $CDCl_3$) δ 7.23–7.15 (m, 2 H, 2 × HC_{Ar}), 7.04–6.96 (m, 2 H, 2 × HC_{Ar}), 4.13 (br s, 1 H, NH), 3.52 (td, *J* = 7.9, 4.0 Hz, 1 H, C*H*HOH), 3.41 (dt, *J* = 9.7, 7.9 Hz, 1 H, CH*H*OH), 3.27 (ddd, *J* = 11.0, 7.9, 4.0 Hz, 1 H, C*H*CH_2OH), 3.19–3.08 (m, 2 H, NC*H*HCH_2 and CHAr), 3.02 (td, *J* = 11.1, 8.6 Hz, 1 H, NCH*H*CH_2), 2.25–2.07 (m, 2 H, NCH_2CH_2); ^{13}C NMR (101 MHz, $CDCl_3$) δ 161.8 (d, *J* = 266.8 Hz, FC_{Ar} quat), 134.3 (d, J_{CF} = 3.2 Hz, F-*p*-C_{Ar} quat), 129.6 (d, J_{CF} = 7.8 Hz, 2 × F-*m*-C_{Ar}), 115.3 (d, J_{CF} = 21.5 Hz, 2 × F-*o*-C_{Ar}), 62.6 (CH_2OH), 61.0 ($CHCH_2OH$), 45.8 (NCH_2), 44.9 (CHAr), 30.3 (NCH_2CH_2); $^{19}F\{^1H\}$ NMR (376 MHz, $CDCl_3$) δ –118.67 (s); HRMS (ESI) *m/z* Calculated for $C_{11}H_{15}NOF$ [M+H] 196.1138; Found 196.1140.

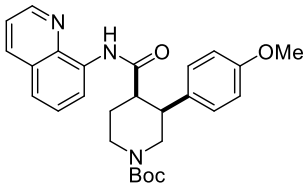
cis-(±)-3-(4-Methoxyphenyl)pyrrolidin-2-yl)methanol (93)



Prepared according to **General Procedure I** using Pd/C (80 mg) and **91** (117 mg, 0.30 mmol, 1.0 equiv) in EtOH (3 mL). Concentration of the filtrate under reduced pressure afforded **93** as a white foam (64 mg, 0.31 mmol, 91%); R_f 0.11 (10% $MeOH/CH_2Cl_2$); mp = 75–80 °C; IR (film)/cm^{-1} 3424 (br OH), 2937, 2837, 1513, 1409, 1249, 1182, 1036, 835; ^1H NMR (400 MHz, $CDCl_3$) δ 7.21–7.15 (m, 2 H, 2 × HC_{Ar}), 6.93–6.81 (m, 2 H, 2 × HC_{Ar}), 3.82 (s, 3 H, OCH_3), 3.51 (td, *J* = 7.8, 4.8 Hz, 1 H, C*H*HOH), 3.40 (dt, *J* = 10.0, 7.8 Hz, 1 H, CH*H*OH), 3.24 (ddd, *J* = 11.0, 7.8, 3.3 Hz, 1 H, C*H*CH_2OH), 3.18–3.10 (m, 2 H, NC*H*HCH_2 and CHAr), 3.04 (dd, *J* = 10.9, 8.5 Hz, 1 H, NCH*H*CH_2), 2.25–2.05 (m, 2 H, NCH_2CH_2); ^{13}C NMR (101 MHz, $CDCl_3$) δ 154.3 (C_{Ar} quat), 127.6 (C_{Ar} quat), 125.1 (2 × C_{Ar}), 109.8 (2 × C_{Ar}), 58.4 (CH_2OH), 57.8 ($CHCH_2OH$), 51.3 (OCH_3), 42.3 (NCH_2), 41.3 (CHAr), 26.6 (NCH_2CH_2); HRMS (ESI) *m/z* Calculated for $C_{12}H_{18}NO_2$ [M+H] 208.2810; Found 208.2806.

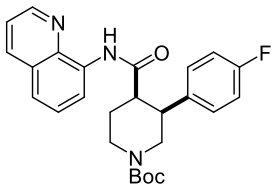
4.3.2 Aminoquinoline Deprotection on the 4,3-Disubstitution Pattern

***tert*-Butyl-*cis*-(±)-3-(4-methoxyphenyl)-4-(quinolin-8-ylcarbamoyl)piperidine-1-carboxylate (29a)**



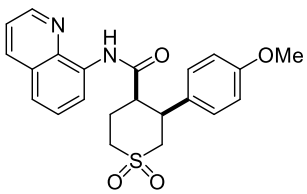
See Section 4.24 Gram-Scale Arylation of Piperidine Amide 29a

***tert*-Butyl-*cis*-(±)-3-(4-fluorophenyl)-4-(quinolin-8-ylcarbamoyl)piperidine-1-carboxylate (46b)**



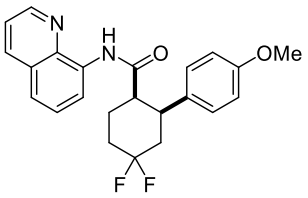
A flask was charged with amide **25** (1.42 g, 4.00 mmol, 1.0 equiv),1-fluoro-4-iodobenzene (1.78 g, 8.00 mmol, 2.0 equiv), Ag_2CO_3 (1.38 g, 5.00 mmol, 1.25 equiv), 2,4,6-trimethylbenzoic acid (MesCOOH, 197 mg, 1.2 mmol, 0.3 equiv) and $Pd(OAc)_2$ (90 mg, 0.4 mmol, 0.1 equiv) in this order. The reaction vessel was covered with a suba seal and purged with argon, then $PhCF_3$ (13.4 mL, 0.3 M) was added by syringe. The flask was placed in a preheated oil bath and stirred at 45 ºC for 18 h under an atmosphere of argon. The mixture was then allowed to cool to rt and EtOAc (20 mL) was added before filtering through a pad of Celite, eluting with further EtOAc (2 × 50 mL). The solvent was removed under reduced pressure and the residue purified by sequential flash column chromatography (5% to 8% Et_2O/CH_2Cl_2, followed by 20% acetone/pentane). The product containing fractions were combined and the solvent was removed under reduced pressure. Et_2O (5 mL) and pentane (10 mL) were added and the solvent was removed under reduced pressure to afford arylated piperidine **46b** as a yellow foamy solid (980 mg, 2.18 mmol, 56%). All characterisation information in agreement with data previously reported for **46b**.

***cis*-(±)-3-(4-Methoxyphenyl)-*N*-(quinolin-8-yl)tetrahydro-2H-thiopyran-4-carboxamide 1,1-dioxide (54)**



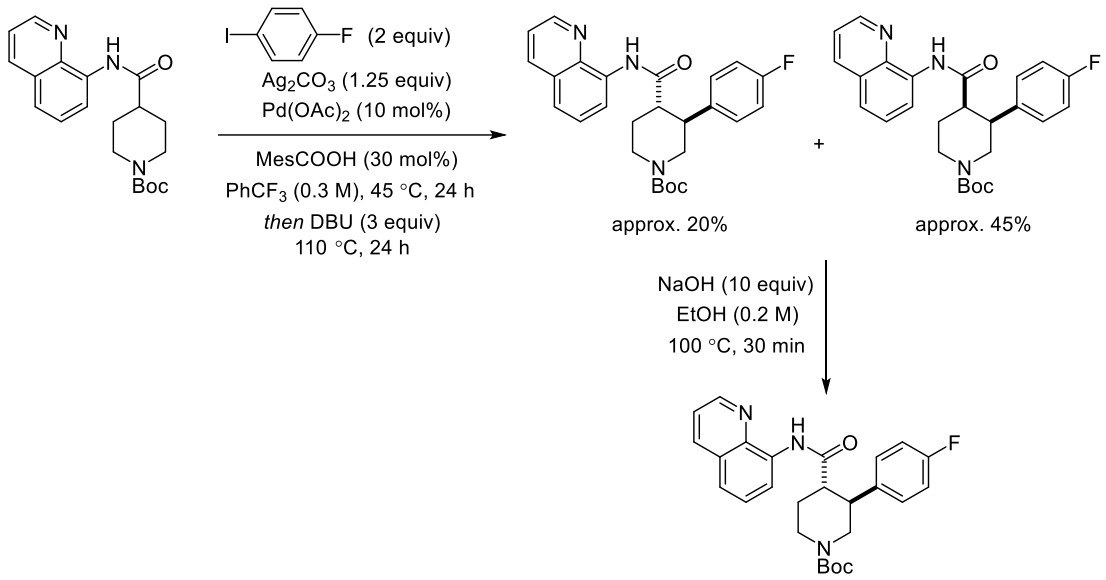
A flask was charged with amide **50** (1.21 g, 4.00 mmol, 1.0 equiv), 4-iodoanisole (2.80 g, 12.00 mmol, 3.0 equiv), Ag_2CO_3 (2.2 g, 8.00 mmol, 2.0 equiv), MesCOOH (197 mg, 1.20 mmol, 0.3 equiv) and $Pd(OAc)_2$ (90 mg, 0.40 mmol, 0.1 equiv) in this order. The reaction vessel was covered with a suba seal and purged with argon, then $PhCF_3$ (13.34 mL, 0.3 M) was added by syringe. The flask was placed in a preheated oil bath and stirred at 75 °C for 24 h. The mixture was then allowed to cool to rt and diluted with EtOAc (10 mL) before filtering through a pad of Celite, eluting with further EtOAc (2 × 15 mL). The solvent was removed under reduced pressure and the crude material purified by flash column chromatography (40% to 60% acetone/pentane). Et_2O (5 mL), followed by pentane (5 mL) were added to the isolated product, with the resulting suspension concentrated under reduced pressure. This procedure was repeated three times to eliminate residual solvent and afford **54** as a pale pink crystalline solid (409 mg, 1.00 mmol, 25%). All characterisation information in agreement with data previously reported for **54**.

cis-(±)-4,4-Difluoro-2-(4-methoxyphenyl)-_N_-(quinolin-8-yl)cyclohexane-1-carboxamide (55)



A flask was charged with amide **51** (1.16 g, 4.00 mmol, 1.0 equiv), 4-iodoanisole (1.87 g, 8.00 mmol, 2.0 equiv), Ag_2CO_3 (1.38 g, 5.00 mmol, 1.25 equiv), MesCOOH (197 mg, 1.20 mmol, 0.3 equiv) and $Pd(OAc)_2$ (90 mg, 0.40 mmol, 0.1 equiv) in this order. The reaction vessel was covered with a suba seal and purged with argon, then $PhCF_3$ (13.4 mL) was added by syringe. The flask was placed in a preheated oil bath and stirred at 45 °C for 24 h. The mixture was then allowed to cool to rt and diluted with EtOAc (5 mL) before filtering through a pad of Celite, eluting with further EtOAc (2 × 10 mL). The solvent was removed under reduced pressure and the crude material was purified by flash column chromatography (20% EtOAc/pentane) to afford **55** as an off-white solid (906 mg, 2.29 mmol, 57%). All characterisation information in agreement with data previously reported for **55**.

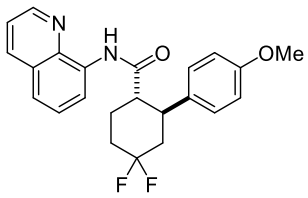
***tert*-Butyl-*trans*-(±)-3-(4-fluorophenyl)-4-(quinolin-8-ylcarbamoyl)piperidine-1-carboxylate (57)**



A flame-dried microwave vial (25 mL) was charged sequentially with amide **25** (1.42 g, 4.00 mmol, 1.0 equiv), 4-fluoroiodobenzene (1.77 g, 8.00 mmol, 2.0 equiv), Ag_2CO_3 (1.38 g, 5.00 mmol, 1.25 equiv), MesCOOH (197 mg, 1.20 mmol, 0.3 equiv) and $Pd(OAc)_2$ (90 mg, 0.40 mmol, 0.1 equiv) in this order. The reaction vessel was sealed and purged with argon, then $PhCF_3$ (13.4 mL) was added by syringe. The reaction tube was placed in a preheated oil bath and stirred at 45 ºC for 24 h. The reaction mixture was then allowed to cool to rt and 1,8-diazabicyclo[5.4.0]undec-7-ene (DBU, 1.8 mL, 12.00 mmol, 3.0 equiv) was added by syringe. The reaction was stirred at 110 °C for additional 24 h before cooling to rt and diluting with EtOAc (20 mL). The resulting mixture was filtered through a pad of Celite, eluting with further EtOAc (2 × 50 mL), and the solvent removed under reduced pressure. The residue was purified by flash column chromatography (5% to 10% Et_2O/CH_2Cl_2) to afford a mixture of mono-*trans* and mono-*cis* arylated piperidines (1.16 g, combined yield 65%, d.r. 7:3 *cis*:*trans*) which was subjected to NaOH-mediated epimerisation to promote full conversion of the remaining mono-*cis* isomer to mono-*trans*.

NaOH (480 mg, 12.00 mmol, 10.0 equiv) was added to the mixture of *cis* and *trans*-arylated piperidines from above. The reaction vessel was sealed and purged with argon, then EtOH (18 mL) was added by syringe. The reaction tube was gradually heated to 100 °C in an oil bath, followed by stirring at 100 °C for 30 min. The mixture was then allowed to cool down to rt and the solvent evaporated. EtOAc (10 mL) and distilled water (10 mL) were added and the organic phase separated and washed with brine (2 × 5 mL). The organic phase was dried over Na_2SO_4, filtered and concentrated under reduced pressure to afford *trans*-arylated piperidine **57** as an orange solid which did not require further purification (1.03 g, 2.28 mmol, 57% from **25**). All characterisation information in full agreement with data previously reported for **57**.

***trans*-(±)-4,4-Difluoro-2-(4-methoxyphenyl)-N-(quinolin-8-yl)cyclohexane-1-carboxamide (94)**



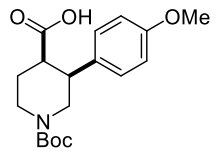
A reaction tube was charged with *cis*-arylated **55** (435 mg, 1.50 mmol, 1.0 equiv) and NaOH (600 mg, 15.00 mmol, 10.0 equiv). The reaction vessel was sealed and purged with argon, then EtOH (7.5 mL) was added by syringe. The reaction tube was gradually heated to 100 °C in an oil bath, followed by stirring at 100 °C for 30 min. The mixture was then allowed to cool down to rt and the solvent evaporated. EtOAc (10 mL) and distilled water (10 mL) were added and the organic phase separated and washed with brine (2 × 5 mL). The organic phase was dried over Na_2SO_4, filtered and concentrated under reduced pressure to afford the *trans*-arylated piperidine **94** as a yellow solid which did not require further purification (360 mg, 0.84 mmol, 84%). R_f 0.45 (20% acetone/pentane); mp = 153–154 °C (from acetone/pentane); IR (film)/cm^{-1} 3347 (NH br), 2937, 1685 (C=O), 1521, 1372, 1252, 1163, 1096, 969, 828; ^{1}H NMR (400 MHz, $CDCl_3$) δ 9.49 (s, 1 H, NH), 8.74 (dd, *J* = 4.2, 1.7 Hz, 1 H, HC_{Ar}), 8.60 (dd, *J* = 5.3, 3.7 Hz, 1 H, HC_{Ar}), 8.11 (dd, *J* = 8.3, 1.7 Hz, 1 H, HC_{Ar}), 7.48–7.37 (m, 3 H, 3 × HC_{Ar}), 7.24–7.13 (m, 2 H, 2 × HC_{Ar}), 6.81–6.67 (m, 2 H, 2 × HC_{Ar}), 3.60 (s, 3 H, OCH_3), 3.34 (ddd, *J* = 13.1, 11.3, 4.0 Hz, 1 H, CHAr), 2.69 (ddd, *J* = 10.6, 7.8, 5.9 Hz, 1 H, CH(C=O)), 2.45–2.31 (m, 2 H, F_2CC*H*HCHAr and F_2CC*H*HCH_2), 2.28–2.17 (m, 2 H, F_2CCH*H*CHAr and F_2CCH*H*CH_2), 2.17–1.86 (m, 2 H, F_2CCH_2C*H*$_2$); ^{13}C NMR (101 MHz, $CDCl_3$) δ 171.7 (C=O amide), 158.4 (C_{Ar} quat), 147.9 (C_{Ar}), 138.1 (C_{Ar} quat), 136.2 (C_{Ar}), 134.0 (C_{Ar} quat), 133.6 (C_{Ar} quat), 128.1 (2 × C_{Ar}), 127.7 (C_{Ar} quat), 127.2 (C_{Ar}), 122.6 (dd, J_{CF} = 243.8, 240.8 Hz, CF_2), 121.5 (C_{Ar}), 116.4 (C_{Ar}), 114.1 (2 × C_{Ar}), 55.0 (OCH_3), 52.3 (*C*H(C=O)), 42.7 (d, J_{CF} = 10.0 Hz, CHAr), 40.8 (t, J_{CF} = 24.0 Hz, F_2CCH_2CHAr), 32.9 (t, J_{CF} = 24.1 Hz, $F_2CCH_2CH_2$), 26.7 (d, J_{CF} = 10.6 Hz, $F_2CCH_2CH_2$); ^{19}F{^{1}H} NMR (376 MHz, $CDCl_3$) δ –90.49 (d, J_{FF} = 238.6 Hz), –101.24 (d, J_{FF} = 238.7 Hz); HRMS (ESI) *m/z* Calculated for $C_{23}H_{23}N_2O_2F_2$ [M+H] 397.1728; Found 397.1721.

General Procedure J for Aminoquinoline Deprotection to Carboxylic Acids

A flame-dried microwave vial (25 mL) was charged with the requisite C(3)-arylated piperidine (1.0 equiv), di-*tert*-butyl dicarbonate (Boc_2O, 5.0 equiv) and 4-(dimethylamino)pyridine (DMAP, 0.2 equiv). The reaction vessel was sealed and purged with argon, then MeCN (0.5 M) was added by syringe. The vial was placed in an oil bath and gradually warmed up to 70 ºC, then stirred for 3 h at 70 °C. The mixture was allowed to cool down and sat. aq. NH_4Cl (10 mL) and CH_2Cl_2 (15 mL) were added. The phases were separated, and the aqueous layer was extracted with CH_2Cl_2 (3 × 10 mL). The combined organic

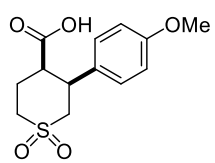
extracts were dried over Na_2SO_4 and filtered and the solvent was removed under reduced pressure to afford the crude *N*-Boc protected amide derivative, which was carried forward to the hydrolysis step without further purification. A solution of H_2O_2 (30 wt.% in H_2O, 4.0 equiv) in THF (0.1 M) was added to a solution of $LiOH{\cdot}H_2O$ (1.6 equiv) in H_2O (0.1 M) at 0 °C under argon. The resulting mixture was added dropwise to a solution of the crude *N*-Boc protected amide in THF (0.5 M) at 0 °C under argon. The reaction was then stirred at 45 °C for 2 h. The reaction mixture was then allowed to cool down to rt and sat. aq. $Na_2S_2O_3$ (10 mL), EtOAc (10 mL) and 1 M NaOH (5 mL) were added. The aqueous alkaline layer was collected, and the organic layer extracted with 1 M NaOH (3 × 15 mL). All the aqueous alkaline layers were combined and acidified to pH ~ 1 with 1 M HCl, then extracted with EtOAc (3 × 50 mL). The combined organic extracts were dried over Na_2SO_4, filtered, and the solvent evaporated under reduced pressure to afford the desired acid.

cis-(±)-1-(_tert_-Butoxycarbonyl)-3-(4-methoxyphenyl)piperidine-4-carboxylic acid (_cis_-95)



Prepared according to **General Procedure J** using **29a** (0.46 g, 1.00 mmol), Boc_2O (1.10 g, 5.00 mmol), DMAP (25 mg, 0.20 mmol) and MeCN (2.0 mL), then H_2O_2 (30 wt.% in H_2O, 0.40 mL) in THF (1.1 mL), $LiOH{\cdot}H_2O$ (68 mg, 1.60 mmol) in H_2O (1.6 mL) and THF (2.0 mL). Acid-base work-up afforded *cis* acid ***cis*-95** as a white solid (255 mg, 0.71 mmol, 71% over 2 steps). R_f 0.27 (25% acetone/pentane); mp = 140–142 °C (from EtOAc); IR (film)/cm^{-1} 3206 (OH br), 2971, 2933, 1733 (C=O), 1651 (C=O), 1513, 1431, 1260, 1152, 1118, 1025, 820, 757; ^{1}H NMR (500 MHz, DMSO-*d*$_6$, 373 K) δ 7.18 (dd, J = 8.9, 0.6 Hz, 2 H, 2 × HCAr), 6.82 (d, J = 8.8 Hz, 2 H, 2 × HCAr), 3.93 (ddd, J = 13.1, 7.2, 0.8 Hz, 1 H, NC*H*HCHAr), 3.74 (s, 3 H, OCH_3), 3.66 (ddd, J = 13.2, 7.6, 4.0 Hz, 1 H, NC*H*HCH_2), 3.58 (dd, J = 13.1, 4.1 Hz, 1 H, NCH*H*CHAr), 3.37 (ddd, J = 13.2, 7.6, 4.2 Hz, 1 H, NCH*H*CH_2), 3.09 (dt, J = 7.2, 4.4 Hz, 1 H, CHAr), 2.90 (dt, J = 7.5, 4.8 Hz, 1 H, CH(C=O)), 1.87 (dtd, J = 13.9, 7.5, 4.0 Hz, 1 H, NCH_2C*H*H), 1.77 (ddt, J = 13.9, 7.6, 4.4 Hz, 1 H, NCH_2CH*H*), 1.39 (s, 9 H, $C(CH_3)_3$); ^{13}C NMR (126 MHz, DMSO-*d*$_6$, 373 K) δ 173.6 (C=O acid), 157.6 (C_{Ar} quat), 153.6 (C=O carbamate), 132.8 (C_{Ar} quat), 128.5 (2 × C_{Ar}), 113.1 (2 × C_{Ar}), 78.2 (*C*$(CH_3)_3$), 54.6 (OCH_3), 45.8 (N*C*H_2CHAr), 43.5 (*C*H(C=O)), 40.6 (N*C*H_2CH_2), 40.1 (CHAr), 27.6 (C(*C*$H_3)_3$), 24.7 (NCH_2*C*H_2); HRMS (ESI) m/z Calculated for $C_{18}H_{26}NO_5$ [M+H] 336.1811; Found 336.1822.

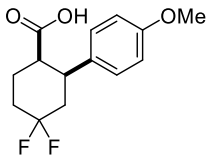
cis-(±)-3-(4-Methoxyphenyl)tetrahydro-2*H*-thiopyran-4-carboxylic acid 1,1-dioxide (_cis_-97)



Prepared according to **General Procedure J** using *cis*-arylated **54** (0.37 g, 0.90 mmol), Boc_2O (981 mg, 4.50 mmol), DMAP (22 mg, 0.18 mmol) and MeCN (1.8 mL). The oxidative cleavage step was conducted using a solution of H_2O_2 (30 wt.% in H_2O, 0.36 mL) in THF (0.9 mL), a solution of $LiOH{\cdot}H_2O$ (61 mg, 1.44 mmol) in H_2O (1.5 mL) and a solution of crude *N*-Boc protected amide from the previous step in THF (1.8 mL). Acid-base work-up afforded acid ***cis*-97** as a pale orange solid (121 mg, 0.43 mmol, 48% over 2 steps, 35% recovery of starting **54**). R_f 0.27 (40% acetone/pentane); mp = 255–257 °C (from Et_2O/pentane); IR (film)/cm^{-1} 3220 (br OH), 2914, 2847, 1707 (C=O), 1513, 1416, 1252 (S=O), 1177 (S=O), 1111, 1013, 820; ^{1}H NMR (400 MHz, CD_3CN) δ 9.10 (br s, 1 H, COOH), 7.21–7.12 (m, 2 H, 2 × HC_{Ar}), 6.92–6.82 (m,

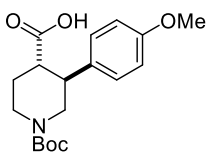
2 H, 2 × HC_{Ar}), 4.09 (t, *J* = 13.6 Hz, 1 H, SC*H*HCHAr), 3.76 (s, 3 H, OCH_3), 3.56 (dt, *J* = 13.4, 3.6 Hz, 1 H, CH(C=O)), 3.32 (ddd, *J* = 14.2, 13.1, 4.5 Hz, 1 H, SC*H*HCH_2), 3.04 (dt, *J* = 13.8, 3.6 Hz, 1 H, SCH*H*CHAr), 3.02–2.89 (m, 2 H, CHAr and SCH*H*CH_2), 2.48–2.28 (m, 2 H, $O_2SCH_2CH_2$); ^{13}C NMR (101 MHz, CD_3CN) δ 174.4 (C=O acid), 159.9 (C_{Ar} quat), 133.2 (C_{Ar} quat), 129.4 (2 × C_{Ar}), 114.8 (2 × C_{Ar}), 55.8 (OCH_3), 52.1 (SCH_2CHAr), 47.6 (SCH_2CH_2), 44.1 (CHAr), 42.5 (*C*H(C=O)), 27.0 (CH_2CH_2); HRMS (ESI) *m/z* Calculated for $C_{13}H_{15}O_5S$ [M+H] 283.0640; Found 283.0649.

cis-(±)-4,4-Difluoro-2-(4-methoxyphenyl)cyclohexane-1-carboxylic acid (_cis_-98)



Prepared according to **General Procedure J** using *cis*-arylated **55** (396 mg, 1.00 mmol), Boc_2O (1.10 g, 5.00 mmol), DMAP (25 mg, 0.20 mmol) and MeCN (2.0 mL). The oxidative cleavage step was conducted using a solution of H_2O_2 (30 wt.% in H_2O, 0.40 mL) in THF (1.1 mL), a solution of LiOH·H_2O (68 mg, 1.60 mmol) in H_2O (1.6 mL) and a solution of crude *N*-Boc protected amide from the previous step in THF (2.0 mL). Acid-base work-up afforded acid ***cis*-98** as a yellow solid (54 mg, 0.20 mmol, 20% over 2 steps). R_f 0.30 (15% acetone/pentane); mp = 127–129 °C (from Et_2O/pentane); IR (film)/cm^{-1} 2945 (br OH), 1707 (C=O), 1513, 1453, 1245, 1103, 1036, 969; ^{1}H NMR (400 MHz, $CDCl_3$) δ 7.17–7.09 (m, 2 H, 2 × HC_{Ar}), 6.89–6.80 (m, 2 H, 2 × HC_{Ar}), 3.80 (s, 3 H, OCH_3), 3.18 (dt, *J* = 13.7, 4.7 Hz, 1 H, CHAr), 2.98 (d, *J* = 4.6 Hz, 1 H, CH(C=O)), 2.81 (dtd, *J* = 33.9, 13.5, 3.9 Hz, 1 H, F_2CC*H*HCHAr), 2.26–2.15 (m, 2 H, F_2CC*H*HCH_2 and F_2CCH*H*CHAr), 2.23–1.98 (ddt, *J* = 17.9, 6.9, 3.2 Hz, 3 H, F_2CCH*H*CH_2 and $F_2CCH_2CH_2$); ^{13}C NMR (101 MHz, $CDCl_3$) δ 178.7 (C=O acid), 158.6 (C_{Ar} quat), 133.2 (C_{Ar} quat), 128.2 (2 × C_{Ar}), 122.1 (t, J_{CF} = 241.5 Hz, CF_2), 114.1 (2 × C_{Ar}), 55.2 (OCH_3), 48.4 (*C*H(C=O)), 41.9 (d, J_{CF} = 10.1 Hz, CHAr), 40.9 (t, J_{CF} = 24.3 Hz, F_2CCH_2CHAr), 32.7 (t, J_{CF} = 25.2 Hz, $F_2CCH_2CH_2$), 26.2 (d, J_{CF} = 10.1 Hz, $F_2CCH_2CH_2$); ^{19}F{^{1}H} NMR (376 MHz, $CDCl_3$) δ –88.66 (d, J_{FF} = 238.0 Hz), –100.84 (d, J_{FF} = 237.8 Hz); HRMS (ESI) *m/z* Calculated for $C_{14}H_{15}O_3F_2$ [M+H] 269.0989; Found 269.0994.

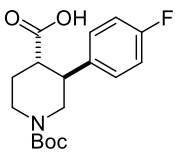
***tert*-Butoxycarbonyl-*trans*-(±)-3-(4-methoxyphenyl)piperidine-4-carboxylic acid (*trans*-95)**



Prepared according to **General Procedure J** using *trans*-arylated **29b** (369 mg, 0.80 mmol), Boc_2O (0.88 g, 4.00 mmol), DMAP (20 mg, 0.16 mmol) and MeCN (1.6 mL). The oxidative cleavage step was conducted using a solution of H_2O_2 (30 wt.% in H_2O, 0.32 mL) in THF (0.9 mL), a solution of LiOH·H_2O (55 mg, 1.28 mmol) in H_2O (1.3 mL) and a solution of crude *N*-Boc protected amide from the previous step in THF (1.6 mL). Acid-base work-up afforded acid ***trans*-95** as a yellow solid (161 mg, 0.48 mmol, 60% over 2 steps). R_f 0.25 (20% acetone/pentane); mp = 173–174 °C (from Et_2O/pentane); IR (film)/cm^{-1} 2999, 2972, 2928, 2859, 1730 (C=O), 1689 (C=O), 1512, 1423, 1293, 1244, 1158, 910, 828, 732; ^{1}H NMR (400 MHz, DMSO-d_6, 373 K) δ 7.17 (d, *J* = 8.7 Hz, 2 H, 2 × HC_{Ar}), 6.86 (d, *J* = 8.8 Hz, 2 H, 2 × HC_{Ar}), 4.05 (ddd, *J* = 13.3, 4.4, 2.6 Hz, 1 H, NC*H*HCH_2), 3.91 (dt, *J* = 10.8, 1.6 Hz, 1 H, NC*H*HCHAr), 3.75 (s, 3 H, OCH_3), 2.87 (td, J = 13.0, 2.9 Hz, 1 H, NCH*H*CH_2), 2.84–2.70 (m, 3 H, NCH*H*CHAr, CH(C=O) and CHAr), 1.93 (dq, J = 13.3, 3.0 Hz, 1 H, NCH_2CH*H*), 1.62–1.51 (m, 1 H, NCH_2CH*H*), 1.43 (s, 9 H, $C(CH_3)_3$); ^{13}C NMR (101 MHz, DMSO-d_6, 373 K) δ 174.0 (C=O acid), 157.8 (C_{Ar} quat), 153.4 (C=O carbamate), 132.8 (C_{Ar} quat), 128.0 (2 × C_{Ar}), 113.5 (2 × C_{Ar}), 78.4 (*C*$(CH_3)_3$), 54.6 (OCH_3), 49.0 (N*C*H_2CHAr), 46.8 (*C*H(C=O)),

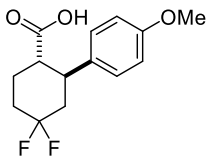
43.2 (N*C*H_2CH_2), 42.4 (*C*HAr), 28.2 (NCH$_2$*C*H$_2$), 27.6 (C(*C*H$_3$)$_3$); HRMS (ESI) ***m/z*** Calculated for $C_{18}H_{26}NO_5$ [M+H] 336.1811; Found 336.1820.

***tert*-Butoxycarbonyl-*trans*-(±)-3-(4-fluorophenyl)piperidine-4-carboxylic acid (*trans*-96)**



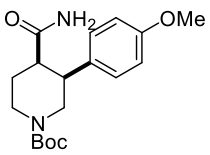
Prepared according to **General Procedure J** using *trans*-arylated **57** (396 mg, 1.00 mmol), Boc_2O (1.10 g, 5.00 mmol), DMAP (25 mg, 0.20 mmol) and MeCN (2.0 mL). The oxidative cleavage step was conducted using a solution of H_2O_2 (30 wt.% in H_2O, 0.40 mL) in THF (1.1 mL), a solution of LiOH·H_2O (68 mg, 1.60 mmol) in H_2O (1.6 mL) and a solution of crude *N*-Boc protected amide from the previous step in THF (2.0 mL). Acid-base work-up afforded acid ***trans*-96** as a pale yellow powder (257 mg, 79% over 2 steps). R_f 0.31 (20% acetone/pentane); mp = 148–150 °C (from Et_2O/pentane); IR (film)/cm^{-1} 2982, 1685 (C=O), 1513, 1424, 1297, 1230, 1163, 910, 835, 731; ^{1}H NMR (400 MHz, DMSO-*d*$_6$, 373 K) δ 7.34–7.22 (m, 2 H, 2 × HC_{Ar}), 7.09 (t, *J* = 9.0 Hz, 2 H, 2 × HC_{Ar}), 4.05 (dddd, *J* = 13.3, 4.4, 2.7, 1.7 Hz, 1 H, NC*H*HCH$_2$), 3.92 (dq, *J* = 9.3, 1.9 Hz, 1 H, NC*H*HCHAr), 2.90 (td, *J* = 13.0, 3.0 Hz, 1 H, NCH*H*CH$_2$), 2.84–2.71 (m, 3 H, NCH*H*CHAr, CH(C=O), CHAr), 1.95 (dq, J = 13.2, 2.9 Hz, 1 H, NCH$_2$C*H*H), 1.64–1.51 (m, 1 H, NCH$_2$CH*H*), 1.43 (s, 9 H, C(CH$_3$)$_3$); ^{13}C NMR (101 MHz, DMSO-*d*$_6$, 373 K) δ 173.9 (C=O acid), 160.7 (d, J_{CF} = 241.7 Hz, FC_{Ar} quat), 153.4 (C=O carbamate), 136.9 (d, J_{CF} = 3.2 Hz, F-*p*-C_{Ar} quat), 128.8 (d, J_{CF} = 8.9 Hz, 2 × F-*m*-C_{Ar}), 114.4 (d, J_{CF} = 22.6 Hz, 2 × F-*o*-C_{Ar}), 78.5 (*C*(CH$_3$)$_3$), 48.7 (N*C*H$_2$CHAr), 46.7 (*C*H(C=O)), 43.3 (CHAr), 42.4 (N*C*H$_2$CH$_2$), 28.1 (NCH$_2$*C*H$_2$), 27.6 (C(*C*H$_3$)$_3$); ^{19}F{^{1}H} NMR (376 MHz, DMSO-*d*$_6$, 373 K) δ –116.25 (s); HRMS (ESI) ***m/z*** Calculated for $C_{17}H_{21}NO_4F$ [M+H] 322.1455; Found 322.1462.

***trans*-(±)-4,4-Difluoro-2-(4-methoxyphenyl)cyclohexane-1-carboxylic acid (*trans*-98)**



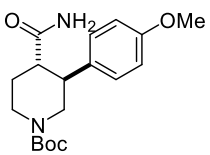
Prepared according to **General Procedure J** using *trans*-arylated **94** (160 mg, 0.40 mmol), Boc_2O (0.44 g, 2.00 mmol), DMAP (10 mg, 0.08 mmol) and MeCN (0.8 mL). The oxidative cleavage step was conducted using a solution of H_2O_2 (30 wt.% in H_2O, 0.16 mL) in THF (0.4 mL), a solution of LiOH·H_2O (27 mg, 0.64 mmol) in H_2O (0.7 mL) and a solution of crude *N*-Boc protected amide from the previous step in THF (0.8 mL). Acid-base work-up afforded acid ***trans*-98** as a yellow solid (51 mg, 0.19 mmol, 47% over 2 steps). R_f 0.37 (20% acetone/pentane); mp = 134–136 °C (from Et_2O/pentane); IR (film)/cm^{-1} 2967 (br OH), 1707 (C=O), 1513, 1461, 1252, 1174, 1036, 962, 835; ^{1}H NMR (400 MHz, $CDCl_3$) δ 7.16–7.06 (m, 2 H, 2 × HC_{Ar}), 6.89–6.78 (m, 2 H, 2 × HC_{Ar}), 3.79 (s, 3 H, OCH_3), 3.19–3.03 (td, *J* = 12.5, 3.6 Hz, 1 H, CHAr), 2.57 (td, *J* = 12.0, 3.0 Hz, 1 H, CH(C=O)), 2.34–2.20 (m, 2 H, F_2CC*H*HCHAr and F_2CC*H*HCH$_2$), 2.18–2.08 (m, 1 H, F_2CCH$_2$C*H*H), 1.99–1.73 (m, 3 H, F_2CCH*H*CH$_2$, F_2CCH*H*CHAr and F_2CCH$_2$CH*H*); ^{13}C NMR (101 MHz, $CDCl_3$) δ 178.7 (C=O acid), 158.6 (C_{Ar} quat), 133.2 (C_{Ar} quat), 128.2 (2 × C_{Ar}), 122.1 (t, J_{CF} = 241.5 Hz, CF_2), 114.1 (2 × C_{Ar}), 55.2 (OCH_3), 48.4 (*C*H(C=O)), 41.9 (d, J_{CF} = 10.6 Hz, CHAr), 40.9 (t, J_{CF} = 23.5 Hz, F_2C*C*H$_2$CHAr), 32.7 (t, J_{CF} = 24.9 Hz, F_2C*C*H$_2$CH$_2$), 26.2 (d, J_{CF} = 10.2 Hz, F_2CCH$_2$*C*H$_2$); ^{19}F{^{1}H} NMR (376 MHz, $CDCl_3$) δ –90.97 (d, J_{FF} = 239.2 Hz), –101.44 (J_{FF} = 237.5 Hz); HRMS (APCI) ***m/z*** Calculated for $C_{14}H_{15}O_2F_2$ [M+H] 269.0995; Found 269.0996.

tert-Butyl-_cis_-(±)-4-carbamoyl-3-(4-methoxyphenyl)piperidine-1-carboxylate (_cis_-102)



Adapting a procedure reported by O'Brien,[223] a flame-dried microwave vial (25 mL) was charged with *cis*-arylated piperidine carboxylic acid ***cis*-95** (260 mg, 0.78 mmol, 1.0 equiv), freshly distilled Et_3N (0.98 mL, 0.78 mmol, 1.0 equiv) and THF (7.8 mL). The reaction vessel was sealed and purged with argon, then cooled to –20 °C before isobutyl chloroformate (127 mg, 0.93 mmol, 1.2 equiv) was added dropwise. The resulting solution was stirred at –20 °C for 40 min, then 35% aq. NH_4OH (7.8 mL) was added and the mixture allowed to warm to rt over 30 min. The solvent was evaporated under reduced pressure and the residue dissolved in EtOAc (15 mL), washed with sat. aq. $NaHCO_3$ (2 × 10 mL), then brine (15 mL) and dried over Na_2SO_4. The organic layer was evaporated under reduced pressure to give the crude product, which was purified by flash column chromatography (78:20:2 pentane/acetone/Et_3N to 63:35:2 pentane/acetone/Et_3N). The product containing fractions were combined and concentrated under reduced pressure. To remove any residual solvent, Et_2O (10 mL) and pentane (10 mL) were added and the mixture was evaporated again to afford amide ***cis*-102** as a white solid (192 mg, 0.57 mmol, 73% over 2 steps). R_f 0.19 (20% acetone/pentane); mp = 177–179 °C (from Et_2O/pentane); IR (film)/cm^{-1} 3459 (NH), 3326 (NH br), 2999, 2972, 2929, 1663 (C=O), 1610 (C=O), 1511, 1463, 1425, 1247, 1163, 1119, 1032, 909, 830, 732; ^{1}H NMR (500 MHz, DMSO-d_6, 373 K) δ 7.18 (d, *J* = 8.7 Hz, 2 H, 2 × HC_{Ar}), 6.81 (d, *J* = 8.7 Hz, 2 H, 2 × HC_{Ar}), 6.49 (br s, 2 H, NH_2), 3.99 (dd, *J* = 12.8, 8.6 Hz, 1 H, NC*H*HCHAr), 3.74 (s, 3 H, OCH_3), 3.64 (ddd, *J* = 12.9, 8.9, 3.8 Hz, 1 H, NC*H*HCH_2), 3.59 (dd, *J* = 12.7, 4.3 Hz, 1 H, NCH*H*CHAr), 3.46 (ddd, *J* = 12.9, 6.1, 4.3 Hz, 1 H, NCH*H*CH_2), 2.99 (dt, *J* = 8.7, 4.4 Hz, 1 H, CHAr), 2.76 (dt, *J* = 6.2, 4.8 Hz, 1 H, CH(C=O)), 1.82 (dtd, *J* = 13.7, 6.2, 3.8 Hz, 1 H, NCH_2C*H*H), 1.71 (ddt, *J* = 13.6, 9.1, 4.6 Hz, 1 H, NCH_2CH*H*), 1.40 (s, 9 H, C(C*H*$_3$)$_3$); ^{13}C NMR (126 MHz, DMSO-d_6, 373 K) δ 174.4 (C=O amide), 157.5 (C_{Ar} quat), 153.7 (C=O carbamate), 133.2 (C_{Ar} quat), 128.5 (2 × C_{Ar}), 113.1 (2 × C_{Ar}), 78.0 (*C*$(CH_3)_3$), 54.6 (OCH_3), 45.5 (N*C*H_2CHAr), 43.1 (CH(C=O)), 41.2 (CHAr), 40.3 (N*C*H_2CH-$_2$), 27.7 (C(*C*$H_3)_3$), 26.0 (NCH_2*C*H_2); HRMS (ESI) *m/z* Calculated for $C_{18}H_{27}N_2O_4$ [M+H] 335.1971; Found 335.1977.

tert-Butyl-_trans_-(±)-4-carbamoyl-3-(4-methoxyphenyl)piperidine-1-carboxylate (_trans_-102)



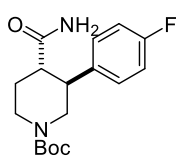
Adapting a procedure reported by O'Brien, [223] a flame-dried microwave vial (25 mL) was charged with *trans*-arylated piperidine carboxylic acid ***trans*-95** (228 mg, 0.70 mmol, 1.0 equiv), freshly distilled Et_3N (0.91 mL, 0.70 mmol, 1.0 equiv) and THF (7.0 mL). The reaction vessel was sealed and purged with argon, then cooled to –20 °C before isobutyl chloroformate (112 mg, 0.84 mmol, 1.2 equiv) was added dropwise. The resulting solution was stirred at –20 °C for 40 min, then 35% aq. NH_4OH (7.0 mL) was added and the mixture allowed to warm to rt over 30 min. The solvent was evaporated under reduced pressure and the residue dissolved in EtOAc (15 mL), washed with sat. aq. $NaHCO_3$ (2 × 10 mL), then brine (15 mL) and dried over Na_2SO_4. The organic layer was evaporated under reduced pressure to give the crude product, which was purified by flash column chromatography (78:20:2 pentane/acetone/Et_3N to 63:35:2 pentane/acetone/Et_3N). The product containing fractions were combined and concentrated under reduced pressure. To remove any residual solvent, Et_2O (10 mL) and pentane (10 mL) were added and

the mixture was evaporated again to afford amide ***trans*-102** as a white solid (175 mg, 0.51 mmol, 74% over 2 steps). R_f 0.15 (20% acetone/pentane); mp = 177–179 °C (from Et_2O/pentane); IR (film)/cm^{-1} 3325 (NH br), 3191, 2974, 2855, 1662 (C=O), 1513, 1416, 1238, 1163, 1036, 910, 828, 731; ^{1}H NMR (400 MHz, DMSO-d_6, 373 K) δ 7.16 (dd, *J* = 8.2, 1.5 Hz, 2 H, 2 × HC_{Ar}), 6.91–6.80 (m, 2 H, 2 × HC_{Ar}), 4.06 (dt, *J* = 13.1, 3.7 Hz, 1 H, NC*H*HCH_2), 3.99–3.87 (m, 1 H, NC*H*HCHAr), 3.74 (s, 3 H. OCH_3), 2.90–2.69 (m, 3 H, NCH*H*CH_2, NCH*H*CHAr and CHAr), 2.62 (td, *J* = 11.1, 10.7, 3.8 Hz, 1 H, CH(C=O)), 1.82 (dd, *J* = 13.1, 3.3 Hz, 1 H, NCH_2C*H*H), 1.57 (qd, *J* = 12.6, 4.6 Hz, 1 H, NCH_2CH*H*), 1.43 (s, 9 H, C(C*H*$_3$)$_3$); ^{13}C NMR (101 MHz, DMSO-d_6, 373 K) δ 174.3 (C=O amide), 157.7 (C_{Ar} quat), 153.4 (C=O carbamate), 133.1 (C_{Ar} quat), 128.0 (2 × C_{Ar}), 113.4 (2 × C_{Ar}), 78.2 (*C*$(CH_3)_3$), 54.6 (OCH_3), 49.3 (N*C*H_2CHAr), 47.4 (*C*H(C=O)), 42.8 (CHAr), 42.7 (N*C*H_2CH_2), 28.7 (NCH_2*C*H_2), 27.6 (C(*C*$H_3)_3$); HRMS (ESI) *m/z* Calculated for $C_{18}H_{27}N_2O_4$ [M+H] 335.1971; Found 335.1979.

General Procedure K for the Synthesis of *trans* Amides by Aminoquinoline Oxidation

Adapting a previously reported protocol by Chen,[231] a flask was charged with the corresponding *trans*-arylated piperidine (1.0 equiv) and 2-iodoxybenzoic acid (IBX, 30 wt.%, 2.0 equiv) under air. H_2O (0.3 M) and 1,1,1,3,3,3-hexafluoro-2-propanol (HFIP, 0.3 M) were added, and the resulting solution (0.15 M) was stirred at 60 °C for 1.5 h. The reaction mixture was then allowed to cool to rt and sat. aq. $NaHCO_3$ (10 mL) and CH_2Cl_2 (10 ml) were added. The phases were separated and the aqueous layer was extracted with CH_2Cl_2 (3 × 15 mL). The combined organic extracts were dried over Na_2SO_4, filtered and concentrated under reduced pressure. The crude material was purified by flash column chromatography under the specified conditions. The product containing fractions were combined and concentrated under reduced pressure. Et_2O (5 mL) and pentane (5 mL) were added and the mixture was evaporated again to afford the desired free amide.

***tert*-Butyl-*trans*-(±)-4-carbamoyl-3-(4-fluorophenyl)piperidine-1-carboxylate (*trans*-100)**



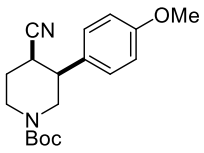
Prepared according to **General Procedure K** using *trans*-arylated piperidine carboxylic acid **57** (400 mg, 0.90 mmol, 1.0 equiv), IBX (513 mg, 1.80 mmol, 2.0 equiv), H_2O (3.0 mL) and HFIP (3.0 mL). Purification by flash column chromatography (78:20:2 pentane:acetone:Et_3N) afforded amide ***trans*-100** as a pale orange solid (195 mg, 0.61 mmol, 68%). R_f = 0.12 (40% acetone/pentane). mp = 204–206 °C (from Et_2O/pentane); IR (film)/cm^{-1} 3398, 3326 (NH br), 2974, 2924, 1661 (C=O), 1510, 1418, 1366, 1229, 1161, 909, 830, 732; ^{1}H NMR (400 MHz, DMSO-d_6, 373 K) δ 7.27 (dd, *J* = 8.7, 5.5 Hz, 2 H, 2 × HC_{Ar}), 7.06 (t, *J* = 8.9 Hz, 2 H, 2 × HC_{Ar}), 4.12–4.02 (m, 1 H, NC*H*HCH_2), 3.93 (ddd, *J* = 12.7, 3.8, 1.5 Hz, 1 H, NC*H*HCHAr), 2.88–2.80 (m, 2 H, NHCH*H*CH_2 and NCH*H*CHAr), 2.81–2.73 (m, 1 H, CHAr), 2.64 (td, *J* = 11.2, 3.9 Hz, 1 H, CH(C=O)), 1.83 (ddt, *J* = 13.2, 3.9, 2.8 Hz, 1 H, NCH_2C*H*H), 1.57 (tdd, *J* = 13.0, 11.7, 4.5 Hz, 1 H, NCH_2CH*H*), 1.43 (s, 9 H, C($CH_3)_3$); ^{13}C NMR (101 MHz, DMSO-d_6, 373 K) δ 174.3 (C=O amide), 160.7 (d, J_{CF} = 243.6 Hz, FC_{Ar} quat), 153.5 (C=O carbamate), 137.2 (d, J_{CF} = 3.2 Hz, F-*p*-C_{Ar} quat), 129.0 (d, J_{CF} = 8.2 Hz, 2 × F-*m*-C_{Ar}), 114.3 (d, J_{CF} = 22.6 Hz, 2 × F-*o*-C_{Ar}), 78.5 (*C*$(CH_3)_3$), 49.1 (N*C*H_2CHAr), 47.4 (*C*H(C=O)), 43.0 (CHAr), 42.7 (N*C*H_2CH_2), 28.7 (NCH_2*C*H_2), 27.7 (C(*C*$H_3)_3$); ^{19}F{^{1}H} NMR (376

MHz, DMSO-d_6, 373 K) δ –116.58 (s); HRMS (ESI) m/z Calculated for $C_{17}H_{24}N_2O_3F$ [M+H] 323.1771; Found 323.1764.

General Procedure L for the Synthesis of Nitrile by Dehydration of Amides

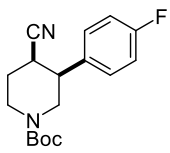
Adapting the procedure reported by Naka,[234] a flame-dried reaction tube was charged with the corresponding *cis*-amide (1.0 equiv), $Pd(OAc)_2$ (0.1 equiv), dichloroacetonitrile (10.0 equiv), dry MeCN (1 M) and H_2O (1 M). The reaction vessel was sealed and purged with argon. The reaction tube was then placed in a preheated oil bath and stirred at 60 ºC for 18 h. The reaction mixture was allowed to cool to rt and MeOH (4 mL per 1 mmol starting amide) was added. The resulting mixture was filtered through a pad of Celite, eluting with further MeOH (2 × 5 mL). The solvent was removed under reduced pressure, and the crude material was purified by flash column chromatography under the specified conditions to afford the desired nitriles.

***tert*-Butyl-*cis*-(±)-4-carbamoyl-3-(4-methoxyphenyl)piperidine-1-carboxylate (*cis*-103)**



Prepared according to **General Procedure L** using *cis* amide ***cis*-102** (172 mg, 0.51 mmol), $Pd(OAc)_2$ (11.2 mg ,0.05 mmol), dichloroacetonitrile (0.41 mL, 5.1 mmol), MeCN (0.5 mL) and H_2O (0.5 mL). Purification by flash column chromatography (40% Et_2O/pentane) afforded ***cis*-103** as a pale yellow solid (125 mg, 0.39 mmol, 77%). R_f 0.21 (40% Et_2O/pentane); mp = 125–127 °C (from Et_2O/pentane); IR (film)/cm^{-1} 2974, 1692 (C=O), 1513, 1416, 1252, 1163, 1036, 835; ^{1}H NMR (500 MHz, DMSO-d_6, 373 K) δ 7.29–7.25 (m, 2 H, 2 × HC_{Ar}), 6.93 (d, *J* = 8.7 Hz, 2 H, 2 × HC_{Ar}), 4.05 (ddd, *J* = 13.5, 2.5, 1.4 Hz, 1 H, NC*H*HCHAr), 4.02–3.94 (m, 1 H, NC*H*HCH_2), 3.78 (s, 3 H, OCH_3), 3.45 (q, *J* = 4.1 Hz, 1 H, CHCN), 3.26 (dd, *J* = 13.5, 11.3 Hz, 1 H, NCH*H*CHAr), 3.06 (ddd, *J* = 13.8, 11.8, 3.3 Hz, 1 H, NCH*H*CH_2), 2.97 (d, *J* = 4.1 Hz, 1 H, CHAr), 2.01–1.92 (m, 1 H, NCH_2CHH), 1.92–1.84 (m, 1 H, NCH_2CHH), 1.43 (s, 9 H, $C(CH_3)_3$); ^{13}C NMR (126 MHz, DMSO-d_6, 373 K) δ 158.2 (C_{Ar} quat), 153.4 (C=O carbamate), 131.1 (C_{Ar} quat), 127.8 (2 × C_{Ar}), 119.1 (nitrile CN), 113.7 (2 × C_{Ar}), 78.8 ($C(CH_3)_3$), 54.7 (OCH_3), 44.5 (NCH_2CHAr), 40.1 (CHAr), 39.7 (NCH_2CH_2), 32.9 (*C*HCN), 27.6 ($C(CH_3)_3$), 27.3 (NCH_2CH_2); HRMS (ESI) ***m/z*** Calculated for $C_{18}H_{25}N_2O_3$ [M+H] 317.1865; Found 317.1850.

***tert*-Butyl-*cis*-(±)-4-cyano-3-(4-fluorophenyl)piperidine-1-carboxylate (*cis*-104)**



Prepared according to **General Procedure L** using the corresponding *cis* arylated piperidine amide ***cis*-100** provided by Dr. Natalia Larionova (0.22 g, 0.68 mmol), $Pd(OAc)_2$ (15.7 mg, 0.07 mmol), dichloroacetonitrile (0.41 mL, 5.1 mmol), MeCN (0.7 mL) and H_2O (0.7 mL). Purification by flash column chromatography (20% to 30% acetone/pentane) afforded ***cis*-104** as a pale yellow paste (190 mg, 0.62 mmol, 91%). R_f 0.05 (10% acetone/pentane); IR (film)/cm^{-1} 2972, 2233 (C=N), 1690 (C=O), 1511, 1418, 1365, 1281, 1160, 1005, 961, 835; ^{1}H NMR (500 MHz, DMSO-d_6, 373 K) δ 7.44–7.35 (m, 2 H, 2 × HC_{Ar}), 7.21–7.12 (m, 2 H, 2 × HC_{Ar}), 4.06 (ddt, *J* = 13.5, 3.9, 1.4 Hz, 1 H, NC*H*HCHAr), 4.03–3.94 (m, 1 H, NC*H*HCH_2), 3.53–3.46 (m, 1 H, CHAr), 3.30 (dd, *J* = 13.5, 11.2 Hz, 1 H, NCH*H*CHAr), 3.12–3.01 (m, 2 H, NHCH*H*CH_2 and CHCN), 1.97 (dq, *J* = 13.8, 3.4 Hz, 1 H, NCH_2CHH), 1.90 (ddt, *J* = 13.8, 11.7, 4.3 Hz, 1 H, NCH_2CHH), 1.43 (s,

9 H, C(CH_3)$_3$); ^{13}C NMR (126 MHz, DMSO-d_6, 373 K) δ 161.0 (d, J = 244.1 Hz, FC_{Ar} quat), 153.4 (C=O carbamate), 135.2 (d, J = 3.2 Hz, F-*p*-C_{Ar} quat), 128.7 (d, J = 8.1 Hz, 2 × F-*m*-C_{Ar}), 118.9 (nitrile CN), 114.6 (d, J = 21.3 Hz, 2 × F-*o*-C_{Ar}), 78.8 (C(CH_3)$_3$), 44.3 (NCH_2CHAr), 40.1 (CHCN), 39.7 (NCH_2CH_2), 32.7 (CHAr), 27.6 (C(CH_3)$_3$), 27.2 (NCH$_2$$CH_2$); ^{19}F{^{1}H} NMR (471 MHz, DMSO-d_6, 373 K) δ –115.69 (s); HRMS (ESI) m/z Calculated for $C_{17}H_{25}N_3O_2F$ [M+NH_4] 322.1931; Found 322.1936.

General Procedure M for the Synthesis of Alcohols by Aminoquinoline Deprotection

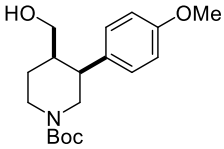
A flame-dried microwave vial (25 mL) was charged with the corresponding *cis*-arylated piperidine (1.0 equiv), di-*tert*-butyl dicarbonate (Boc_2O, 5.0 equiv) and 4-(dimethylamino)pyridine (DMAP, 0.2 equiv). The reaction vessel was sealed and purged with argon, then MeCN (0.5 M) was added by syringe. The vial was placed in an oil bath and gradually warmed up to 70 ºC, then stirred for 3 h at 70 °C. The mixture was allowed to cool down and sat. aq. NH_4Cl (10 mL) and CH_2Cl_2 (15 mL) were added. The phases were separated, and the aqueous layer was extracted with CH_2Cl_2 (3 × 10 mL). The combined organic extracts were dried over Na_2SO_4 and filtered. The solvent was removed under reduced pressure to afford the crude *N*-Boc protected amide derivative which was carried forward to the reductive cleavage step without further purification.

A solution of the crude *N*-Boc-protected amide in dry THF (0.2 M) was added dropwise to a suspension of $LiAlH_4$ (4.0 equiv) in dry THF (0.5 M) at 0 °C under argon atmosphere. The mixture was then stirred at 25 °C for 1 h or until TLC showed reaction completion. The reaction mixture was then quenched by slow addition of sat. aq. NH_4Cl (2-3 mL) at 0 °C and stirred at rt for 30 min. The suspension was filtered through a pad of Celite, eluting with EtOAc (3 × 5 mL). The phases were separated and the aqueous layer extracted with EtOAc (3 × 10 mL). The combined organic extracts were dried over Na_2SO_4 and filtered. The solvent was removed under reduced pressure and the crude residue purified by flash column chromatography under the specified conditions. The product containing fractions were combined and concentrated. Et_2O (10 mL) and pentane (10 mL) were added and the solvent was removed under reduced pressure to afford the desired primary alcohol.

General Procedure N for the Synthesis of Alcohols by Carboxylic Acid Reduction

BH_3·SMe_2 (2.2 equiv) was added to a solution of *cis* carboxylic acid (1.0 equiv) in THF (0.2 M) at 0 °C. The reaction mixture was stirred at 0 °C for 3 h, then at rt for 18 h. The mixture was then cooled again to 0 °C and quenched by dropwise addition of H_2O (3 mL). After dilution with EtOAc (10 mL), the layers were separated and the organic layer washed with sat. aq. NaCl (10 mL), $NaHCO_3$ (10 mL), H_2O (5 mL) and again sat. aq. NaCl (5 mL). The organic layer was dried over Na_2SO_4 and concentrated under reduced pressure. The crude product was purified by flash column chromatography under the specified conditions to afford the desired primary alcohol.

***tert*-Butyl-*cis*-(±)-4-(hydroxymethyl)-3-(4-methoxyphenyl)piperidine-1-carboxylate (*cis*-105)**

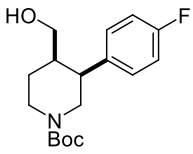


Prepared according to **General Procedure M** using *cis*-arylated piperidine **29a** (324 mg, 0.70 mmol), Boc_2O (763 mg, 3.50 mmol), DMAP (18 mg, 0.14 mmol) in MeCN (1.4 mL), then $LiAlH_4$ (110 mg, 2.80 mmol) and THF (3.5 mL + 1.4 mL).

Purification by flash column chromatography (10% to 20% acetone/pentane) afforded ***cis*-105** as a pale yellow oil (138 mg, 0.43 mmol, 62% over 2 steps). R_f 0.25 (20% acetone/pentane); IR (film)/cm^{-1} 3442 (OH br), 2974, 2930, 1689 (C=O), 1511, 1430, 1366, 1249, 1161, 1036, 829; ^{1}H NMR (500 MHz, DMSO-d_6, 373 K) δ 7.16 (dd, *J* = 8.9, 0.5 Hz, 2 H, 2 × HC_{Ar}), 6.83 (d, *J* = 8.8 Hz, 2 H, 2 × HC_{Ar}), 3.97 (t, *J* = 5.0 Hz, 1 H, OH), 3.82–3.75 (m, 2 H, NC*H*HCHAr and NC*H*HCH_2), 3.75 (s, 3 H, OCH_3), 3.40 (dd, *J* = 13.2, 4.2 Hz, 1 H, NCH*H*CH_2), 3.23–3.16 (m, 2 H, C*H*HOH and NCH*H*CHAr), 3.11 (ddd, *J* = 10.7, 6.1, 4.9 Hz, 1 H, CH*H*OH), 2.99–2.94 (m, 1 H, CHAr, *superimposed onto H_2O peak*), 2.01–1.94 (m, 1 H, C*H*CH_2OH), 1.62–1.53 (m, 2 H, NCH_2CH_2), 1.40 (s, 9 H, $C(CH_3)_3$); ^{13}C NMR (126 MHz, DMSO-d_6, 373 K) δ 157.4 (C_{Ar} quat), 153.7 (C=O carbamate), 133.3 (C_{Ar} quat), 128.8 (2 × C_{Ar}), 113.1 (2 × C_{Ar}), 78.0 (*C*$(CH_3)_3$), 60.8 (CH_2OH), 54.6 (OCH_3), 46.4 (N*C*H_2CHAr), 41.3 (N*C*H_2CH_2), 40.6 (CHAr), 40.0 (*C*HCH_2OH), 27.7 (C(*C*$H_3)_3$), 23.9 (NCH_2*C*H_2); HRMS (ESI) *m/z* Calculated for $C_{18}H_{28}NO_4$ [M+H] 322.2018; Found 322.2023.

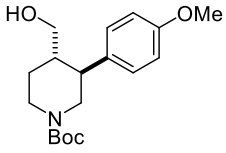
Alternatively prepared according to **General Procedure N** using ***cis*-95** (34 mg, 0.10 mmol), BH_3·SMe_2 (20 µL, 0.22 mmol) and THF (0.5 mL). Purification by flash column chromatography (10% to 35% EtOAc/hexane) afforded ***cis*-105** as a pale yellow oil (23 mg, 0.07 mmol, 72%). R_f 0.55 (35% EtOAc/Hexane); All characterisation information in agreement with data previously reported for ***cis*-105**.

***tert*-Butyl-*cis*-(±)-3-(4-fluorophenyl)-4-(hydroxymethyl)piperidine-1-carboxylate (*cis*-106)**



Prepared according to **General Procedure M** using *cis*-arylated piperidine **46b** (252 mg, 0.56 mmol), Boc_2O (610 mg, 2.80 mmol), DMAP (14 mg, 0.11 mmol) in MeCN (1.2 mL), then $LiAlH_4$ (88 mg, 2.24 mmol) and THF (2.8 mL + 1.2 mL). Purification by flash column chromatography (10% to 20% acetone/pentane) afforded ***cis*-106** as a colourless paste (97 mg, 0.31 mmol, 56% over 2 steps). R_f 0.25 (20% acetone/pentane); IR (film)/cm^{-1} 3437 (OH br), 2920, 2850, 1689 (C=O), 1683, 1667, 1507, 1427, 1364, 1242, 1158, 1114, 1034, 925, 834, 767; ^{1}H NMR (500 MHz, DMSO-d_6, 373 K) δ 7.31–7.26 (m, 2 H, 2 × HC_{Ar}), 7.09–7.00 (m, 2 H, 2 × HC_{Ar}), 3.87–3.76 (m, 2 H, NC*H*HCHAr and NC*H*HCH_2), 3.40 (dd, *J* = 13.2, 4.1 Hz, 1 H, NCH*H*CHAr), 3.22–3.15 (m, 2 H, C*H*HOH and NCH*H*CH_2), 3.10–3.06 (m, 1 H, CH*H*OH), 3.04 (q, *J* = 4.9 Hz, 1 H, CHAr), 2.01 (dddd, *J* = 11.3, 7.8, 7.1, 5.6 Hz, 1 H, C*H*CH_2OH), 1.62–1.50 (m, 2 H, NCH_2CH_2), 1.39 (s, 9 H, $C(CH_3)_3$); ^{13}C NMR (126 MHz, DMSO-d_6, 373 K) δ 160.4 (d, *J* = 242.2 Hz, FC_{Ar} quat), 153.7 (C=O carbamate), 137.3 (d, *J* = 3.2 Hz, F-*p*-C_{Ar} quat), 129.6 (d, *J* = 7.6 Hz, 2 × F-*m*-C_{Ar}), 113.8 (d, *J* = 20.7 Hz, 2 × F-*o*-C_{Ar}), 78.1 (*C*$(CH_3)_3$), 60.9 (*C*H_2OH), 46.3 (N*C*H_2CHAr), 41.4 (N*C*H_2CH_2), 40.5 (*C*HCH$_2$OH), 39.9 (CHAr), 27.6 (C(*C*$H_3)_3$), 23.8 (NCH_2*C*H_2); ^{19}F{^{1}H} NMR (471 MHz, DMSO-d_6, 373 K) δ –117.25 (s); HRMS (ESI) m/z Calculated for $C_{17}H_{25}NO_3F$ [M+H] 310.1818; Found 310.1824.

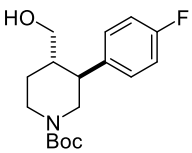
***tert*-Butyl-*trans*-(±)-4-(hydroxymethyl)-3-(4-methoxyphenyl)piperidine-1-carboxylate (*trans*-105)**



Prepared according to **General Procedure M** using *trans*-arylated piperidine **29b** (462 mg, 1.00 mmol), Boc_2O (1.10 g, 5.00 mmol), DMAP (25 mg, 0.20 mmol) in MeCN (2 mL), then $LiAlH_4$ (156 mg, 4.00 mmol) and THF (5 mL + 2 mL). Purification by flash column chromatography (10% to 20% acetone/pentane)

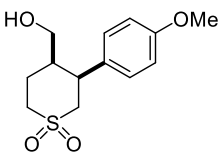
afforded ***trans*-105** as a white solid (198 mg, 0.62 mmol, 62% over 2 steps). R_f 0.34 (20% acetone/pentane); mp = 55–57 °C (from Et_2O/pentane); IR (film)/cm^{-1} 3443 (OH br), 2997, 2971, 2908, 1668 (C=O), 1511, 1422, 1364, 1245, 1164, 1131, 1035, 828, 732; ^{1}H NMR (400 MHz, DMSO-d_6, 373 K) δ 7.17–7.11 (m, 2 H, 2 × HC_{Ar}), 6.90–6.85 (m, 2 H, 2 × HC_{Ar}), 4.05 (ddt, *J* = 13.1, 4.5, 2.3 Hz, 1 H, NC*H*HCH_2), 3.87 (ddd, J = 12.9, 4.4, 1.8 Hz, 1 H, NC*H*HCHAr), 3.75 (s, 3 H, OCH_3), 3.22 (dt, *J* = 10.9, 3.2 Hz, 1 H, C*H*HOH), 3.07–3.05 (m, 1 H, CH*H*OH), 2.83 (td, *J* = 12.9, 2.9 Hz, 1 H, NCH*H*CH_2), 2.76 (dd, *J* = 13.0, 11.6 Hz, 1 H, NCH*H*CHAr), 2.39 (td, *J* = 11.3, 4.4 Hz, 1 H, CHAr), 1.92–1.84 (m, 1 H, NCH_2C*H*H), 1.79 (dtq, *J* = 10.9, 7.2, 3.5 Hz, 1 H, C*H*CH_2OH), 1.41 (s, 9 H, $C(CH_3)_3$), 1.38–1.25 (m, 1 H, NCH_2CH*H*); ^{13}C NMR (101 MHz, DMSO-d_6, 373 K) δ 157.7 (C_{Ar} quat), 153.6 (C=O carbamate), 133.6 (C_{Ar} quat), 128.1 (2 × C_{Ar}), 113.7 (2 × C_{Ar}), 78.2 (*C*$(CH_3)_3$), 62.6 (CH_2OH), 54.8 (OCH_3), 49.9 (N*C*H_2CHAr), 43.34 (N*C*H_2CH_2), 43.27 (CHAr), 42.6 (*C*HCH_2OH), 28.0 (NCH_2*C*H_2), 27.8 (C(*C*$H_3)_3$); HRMS (ESI) *m/z* Calculated for $C_{18}H_{28}NO_4$ [M+H] 322.2018; Found 322.2025.

tert-Butyl-_trans_-(±)-3-(4-fluorophenyl)-4-(hydroxymethyl)piperidine-1-carboxylate (_trans_-106)



Prepared according to **General Procedure M** using *trans*-arylated piperidine **57** (450 mg, 1.00 mmol), Boc_2O (1.10 g, 5.00 mmol), DMAP (25 mg, 0.20 mmol) in MeCN (2 mL), then $LiAlH_4$ (156 mg, 4.00 mmol) and THF (5 mL + 2 mL). Purification by flash column chromatography (10% to 20% acetone/pentane) afforded ***trans*-106** as an orange solid (163 mg, 0.53 mmol, 53% over 2 steps). R_f 0.28 (20% acetone/pentane); mp = 65–67 °C (from Et_2O/pentane); IR (film)/cm^{-1} 3430 (OH br), 3001, 2974, 2920, 1669 (C=O), 1509, 1425, 1365, 1225, 1160, 1131, 908, 829, 731; ^{1}H NMR (400 MHz, DMSO-d_6, 373 K) δ 7.24–7.20 (m, 2 H, 2 × HC_{Ar}), 7.07–7.01 (m, 2 H, 2 × HC_{Ar}), 4.05–3.96 (m, 1 H, NC*H*HCH_2), 3.82 (ddd, *J* = 13.0, 4.4, 1.9 Hz, 1 H, NC*H*HCHAr), 3.20–3.16 (m, 1 H, C*H*HOH), 3.00 (dd, *J* = 10.7, 6.7 Hz, 1 H, CH*H*OH), 2.81 (td, *J* = 12.8, 2.5 Hz, 1 H, NCH*H*CH_2), 2.74 (dd, *J* = 13.0, 11.5 Hz, 1 H, NCH*H*CHAr), 2.41 (td, *J* = 11.0, 4.3 Hz, 1 H, CHAr), 1.86–1.73 (m, 2 H, NCH_2C*H*H and C*H*CH_2OH), 1.36 (s, 9 H, $C(CH_3)_3$), 1.33–1.24 (m, 1 H, NCH_2CH*H*); ^{13}C NMR (101 MHz, DMSO-d_6, 373 K) δ 161.2 (d, *J* = 241.8 Hz, FC_{Ar} quat), 154.4 (C=O carbamate), 138.1 (d, *J* = 2.6 Hz, F-*p*-C_{Ar} quat), 129.5 (d, *J* = 7.6 Hz, 2 × F-*m*-C_{Ar}), 115.1 (d, *J* = 21.2 Hz, 2 × F-*o*-C_{Ar}), 79.2 (*C*$(CH_3)_3$), 63.1 (*C*H_2OH), 50.2 (N*C*H_2CHAr), 43.9 (CHAr), 43.8 (N*C*H_2CH_2), 42.9 (*C*HCH$_2$OH), 28.3 (NCH_2*C*H_2), 28.2 (C(*C*$H_3)_3$); ^{19}F{^{1}H} NMR (471 MHz, DMSO-d_6, 373 K) δ –116.50 (s); HRMS (ESI) m/z Calculated for $C_{17}H_{25}NO_3F$ [M+H] 310.1818; Found 310.1809.

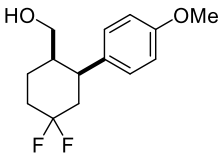
***cis*-(±)-4-(Hydroxymethyl)-3-(4-methoxyphenyl)tetrahydro-2*H*-thiopyran 1,1-dioxide (*cis*-108)**



Prepared according to **General Procedure N** using ***cis*-97** (95 mg, 0.35 mmol), BH_3·SMe_2 (70 µL, 0.77 mmol) and THF (1.8 mL). Purification by flash column chromatography (10% to 35% EtOAc/hexane) afforded ***cis*-108** as a white powder (61 mg, 0.23 mmol, 64%). R_f 0.67 (100% EtOAc); mp = 136–138 °C (from Et_2O/pentane); IR (film)/cm^{-1} 3504 (br OH), 2937, 1513, 1305, 1245 (S=O), 1118 (S=O), 1029, 835; ^{1}H NMR (400 MHz, $CDCl_3$) δ 7.15–7.06 (m, 2 H, 2 × HC_{Ar}), 6.89 (d, *J* = 8.7 Hz, 2 H, 2 × HC_{Ar}), 3.82 (dd, *J* = 12.8, 12.7 Hz, 1 H, SC*H*HCHAr), 3.81 (s, 3 H, OCH_3), 3.73–3.65 (m, 2 H, C*H*HOH and CHAr), 3.62 (dt, *J* = 10.4, 3.4 Hz, 1 H, CH*H*OH), 3.50 (ddd, *J* = 14.1, 11.2, 6.7 Hz, 1 H, SC*H*HCH_2), 3.12–3.04 (m, 1

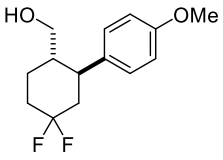
H, SCH*H*CHAr), 2.99 (dq, *J* = 14.1, 3.7 Hz, 1 H, SCH*H*CH_2), 2.48–2.40 (m, 2 H, SCH_2CH_2), 2.04 (dp, *J* = 7.8, 3.9 Hz, 1 H, C*H*CH_2OH), 1.40 (t, *J* = 3.7 Hz, 1 H, OH); ^{13}C NMR (101 MHz, $CDCl_3$) δ 158.7 (C_{Ar} quat), 132.2 (C_{Ar} quat), 128.2 (2 × C_{Ar}), 114.2 (2 × C_{Ar}), 61.6 (*C*H_2OH), 55.3 (OCH_3), 52.4 (S*C*H_2CHAr), 47.7 (S*C*H_2CH_2), 42.7 (CHAr), 39.0 (*C*HCH_2OH), 26.9 (SCH_2CH_2); HRMS (ESI) ***m/z*** Calculated for $C_{15}H_{21}NO_4NaS$ [M+CH_3CN+Na] 334.1089; Found 334.1096.

cis-(±)-4,4-Difluoro-2-(4-methoxyphenyl)cyclohexyl)methanol (_cis_-107)



Prepared according to **General Procedure M** using **55** (396 mg, 1.00 mmol), Boc_2O (1.10 g, 5.00 mmol), DMAP (25 mg, 0.20 mmol) in MeCN (2 mL), then $LiAlH_4$ (156 mg, 4.00 mmol) and THF (5 mL + 2 mL). Purification by flash column chromatography (20% to 40% EtOAc/hexane) afforded ***cis*-107** as a yellow oil (69 mg, 0.27 mmol, 27% over 2 steps). R_f 0.30 (30% EtOAc/hexane); IR (film)/cm^{-1} 3370 (br OH), 2937, 1513, 1461, 1372, 1245 (S=O), 1103, 1005, 969; ^{1}H NMR (400 MHz, $CDCl_3$) δ 7.16–7.06 (m, 2 H, 2 × HC_{Ar}), 6.94–6.82 (m, 2 H, 2 × HC_{Ar}), 3.81 (s, 3 H, OCH_3), 3.54 (ddd, *J* = 10.8, 8.7, 6.3 Hz, 1 H, C*H*HOH), 3.46 (dt, *J* = 10.8, 4.1 Hz, 1 H, CH*H*OH), 3.25 (dd, *J* = 11.6, 5.6 Hz, 1 H, CHAr), 2.30–2.20 (m, 1 H, F_2CC*H*HCHAr), 2.20–2.10 (m, 3 H, C*H*CH_2OH, F_2CCH*H*CHAr and F_2CCH_2CH*H*), 2.07–1.99 (m, 1 H, F_2CC*H*HCH_2), 1.92–1.88 (m, 2 H, F_2CC*H*HCH_2 and F_2CCH_2CH*H*), 0.93 (dd, *J* = 6.5, 4.0 Hz, 1 H, OH); ^{13}C NMR (101 MHz, $CDCl_3$) δ 158.3 (C_{Ar} quat), 133.7 (C_{Ar} quat), 128.0 (2 × C_{Ar}), 124.0 (t, J_{CF} = 246.0 Hz, CF_2), 114.0 (2 × C_{Ar}), 59.6 (CH_2OH), 55.3 (OCH_3), 40.9 (*C*HCH_2OH), 40.4 (d, J_{CF} = 9.5 Hz, CHAr), 34.2 (dd, J_{CF} = 25.2, 22.8 Hz, F_2CCH_2CHAr), 29.1 (dd, J_{CF} = 25.2, 22.8 Hz, $F_2CCH_2CH_2$), 24.0 (d, J_{CF} = 9.5 Hz, $F_2CCH_2CH_2$); ^{19}F NMR (376 MHz, $CDCl_3$, 298 K) δ –87.13–-87.79 (m), –99.75–-100.62 (m); HRMS (APCI) ***m/z*** Calculated for $C_{14}H_{18}O_2F_2^+$ $[M+H]^+$ 256.1269; Found 256.1261.

trans-(±)-4,4-Difluoro-2-(4-methoxyphenyl)cyclohexyl)methanol (_trans_-98)

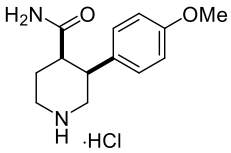


Prepared according to **General Procedure M** using **94** (300 mg, 0.75 mmol), Boc_2O (817 mg, 3.75 mmol), DMAP (19 mg, 0.15 mmol) in MeCN (2 mL), then $LiAlH_4$ (117 mg, 3.00 mmol) and THF (3.8 mL + 1.5 mL). Purification by flash column chromatography (20% to 40% EtOAc/hexane) afforded ***trans*-98** as an orange oil (63 mg, 0.25 mmol, 33% over 2 steps). R_f 0.35 (30% EtOAc/Hexane); IR (film)/cm^{-1} 3360 (OH), 2937, 1513, 1446, 1372, 1238, 1074, 962; ^{1}H NMR (400 MHz, $CDCl_3$) δ 7.17–7.06 (m, 2 H, 2 × HC_{Ar}), 6.93–6.80 (m, 2 H, 2 × HC_{Ar}), 3.80 (s, 3 H, OCH_3), 3.43 (dd, *J* = 10.8, 3.7 Hz, 1 H, C*H*HOH), 3.24 (dd, *J* = 10.8, 6.4 Hz, 1 H, CH*H*OH), 2.68 (ddd, *J* = 13.0, 11.2, 4.0 Hz, 1 H, CHAr), 2.31–2.14 (m, 2 H, F_2CC*H*HCHAr and F_2CC*H*HCH_2), 2.12–2.01 (m, 1 H, F_2CCH_2CHH), 1.98–1.75 (m, 2 H, F_2CCH*H*CHAr and F_2CCH*H*CH_2), 1.76–1.66 (m, 1 H, C*H*CH_2OH), 1.59 (ddd, *J* = 13.6, 12.3, 3.9 Hz, 1 H, F_2CCH_2CH*H*), 1.21 (s, 1 H, OH); ^{13}C NMR (101 MHz, $CDCl_3$) δ 158.5 (C_{Ar} quat), 134.5 (C_{Ar} quat), 128.2 (2 × C_{Ar}),123.2 (dd, J_{CF} = 243.0, 239.1 Hz, CF_2), 114.2 (2 × C_{Ar}), 65.0 (CH_2OH), 55.2 (OCH_3), 43.9 (*C*HCH_2OH), 42.4 (d, J_{CF} = 10.6 Hz, CHAr), 41.8 (dd, J_{CF} = 25.4, 22.2 Hz, F_2CCH_2CHAr), 33.4 (dd, J_{CF} = 25.4, 22.2 Hz, $F_2CCH_2CH_2$), 25.8 (d, J_{CF} = 10.6 Hz, $F_2CCH_2CH_2$); ^{19}F NMR (376 MHz, $CDCl_3$) δ –90.09–-95.75 (m), –101.19–-102.06 (m); HRMS (APCI) ***m/z*** Calculated for $C_{14}H_{18}O_2F_2^+$ $[M+H]^+$ 256.1269; Found 256.1269.

General Procedure O for the Boc-deprotection of Piperidine Substrates

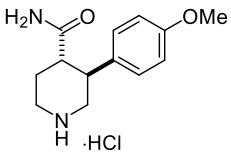
4 N HCl in 1,4-dioxane (10.0 equiv) was added to *N*-Boc protected piperidine (1.0 equiv) at 0 °C. The resulting solution was allowed to warm to rt and the reaction mixture stirred until a dense precipitate formed (1-3 h). Ice-cold Et_2O (5 mL) was added and the precipitate was separated by filtration under reduced pressure, washing with further ice-cold Et_2O (2 × 5 mL). The precipitate was then dried under reduced pressure to afford the deprotected piperidine product as the corresponding hydrochloride salt.

***cis*-(±)-4-Carbamoyl-3-(4-methoxyphenyl)piperidin-1-ium chloride (*cis*-111)**



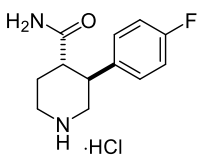
Prepared according to **General Procedure O** using *N*-Boc protected piperidine ***cis*-102** (100 mg, 0.30 mmol) and 4 N HCl in dioxane (0.8 mL, 3.20 mmol) to afford ***cis*-111** as a pale yellow solid (74 mg, 0.27 mmol, 92%). mp = 271–272 °C (from dioxane/Et_2O); IR (film)/cm^{-1} 3421 (NH br), 2995, 2957, 2833, 2533, 2363, 2115, 1641 (C=O), 1513, 1451, 1248, 1183, 1027, 831; ^{1}H NMR (400 MHz, CD_3OD) δ 7.22–7.14 (m, 2 H, 2 × HC_{Ar}), 6.91–6.86 (m, 2 H, 2 × HC_{Ar}), 4.17 (t, *J* = 12.3 Hz, 1 H, NC*H*HCHAr), 3.77 (s, 3 H, OCH_3), 3.76–3.65 (m, 1 H, NC*H*HCH_2), 3.31–3.20 (m, 3 H, NCH*H*CHAr, NCH*H*CH_2 and CHAr), 2.92 (dt, *J* = 6.8, 3.2 Hz, 1 H, CH(C=O)), 2.27–2.08 (m, 2 H, NCH_2CH_2); ^{13}C NMR (101 MHz, CD_3OD) δ 178.1 (C=O amide), 160.6 (C_{Ar} quat), 132.0 (C_{Ar} quat), 129.6 (2 × C_{Ar}), 115.1 (2 × C_{Ar}), 55.7 (OCH_3), 44.7 (NCH_2CHAr), 43.0 (*C*H(C=O)), 41.6 (CHAr), 41.0 (NCH_2CH_2), 27.1 (NCH_2CH_2); HRMS (ESI) *m/z* Calculated for $C_{13}H_{19}N_2O_2$ [M–Cl] 235.1447; Found 235.1454.

***trans*-(±)-4-Carbamoyl-3-(4-methoxyphenyl)piperidin-1-ium chloride (*trans*-111)**



Prepared according to **General Procedure O** using *N*-Boc protected piperidine ***trans*-102** (116 mg, 0.35 mmol) and 4 N HCl in dioxane (0.9 mL, 3.60 mmol) to afford ***trans*-111** as a pale yellow solid (78 mg, 0.29 mmol, 83%). mp not observed up to 280 °C (from dioxane/Et_2O); IR (film)/cm^{-1} 3355 (br NH), 3183 (br NH), 2952, 2803, 1670 (C=O), 1513, 1446, 1252, 1185, 835; ^{1}H NMR (400 MHz, CD_3OD) δ 7.31–7.19 (m, 2 H, 2 × HC_{Ar}), 6.96–6.85 (m, 2 H, 2 × HC_{Ar}), 3.78 (s, 3 H, OCH_3), 3.53 (ddt, *J* = 12.9, 4.3, 2.1 Hz, 1 H, NC*H*HCH_2), 3.37 (dd, *J* = 8.0, 1.4 Hz, 1 H, NC*H*HCHAr), 3.24–3.11 (m, 3 H, CHAr, NCH*H*CHAr and NCH*H*CH_2), 2.87 (ddt, *J* = 11.6, 8.4, 3.5 Hz, 1 H, CH(C=O)), 2.21–2.12 (m, 1 H, NCH_2CHH), 2.11–1.98 (m, 1 H, NCH_2CHH); ^{13}C NMR (101 MHz, CD_3OD) δ 177.4 (C=O amide), 160.7 (C_{Ar} quat), 131.6 (C_{Ar} quat), 130.0 (2 × C_{Ar}), 115.3 (2 × C_{Ar}), 55.7 (OCH_3), 49.4 (NCH_2CHAr), 47.7 (*C*H(C=O)), 44.3 (NCH_2CH_2), 42.8 (CHAr), 27.7 (NCH_2CH_2); HRMS (ESI) *m/z* Calculated for $C_{13}H_{19}N_2O_2$ [M-Cl] 235.1447; Found 235.1449.

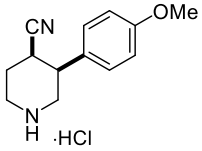
***trans*-(±)-4-Carbamoyl-3-(4-fluorophenyl)piperidin-1-ium chloride (*trans*-112)**



Prepared according to **General Procedure O** using *N*-Boc protected piperidine ***trans*-100** (145 mg, 0.45 mmol) and 4 N HCl in dioxane (1.2 mL, 4.80 mmol) to afford ***trans*-112** as a pale yellow solid (65 mg, 0.25 mmol, 55%). mp not observed up to 280 °C (from dioxane/Et_2O); IR (film)/cm^{-1} 3336 (br NH), 3178 (br NH), 2953, 2764, 2124, 1664 (C=O), 1605, 1510, 1422, 1224, 835, 538; ^{1}H NMR (400 MHz, CD_3OD) δ 7.43–7.27

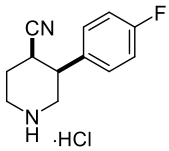
(m, 2 H, 2 × HC_{Ar}), 7.12–7.01 (m, 2 H, 2 × HC_{Ar}), 3.53 (dq, *J* = 12.7, 2.0 Hz, 1 H, NC*H*HCH_2), 3.38 (dq, *J* = 8.2, 1.8 Hz, 1 H, NC*H*HCHAr), 3.27–3.13 (m, 3 H, NCH*H*CH_2, NCH*H*CHAr and CHAr), 2.88 (td, *J* = 11.1, 4.0 Hz, 1 H, CH(C=O)), 2.16 (dtd, *J* = 14.5, 3.6, 2.3 Hz, 1 H, NCH_2C*H*H), 2.03 (dddd, *J* = 14.5, 13.6, 11.9, 4.2 Hz, 1 H, NCH_2CH*H*); ^{13}C NMR (101 MHz, CD_3OD) δ 177.0 (C=O amide), 163.8 (d, J_{CF} = 243.5 Hz, FC_{Ar} quat), 135.8 (d, J_{CF} = 3.2 Hz, F-*p*-C_{Ar} quat), 131.0 (d, J_{CF} = 8.2 Hz, 2 × F-*m*-C_{Ar}), 116.6 (d, J_{CF} = 22.0 Hz, 2 × F-*o*-C_{Ar}), 49.1 (N*C*H_2CHAr), 47.6 (*C*H(C=O)), 44.3 (N*C*H_2CH_2), 42.8 (CHAr), 27.7 (NCH_2*C*H_2); ^{19}F{^{1}H} NMR (376 MHz, CD_3OD) δ –116.68 (s); HRMS (ESI) *m/z* Calculated for $C_{12}H_{16}N_2OF$ [M-Cl] 223.1247; Found 223.1242.

cis-(±)-4-Cyano-3-(4-methoxyphenyl)piperidin-1-ium chloride (_cis_-109)



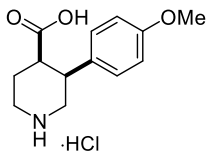
Prepared according to **General Procedure O** using *N*-Boc protected piperidine ***cis*-103** (110 mg, 0.35 mmol) and 4 N HCl in dioxane (0.9 mL, 3.60 mmol) to afford ***cis*-109** as a pale yellow solid (97 mg, 0.33 mmol, 94%). mp not observed up to 280 °C (from dioxane/Et_2O); IR (film)/cm^{-1} 3124, 2962, 2919, 2704, 2598, 1514, 1440, 1251 (CN), 1183, 1119, 1031, 817, 787; ^{1}H NMR (400 MHz, CD_3OD) δ 7.29 (d, *J* = 8.3 Hz, 2 H, 2 × HC_{Ar}), 6.96 (d, *J* = 8.4 Hz, 2 H, 2 × HC_{Ar}), 3.80 (s, 3 H, OCH_3), 3.61–3.49 (m, 4 H, NC*H*$_2$CHAr, CHCN and NC*H*HCH_2), 3.39 (dt, *J* = 11.9, 4.2 Hz, 1 H, CHAr), 3.29–3.17 (m, 1 H, NCH*H*CH_2), 2.36–2.26 (m, 2 H, NCH_2C*H*$_2$); ^{13}C NMR (101 MHz, CD_3OD) δ 161.1 (C_{Ar} quat), 130.4 (C_{Ar} quat), 129.4 (2 × C_{Ar}), 119.6 (CN), 115.4 (2 × C_{Ar}), 55.8 (OCH_3), 45.3 (N*C*H_2CHAr), 41.5 (N*C*H_2CH_2), 40.4 (CHAr), 34.2 (CHCN), 26.9 (NCH_2*C*H_2); HRMS (ESI) *m/z* Calculated for $C_{15}H_{20}N_3O$ [M+CH_3CN–Cl] 258.1606; Found 258.1613.

cis-(±)-3-(4-Fluorophenyl)piperidine-4-carbonitrile (_cis_-110)



Prepared according to **General Procedure O** using *N*-Boc protected piperidine ***cis*-104** (110 mg, 0.35 mmol) and 4 N HCl in dioxane (0.9 mL, 3.60 mmol) to afford ***cis*-110** as a pale yellow solid (70 mg, 0.28 mmol, 80%). mp = 250–252 °C (from dioxane/Et_2O); IR (film)/cm^{-1} 2918 (NH br), 2698 (NH br), 2234 (C=N), 1704, 1509, 1432, 1356, 1221, 1112, 1011, 968, 831; ^{1}H NMR (400 MHz, CD_3OD) δ 7.43–7.36 (m, 2 H, 2 × HC_{Ar}), 7.20–7.09 (m, 2 H, 2 × HC_{Ar}), 3.66–3.48 (m, 4 H, NC*H*$_2$CHAr *and* NC*H*$_2CH_2$), 3.40 (s, 1 H, CHAr), 3.23 (ddd, *J* = 13.5, 12.3, 4.7 Hz, 1 H, CHCN), 2.36–2.21 (m, 2 H, NCH_2C*H*$_2$); ^{13}C NMR (101 MHz, CD_3OD) δ 162.1 (d, J_{CF} = 243.5 Hz, FC_{Ar} quat), 134.8 (d, J_{CF} = 3.2 Hz, F-*p*-C_{Ar} quat), 131.3 (CN), 130.4 (d, J_{CF} = 8.4 Hz, 2 × F-*m*-CAr), 116.9 (d, J_{CF} = 21.7 Hz, 2 × F-*o*-CAr), 45.1 (N*C*H_2CHAr), 41.5 (CHAr), 40.5 (N*C*H_2CH_2), 34.0 (*C*HCN), 26.9 (NCH_2*C*H_2); ^{19}F{^{1}H} NMR (376 MHz, CD_3OD) δ –115.64 (s); HRMS (ESI) *m/z* Calculated for $C_{12}H_{14}N_2F$ [M–Cl] 205.1141; Found 205.1148.

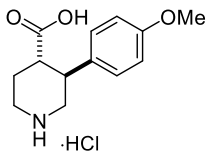
cis-(±)-4-Carboxy-3-(4-methoxyphenyl)piperidin-1-ium chloride (_cis_-113)



Prepared according to **General Procedure O** using *N*-Boc protected piperidine ***cis*-95** (151 mg, 0.45 mmol) and 4 N HCl in dioxane (1.2 mL, 4.80 mmol) to afford ***cis*-113** as a pale yellow solid (105 mg, 0.39 mmol, 86%). mp = 256–258 °C (from dioxane/Et_2O); IR (film)/cm^{-1} 3012 (OH br), 2937, 2825, 1707 (C=O), 1517, 1420,

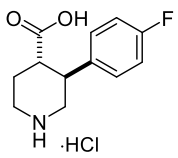
1252, 1156, 1122, 1029, 824, 705; ^{1}H NMR (400 MHz, CD_3OD) δ 7.20 (d, *J* = 8.7 Hz, 2 H, 2 × HC_{Ar}), 6.90 (d, *J* = 8.8 Hz, 2 H, 2 × HC_{Ar}), 4.01 (t, *J* = 12.5 Hz, 1 H, NC*H*HCHAr), 3.77 (s, 3 H, OCH_3), 3.47 (td, *J* = 12.3, 4.9 Hz, 1 H, NC*H*HCH_2), 3.42–3.32 (m, 2 H, NCH*H*CHAr, NCH*H*CH_2), 3.30–3.26 (m, 1 H, CHAr), 3.09 (q, *J* = 4.2 Hz, 1 H, CH(C=O)), 2.32–2.15 (m, 2 H, NCH_2C*H*$_2$); ^{13}C NMR (101 MHz, CD_3OD) δ 176.2 (C=O acid), 160.5 (C_{Ar} quat), 131.8 (C_{Ar} quat), 129.4 (2 × C_{Ar}), 115.1 (2 × C_{Ar}), 55.7 (OCH_3), 44.6 (N*C*H_2CHAr), 43.4 (*C*H(C=O)), 40.9 (N*C*H_2CH_2), 40.8 (CHAr), 26.2 (NCH_2*C*H_2); HRMS (ESI) *m/z* Calculated for $C_{13}H_{18}NO_3$ [M–Cl] 236.1287; Found 236.1290.

trans-(±)-4-Carboxy-3-(4-methoxyphenyl)piperidin-1-ium chloride (_trans_-113)



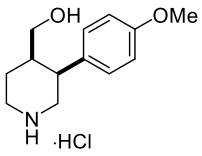
Prepared according to **General Procedure O** using *N*-Boc protected piperidine ***trans*-96** (110 mg, 0.33 mmol) and 4 N HCl in dioxane (0.8 mL, 3.20 mmol) to afford ***trans*-113** as a pale yellow solid (86 mg, 0.32 mmol, 98%). mp = 278–280 °C (from dioxane/Et_2O); IR (film)/cm^{-1} 2961 (OH), 2934, 2781, 1718 (C=O), 1513, 1249, 1182, 1125, 1026, 821; ^{1}H NMR (400 MHz, CD_3OD) δ 7.24 (d, *J* = 8.7 Hz, 2 H, 2 × HC_{Ar}), 6.89 (d, *J* = 8.7 Hz, 2 H, 2 × HC_{Ar}), 3.77 (s, 3 H, OCH_3), 3.52 (ddd, *J* = 12.0, 4.7, 2.6 Hz, 1 H, NC*H*HCH_2), 3.35 (ddd, *J* = 6.3, 3.6, 2.2 Hz, 1 H, NC*H*HCHAr), 3.23–3.08 (m, 3 H, NCH*H*CHAr, NCH*H*CH_2 and CHAr), 2.95 (td, *J* = 11.8, 3.6 Hz, 1 H, CH(C=O)), 2.27 (dq, *J* = 14.4, 3.1 Hz, 1 H, NCH_2C*H*H), 2.09–1.94 (m, 1 H, NCH_2CH*H*); ^{13}C NMR (101 MHz, CD_3OD) δ 176.1 (C=O acid), 160.8 (C_{Ar} quat), 131.7 (C_{Ar} quat), 130.0 (2 × C_{Ar}), 115.3 (2 × C_{Ar}), 55.7 (OCH_3), 48.6 (N*C*H_2CHAr), 47.1 (*C*H(C=O)), 44.2 (N*C*H_2CH_2), 43.0 (CHAr), 27.6 (NCH_2*C*H_2); HRMS (ESI) *m/z* Calculated for $C_{13}H_{18}NO_3$ [M-Cl] 236.1287; Found 236.1294.

trans-(±)-4-Carboxy-3-(4-fluorophenyl)piperidin-1-ium chloride (_trans_-114)



Prepared according to **General Procedure O** using *N*-Boc protected piperidine ***trans*-96** (114 mg, 0.35 mmol) and 4 N HCl in dioxane (0.9 mL, 3.60 mmol) to afford ***trans*-114** as a pale yellow solid (68 mg, 0.26 mmol, 75%). mp = 276–278 °C (from dioxane/Et_2O); IR (film)/cm^{-1} 3399 (br OH), 2949, 2806, 1720 (C=O), 1511, 1418, 1224, 1184, 1160, 1122, 833; ^{1}H NMR (400 MHz, CD_3OD) δ 7.40–7.32 (m, 2 H, 2 × HC_{Ar}), 7.12–7.03 (m, 2 H, 2 × HC_{Ar}), 3.58–3.49 (m, 1 H, NC*H*HCH_2), 3.38 (ddd, *J* = 12.0, 3.4, 1.3 Hz, 1 H, NC*H*HCHAr), 3.27–3.12 (m, 3 H, NCH*H*CH_2, NCH*H*CHAr and CHAr), 3.05–2.94 (m, 1 H, CH(C=O)), 2.29 (dq, *J* = 14.4, 2.9 Hz, 1 H, NCH_2C*H*H), 2.09–1.95 (m, 1 H, NCH_2CH*H*); ^{13}C NMR (101 MHz, CD_3OD) δ 175.8 (C=O acid), 163.7 (d, J_{CF} = 245 Hz, FC_{Ar} quat), 136.0 (d, J_{CF} = 3.2 Hz, F-*p*-C_{Ar} quat), 130.9 (d, J_{CF} = 8.3 Hz, 2 × F-*m*-C_{Ar}), 116.6 (d, J_{CF} = 21.7 Hz, 2 × F-*o*-C_{Ar}), 49.1 (N*C*H_2CHAr), 47.0 (*C*H(C=O)), 44.2 (N*C*H_2CH_2), 43.0 (CHAr), 27.5 (NCH_2*C*H_2); ^{19}F{^{1}H} NMR (376 MHz, CD_3OD) δ –116.62 (s); HRMS (ESI) *m/z* Calculated for $C_{12}H_{15}NO_2F$ [M-Cl] 224.1087; Found 224.1094.

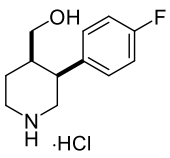
cis-(±)-4-(Hydroxymethyl)-3-(4-methoxyphenyl)piperidin-1-ium chloride (_cis_-115)



Prepared according to **General Procedure O** using *N*-Boc protected piperidine ***cis*-105** (115 mg, 0.36 mmol) and 4 N HCl in dioxane (0.9 mL, 3.60 mmol) to afford ***cis*-115** as a white solid (75 mg, 0.30 mmol, 82%). mp= 268–269 °C (from dioxane/Et_2O); IR (film)/cm^{-1} 3370 (OH br), 2958, 2835, 2490, 2126, 1515, 1249, 1183, 1033, 988;

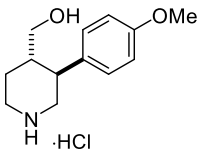
^{1}H NMR (400 MHz, CD_3OD) δ 7.19–7.11 (m, 2 H, 2 × HC_{Ar}), 6.96–6.89 (m, 2 H, 2 × HC_{Ar}), 3.78 (s, 3 H, OCH_3), 3.70–3.60 (m, 2 H, CH_2OH), 3.42–3.32 (m, 5 H, NC*H*$_2$CHAr, NC*H*$_2$CH$_2$ and CHAr), 2.25 (dq, *J* = 14.7, 2.8 Hz, 1 H, NCH$_2$C*H*H), 2.14 (m, 1 H, C*H*CH$_2$OH), 2.11–2.01 (m, 1 H, NCH$_2$CH*H*); ^{13}C NMR (101 MHz, CD_3OD) δ 160.3 (C_{Ar} quat), 132.4 (C_{Ar} quat), 129.4 (2 × C_{Ar}), 115.2 (2 × C_{Ar}), 60.2 (CH_2OH), 55.7 (OCH_3), 45.1 (N*C*H$_2$CHAr), 41.7 (CHAr), 41.3 (N*C*H$_2$CH$_2$), 39.7 (*C*HCH$_2$OH), 25.2 (NCH$_2$*C*H$_2$); HRMS (ESI) ***m/z*** Calculated for $C_{13}H_{20}NO_2$ [M–Cl] 222.1494; Found 222.1503.

cis-(±)-3-(4-Fluorophenyl)piperidin-4-yl)methanol (_cis_-116)



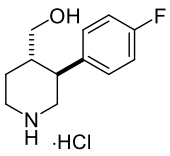
Prepared according to **General Procedure O** using *N*-Boc protected piperidine ***cis*-106** (95 mg, 0.30 mmol) and 4 N HCl in dioxane (0.8 mL, 3.20 mmol) to afford ***cis*-116** as a pale yellow solid (67 mg, 0.29 mmol, 97%). mp = 200–203 °C (from dioxane/Et_2O); IR (film)/cm^{-1} 3351 (OH br), 2927 (NH br), 2793, 1688, 1600, 1510, 1444,1363, 1225, 1161, 1020, 940, 821, 753; ^{1}H NMR (400 MHz, CD_3OD) δ 7.32–7.21 (m, 2 H, 2 × HC_{Ar}), 7.14–7.03 (m, 2 H, 2 × HC_{Ar}), 3.73–3.56 (m, 2 H, NC*H*HCH and C*H*HOH), 3.42–3.25 (m, 5 H, NC*H*$_2$CH$_2$, NCH*H*CH, CHAr, CH*H*OH), 2.24 (dq, *J* = 14.6, 2.8 Hz, 1 H, NCH$_2$C*H*H), 2.16–2.03 (m, 2 H, NCH$_2$CH*H* and C*H*CH$_2$OH); ^{13}C NMR (101 MHz, CD_3OD) δ 164.6 (d, *J* = 242.8 Hz, FC_{Ar} quat), 136.6 (d, *J* = 3.2 Hz, F-*p*-C_{Ar} quat), 130.2 (d, *J* = 8.1 Hz, 2 × F-*m*-C_{Ar}), 116.5 (d, *J* = 21.4 Hz, 2 × F-*o*-C_{Ar}), 60.3 (*C*H$_2$OH), 44.9 (N*C*H$_2$CH), 41.7 (N*C*H$_2$CH$_2$), 41.3 (CHAr), 39.5 (*C*HCH$_2$OH), 25.8 (NCH$_2$*C*H$_2$); ^{19}F NMR (376 MHz, CD_3OD) δ –117.45; HRMS (ESI) ***m/z*** Calculated for $C_{12}H_{17}NOF$ [M–Cl] 210.1294; Found 210.1297.

trans-(±)-4-(Hydroxymethyl)-3-(4-methoxyphenyl)piperidin-1-ium chloride (_trans_-115)



Prepared according to **General Procedure O** using *N*-Boc protected piperidine ***trans*-105** (140 mg, 0.43 mmol) and 4 N HCl in dioxane (1.1 mL, 4.40 mmol) to afford ***trans*-115** as a white solid (90 mg, 0.36 mmol, 83%). mp = 218–220 °C (from Et_2O/dioxane); IR (film)/cm^{-1} 3370 (br OH), 2952, 2803, 1513, 1252, 1178, 1029, 828; ^{1}H NMR (400 MHz, CD_3OD) δ 7.22 (d, *J* = 8.7 Hz, 2 H, 2 × HC_{Ar}), 6.92 (d, *J* = 8.7 Hz, 2 H, 2 × HC_{Ar}), 3.78 (s, 3 H, OCH_3), 3.52 (ddt, *J* = 12.7, 4.2, 2.0 Hz, 1 H, NC*H*HCH$_2$), 3.36 (dd, *J* = 10.9, 3.0 Hz, 1 H, C*H*HOH), 3.30–3.25 (m, 1 H, NC*H*HCHAr), 3.22–3.06 (m, 3 H, CH*H*OH, NCH*H*CH$_2$ and NCH*H*CHAr), 2.81 (td, *J* = 12.0, 4.2 Hz, 1 H, CHAr), 2.18 (dq, *J* = 14.5, 3.1 Hz, 1 H, NCH$_2$C*H*H), 2.07–1.93 (m, 1 H, C*H*CH$_2$OH), 1.75 (tdd, *J* = 14.1, 11.8, 4.3 Hz, 1 H, NCH$_2$CH*H*); ^{13}C NMR (101 MHz, CD_3OD) δ 160.7 (C_{Ar} quat), 132.2 (C_{Ar} quat), 129.9 (2 × C_{Ar}), 115.4 (2 × C_{Ar}), 63.8 (CH_2OH), 55.7 (OCH_3), 50.3 (N*C*H$_2$CHAr), 45.3 (N*C*H$_2$CH$_2$), 42.8 (CHAr), 42.6 (*C*HCH$_2$OH), 27.0 (NCH$_2$*C*H$_2$); HRMS (ESI) ***m/z*** Calculated for $C_{13}H_{20}NO_2$ [M-Cl] 222.1494; Found 222.1493.

trans-(±)-4-(Hydroxymethyl)-3-(4-fluorophenyl)piperidin-1-ium chloride (_trans_-116)

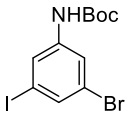


Prepared according to **General Procedure O** using *N*-Boc protected piperidine ***trans*-106** (155 mg, 0.50 mmol) and 4 N HCl in dioxane (1.3 mL, 5.20 mmol) to afford ***trans*-116** as a pale yellow solid (69 mg, 0.28 mmol, 56%). mp = 214–216 °C (from Et_2O/dioxane); IR (film)/cm^{-1} 3366 (br OH), 2984, 2796, 1510, 1224, 1161, 1093, 1068, 1032, 833; ^{1}H NMR (400 MHz, CD_3OD) δ 7.42–7.34 (m, 2 H, 2 × HC_{Ar}), 7.19–7.11 (m, 2 H, 2 × HC_{Ar}),

3.56 (ddt, *J* = 12.6, 4.1, 2.0 Hz, 1 H, NC*H*HCH$_2$), 3.41–3.33 (m, 2 H, C*H*HOH, NC*H*HCHAr), 3.26–3.13 (m, 3 H, NCH*H*CH$_2$, CH*H*OH and NCH*H*CHAr), 2.99–2.88 (m, 1 H, CHAr), 2.21 (dq, *J* = 14.5, 3.1 Hz, 1 H, NCH$_2$C*H*H), 2.05 (tdd, *J* = 11.7, 6.4, 3.2 Hz, 1 H, C*H*CH$_2$OH), 1.90–1.76 (m, 1 H, NCH$_2$CH*H*); ^{13}C NMR (101 MHz, CD$_3$OD) δ 164.6 (d, J_{CF} = 244.5 Hz, FC$_{Ar}$ quat), 136.4 (d, J_{CF} = 3.2 Hz, F-*p*-C$_{Ar}$ quat), 130.8 (d, J_{CF} = 8.0 Hz, 2 × F-*m*-C$_{Ar}$), 116.7 (d, J_{CF} = 21.4 Hz, 2 × F-*o*-C$_{Ar}$), 63.6 (CH$_2$OH), 50.0 (N*C*H$_2$CHAr), 45.2 (N*C*H$_2$CH$_2$), 42.7 (CHAr), 42.6 (*C*HCH$_2$OH), 26.9 (NCH$_2$*C*H$_2$); ^{19}F{^{1}H} NMR (376 MHz, CD$_3$OD) δ –116.85 (s); HRMS (ESI) *m/z* Calculated for C$_{12}$H$_{17}$NOF [M-Cl] 210.1294; Found 210.1303.

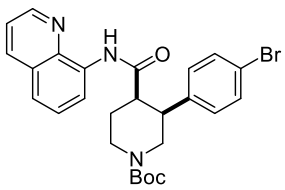
4.3.3 Synthesis of Building Blocks for DNA Encoded Libraries (DEL)

***tert*-Butyl 3-bromo-5-iodophenylcarbamate (136)**



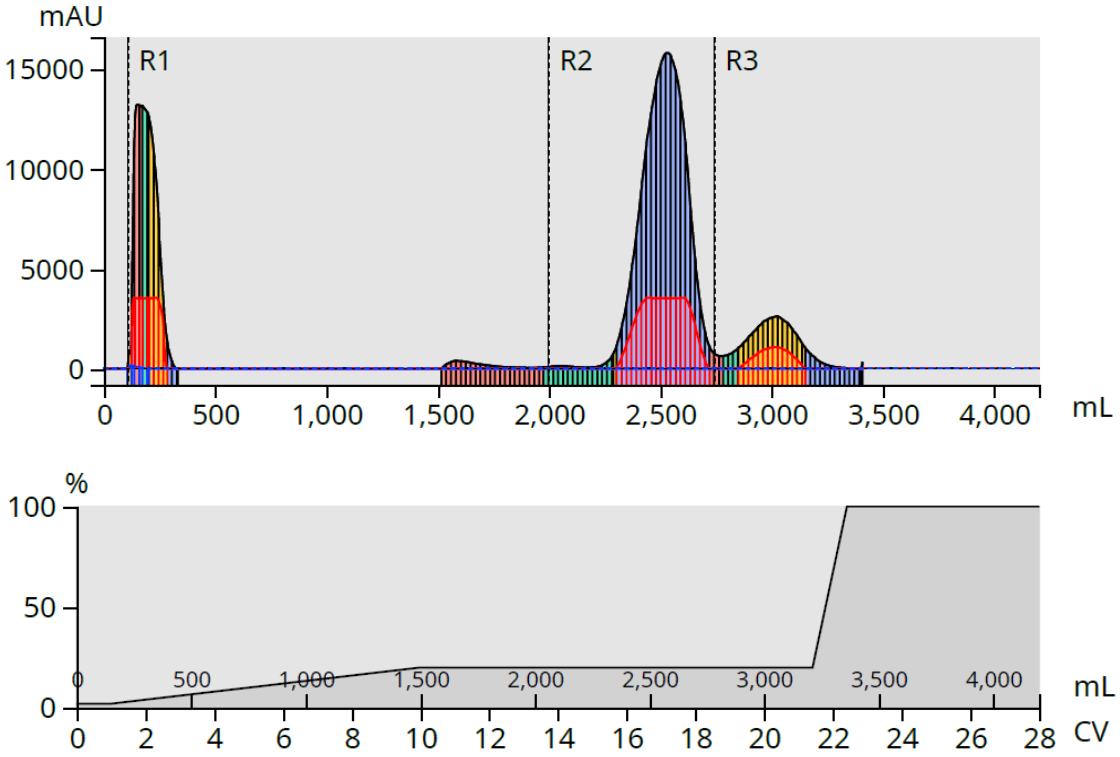
Freshly distilled triethylamine (Et$_3$N, 3.6 mL, 26.00 mmol, 1.3 equiv) and diphenylphosphorylazide (4.8 mL, 22.00 mmol, 1.1 equiv) were added to a solution of 3-bromo-5-iodobenzoic acid (6.54 g, 20.0 mmol 1.0 equiv) in *t*-butanol (40 mL) containing activated 4 Å molecular sieves. The reaction mixture was heated under reflux for 24 h, then concentrated under reduced pressure, diluted with Et$_2$O (30 mL), and washed with a 10% aq. NaOH solution (2 × 15 mL) and brine (2 × 15 mL). The organic layer was dried over Na$_2$SO$_4$, concentrated and the crude purified by flash column chromatography (10% EtOAc/hexane) to afford **136** as a white solid (6.10 g, 15.32 mmol, 77%). R$_f$ 0.35 (10% EtOAc/hexane); mp = 97–100 °C; ^{1}H NMR (400 MHz, CDCl$_3$,) δ 7.65 (s, 1 H, HC$_{Ar}$), 7.54 (s, 1 H, HC$_{Ar}$), 7.48 (s, 1 H, HC$_{Ar}$), 6.44 (br s, 1 H, NHBoc), 1.49 (s, 9 H, C(CH$_3$)$_3$); ^{13}C NMR (400 MHz, CDCl$_3$) 152.2 (C=O carbamate), 140.7 (C$_{Ar}$), 134.2 (C$_{Ar}$ quat), 125.8 (C$_{Ar}$ quat), 123.2 (C$_{Ar}$), 120.8 (C$_{Ar}$ quat), 94.3 (C$_{Ar}$), 81.7 (*C*(CH$_3$)$_3$), 28.5 (C(*C*H$_3$)$_3$); All characterisation information in agreement with data previously reported for the same compound.[249]

***tert*-Butyl-*cis*-(±)-3-(4-bromophenyl)-4-(quinolin-8-ylcarbamoyl)piperidine-1-carboxylate (46d)**

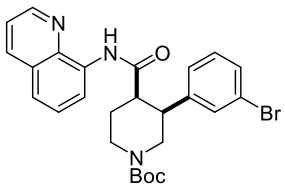


A flame-dried microwave vial (25 mL volume) was sequentially charged with amide **25** (710 mg, 2.00 mmol, 1.0 equiv), 1-bromo-4-iodobenzene (1.14 g, 4.00 mmol, 2.0 equiv), Ag$_2$CO$_3$ (690 mg, 2.50 mmol, 1.25 equiv), mesityl carboxylic acid (MesCOOH, 99 mg, 0.60 mmol, 0.3 equiv) and Pd(OAc)$_2$ (45 mg, 0.20 mmol, 0.1 equiv) in this order. The reaction vessel was sealed and purged with argon, then PhCF$_3$ (6.7 mL, 0.3 M) was added by syringe. The tube was placed in a preheated oil bath and stirred at 45 ºC for 24 h before cooling to rt and diluting with EtOAc (20 mL). The resulting mixture was filtered through a pad of Celite, eluting with further EtOAc (2 × 50 mL). The solvent was removed under reduced pressure, and the crude material was purified by automated flash column chromatography (silica, 0% to 100% acetone in pentane, see chromatogram below). The product containing fractions were combined and concentrated. Et$_2$O (10 mL) and pentane (10 mL) were added and the solvent was removed under reduced pressure to afford *cis*-arylated piperidine **46d** as a pale yellow crystalline solid (521 mg, 1.02 mmol, 51%). R$_f$ = 0.50 (5% Et$_2$O/CH$_2$Cl$_2$); mp = 128–130 °C (from CH$_2$Cl$_2$/Et$_2$O); All characterisation information in agreement with data previously reported for **46d**.

Automated Column Conditions: Run on Biotage® Selekt. Column Type: Biotage® Sfär HC 100 g. Flow Rate: 120 mL/min. Sample Mass: 3000 mg. Solvent A: pentane, Solvent B: acetone. UV wavelength detection: λ 200–400 nm. See trace and gradient below. From the left: 1st peak: unreacted aryl iodide. 2nd peak (red and green): mono-*trans* and di-*cis*-*trans* arylated side-products. 3rd peak (blue): *cis*-arylated product **46d**. 4th peak (yellow): unreacted **25**.



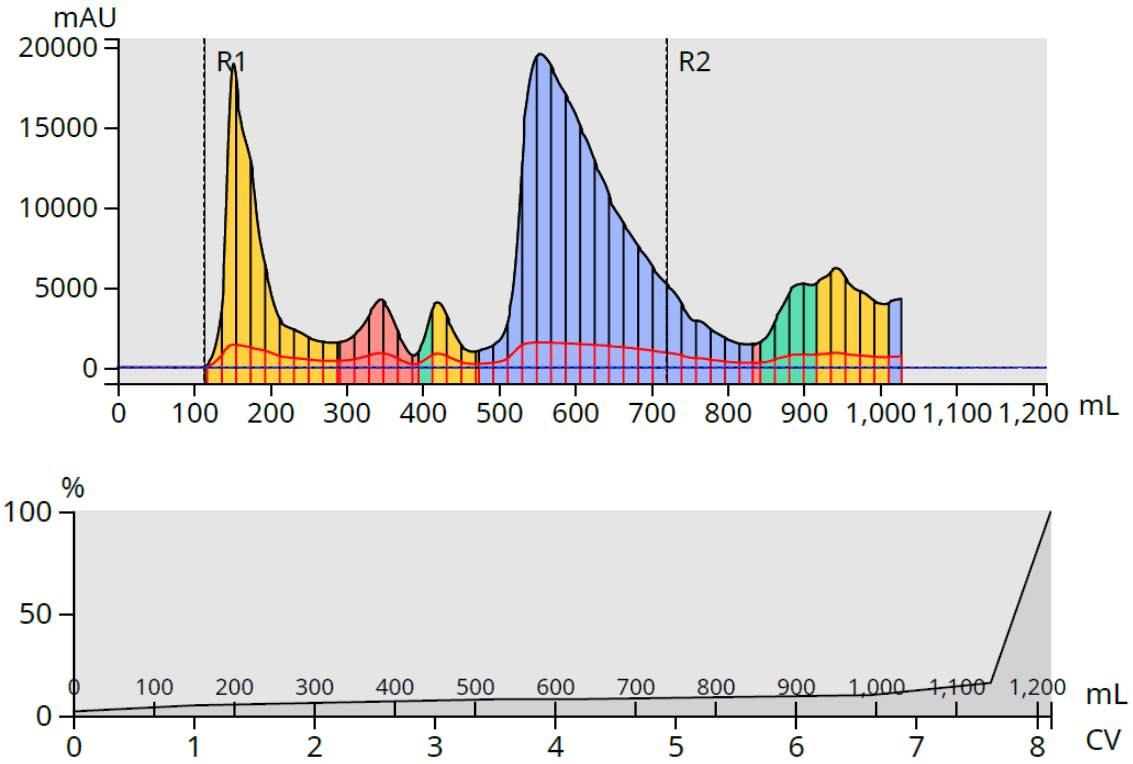
***tert*-Butyl-*cis*-(±)-3-(3-bromophenyl)-4-(quinolin-8-ylcarbamoyl)piperidine-1-carboxylate (46m)**



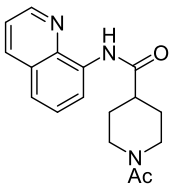
A flame-dried microwave vial (25 mL volume) was charged sequentially with amide **25** (1.06 g, 3.00 mmol, 1.0 equiv), 3-bromoiodobenzene (1.70 g, 6.00 mmol, 2.0 equiv), Ag_2CO_3 (1.03 g, 3.75 mmol, 1.25 equiv), MesCOOH (114 mg, 0.90 mmol, 0.3 equiv) and $Pd(OAc)_2$ (67 mg, 0.30 mmol, 0.1 equiv) in this order. The reaction vessel was sealed and purged with argon, then $PhCF_3$ (10 mL, 0.3 M) was added by syringe. The vial was placed in a preheated oil bath and stirred at 45 ºC for 24 h before cooling to rt and diluting with EtOAc (20 mL). The resulting mixture was filtered through a pad of Celite, eluting with further EtOAc (2 × 50 mL). The solvent was removed under reduced pressure, and the crude material was purified by automated flash column chromatography (2% to 5% Et_2O/CH_2Cl_2, see chromatogram below). The product containing fractions were combined and concentrated. Et_2O (10 mL) and pentane (10 mL) were added and the solvent was removed under reduced pressure to afford *cis*-arylated piperidine **46m** as a light pink crystalline solid (812 mg, 1.59 mmol, 53%). All characterisation information in agreement with data previously reported for **46m**.

Automated Column Conditions: Run on Biotage® Selekt. Column Type: Biotage® Sfär HC 100 g. Flow Rate: 120 mL/min. Sample Mass: 2500 mg. Solvent A: Dichloromethane, Solvent B: Diethyl Ether. UV

wavelength detection: λ 200–400 nm. See trace and gradient below. From the left: 1st peak (yellow): unreacted aryl iodide. 2nd and 3rd peaks (red and yellow): mono-*trans* and di-*cis*-*trans* arylated side-products. 3rd peak (blue): *cis*-arylated product **46m**. 4th peak (green/yellow): unreacted **25**.

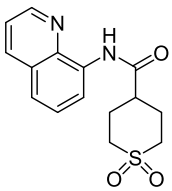


1-Acetyl-*N*-(quinolin-8-yl)piperidine-4-carboxamide (41)



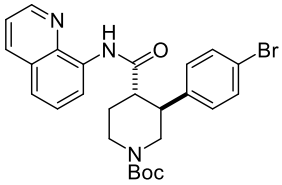
See Section 4.2.2 Scope of N-Protecting Group and Aryl Iodide for synthesis and characterisation

***N*-(Quinolin-8-yl)tetrahydro-2*H*-thiopyran-4-carboxamide 1,1-dioxide (51)**



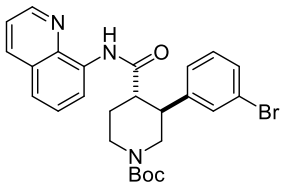
See Section 4.2.3 Heterocycle Scope for synthesis and characterisation

***tert*-Butyl-*trans*-(±)-3-(4-bromophenyl)-4-(quinolin-8-ylcarbamoyl)piperidine-1-carboxylate (61)**



See Section 4.2.8 One-Pot Arylation Epimerisation for synthesis, characterisation and chromatogram

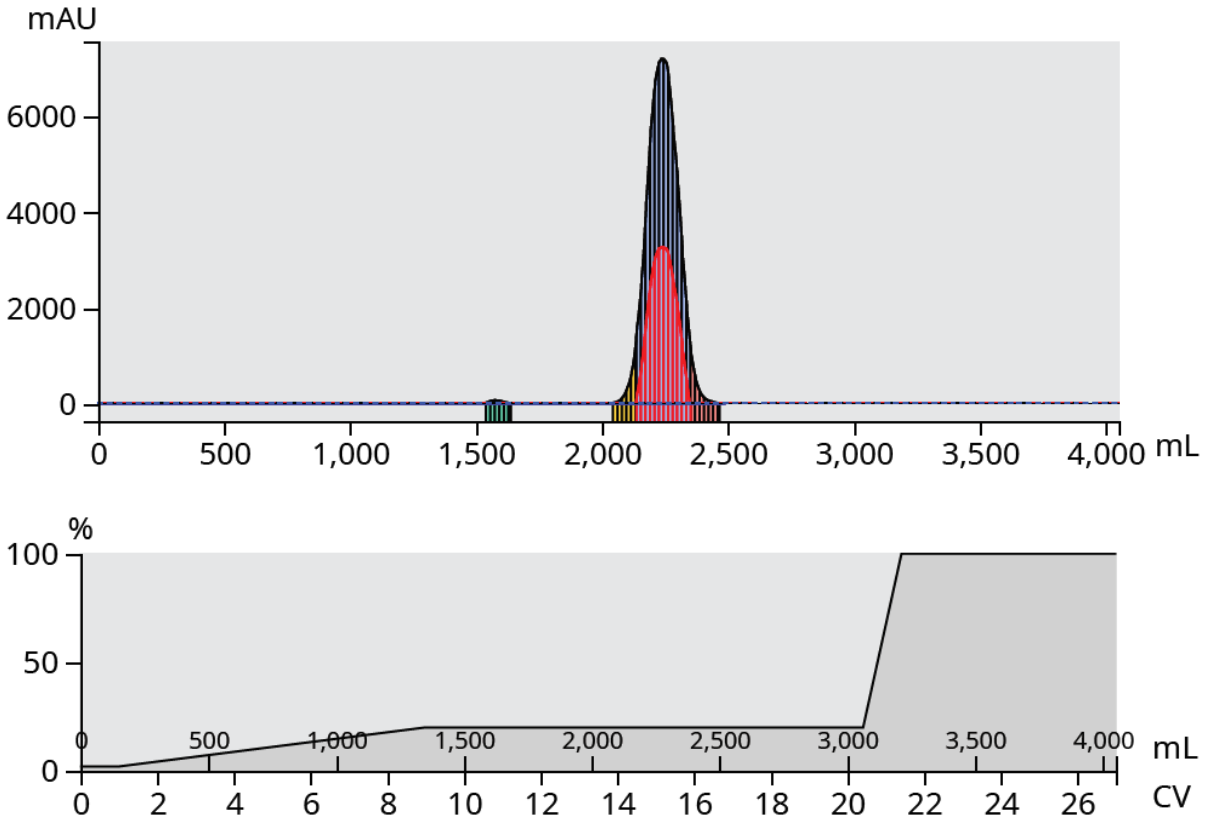
***tert*-Butyl-*trans*-(±)-3-(3-bromophenyl)-4-(quinolin-8-ylcarbamoyl)piperidine-1-carboxylate (*trans*-46m)**



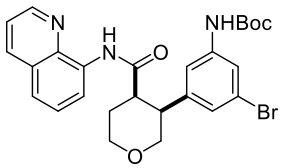
A flame-dried microwave vial (25 mL volume) was sequentially charged with amide **25** (710 mg, 2.00 mmol, 1.0 equiv), 3-bromoiodobenzene (1.14 g, 4.00 mmol, 2.0 equiv), Ag_2CO_3 (690 mg, 2.50 mmol, 1.25 equiv), MesCOOH (99 mg, 0.60 mmol, 0.3 equiv) and $Pd(OAc)_2$ (45 mg, 0.20 mmol, 0.1 equiv) in this order. The reaction vessel was sealed and purged with argon, then $PhCF_3$ (6.7 mL, 0.3 M) was added by syringe. The vial was placed in a preheated oil bath and stirred at 45 ºC for 24 h before cooling to rt and diluting with EtOAc (20 mL). The resulting mixture was filtered through a pad of Celite, eluting with further EtOAc (2 × 50 mL). The solvent was removed under reduced pressure, and the crude material was purified by flash column chromatography (5% to 8% Et_2O/CH_2Cl_2) to separate a mixture of *cis*-arylated piperidine **46m** (R_f 0.44 in 5% Et_2O/CH_2Cl_2) and *trans*-arylated piperidine ***trans*-46m** (R_f 0.37 in 5% Et_2O/CH_2Cl_2) in a 95:5 *cis*:*trans* d.r. (525 mg, 52% combined yield). A flame-dried microwave vial (25 mL volume) was charged with the mixture of *cis* and *trans*-arylated amides from the preivous step (95:5 d.r., 525 mg, 1.03 mmol, 1.0 equiv) and EtOH (7.0 mL, 0.15 M). NaOH powder (480 mg, 8.25 mmol, 8.0 equiv) was then added and the resulting mixture was stirred at 80 °C over an oil bath for 30 min. The reaction was allowed to cool down to rt and diluted with EtOAc (5 mL) and H_2O (5 mL). The phases were separated, and the aqueous layer was extracted with EtOAc (3 × 10 mL). The combined organic extracts were dried over Na_2SO_4 and filtered. The solvent was removed under reduced pressure and the crude material purified by automated flash column chromatography (2% to 20% acetone/pentane, see chromatogram below). The product containing fractions were combined and the solvent was removed under reduced pressure to afford *trans*-arylated piperidine ***trans*-46m** as a pale orange foam (425 mg, 0.82 mmol, 42% over 2 steps). R_f 0.35 (17% acetone/pentane); mp = 95–98 °C (from Et_2O/pentane); IR (film)/cm^{-1} 3388 (NH br), 2998, 2974, 2888, 1655 (C=O), 1525 (C=O), 1483, 1423, 1245, 1163, 910, 828, 731; ^{1}H NMR (500 MHz, DMSO-d_6, 373 K) δ 9.74 (br s, 1 H, NH), 8.87 (dd, *J* = 4.2, 1.7 Hz, 1 H, HC_{Ar}), 8.40 (dd, *J* = 7.7, 1.3 Hz, 1 H, HC_{Ar}), 8.31 (dd, *J* = 8.3, 1.7 Hz, 1 H, HC_{Ar}), 7.63–7.53 (m, 3 H, 3 × HC_{Ar}), 7.46 (t, *J* = 7.9 Hz, 1 H, HC_{Ar}), 7.34 (ddd, *J* = 7.7, 1.7, 1.1 Hz, 1 H, HC_{Ar}), 7.26 (ddd, *J* = 8.0, 2.0, 1.0 Hz, 1 H, HC_{Ar}), 7.22–7.12 (m, 1 H, HC_{Ar}), 4.13 (ddt, *J* = 13.3, 4.4, 2.2 Hz, 1 H, NC*H*HCH), 4.05–3.98 (m, 1 H, NC*H*HCH_2), 3.35–3.28 (m, 1 H, NCH*H*CH), 3.03–2.95 (m, 3 H, NCH*H*CH_2, CH(C=O) and CHAr), 2.04 (dq, *J* = 13.1, 2.8 Hz, 1 H, NCH_2CHH), 1.73 (tdd, *J* = 12.9, 11.6, 4.5 Hz, 1 H, NCH_2CH*H*), 1.45 (s, 9 H, $C(CH_3)_3$); ^{13}C NMR (126 MHz, DMSO-d_6, 373 K) δ 171.2 (C=O amide), 153.5 (C=O carbamate), 148.0 (C_{Ar}), 143.5 (C_{Ar} quat), 137.7 (C_{Ar} quat), 135.8 (C_{Ar}), 133.6 (C_{Ar} quat), 129.9 (C_{Ar}), 129.8 (C_{Ar}), 129.1 (C_{Ar}), 127.2 (C_{Ar} quat), 126.3 (C_{Ar}), 126.1 (C_{Ar}), 121.3 (C_{Ar} and C_{Ar} quat), 121.2 (C_{Ar}), 116.0 (C_{Ar}), 78.5 (*C*$(CH_3)_3$), 48.7 (N*C*H_2CH), 48.5 (*C*H(C=O)), 44.1 (CHAr), 42.5 (N*C*H_2CH_2), 28.6 (NCH_2*C*H_2), 27.6 (C(*C*$H_3)_3$); HRMS (ESI) *m/z* Calculated for $C_{26}H_{29}{}^{79}BrN_3O_3$ [M+H] 510.1392; Found 510.1410.

Automated Column Conditions: Run on Biotage® Selekt. Column Type: Biotage® Sfär HC 100 g. Flow Rate: 120 mL/min. Sample Mass: 3000 mg. Solvent A: pentane, Solvent B: acetone. UV wavelength

detection: λ 200–400 nm. See trace and gradient below. From the left: 1st peak (green): unreacted mono-*cis* arylated piperidine. 2nd peak (blue): desired epimerised product ***trans*-46m**.



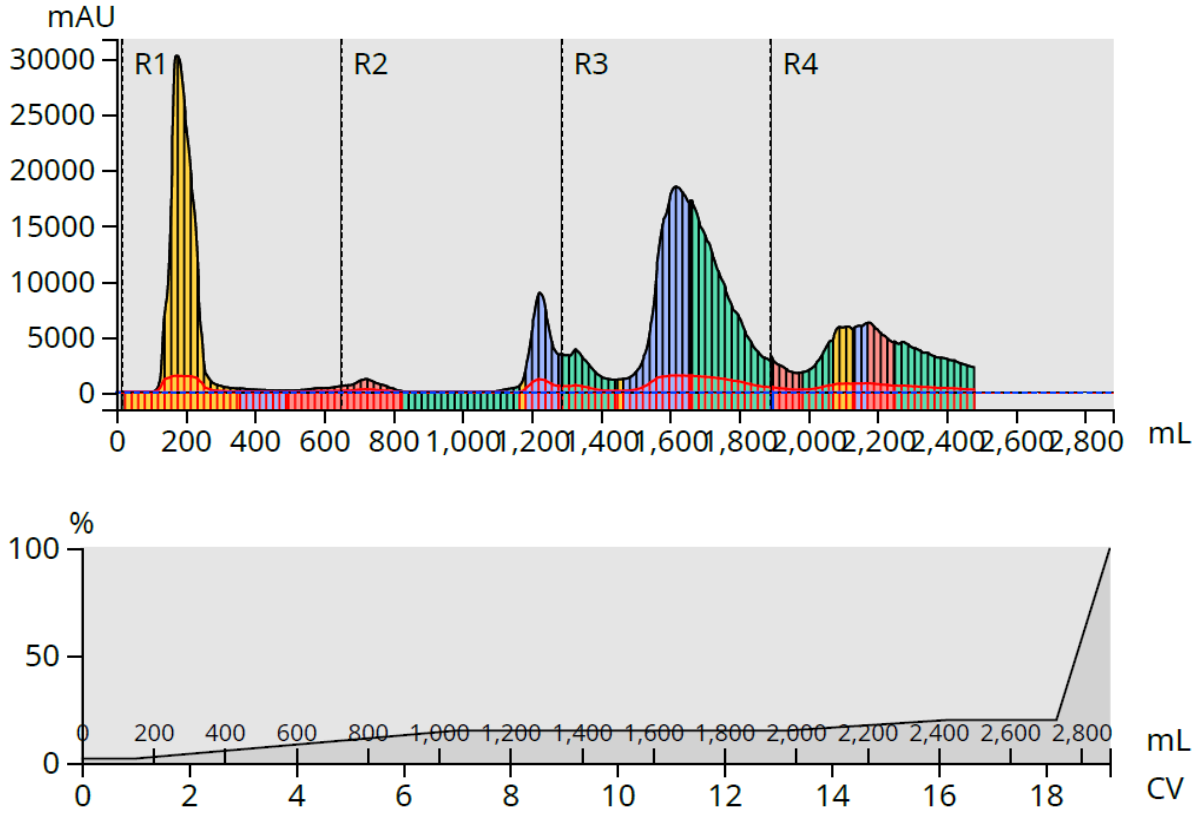
***tert*-Butyl-*cis*-(±)-(3-bromo-5-4-(quinolin-8-ylcarbamoyl)tetrahydro-2*H*-pyran-3-yl)phenyl) carbamate (53j)**



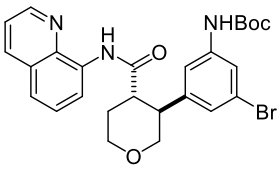
A flask was charged with amide **49** (1.03 g, 4.00 mmol, 1.0 equiv), *tert*-butyl (3-bromo-5-iodophenyl)carbamate (4.70 g, 12.00 mmol, 3.0 equiv), Ag_2CO_3 (1.65 g, 6.00 mmol, 1.50 equiv), MesCOOH (197 mg, 1.2 mmol, 0.3 equiv) and $Pd(OAc)_2$ (90 mg, 0.40 mmol, 0.1 equiv) in this order. The reaction vessel was covered with a suba seal and purged with argon, then $PhCF_3$ (16 mL) was added by syringe. The flask was placed in a preheated oil bath and stirred at 50 °C for 24 h before cooling to rt and diluting with EtOAc (10 mL). The resulting mixture was filtered through a pad of Celite, eluting with further EtOAc (2 × 15 mL). The solvent was removed under reduced pressure and the crude material purified by automated flash column chromatography (3% to 8% MeCN/CH_2Cl_2, see chromatogram below). Et_2O (5 mL), followed by pentane (5 mL) were added to the isolated product, with the resulting suspension concentrated under reduced pressure. This procedure was repeated three times to eliminate residual solvent and afford **53j** as a pale yellow crystalline solid (536 mg, 1.02 mmol, 26%). All characterisation information in agreement with data previously reported for **53j**.

Automated Column Conditions: Run on Biotage® Selekt. Column Type: Biotage® Sfär HC 100 g. Flow Rate: 120 mL/min. Sample Mass: 3000 mg. Solvent A: Dichloromethane, Solvent B: Acetonitrile. UV

wavelength detection: λ 200–400 nm. See trace and gradient below. From the left: 1st peak (yellow): unreacted aryl iodide. 2nd peak (red): di-*cis*-*trans* arylated side-product. 3rd peak (blue and green): di-*cis*-*cis* arylated side-product. 4th peak (blue/green): *cis*-arylated product **53j**. 5th peak: unreacted **49** and traces of mono-*trans* arylated side-product.



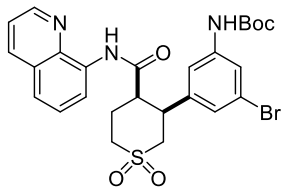
tert-Butyl-_trans_-(±)-(3-bromo-5-4-(quinolin-8-ylcarbamoyl)tetrahydro-2*H*-pyran-3-yl)phenyl) carbamate (_trans_-53j)



A flame-dried microwave vial (25 mL volume) was sequentially charged with amide **49** (1.03 g, 4.00 mmol, 1.0 equiv), *tert*-butyl (3-bromo-5-iodophenyl)carbamate (4.70 g, 12.00 mmol, 3.0 equiv), Ag_2CO_3 (1.65 g, 6.00 mmol, 1.50 equiv), MesCOOH (197 mg, 1.2 mmol, 0.3 equiv) and $Pd(OAc)_2$ (90 mg, 0.40 mmol, 0.1 equiv). The reaction vessel was covered with a suba seal and purged with argon, then $PhCF_3$ (16 mL) was added by syringe. The tube was placed in a preheated oil bath and stirred at 50 °C for 24 h. The reaction was allowed to cool to rt and 1,8-diazabicyclo[5.4.0]undec-7-ene (DBU, 0.6 mL, 3.90 mmol, 3.0 equiv) was added by syringe. The mixture was then stirred at 110 °C for an additional 24 h before cooling to rt and diluting with EtOAc (15 mL). The suspension was filtered through a pad of Celite, eluting with further EtOAc (2 × 40 mL). The solvent was removed under reduced pressure, and the crude material was purified by flash column chromatography (10% to 30% acetone/pentane) affording the *trans*-arylated product ***trans*-53j** as a white solid (255 mg, 0.50 mmol, 13%). R_f 0.31 (20% acetone/pentane); mp = 165–167 °C; IR (film)/cm^{-1} 3317 (NH br), 2967, 2837, 1722 (C=O), 1677 (C=O), 1599, 1453, 1521, 1424, 1323, 1238, 1156, 1092, 828, 790, 690; ^1H NMR (400 MHz, $CDCl_3$) δ 9.66 (br

s, 1 H, NH), 8.78 (dd, *J* = 4.2, 1.7 Hz, 1 H, HC_{Ar}), 8.61 (dd, *J* = 5.0, 4.0 Hz, 1 H, HC_{Ar}), 8.12 (dd, *J* = 8.3, 1.7 Hz, 1 H, HC_{Ar}), 7.51–7.40 (m, 4 H, 4 × HC_{Ar}), 7.15 (t, *J* = 1.6 Hz, 1 H, HC_{Ar}), 7.11 (t, *J* = 1.8 Hz, 1 H, HC_{Ar}), 6.44 (br s, 1 H, NHBoc), 4.23–4.12 (m, 1 H, OC*H*HCHAr), 4.01 (dd, *J* = 11.5, 4.4 Hz, 1 H, OC*H*HCH$_2$), 3.61 (td, *J* = 12.1, 2.3 Hz, 1 H, OCH*H*CHAr), 3.49–3.40 (m, OCH*H*CH$_2$), 3.22 (td, *J* = 11.2, 4.4 Hz, 1 H, CHAr), 3.04–2.89 (m, 1 H, CH(C=O)), 2.25–2.12 (m, 1 H, OCH$_2$C*H*H), 2.12–1.98 (m, 1 H, OCH$_2$CH*H*), 1.46 (s, 9 H, C(C*H*$_3$)$_3$); ^{13}C NMR (101 MHz, $CDCl_3$) δ 171.3 (C=O amide), 152.0 (C=O carbamate), 148.0 (C_{Ar}), 142.7 (C_{Ar} quat), 139.3 (C_{Ar} quat), 138.8 (C_{Ar} quat), 136.3 (C_{Ar}), 133.7 (C_{Ar} quat), 127.8 (C_{Ar} quat), 127.2 (C_{Ar}), 126.3 (C_{Ar}), 122.8 (C_{Ar} quat), 121.7 (C_{Ar}), 121.6 (C_{Ar}), 119.7 (C_{Ar}), 117.2 (C_{Ar}), 116.6 (C_{Ar}), 80.7 (*C*(CH$_3$)$_3$), 69.8 (O*C*H$_2$CH), 66.0 (O*C*H$_2$CH$_2$), 47.1 (CH(C=O)), 42.8 (*C*HAr), 28.2 (C(*C*H$_3$)$_3$), 25.5 (OCH$_2$*C*H$_2$); HRMS (ESI) *m/z* Calculated for $C_{26}H_{29}{}^{79}BrN_3O_4$ [M+H] 526.1341; Found 526.1356.

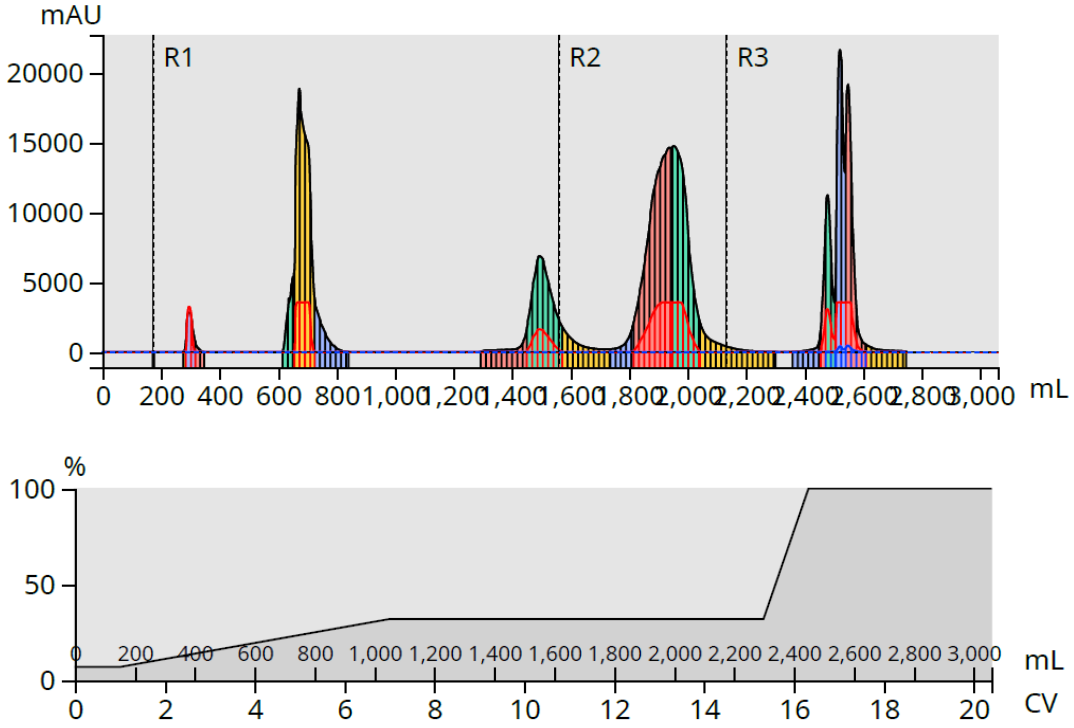
tert-Butyl-_cis_-(±)-(3-bromo-5-1,1-dioxido-4-(quinolin-8-ylcarbamoyl)tetrahydro-2_H_-thiopyran-3-yl)phenyl)carbamate (147)



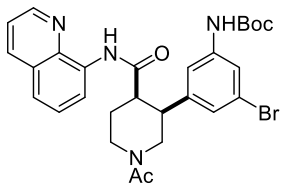
A flask was charged with amide **51** (1.22 g, 4.00 mmol, 1.0 equiv), *tert*-butyl (3-bromo-5-iodophenyl)carbamate (4.70 g, 12.00 mmol, 3.0 equiv), Ag_2CO_3 (138 mg, 8.00 mmol, 2.0 equiv), MesCOOH (197 mg, 1.20 mmol, 0.3 equiv) and $Pd(OAc)_2$ (90 mg, 0.40 mmol, 0.1 equiv) in this order. The reaction vessel was covered with a suba seal and purged with argon, then $PhCF_3$ (16 mL) was added by syringe. The flask was placed in a preheated oil bath and stirred at 50 °C for 24 h before cooling to rt and diluting with EtOAc (10 mL). The resulting mixture was filtered through a pad of Celite, eluting with further EtOAc (2 × 15 mL). The solvent was removed under reduced pressure and the crude material purified by automated flash column chromatography (2% to 100% acetone/pentane, see chromatogram below) to afford arylated sulfone **147** as a white solid (1.12 g, 1.92 mmol, 48%). R_f 0.31 (20% acetone/pentane); mp = 210–212 °C; IR (film)/cm^{-1} 3323 (NH br), 2974, 2926, 1723 and 1674 (C=O), 1580 (C=O), 1525, 1483, 1315, 1282, 1156 (S=O), 1118 (S=O), 849, 790, 530, 447; ^{1}H NMR (400 MHz, $CDCl_3$) δ 9.36 (br s, 1 H, NH amide), 8.64 (dd, *J* = 4.3, 1.6 Hz, 1 H, HC_{Ar}), 8.59 (dd, *J* = 4.9, 4.0 Hz, 1 H, HC_{Ar}), 8.11 (dd, *J* = 8.3, 1.7 Hz, 1 H, HC_{Ar}), 7.53–7.46 (m, 2 H, 2 × HC_{Ar}), 7.41 (dd, *J* = 8.3, 4.2 Hz, 1 H, HC_{Ar}), 7.34 (s, 1 H, HC_{Ar}), 7.09 (t, *J* = 1.8 Hz, 1 H, HC_{Ar}), 7.01 (t, *J* = 1.7 Hz, 1 H, HC_{Ar}), 6.37 (s, 1 H, NHBoc), 4.35 (t, *J* = 13.3 Hz, 1 H, SC*H*HCHAr), 4.03 (td, *J* = 13.4, 4.5 Hz, 1 H, SC*H*HCH$_2$), 3.77 (dt, *J* = 13.6, 3.5 Hz, 1 H, SCH*H*CHAr), 3.13–2.96 (m, 3 H, SCH*H*CH$_2$, CH(C=O) and CHAr), 2.57 (tdt, *J* = 18.1, 10.7, 4.0 Hz, 2 H, SCH$_2$C*H*H and SCH$_2$CH*H*), 1.45 (s, 9 H, C(CH$_3$)$_3$); ^{13}C NMR (126 MHz, $CDCl_3$) δ 170.4 (C=O amide), 151.9 (C=O carbamate), 148.1 (C_{Ar}), 142.0 (C_{Ar} quat), 140.1 (C_{Ar} quat), 138.1 (C_{Ar} quat), 136.3 (C_{Ar}), 133.2 (C_{Ar} quat), 127.7 (C_{Ar} quat), 127.0 (C_{Ar}), 124.5 (C_{Ar}), 123.2 (C_{Ar} quat), 122.3 (C_{Ar}), 121.7 (C_{Ar}), 120.3 (C_{Ar}), 116.9 (C_{Ar}), 115.4 (C_{Ar}), 81.1 (*C*(CH$_3$)$_3$), 51.1 (S*C*H$_2$CHAr), 47.0 (S*C*H$_2$CH$_2$), 45.4 (*C*H(C=O)), 43.8 (CHAr), 28.2 (C(*C*H$_3$)$_3$), 27.2 (SCH$_2$*C*H$_2$); HRMS (ESI) *m/z* Calculated for $C_{26}H_{29}{}^{79}BrN_3O_5S$ [M+H] 574.0888; Found 574.0880.

Automated Column Conditions: Run on Biotage® Selekt. Column Type: Biotage® Sfär HC 100 g. Flow Rate: 120 mL/min. Sample Mass: 3000 mg. Solvent A: pentane, Solvent B: acetone. UV wavelength

detection: λ 200–400 nm. See trace and gradient below. From the left: 1st peak (yellow): unreacted aryl iodide with traces of $PhCF_3$ solvent. 2nd peak (green): di-arylated side-products. 3rd peak (red/green): *cis*-arylated product **146**. 4th peak: mono-*trans* arylated side-product and unreacted **51**.



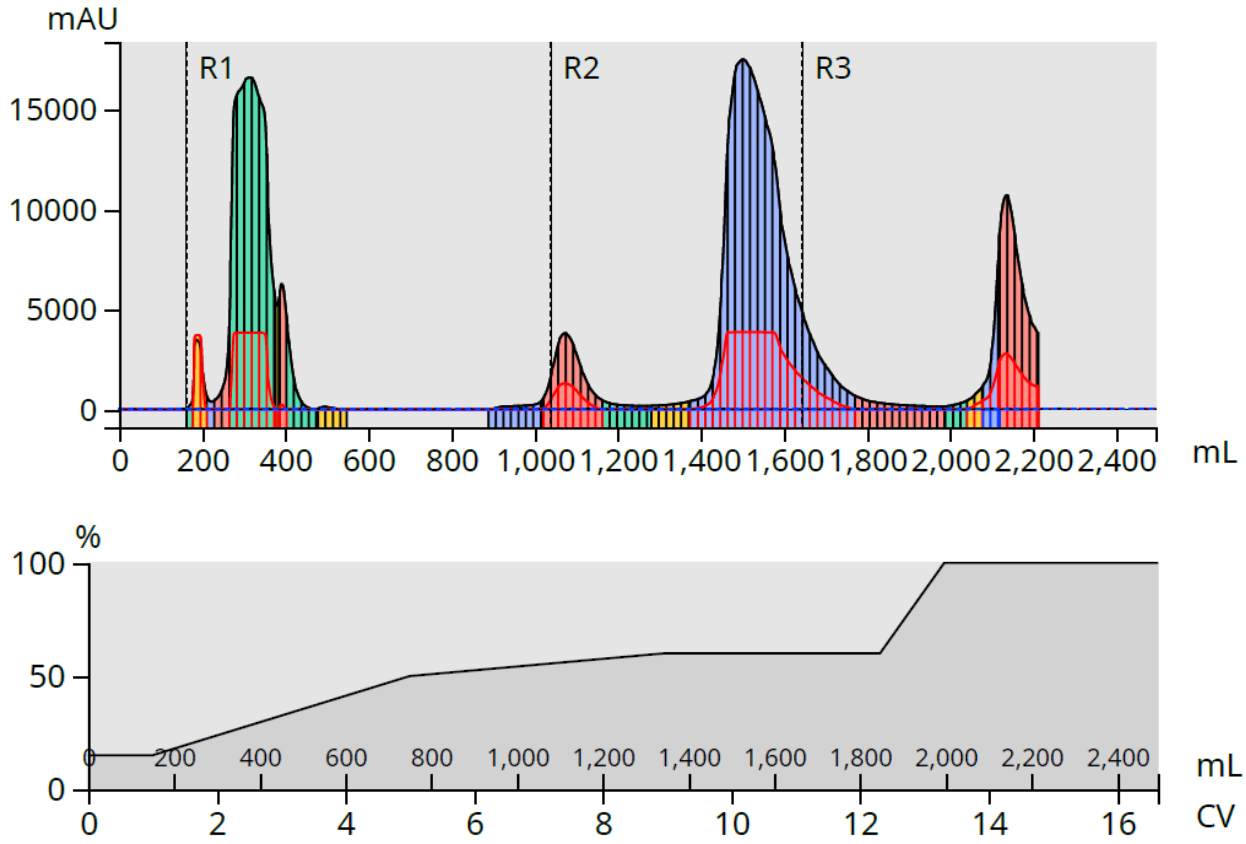
***tert*-Butyl-*cis*-(±)-1-acetyl-4-(quinolin-8-ylcarbamoyl)piperidin-3-yl)-5-bromophenyl)carbamate (144)**



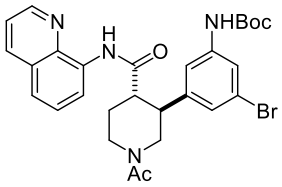
A flame-dried microwave vial (25 mL volume) was charged sequentially with amide **41** (1.20 g, 4.00 mmol, 1.0 equiv), *tert*-butyl (3-bromo-5-iodophenyl)carbamate (3.20 g, 8.04 mmol, 2.0 equiv), Ag_2CO_3 (1.37 g, 5.00 mmol, 1.25 equiv), MesCOOH (152 mg, 1.20 mmol, 0.3 equiv) and $Pd(OAc)_2$ (89 mg, 0.40 mmol, 0.1 equiv) in this order. The reaction vessel was sealed and purged with argon, then $PhCF_3$ (13.4 mL) was added by syringe. The vial was placed in a preheated oil bath and stirred at 45 ºC for 24 h before cooling to rt and diluting with EtOAc (20 mL). The resulting mixture was filtered through a pad of Celite, eluting with further EtOAc (2 × 50 mL). The solvent was removed under reduced pressure, and the crude material was purified by automated flash column chromatography (2% to 100% acetone/pentane, see chromatogram below). The product containing fractions were combined and concentrated. Et_2O (10 mL) and pentane (10 mL) were added and the solvent was removed under reduced pressure to afford *cis*-arylated piperidine 1**44** as a bright yellow foam (1.28 g, 2.24 mmol, 56%). R_f 0.48 (50% acetone/pentane); mp = 140–142 °C; IR (film)/cm^{-1} 3668 (NH br), 3324 (NH br), 2974, 2926, 1722 (C=O), 1681 (C=O), 1629 (C=O), 1528, 1453, 1368, 1245, 1159, 1055; ^{1}H NMR (400 MHz, DMSO-d_6, 373 K) δ 9.63 (br s, 1 H, NH amide), 8.97 (s, 1 H, NBoc), 8.81 (dd, J = 4.2, 1.7 Hz, 1 H, HC_{Ar}), 8.43 (dd, J = 7.7, 1.4 Hz, 1 H, HC_{Ar}), 8.35–8.28 (m, 1 H, HC_{Ar}), 7.61–7.54 (m, 2 H, 2 × HC_{Ar}), 7.50 (d, J = 7.9 Hz, 1 H, HC_{Ar}), 7.44–7.38 (m, 2 H, 2 × HC_{Ar}), 7.05 (t, J =

1.7 Hz, 1 H, HC_{Ar}), 3.97 (br s, 1 H, NC*H*HCHAr), 3.87 (br s, 2 H, NC*H*HCH$_2$ and NCH*H*CHAr), 3.70 (br s, 1 H, NCH*H*CH$_2$), 3.43–3.36 (m, 1 H, CH(C=O)), 3.26 (br s, 1 H, CHAr), 2.18–2.09 (m, 1 H, NCH$_2$C*H*H), 2.05 (s, 3 H, (C=O)CH$_3$), 1.94 (td, J = 8.8, 3.8 Hz, 1 H, NCH$_2$CH*H*), 1.44 (s, 9 H, C(CH$_3$)$_3$); ^{13}C NMR (101 MHz, DMSO-*d*$_6$, 373 K) δ 171.1 (C=O amide), 168.0 (C=O acetyl), 151.9 (C=O carbamate), 147.9 (C_{Ar}), 143.2 (C_{Ar} quat), 140.5 (C_{Ar} quat), 137.8 (C_{Ar} quat), 135.7 (C_{Ar}), 133.6 (C_{Ar} quat), 127.4 (C_{Ar} quat), 126.1 (C_{Ar}), 123.8 (C_{Ar}), 121.2 (2 × C_{Ar}), 120.7 (C_{Ar} quat), 118.5 (C_{Ar}), 116.3 (C_{Ar}), 116.2 (C_{Ar}), 78.9 (*C*(CH$_3$)$_3$), 44.8 (*C*H(C=O)), 42.1 (N*C*H$_2$CH$_2$), 40.2 (CHAr), 27.6 (C(*C*H$_3$)$_3$), 26.1 (NCH$_2$*C*H$_2$), 20.5 ((C=O)*C*H$_3$); Due to rotamer interconversion occurring even at high temperatures (373 K) and resulting in peak broadening, N*C*H$_2$CH was not observed; HRMS (ESI) *m/z* Calculated for $C_{28}H_{32}{}^{79}BrN_4O_4$ [M+H] 566.1529; Found 566.1522.

Automated Column Conditions: Run on Biotage® Selekt. Column Type: Biotage® Sfär HC 100 g. Flow Rate: 120 mL/min. Sample Mass: 3000 mg. Solvent A: pentane, Solvent B: acetone. UV wavelength detection: λ 200–400 nm. See trace and gradient below. From the left: 1st peak (green): unreacted aryl iodide with traces of $PhCF_3$ solvent. 2nd peak (red): di-arylated side-products. 3rd peak (blue): *cis*-arylated product **144**. 4th peak (red): mono-*trans* arylated side-product and unreacted **41**.

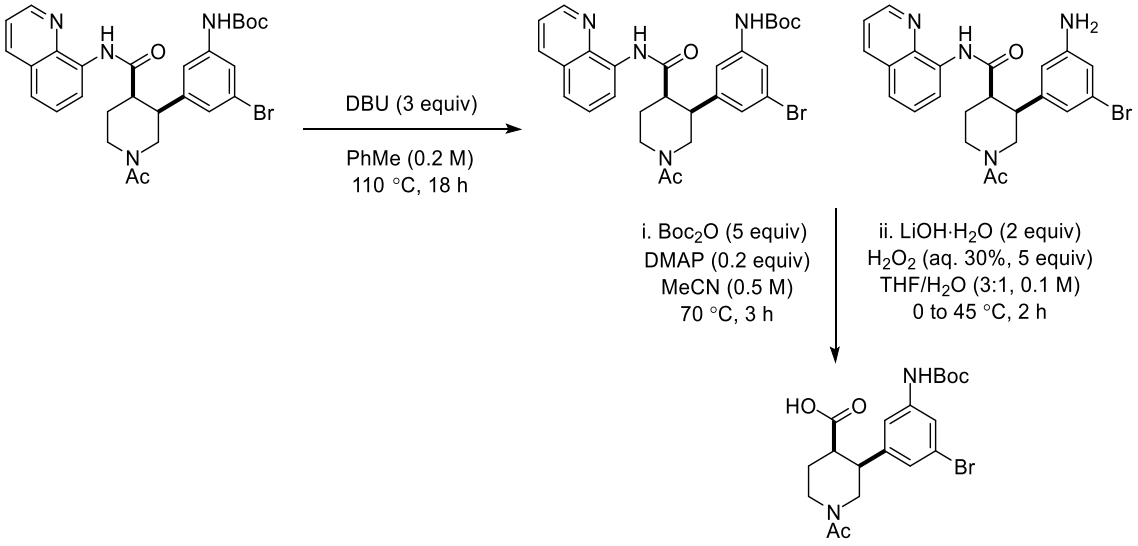


***tert*-Butyl-*trans*-(±)-1-acetyl-4-(quinolin-8-ylcarbamoyl)piperidin-3-yl)-5-bromophenyl)carbamate (*trans*-144)**



Carried forward to the aminoquinoline deprotection step. See below for full procedure

***trans*-(±)-1-Acetyl-3-(3-bromo-5-((*tert*-butoxycarbonyl)amino)phenyl)piperidine-4-carboxylic acid (*trans*-156)**



Epimerisation: A flame-dried microwave vial (25 mL volume) was charged with *cis*-arylated **144** (854 mg, 1.50 mmol, 1.0 equiv) and DBU (0.70 mL, 4.50 mmol, 3.0 equiv). The reaction vessel was sealed and purged with argon, then PhMe (7.5 mL) was added by syringe. The tube was gradually heated to 110 °C in an oil bath, followed by stirring at 110 °C for 18 h. The mixture was then allowed to cool down to rt and evaporated. The brown residue was re-dissolved in EtOAc (5 mL) and filtered through a plug of silica, washing with EtOAc. (approx. 25 mL). The filtrate was concentrated and the residue, consisting of a mixture of approx. 3:1 (molar ratio) of Boc-protected aniline: free aniline was subjected to the Boc re-protection and AQ removal steps.

Boc re-protection: Di-*tert*-butyl dicarbonate (Boc_2O, 1.64 g, 7.50 mmol, 5.0 equiv) and 4-(dimethylamino)pyridine (DMAP, 38 mg, 0.30 mmol, 0.2 equiv) were added to a solution of the mixture from above in MeCN (3 mL). The reaction vessel was sealed and purged with argon and the vial was placed in an oil bath and gradually warmed up to 70 ºC, then stirred at 70 °C for 3 h. The mixture was allowed to cool down and sat. aq. NH_4Cl (10 mL) and CH_2Cl_2 (15 mL) were added. The phases were separated, and the aqueous layer was extracted with CH_2Cl_2 (3 × 10 mL). The combined organic extracts were dried over Na_2SO_4 and filtered and the solvent was removed under reduced pressure to afford the crude tri-Boc protected derivative (di-Boc protected on aniline, mono-Boc protected on amide), which was carried forward to the hydrolysis step without further purification.

AQ hydrolysis: A solution of H_2O_2 (30 wt.% in H_2O, 0.9 mL, 7.50 mmol, 5.0 equiv) in THF (9 mL) was added to a solution of $LiOH{\cdot}H_2O$ (126 mg, 3.00 mmol, 2.0 equiv) in H_2O (6 mL) at 0 °C under argon. The resulting mixture was added dropwise to a solution of the crude *N*-Boc protected amide in THF (7 mL) at 0 °C under argon. The reaction was then stirred at 45 °C for 2 h. The reaction mixture was then allowed to cool down to rt and sat. aq. $Na_2S_2O_3$ (10 mL), EtOAc (10 mL) and 1 M NaOH (5 mL) were added. The aqueous alkaline layer was collected, and the organic layer extracted with 1 M NaOH (3 × 15 mL). All the aqueous alkaline layers were combined and acidified to pH ~ 1 with 1 M HCl, then extracted with EtOAc (3 × 50 mL). The combined organic extracts were dried over Na_2SO_4, filtered and concentrated. Et_2O (10 mL) and pentane (10 mL) were added to the residue and the solvent was removed under reduced pressure to afford piperidine *trans* carboxylic acid ***trans*-156** as an orange solid (135 mg, 20% over 3 steps). R_f 0.23 (35% acetone/pentane); mp = 158–160 °C (from Et_2O/pentane); IR (film)/cm^{-1} 3280 (br OH), 3071, 2982, 1715 (C=O), 1580, 1454, 1372, 1245, 1163, 910, 850; ^1H NMR (400 MHz, DMSO-d_6, 373 K) δ 9.12 (s, 1 H, NHBoc), 7.60 (s, 1 H, HC_{Ar}), 7.34 (s, 1 H, HC_{Ar}), 7.09 (s, 1 H, HC_{Ar}), 2.97 (br s, 4 H, NCH_2CHAr, $NCHCH_2$ and NCH_2CHH), 2.85–2.65 (m, 3 H, CH(C=O), $NCHCH_2$ and NCH_2CHH), 2.03 (s, 3 H, $(C=O)CH_3$), 2.02–1.95 (m, 1 H, CHAr), 1.50 (s, 9 H, $C(CH_3)_3$); ^{13}C NMR (101 MHz, DMSO-d_6, 373 K) δ 173.6 (C=O acid), 167.6 (C=O acetate), 152.1 (C=O carbamate), 143.5 (C_{Ar} quat), 140.6 (C_{Ar} quat), 123.3 (C_{Ar} quat), 120.9 (C_{Ar}), 118.9 (C_{Ar}), 116.4 (C_{Ar}), 79.1 ($C(CH_3)_3$), 46.3 (CH(C=O)), 44.5 (NCH_2CH_2), 28.7 (CHAr), 27.6 ($C(CH_3)_3$), 20.3 ($(C=O)CH_3$); Due to rotamer interconversion occurring even at high temperatures (373 K) and resulting in peak broadening, NCH_2CH was not observed; HRMS (ESI) *m/z* Calculated for $C_{19}H_{26}N_2O_5{}^{79}Br$ [M+H] 441.1025; Found 441.1024.

General Procedure P for Aminoquinoline Amide Activation and Cleavage to Carboxylic Acids

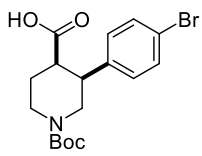
A flame-dried microwave vial (25 mL volume) was charged with the arylated amide (1.0 equiv), followed by di-*tert*-butyl dicarbonate (Boc_2O, 5.0 equiv) and 4-(dimethylamino)pyridine (DMAP, 0.2 equiv). The reaction vessel was sealed and purged with argon, then MeCN (0.5 M) was added by syringe. The reaction mixture was then placed in an oil bath and gradually warmed up to 70 ºC. The reaction was then stirred at 70 °C for 3 h. The reaction mixture was allowed to cool to rt and sat. aq. NH_4Cl (10 mL) and CH_2Cl_2 (15 mL) were added. The phases were separated, and the aqueous layer was extracted with CH_2Cl_2 (3 × 5 mL). The combined organic extracts were dried over Na_2SO_4 and filtered. The solvent was removed under reduced pressure to afford the crude *N*-Boc protected amide derivative which was carried forward to the oxidative cleavage step without further purification. A solution of H_2O_2 (30 wt.% in H_2O, 4.0 equiv) in THF (4 M) was added to a solution of $LiOH{\cdot}H_2O$ (1.6 equiv) in H_2O (1 M) at 0 °C under argon. The resulting mixture was added dropwise to a solution of crude *N*-Boc protected piperidine in THF (0.5 mL) at 0 °C under argon. The reaction was then stirred at 45 °C for 3 h. The reaction mixture was then allowed to cool down to rt and sat. aq. $Na_2S_2O_3$ (10 mL), EtOAc (5 mL) and 1 M NaOH (5 mL) were added. The aqueous alkaline layer was collected, and the organic layer extracted with 1 M NaOH (3 × 15 mL). All the aqueous alkaline layers were combined, washed with EtOAc (10 mL), and acidified to pH ~ 1 with 1 M HCl. The acidic layer was extracted with EtOAc (3 × 50 mL). The combined organic extracts were dried over Na_2SO_4 and filtered. Solvent was removed under reduced pressure. Et_2O (5

mL) and pentane (5 mL) were added and the solvent was removed under reduced pressure to afford the pure carboxylic acid.

General Procedure Q for Aminoquinoline Amide Activation and Cleavage to Carboxylic Acids

A flame-dried microwave vial (25 mL volume) was charged with the arylated amide (1.0 equiv), followed by di-*tert*-butyl dicarbonate (Boc_2O, 5.0 equiv) and 4-(dimethylamino)pyridine (DMAP, 0.2 equiv). The reaction vessel was sealed and purged with argon, then MeCN (0.5 M) was added by syringe. The reaction mixture was then placed in an oil bath and gradually warmed up to 70 ºC. The reaction was then stirred at 70 °C for 1 h, then cooled to rt before a second addition of di-*tert*-butyl dicarbonate (Boc_2O, 5.0 equiv). After stirring for an additional 2 h at 70 °C, the reaction mixture was allowed to cool to rt and sat. aq. NH_4Cl (10 mL) and CH_2Cl_2 (15 mL) were added. The phases were separated, and the aqueous layer was extracted with CH_2Cl_2 (3 × 5 mL). The combined organic extracts were dried over Na_2SO_4 and filtered. The solvent was removed under reduced pressure to afford the crude *N*-Boc protected amide derivative which was carried forward to the oxidative cleavage step without further purification. A solution of H_2O_2 (30 wt.% in H_2O, 4.0 equiv) in THF (0.7 M) was added to a solution of $LiOH·H_2O$ (1.6 equiv) in H_2O (0.8 M) at 0 °C under argon. The resulting mixture was added dropwise to a solution of crude *N*-Boc protected piperidine in THF (0.3 mL) at 0 °C under argon. The reaction was then stirred at 45 °C for 1 h, before cooling to 0 °C again. The previous step consisting in mixing a solution of H_2O_2 in THF with a solution of $LiOH·H_2O$ in H_2O was repeated using the same quantities as before. The LiOOH solution was added dropwise to the reaction mixture at 0 °C, folowed by gradual heating to 45 °C and stirring for an extra 2 h. The reaction was allowed to cool down to rt and sat. aq. $Na_2S_2O_3$ (10 mL), EtOAc (10 mL) and sat. aq $NaHCO_3$ (10 mL) were added. The aqueous layer was collected, and the organic layer extracted with sat. aq $NaHCO_3$ (3 × 25 mL). All the aqueous alkaline layers were combined, washed with EtOAc (20 mL), and acidified to pH ~ 1 with 1 M HCl. The acidic layer was extracted with EtOAc (3 × 50 mL). The combined organic extracts were dried over Na_2SO_4 and filtered. Solvent was removed under reduced pressure. Et_2O (5 mL) and pentane (5 mL) were added and the solvent was removed under reduced pressure to afford the pure carboxylic acid bearing a mono-Boc protected aniline.

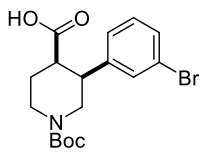
***cis*-(±)-3-(4-Bromophenyl)-1-(*tert*-butoxycarbonyl)piperidine-4-carboxylic acid (149)**



Prepared according to **General Procedure P** using *cis*-arylated **46d** (409 mg, 0.80 mmol), Boc_2O (872 mg, 4.00 mmol), DMAP (20 mg, 0.16 mmol) and MeCN (1.6 mL). The oxidative cleavage step was conducted using a solution of H_2O_2 (30 wt.% in H_2O, 0.32 mL, 3.20 mmol) in THF (0.8 mL), a solution of $LiOH·H_2O$ (80 mg, 1.90 mmol) in H_2O (1.9 mL) and a solution of crude *N*-Boc protected amide from the previous step in THF (1.6 mL). Acid-base work-up afforded acid **149** as a white solid (135 mg, 0.35 mmol, 45% over 2 steps). R_f 0.24 (25% acetone/pentane); mp = 128–130 °C (from Et_2O/pentane); IR (film)/cm^{-1} 3664 (OH br), 2974, 2904, 1692 (C=O), 1487, 1409, 1249, 1163, 1055, 910, 829, 734; ^1H NMR (400 MHz, DMSO-d_6, 373 K) δ 7.46–7.42 (m, 2 H, 2 × HC_{Ar}), 7.24–7.20 (m, 2 H, 2 × HC_{Ar}), 3.93 (dd, *J* = 13.1, 7.0, Hz, 1 H, NC*H*HCHAr), 3.66 (ddd, *J* = 13.3, 7.4, 4.1 Hz, 1 H, NC*H*HCH_2), 3.59 (dd, *J* = 13.2, 4.1 Hz, 1 H,

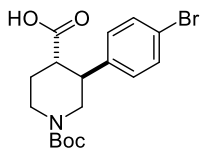
NCH*H*CHAr), 3.36 (ddd, *J* = 13.2, 7.7, 4.2 Hz, 1 H, NCH*H*CH_2), 3.15 (dt, *J* = 7.0, 4.4 Hz, 1 H, CHAr), 2.96 (dt, *J* = 7.7, 4.9 Hz, 1 H, CH(C=O)), 1.89 (dtd, *J* = 14.0, 7.7, 4.1 Hz, 1 H, NCH_2CHH), 1.79 (ddt, *J* = 13.9, 7.4, 4.4 Hz, 1 H, NCH_2CHH), 1.38 (s, 9 H, $C(CH_3)_3$); ^{13}C NMR (101 MHz, DMSO-*d*$_6$, 373 K) δ 173.3 (C=O acid), 153.5 (C=O carbamate), 140.2 (C_{Ar} quat), 130.2 (2 × C_{Ar}), 129.7 (2 × C_{Ar}), 119.0 (C_{Ar} quat), 78.3 ($C(CH_3)_3$), 45.5 (NCH_2CHAr), 43.1 (*C*H(C=O)), 40.6 (NCH_2CH_2), 40.2 (CHAr), 27.6 ($C(CH_3)_3$), 24.6 (NCH_2CH_2); HRMS (ESI) *m/z* Calculated for $C_{12}H_{15}{}^{79}BrNO_2$ [M–$C_5H_9O_2$+H_2] 284.0286; Found 284.0295.

cis-(±)-3-(3-Bromophenyl)-1-(_tert_-butoxycarbonyl)piperidine-4-carboxylic acid (150)



Prepared according to **General Procedure P** using *cis*-arylated **46m** (357 mg, 0.70 mmol), Boc_2O (763 mg, 3.50 mmol), DMAP (18 mg, 0.14 mmol) and MeCN (1.4 mL). The oxidative cleavage step was conducted using a solution of H_2O_2 (30 wt.% in H_2O, 0.28 mL, 2.80 mmol) in THF (0.7 mL), a solution of $LiOH·H_2O$ (47 mg, 1.12 mmol) in H_2O (1.2 mL) and a solution of crude *N*-Boc protected amide from the previous step in THF (1.4 mL). Acid-base work-up afforded acid **150** as a pale yellow solid (203 mg, 0.53 mmol, 76% over 2 steps). R_f 0.21 (25% acetone/pentane); mp = 161-163 °C (from Et_2O/pentane); IR (film)/cm^{-1} 3004 (OH br), 2967, 2930, 1726 (C=O acid), 1621 (C=O carbamate), 1476, 1431, 1279, 1249, 1159, 1122, 790; ^{1}H NMR (400 MHz, DMSO-*d*$_6$, 373 K) δ 7.46 (td, *J* = 1.9, 0.6 Hz, 1 H, HC_{Ar}), 7.39 (ddd, *J* = 7.7, 2.0, 1.2 Hz, 1 H, HC_{Ar}), 7.30–7.24 (m, 1 H, HC_{Ar}), 7.27–7.19 (m, 1 H, HC_{Ar}), 3.97 (dd, *J* = 13.2, 6.6, Hz, 1 H, NC*H*HCH_2), 3.76–3.67 (m, 1 H, NC*H*HCHAr), 3.56 (dd, *J* = 13.2, 4.1 Hz, 1 H, NCH*H*CHAr), 3.32 (ddd, *J* = 12.8, 8.1, 4.1 Hz, 1 H, NCH*H*CH_2), 3.19 (dt, *J* = 6.7, 4.5 Hz, 1 H, CHAr), 2.96 (dt, *J* = 8.1, 4.8 Hz, 1 H, CH(C=O)), 1.87 (dtd, *J* = 14.0, 8.1, 4.2 Hz, 1 H, NCH_2CHH), 1.79 (ddt, *J* = 13.9, 6.9, 4.4 Hz, 1 H, NCH_2CHH), 1.38 (s, 9 H, $C(CH_3)_3$); ^{13}C NMR (101 MHz, DMSO-*d*$_6$, 373 K) δ 173.3 (C=O acid), 153.5 (C=O carbamate), 143.6 (C_{Ar} quat), 130.4 (C_{Ar}), 129.4 (C_{Ar}), 128.7 (C_{Ar}), 126.7 (C_{Ar}), 120.8 (C_{Ar} quat), 78.3 ($C(CH_3)_3$), 45.7 (NCH_2CHAr), 43.2 (*C*H(C=O)), 40.8 (NCH_2CH_2), 40.3 (CHAr), 27.6 ($C(CH_3)_3$), 24.4 (NCH_2CH_2); HRMS (ESI) *m/z* Calculated for $C_{12}H_{15}{}^{79}BrNO_2$ [M–$C_5H_9O_2$+H_2] 284.0281; Found 284.0276.

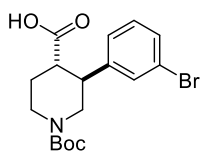
trans-(±)-3-(4-Bromophenyl)-1-(_tert_-butoxycarbonyl)piperidine-4-carboxylic acid (_trans_-149)



Prepared according to **General Procedure P** using *trans*-arylated **61** (390 mg, 0.76 mmol), Boc_2O (828 mg, 3.80 mmol), DMAP (19 mg, 0.15 mmol) and MeCN (1.5 mL). The oxidative cleavage step was conducted using a solution of H_2O_2 (30 wt.% in H_2O, 0.32 mL, 3.10 mmol) in THF (0.8 mL), a solution of $LiOH·H_2O$ (51 mg, 1.20 mmol) in H_2O (1.6 mL) and a solution of crude *N*-Boc protected amide from the previous step in THF (2.0 mL). Acid-base work-up afforded acid ***trans*-149** as a white solid (205 mg, 0.54 mmol, 71% over 2 steps). R_f 0.27 (20% acetone/pentane); mp = 95–98 °C (from Et_2O/pentane); IR (film)/cm^{-1} 3100 (OH br), 2974, 2930, 2863, 1733 (C=O acid), 1689 (C=O carbamate), 1424, 1368, 1297, 1156, 1010, 910, 731; ^{1}H NMR (400 MHz, DMSO-*d*$_6$, 373 K) δ 7.48 (d, *J* = 8.5 Hz, 2 H, 2 × HC_{Ar}), 7.23 (d, *J* = 8.5 Hz, 2 H, 2 × HC_{Ar}), 4.05 (ddd, *J* = 13.4, 4.4, 2.6 Hz, 1 H, NC*H*HCH_2), 3.92 (dt, *J* = 10.6, 1.4 Hz, 1 H, NC*H*HCHAr), 2.97–2.84 (m, 1 H, NCH*H*CHAr), 2.88–2.77 (m, 1 H, NCH*H*CH_2), 2.83–2.74 (m, 2 H, CH(C=O) and CHAr), 1.96 (dq, *J* = 13.0, 2.9 Hz, 1 H, NCH_2CHH), 1.62–1.51 (m, 1 H, NCH_2CHH), 1.43 (s, 9 H,

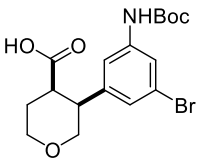
$C(CH_3)_3$); ^{13}C NMR (101 MHz, DMSO-d_6, 373 K) δ 173.8 (C=O acid), 153.4 (C=O carbamate), 140.2 (C_{Ar} quat), 130.7 (2 × C_{Ar}), 129.3 (2 × C_{Ar}), 119.3 (C_{Ar} quat), 78.5 ($C(CH_3)_3$), 48.4 (NCH_2CHAr), 46.4 ($CH(C=O)$), 43.5 (CHAr), 42.4 (NCH_2CH_2), 28.0 (NCH_2CH_2), 27.6 ($C(CH_3)_3$); HRMS (ESI) *m/z* Calculated for $C_{12}H_{15}{}^{79}BrNO_2$ [M–$C_5H_9O_2$+H_2] 284.0281 ; Found 284.0279.

trans-(±)-3-(3-Bromophenyl)-1-(_tert_-butoxycarbonyl)piperidine-4-carboxylic acid (_trans_-150)



Prepared according to **General Procedure P** using *trans*-arylated ***trans*-46m** (370 mg, 0.72 mmol), Boc_2O (784 mg, 3.60 mmol), DMAP (18 mg, 0.15 mmol) and MeCN (1.4 mL). The oxidative cleavage step was conducted using a solution of H_2O_2 (30 wt.% in H_2O, 0.30 mL, 2.90 mmol) in THF (0.8 mL), a solution of $LiOH{\cdot}H_2O$ (49 mg, 1.15 mmol) in H_2O (1.6 mL) and a solution of crude *N*-Boc protected amide from the previous step in THF (2.0 mL). Acid-base work-up afforded ***trans*-150** as a white solid (235 mg, 0.60 mmol, 82% over 2 steps). R_f 0.26 (20% acetone/pentane); mp = 168–170 °C (from Et_2O/pentane); IR (film)/cm^{-1} 3083 (OH br), 3015, 2974, 1722 (C=O acid), 1640 (C=O carbamate), 1476, 1428, 1364, 1297, 1148, 1051, 939, 850, 790; ^1H NMR (400 MHz, DMSO-d_6, 373 K) δ 7.48–7.46 (m, 1 H, HC_{Ar}), 7.41 (ddd, *J* = 6.2, 2.6, 2.0 Hz, 1 H, HC_{Ar}), 7.31–7.22 (m, 2 H, 2 × HC_{Ar}), 4.04 (ddd, *J* = 13.3, 4.5, 2.7 Hz, 1 H, $NCHHCH_2$), 3.92 (dq, *J* = 12.8, 1.5 Hz, 1 H, $NCHHCHAr$), 2.97–2.91 (m, 2 H, $NCHHCH_2$ and $NCHHCHAr$), 2.84–2.75 (m, 2 H, CH(C=O) and CHAr), 1.95 (dq, *J* = 13.2, 3.1 Hz, 1 H, NCH_2CHH), 1.62–1.50 (m, 1 H, NCH_2CHH), 1.44 (s, 9 H, $C(CH_3)_3$); ^{13}C NMR (101 MHz, DMSO-d_6, 373 K) δ 173.8 (C=O acid), 153.4 (C=O carbamate), 143.7 (C_{Ar} quat), 129.9 (C_{Ar}), 129.1 (C_{Ar}), 126.3 (C_{Ar}), 121.1 (C_{Ar} quat), 78.5 ($C(CH_3)_3$), 48.4 (NCH_2CHAr), 46.3 ($CH(C=O)$), 43.7 (CHAr), 42.3 (NCH_2CH_2), 28.0 (NCH_2CH_2), 27.6 ($C(CH_3)_3$); HRMS (ESI) *m/z* Calculated for $C_{12}H_{15}{}^{79}BrNO_2$ [M–$C_5H_9O_2$+H_2] 284.0281 ; Found 284.0278.

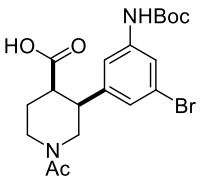
cis-(±)-3-(3-Bromo-5-((_tert_-butoxycarbonyl)amino)phenyl)tetrahydro-2_H_-pyran-4-carboxylic acid (152)



Prepared acording to **General Procedure Q** using *cis*-arylated **53j** (395 mg, 0.75 mmol), Boc_2O (2 × 818 mg, 2 × 3.75 mmol), DMAP (19 mg, 0.15 mmol) and MeCN (1.5 mL). The oxidative cleavage step was conducted using a solution of crude *N*-Boc protected amide from the previous step in THF (2.5 mL) and twice the addition of a mixture of the following at 0 °C: a solution of H_2O_2 (30 wt.% in H_2O, 0.30 mL, 3.00 mmol) in THF (1.8 mL) and a solution of $LiOH{\cdot}H_2O$ (51 mg, 1.20 mmol) in H_2O (1.5 mL). Acid-base work-up afforded **152** as a pale yellow powder (217 mg, 0.53 mmol, 70% over 2 steps). R_f 0.19 (25% acetone/pentane); mp = 150–151 °C (from Et_2O/pentane); IR (film)/cm^{-1} 3664 and 3332 (OH br), 2978, 1707 (C=O), 1603, 1536, 1454, 1245, 1156, 1088, 909, 857, 730; ^1H NMR (400 MHz, $CDCl_3$) δ 7.63 (s, 1 H, HC_{Ar}), 7.28 (s, 1 H, HC_{Ar}), 7.20 (s, 1 H, HC_{Ar}), 6.76 (br s, 1 H, NHBoc), 4.23 (dd, *J* = 11.7, 3.6 Hz, 1 H, $OCHHCHAr$), 4.11 (dt, *J* = 11.7, 4.2 Hz, 1 H, $OCHHCHAr$), 3.82 (dd, *J* = 11.6, 3.6 Hz, 1 H, $OCHHCH_2$), 3.64–3.53 (m, 1 H, $OCHHCH_2$), 3.15 (app q, *J* = 4.0 Hz, 1 H, CH(C=O)), 3.00 (dt, *J* = 9.8, 4.6 Hz, 1 H, CHAr), 2.03 (ddd, *J* = 14.2, 11.6, 6.5 Hz, 1 H, OCH_2CHH), 1.80–1.71 (m, 1 H, OCH_2CHH), 1.51 (s, 9 H, $C(CH_3)_3$); ^{13}C NMR (101 MHz, $CDCl_3$) δ 177.0 (C=O acid), 152.9 (C=O carbamate), 142.7 (C_{Ar} quat), 139.2 (C_{Ar}

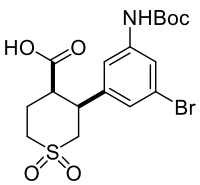
quat), 126.7 (C_{Ar}), 122.5 (C_{Ar} quat), 120.1 (C_{Ar}), 117.9 (C_{Ar}), 77.3 ($C(CH_3)_3$), 70.3 (OCH_2CHAr), 66.2 (OCH_2CH_2), 44.0 (CHAr), 41.2 ($CH(C=O)$), 28.3 ($C(CH_3)_3$), 24.0 (OCH_2CH_2); HRMS (ESI) *m/z* Calculated for $C_{17}H_{22}{}^{79}BrNO_5Na^+$ $[M+Na]^+$ 422.0579; Found 422.0576.

cis-(±)-1-Acetyl-3-(3-bromo-5-((_tert_-butoxycarbonyl)amino)phenyl)piperidine-4-carboxylic acid (156)



Prepared according to **General Procedure Q** using *cis*-arylated **144** (285 mg, 0.50 mmol), Boc_2O (2 × 545 mg, 2 × 2.5 mmol), DMAP (13 mg, 0.10 mmol) and MeCN (1.0 mL). The oxidative cleavage step was conducted using a solution of crude *N*-Boc protected amide from the previous step in THF (1.7 mL) and twice the addition of the mixture of the following at 0 °C: a solution of H_2O_2 (30 wt.% in H_2O, 0.20 mL, 2.00 mmol) in THF (1.2 mL) and a solution of $LiOH{\cdot}H_2O$ (34 mg, 0.80 mmol) in H_2O (1.0 mL). Acid-base work-up afforded acid **156** as a white powder (135 mg, 0.31 mmol, 61% over 2 steps). R_f 0.25 (25% acetone/pentane); IR (film)/cm^{-1} 3377 (br OH acid), 2982, 2926, 2482, 1714 (C=O), 1603, 1590, 1461, 1390, 1252, 1163, 1085, 973, 857; ^{1}H NMR (400 MHz, DMSO-d_6, 373 K) δ 9.12 (br s, 1 H, NHBoc), 7.60 (d, J = 2.1 Hz, 1 H, HC_{Ar}), 7.35 (t, J = 1.8 Hz, 1 H, HC_{Ar}), 7.02 (s, 1 H, HC_{Ar}), 3.91 (dd, J = 13.2, 7.7 Hz, 1 H, NC*H*HCHAr), 3.69 (ddd, J = 12.5, 8.1, 3.9 Hz, 2 H, NCH*H*CHAr and NC*H*HCH$_2$), 3.51 (ddd, J = 12.9, 7.1, 4.4 Hz, 1 H, NCH*H*CH$_2$), 3.00–2.96 (m, 2 H, CH(C=O) and CHAr), 1.97 (br s, 4 H, $(C=O)CH_3$ and NCH_2CHH), 1.88–1.75 (m, 1 H, NCH_2CHH), 1.49 (s, 9 H, $C(CH_3)_3$); ^{13}C NMR (101 MHz, DMSO-d_6, 373 K) δ 173.2 (C=O acid), 167.9 (C=O acetyl), 152.1 (C=O carbamate), 143.5 (C_{Ar} quat), 140.4 (C_{Ar} quat), 123.9 (C_{Ar}), 120.6 (C_{Ar} quat), 118.5 (C_{Ar}), 116.6 (C_{Ar}), 79.0 ($C(CH_3)_3$), 43.0 ($CH(C=O)$), 40.8 (CHAr), 27.6 ($C(CH_3)_3$), 25.3 (NCH_2CH_2), 20.4 ($(C=O)CH_3$); Due to rotamer interconversion occurring even at high temperatures (373 K) and resulting in peak broadening, N*C*H$_2$CH and N*C*H$_2$CH$_2$ were not observed; HRMS (ESI) *m/z* Calculated for $C_{19}H_{26}{}^{79}BrN_2O_5$ $[M+H]$ 441.1025; Found 441.1024.

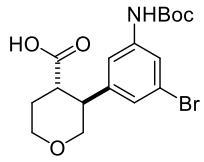
cis-(±)-3-(3-Bromo-5-((_tert_-butoxycarbonyl)amino)phenyl)tetrahydro-2_H_-thiopyran-4-carboxylic acid 1,1-dioxide (155)



Prepared according to **General Procedure Q** using *cis*-arylated **147** (338 mg, 0.50 mmol), Boc_2O (2 × 545 mg, 2 × 2.5 mmol), DMAP (13 mg, 0.1 mmol) and MeCN (1.0 mL). The oxidative cleavage step was conducted using a solution of crude *N*-Boc protected amide from the previous step in THF (1.7 mL) and twice the addition of the mixture of the following at 0 °C: a solution of H_2O_2 (30 wt.% in H_2O, 0.20 mL, 2.00 mmol) in THF (1.2 mL) and a solution of $LiOH{\cdot}H_2O$ (34 mg, 0.80 mmol) in H_2O (1.0 mL). Acid-base work-up afforded acid **155** as a yellow powder (96 mg, 0.28 mmol, 55% over 2 steps). R_f 0.29 (25% acetone/pentane); mp = 189–191 °C (from Et_2O/pentane); IR (film)/cm^{-1} 3332 (br OH acid), 2982, 2933, 1707 (C=O), 1603, 1535, 1424, 1453, 1368, 1312, 1241, 1279, 1241, 1156 (S=O), 1118 (S=O), 910, 854, 734; ^{1}H NMR (400 MHz, DMSO-d_6, 373 K) δ 8.87 (br s, 1 H, NHBoc), 7.51 (s, 1 H, HC_{Ar}), 7.16 (s, 1 H, HC_{Ar}), 7.00 (s, 1 H, HC_{Ar}), 4.26 (t, J = 13.6 Hz, 1 H, SC*H*HCHAr), 3.59 (dt, J = 13.6, 3.5 Hz, 1 H, SC*H*HCH$_2$), 3.43 (ddd, J = 17.9, 12.0, 5.0 Hz, 1 H, SCH*H*CHAr), 3.14–2.96 (m, 3 H, SCH*H*CH$_2$, CH(C=O) and CHAr), 2.63–2.42 (m, 2 H, SCH_2CH_2), 1.50 (s, 9 H, $C(CH_3)_3$); ^{13}C NMR (101 MHz, DMSO-

d_6, 373 K) δ 175.4 (C=O acid), 141.8 (C_{Ar}), 140.0 (C_{Ar} quat), 125.0 (C_{Ar} quat), 123.0 (C_{Ar}), 121.0 (C_{Ar} quat), 116.1 (C_{Ar}), 51.1 (S*C*H_2CHAr), 46.8 (S*C*H_2CH_2), 42.9 (*C*H(C=O)), 42.4 (CHAr), 28.2 (C(*C*$H_3)_3$), 26.5 (SCH_2*C*H_2); HRMS (ESI) *m/z* Calculated for $C_{17}H_{22}{}^{79}BrNO_6SNa^+$ [M+Na]$^+$ 470.0249; Found 470.0237.

trans-(±)-3-(3-Bromo-5-((_tert_-butoxycarbonyl)amino)phenyl)tetrahydro-2_H_-pyran-4-carboxylic acid (_trans_-152)

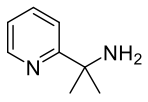


Prepared according to **General Procedure Q** using *trans*-arylated ***trans*-53j** (255 mg, 0.48 mmol), Boc_2O (2 × 528 mg, 2 × 2.42 mmol), DMAP (13 mg, 0.10 mmol) and MeCN (1.0 mL). The oxidative cleavage step was conducted using a solution of crude *N*-Boc protected amide from the previous step in THF (1.7 mL) and twice the addition of the mixture of the following at 0 °C: a solution of H_2O_2 (30 wt.% in H_2O, 0.20 mL, 2.00 mmol) in THF (1.2 mL) and a solution of LiOH·H_2O (34 mg, 0.80 mmol) in H_2O (1.0 mL). Acid-base work-up afforded acid ***trans*-152** as an orange foam (34 mg, 0.09 mmol, 20% over 2 steps). R_f 0.28 (20% acetone/pentane); mp = 138–140 °C (from Et_2O/pentane); IR (film)/cm^{-1} 3329 (OH acid br), 2979, 2933, 2855, 1711 (C=O), 1603, 1536, 1454, 1260, 1156, 842; ^{1}H NMR (400 MHz, $CDCl_3$) δ 9.23 (s, 1 H, NHBoc), 7.54 (s, 1 H, HC_{Ar}), 7.11–6.93 (m, 2 H, 2 × HC_{Ar}), 4.16–4.01 (m, 1 H, OC*H*HCHAr), 3.91 (dd, *J* = 11.6, 4.4 Hz, 1 H, OC*H*HCH_2), 3.50 (td, *J* = 11.9, 2.5 Hz, 1 H, OCH*H*CHAr), 3.33 (t, *J* = 11.3 Hz, 1 H, OCH*H*CH_2), 3.04 (td, *J* = 11.2, 4.5 Hz, 1 H, CH(C=O)), 2.82 (td, *J* = 11.4, 4.1 Hz, 1 H, CHAr), 2.03–1.86 (m, 2 H, OCH_2CH_2), 1.50 (s, 9 H, C($CH_3)_3$); ^{13}C NMR (101 MHz, $CDCl_3$) δ 178.1 (C=O acid), 142.1 (C_{Ar}), 139.7 (C_{Ar} quat), 130.0 (C_{Ar} quat), 125.0 (C_{Ar}), 122.8 (C_{Ar}), 120.4 (C_{Ar} quat), 71.9 (*C*($CH_3)_3$), 67.0 (O*C*H_2CHAr), 46.0 (O*C*H_2CH_2), 44.1 (*C*H(C=O)), 29.1 (OCH_2*C*H_2), 28.2 (C(*C*$H_3)_3$); C=O carbamate and *C*HAr *not observed*; HRMS (ESI) *m/z* Calculated for $C_{17}H_{22}{}^{79}BrNO_5Na^+$ [M+Na]$^+$ 422.0579; Found 422.0576.

4.4 Compounds for Chapter 2.3

4.4.1 Synthesis of Amides

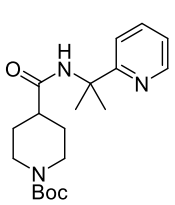
2-(Pyridin-2-yl)propan-2-amine (160)



Using a previously reported literature protocol,[169] MeMgBr (9.4 mL, 30.00 mmol, 3.2 M in 2-MeTHF, 3.0 equiv) was added dropwise over 15 min to a solution of 2-cyanopyridine (920 mg, 10.00 mmol, 1.0 equiv) in toluene (17 mL) at 0 ºC, whilst maintaining a maximum stirring rate (1500 rpm). The solution was heated to reflux for 18 h, then allowed to cool to rt. Upon cooling to 0 °C, a solution of ammonium hydroxide (20 mL, 28% NH_3 in H_2O) was added portionwise until a yellow dense precipitate formed. The resulting mixture was allowed to warm to rt and stirred for 20 min, then filtered through a pad of Celite, washing with THF (200 mL). The solvent was removed under reduced pressure, affording title amine **160** as a brown oil (1.30 g crude, approx. 90% desired **160** by ^{1}H NMR) which was used in the next step without further purification. IR (film)/cm^{-1} 3355 (br NH), 2971, 1591, 1569, 1475, 1433, 1383, 1125, 1049, 995, 789, 751; ^{1}H NMR (400 MHz, $CDCl_3$) δ 8.57 (dd, J = 5.0 Hz, 1 H, HC_{Ar}), 7.68–7.62 (m, 1 H, HC_{Ar}), 7.45 (dd, J = 8.1 Hz, 1 H, HC_{Ar}), 7.20–7.11

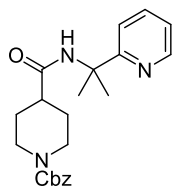
(m, 1 H, HC_{Ar}), 2.31 (br s, 2 H, NH_2), 1.52 (s, 6 H, 2 × CH_3); ^{13}C NMR (101 MHz, $CDCl_3$) δ 168.0 (C_{Ar} quat), 148.5 (C_{Ar}), 136.3 (C_{Ar}), 121.1 (C_{Ar}), 118.2 (C_{Ar}), 53.9 ($C(CH_3)_2$), 31.1 (2 × CH_3). All characterisation information in agreement with literature data previously reported for the same compound.[169]

***tert*-Butyl 4-((2-(pyridin-2-yl)propan-2-yl)carbamoyl)piperidine-1-carboxylate (161)**



HOBt · H_2O (1.15 g, 6.00 mmol, 1.2 equiv, wetted with ≥ 20% H_2O) and EDC·HCl (1.15 g, 6.00 mmol, 1.2 equiv) were added to a solution of *N*-Boc-piperidine-4-carboxylic acid (1.15 g, 5.00 mmol, 1.0 equiv) and 2-(pyridin-2-yl)propan-2-amine **160** (90% purity, 831 mg, 5.50 mmol, 1.1 equiv) in CH_2Cl_2 (17 mL). After stirring at rt for 72 h, the reaction was diluted with CH_2Cl_2 (20 mL), then sat. aq. $NaHCO_3$ (30 mL) was added and the aqueous layer extracted with CH_2Cl_2 (3 x 20 mL). The combined organic extracts were dried over Na_2SO_4, filtered, and the solvent removed under reduced pressure. Purification of the residue by flash column chromatography (50% acetone/pentane) afforded amide **161** as a brown powder (852 mg, 2.40 mmol, 48%). R_f 0.45 (50% acetone/pentane); mp = 129–131 °C (from acetone/pentane); IR (film)/cm^{-1} 3320 (br NH), 2859, 2985, 2943, 1687 (C=O), 1650 (C=O), 1540, 1419, 1219, 1170, 1122, 939, 783, 650; ^1H NMR (400 MHz, $CDCl_3$) δ 8.52 (dd, *J* = 5.0, 1.8 Hz, 1 H, HC_{Ar}), 7.97 (s, 1 H, HC_{Ar}), 7.75 (td, *J* = 7.8, 1.8 Hz, 1 H, HC_{Ar}), 7.42 (dt, *J* = 8.2, 1.0 Hz, 1 H, HC_{Ar}), 7.23 (ddd, *J* = 7.5, 5.0, 1.0 Hz, 1 H, HC_{Ar}), 4.15 (br s, 2 H, 2 × NC*H*HCH_2), 2.77 (q, *J* = 9.0, 5.1 Hz, 2 H, 2 × NCH*H*CH_2), 2.34 (tt, *J* = 11.6, 3.7 Hz, 1 H, CH(C=O)), 1.91–1.87 (m, 2 H, 2 × NCH_2CHH), 1.75 (s, 6 H, $C(CH_3)_2$), 1.67 (qd, *J* = 11.6, 11.0, 3.7 Hz, 2 H, 2 × NCH_2CH*H*), 1.46 (s, 9 H, $C(CH_3)_3$); ^{13}C NMR (101 MHz, $CDCl_3$) δ 173.6 (C=O amide), 164.5 (C_{Ar} quat), 154.8 (C=O carbamate), 147.3 (C_{Ar}), 137.4 (C_{Ar}), 122.0 (C_{Ar}), 119.6 (C_{Ar}), 79.5 ($C(CH_3)_3$), 56.1 ($C(CH_3)_2$), 44.2 (*C*H(C=O)), 43.7 (2 × N*C*H_2CH_2), 28.7 ($C(CH_3)_3$), 28.5 (2 × NCH_2CH_2), 27.5 ($C(CH_3)_2$); HRMS (APCI) *m/z* Calculated for $C_{19}H_{30}N_3O_3^+$ $[M+H]^+$ 384.2282; Found 384.2289.

Benzyl 4-((2-(pyridin-2-yl)propan-2-yl)carbamoyl)piperidine-1-carboxylate (163)

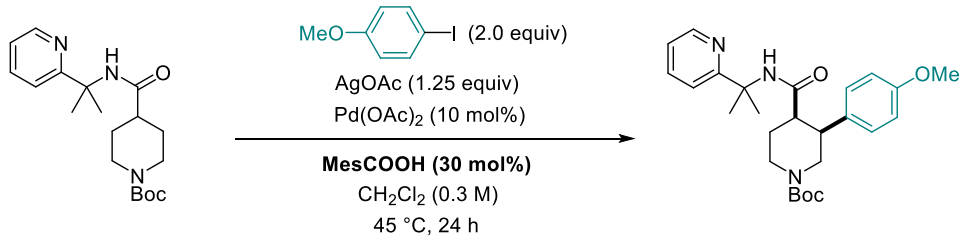


HOBt · H_2O (1.15 g, 6.00 mmol, 1.2 equiv, wetted with ≥ 20% H_2O) and EDC·HCl (1.15 g, 6.00 mmol, 1.2 equiv) were added to a solution of *N*-Boc-piperidine-4-carboxylic acid (1.31 g, 5.00 mmol, 1.0 equiv) and 2-(pyridin-2-yl)propan-2-amine **160** (90% purity, 831 mg, 5.50 mmol, 1.1 equiv) in CH_2Cl_2 (17 mL). After stirring at rt for 72 h, the reaction was diluted with CH_2Cl_2 (20 mL), then sat. aq. $NaHCO_3$ (30 mL) was added and the aqueous layer extracted with CH_2Cl_2 (3 x 20 mL). The combined organic extracts were dried over Na_2SO_4, filtered, and the solvent removed under reduced pressure. Purification of the residue reverse phase chromatography (0% to 100% MeOH/H_2O) afforded amide **163** as a yellow powder (810 mg, 2.15 mmol, 43%). R_f 0.51 (50% acetone/pentane); mp = 85–87 °C (from MeOH/H_2O); IR (film)/cm^{-1} 3302 (NH), 2861, 2953, 2929, 1689 (C=O), 1646 (C=O), 1539, 1429, 1325, 1212, 1122, 1088, 1024, 692; ^1H NMR (400 MHz, $CDCl_3$) δ 8.57–8.47 (m, 1 H, HC_{Ar}), 8.00 (s, 1 H, NH), 7.83–7.70 (m, 1 H, HC_{Ar}), 7.46–7.31 (m, 5 H, 5 × HC_{Ar}), 7.31–7.22 (m, 2 H, 2 × HC_{Ar}), 5.14 (s, 2 H, CH_2Ph), 4.23 (br s, 2 H, 2 × NC*H*HCH_2), 2.88 (br s, 2 H, 2 × NCH*H*CH_2), 2.36 (tt, *J* = 11.5, 3.8 Hz, 1 H, CH(C=O)), 1.91 (br s, 2 H,

2 × NCH_2CHH), 1.75 (s, 6 H, $C(CH_3)_2$), 1.74–1.63 (m, 2 H, 2 × NCH_2CHH); ^{13}C NMR (101 MHz, $CDCl_3$) δ 173.4 (C=O amide), 164.3 (C_{Ar} quat), 155.2 (C=O carbamate), 147.1 (C_{Ar}), 137.6 (C_{Ar}), 136.8 (C_{Ar} quat), 128.4 (2 × C_{Ar}), 127.9 (C_{Ar}), 127.8 (2 × C_{Ar}), 122.0 (C_{Ar}), 119.7 (C_{Ar}), 67.1 (CH_2Ph), 56.1 ($C(CH_3)_2$), 43.9 (*C*H(C=O)), 43.5 (2 × NCH_2CH_2), 28.6 (2 × NCH_2CH_2), 27.4 ($C(CH_3)_2$); HRMS (ESI) *m/z* Calculated for $C_{22}H_{28}N_3O_3$ [M+H] 382.2131; Found 382.2148.

4.4.2 Representative Procedures for the Synthesis of Racemic Compounds

tert-Butyl-_cis_-(±)-3-(4-methoxyphenyl)-4-((2-(pyridin-2-yl)propan-2-yl)carbamoyl)piperidine-1-carboxylate (_rac_-162)

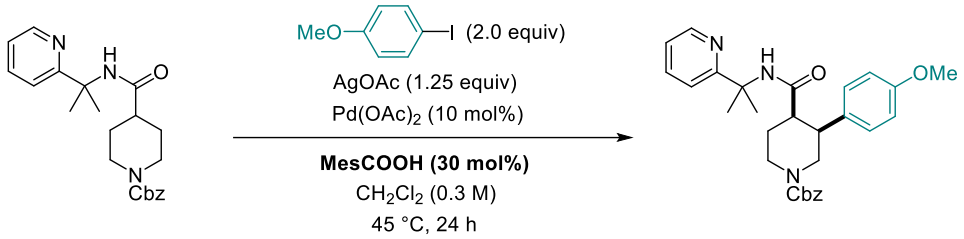


A flame-dried microwave vial was charged with amide **161** (138 mg, 0.40 mmol, 1.0 equiv), 4-iodoanisole (187 mg, 0.80 mmol, 2.0 equiv), Ag_2CO_3 (138 mg, 0.50 mmol, 1.25 equiv), 2,4,6-trimethylbenzoic acid (MesCOOH, 20 mg, 0.12 mmol, 0.3 equiv) and $Pd(OAc)_2$ (9 mg, 0.04 mmol, 0.1 equiv) in this order. The reaction vessel was sealed and purged with argon, then CH_2Cl_2 (1.3 mL, 0.3 M) was added by syringe. The reaction tube was placed in a preheated oil bath and stirred at 45 °C for 24 h. The reaction mixture was then allowed to cool to rt, diluted with EtOAc (5 mL) and filtered through a pad of Celite, eluting with further EtOAc (2 × 10 mL). The solvent was removed under reduced pressure and the crude material purified by flash column chromatography (10% to 25% MeCN/CH_2Cl_2). Et_2O (5 mL), followed by pentane (5 mL) were added to the isolated product, with the resulting suspension concentrated under reduced pressure. This procedure was repeated three times to eliminate residual solvent and afford ***rac*-162** as a yellow solid (98 mg, 0.21 mmol, 52%). R_f 0.49 (25% MeCN/CH_2Cl_2); mp = 70–71 °C (from Et_2O/pentane); IR (film)/cm^{-1} 3330 (br NH), 2975, 2931, 1658 (C=O), 1511, 1471, 1425, 1243, 1160, 1035, 910, 728; ^1H NMR (500 MHz, DMSO-d_6, 373 K) δ 8.40 (ddd, *J* = 4.8, 1.9, 1.0 Hz, 1 H, NH), 7.59–7.46 (m, 2 H, 2 × HC_{At}), 7.18–7.14 (m, 2 H, 2 × HC_{At}), 7.12 (ddd, *J* = 7.4, 4.8, 1.1 Hz, 1 H, HC_{At}), 7.03 (dt, *J* = 8.0, 1.0 Hz, 1 H, HC_{At}), 6.84–6.78 (m, 2 H, 2 × HC_{At}), 3.90 (dd, *J* = 12.7, 9.4 Hz, 1 H, NC*H*HCHAr), 3.74 (s, 3 H, OCH_3), 3.66 (dd, *J* = 12.7, 4.3 Hz, 1 H, NCH*H*CHAr), 3.60–3.51 (m, 2 H, NCH_2CH_2), 3.00–2.95 (m, 1 H, CHAr), 2.90 (q, *J* = 5.0 Hz, 1 H, CH(C=O)), 1.85 (dtd, *J* = 14.0, 5.2, 3.8 Hz, 1 H, NCH_2CHH), 1.81–1.71 (m, 1 H, NCH_2CHH), 1.43 (d, *J* = 5.4 Hz, 6 H, $C(CH_3)_2$), 1.39 (s, 9 H, $C(CH_3)_3$); ^{13}C NMR (126 MHz, DMSO-d_6, 373 K) δ 171.6 (C=O amide), 164.6 (C_{Ar} quat), 157.5 (C=O carbamate), 153.7 (C_{Ar} quat), 147.0 (C_{Ar}), 135.5 (C_{Ar}), 133.1 (C_{Ar} quat), 128.5 (2 × C_{Ar}), 120.4 (C_{Ar}), 118.5 (C_{Ar}), 113.1 (2 × C_{Ar}), 77.9 ($C(CH_3)_3$), 55.9 ($C(CH_3)_2$), 54.7 (OCH_3), 44.9 (NCH_2CHAr), 43.4 (CH(C=O)), 41.4 (CHAr), 40.0 (NCH_2CH_2), 27.6 ($C(CH_3)_3$), 27.2 and 27.1 ($C(CH_3)_2$), 26.5 (NCH_2CH_2); HRMS (ESI) *m/z* Calculated for $C_{26}H_{36}N_3O_4$ [M+H] 454.2706; Found 454.2710.

Approx. 1 mg of sample was dissolved in *i*-PrOH/*n*-hexane (1 mL, 5:95 v/v) and separated by HPLC into the 2 corresponding *cis* enantiomers.

HPLC Conditions: Chiralpak ID column, 80:20 *n*-hexane: *i*-PrOH, flow rate: 1 mL min^{-1}, 35 °C, UV detection wavelength: 254 nm.

Benzyl-*cis*-(±)-3-(4-methoxyphenyl)-4-((2-(pyridin-2-yl)propan-2-yl)carbamoyl)piperidine-1-carboxylate (*rac*-164)

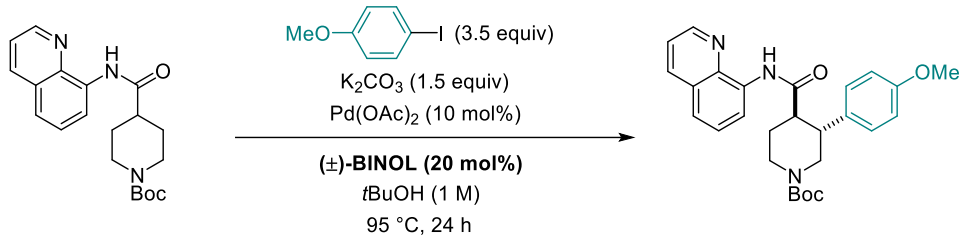


A flame-dried microwave vial was charged with amide **163** (152 mg, 0.40 mmol, 1.0 equiv), 4-iodoanisole (187 mg, 0.80 mmol, 2.0 equiv), Ag_2CO_3 (138 mg, 0.50 mmol, 1.25 equiv), 2,4,6-trimethylbenzoic acid (MesCOOH, 20 mg, 0.12 mmol, 0.3 equiv) and $Pd(OAc)_2$ (9 mg, 0.04 mmol, 0.1 equiv) in this order. The reaction vessel was sealed and purged with argon, then CH_2Cl_2 (1.3 mL, 0.3 M) was added by syringe. The reaction tube was placed in a preheated oil bath and stirred at 45 °C for 24 h. The reaction mixture was then allowed to cool to rt, diluted with EtOAc (5 mL) and filtered through a pad of Celite, eluting with further EtOAc (2 × 10 mL). The solvent was removed under reduced pressure and the crude material purified by flash column chromatography (10% to 25% MeCN/CH_2Cl_2). Et_2O (5 mL), followed by pentane (5 mL) were added to the isolated product, with the resulting suspension concentrated under reduced pressure. This procedure was repeated three times to eliminate residual solvent and afford ***rac*-164** as a dark orange oil (112 mg, 0.23 mmol, 58%). R_f 0.51 (25% MeCN/CH_2Cl_2); IR (film)/cm^{-1} 3343 (br NH), 3000, 2934, 1696 (C=O), 1667 (C=O), 1513, 1471, 1432, 1245, 1115, 1034, 832, 788, 748; ^{1}H NMR (500 MHz, DMSO-d_6, 373 K) δ 8.40 (ddd, *J* = 4.8, 1.9, 1.0 Hz, 1 H, HC_{Ar}), 7.59–7.50 (m, 2 H, 2 × HC_{Ar}), 7.39–7.27 (m, 4 H, 4 × HC_{Ar}), 7.18–7.13 (m, 2 H, 2 × HC_{Ar}), 7.14–7.10 (m, 1 H, HC_{Ar}), 7.02 (dt, *J* = 8.0, 1.1 Hz, 1 H, HC_{Ar}), 6.84–6.79 (m, 2 H, 2 × HC_{Ar}), 5.08 (s, 2 H, CH_2Ph), 3.98 (dd, *J* = 12.7, 9.7 Hz, 1 H, NC*H*HCHAr), 3.79–3.74 (m, 1 H, NCH*H*CHAr), 3.73 (s, 3 H, OCH_3), 3.70–3.64 (m, 1 H, NC*H*HCH_2), 3.57 (ddd, *J* = 13.3, 10.0, 3.7 Hz, 1 H, NCH*H*CH_2), 3.01 (dt, *J* = 9.5, 4.6 Hz, 1 H, CHAr), 2.93 (q, *J* = 4.9 Hz, 1 H, CH(C=O)), 1.88 (dtd, *J* = 13.7, 5.0, 3.8 Hz, 1 H, NCH_2CHH), 1.79 (ddt, *J* = 13.8, 9.8, 4.8 Hz, 1 H, NCH_2CHH), 1.45 (d, *J* = 5.4 Hz, 6 H, $C(CH_3)_2$); ^{13}C NMR (126 MHz, DMSO-d_6, 373 K) δ 171.6 (C=O amide), 164.6 (C_{Ar} quat), 157.6 (C=O carbamate), 154.3 (C_{Ar} quat), 147.1 (C_{Ar}), 136.7 (C_{Ar} quat), 135.4 (C_{Ar}), 132.9 (C_{Ar} quat), 128.4 (2 × C_{Ar}), 127.7 (2 × C_{Ar}), 127.0 (C_{Ar}), 126.8 (2 × C_{Ar}), 120.4 (C_{Ar}), 118.5 (C_{Ar}), 113.1 (2 × C_{Ar}), 65.6 (CH_2Ph), 55.9 ($C(CH_3)_2$), 54.7 (OCH_3), 45.0 (NCH_2CHAr), 43.2 (CH(C=O)), 41.4 (CHAr), 40.2 (NCH_2CH_2), 27.2 and 27.1 ($C(CH_3)_2$), 26.6 (NCH_2CH_2); HRMS (ESI) *m/z* Calculated for $C_{26}H_{34}N_3O_4$ [M+H] 488.2549; Found 488.2569.

Approx. 1 mg of sample was dissolved in *i*-PrOH/*n*-hexane (1 mL, 5:95 v/v) and separated by HPLC into the 2 corresponding *cis* enantiomers.

HPLC Conditions: Chiralpak IA column, 85:15 *n*-hexane: *i*-PrOH, flow rate: 1 mL min^{-1}, 35 °C, UV detection wavelength: 254 nm.

***tert*-Butyl-*cis*-(±)-3-(4-methoxyphenyl)-4-(quinolin-8-ylcarbamoyl)piperidine-1-carboxylate (*rac*-29b)**



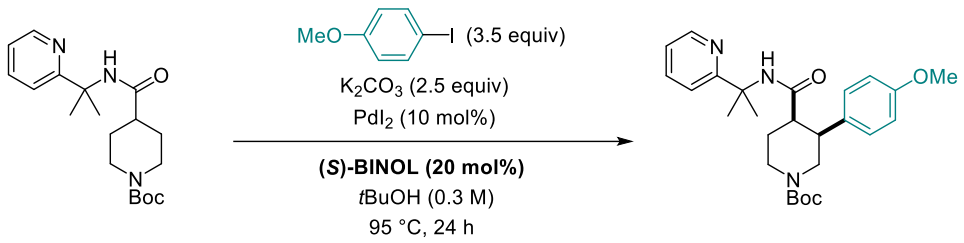
A flame-dried microwave vial was charged with amide **25** (36 mg, 0.10 mmol, 1.0 equiv), 4-iodoanisole (82 mg, 0.35 mmol, 3.5 equiv), K_2CO_3 (21 mg, 0.15 mmol, 1.5 equiv), (±)-BINOL (5.7 mg, 0.02 mmol, 0.2 equiv) and $Pd(OAc)_2$ (2.4 mg, 0.01 mmol, 0.1 equiv) in this order. The reaction vessel was sealed and purged with argon, then *t*BuOH (0.1 mL, 1 M) was added by syringe. The reaction tube was placed in a preheated oil bath and stirred at 95 °C for 24 h. The reaction mixture was then allowed to cool to rt, diluted with EtOAc (5 mL) and filtered through a pad of Celite, eluting with further EtOAc (2 × 10 mL). The solvent was removed under reduced pressure and the crude material purified by preparative TLC (20% acetone/pentane, then a second preparative TLC using 5% Et_2O/CH_2Cl_2) to isolate a small sample (5-10 mg) of *trans*-3-arylated piperidine for HPLC analysis. All characterisation information in agreement with data previously reported for **29b**.

Approx. 1 mg of sample was dissolved in *i*-PrOH/*n*-hexane (1 mL, 5:95 v/v) and separated by HPLC into the 2 corresponding *trans* enantiomers.
HPLC Conditions: Chiralpak IA column, 90:10 *n*-hexane: *i*-PrOH, flow rate: 1 mL min^{-1}, 35 °C, UV detection wavelength: 254 nm.

The preparation of structurally similar racemates followed the same protocol, by replacing 4-iodoanisole with the aryl iodide of choice. HPLC conditions were screened to obtain separation of the 1:1 mixture of enantiomers. Based on retention times of individual enantiomers, e.r. ratios for corresponding enantioenriched products could be calculated (See HPLC Traces in Section 4.4.5).

4.4.3 General Procedure for the Synthesis of Enantioenriched Compounds

Representative PIP-directed Enantioselective Arylation



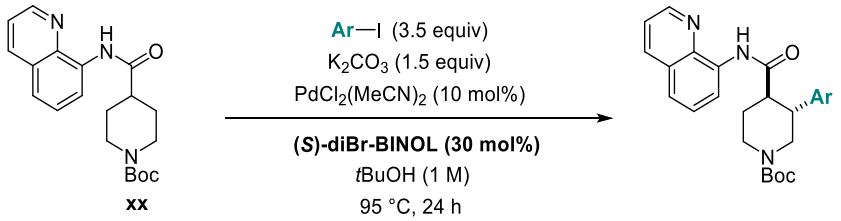
***tert*-Butyl-*cis*-(±)-3-(4-methoxyphenyl)-4-((2-(pyridin-2-yl)propan-2-yl)carbamoyl)piperidine-1-carboxylate (162)**

A flame-dried microwave vial was charged with amide **161** (77 mg, 0.20 mmol, 1.0 equiv), 4-iodoanisole (164 mg, 0.70 mmol, 1.0 equiv), K_2CO_3 (70 mg, 0.50 mmol, 2.5 equiv), (*S*)-BINOL (11.5 mg, 0.04 mmol, 0.2 equiv) and PdI_2 (7.2 mg, 0.02 mmol, 0.1 equiv) in this order. The reaction vessel was sealed and purged with argon, then the solvent (0.6 mL, 0.3 M) was added by syringe. The reaction tube was placed in a preheated oil bath and stirred at 95 °C for 24 h. The reaction mixture was then allowed to cool to rt, diluted with EtOAc (5 mL) and filtered through a pad of Celite, eluting with further EtOAc (2 × 10 mL). The solvent was removed under reduced pressure and the crude material purified by flash column chromatography (10% to 25% MeCN/CH_2Cl_2) to afford **162** as a yellow solid (8.9 mg, 0.02 mmol, 12%, **e.r. 65.5:34.5**). All characterisation information in agreement with data previously reported for **162**.

Approx. 1 mg of sample was dissolved in *i*-PrOH/*n*-hexane (1 mL, 5:95 v/v) and separated by HPLC, with enantiomeric ratios (e.r.) calculated based on the integrations of the areas under each enantiomer peak.

HPLC Conditions: Chiralpak ID column, 80:20 *n*-hexane: *i*-PrOH, flow rate: 1 mL min^{-1}, 35 °C, UV detection wavelength: 254 nm. *See HPLC traces in Section 4.4.5.*

General Procedure R for AQ-directed Enantioselective Arylation



A reaction tube was charged with amide **25** (71 mg, 0.20 mmol, 1.0 equiv), the requisite aryl iodide (0.70 mmol, 3.5 equiv), K_2CO_3 (41 mg, 0.30 mmol, 1.5 equiv), (*S*)-diBr-BINOL (27 mg, 0.06 mmol, 0.3 equiv) and $PdCl_2(MeCN)_2$ (2.6 mg, 0.02 mmol, 0.1 equiv) in this order. The reaction vessel was sealed and purged with argon, then *t*BuOH (0.2 mL, 1 M) was added by syringe. The reaction tube was placed in a

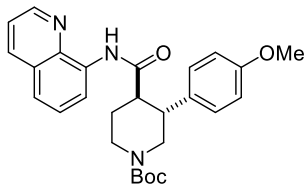
preheated oil bath and stirred at 95 °C for 24 h. The reaction mixture was then allowed to cool to rt, diluted with EtOAc (5 mL) and filtered through a pad of Celite, eluting with further EtOAc (2 × 10 mL). The solvent was removed under reduced pressure and the crude material purified by column chromatography (10% to 20% acetone/pentane). Et_2O (5 mL), followed by pentane (5 mL) were added to the isolated *trans*-3-arylated piperidine, with the resulting suspension concentrated under reduced pressure. This procedure was repeated three times to eliminate residual solvent and afford the desired enantioenriched piperidines.

Where the trans isomer could not be separated from traces of cis-trans arylated product, a second flash column chromatography (5% Et_2O/CH_2Cl_2) was performed. These sequential purifications are denoted accordingly in the individual experimental procedures below.

Approx. 1 mg of sample was dissolved in *i*-PrOH/*n*-hexane (1 mL, 5:95 v/v) and separated by HPLC, with enantiomeric ratios (e.r.) calculated based on the integrations of the areas under each enantiomer peak.

HPLC Conditions: *see individual experimental procedures and HPLC traces in Section 4.4.5.*

***tert*-Butyl-*trans*-3-(4-methoxyphenyl)-4-(quinolin-8-ylcarbamoyl)piperidine-1-carboxylate (29b)**

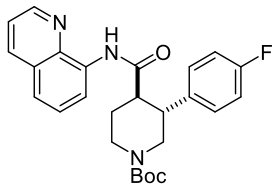


Prepared according to **General Procedure R** using 4-iodoanisole (164 mg) to afford **29b** as a white solid (73 mg, 0.16 mmol, 79%, **e.r. 98:2**). All characterisation information in agreement with data previously reported for **29b**.

Scale-up procedure: A reaction tube was charged with amide **25** (355 mg, 1.00 mmol, 1.0 equiv), 4-iodoanisole (819 mg, 3.50 mmol, 3.5 equiv), K_2CO_3 (137 mg, 1.50 mmol, 1.5 equiv), (S)-diBr-BINOL (135 mg, 0.30 mmol, 0.3 equiv) and $PdCl_2(MeCN)_2$ (26 mg, 0.20 mmol, 0.1 equiv) in this order. The reaction vessel was sealed and purged with argon, then *t*BuOH (1 mL) was added by syringe. The reaction tube was placed in a preheated oil bath and stirred at 95 °C for 24 h. The reaction mixture was then allowed to cool to rt, diluted with EtOAc (5 mL) and filtered through a pad of Celite, eluting with further EtOAc (2 × 10 mL). The solvent was removed under reduced pressure and the crude material purified by column chromatography (10% to 20% acetone/pentane). Et_2O (5 mL), followed by pentane (5 mL) were added to the isolated *trans*-3-arylated piperidine, with the resulting suspension concentrated under reduced pressure. This procedure was repeated three times to eliminate residual solvent and afford **29b** as a white solid (206 mg, 0.45 mmol, 45%, **e.r. 97:3**). All characterisation information in agreement with data previously reported for **29b**.

HPLC Conditions: Chiralpak IA column, 90:10 *n*-hexane: *i*-PrOH, flow rate: 1 mL min^{-1}, 35 °C, UV detection wavelength: 254 nm.

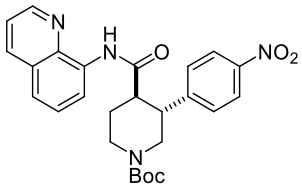
***tert*-Butyl-*trans*-3-(4-fluorophenyl)-4-(quinolin-8-ylcarbamoyl)piperidine-1-carboxylate (57)**



Prepared according to **General Procedure R** using 1-fluoro-4-iodobenzene (155 mg) to afford **57** as a white solid (54 mg, 0.12 mmol, 60%, **e.r. 95:5**). All characterisation information in agreement with data previously reported for **57**.

HPLC Conditions: Chiralpak IA column, 97:3 *n*-hexane: *i*-PrOH, flow rate: 1 mL min^{-1}, 35 °C, UV detection wavelength: 254 nm.

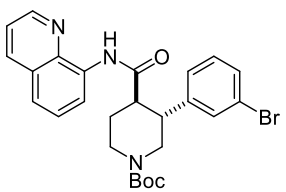
***tert*-Butyl-*trans*-3-(4-nitrophenyl)-4-(quinolin-8-ylcarbamoyl)piperidine-1-carboxylate (165)**



Prepared according to **General Procedure R** using 1-iodo-4-nitrobenzene (174 mg). Purification by sequential flash column chromatography (10% to 20% acetone/pentane, followed by 5% Et_2O/CH_2Cl_2) afforded **165** as a yellow solid (33 mg, 0.07 mmol, 35%, **e.r. 98:2**). R_f 0.27 (20% acetone/pentane); mp = 170–171 °C (from Et_2O/pentane); IR (film)/cm^{-1} 3341 (br NH), 2971, 2928, 1689 (C=O), 1523, 1484, 1422, 1346, 1241, 1159, 951, 829; ^{1}H NMR (500 MHz, DMSO-d_6, 373 K) δ 9.75 (br s, 1 H, NH), 8.83 (dd, *J* = 4.2, 1.7 Hz, 1 H, HC_{Ar}), 8.38 (dd, *J* = 7.7, 1.3 Hz, 1 H, HC_{Ar}), 8.30 (ddd, *J* = 8.3, 1.7, 0.4 Hz, 1 H, HC_{Ar}), 8.09–8.04 (m, 2 H, 2 × HC_{Ar}), 7.70–7.62 (m, 2 H, 2 × HC_{Ar}), 7.60–7.53 (m, 2 H, 2 × HC_{Ar}), 7.49–7.42 (m, 1 H, HC_{Ar}), 4.17 (ddt, *J* = 13.3, 4.4, 2.2 Hz, 1 H, NC*H*HCHAr), 4.07 (ddd, *J* = 13.0, 4.1, 1.6 Hz, 1 H, NC*H*HCH_2), 3.41 (td, *J* = 11.4, 3.9 Hz, 1 H, NCH*H*CH_2), 3.14 (td, *J* = 11.3, 4.1 Hz, 1 H, CHAr), 3.08–2.99 (m, 2 H, CH(C=O) and NCH*H*CHAr), 2.15–2.06 (m, 1 H, NCH_2CHH), 1.77 (tdd, *J* = 12.9, 11.6, 4.5 Hz, 1 H, NCH_2CH*H*), 1.46 (s, 9 H, $C(CH_3)_3$); ^{13}C NMR (126 MHz, DMSO-d_6, 373 K) δ 171.0 (C=O amide), 153.4 (C_{Ar} quat), 148.6 (C=O carbamate), 148.0 (C_{Ar}), 146.2 (C_{Ar} quat), 137.7 (C_{Ar} quat), 135.8 (C_{Ar}), 133.5 (C_{Ar} quat), 128.5 (2 × C_{Ar}), 127.2 (C_{Ar} quat), 126.1 (2 × C_{Ar}), 122.8 (2 × C_{Ar}), 121.3 (C_{Ar}), 116.2 (C_{Ar}), 78.6 (*C*$(CH_3)_3$), 48.34 (N*C*H_2CH_2), 48.25 (*C*H(C=O)), 44.3 (CHAr), 42.5 (N*C*H_2CHAr), 28.5 (NCH_2*C*H_2), 27.6 (C(*C*$H_3)_3$); HRMS (ESI) *m/z* Calculated for $C_{26}H_{29}N_4O_5$ [M+H] 477.2138; Found 477.2123.

HPLC Conditions: Chiralpak IF column, 80:20 *n*-hexane: *i*-PrOH, flow rate: 1 mL min^{-1}, 35 °C, UV detection wavelength: 254 nm.

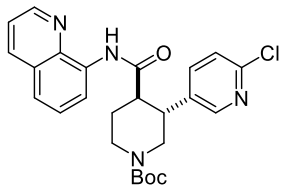
***tert*-Butyl-*trans*-3-(3-bromophenyl)-4-(quinolin-8-ylcarbamoyl)piperidine-1-carboxylate (*trans*-46m)**



Prepared according to **General Procedure R** using 3-bromoiodobenzene (200 mg). Purification by sequential flash column chromatography (10% to 20% acetone/pentane, followed by 5% Et_2O/CH_2Cl_2) afforded ***trans*-46m** as a yellow foam (65 mg, 0.13 mmol, 64%, **e.r. 97:3**). All characterisation information in agreement with data previously reported for ***trans*-46m**.

HPLC Conditions: Chiralpak IA column, 90:10 *n*-hexane: *i*-PrOH, flow rate: 1 mL min^{-1}, 35 °C, UV detection wavelength: 254 nm.

***tert*-Butyl-*trans*-3-(6-chloropyridin-3-yl)-4-(quinolin-8-ylcarbamoyl)piperidine-1-carboxylate (167)**

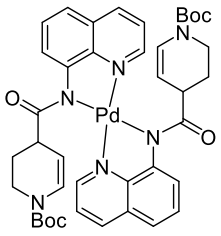


Prepared according to **General Procedure R** using 2-chloro-5-iodopyridine (165 mg). Purification by sequential flash column chromatography (20% to 30% acetone/pentane, followed by 10% Et_2O/CH_2Cl_2) afforded **167** as a white foam (56 mg, 0.12 mmol, 60%, **e.r. 90:10**). R_f 0.21 (10% Et_2O/CH_2Cl_2); mp = 120–121 °C (from Et_2O/pentane); IR (film)/cm^{-1} 3340 (NH br), 2974, 2925, 2859, 1689 (C=O), 1527, 1484, 1460, 1423, 1242, 1160, 828; ^{1}H NMR (500 MHz, DMSO-d_6, 373 K) δ 9.79 (br s, 1 H, NH), 8.92–8.82 (m, 1 H, HC_{Ar}), 8.44–8.35 (m, 2 H, 2 × HC_{Ar}), 8.35–8.29 (m, 1 H, HC_{Ar}), 7.93–7.80 (m, 1 H, HC_{Ar}), 7.64–7.56 (m, 2 H, 2 × HC_{Ar}), 7.56–7.44 (m, 1 H, HC_{Ar}), 7.35 (d, *J* = 8.2 Hz, 1 H, HC_{Ar}), 4.16 (ddt, *J* = 13.2, 4.3, 2.2 Hz, 1 H, NC*H*HCH_2), 4.08–4.03 (m, 1 H, NC*H*HCHAr), 3.36 (td, *J* = 11.4, 3.9 Hz, 1 H, CH(C=O)), 3.05–3.02 (m, 3 H, NCH*H*CH_2, NCH*H*CHAr and CHAr), 2.12–2.05 (m, 1 H, NCH_2CH*H*), 1.80–1.71 (m, 1 H, NCH_2CH*H*), 1.46 (s, 9 H, $C(CH_3)_3$); ^{13}C NMR (126 MHz, DMSO-d_6, 373 K) δ 171.0 (C=O amide), 153.4 (C=O carbamate), 148.7 (C_{Ar}), 148.3 (C_{Ar} quat), 148.1 (C_{Ar}), 138.1 (C_{Ar}), 137.7 (C_{Ar} quat), 135.8 (C_{Ar}), 135.6 (C_{Ar} quat), 133.5 (C_{Ar} quat), 127.2 (C_{Ar} quat), 126.1 (C_{Ar}), 123.4 (C_{Ar}), 121.4 (C_{Ar}), 121.3 (C_{Ar}), 116.3 (C_{Ar}), 78.6 (*C*$(CH_3)_3$), 48.2 (N*C*H_2CHAr), 48.1 (*C*H(C=O)), 42.4 (N*C*H_2CH_2), 41.1 (CHAr), 28.6 (NCH_2*C*H_2), 27.6 (C(*C*$H_3)_3$); HRMS (ESI) *m/z* Calculated for $C_{25}H_{28}N_4O_3Cl$ [M+H] 467.1850; Found 467.1859.

HPLC Conditions: Chiralpak IB column, 90:10 *n*-hexane: *i*-PrOH, flow rate: 1 mL min^{-1}, 35 °C, UV detection wavelength: 254 nm.

4.4.4 Palladacycle Formation

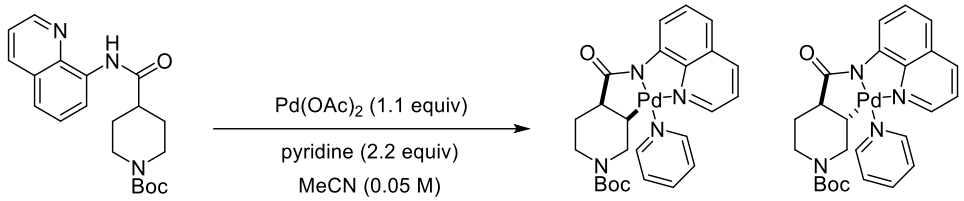
***tert*-Butyl 4-(quinolin-8-ylcarbamoyl)-3,4-dihydropyridine-1(2*H*)-carboxylate – dimer (168)**



$Pd(OAc)_2$ (22.4 mg, 0.10 mmol, 1.0 equiv) and (*S*)-BINOL (57 mg, 0.20 mmol, 2.0 equiv) were added to a solution of amide **25** (36 mg, 0.10 mmol, 1.0 equiv) in *t*BuOD (0.1 mL). The resulting mixture was gradually heated to 95 °C and stirred at this temperature for 18 h, resulting in the formation of a black precipitate. Upon cooling to rt, the black precipitate was separated by gravity filtration and was found to consist of a mixture of unidentified BINOL-containing side-products. The filtrate was concentrated under reduced pressure and purified by flash column chromatography (20% $MeCN/CH_2Cl_2$) to afford **168** as a yellow glass (24 mg, 0.03 mmol, 15%). R_f 0.45 (20% $MeCN/CH_2Cl_2$); IR (film)/cm^{-1} 2962, 2924, 2862, 1732 (C=O), 1617, 1502, 1460, 1382, 1313, 1286, 1257, 1153, 1055, 1032, 824, 760; ^{1}H NMR (400 MHz, $CDCl_3$) δ 9.18 (dd, *J* = 5.1, 1.6 Hz, 1 H, HC_{Ar}), 9.01 (dd, *J* = 7.9, 1.2 Hz, 1 H, HC_{Ar}), 8.82 (d, *J* = 6.0 Hz, 1 H, NC*H*=CH), 8.37 (dd, *J* = 8.3, 1.5 Hz, 1 H, HC_{Ar}), 7.62–7.51 (m, 2 H, 2 × HC_{Ar}), 7.45 (d, *J* = 8.0 Hz, 1 H, HC_{Ar}), 4.99 (t, *J* = 6.0 Hz, 1 H, NCH=C*H*), 4.13 (d, *J* = 13.9 Hz, 1 H, NC*H*HCH_2), 3.45 (br t, *J* = 5.0 Hz, 1 H, CH(C=O)), 3.20–3.04 (m, 1 H, NCH*H*CH_2), 2.51–2.46 (m, 1 H, NCH_2CH*H*), 1.81–1.69 (m, 1 H, NCH_2CH*H*), 1.61 (s, 12 H, $C(CH_3)_3$ and CH_3CN); ^{13}C NMR (101 MHz, $CDCl_3$) δ 171.5 (C=O amide), 154.2 (C=O carbamate), 148.6 (C_{Ar}), 139.2 (C_{Ar} quat), 131.6 (N*C*H=CH), 130.1 (C_{Ar}), 129.6 (C_{Ar} quat), 127.2 (C_{Ar} quat), 122.9 (C_{Ar}), 121.7 (C_{Ar}), 121.0 (C_{Ar}), 85.0

(*C*(CH_3)$_3$), 54.3 (NCH=*C*H), 41.9 (*C*H(C=O)), 39.3 (N*C*H_2*C*H_2), 28.0 (C(*C*H_3)$_3$), 25.7 (NCH_2*C*H_2); *Peaks for CH_3CN not observed, presumably due to dimerisation of the complex in $CDCl_3$ during the longer timeframe required for running ^{13}C.* HRMS (ESI) *m/z* Calculated for $C_{22}H_{25}N_4O_3{}^{106}Pd^+$ [M-$C_{20}H_{22}N_3O_3$+CH_3CN]$^+$ 499.0961; Found 499.0959.

6-Membered-(±)-palladacycle-pyridine *cis*- and *trans*-complexes 169 and *trans*-169

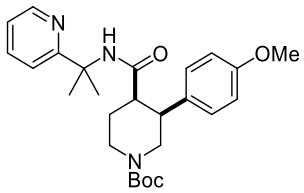


A flame-dried microwave vial was charged with amide **25** (36 mg, 0.10 mmol, 1.0 equiv) and $Pd(OAc)_2$ (25 mg, 0.11 mmol, 1.1 equiv). The reaction vessel was sealed and purged with argon, then MeCN (2 mL), followed by pyridine (0.2 mL, 0.22 mmol, 2.2 equiv) were added by syringe. The tube was placed in a preheated oil bath and the mixture stirred at 60 °C for 18 h. Upon cooling to rt, the mixture was filtered through Celite, eluting with further MeCN (2 × 10 mL). The mixture was then concentrated under reduced pressure and the residue purified by flash column chromatography (30% to 50% EtOAc/CH_2Cl_2) to afford **169** and ***trans*-169** as a yellow oil and an inseparable mixture of diastereomers (40 mg, 0.08 mmol, 80%). R_f 0.15 (30% EtOAc/CH_2Cl_2). IR (film)/cm^{-1} 3329, 2938, 2973, 1674 (C=O), 1602, 1480, 1248, 1389, 1162, 904, 723, 645; Due to extensive rotamer interconversion, full characterization by NMR could not be performed and the identity was assigned based on analogy to a *cis*-palladacycle analogue of **169**, previously isolated as a single diastereomer by Dr. Daniele Antermite.[232] HRMS (ESI) *m/z* Calculated for $C_{25}H_{29}N_4O_3{}^{106}Pd$ [M+H] 539.1274; Found 539.1295..

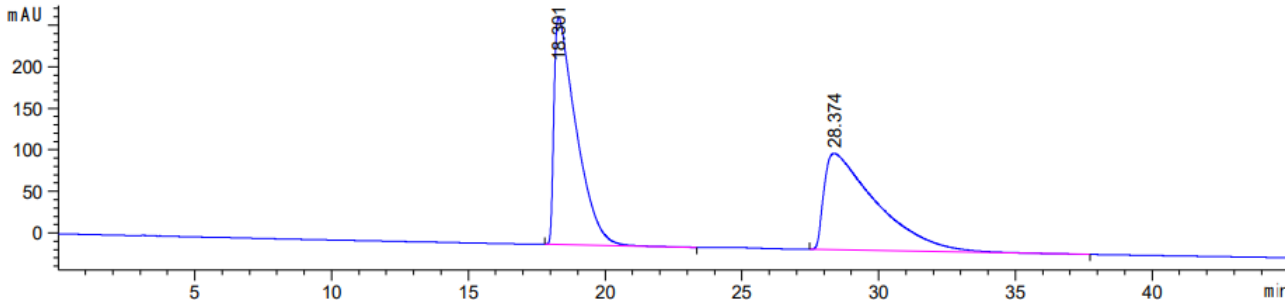
4.4.5 HPLC Traces for Enantioenriched 3,4-Disubstituted Piperidines

***tert*-Butyl-*cis*-(±)-3-(4-methoxyphenyl)-4-((2-(pyridin-2-yl)propan-2-yl)carbamoyl)piperidine-1-carboxylate**

Conditions: Chiralpak ID column, 80:20 *n*-hexane: *i*-PrOH, flow rate: 1 mL min^{-1}, 35 °C, UV detection wavelength: 254 nm.

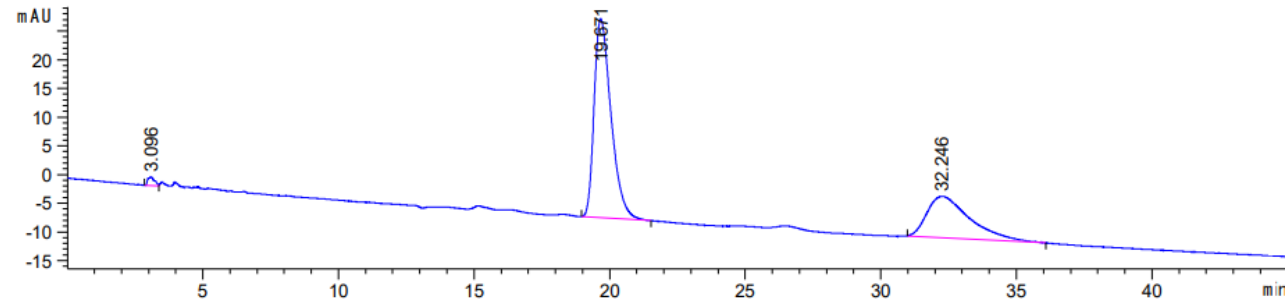


***rac*–162**



Peak #	RetTime [min]	Type	Width [min]	Area [mAU*s]	Height [mAU]	Area %
1	18.301	BB	0.8103	1.54394e4	273.62961	49.8736
2	28.374	BBA	1.7383	1.55177e4	116.17842	50.1264
Totals :				3.09571e4	389.80803	

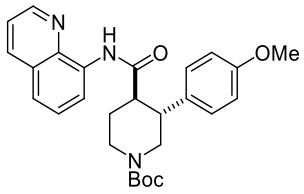
162



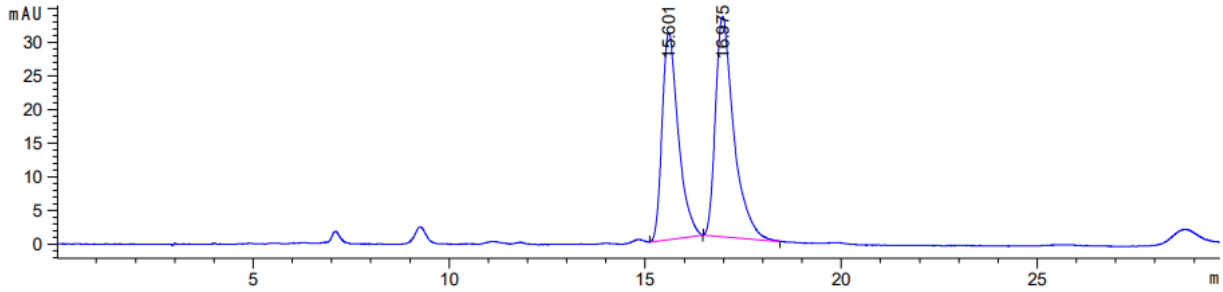
Peak #	RetTime [min]	Type	Width [min]	Area [mAU*s]	Height [mAU]	Area %
1	3.096	BV	0.2270	26.34017	1.51407	1.1343
2	19.671	BB	0.6353	1503.47144	34.71498	64.7430
3	32.246	BB	1.2927	792.40228	7.18478	34.1227
Totals :				2322.21389	43.41384	

***tert*-Butyl-*trans*-3-(4-methoxyphenyl)-4-(quinolin-8-ylcarbamoyl)piperidine-1-carboxylate**

Conditions: Chiralpak IA column, 90:10 *n*-hexane: *i*-PrOH, flow rate: 1 mL min^{-1}, 35 °C, UV detection wavelength: 254 nm.

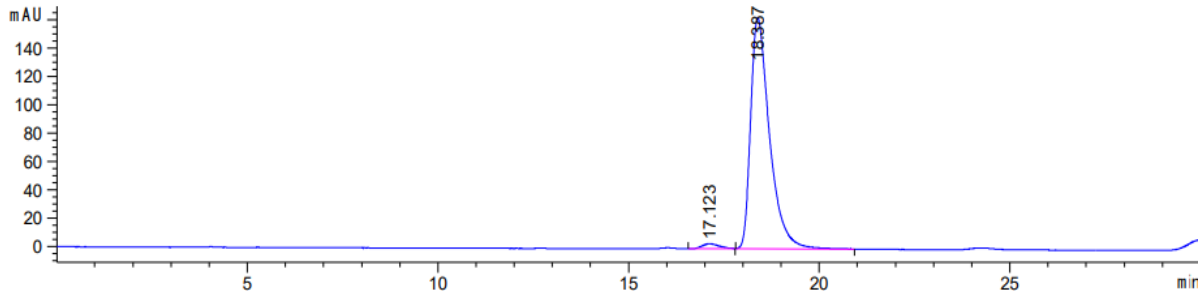


***rac*–29b**



Peak #	RetTime [min]	Type	Width [min]	Area [mAU*s]	Height [mAU]	Area %
1	15.601	BB	0.4358	880.60846	30.78279	45.3019
2	16.975	BB	0.4850	1063.25659	32.73140	54.6981
Totals :				1943.86505	63.51419	

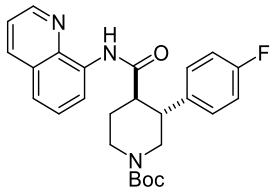
29b



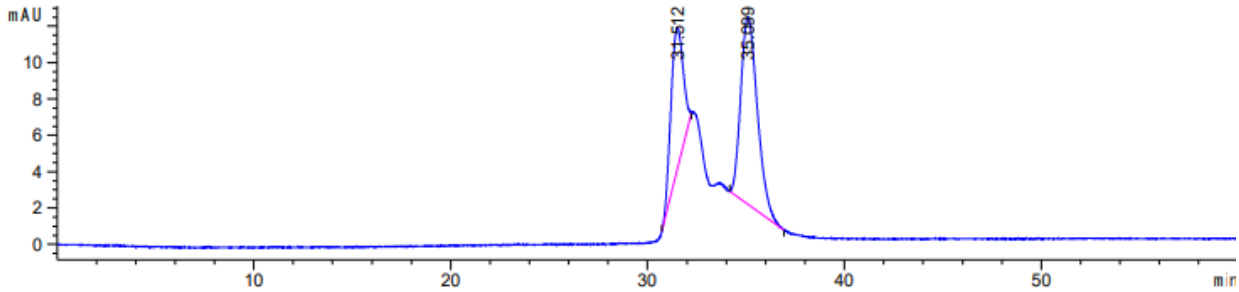
Peak #	RetTime [min]	Type	Width [min]	Area [mAU*s]	Height [mAU]	Area %
1	17.123	BB	0.4024	106.67000	3.45325	1.8699
2	18.387	BB	0.5147	5597.83350	163.00301	98.1301
Totals :				5704.50349	166.45626	

***tert*-Butyl-*trans*-3-(4-fluorophenyl)-4-(quinolin-8-ylcarbamoyl)piperidine-1-carboxylate**

Conditions: Chiralpak IA column, 97:3 *n*-hexane: *i*-PrOH, flow rate: 1 mL min^{-1}, 35 °C, UV detection wavelength: 254 nm.

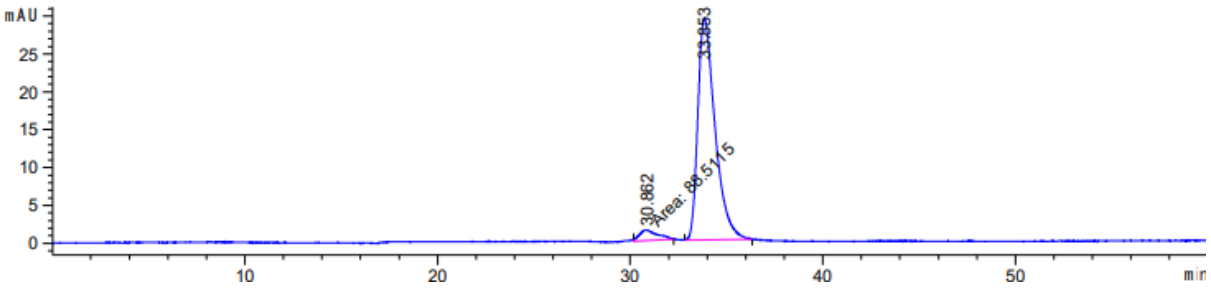


rac*–57 – *presents impurity not visible by NMR that is inseparable by standard chromatographic methods



Peak #	RetTime [min]	Type	Width [min]	Area [mAU*s]	Height [mAU]	Area %
1	31.512	BB	0.5140	334.56534	7.80631	35.6271
2	35.099	BB	0.7565	604.51068	10.27388	64.3729
Totals :				939.07602	18.08019	

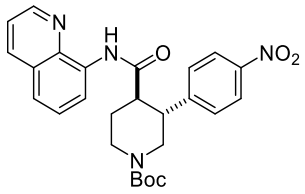
57



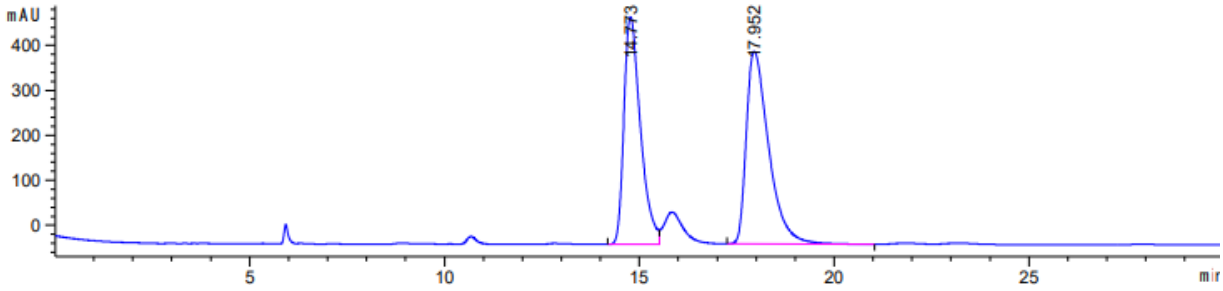
Peak #	RetTime [min]	Type	Width [min]	Area [mAU*s]	Height [mAU]	Area %
1	30.862	MM	1.0626	88.51151	1.38834	4.6515
2	33.853	BB	0.8911	1814.34241	29.27183	95.3485
Totals :				1902.85391	30.66017	

***tert*-Butyl-*trans*-3-(4-nitrophenyl)-4-(quinolin-8-ylcarbamoyl)piperidine-1-carboxylate**

Conditions: Chiralpak IF column, 80:20 *n*-hexane: *i*-PrOH, flow rate: 1 mL min^{-1}, 35 °C, UV detection wavelength: 254 nm.

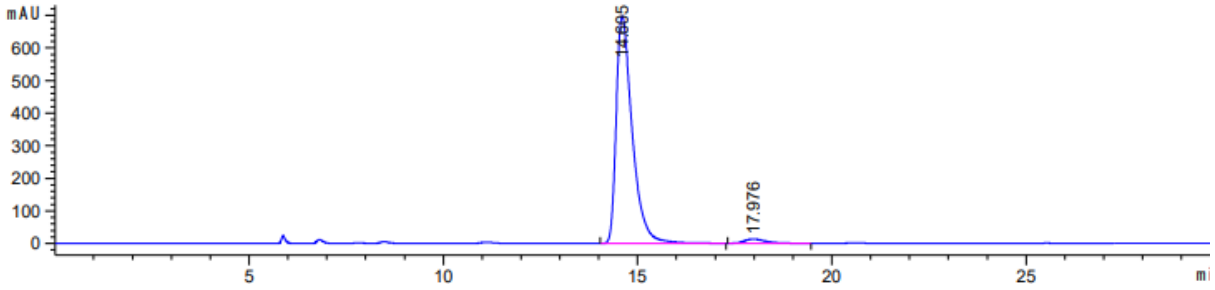


***rac*–165**



Peak #	RetTime [min]	Type	Width [min]	Area [mAU*s]	Height [mAU]	Area %
1	14.773	BV	0.4447	1.16549e4	399.10559	46.5414
2	17.952	BB	0.6025	1.33871e4	336.21564	53.4586
Totals :				2.50419e4	735.32123	

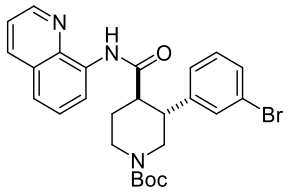
165



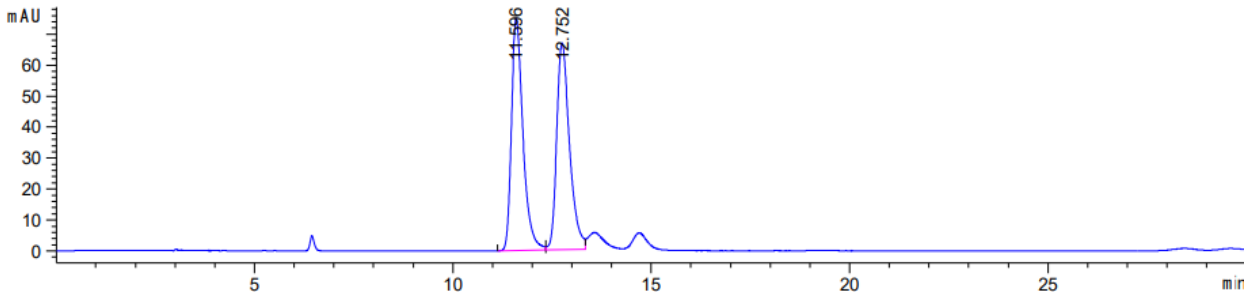
Peak #	RetTime [min]	Type	Width [min]	Area [mAU*s]	Height [mAU]	Area %
1	14.605	BB	0.4324	1.99776e4	696.97821	97.6459
2	17.976	BB	0.5419	481.62881	13.01085	2.3541
Totals :				2.04593e4	709.98906	

***tert*-Butyl-*trans*-3-(3-bromophenyl)-4-(quinolin-8-ylcarbamoyl)piperidine-1-carboxylate**

Conditions: Chiralpak IA column, 90:10 *n*-hexane: *i*-PrOH, flow rate: 1 mL min^{-1}, 35 °C, UV detection wavelength: 254 nm.

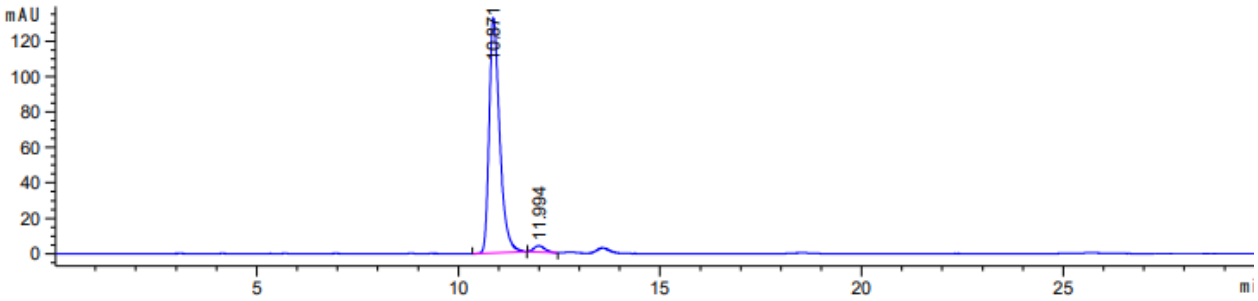


***rac–trans*-46m**



Peak #	RetTime [min]	Type	Width [min]	Area [mAU*s]	Height [mAU]	Area %
1	11.596	BV	0.3055	1511.94519	74.89310	50.1718
2	12.752	VV	0.3407	1501.59351	66.69091	49.8282
Totals :				3013.53870	141.58401	

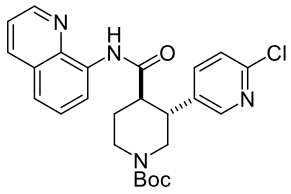
***trans*-46m**



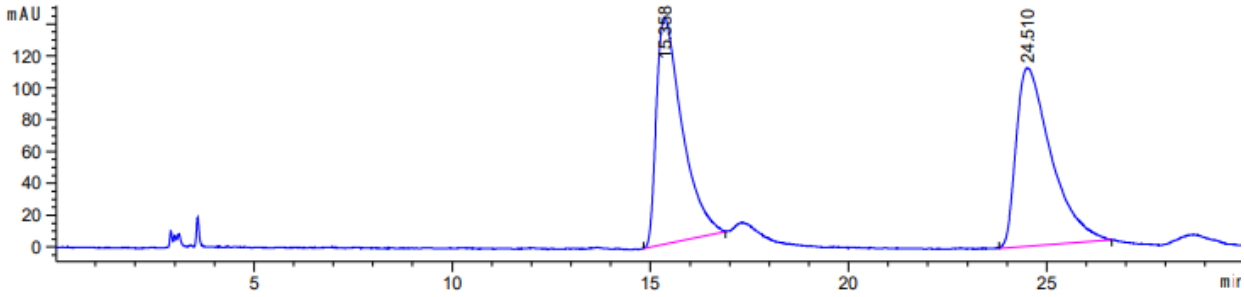
Peak #	RetTime [min]	Type	Width [min]	Area [mAU*s]	Height [mAU]	Area %
1	10.871	BB	0.2740	2408.47412	132.54710	97.3259
2	11.994	BB	0.2854	66.17393	3.55039	2.6741
Totals :				2474.64806	136.09750	

***tert*-Butyl-*trans*-3-(6-chloropyridin-3-yl)-4-(quinolin-8-ylcarbamoyl)piperidine-1-carboxylate**

Conditions: Chiralpak IB column, 90:10 *n*-hexane: *i*-PrOH, flow rate: 1 mL min^{-1}, 35 °C, UV detection wavelength: 254 nm.

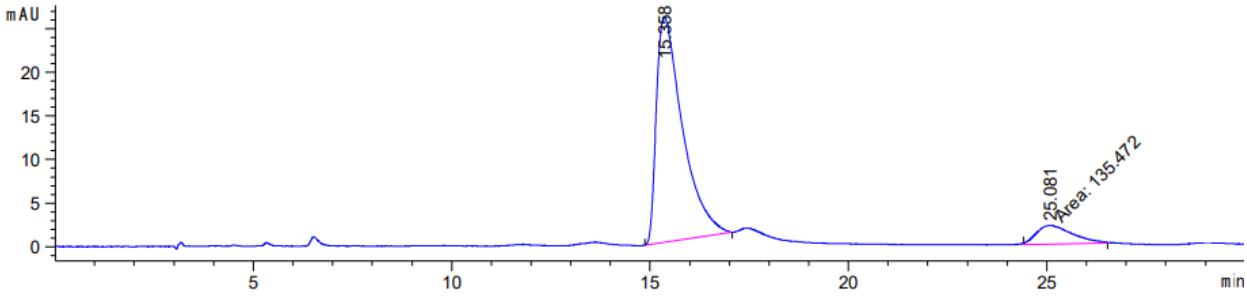


***rac*–167**



Peak #	RetTime [min]	Type	Width [min]	Area [mAU*s]	Height [mAU]	Area %
1	15.358	BB	0.6387	6438.67871	142.61279	48.3957
2	24.510	VB	0.7344	6865.55957	111.81297	51.6043
Totals :				1.33042e4	254.42577	

167



Peak #	RetTime [min]	Type	Width [min]	Area [mAU*s]	Height [mAU]	Area %
1	15.358	BB	0.6744	1185.42761	25.87770	89.7439
2	25.081	MM	1.0673	135.47231	2.11550	10.2561
Totals :				1320.89992	27.99320	

References

1 Maehr, H. *J. Chem. Educ.* **1985**, 62, 114.

2 Lichtenberg, F. R. *Int. Health* **2019**, *11*, 403–416.

3 Nurk, S.; Koren, S.; Rhie, A.; Rautiainen, M.; Bzikadze, A. V.; Mikheenko, A.; Vollger, M. R.; Altemose, N. et al *Science* **2022**, *376*, 44–53.

4 Kabadi, A.; McDonnell, E.; Frank, C. L.; Drowley, L. *SLAS Discovery* **2020**, *25*, 823–842.

5 Suthram, S.; Dudley, J. T.; Chiang, A. P.; Chen, R.; Hastie, T. J.; Butte, A. J. *PLOS Comput. Biol.* **2010**, *6*, e1000662.

6 Deeks, S. G.; Archin, N.; Cannon, P.; Collins, S.; Jones, R. B.; de Jong, M. A. W. P.; Lambotte, O.; Lamplough, R.; Ndung'u, T.; Sugarman, J.; Tiemessen, C. T.; Vandekerckhove, L.; Lewin, S. R. *Nat. Med.* **2021**, *27*, 2085–2098.

7 Hughes, R. E.; Elliott, R. J. R.; Dawson, J. C.; Carragher, N. O. *Cell Chem. Biol.* **2021**, *28*, 338–355.

8 Zhu, N.; Zhang, D.; Wang, W.; Li, X.; Yang, B.; Song, J.; Zhao, X.; Huang, B.; Shi, W.; Lu, R.; Niu, P.; Zhan, F.; Ma, X.; Wang, D.; Xu, W.; Wu, G.; Gao, G. F.; Tan, W. *N. Engl. J. Med.* **2020**, *382*, 727–733.

9 Ventola, C. L. *P T.* **2015**, *40*, 277–283.

10 Gormely, G.; Salazar, D. E. Modern Drug Discovery and Development. In *Clinical and Translational Science: Principles of Human Research, 2nd Edition*; Robertson, D., Williams, G. H. Eds.; Elsevier – Academic Press: Cambridge, MA, 2017; pp 719–743.

11 Holenz, J.; Stoy, P. *Bioorg. Med. Chem. Lett.* **2019**, *29*, 517–524.

12 Bleicher, K. H.; Böhm, H.-J.; Müller, K.; Alanine, A. I. *Nat. Rev. Drug Discov.* **2003**, *2*, 369–378.

13 Wouters O. J.; McKee M.; Luyten J. *JAMA* **2020**, *323*, 844–853.

14 Mullard, A. *Nat. Rev. Drug Discov.* **2019**, *18*, 85–89.

15 Dowden, H.; Munro, J. *Nat. Rev. Drug Discov.* **2019**, *18*, 495–496.

16 Hay, M.; Thomas, D. W.; Craighead, J. L.; Economides, C.; Rosenthal, J. *Nat. Biotechnol.* **2014**, *32*, 40-51.

17 Waring, M. J.; Arrowsmith, J.; Leach, A. R.; Leeson, P. D.; Mandrell, S.; Owen, R. M.; Pairaudeau, G.; Pennie, W. D.; Pickett, S. D.; Wang, J.; Wallace, O.; Weir, A. *Nat. Rev. Drug Discov.* **2015**, *14*, 475–486.

18 Kola, I.; Landis, J. *Nat. Rev. Drug Discov.* **2004**, *3*, 711–716.

19 Harrison, R. K. *Nat. Rev. Drug Discov.* **2016**, *15*, 817–818.

20 Hutchinson, L.; Kirk, R. *Nat. Rev. Clin. Oncol.* **2011**, *8*, 189–190.

21 Leeson, P. D.; Springthorpe, B. *Nat. Rev. Drug Discov.* **2007**, *6*, 881–890.

22 Blakemore, D. C.; Castro, L.; Churcher, I.; Rees, D. C.; Thomas, A. W.; Wilson, D. M.; Wood, A. *Nat. Chem.* **2018**, *10*, 383–394.

23 Inglese, J.; Johnson, R. L.; Simeonov, A.; Xia, M.; Zheng, W.; Austin, C. P.; Auld, D. S. *Nat. Chem. Biol.* **2007**, *3*, 466–479.

24 Lane, S. J.; Eggleston, D. S.; Brinded, K. A.; Hollerton, J. C.; Taylor, N. L.; Readshaw, S. A. *Drug Discov.* **2006**, *11*, 267–272.

25 Lipinski, C. A.; Lombardo, F.; Dominy, B. W.; Feeney, P. J. *Adv. Drug Deliv. Rev.* **2001**, *46*, 3–26.
26 Lahana, R. *Drug Discov.* **2003**, *8*, 655–656.
27 Hughes, J.; Rees, S.; Kalindjian, S.; Philpott, K. *Br. J. Pharmacol.* **2011**, *162*, 1239–1249.
28 Carr, R.; Jhoti, H. *Drug Discov.* **2002**, *7*, 522–527.
29 Shuker, S. B.; Hajduk, P. J.; Meadows, R. P.; Fesik, S. W. *Science* **1996**, *274*, 1531–1534.
30 Erlanson, D. A.; Fesik, S. W.; Hubbard, R. E.; Jahnke, W.; Jhoti, H. *Nat. Rev. Drug Discov.* **2016**, *15*, 605–619.
31 de Souza Neto, L. R.; Moreira-Filho, J. T.; Neves, B. J.; Maidana, R. L. B. R.; Guimarães, A. C. R.; Furnham, N.; Andrade, C. H.; Silva, F. P. *Front. Chem.* **2020**, *8*, 93.
32 Al-Ali, H. *Med. Chem. Commun.* **2016**, *7*, 788–798.
33 Childers, W. E.; Elokely, K. M.; Abou-Gharbia, M. *ACS Med. Chem. Lett.* **2020**, *11*, 1820–1828.
34 Moffat, J. G.; Vincent, F.; Lee, J. A.; Eder, J.; Prunotto, M. *Nat. Rev. Drug Discov.* **2017**, *16*, 531–543.
35 Martín, A.; Nicolaou, C. A.; Toledo, M. A. *Commun. Chem.* **2020**, *3*, 127.
36 Brenner, S.; Lerner, R. A. *Proc. Natl. Acad. Sci. U.S.A* **1992**, *89*, 5381–5383.
37 Lerner R., Janda K., Brenner S., Nielsen J., ENCODED COMBINATORIAL CHEMICAL LIBRARIES, PCT Int. Appl. WO9320242, 1993.
38 Song, M.; Hwang, G. T. *J. Med. Chem.* **2020**, *63*, 6578–6599.
39 Seifert, M. H. J.; Wolf, K.; Vitt, D. *BIOSILICO* **2003**, *1*, 143–149.
40 Leach, A. *Drug Discov.* **2000**, *5*, 326–336.
41 Lipinski, C. A.; Lombardo, F.; Dominy, B. W.; Feeney, P. J. *Adv. Drug Deliv. Rev.* **1997**, *23*, 3–25.
42 Jimenez, D. G.; Sebastiano, M. R.; Caron, G.; Ermondi, G. *ADMET DMPK* **2021**, *9*, 243–254.
43 Gleeson, M. P. J. *Med. Chem.* **2008**, *51*, 817–834.
44 Hughes, J. D.; Blagg, J.; Price, D. A.; Bailey, S.; DeCrescenzo, G. A.; Devraj, R. V.; Ellsworth, E.; Fobian, Y. M.; Gibbs, M. E.; Gilles, R. W.; Greene, N.; Huang, E.; Krieger-Burke, T.; Loesel, J.; Wager,T.; Whiteley, L.; Zhang, Y. *Bioorg. Med. Chem. Lett.* **2008**, *18*, 4872–4875.
45 Nadin, A.; Hattotuwagama, C.; Churcher, I. *Angew. Chem. Int. Ed.* **2012**, *51*, 1114–1122.
46 P. D. Leeson, B. Springthorpe, *Nat. Rev. Drug Discov.* **2007**, *6*, 881–890.
47 Waring, M. J. *Expert Opin. Drug Discov.* **2010**, *5*, 235–248.
48 Waring, M. J. *Bioorg. Med. Chem. Lett.* **2009**, *19*, 2844–2851.
49 Wildman, S.; Crippen, G. J. *Chem. Inf. Model.* **1999**, *39*, 868–873.
50 Savjani, K. T.; Gajjar, A. K.; Savjani, J. K. *ISRN Pharm* **2012**, *2012*, 195727.
51 Hann, M. M. *Med. Chem. Commun*. **2011**, *2*, 349–355.
52 Waring, M. J. *Expert Opin. Drug Discov.* **2010**, *5*, 235–248.
53 Nassar, A.-E. F.; Kamel, A. M.; Clarimont, C. *Drug Discov.* **2004**, *9*, 1020–1028.
54 Veber, D. F.; Johnson, S. R.; Cheng, H.; Smith, B. R.; Ward, K. W.; Kopple, K. D. *J. Med. Chem.* **2002**, *45*, 2615–2623.
55 Pajouhesh, H.; Lenz, G. R. *NeuroRx* **2005**, *2*, 541–553.

56 Daina, A.; Michielin, O.; Zoete, V. *Sci. Rep.* **2017**, *7*, 42717.

57 Daina, A.; Zoete, V. *ChemMedChem* **2016**, *11*, 1117–1121.

58 Lovering, F.; Bikker, J.; Humblet, C. *J. Med. Chem.* **2009**, *52*, 6752–6756.

59 Lovering, F. *Med. Chem. Commun.* **2013**, *4*, 515–519.

60 Ritchie, T. J.; Macdonald, S. J. F. *Drug Discov.* **2009**, *14*, 1011–1020.

61 Ishikawa, M.; Hashimoto, Y. *J. Med. Chem.* **2011**, *54*, 1539−1554.

62 Ritchie, T. J.; Macdonald, S. J. F.; Peace, S.; Pickett, S. D.; Luscombe, C. N. *Med. Chem. Commun.* **2012**, *3*, 1062–1069.

63 Gunaydin, H.; Bartberger, M. D. *ACS Med. Chem. Lett.* **2016**, *7*, 341–344.

64 Campos, K. R.; Coleman, P. J.; Alvarez, J. C.; Dreher, S. D.; Garbaccio, R. M.; Terrett, N. K.; Tillyer, R. D.; Truppo, M. D.; Parmee, E. R. *Science* **2019**, *363*, eaat0805.

65 Grygorenko, O. O.; Volochnyuk, D. M.; Ryabukhin, S. V.; Judd, D. B. *Chem. Eur. J.* **2020**, *26*, 1196–1237.

66 Roughley, S. D.; Jordan, A. M. *J. Med. Chem.* **2011**, *54*, 3451–3479.

67 Brown, D. G.; Boström, J. *J. Med. Chem.* **2016**, *59*, 4443–4458.

68 Silvestri, I. P.; Colbon, P. J. J. *ACS Med. Chem. Lett.* **2021**, *12*, 1220–1229.

69 Rej, S.; Das, A.; Chatani, N. *Coord. Chem. Rev.* **2021**, *431*, 213683.

70 Vitaku, E.; Smith, D. T.; Njardarson, J. T. *J. Med. Chem.* **2014**, *57*, 10257–10274.

71 DeWire, S. M.; Yamashita, D. S.; Rominger, D. H.; Liu, G.; Cowan, C. L.; Graczyk, T. M.; Chen, X.-T.; Pitis, P. M.; Gotchev, D.; Yuan, C.; Koblish, M.; Lark, M. W.; Violin, J. D. *J. Pharmacol. Exp. Ther.* **2013**, *344*, 708–717.

72 Chang, C. A.; W.; Gilson, M. K. *Proc. Natl. Acad. Sci. U.S.A* **2007**, *104*, 1534–1539.

73 For a more recent review, see: Katritzky, A. R.; Ramsden, C. A.; Joule, J. A.; Zhdankin, V. V. Synthesis of Monocyclic Rings with One Heteroatom. In *Handbook of Heterocyclic Chemistry*, 3rd Edition; Katritzky, A. R., Ramsden, C. A., Joule, J. A., Zhdankin, V. V., Eds.; Elsevier: Amsterdam, 2010; pp 652–703.

74 For selected cyclisaion examples, see: (a) Larsen, M. A.; Hennessy, E. T.; Deem, M. C.; Lam, Y.; Saurí, J.; Sather, A. C. A *J. Am. Chem. Soc.* **2020**, *142*, 726–732; (b) Chamberlain, A. E. R.; Paterson, K. J.; Armstrong, R. J.; Twin, H. C.; Donohoe, T. J. *Chem. Commun.* **2020**, *56*, 3563–3566; (c) Boddy, A. J.; Affron, D. P.; Cordier, C. J.; Rivers, E. L.; Spivey, A. C.; Bull, J. A. *Angew. Chem. Int. Ed.* **2019**, *58*, 1458–1462; (d) Sandmeier, T.; Krautwald, S.; Carreira, E. M. *Angew. Chem. Int. Ed.* **2017**, *56*, 11515–11519.

75 For recent examples of asymmetric cyclisations, see: (a) Dai, X.-J.; Engl, O. D.; León, T.; Buchwald, S. L. *Angew. Chem. Int. Ed.* **2019**, *58*, 3407–3411; (b) Ma, X.; Hazelden, I. R.; Langer, T.; Munday, R. H.; Bower, J. F. *J. Am. Chem. Soc.* **2019**, *141*, 3356–3360.

76 For a review of transition metal catalysed intramolecular amination, see: Zhang, M.; Wang, Q.; Peng, Y.; Chen, Z.; Wan, C.; Chen, J.; Zhao, Y.; Zhang, R.; Zhang, A. Q. *Chem. Commun.* **2019**, *55*, 13048–13065.

77 Wiesenfeldt, M. P.; Nairoukh, Z.; Dalton, T.; Glorius, F. *Angew. Chem. Int. Ed.* **2019**, *58*, 10460–10476.

78 Adrio, J.; Carretero, J. C. *Chem. Commun.* **2019**, *55*, 11979–11991.

79 Liu, G.-Q.; Opatz, T. Recent Advances in the Synthesis of Piperidines: Functionalization of Preexisting Ring Systems. In *Advances in Heterocyclic Chemistry*, 1st Edition; Scriven, E. F. V, Ramsden, C., Eds.; Elsevier – Academic Press: Cambridge, MA, 2018; Vol. 125, pp 107–234.

80 González-Bobes, F.; Fu, G. C. *J. Am. Chem. Soc.* **2006**, *128*, 5360–5361.

81 Strotman, N. A.; Sommer, S.; Fu, G. C. *Angew. Chem. Int. Ed.* **2007**, *46*, 3556–3558.

82 Yang, Y.; Niedermann, K.; Han, C.; Buchwald, S. L. *Org. Lett.* **2014**, *16*, 4638–4641.

83 (a) Vechorkin, O.; Proust, V.; Hu, X. *J. Am. Chem. Soc.* **2009**, *131*, 9756–9766; (b) Gonnard, L.; Guérinot, A.; Cossy, J. *Chem. Eur. J.* **2015**, *21*, 12797–12803; (c) Hofmayer, M. S.; Hammann, J. M.; Haas, D.; Knochel, P. *Org. Lett.* **2016**, *18*, 6456–6459.

84 Bhonde, V. R.; O'Neill, B. T.; Buchwald, S. L. *Angew. Chem. Int. Ed.* **2016**, *55*, 1849–1853.

85 Cornella, J.; Edwards, J. T.; Qin, T.; Kawamura, S.; Wang, J.; Pan, C.-M.; Gianatassio, R.; Schmidt, M.; Eastgate, M. D.; Baran, P. S. *J. Am. Chem. Soc.* **2016**, *138*, 2174–2177.

86 Sandfort, F.; O'Neill, M. J.; Cornella, J.; Wimmer, L.; Baran, P. S. *Angew. Chem. Int. Ed.* **2017**, *56*, 3319–3323.

87 Merchant, R. R.; Edwards, J. T.; Qin, T.; Kruszyk, M. M.; Bi, C.; Che, G.; Bao, D.-H.; Qiao, W.; Sun, L.; Collins, M. R.; Fadeyi, O. O.; Gallego, G. M.; Mousseau, J. J.; Nuhant, P.; Baran, P. S. *Science*, **2018**, *360*, 75–80.

88 Molander, G. A.; Traister, K. M.; O'Neill, B. T. *J. Org. Chem.* **2014**, *79*, 5771–5780.

89 Wang, X.; Ma, G.; Peng, Y.; Pitsch, C. E.; Moll, B. J.; Ly, T. D.; Wang, X.; Gong, H. *J. Am. Chem. Soc.* **2018**, *140*, 14490–14497.

90 Hughes, J. M. E.; Fier, P. S. *Org. Lett.* **2019**, *21*, 5650–5654.

91 Mennie, K. M.; Vara, B. A.; Levi, S. M. *Org. Lett.* **2020**, *22*, 556–559.

92 Shaw, M. H.; Twilton, J.; MacMillan, D. W. C. *J. Org. Chem.* **2016**, *81*, 6898–6926.

93 Zuo, Z.; Ahneman, D. T.; Chu, L.; Terrett, J. A.; Doyle, A. G.; MacMillan, D. W. C. *Science* **2014**, *345*, 437–440.

94 For reviews on α-functionalization of piperidines, see: (a) Mitchell E. A.; Peschiulli, A.; Lefevre, N.; Meerpoel, L.; Maes, B. U. W. *Chem. Eur. J.* **2012**, *18*, 10092–10142; (b) Liu, G.-Q.; Opatz, T. Chapter Two - Recent Advances in the Synthesis of Piperidines: Functionalization of Preexisting Ring Systems. In *Advances in Heterocyclic Chemistry*; E. F. V. Scriven, C. A. Ramsden, Eds.; Academic Press, 2018; Vol. 125, pp 107–234.

95 Luo, Y.-R.; *Comprehensive Handbook of Chemical Bond Energies*; CRC Press: Boca Raton; 2007.

96 Bordwell pKa Table, http://www.chem.wisc.edu/areas (accessed August 2022).

97 Kerrick, S. T.; Beak, P. *J. Am. Chem. Soc.* **1991**, *113*, 9708–9710.

98 Stead, D.; Carbone, G.; O'Brien, P.; Campos, K. R.; Coldham, I.; Sanderson, A. *J. Am. Chem. Soc.* **2010**, *132*, 7260–7261.

99 Selected examples: (a) Ghobrial, M.; Schnürch, M.; Mihovilovic, M. D. *J. Org. Chem.* **2011**, *76*, 8781–8793; (b) Alagiri, K.; Kumara, G. S. R.; Prabhu, K. R. *Chem. Commun.* **2011**, *47*, 11787–11789; (c) Li, Z.; Li, C.-J. *J. Am. Chem. Soc.* **2005**, *127*, 6968–6969.

100 (a) Seidel, D. *Acc. Chem. Res.* **2015**, *48*, 317–328. (b) Jurberg, I. D.; Peng, B.; Wöstefeld, E.; Wasserloos, M.; Maulide, N. *Angew. Chem. Int. Ed.* **2012**, *51*, 1950–1953.

101 Chen, W.; Wilde, R. G.; Seidel, D. *Org. Lett.* **2014**, *16*, 730–732.

102 McNally, A.; Prier, C. K.; MacMillan, D. W. C. *Science* **2011**, *334*, 1114–1117.

103 (a) Ahneman, D. T.; Doyle, A. G. *Chem. Sci.* **2016**, *7*, 7002–7006; (b) MacMillan, D. W. C.; Cuthbertson, J. D.; Terrett, J. A.; Shurtleff, V. W.; Shaw, M. H. *Science*, **2016**, *352*, 1304–1308.

104 Grainger, R.; Heightman, T. D.; Ley, S. V.; Lima, F.; Johnson, C. N. *Chem. Sci.* **2019**, *10*, 2264–2271.

105 Pastine, S. J.; Gribkov, D. V.; Sames, D. *J. Am. Chem. Soc.* **2006**, *128*, 14220–14221.

106 Prokopcová, H.; Bergman, S. D.; Aelvoet, K.; Smout, V.; Herrebout, W.; Van der Veken, B.; Meerpoel, L.; Maes, B. U. W. *Chem. Eur. J.* **2010**, *16*, 13063–13067.

107 For general reviews of C(sp^3)–H functionalization, see: (a) Godula, K.; Sames, D. *Science* **2006**, *312*, 67. (b) Yamaguchi, J.; Yamaguchi, A. D.; Itami, K. *Angew. Chem. Int. Ed.* **2012**, *51*, 8960. (c) He, J.; Wasa, M.; Chan, K. S. L.; Shao, Q.; Yu, J.-Q. *Chem. Rev.* **2017**, *117*, 8754.

108 Balcells, D.; Clot, E.; Eisenstein, O. *Chem. Rev.* **2010**, *110*, 749–823.

109 Boutadla, Y.; Davies, D. L.; Macgregor, S. A.; Poblador-Bahamonde, A. I. *Dalton Trans.* **2009**, *30*, 5820–5831.

110 Ryabov, A. D.; Sakodinskaya, I. K.; Yatsimirsky, A. K. *J. Chem. Soc., Dalton Trans.* **1985**, *12*, 2629–2638.

111 (a) Park, C.-H.; Ryabova, V.; Seregin, I. V.; Sromek, A. W.; Gevorgyan, V. *Org. Lett.* **2004**, *6*, 1159–1162; (b) Lane, B. S.; Brown, M. A.; Sames, D. *J. Am. Chem. Soc.* **2005**, *127*, 8050–8057.

112 Davies, D. L.; Donald, S. M. A.; Macgregor, S. A. *J. Am. Chem. Soc.* **2005**, *127*, 13754–13755.

113 Davies, D. L.; Macgregor, S. A.; McMullin, C. L. *Chem. Rev.* **2017**, *117*, 8649–8709.

114 Lapointe, D.; Fagnou, K. *Chem. Lett.* **2010,** *39*, 1118–1126.

115 Lafrance, M.; Fagnou, K. *J. Am. Chem. Soc.* **2006**, *128*, 16496–16497.

116 Gorelsky, S. I.; Lapointe, D.; Fagnou, K. *J. Am. Chem. Soc.* **2008**, *130*, 10848–10849.

117 Gorelsky, S. I.; Lapointe, D.; Fagnou, K. *J. Org. Chem.* **2012**, *77*, 658–668.

118 Lafrance, M.; Gorelsky, S. I.; Fagnou, K. *J. Am. Chem. Soc.* **2007**, *129*, 14570–14571.

119 Weibel, J.-M.; Blanc, A.; Pale, P. *Chem. Rev.* **2008**, *108*, 3149–3173.

120 Daugulis, O.; Do, H.-Q.; Shabashov, D. *Acc. Chem. Res.* **2009**, *42*, 1074–1086.

121 Feng, W.; Wang, T.; Liu, D.; Wang, X.; Dang, Y. *ACS Catal.* **2019**, *9*, 6672–6680.

122 Examples of outer-sphere acetate-assisted CMD: (a) Shi, B.-F.; Maugel, N.; Zhang, Y.-H.; Yu, J.-Q. *Angew. Chem. Int. Ed.* **2008**, *47*, 4882–4886. (b) Musaev, D. G.; Kaledin, A.; Shi, B.-F.; Yu, J.-Q. *J. Am. Chem. Soc.* **2012**, *134*, 1690–1698.

123 (a) Liu, B.; Romine, A. M.; Rubel, C. Z.; Engle, K. M.; Shi, B.-F. *Chem. Rev.* **2021**, *121*, 14957–15074; (b) Sambiagio, C.; Schönbauer, D.; Blieck, R.; Dao-Huy, T.; Pototschnig, G.; Schaaf, P.; Wiesinger, T.; Zia, M. F.; Wencel-Delord, J.; Besset, T.; Maes, B. U. W.; Shnürch, M. *Chem. Soc. Rev*. **2018**, *47*, 6603–6743.

124 Alberico, D.; Scott, M. E.; Lautens, M. *Chem. Rev.* **2007**, *107*, 174–238.

125 Zaitsev, V. G.; Shabashov, D.; Daugulis, O. *J. Am. Chem. Soc.* **2005**, *127*, 13154–13155.

126 Shabashov, D.; Daugulis, O. *J. Am. Chem. Soc.* **2010**, *132*, 3965–3972.

127 Wei, Y.; Tang, H.; Cong, X.; Rao, B.; Wu, C.; Zeng, X. *Org. Lett.* **2014**, *16*, 2248–2251.

128 Vicente, J.; Arcas, A.; Juliá-Hernández, F.; Bautista, D. *Angew. Chem. Int. Ed.* **2011**, *50*, 6896–6899.

129 Kinsinger, T.; Kazmaier, U. *Org. Lett.* **2018**, *20*, 7726–7730.

130 Zhang, X.; Lu, G.; Sun, M.; Mahankali, M.; Ma, Y.; Zhang, M.; Hua, W.; Hu, Y.; Wang, Q.; Chen, J.; He, G.; Qi, X.; Shen, W.; Liu, P.; Chen, G. *Nat. Chem.* **2018**, *10*, 540–548.

131 (a) Chapman, L. M.; Beck, J. C.; Wu, L.; Reisman, S. E. *J. Am. Chem. Soc.* **2016**, *138*, 9803–9806; (b) Gutekunst, W. R.; Gianatassio, R.; Baran, P. S. *Angew. Chem. Int. Ed.* **2012**, *51*, 7507−7510.

132 (a) Powers, D. C.; Geibel, M. A. L.; Klein, J. E. M. N.; Ritter, T. *J. Am. Chem. Soc.* **2009**, *131*, 17050–17051; (b) Zhang, L.-L.; Zhang, L.; Li, S.-J.; Fang, D.-C. *Dalton Trans.* **2018**, *47*, 6102–6111.

133 Rej, S.; Ano, Y.; Chatani, N. *Chem. Rev*. **2020**, *120*, 1788–1887.

134 Affron, D. P.; Davis, O. A.; Bull, J. A. *Org. Lett.* **2014**, *16*, 4956–4959.

135 He, G.; Zhang, S.-Y.; Nack, W. A.; Li, Q.; Chen, G. *Angew. Chem. Int. Ed.* **2013**, *52*, 11124–11128.

136 Parella, R.; Babu, S. A. *J. Org. Chem.* **2015**, *80*, 2339–2355.

137 Feng, R.; Wang, B.; Liu, Y.; Liu, Z.; Zhang, Y. *Eur. J. Org. Chem.* **2015**, *2015*, 142–151.

138 Mondal, B.; Roy, B.; Kazmaier, U. *J. Org. Chem.* **2016**, *81*, 11646–11655.

139 Yu, Q.-Y.; Zhong, H.-M.; Sun, W.-W.; Zhang, S.-J.; Cao, P.; Dong, X.-P.; Qin, H.-B.; Liu, J.-K.; Wu, B. *Asian J. Org. Chem.* **2016**, *5*, 608–612.

140 (a) Shan, G.; Yang, X.; Zong, Y.; Rao, Y. *Angew. Chem. Int. Ed.* **2013**, *52*, 13606–13610; (b) Chen, F.-J.; Zhao, S.; Hu, F.; Chen, K.; Zhang, Q.; Zhang, S.-Q.; Shi, B.-F. *Chem. Sci.* **2013**, *4*, 4187–4192.

141 Zhang, S.-Y.; Li, Q.; He, G.; Nack, W. A.; Chen, G. *J. Am. Chem. Soc.* **2013**, *135*, 12135–12141.

142 Yang, Q.; Yang, S.-D. *ACS Catal.* **2017**, *7*, 5220–5224.

143 Zhu, Q.; Ji, D.; Liang, T.; Wang, X.; Xu, Y. *Org. Lett.* **2015**, *17*, 3798–3801.

144 Miao, J.; Yang, K.; Kurek, M.; Ge, H. *Org. Lett.* **2015**, *17*, 3738–3741.

145 Wang, B.; He, G.; Chen, G. *Sci. China Chem.* **2015**, *58*, 1345–1348.

146 Shang, M.; Feu, K. S.; Vantourout, J. C.; Barton, L. M.; Osswald, H. L.; Kato, N.; Gagaring, K.; McNamara, C. W.; Chen, G.; Hu, L.; Ni, S.; Fernández-Canelas, P.; Chen, M.; Merchant, R. R.; Qin, T.; Schreiber, S. L.; Melillo, B.; Yu, J.-Q.; Baran, P. S. *Proc. Natl. Acad. Sci. U.S.A* **2019**, *116*, 8721–8727.

147 Maetani, M.; Kato, N.; Jabor, V. A. P.; Calil, F. A.; Nonato, M. C.; Scherer, C. A.; Schreiber, S. L. *ACS Med. Chem. Lett.* **2017**, *8*, 438–442.

148 Verho, O.; Maetani, M.; Melillo, B.; Zoller, J.; Schreiber, S. L. *Org. Lett.* **2017**, *19*, 4424–4427.

149 Hutskalova, V.; Mykhailiuk, P. K. *Org. Biomol. Chem.* **2019**, *17*, 4342–4349.
150 (a) Sun, W.-W.; Cao, P.; Mei, R.-Q.; Li, Y.; Ma, Y.-L.; Wu, B. *Org. Lett.* **2014**, *16*, 480–483; (b) Zhang, S.-J.; Sun, W.-W.; Cao, P.; Dong, X.-P.; Liu, J.-K.; Wu, B. *J. Org. Chem.* **2016**, *81*, 956–968.
151 Ye, S.; Yang, W.; Coon, T.; Fanning, D.; Neubert, T.; Stamos, D.; Yu, J.-Q. *Chem. Eur. J.* **2016**, *22*, 4748–4752.
152 Van Steijvoort, B. F.; Kaval, N.; Kulago, A. A.; Maes, B. U. W. *ACS Catal.* **2016**, *6*, 4486–4490.
153 Biswas, S.; Van Steijvoort, B. F.; Waeterschoot, M.; Bheemireddy, N. R.; Evano, G.; Maes, B. U. W. *Angew. Chem. Int. Ed.* **2021**, *60*, 21988–21996.
154 Landge, V. G.; Parveen, A.; Nandakumar, A.; Balaraman, E. *Chem. Commun.* **2018**, *54*, 7483–7486.
155 For a review of recent transient directing group strategies for C–H functionalisation, see: Higham, J. I.; Bull, J. A. *Org. Biomol. Chem.* **2020**, *18*, 7291–7315.
156 Chen, Y.-Q.; Wang, Z.; Wu, Y.; Wisniewski, S. R.; Qiao, J. X.; Ewing, W. R.; Eastgate, M. D.; Yu, J.-Q. *J. Am. Chem. Soc.* **2018**, *140*, 17884–17894.
157 Xia, G.; Zhuang, Z.; Liu, L.-Y.; Schreiber, S. L.; Melillo, B.; Yu, J.-Q. *Angew. Chem. Int. Ed.* **2020**, *59*, 7783–7787.
158 Topczewski, J. J.; Cabrera, P. J.; Saper, N. I.; Sanford, M. S. *Nature* **2016**, *531*, 220–224.
159 Aguilera, E. Y.; Sanford, M. S. *Organometallics* **2019**, *38*, 138–142.
160 Cabrera, P. J.; Lee, M.; Sanford, M. S. *J. Am. Chem. Soc.* **2018**, *140*, 5599–5606.
161 Li, Z.; Dechantsreiter, M.; Dandapani, S. *J. Org. Chem.* **2020**, *85*, 6747–6760.
162 Aguilera, E. Y.; Sanford, M. S. *Angew. Chem Int. Ed.* **2021**, *60*, 11227–11230.
163 Wasa, M.; Chan, K. S. L.; Zhang, X.-G.; He, J.; Miura, M.; Yu, J.-Q. *J. Am. Chem. Soc.* **2012**, *134*, 18570–18572.
164 He, J.; Wasa, M.; Chan, K. S. L.; Yu, J.-Q. *J. Am. Chem. Soc.* **2013**, *135*, 3387–3390.
165 He, C.; Gaunt, M. J. *Angew. Chem. Int. Ed.* **2015**, *54*, 15840–15844.
166 Ghouilem, J.; Tran, C.; Grimblat, N.; Retailleau, P.; Alami, M.; Gandon, V.; Messaoudi, S. *ACS Catal.* **2021**, *11*, 1818–1826.
167 Coomber, C. E.; Porter, M. J.; Aliev, A. E.; Smith, P. D.; Sheppard, T. D. *Adv. Synth. Catal.* **2020**, *362*, 5105–5115.
168 Piticari, A.-S.; Antermite, D.; Higham, J. I.; Moore, J. H.; Webster, M. P.; Bull, J. A. *Adv. Synth. Catal.* **2022**, *364*, 1488–1497.
169 Affron, D. P.; Bull, J. A. *Eur. J. Org. Chem.* **2016**, *2016*, 139–149.
170 Antermite, D.; Affron, D. P.; Bull, J. A. *Org. Lett.* **2018**, *20*, 3948–3952.
171 Jerhaoui, S.; Chahdoura, F.; Rose, C.; Djukic, J.-P.; Wencel-Delord, J.; Colobert, F. *Chem. Eur. J.* **2016**, *22*, 17397–17406.
172 Karplus, Martin. *J. Am. Chem. Soc.* **1963**, *85*, 2870–2871.
173 Forrest, T. P. *J. Am. Chem. Soc.* **1975**, *97*, 2628–2630.
174 Lambert, J. B. *J. Am. Chem. Soc.* **1967**, *89*, 1836–1840.

175 Rubiralta, M. ^{1}H NMR Properties of Piperidine Derivatives. In *Piperidine – structure, preparation, reactivity, and synthetic applications of piperidine and its derivatives*; Rubiralta, M., Giralt, E., Diez, A., Eds.; Elsevier, 1991; Vol. 43; pp 34–87.
176 Haasnoot, C. A. G. *J. Am. Chem. Soc.* **1993**, *115*, 1460–1468.
177 Jensen, F. R.; Noyce, D. S.; Sederholm, C. H.; Berlin, A. J. *J. Am. Chem. Soc.* **1962**, *84*, 386–389.
178 Hamlow, H. P.; Okuda, S.; Nakagawa, N. *Tetrahedron Lett.* **1964**, *5*, 2553–2559.
179 Blackburne, I. D.; Katritzky, A. R.; Takeuchi, Y. *Acc. Chem. Res.* **1975**, *8*, 300–306.
180 Abraham, R. J.; Mobli, M.; Smith, R. *J. Magn. Reson. Chem.* **2003**, *41*, 26–36.
181 Hirsch, J. A. Table of Conformational Energies–1967. In *Topics in Stereochemistry*; Allinger, N. L., Eliel, E. L. Eds.; John Wiley & Sons, Inc.: New York, 1967; Vol. 1; pp 199–222.
182 Nack, W. A.; Wang, B.; Wu, X.; Jiao, R.; He, G.; Chen, G. *Org. Chem. Front.* **2016**, *3*, 561–564.
183 Ogawa, A.; Curran, D. P. *J. Org. Chem.* **1997**, *62*, 450–451.
184 Bhattacharya, T.; Ghosh, A.; Maiti, D. *Chem. Sci.* **2021**, *12*, 3857–3870.
185 Wang, P.; Farmer, M. E.; Huo, X.; Jain, P.; Shen, P.-X.; Ishoey, M.; Bradner, J. E.; Wisniewski, S. R.; Eastgate, M. D.; Yu, J.-Q. *J. Am. Chem. Soc.* **2016**, *138*, 9269–9276.
186 Zerella, M.; Mukhopadhyay, S.; Bell, A. T. *Chem. Commun.* **2004**, *17*, 1948–1949.
187 Anand, M.; Sunoj, R. B.; Schaefer, H. F. *J. Am. Chem. Soc.* **2014**, *136*, 5535–5538.
188 JMP®, Version 14. SAS Institute Inc., Cary, NC, 1989–2021.
189 Santos, C. P.; Rato, T. J.; Reis, M. S. *J. Chemom.* **2019**, *33*, e3087.
190 Moore, H. J. Palladium-catalysed C(sp^3)–H Functionalisation of Tetrahydropyran Derivatives. MSci Thesis, Imperial College London, May 2020.
191 Yang, X.; Sun, T.-Y.; Rao, Y. *Chem. Eur. J.* **2016**, *22*, 3273–3277.
192 Probst, N.; Grelier, G.; Dahaoui, S.; Alami, M.; Gandon, V.; Messaoudi, S. *ACS Catal.* **2018**, *8*, 7781–7786.
193 de Esch, I. J. P.; Erlanson, D. A.; Jahnke, W.; Johnson, C. N.; Walsh, L. *J. Med. Chem.* **2022**, *65*, 84–99.
194 Osbourn, J. K. 1.10 - Biological Macromolecules. In *Comprehensive Medicinal Chemistry II*; Taylor, J. B., Triggle, D. J., Eds.; Elsevier: Oxford, 2007; pp 431–447.
195 Scott, D. E.; Coyne, A. G.; Hudson, S. A.; Abell, C. *Biochemistry* **2012**, *51*, 4990–5003.
196 Bollag, G.; Tsai, J.; Zhang, J.; Zhang, C.; Ibrahim, P.; Nolop, K.; Hirth, P. *Nat. Rev. Drug Discov.* **2012**, *11*, 873–886.
197 Bollag, G.; Hirth, P.; Tsai, J.; Zhang, J.; Ibrahim, P. N.; Cho, H.; Spevak, W.; Zhang, C.; Zhang, Y.; Habets, G.; Burton, E. A.; Wong, B.; Tsang, G.; West, B. L.; Powell, B.; Shellooe, R.; Marimuthu, A.; Nguyen, H.; Zhang, K. Y. J.; Artis, D. R.; Schlessinger, J.; Su, F.; Higgins, B.; Iyer, R.; D'Andrea, K.; Koehler, A.; Stumm, M.; Lin, P. S.; Lee, R. J.; Grippo, J.; Puzanov, I.; Kim, K. B.; Ribas, A.; McArthur, G. A.; Sosman, J. A.; Chapman, P. B.; Flaherty, K. T.; Xu, X.; Nathanson, K. L.; Nolop, K. *Nature* **2010**, *467*, 596–599.
198 Kirsch, P.; Hartman, A. M.; Hirsch, A. K. H.; Empting, M. *Molecules* **2019**, *24*, 4309.

199 Chilingaryan, Z.; Yin, Z.; Oakley, A. J. *Int. J. Mol. Sci.* **2012**, *13*, 12857–12879.

200 Carr, R. A. E.; Congreve, M.; Murray, C. W.; Rees, D. C. *Drug Discov.* **2005**, *10*, 987–992.

201 Congreve, M.; Carr, R.; Murray, C.; Jhoti, H. *Drug Discov.* **2003**, *8*, 876–877.

202 Murray, C. W.; Rees, D. C. *Angew. Chem. Int. Ed.* **2016**, *55*, 488–492.

203 O'Reilly, M.; Cleasby, A.; Davies, T. G.; Hall, R. J.; Ludlow, R. F.; Murray, C. W.; Tisi, D.; Jhoti, H. *Drug Discov.* **2019**, *24*, 1081–1086.

204 Feng, K.; Quevedo, R. E.; Kohrt, J. T.; Oderinde, M. S.; Reilly, U.; White, M. C. *Nature* **2020**, *580*, 621–627.

205 Twilton, J.; Le, C. (Chip); Zhang, P.; Shaw, M. H.; Evans, R. W.; MacMillan, D. W. C. *Nat. Rev. Chem.* **2017**, *1*, 1–19.

206 Cernak, T.; Dykstra, K. D.; Tyagarajan, S.; Vachal, P.; Krska, S. W. *Chem. Soc. Rev.* **2016**, *45*, 546–576.

207 Grainger, R.; Heightman, T. D.; Ley, S. V.; Lima, F.; Johnson, C. N. *Chem. Sci.* **2019**, *10*, 2264–2271.

208 Troelsen, N. S.; Clausen, M. H. *Chem. Eur. J.* **2020**, *26*, 11391–11403

209 Keserű, G. M.; Erlanson, D. A.; Ferenczy, G. G.; Hann, M. M.; Murray, C. W.; Pickett, S. D. *J. Med. Chem.* **2016**, *59*, 8189–8206.

210 Cox, O. B.; Krojer, T.; Collins, P.; Monteiro, O.; Talon, R.; Bradley, A.; Fedorov, O.; Amin, J.; Marsden, B. D.; Spencer, J.; Delft, F. von; Brennan, P. E. *Chem. Sci.* **2016**, *7*, 2322–2330.

211 Denis, J. D. S.; Hall, R. J.; Murray, C. W.; Heightman, T. D.; Rees, D. C. *RSC Med. Chem.* **2021**, *12*, 321–329.

212 Hall, R. J.; Murray, C. W.; Verdonk, M. L. *J Med. Chem.* **2017**, *60*, 6440–6450.

213 Lovering, F.; Bikker, J.; Humblet, C. *J. Med. Chem.* **2009**, *52*, 6752–6756.

214 Imbernon, J. R.; Jacquemard, C.; Bret, G.; Marcou, G.; Kellenberger, E. *RSC Med. Chem.* **2022**, *13*, 300–310.

215 Klein, H. F.; Hamilton, D. J.; de Esch, I. J. P.; Wijtmans, M.; O'Brien, P. *Drug Discov.* **2022**, *27*, 2484-2496.

216 Zhang, C.; Ibrahim, P. N.; Zhang, J.; Burton, E. A.; Habets, G.; Zhang, Y.; Powell, B.; West, B. L.; Matusow, B.; Tsang, G.; Shellooe, R.; Carias, H.; Nguyen, H.; Marimuthu, A.; Zhang, K. Y. J.; Oh, A.; Bremer, R.; Hurt, C. R.; Artis, D. R.; Wu, G.; Nespi, M.; Spevak, W.; Lin, P.; Nolop, K.; Hirth, P.; Tesch, G. H.; Bollag, G. *Proc. Natl. Acad. Sci. U.S.A.* **2013**, *110*, 5689−5694.

217 Kwiatkowski, J.; Liu, B.; Tee, D. H. Y.; Chen, G.; Ahmad, N. H. B.; Wong, Y. X.; Poh, Z. Y.; Ang, S. H.; Tan, E. S. W.; Ong, E. H.; Nurul Dinie; Poulsen, A.; Pendharkar, V.; Sangthongpitag, K.; Lee, M. A.; Sepramaniam, S.; Ho, S. Y.; Cherian, J.; Hill, J.; Keller, T. H.; Hung, A. W. *J. Med. Chem.* **2018**, *61*, 4386−4396.

218 King, T. A.; Stewart, H. L.; Mortensen, K. T.; North, A. J. P.; Sore, H. F.; Spring, D. R. *Eur. J. Org. Chem*. **2019**, *2019*, 5219–5229.

219 Chalyk, B. A.; Isakov, A. A.; Butko, M. V.; Hrebeniuk, K. V.; Savych, O. V.; Kucher, O. V.; Gavrilenko, K. S.; Druzhenko, T. V.; Yarmolchuk, V. S.; Zozulya, S.; Mykhailiuk, P. K. *Eur. J. Org. Chem.* **2017**, *2017*, 4530–4542.

220 Garner, P.; Cox, P. B.; Rathnayake, U.; Holloran, N.; Erdman, P. *ACS Med. Chem. Lett.* **2019**, *10*, 811–815.

221 Chawner, S. J.; Cases-Thomas, M. J.; Bull, J. A. *Eur. J. Org. Chem.* **2017**, *2017*, 5015–5024.

222 Lee, M.; Adams, A.; Cox, P. B.; Sanford, M. S. *Synlett.* **2019**, *30*, 417–422.

223 Downes, T. D.; Jones, S. P.; Klein, H. F.; Wheldon, M. C.; Atobe, M.; Bond, P. S.; Firth, J. D.; Chan, N. S.; Waddelove, L.; Hubbard, R. E.; Blakemore, D. C.; De Fusco, C.; Roughley, S. D.; Vidler, L. R.; Whatton, M. A.; Woolford, A. J.-A.; Wrigley, G. L.; O'Brien, P. *Chem. Eur. J.* **2020**, *26*, 8969–8975.

224 Caplin, M. J.; Foley, D. J. *Chem. Sci.* **2021**, *12*, 4646–4660.

225 Berger, M.; Chauhan, R.; Rodrigues, C. A. B.; Maulide, N. *Chem. Eur. J.* **2016**, *22*, 16805–16808.

226 Affron, D. P. Functionalisation of Saturated Heterocycles at Unactivated Positions by Palladium-Catalysed Directed C(sp^3)–H Arylation. PhD Thesis, Imperial College London, 2016.

227 Sambiagio, C.; Schönbauer, D.; Blieck, R.; Dao-Huy, T.; Pototschnig, G.; Schaaf, P.; Wiesinger, T.; Zia, M. F.; Wencel-Delord, J.; Besset, T.; Maes, B. U. W.; Shnürch, M. *Chem. Soc. Rev.* **2018**, *47*, 6603–6743.

228 (a) Evans, D. A.; Carter, P. H.; Dinsmore, C. J.; Barrow, J. C.; Katz, J. L.; Kung, D. W. *Tetrahedron Lett.* **1997**, *38*, 4535–4538. (b) Flynn, D. L.; Zelle, R. E.; Grieco, P. A. *J. Org. Chem.* **1983**, *48*, 2424–2426.

229 Jung, M. F.; Lyster, M. A. *J. Am. Chem. Soc.* **1977**, *99*, 968–969.

230 Zhang, Z.; Zheng, D.; Wan, Y.; Zhang, G.; Bi, J.; Liu, Q.; Liu, T.; Shi, L. *J. Org. Chem.* **2018**, *83*, 1369–1376.

231 Zhang, Z.; Li, X.; Song, M.; Wan, Y.; Zheng, D.; Zhang, G.; Chen, G. *J. Org. Chem.* **2019**, *84*, 12792–12799.

232 Antermite, D. Palladium-Catalysed Directed C(sp^3)–H Functionalisation of Saturated *N*-Heterocycles at Unactivated C4 Positions. PhD Thesis, Imperial College London, 2020.

233 Dohi, T.; Maruyama, A.; Minamitsuji, Y.; Takenaga, N.; Kita, Y. *Chem. Commun.* **2007**, *12*, 1224–1226.

234 Okabe, H.; Naraoka, A.; Isogawa, T.; Oishi, S.; Naka, H..*Org. Lett.* **2019**, *21*, 4767–4770.

235 Daina, A.; Michielin, O.; Zoete, V. *Sci. Rep.* **2017**, *7*, 42717.

236 Wildman, S. A.; Crippen, G. M. *J. Chem. Inf. Comput. Sci.* **1999**, *39*, 868–873.

237 Colomer, I.; Empson, C. J.; Craven, P.; Owen, Z.; Doveston, R. G.; Churcher, I.; Marsden, S. P.; Nelson, A. *Chem. Commun.* **2016**, *52*, 7209–7212.

238 Firth, N. C.; Brown, N.; Blagg, J. *J. Chem. Inf. Model.* **2012**, *52*, 2516–2525.

239 Irwin, J. J.; Sterling, T.; Mysinger, M. M.; Bolstad, E. S.; Coleman, R. G. *J. Chem. Inf. Model.* **2012**, *52*, 1757–1768.

240 Belyanskaya, S. L.; Ding, Y.; Callahan, J. F.; Lazaar, A. L.; Israel, D. I. *ChemBioChem* **2017**, *18*, 837–842.

241 Madsen, D.; Azevedo, C.; Micco, I.; Petersen, L. K.; Hansen, N. J. V. An overview of DNA-encoded libraries: A versatile tool for drug discovery in Progress. In *Medicinal Chemistry*; Witty, D. R., Brian Cox, B., Eds.; Elsevier, 2020; pp 181−249.

242 Shi, Y.; Wu, Y.; Yu, J.; Zhang, W.; Zhuang, C. *RSC Adv.* **2021**, *11*, 2359–2376.

243 Kölmel, D. K.; Loach, R. P.; Knauber, T.; Flanagan, M. E. *ChemMedChem* **2018**, *13*, 2159–2165.

244 Fan, Z.; Zhao, S.; Liu, T.; Shen, P.-X.; Cui, Z.-N.; Zhuang, Z.; Shao, Q.; Chen, J. S.; Ratnayake, A. S.; Flanagan, M. E.; Kölmel, D. K.; Piotrowski, D. W.; Richardson, P.; Yu, J.-Q. *Chem. Sci.* **2020**, *11*, 12282–12288.

245 Arico-Muendel, C. C. *MedChemComm* **2016**, *7*, 1898−1909.

246 Satz, A. L. Foundations of a DNA-Encoded Library (DEL). In *A Handbook for DNA-Encoded Chemistry: Theory and Applications for Exploring Chemical Space and Drug Discovery*; Goodnow, R. A., Eds.; Wiley, 2014; pp 99−121.

247 Gerry, C. J.; Wawer, M. J.; Clemons, P. A.; Schreiber, S. L. *J. Am. Chem. Soc.* **2019**, *141*, 10225–10235.

248 Maetani, M.; Zoller, J.; Melillo, B.; Verho, O.; Kato, N.; Pu, J.; Comer, E.; Schreiber, S. L. *J. Am. Chem. Soc.* **2017**, *139*, 11300–11306.

249 Kumar, A. B.; Anderson, J. M.; Manetsch, R. *Org. Biomol. Chem.* **2011**, *9*, 6284–6292.

250 Basel, Y.; Hassner, A. *J. Org. Chem.* **2000**, *65*, 6368–6380.

251 Bordwell, F. G.; Imes, R. H.; Steiner, E. C. Acidities of Sulfones. *J. Am. Chem. Soc.* **1967**, *89*, 3905–3906.

252 Blackmond, D. G. *Cold Spring Harb. Perspect. Biol.* **2010**, *2*, a002147.

253 Ariëns, E. J. *Eur. J. Clin. Pharmacol.* **1991**, *41*, 89–93.

254 Tokunaga, E.; Yamamoto, T.; Ito, E.; Shibata, N. *Sci. Rep.* **2018**, *8*, 17131.

255 Rentsch, K. M. *J Biochem Biophys Methods* **2002**, *54*, 1–9.

256 Calcaterra, A.; D'Acquarica, I. *J. Pharm. Biomed.* **2018**, *147*, 323–340.

257 Nguyen, L. A.; He, H.; Pham-Huy, C. *Int. J. Biomed. Sci.* **2006**, *2*, 85–100.

258 Farina, V.; Reeves, J. T.; Senanayake, C. H.; Song, J. J. *Chem. Rev.* **2006**, *106*, 2734–2793.

259 Jain, P.; Verma, P.; Xia, G.; Yu, J.-Q. *Nature Chem.* **2017**, *9*, 140–144.

260 Campos, K. R.; Klapars, A.; Waldman, J. H.; Dormer, P. G.; Chen, C. *J. Am. Chem. Soc.* **2006**, *128*, 3538–3539.

261 Cordier, C. J.; Lundgren, R. J.; Fu, G. C. *J. Am. Chem. Soc.* **2013**, *135*, 10946–10949.

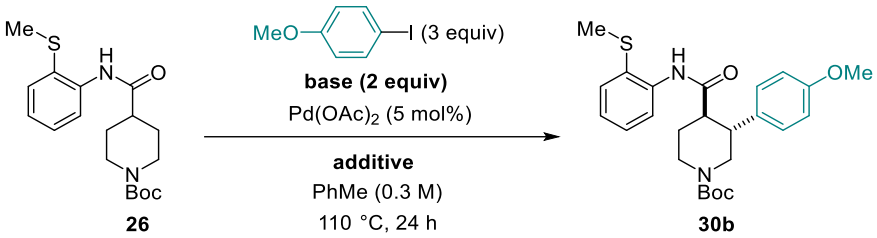
262 (a) He, C.; Gaunt, M. J. *Angew. Chem. Int. Ed.* **2015**, *54*, 15840–15844. Enantioselective variant: (b) Smalley, A. P.; Cuthbertson, J. D.; Gaunt, M. J. *J. Am. Chem. Soc.* **2017**, *139*, 1412–1415.

263 Andrä, M. S.; Schifferer, L.; Pollok, C. H.; Merten, C.; Gooßen, L. J.; Yu, J.-Q. *Chem. Eur. J.* **2019**, *25*, 8503–8507.

264 Yan, S.-B.; Zhang, S.; Duan, W.-L. *Org. Lett.* **2015**, *17*, 2458–2461.

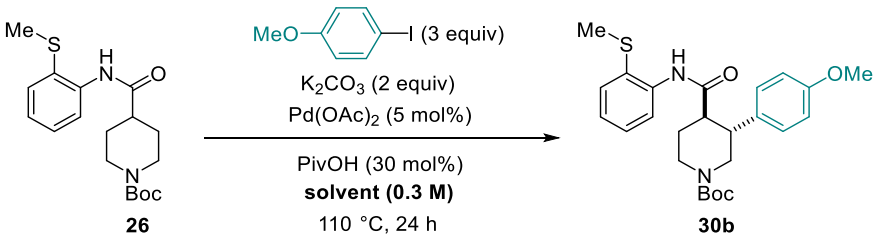
265 Zhang, J. *Org. Biomol. Chem.* **2018**, *16*, 8064–8071.
266 Zaitsev, V. G.; Shabashov, D.; Daugulis, O. *J. Am. Chem. Soc.* **2005**, *127*, 13154–13155.
267 Wang, H.; Tong, H.-R.; He, G.; Chen, G. *Angew. Chem. Int. Ed.* **2016**, *55*, 15387–15391.
268 Bay, K. L.; Yang, Y.-F.; Houk, K. N. *J. Org. Chem.* **2018**, *83*, 14786–14790.
269 Tong, H.-R.; Zheng, S.; Li, X.; Deng, Z.; Wang, H.; He, G.; Peng, Q.; Chen, G. *ACS Catal.* **2018**, *8*, 11502–11512.
270 Yan, S.-Y.; Han, Y.-Q.; Yao, Q.-J.; Nie, X.-L.; Liu, L.; Shi, B.-F. *Angew. Chem. Int. Ed.* **2018**, *57*, 9093–9097.
271 Lv, J.-Z.; Wei, Y.-T.; Yang, L.-Y.; Yang, D.-F.; Li, H.-L. *Catalysts* **2022**, *12*, 537.
272 Han, Y.-Q.; Ding, Y.; Zhou, T.; Yan, S.-Y.; Song, H.; Shi, B.-F. *J. Am. Chem. Soc.* **2019**, *141*, 4558–4563.
273 Zhou, T.; Jiang, M.-X.; Yang, X.; Yue, Q.; Han, Y.-Q.; Ding, Y.; Shi, B.-F. *Chin. J. Chem.* **2020**, *38*, 242–246.
274 Han, Y.-Q.; Yang, X.; Kong, K.-X.; Deng, Y.-T.; Wu, L.-S.; Ding, Y.; Shi, B.-F. *Angew. Chem. Int. Ed.* **2020**, *59*, 20455–20458.
275 Yang, X.; Jiang, M.-X.; Zhou, T.; Han, Y.-Q.; Xu, X.-T.; Zhang, K.; Shi, B.-F. *Chem. Commun.* **2021**, *57*, 5562–5565.
276 Han, Y.-Q.; Zhang, Q.; Yang, X.; Jiang, M.-X.; Ding, Y.; Shi, B.-F. *Org. Lett.* **2021**, *23*, 97–101.
277 Jiang, M.-X.; Yang, X.; Han, Y.-Q.; Zhou, T.; Xu, X.-T.; Zhang, K.; Shi, B.-F. *Org. Chem. Front.* **2021**, *8*, 2903–2908.
278 Dang, Y.; Qu, S.; Nelson, J. W.; Pham, H. D.; Wang, Z.-X.; Wang, X. *J. Am. Chem. Soc.* **2015**, *137*, 2006–2014.
279 Oliveira, M. T.; Lee, J.-W. *ChemCatChem* **2017**, *9*, 377–384.
280 Yan, H.; Jang, H. B.; Lee, J.-W.; Kim, H. K.; Lee, S. W.; Yang, J. W.; Song, C. E. *Angew. Chem. Int. Ed.* **2010**, *49*, 8915–8917.
281 Engle, K. M. *Pure and Applied Chemistry* **2016**, *88*, 119–138.
282 Lee, J. W.; Yan, H.; Jang, H. B.; Kim, H. K.; Park, S.-W.; Lee, S.; Chi, D. Y.; Song, C. E. *Angew. Chem. Int. Ed.* **2009**, *48*, 7683–7686.
283 Bergens, S. H.; Leung, P. H.; Bosnich, B.; Rheingold, A. L. *Organometallics* **1990**, *9*, 2406–2408.
284 Pichette Drapeau, M.; Gooßen, L. J. *Chem. Eur. J.* **2016**, *22*, 18654–18677.
285 Dai, H.-X.; Stepan, A. F.; Plummer, M. S.; Zhang, Y.-H.; Yu, J.-Q. *J. Am. Chem. Soc.* **2011**, *133*, 7222–7228.
286 Bull, J. A.; Mousseau, J. J.; Charette, A. B. *Org. Lett.* **2008**, *10*, 5485–5488.

Appendix 1 – Optimisation Screen in the Presence of 2-(Methylthio)aniline Directing Group



Entry	Base	Additive	Product (%)[a]	RSM (%)[a]
1	K_2CO_3	PivOH (30 mol%)	**30b** (29)	67
2	K_2CO_3	PivOH (200 mol%)	**30b** (16)	72
3	Ag_2CO_3	PivOH (30 mol%)	**none**	84
4	Cs_2CO_3	PivOH (30 mol%)	**30b** (9)	80
5	AgOAc	PivOH (30 mol%)	**none**	86
6	CsOAc	PivOH (30 mol%)	**30b** (15)	70

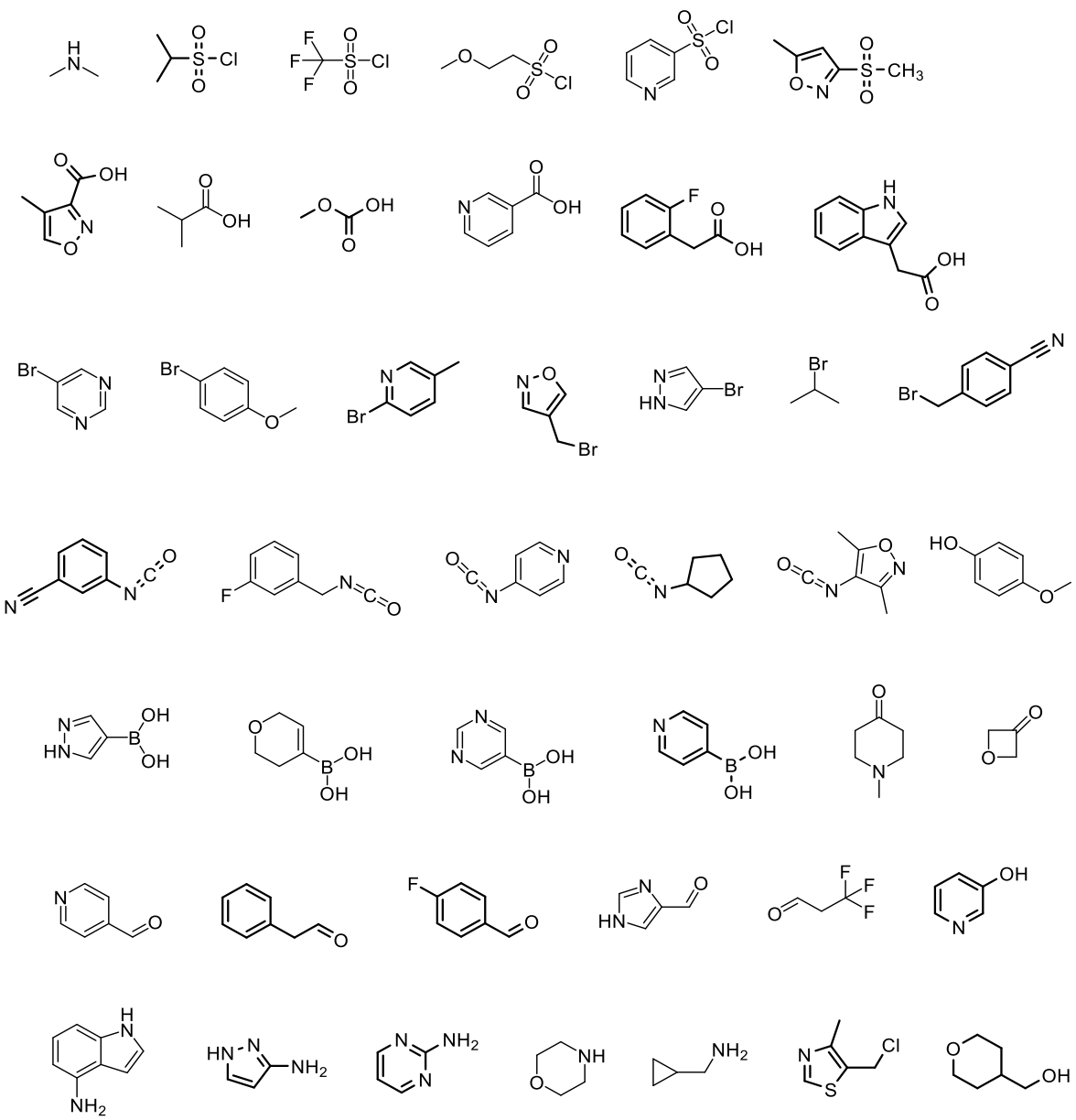
Table S1 Base screen using the 2-(methylthio)aniline directing group. Reaction scale: 0.2 mmol. [a]Calculated by ^{1}H NMR using 1,3,5-trimethoxybenzene as internal standard.



Entry	Solvent	Product (%)[a]	RSM (%)[a]
1	toluene	**30b** (26)	70
2	xylenes	**30b** (23)	76
3	dioxane	**none**	90
4	*t*-amylOH	**30b** (20)	68
5	HFIP	**none**	99
6	DCE	**30b** (32)	66
7[b]	CH_2Cl_2	**none**	88
8	MeCN	**30b** (12)	72

Table S2 Base screen using the 2-(methylthio)aniline directing group. Reaction scale: 0.2 mmol. [a]Calculated by ^{1}H NMR using 1,3,5-trimethoxybenzene as internal standard.[b]Reaction conducted at 45 °C.

Appendix 2 – List of Default Reagents Used in LLAMA Scaffold Decoration



Virtual scaffold elaboration reactions used: Alcohol alkylation; Amide formation; Alcohol arylation; Buchwald-Hartwig amination; Carbamate formation; Esterification; Secondary amide formation; Secondary amide alkylation; Reductive amination; Suzuki coupling; Sulfonamide formation; Urea alkylation; Urea arylation. Urea formation.